

ICBME 2013

The 15th International Conference on
Biomedical Engineering

4 – 7 December 2013, Singapore

www.icbme.org



PROGRAMME
& ABSTRACTS

Jointly organised by



Department of
Biomedical Engineering



Biomedical Engineering Society
(Singapore)

ICBME 2013 : Programme-At-A-Glance

Wednesday, 04 December 2013

Time	Venue/Description					
09:15	Conference Opening Ceremony @ Auditorium					
10:00	Tea Break					
10:30	Plenary Lecture 1 @ Auditorium					
11:00	Biomaterials for Tissue Engineering by Antonios G. Mikos, <i>Rice University, USA</i>					
11:15	Auditorium	SR 1&2	SR 3&4	SR 5&6	SR 7&8	SR 12
	SYM-01: Musculoskeletal Tissue Engineering	A1: Medical Imaging	B1: Regenerative Medicine	C1: Cardiovascular Mechanics	D1: Biomedical Devices and Biomedical Instrumentation	E1: Assisted Technologies
12:45	Lunch					
13:45	Plenary Lecture 2 @ Auditorium Biomechanics of Arterial Walls in Health and Disease: State of the Art and Challenges Ahead by Gerhard A. Holzapfel, <i>Graz University of Technology, Austria</i>					
14:30	Short Break					
14:45	Auditorium	SR 1&2	SR 3&4	SR 5&6	SR 7&8	SR 12
	SYM-02A: Gastrointestinal Motility Symposium	A2: Biosignal Processing	B2: Regenerative Medicine Tissue Engineering	C2: Musculoskeletal Mechanics	D2: Diagnostic Devices Implantable Devices	SYM-03A: Micro and Nanofluidics for Biomedical Applications
16:15	Tea Break					
16:45	Auditorium	SR 1&2	SR 3&4	SR 5&6	SR 7&8	SR 12
	SYM-02B (cont'd): Gastrointestinal Motility Symposium	A3: Bioelectronics	B3: Biological Materials	C3: Cardiovascular Mechanics Computational Mechanics	Edn: Biomedical Engineering Education Session	SYM-03B (cont'd): Micro and Nanofluidics for Biomedical Applications
End of Day 1						

Poster Session 1

Thursday, 05 December 2013

Time	Venue/Description					
9:00	Plenary Lecture 3 @ Auditorium Integration of Computer Assisted Surgical Guidance and Surgical Robotics for Robotics for Minimally Invasive Surgery by Ichiro Sakuma, <i>The University of Tokyo, Japan</i>					
9:45	Plenary Lecture 4 @ Auditorium Autodigestion: A missing link to inflammation and disease by Geert W. Schmid-Schönbein, <i>University of California San Diego, United States of America</i>					
10:30	Tea Break					
11:00	Auditorium	SR 1&2	SR 3&4	SR 5&6	SR 7&8	SR 12
	SYM-04: Biomechanics in Nature and Bioinspired Engineering	A4: Biosignal Processing	B5: Controlled Drug Delivery	C4: Musculoskeletal Mechanics	YIA-01: Young Investigator Award I	B4: Tissue Engineering
12:30	Lunch					
13:30	Plenary Lecture 5 @ Auditorium Biomedical Micro and Nanotechnology: From Lab-on-Chip to Building Systems with Cells by Rashid Bashir, <i>University of Illinois, United States of America</i>					
14:15	Short Break					
14:30	Auditorium	SR 1&2	SR 3&4	SR 5&6	SR 7&8	SR 12
	SYM-05: Supramolecular and Nano-Biomaterials	A5: Biosignal Processing	B6: Pharmaceutical Science & Engineering	C5: Orthopaedics	YIA-02: Young Investigator Award II	SYM-06: Reproductive Bioengineering
16:00	Tea Break					
16:30	Auditorium	SR 1&2	SR 3&4	SR 5&6	SR 7&8	SR 12
	SYM-07: Virtual Physiological Rat Project	A6: Medical Imaging	SYM-09: Pharmaceutical Science and Engineering	C6: Computational Mechanics	E2: Assisted Technologies	SYM-08: Tissue Mechanobiology: Tissue on the move
End of Day 2						

Poster Session 2

Foreword

On behalf of the organising committee of the International Conference on Biomedical Engineering (ICBME) 2013, we would like to warmly welcome you to this meeting. This conference is part of a series that began in 1983 and is jointly organised by the Faculty of Engineering of the National University of Singapore (NUS) and the Biomedical Engineering Society (Singapore) (BES). This conference is also endorsed by the International Federation for Medical and Biological Engineering (IFMBE).

We are happy to report that we have more than 600 participants from 35 countries. We have received very high quality papers and as a result, we had to decline a substantial number of papers. In this conference proceedings, we have published 245 papers with 6 being symposium papers, 11 Young Investigator Awards (YIA) papers, 118 oral presentation papers and 110 Poster papers. We are also very honoured to have invited very prominent speakers. Each of these speakers is an authority in their own field of expertise and we are grateful that they are able to take time to participate in this conference.

In this conference, we have also included a design competition jointly organised by the BES and the Society of Engineers for the Community (SEC). The focus of the competition is on the design of a low-cost medical device to improve healthcare in resource-scarce communities. The competition is opened to teams comprising up to five bona-fide students. We are pleased to report that we have 12 entries from 8 countries.

While the success of this conference lies in the participation of the delegates and the quality of papers presented, we are also mindful of the efforts put in by many of the volunteers, reviewers, as well as the members of the Organising Committee and the International Advisory Committee. Their dedicated contributions to this meeting are very much acknowledged and appreciated. We would also like to sincerely thank our sponsors, supporters and exhibitors for contributing to the success of this conference. Finally, we would like to thank the staff of INMEET CMS who has ensured the smooth running of the conference.

Finally, to all our delegates, I hope the 15th ICBME 2013 will not only be one where excellent scientific exchanges are facilitated, but also one where old friendships are renewed and new friends made. Do enjoy the conference as well as the sights and sounds of Singapore!

Best wishes,

Prof. James GOH
Chairman

Prof. Chwee Teck LIM
Scientific Program Chair

15th ICBME Organising Committee

Table of Contents

<i>Foreword</i>	i
<i>About ICBME Conference Series</i>	iv
<i>Organisers</i>	iv
<i>Committees</i>	vii
<i>Themes & Topics</i>	x
<i>Speakers</i>	xi
<i>Symposia</i>	xiii
<i>Acknowledgements</i>	xv
<i>General Information</i>	xvi
Programme	
Day 1 — Wednesday, 4 December 2013	P-3
Day 2 — Thursday, 5 December 2013	P-15
Day 3 — Friday, 6 December 2013	P-28
Day 4 — Saturday, 7 December 2013	P-41
Abstracts	
Day 1 — Wednesday, 4 December 2013	3
Day 2 — Thursday, 5 December 2013	44
Day 3 — Friday, 6 December 2013	88
Day 4 — Saturday, 7 December 2013	130
Poster Abstracts	
Day 1 — Wednesday, 4 December 2013	155
Day 2 — Thursday, 5 December 2013	180
Day 3 — Friday, 6 December 2013	204
<i>Author Index</i>	231

About ICBME Conference Series

The ICBME is a series of international conference in biomedical engineering held in Singapore. Our past conferences have been successful in attracting over 600 participants from more than 40 countries. The next conference will be hosted from 4-7 December 2013 in Singapore.

Biomedical engineering is applied in most aspects of our healthcare ecosystem. From electronic health records to diagnostic tools to therapeutic, rehabilitative and regenerative treatments, the work of biomedical engineers is evident. Biomedical engineers work at the intersection of engineering, life sciences and healthcare. The engineers would use principles from applied science including mechanical, electrical, chemical and computer engineering together with physical sciences including physics, chemistry and mathematics to apply them to biology and medicine. Applying such concepts to the human body is very much the same concepts that go into building and programming a machine. The goal is to better understand, replace or fix a target system to ultimately improve the quality of healthcare.

With this understanding, we have created the International Conference in BioMedical Engineering to offer a single platform for individuals and organisations working in the biomedical engineering related field to gather and network with each other in so doing create the catalyst for future development of biomedical engineering in Asia.

The 15th International Conference on Biomedical Engineering is endorsed by the International Federation for Medical and Biological Engineering (IFMBE).



Organisers



Biomedical Engineering Society (Singapore)

The Biomedical Engineering Society (Singapore) had its humble beginning in 1991, when a group of doctors and engineers who had been working together on biomedical engineering research projects decided to form a society to promote the field of Biomedical Engineering in Singapore.

The Founding President was Prof Kamal Bose an Orthopaedic Surgeon with a passion for interdisciplinary collaboration. He steered the Society during its early years and set the sight for academic excellence in biomedical engineering. He left a lasting legacy of successful conferences on biomedical engineering organised by the Society. Prof Chew Yong Tian succeeded Prof Bose as the second President of BES. Prof Chew, a Mechanical Engineer led the Society to greater heights. The conferences organised by the Society achieved international status. Indeed, BES successfully hosted the 6th World Congress on Biomechanics in 2010 which saw 1600 participants from 42 countries around the world congregating in Singapore's Suntec City Convention Centre. Prof Bose and Prof Chew had laid the strong foundation for the building of the Society.

In view of BES' academic strength and its association to the various tertiary institutions, BES set up a Student Chapter in 2009. The Student Chapter organises the BES' Scientific Meetings with participation of students from Junior Colleges, Polytechnics and Universities. BES launched the Industry Chapter on the 12th November 2011 as part of its 20th Anniversary Celebration.

Apart from creating these two synergistic platforms to address human capital development for the biomedical industry locally and regionally, BES is also well connected around the world. BES is affiliated to the International Federation of Medical and Biological Engineering (IFMBE) since 1994. It allows the Society to plug into 65 sister societies around the world, boasting a total membership of 120,000 biomedical engineers.



National University of Singapore, Department of Biomedical Engineering, Faculty of Engineering

The NUS' Department of Biomedical Engineering is a University Department which was established in 2002. Our talented academic staff has varied background in engineering, life sciences and medicine. Many of whom has joint appointments with either the YLL School of Medicine, Faculty of Science, Faculty of Engineering, Mechanobiology Institute or A*STAR Research Institutes. This is a reflection of the multidisciplinary and integrative approach we take in bioengineering research and education.

Broadly speaking, the core research expertise available in the department include Biomaterials, Biomechanics, Bionanotechnology, Biosignal Processing, Biosensors, Biomicrofluidics, Computational Methods with application in areas of Tissue Engineering, Therapeutic Delivery Systems, Biomedical Imaging and Instrumentation, and Medical Devices just to name a few. Last

year, the total research funding received was more than S\$4.5 million. Several breakthrough projects were undertaken, for example, Associate Professor Zhang Yong led a team to develop a user-friendly method to produce nanocrystals with strong “up-conversion” fluorescence at low temperature which could be used for treating malignant melanoma. Another team led by Assistant Professor Chen Nanguang made significant headway in the development of diffuse optical tomography which may lead to a potential clinical imaging tool for applications such as breast cancer detection and brain function study.

The undergraduate programme while designed to provide students with strong fundamental and broad based learning in engineering and life sciences, its approach is integrative and students are exposed to clinical applications as well. There is strong emphasis in engineering design in the curriculum. In fact students have a choice to enroll in the Design-Centric Curriculum (DCC) under the theme “Engineering in Medicine”. In the final year, students are required to take on individual research projects. Past students had done extremely well, winning regional and international awards. For example, last year Natalie Lim Sheng Jie won the National Research and Innovation Competition’s Best Award held in Universiti Sains Malaysia beating 130 other entries from over 20 universities. Her research work focused on detecting early signs of cartilage damage using microspectroscopy technology.

Outstanding undergraduate students can enrolled in the accelerated programme, the Global Engineering Programme (GEP) leading to the award of two degrees in 4 years, ie a Bachelor of Engineering (B.Eng.) at NUS and for those who qualify for admission to a top partner university, a Master degree in Engineering. We also have an excellent PhD graduate programme that aims to train graduate students in multidisciplinary bioengineering research. Highly competitive research scholarships are offered to students that demonstrate potential in research.

Committees

Organising Committee

Chairperson	James Goh
Co-Chair & Treasurer	Siew Lok Toh
Scientific Program Chair	Chwee Teck Lim
YIA Awards Chair	Sierin Lim
BES-SEC Design Competition Chair	Alberto Corrias
Members	Peck Ha Khoo-Tan Jeff Schmidt

International Advisory Committee

Taiji Adachi <i>Kyoto University</i>	Yubo Fan <i>Beihang University</i>
Kainan An <i>Mayo Clinic</i>	Janie Fouke <i>Nanyang Technological University</i>
Cholid Badri <i>Universitas Indonesia</i>	Bin He <i>University of Minnesota</i>
Gang Bao <i>Georgia Institute of Technology</i>	Herbert Voigt <i>Boston University</i>
Rashid Bashir <i>University of Illinois at Urbana-Champaign</i>	Walter Herzog <i>University of Calgary</i>
Cheng-Kung Cheng <i>National Yang Ming University</i>	I-Ming Hsing <i>The Hong Kong University of Science & Technology</i>
Shu Chien <i>University of California, San Diego</i>	Peter Hunter <i>University of Auckland</i>
J.E. Davies <i>University of Toronto</i>	Dietmar Hutmacher <i>Queensland University of Technology</i>
Yiping Du <i>Zhejiang University</i>	Zhonglai Jiang <i>Shanghai Jiao Tong University</i>
David Elad <i>Tel Aviv University</i>	Roger Kamm <i>Massachusetts Institute of Technology</i>
Ross Ethier <i>Georgia Institute of Technology</i>	Young-Ho Kim <i>Yonsei University</i>
Jing Fan <i>Peking University</i>	Eng Hin Lee <i>National University of Singapore</i>

Kam Leong
Duke University

Kangping Lin
Chung-Yuan Christian University

Feng Huai Lin
National Taiwan University

Hao Liu
Chiba University

Mian Long
Chinese Academy of Sciences

Ratko Magjarević
University of Zagreb

Arthur Mak
Chinese University of Hong Kong

Takeo Matsumoto
Nagoya Institute of Technology

Karol Miller
University of Western Australia

Ralph Muller
Eidgenössische Technische Hochschule Zürich

Nigel Novell
University of New South Wales

Teruo Okano
Tokyo Women's Medical University

Marcus Pandy
University of Melbourne

Mark Pearcy
Queensland University of Technology

Robert Ritchie
University of California, Berkeley

Ichiro Sakuma
Tokyo University

Masaaki Sato
Tohoku University

Michael Sheetz
National University of Singapore

Molly Shoichet
University of Toronto

Fong Chin Su
National Cheng Kung University

Toshiyo Tamura
Osaka Electro-Communication University

Kazuo Tanishita
Waseda University

David Townsend
National University Health System

Shigeo Wada
Osaka University

Jawlin Wang
National Taiwan University

David F. Williams
Wake Forest University

Ed X. Wu
University of Hong Kong

Takami Yamaguchi
Tohoku University

Ajit Yoganathan
Georgia Institute of Technology

Haishan Zeng
University of British Columbia

Yuan-Ting Zhang
Chinese University of Hong Kong

Scientific Program Committee

Scientific Program Chair

Chwee Teck Lim, *National University of Singapore*

Members

Biomedical Imaging

Anqi Qiu, *National University of Singapore*

Biomedical Instrumentation

Zhiwei Huang, *National University of Singapore*
Changyuan Yu, *National University of Singapore*
Chengkuo Lee, *National University of Singapore*

Biosignal Processing

Nanguang Chen, *National University of Singapore*
Shanbao Tong, *Shanghai Jiaotong University*
Linbo Liu, *Nanyang Technological University*

Clinical Engineering

Peck Ha Khoo-Tan, *Ngee Ann Polytechnic*

Neuroengineering

Shih Cheng Yen, *National University of Singapore*
Zhi Yang, *National University of Singapore*

Telemedicine & Healthcare

Johnny Chee, *Ngee Ann Polytechnic*
Karen Chua, *Tan Tock Seng Hospital*

Biosensors and BioMEMs

Dieter Trau, *National University of Singapore*

Micro/Nano Biomedical Devices

Chia Hung Chen, *National University of Singapore*

Nanobiotechnology

Yong Zhang, *National University of Singapore*
Long Ping Wen, *University of Science & Technology of China*
James Kah, *National University of Singapore*

Computer-Integrated & Robot-Assisted Surgery

Chee Kong Chui, *National University of Singapore*
Jimmy Liu, *A*Star*

Ergonomics & Human Factors

Kay Chuan Tan, *National University of Singapore*
John Brian Peacock, *National University of Singapore*

Bio-Robotics

Chee Meng Chew, *National University of Singapore*
Peter Chen, *National University of Singapore*

Rehabilitation Engineering & Assistive Technology

Hao Yong Yu, *National University of Singapore*
Domenico Campolo, *Nanyang Technological University*
Yue Hong Yin, *Shanghai Jiaotong University*

Artificial Organs

Hwa Liang Leo, *National University of Singapore*
Yan Wang, *Zhujiang Hospital & Southern Medical University*

Biomaterials

Jun Li, *National University of Singapore*

Controlled Drug Delivery

Chi Hwa Wang, *National University of Singapore*
Yi Yan Yang, *A*Star*

Pharmaceutical Sciences & Engineering

Sierin Lim, *Nanyang Technological University*
Kathy Luo, *Nanyang Technological University*

Regenerative Medicine & Tissue Engineering

Evelyn Yim, *National University of Singapore*
Andrew Wan, *A*Star*

Sports Biomechanics & Human Performance

Fook Rhu Ong, *Singapore Polytechnic*
Veni Kong, *National Institute of Education Singapore*

Cardiovascular Bioengineering

Sangho Kim, *National University of Singapore*

Cell & Molecular Bioengineering

Pakorn Kanachawang, *National University of Singapore*
Jean-Cheng Kuo, *National Yang Ming University*

Computational Bioengineering

Martin Buist, *National University of Singapore*
Cheng Leo, *University of Auckland*

Dental Bioengineering

Tong Cao, *National University of Singapore*
Amr Sherif Fawzy, *National University of Singapore*

Organ and Tissue Mechanics

Yusuke Toyama, *National University of Singapore*
Lance Davidson, *University of Pittsburgh*

Orthopaedic Biomechanics

Peter Lee, *University of Melbourne*
Tae Yong Lee, *National University of Singapore*

Biomedical Engineering Education

Siew Lok Toh, *National University of Singapore*

Themes and Topics

The conference is divided into the following major themes, with its respective topics (but not limited to) as follows:

A. Bioimaging and Biosignals

1. Bioelectronics
2. Biosignal Processing
3. Image Guided Intervention
4. Medical Imaging
5. Optical Imaging

B. Biomaterials and Tissue Engineering

1. Biological Materials
2. Controlled Drug Delivery
3. Diagnostics and Therapeutics
4. Gene Vectors Delivery
5. Host Response
6. Pharmaceutical Science and Engineering
7. Polymer Synthesis and Characterization
8. Regenerative Medicine
9. Tissue Engineering

C. Biomechanics and Computational Bioengineering

1. Biomimetics
2. Cardiovascular Mechanics
3. Cell Mechanics
4. Computational Mechanics
5. Insect and Animal Biomechanics
6. Mechanobiology
7. Molecular Biomechanics
8. Musculoskeletal Mechanics
9. Orthopaedics
10. Tissue Mechanics
11. Organ Mechanics

D. Biomedical Devices and Biomedical Instrumentation

1. Biochips
2. Biomedical Devices
3. BioMEMS
4. Diagnostic Devices
5. Implantable Devices
6. Lab-on-Chip
7. Microarrays
8. Micro/Nanofabrication
9. Micro/Nanofluidics
10. Micro-Total Analysis Systems
11. Organ-on-Chip
12. Surgical Tools

E. Biomedical Robotics and Surgical Technology

1. Assisted Technologies
2. Bio- and Medical Robotics
3. Bioinstrumentation and Control
4. Rehabilitation
5. Soft Robotics

F. Neuroengineering and Rehabilitation Engineering

1. Clinical and Translational Neuroengineering
2. Cognitive Engineering
3. Neurotechnology
4. Neurotherapeutics

G. Special Topics

1. Bioethics
2. Biomedical Engineering Education
3. Manuscript Writing

Speakers

Plenary Speakers

Plenary 1 : Biomaterials for Tissue Engineering

Antonios G. Mikos

*John W. Cox Laboratory of Biomedical Engineering, Center for Excellence in Tissue Engineering,
Rice University*

Plenary 2 : Biomechanics of Arterial Walls in Health and Disease: State of the Art and Challenges Ahead

Gerhard A. Holzapfel

Institute of Biomechanics, Graz University of Technology

Plenary 3 : Integration of Computer Assisted Surgical Guidance and Surgical Robotics for Minimally Invasive Surgery

Ichiro Sakuma

*Department of Precision Engineering/Department of Bioengineering, School of Engineering,
The University of Tokyo*

Plenary 4 : Autodigestion: A Missing Link to Inflammation and Disease

Geert Schmid-Schoenbein

Bioengineering, UCSD Jacob School of Bioengineering

Plenary 5 : Biomedical Micro and Nanotechnology: From Lab-on-Chip to Building Systems with Cells

Rashid Bashir

Department of Electrical and Computing Engineering, University of Illinois

Plenary 6 : Advancing Multi-Modality Clinical Imaging: A Challenge for the Engineer and Physicist

David Townsend

*Director, A*STAR-NUS Clinical Imaging Research Centre (CIRC)*

Plenary 7 : Brain Machine Interface Technology: From Neurons to Prostheses

Nitish Thakor

SiNAPSE, Singapore & Johns Hopkins School of Medicine, USA

Keynote Speakers

Keynote 1

Biomedical Imaging – MRI Visualization of Living Biological Systems

Ed X. Wu

University of Hong Kong, Hong Kong S.A.R. (China)

Keynote 2

Application of Bioimaging to Tissue Engineering and Regenerative Medicine

Kishore Bhakoo

Singapore Bioimaging Consortium, Singapore

Keynote 3

Electrochemistry and Nanotechnology in Biomicrosystems for Point of Care Applications

I-Ming Hsing

The Hong Kong University of Science & Technology, Hong Kong, China

Keynote 4

Robots and the Human

Oussama Khatib

Stanford University, USA

Keynote 5

Nestin-Expressing Multipotent Hair Follicle Stem Cells for Regenerative Medicine

Robert Hoffman

University of California, San Diego, USA

Keynote 6

Drug Delivery Technology for Tissue Regeneration Therapy

Yasuhiko Tabata

Kyoto University, Japan

Keynote 7

Development, Validation of a Degenerated Intervertebral Disc Model and its Application in Disc Research

Jaw-Lin Wang

National Taiwan University, Taiwan

Keynote 8

Current Biomaterials for Tendon / Ligament Tissue Engineering

Hong Wei Ouyang

Zhejiang University, Hangzhou, China

Keynote 9

An Overview of VPH/ Physiome Activities

Peter Hunter

University of Auckland, New Zealand

Keynote 10

Lessons Learnt: Development of Genomics-based Diagnostics Tests

Christopher Wong

Genome Institute of Singapore, Singapore

Keynote 11

Robotics in Gastroenterology: Bench to Beside, and Beyond

Louis Phee

Nanyang Technological University, Singapore

Keynote 12

Title not available at time of print

Theodoros Kofidis

National University Heart Centre, Singapore

Symposia

Symposium	Date / Time	Chair	Co-Chairs
SYM-01 Musculoskeletal Tissue Engineering	Wednesday, 4 Dec 2013 / 11:00–12:30 hrs	Eng Hin Lee National University of Singapore	
SYM-02 Gastrointestinal Motility	Wednesday, 4 Dec 2013 / 14:45–16:15 hrs & 16:45–18:15 hrs	Martin Buist National University of Singapore	Leo Cheng University of Auckland
SYM-03 Micro and Nanofluidics for Biomedical Applications	Wednesday, 4 Dec 2013 / 14:45–16:15 hrs & 16:45–18:15 hrs	Chwee Teck Lim National University of Singapore	Dino Di Carlo The University of California San Diego Jay Han Massachusetts Institute of Technology
SYM-04 Biomechanics in Nature and Bioinspired Engineering	Thursday, 5 Dec 2013 / 11:00–12:30 hrs	Hao Liu Chiba University	Masatsugu Shimomura Tohoku University
SYM-05 Supramolecular and Nano-Biomaterials	Thursday, 5 Dec 2013 / 14:30–16:00 hrs	Jun Li National University of Singapore	Jun Araki Shinshu University
SYM-06 Reproductive Bioengineering	Thursday, 5 Dec 2013 / 14:30–16:00 hrs	David Elad Tel Aviv University	

Symposium	Date / Time	Chair	Co-Chairs
SYM-07 Virtual Physiological Rat Project	Thursday, 5 Dec 2013 / 16:30–18:00 hrs	David Nickerson <i>The University of Auckland</i>	
SYM-08 Tissue Mechanobiology: Tissue on the move	Thursday, 5 Dec 2013 / 16:30–18:00 hrs	Yusuke Toyama <i>National University of Singapore</i>	
SYM-09 Pharmaceutical Science and Engineering	Thursday, 5 Dec 2013 / 16:30–18:00 hrs	Sierin Lim <i>Nanyang Technological University</i>	Kathy Luo Qian <i>Nanyang Technological University</i>
SYM-10 Nanoparticles for Bioimaging and Targeted Therapy	Friday, 6 Dec 2013 / 11:00–12:30 hrs	Yong Zhang <i>National University of Singapore</i>	James Kah <i>National University of Singapore</i>
SYM-11 Biomedical Engineering in Sport Science	Friday, 6 Dec 2013 / 11:00–12:30 hrs	Matthias Lochmann <i>Institut für Sportwissenschaft und Sport</i>	
SYM-12 Emerging Developments for Regenerative & Therapeutic Medicine	Friday, 6 Dec 2013 / 13:30–15:00 hrs	Evelyn Yim <i>National University of Singapore</i>	Andrew Wan <i>Institute of Bioengineering and Nanotechnology, A*STAR</i>

Acknowledgements

The organising committee would like to thank the following organisations for their support towards the conference:



National Institute for Materials Science, Japan

<http://www.nims.go.jp/mmsp/en/>

The mission of NIMS Molecule & Material Synthesis Platform is to provide a research environment where activities ranging from basic research in nanotechnology and bioscience to the creation of innovations useful to society and industry can be carried out. Towards this end, we provide R&D support with a focus on interdisciplinary biotechnology and nanotechnology/materials science research.



Springer

Springer's business is publishing. Throughout the world, Springer provides scientific and professional communities with superior specialist information – produced by authors and colleagues across cultures in a nurtured collegial atmosphere of which we are justifiably proud. Springer fosters communication among our customers – researchers, students and professionals – enabling them to work more efficiently, thereby advancing knowledge and learning. Springer's dynamic growth allows it to invest continually all over the world. Springer thinks ahead, moves fast and promotes change: creative business models, inventive products, and mutually beneficial international partnerships have established Springer as a trusted supplier and pioneer in the information age.

The IFMBE Proceedings book series presents the results of IFMBE Conferences. These scientific conferences – organized or endorsed by the International Federation for Medical and Biological Engineering (IFMBE) – deal with various topics of medical, biological and clinical engineering, and biophysics and they are. The aims of the IFMBE conferences are to encourage research and the application of knowledge, and to disseminate information and promote collaboration. The papers of the IFMBE proceedings present research results of a high impact for the community and their high scientific standard is guaranteed by a double peer-reviewing of every published paper.

The topics included but are not limited to:

- Diagnostic Imaging, Image Processing, Biosignal Processing
- Modeling and Simulation, Biomechanics
- Biomaterials, Cellular and Tissue Engineering
- Information and Communication in Medicine, Telemedicine and e-Health
- Instrumentation and Clinical Engineering
- Surgery, Minimal Invasive Interventions, Endoscopy and Image Guided Therapy
- Audiology, Ophthalmology, Emergency and Dental Medicine Applications
- Radiology, Radiation Oncology and Biological Effects of Radiation

The IFMBE Proceedings series is an official publication of the International Federation for Medical and Biological Engineering (IFMBE).

General Information

Conference Venue

Town Plaza, University Town (UTown)
National University of Singapore

Registration Desk Opening Hours

Level 1, Town Plaza, UTown
Foyer of Auditorium 1

4 December 2013	Wednesday	08:00–16:00 hrs
5 December 2013	Thursday	08:30–15:30 hrs
6 December 2013	Friday	08:30–15:30 hrs
7 December 2013	Saturday	08:30–11:00 hrs

Conference Banquet (Ticketed event)

Date / Time: Friday, 6 December 2013 / 18:30–21:30 hrs

Venue: Roselle Junior Ballroom: 4611-3 & 4711-3,
Sands Expo & Convention Center 10 Bayfront Avenue, Singapore 018956

Menu: Chinese menu (no pork, no lard)

Dress Code: Smart Casual

Ticket price: S\$120 per ticket

Participants who have purchased tickets will receive their tickets in the conference kit issued to them onsite. Complimentary bus service from the conference venue to the banquet venue will be provided. Please check with the registration counter for bus pick up schedule.

Limited tickets are available for sale onsite, on a first-come-first-served basis. Ticket sale closes at 14:00 hrs on 4 December 2013. (Note: Only cash payment will be accepted for onsite purchase).

Badges & Security

All participants will receive their badges upon registration. It is mandatory that participants wear their badges at all times when at the conference venue.

Language

The official language of the conference is English. No translation will be provided

Liability

The Organising Committee is not liable for personal accidents or loss/damage of private properties of registered participants during the conference.

Disclaimer

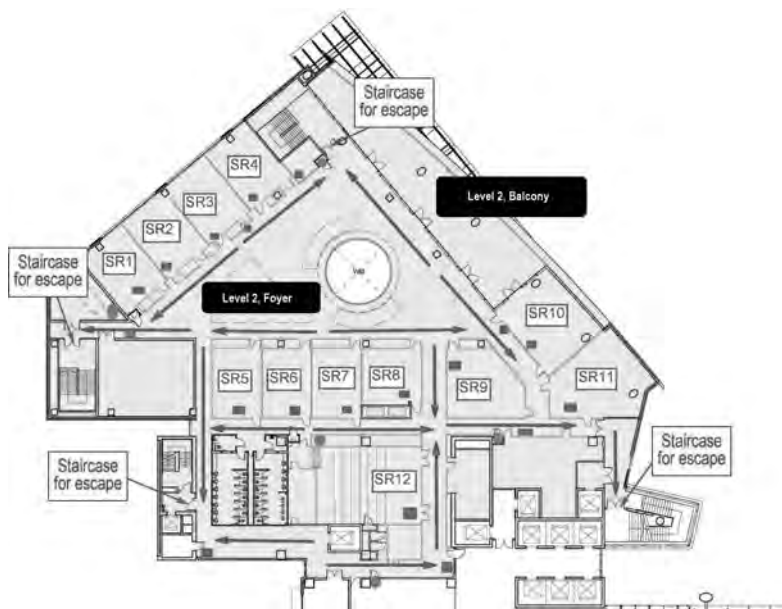
The Organising Committee reserves the right to make any necessary changes in the programme. Whilst every attempt is made to ensure that all aspects of the conference will be carried out as scheduled, the Organising Committee is not responsible for any personal expenses incurred or any loss suffered by any participant or his/her accompanying guest in connection with changes in the conference schedule.

Venue Floor Plan & Activity Locator

Level 1, Town Plaza, U-Town



Level 2, Town Plaza, U-Town



Activity	Location
Opening Session	Level 1, Auditorium 1
Plenary Lectures	Level 1, Auditorium 1
Oral Sessions / Symposia	Level 2, Seminar Rooms
YIA / BES-SEC Design Award Presentations	(SR 1 to 12)
Poster Session	Level 2, Foyer
Closing Session	Level 2, SR 12
Lunch Box Collection Point	Level 2, Balcony
Tea breaks	Level 2, Balcony
Registration Desk	Level 1, Auditorium 1 Foyer

Programme

Day 1 — Wednesday, 4 December 2013

Session	Conference Opening Ceremony
Date/Time	Wednesday, 4 December 2013 / 09:15–10:00 hrs
Venue	Auditorium

10:00–10:30 **Tea Break**

Session	PL1: Plenary Lecture 1
Date/Time	4 December 2013 / 10:30–11:15 hrs
Venue	Auditorium
Chair(s)	Evelyn K. F. Yim

PL1

Biomaterials for tissue engineering Pg. 3
Antonios G. Mikos and F. Kurtis Kasper

Session	SYM-01: Musculoskeletal Tissue Engineering
Date/Time	4 December 2013 / 11:15–12:45 hrs
Venue	Auditorium
Chair(s)	Eng Hin Lee

SYM-01: 1 / 11:15–11:45 hrs

Symposium Keynote

Leveraging biomaterials in translational strategies for craniofacial bone repair Pg. 3
Antonios G. Mikos, Mark E. Wong and F. Kurtis Kasper

SYM-01: 2 / 11:45–12:00 hrs

Create vascularized and innervated tissue and organ from human ESC for wide applications Pg. 3
Tong Cao

SYM-01: 3/ 12:00–12:15 hrs

The roles of mechanics and matrix on teno-differentiation of stem cells Pg. 4
Xiao Chen, Zi Yin and Hong-Wei Ouyang

SYM-01: 4/ 12:15–12:30 hrs

Research strategies for optimisation of chondrogenesis for cartilage tissue engineering Pg. 4
Eng Hin Lee

SYM-01: 5 / 12:30–12:45 hrs

Application of tissue engineering in spinal surgery Pg. 5
Hee Kit Wong

Session	A1: Medical Imaging
Date/Time	4 December 2013 / 11:15–12:45 hrs
Venue	SR-01 & 02
Chair(s)	Ruchir Srivastava and Shyh-Hau Wang

A1: 1 / 11:15–11:45 hrs

Conference Keynote

Biomedical imaging – MRI visualization of living biological systems Pg. 5
Ed X. Wu

A1: 2 / 11:45–12:00 hrs

Exploring image gradients for nuclear cataract grading Pg. 6
Ruchir Srivastava, Xinting Gao, Fengshou Yin, Damon Wong, Jiang Liu, Carol Y. Cheung and Tien Y. Wong

A1: 3 / 12:00–12:15 hrs

Method for determining thickness of the tongue coating by using color histogram Pg. 6
of a tongue image
Chang Jin Jung, Keun Ho Kim and Jaeuk U. Kim

A1: 4 / 12:15–12:30 hrs

A modified synthetic aperture focusing technique using beam characteristics Pg. 6
of transducer for ultrasound image improvement
Chia-Che Ho, Yi-Hsun Lin and Shyh-Hau Wang

A1: 5 / 12:30–12: 45 hrs

Super resolution reconstructed 4D magnetic resonance imaging for lung cancer radiotherapy Pg. 7
Eric Van Reeth, Cher Heng Tan, Ivan W. K. Tham and Chueh Loo Poh

Session	B1: Regenerative Medicine
Date/Time	4 December 2013 / 11:15–12:45 hrs
Venue	SR-03 & 04
Chair(s)	Gary Yam and Robert M. Hoffman

B1: 1 / 11:15 – 11:45 hrs

Conference Keynote

Nestin-expressing multipotent hair follicle stem cells for regenerative medicine Pg. 7
Robert M. Hoffman

B1: 2 / 11:45–12:00 hrs

Directing adult human periodontal ligament-derived stem cells to retinal fate Pg. 7
Gary Yam, Li Huang, Herman S. Cheung and Jodhbir S. Mehta

B1: 3 / 12:00 – 12:15 hrs

Improvement of osteochondral repair by bi-layer electrospun nanofiber scaffold Pg. 8
Shufang Zhang, Longkun Chen, Yangzi Jiang, Youzhi Cai, Tong Tong, Junfeng Ji and Hong Wei Ouyang

B1: 4 / 12:15 – 12:30 hrs

Effect of biphasic calcium phosphate treated with vascular endothelial growth factor on osteogenesis and angiogenesis gene expression *in vitro* Pg. 8
Hamid Enezei, Azlina Ahmad, Mohd Khamis, Roselinda Rahman,
Noor Hayati Abdul Razak, Mutum Singh and Rani Shamsuddin

B1: 5 / 12:30 – 12: 45 hrs

Induction of functional tenocyte-like cells from mesenchymal stem cells by Mohawk Pg. 9
Huanhuan Liu, Can Zhang, Shouan Zhu, Ping Lu, Ting Zhu, Xiao Chen and
Hongwei Ouyang

Session	C1: Cardiovascular Mechanics
Date/Time	4 December 2013 / 11:15–12:45 hrs
Venue	SR-05 & 06
Chair(s)	Hwa Liang Leo and Takeo Matsumoto

C1: 1 / 11:15 –11:45 hrs

Heterogeneity in the intramural mechanical environment of the aorta: Estimation of Pg. 9
stress applied to elastic laminae in a physiological state
Takeo Matsumoto, Yohei Uno and Kazuaki Nagayama

C1: 2 / 11:45 – 12:00 hrs

Quantitative endothelial cell response to wall shear stress in an experimental Pg. 10
cell-structure interaction model simulating stented coronary artery
Nii Armah Armah and Chuh Khiun Chong

C1: 3 / 12:00–12:15 hrs

Influence of increasing oversizing and aortic neck angulation on the proximal fixation Pg. 10
of thoracic stent-grafts
Chen Hsien Chiang, Ming-Long Yeh, Wei-Ling Chen and Chung-Dann Kan

C1: 4 / 12:15 – 12:30 hrs

Effect of wall elasticity on high and low wall shear stresses in human coronary arteries Pg. 11
Ashkan Javadzadegan, Houman Tamaddon, Mehrdad Behnia and Masud Behnia

C1: 5 / 12:30 – 12: 45 hrs

Numerical investigation of blood flow behaviour in different orders of vascular system Pg. 11
Houman Tamaddon, Ashkan Javadzadegan, Mehrdad Behnia and Masud Behnia

Session	D1: Biomedical Devices and Biomedical Instrumentation
Date/Time	4 December 2013 / 11:15–12:45 hrs
Venue	SR-07 & 08
Chair(s)	Chien-Fu Chen and I-Ming Hsing

D1: 1 / 11:15 – 11:45 hrs

Conference Keynote

Electrochemistry and nanotechnology in biomicrosystems for point of care applications Pg. 11
I-Ming Hsing

D1: 2 / 11:45 – 12:00 hrs

A bioimpedance-based sensing system for monitoring cellular dynamics in a 3D culture environment Pg. 12

Chiara Canali, Haseena Bashir Muhammad, Martin Dufva, Anders Wolff, Ørjan Grøttem Martinsen, Arto Heiskanen and Jenny Emnéus

D1: 3 / 12:00 – 12:15 hrs

Diamond MEMS as new promising biochemical sensing transducers Pg. 12

Lionel Rousseau, Alexandre Bongrais, Emmanuel Scorsone, Gaëlle Lissorgues and Philippe Bergonzo

D1: 4 / 12:15 – 12:30 hrs

Surface-modified gold nanoparticles and porous monoliths for colorimetric immunosensing Pg. 13

Shao-Hsuan Chuag, Guan-Hua Chen, Yu-Chun Yen, Jun-You Chen and Chien-Fu Chen

D1: 5 / 12:30 – 12: 45 hrs

Diamond microelectrodes for electrochemical sensing in biofluids and record and stimulate neuronal tissue Pg. 13

Lionel Rousseau, Raphael Kiran, Myline Cottance, Sebastien Joucla, Blaise Yvert, Emmanuel Scorsone, Amel Bendali, Gaelle Lissorgues, Serge Picaud and Philippe Bergonzo

Session E1: Assisted Technologies

Date/Time 4 December 2013 / 11:15–12:45 hrs

Venue SR-12

Chair(s) Khatib Oussama and Stefan Bohn

E1: 1 / 11:15 – 11:45 hrs

Conference Keynote

Robots and the human Pg. 14

Oussama Khatib

E1: 2 / 11:45–12:00 hrs

An interoperability architecture for networked medical devices and its application to neurosurgery Pg. 14

Stefan Bohn, Dirk Lindner, Stefan Franke, Thomas Neumuth and Jürgen Meixensberger

E1: 3 / 12:00–12:15 hrs

Design and development of lower limb exoskeleton for rehabilitation Pg. 15

Yugan Velusamy, Suresh Gobee and Vickneswari Durairajah

E1: 4 / 12:15 –12:30 hrs

Development and testing of a visuo-haptic surgical training simulator for orthognathic surgery Pg. 15

Yanping Lin, Xiaojun Chen, Xudong Wang, Guofang Shen and Chengtao Wang

E1: 5 / 12:30 – 12: 45 hrs

Investigating multimodal displays: reaction times to visual and tactile modality stimuli Pg. 15

Jing Yu and Knut Möller

12:45–13:45 **Lunch & Poster Session**

Session	PL2: Plenary Lecture 2
Date/Time	4 December 2013 / 13:45–14:30 hrs
Venue	Auditorium
Chair(s)	Chwee Teck Lim

PL2

Biomechanics of arterial walls in health and disease: state of the art and challenges ahead Pg. 16
Gerhard A. Holzapfel

14:30–14:45 Short Break

Session	SYM-02A: Gastrointestinal Motility Symposium
Date/Time	4 December 2013 / 14:45–16:15 hrs
Venue	Auditorium
Chair(s)	Leo Cheng and Martin L. Buist

SYM-02A: 1 / 14:45 – 15:15 hrs

Symposium Keynote

Defining the mechanical states of the gut during peristalsis through the use of combined impedance/manometry catheters Pg. 16
Philip Dinning, Lukasz Wiklendt, Taher Omari and Marcello Costa

SYM-02A: 2 / 15:15 – 15:45 hrs

Symposium Keynote

Recirculating flow in the stomach during gastric mixing Pg. 17
Yohsuke Imai, Ikuma Kobayashi, Takuji Ishikawa, Martin Buist and Takami Yamaguchi

SYM-02A: 3 / 15:45 – 16:00 hrs

Dynamics of gastric contents during digestion – a numerical analysis Pg. 17
Maria J. Ferrua, Zhengjun Xue and R. Paul Singh

SYM-02A: 4 / 16:00 – 16:15 hrs

Solid particle motion in the stomach during gastric mixing Pg. 17
Taimei Miyagawa, Yohsuke Imai, Takami Yamaguchi and Takuji Ishikawa

Session	A2: Biosignal Processing
Date/Time	4 December 2013 / 14:45–16:15 hrs
Venue	SR-01 & 02
Chair(s)	Chee Teck Phua

A2: 1 / 14:45 – 15:00 hrs

An adaptable inertial sensor fusion-based approach for energy expenditure estimation Pg. 18
Dominik Schuldhau, Sabrina Dorn, Heike Leutheuser, Alexander Tallner, Jochen Klucken and Bjoern M. Eskofier¹

A2: 2 / 15:00 – 15:15 hrs

The development of behavioral and neuronal activities of animal models with kindling-induced and spontaneous temporal lobe seizures Pg. 18
Yu-Lin Wang, Yin-Lin Chen, Yu-Shin Huang, Sheng-Fu Liang and Fu-Zen Shaw

A2: 3 / 15:15 – 15:30 hrs

Effect of mobile phone radiation on brain using wavelet energy Pg. 19
C. K. Smitha and N. K. Narayanan

A2: 4 / 15:30 – 15:45 hrs

Automatic detection of atrial fibrillation using RR interval from ECG signals Pg. 19
Victoria Gokana, Chee Teck Phua and Gaëlle Lissorgues

A2: 5 / 15:45 –16:00 hrs

Multiclass least-square support vector machine for myoelectric-based facial gesture Pg. 20
recognition
Mahyar Hamedi, Sheikh Hussain Shaikh Salleh, Alias Mohd Noor,
Arief Ruhullah A. Harris and Norazman Abd. Majid

A2: 6 / 16:00 – 16:15 hrs

Hierarchical identification process of a two-parameter gas exchange model Pg. 20
Axel Riedlinger, Jörn Kretschmer and Knut Möller

Session	B2: Regenerative Medicine Tissue Engineering
Date/Time	4 December 2013 / 14:45–16:15 hrs
Venue	SR-03 & 04
Chair(s)	Xiao Chen and Kishore Bhakoo

B2: 1 / 14:45–15:15 hrs

Conference Keynote

Application of bioimaging to tissue engineering and regenerative medicine Pg. 20
Kishore Bhakoo

B2: 2 / 15:15 –15:30 hrs

Dual function of miRNA199a-HIF1-Twist1 cyclic pathway in stage-specific osteogenesis Pg. 21
of mesenchymal stem cells
Xiao Chen, Shen Gu, Hongwei Ouyang, Tin lap Lee and Wai Yee Chan

B2: 3 / 15:30 – 15:45 hrs

Differential effect of biphasic calcium phosphate scaffold ratios on odontoblast cells Pg. 21
Sarah Talib Abdul Qader, Ismail Ab Rahman, Thirumulu Ponnuraj Kannan,
Zuliani Mahmood and Hanafi Ismail

B2: 4 / 15:45 – 16:00 hrs

Comparison of stage specific tendon stem/progenitor cells and the inherent role during Pg. 22
tendon development
Jialin Chen, Wei Zhang, Zeyu Liu, Ting Zhu and Hongwei Ouyang

B2: 5 / 16:00 – 16:15 hrs

Stimulation of angiogenesis in tissue engineered constructs using prolyl hydroxylase Pg. 22
inhibitors
Adeline Sham, Eliana C. Martinez, Sebastian Beyer, Dieter W. Trau and Michael Raghunath

Session	C2: Musculoskeletal Mechanics
Date/Time	4 December 2013 / 14:45–16:15 hrs
Venue	SR-05 & 06
Chair(s)	Desmond Chong and Mark Pearcy

C2: 1 / 14:45 –15:00 hrs

Assessment of the impact of positive heels (plantarflexion) and negative heels (dorsiflexion) shoes on human walking gait Pg. 23
Desmond Y.R. Chong, Ee Xien Ng, Catriona Monkhouse, Paul Wong, Ganit Meyer and Yoav Aloni

C2: 2 / 15:00 – 15:15 hrs

Segmental torso masses and joint torques produced by gravity in the adolescent scoliotic spine Pg. 23
 Bethany E. Keenan, Maree T. Izatt, Geoff N. Askin, Graeme Pettet, Robert D. Labrom, Mark J. Pearcy and Clayton J. Adam

C2: 3 / 15:15 –15:30 hrs

Wheelchair propulsion torque and joint moments during manual wheelchair propulsion on a brake-type dynamometer Pg. 23
Youngho Kim, Jeseong Ryu, Jongsang Son, Seunghyeon Kim and Seonhong Hwang

C2: 4 / 15:30 – 15:45 hrs

Wearable movement analysis system for children with movement disorders – lower extremities assessment system Pg. 24
Yu Zheng Chong and Jasmy Yunus

C2: 5 / 15:45 – 16:00 hrs

Predicting the contact of dual mobility hip implants – effect of bearing geometry and material Pg. 24
M. S. Uddin

C2: 6 / 16:00 – 16:15 hrs

Influence of lower-leg muscle spindle function in irregular surface walking Pg. 25
Akira Obara, Takeshi Yamakoshi, Takayuki Shina, Hiroshi Takkemura and Hiroshi Mizoguchi

Session	D2: Diagnostic Devices Implantable Devices
Date/Time	4 December 2013 / 14:45–16:15 hrs
Venue	SR-07 & 08
Chair(s)	Atsushi Mahara and Weng Kung Peng

D2: 1 / 14:45 – 15:00 hrs

Circulating tumor cell detection system on cell rolling microchip Pg. 25
Atsushi Mahara, Hao Chen, Carlos Agudelo, Kazuhiko Ishihara and Tetsuji Yamaoka

D2: 2 / 15:00 –15:15 hrs

Development of handheld, portable magnetic resonance relaxometry system for rapid blood screening Pg. 26
Weng Kung Peng and Jongyoon Han

- D2: 3 / 15:15 – 15:30 hrs**
Research and development of the primary side frequency controlled transcutaneous energy transmission system for implantable devices Pg. 26
Hidekazu Miura, Isturo Saito, Yasuyuki Shiraishi and Tomoyuki Yambe
- D2: 4 / 15:30 – 15:45 hrs**
Stand-alone integrated microfluidic parasite analysis system Pg. 26
András J. Laki, Gábor Zs. Nagy, Kristóf Iván, Péter Fürjes and Pierluigi Civera
- D2: 5 / 15:45 – 16:00 hrs**
Characterization of the role of contact surface temperature on perception of the hand-transmitted vibration Pg. 27
Manabu Chikai, Mohammad Fard and Hitoshi Miyake
- D2: 6 / 16:00 – 16:15 hrs**
Preliminary study on contactless evaluation of peripheral perfusion during rotary blood pump support Pg. 27
Kyosuke Sano, Tomoya Kitano, Yasuyuki Shiraishi, Tomoyuki Yambe, A. Tanaka and M Yoshizawa

Session	SYM-03A: Micro and Nanofluidics for Biomedical Applications
Date/Time	4 December 2013 / 14:45–16:15 hrs
Venue	SR-12
Chair(s)	Chwee Teck Lim

- SYM-03A: 1 / 14:45 – 15:15 hrs**
Symposium Keynote
Measuring cell mechanics for medicine Pg. 28
Dino Di Carlo
- SYM-03A: 2 / 15:15 – 15:30 hrs**
Integrated microfluidics for cellular functional immunophenotyping Pg. 28
Jianping Fu
- SYM 03A: 3 / 15:30 – 15:45 hrs**
Microfluidic in-vitro platform for imaging metastasis: perfusable microvascular networks and cancer cells on a microfluidic chip Pg. 29
Noo Li Jeon, Sudong Kim, Hyunjae Lee and Minhwan Chung
- SYM 03A: 4 / 15:45 – 16:00 hrs**
Ultra-high throughput enrichment of viable circulating tumor cells Pg. 29
Majid Ebrahimi Warkiani, Guofeng Guan, Bee Luan Khoo, Daniel Shao-Weng Tan, Soo Chin Lee, Chwee Teck Lim, Jongyoon Han, Alvin S.T. Lim, Wan-Teck Lim, Yoon Sim Yap and Ross A. Soo

16:15–16:45 **Tea Break**

Session	SYM-02B: Gastrointestinal Motility Symposium (cont'd)
Date/Time	4 December 2013 / 16:45–18:15 hrs
Venue	Auditorium
Chair(s)	Leo Cheng and Martin L. Buist

SYM-02B: 1 / 16:45 – 17:00 hrs

An interdisciplinary approach to understanding gastrointestinal slow wave electrophysiology Pg. 30
Peng Du and Leo Cheng

SYM-02B: 2 / 17:00 – 17:15 hrs

A biophysically-based tissue model for optimizing gastric pacing Pg. 30
Shameer Sathar, Greg O'Grady, Mark L. Trew and Leo K. Cheng

SYM-02B: 3 / 17:15 – 17:30 hrs

A coupled model of the gastrointestinal smooth muscle cell electromechanics Pg. 30
Nicholas Cheng, Cheuk Wang Chung, Alberto Corrias and Martin Buist

SYM-02B: 4 / 17:30 – 17:45 hr

An image-based model of the interstitial cells of Cajal network in the gastrointestinal tract Pg. 31
Ruchi Vyas, Jerry Gao, Leo K. Cheng and Peng Du

SYM-02B: 5 / 17:45 – 18:00 hrs

Modeling the role of pdgfra+ cells in enteric inhibitory neurotransmission Pg. 31
Jing Wui Yeoh, Alberto Corrias and Martin Lindsay Buist

SYM-02B: 6 / 18:00 –18:15 hrs

Potential pitfalls in the development of electrophysiological models Pg. 31
Martin L. Buist and Alberto Corrias

Session	A3: Bioelectronics
Date/Time	4 December 2013 / 16:45–18:15 hrs
Venue	SR-01 & 02
Chair(s)	Kentaro Doi

A3: 1 / 16:45 – 17:00 hrs

Feature analysis of myocardial ischemia based on T wave alternans Pg. 32
Song Jinzhong, Yan Hong, Xu Zhi, Yu Xinming and Li Yanjun

A3: 2 / 17:00 – 17:15 hrs

Phase detection for electric field body scanner Pg. 32
Ichiro Hieda and Ki-Chang Nam

A3: 3 / 17:15 –17:30 hrs

Theoretical study of non-equilibrium ionic response near electrode surface Pg. 32
Kentaro Doi, Makusu Tsutsui, Takahito Ohshiro, Masateru Taniguchi, Tomoji Kawai, Massimiliano Di Ventra and Satoyuki Kawano

A3: 4 / 17:30 –17:45 hrs

SAR computation and channel modeling of body area networks Pg. 33
Zhangyong Li, Yu Pang, Jinzhao Lin, Jie Liu, Shengrong Liu and Chunyang Li

A3: 5 / 17:45 – 18:00 hrs

Gastric lymph node cancer detection using multiple features support vector machine for pathology diagnosis support system Pg. 33

Takumi Ishikawa, Junko Takahashi, Hiroshi Takemura, Hiroshi Mizoguchi and Takeshi Kuwata

A3: 6 / 18:00 –18:15 hrs

Analysis of SELDI-TOF-MS using support vector regression for ovarian cancer identification Pg. 34

Isye Arieshanti and Yudhi Purwananto

Session B3: Biological Materials

Date/Time 4 December 2013 / 16:45–18:15 hrs

Venue SR-03 & 04

Chair(s) Arghya Paul and Dror Seliktar

B3: 1 / 16:45–17:00 hrs

Nanobioactive hydrogel for myocardial therapy applications Pg. 34

Arghya Paul, Hamood Al Kindi, MD Anwarul Hasan, Akhilesh Gaharwar, Mehdi Nikkhah, Mehmet R. Dokmeci, Dominique Shum-Tim and Ali Khademhosseini

B3: 2 / 17:00 – 17:15 hrs

Natural patches from the heart to the infarct: functional improvements and induced vascularization towards regeneration of a scarred tissue pg. 34

Hadar Sarig, Udi Sarig, Su Yin Chaw, Elio de Bernardinis, Vaibavi S. Ramanujam, Rufaihah B.A. Jalil, Vu D. Thang, Dror Seliktar, Theodoros Kofidis, Freddy Yin Chiang Boey, Subbu Venkatraman and Marcelle Machluf

B3: 3 / 17:15–17:30 hrs

The different roles of collagenous matrices from different origin on Human Tendon Stem/Progenitor Cells fate-decision Pg. 35

Zi Yin, Ting Zhu, Jiajie Hu, Xiao Chen and Hongwei Ouyang

B3: 4 / 17:30 – 17:45 hrs

Protein and cell therapeutics using polymeric hydrogel carriers Pg. 35

Dror Seliktar

B3: 5 / 17:45–18:00 hrs

Polycaprolactone fibers gellation with gelatin ground substance: engineered skin extracellular matrix aims for using as tissue engineering skin Pg. 36

Oraphan Chaisiri, N. Chanunpanich and B. S. Hanpanich

B3: 6 / 18:00– 18:15 hrs

Novel scalable silicone elastomer and poly(2-hydroxyethyl methacrylate) (PHEMA) composite materials for tissue engineering and drug delivery applications Pg. 36

Soumyaranjan Mohanty, Mette Hemmingsen, Magdalena Wojcik, Martin Alm, Peter Thomsen, Martin Dufva, Jenny Emnéus and Anders Wolff

Session	C3: Cardiovascular Mechanics Computational Mechanics	
Date/Time	4 December 2013 / 16:45–18:15 hrs	
Venue	SR-05 & 06	
Chair(s)	Hwa Liang Leo	
C3: 1 / 16:45 – 17:00 hrs	Effects of stent design on an emerging clinical issue of longitudinal stent compression Chun-Ting Yeh, Chun Wang, Dian-Ru Li, Chun-Pei Chen and <u>Hao-Ming Hsiao</u>	pg. 37
C3: 2 / 17:00 –17:15 hrs	In-silico study of the nasal cavity's influence on the pharyngeal wall pressure in anatomically-correct airway models of patients with obstructive sleep apnea <u>Julien Cisonni</u> , Anthony D. Lucey, Andrew J. C. King, Syed M. S. Islam and Mithran S. Goonewardene	Pg. 37
C3: 3 / 17:15 – 17:30 hrs	Simulation of photon propagation in multi-layered tissue for non-invasive fetal pulse oximetry <u>Sebastian Ley</u> , Daniel Laqua and Peter Husar	Pg. 38
C3: 4 / 17:30 – 17:45 hrs	Improvement of thermodynamic control in the newly developed pediatric circulatory assist device for fontan circulation <u>Akihiro Yamada</u> , Yasuyuki Shiraishi, Hidekazu Miura, Takuya Shiga, Mohamed Omran Hashem, Yusuke Tusboko, Takuya Ito, Kyosuke Sano, Yasunori Taira, Tomoyuki Yambe, Masaaki Yamagishi and Dai Homma	Pg. 38
C3: 5 / 17:45 – 18:00 hrs	Hemodynamic studies of flow modulating stent designs for aortic aneurysms <u>Siang Lin Yeow</u> , Hwa Liang Leo, Tsui Ying Rachel Hong, Wee Chuan Melvin Loh and Soo Yeng Benjamin Chua	Pg. 39
C3: 6 / 18:00 –18:15 hrs	Influence of contact angle on the bubble transport in a rectangular bifurcating microchannel <u>Poornima Josyula</u> and S. Vengadesan	Pg. 39
C3: 7 / 18:15 –18:30 hrs	Three-dimensional finite element analysis of foot-ground interface to investigate different landing patterns <u>Jee Chin Teoh</u> and Taeyong Lee	Pg. 39
Session	Edn: Biomedical Engineering Education Session	
Date/Time	4 December 2013 / 16:45–18:15 hrs	
Venue	SR-07 & 08	
Chair(s)	Kang-Ping Lin and Siew Lok Toh	
Edn: 1 / 16:45 – 17:00 hrs	Education of biomedical engineering in the Technical University of Ostrava <u>Martin Augustynek</u> , Marek Penhaker, Martin Cerny, Jindrich Cernohorsky and Iveta Bryjova	Pg. 40

Edn: 2 / 17:00 – 17:15 hrs		
Development of biomedical engineering education in Indonesia		Pg. 40
<u>Cholid Badri</u>		
Edn: 3 / 17:15 –17:30 hrs		
Biomedical engineering education at the University of Sheffield, UK – from biomedical engineering to bioengineering		Pg. 40
<u>Chuh Khiun Chong</u>		
Edn: 4 / 17:30 –17:45 hrs		
Education of biomedical engineering in Taiwan		Pg. 41
<u>Kang-Ping Lin</u>		
Edn: 5 / 17:45–18:00 hrs		
BME education in Hong Kong: rehabilitation engineering, biomedical engineering, medical engineering, and bioengineering		Pg. 41
<u>Yong-Ping Zheng</u>		
Edn: 6 / 18:00–18:15 hrs		
Accreditation of the Bachelor of Engineering (Biomedical Engineering) program – the NUS experience		Pg. 42
<u>Siew Lok Toh</u>		

Session	SYM-03B: Micro and Nanofluidics for Biomedical Applications (cont'd)
Date/Time	4 December 2013 / 16:45–18:15 hrs
Venue	SR-12
Chair(s)	Chwee Teck Lim

SYM-03B: 1 / 16:45–17:15 hrs		
Symposium Keynote		
Ultrafast image cytometry for cancer detection		Pg. 42
<u>Keisuke Goda</u>		
SYM-03B: 2 / 17:15–17:30 hrs		
Toward gut and pancreas on chip for pathological models		Pg. 42
<u>Sungsu Park</u>		
SYM-03B: 3 / 17:30–17:45 hrs		
Nanomechanical mapping cellular migration		Pg. 43
<u>Xiao Dong Chen</u>		
SYM-03B: 4 / 17:45–18:00 hrs		
Proteolytic activity matrix analysis for diagnosis of endometriosis using droplet based microfluidics		Pg. 43
<u>Chia-Hung Chen</u>		

End of Day 1

Day 2 — Thursday, 5 December 2013

Session	PL3: Plenary Lecture 3	
Date/Time	5 December 2013 / 09:00–09:45 hrs	
Venue	Auditorium	
Chair(s)	Haoyong Yu	
PL3		
Integration of computer assisted surgical guidance and surgical robotics for robotics for minimally invasive surgery		pg. 44
<u>Ichiro Sakuma</u>		
Session	PL4: Plenary Lecture 4	
Date/Time	5 December 2013 / 09:45–10:30 hrs	
Venue	Auditorium	
Chair(s)	James Goh	
PL4		
Autodigestion: A missing link to inflammation and disease		Pg. 44
<u>Geert W. Schmid-Schönbein</u>		
10:30–11:00	Tea Break	
Session	SYM-04: Biomechanics in Nature and Bioinspired Engineering	
Date/Time	5 December 2013 / 11:00–12:30 hrs	
Venue	Auditorium	
Chair(s)	Hao Liu	
SYM-04: 1 / 11:00–11:30 hrs		
Symposium Keynote		
Bio-inspired mechanical systems and biomimetics in bio-flights		Pg. 45
<u>Hao Liu</u>		
SYM-04: 2 / 11:30–11:45 hrs		
Mechanobio-materials: design of elastically-micropatterned gels to control cell mechanotaxis and motility-related functions		Pg. 45
<u>Satoru Kidoaki</u>		
SYM 04: 3 / 11:45–12:00 hrs		
Bio-inspired aquatic omnidirectional multi-link propulsion mechanism		Pg. 45
<u>Shunichi Kobayashi</u>		
SYM 04: 4 / 12:00–12:15 hrs		
Tunable optical diffuser based on deformable wrinkles		Pg. 46
<u>Takuya Ohzono, Kosuke Suzuki, Tomohiko Yamaguchi, Nobuko Fukuda</u>		
SYM-04: 5 / 12:15–12:30 hrs		
Biomimetic adhesive superhydrophobic surface for water droplet manipulation		Pg. 46
<u>Daisuke Ishii</u>		

Session	A4: Biosignal Processing
Date/Time	5 December 2013 / 11:00–12:30 hrs
Venue	SR-01 & 02
Chair(s)	Charles T. M. Choi and Marek Penhaker

A4: 1 / 11:00–11:15 hrs

Classification of EEG signals from imagined writing for treating writing disorder Pg. 46
Azlee Zabidi, Wahidah Mansor and Khuan Y. Lee

A4: 2 / 11:15–11:30 hrs

Acoustic cochlear implant models incorporating electrical field interaction between Pg. 47
neighboring electrodes
Charles T. M. Choi, Shang-Yi Huang and Yi-Hsuan Lee

A4: 3 / 11:30–11:45 hrs

A study on the effect of subliminal priming on subjective perception of images: Pg. 47
a machine learning approach
Justin Dauwels, Parmod Kumar, Faisal Mahmood, Ken Wong, Abhishek Agrawal,
Mohamed Elgendi, Srinivasan Kannan, Dhanya Menoth Mohan, Rohit Shukla and
Alice H. D. Chan

A4: 4 / 11:45–12:00 hrs

Unobtrusive, mobile ECG monitoring and arrhythmia detection using mobile phones Pg. 48
Heike Leutheuser, Patrick Kugler, Stefan Gradl, Dominik Schuldhaus, Stephan Achenbach
and Bjoern M. Eskofier

A4: 5 / 12:00–12: 15 hrs

SVM for semi-automatic selection of ICA components of electromyogenic artifacts in Pg. 48
EEG data
Florian Gabsteiger, Heike Leutheuser, Pedro Reis, Matthias Lochmann and
Bjoern M. Eskofier

A4: 6 / 12:15–12:30 hrs

Measurements and data processing in home care telemetry systems Pg. 49
Marek Penhaker and Hoang Tran Minh

Session	B5: Controlled Drug Delivery
Date/Time	5 December 2013 / 11:00–12:45 hrs
Venue	SR-03 & 04
Chair(s)	Chia-Hung Chen and Dieter Trau

B5: 1 / 11:00–11:15 hrs

Evaluation of particle deposition efficiency in human oral passage: A CFD study Pg. 49
Jianhua Zhu, Hong Siang How, De Yun Wang, Shu Jin Lee and Heow Pueh Lee

B5: 2 / 11:15–11:30 hrs

Near-Infrared photothermal activation of microgels incorporating polypyrrole Pg. 49
nanotransducers through droplet microfluidics
Rong-Cong Luo and Chia-Hung Chen

- B5: 3 / 11:30–11:45 hrs**
Objective assessment of the effects of long-duration wearing of N95 and surgical facemasks on upper airway functions Pg. 50
Jian Hua Zhu, Heow Pueh Lee, Shu Jin Lee and De Yun Wang
- B5: 4 / 11:45–12:00 hrs**
Quantifying in vivo resorption and integration of hydrogel scaffolds using bimodal imaging Pg. 50
Sasha Berdichevski, Haneen Simaan Yameen, Hagit Dafni, Michal Neeman and Dror Seliktar
- B5: 5 / 12:00–12: 15 hrs**
Biodegradable nano-conjugates for non invasive insulin delivery Pg. 51
Pooja Hurkat and Sanjay K. Jain
- B5: 6 / 12:15–12:30 hrs**
Controlled release system of antisense molecule from atelocollagen porous gel for hyperlipemia treatment Pg. 51
Genki Mihara, Joeng-Hung Kang, Takahiko Nakaoki, Hidetaka Torigoe, Mariko Harada-Shiba, Satoshi Obika and Tetsuji Yamaoka
- B5:7 / 12:15–12:45 hrs**
Fabrication of spherical multi-shells with discrete porosity differences via organic phase polymer-hydrogel assemblies Pg. 52
Houwen Matthew Pan and Dieter Trau
- | | |
|------------------|-----------------------------------|
| Session | C4: Musculoskeletal Mechanics |
| Date/Time | 5 December 2013 / 11:00–12:45 hrs |
| Venue | SR-05 & 06 |
| Chair(s) | Peter Pivonka and Jaw-Lin Wang |
- C4: 1 / 11:00–11:30 hrs**
Conference Keynote
Development, validation of a degenerated intervertebral disc model and its application in disc research Pg. 52
Jaw-Lin Wang
- C4: 2 / 11:30–11:45 hrs**
Computational study on the effect of the ligaments in knee joint during quasi-static stand-to-sit motion Pg. 52
Chunhui Chung and Bing-Shiang Yang
- C4: 3 / 11:45–12:00 hrs**
Investigation of determinants of atypical femoral fractures using multiscale computational modeling Pg. 53
Peter Pivonka, Saulo Martelli and Peter R. Ebeling
- C4: 4 / 12:00–12: 15 hrs**
Muscle force prediction during knee flexion/extension using EMG-driven model Pg. 53
Saran Keeratihattayakorn and Shigeru Tadano

C4: 5 / 12:15–12:30 hrs

Differences in soccer kick kinematics for left-side and right-side targets Pg. 54
Luis Carlos Hernandez Barraza and Chen-Hua Yeow

C4: 6 / 12:30–12:45 hrs

Biomechanics of artificial elbow joints Pg. 54
Norio Inou, Michael Surjawidjaja, Katsuyuki Kobayashi, Taisuke Osanai,
Ren Kadowaki, Hitoshi Kimura, Jun Ikeda and Katsunoki Inagaki

Session	YIA-01: Young Investigator Award I
Date/Time	5 December 2013 / 11:00–12:30 hrs
Venue	SR-07 & 08
Chair(s)	Yong Tian Chew

YIA-01: 1 / 11:00–11:15 hrs

Synchrotron nano-mechanical imaging techniques to understand how altered bone quality Pg. 54
increases fracture risk in secondary osteoporosis
Angelo Karunaratne, Alan Boyde, Chris T. Esapa, Nick Terrill, Graham R. Davis,
Steve D. M. Brown, Roger D. Cox, Liz Bentley, Rajesh V. Thakker and Himadri S. Gupta

YIA-01:2 / 11:15–11:30 hrs

Design and actuation of a snake-like robot for minimally invasive surgeries Pg. 55
Zeqi Tan and Hongliang Ren

YIA-01: 3 / 11:30–11:45 hrs

Relationship between pathology and hemodynamics of human unruptured cerebral Pg. 55
aneurysms
Yasutaka Tobe, Takanobu Yagi, Yuki Iwabuchi, Momoko Yamanashi, Kenji Takamura,
Takuma Sugiura, Mitsuo Umezu, Yoshifumi Hayashi, Hiroataka Yoshida,
Atsushi Nakajima, Kazutoshi Nishitani, Yoshifumi Okada, Michihito Sugawara,
Shin Hiraguchi, Toshiro Kubo and Shigemi Kitahara

YIA-01: 4 / 11:45–12:00 hrs

Optimal intra-articular injection of parathyroid hormone-related protein Pg. 56
effectively promotes osteochondral defects repair
Wei Zhang, Jialin Chen, Jiadong Tao, Changchang Hu, Junfeng Ji and
Hongwei Ouyang

YIA-01: 5 / 12:00–12: 15 hrs

Correlation between facial trauma and brain injury – a finite element study Pg. 56
Kwong Ming Tse, Long Bin Tan, Shu Jin Lee, Siak Piang Lim and Heow Pueh Lee

YIA-01: 6 / 12:15–12:30 hrs

Understanding nanotopography induced stem cell differentiation: a focus on Pg. 57
focal adhesion kinase
Benjamin Kim Kiat Teo, Sum Thai Wong, Choon Kiat Lim, Terrence Kung,
Chong Hao Yap, Yamini Ramgopal, Lewis H. Romer and Evelyn Yim

Session	B4: Tissue Engineering
Date/Time	5 December 2013 / 11:00–12:30 hrs
Venue	SR-12
Chair(s)	S��verine Le Gac and Yasuhiko Tabata

B4: 1 / 11:00–11:30 hrs

Conference Keynote

Drug delivery technology for tissue regeneration therapy Pg.57
Yasuhiko Tabata

B4: 2 / 11:30–11:45 hrs

Fibroblast growth factor-immobilized polyethylene porous scaffolds via mussel adhesive peptide and heparin for inducing angiogenesis Pg. 58
Yusuke Sakai, Sachiro Kakinoki, Taro Takemura, Nobutaka Hanagata, Thosia Fujisato and Tetsuji Yamaoka

B4: 3 / 11:45–12:00 hrs

In situ non-invasive cellular assays in microfabricated well arrays using scanning electrochemical microscopy (SECM) Pg. 58
Adithya Sridhar, Hans L. de Boer, Albert van den Berg and S  verine Le Gac

B4: 4 / 12:00–12: 15 hrs

Proliferation behavior of mesenchymal stem cells in peptide functionalized chitosan scaffolds Pg. 59
Md. Abdul Kafi, Phanny Yos, Nakamuta Yusuke and Mitsugu Todo

B4: 5 / 12:15–12:30 hrs

Decellularised organs – a tool to enable neovascularisation in tissue-engineered skin Pg. 59
Lindsey Dew, Sheila MacNeil and Chuh Khiun Chong

12:30–13:30 **Lunch & Poster Session**

Session	PL5: Plenary Lecture 5
Date/Time	5 December 2013 / 13:30–14:15 hrs
Venue	Auditorium
Chair(s)	Yen Wah Tong

PL5

Biomedical micro and nanotechnology: from lab-on-chip to building systems with cells Pg. 59
Rashid Bashir

14:15–14:30 **Short Break**

Session	SYM-05: Supramolecular and Nano-Biomaterials
Date/Time	5 December 2013 / 14:30–16:00 hrs
Venue	Auditorium
Chair(s)	Jun Araki

SYM-05: 1 / 14:30–15:00 hrs

Symposium Keynote

Translational nanomedicine from self-assembling prodrugs Pg. 60
Youqing Shen

SYM-05: 2 / 15:00–15:15 hrs

Sliding graft copolymers – supramolecular derivatives equipping promising potentials Pg. 60
Jun Araki

SYM-05: 3 / 15:15–15:30 hrs

Mesoporous polymer materials through solvent nano-crystallization Pg. 60
Sadaki Samitsu and Izumi Ichinose

SYM-05: 4 / 15:30–15:45 hrs

Pillararenes: easy-to-make and versatile receptors for supramolecular chemistry Pg. 61
Tomoki Ogoshi

SYM-05: 5 / 15:45–16:00 hrs

Bioreducible stimuli-responsive cyclodextrin-based star polymer for efficient gene delivery Pg. 61
Yuting Wen

Session A5: Biosignal Processing

Date/Time 5 December 2013 / 14:30–16:00 hrs

Venue SR-01 & 02

Chair(s) Zhiwei Huang and Bing Nan Li

A5: 1 / 14:30–14:45 hrs

NniLSM: A unified level set model for medical image segmentation Pg. 61
Bing Nan Li, Fang Chen, Yi Zhuang Cheng, Jing Qin and Ning An

A5: 2 / 14:45–15:00 hrs

3-D lung visualization using electrical impedance tomography combined with body plethysmography Pg. 62
Stefanie Heizmann, Moritz Baumgärtner, Sabine Krüger-Ziolek, Zhanqi Zhao and Knut Möller

A5: 3 / 15:00–15:15 hrs

ELM based classification and analysis of spirometric pulmonary function data Pg. 62
A. Mythili, C. M. Sujatha and S. Srinivasan

A5: 4 / 15:15–15:30 hrs

Signal quality improvement in time domain optical coherence tomography (TD-OCT) and Doppler optical coherence tomography (DOCT) using wavelet analysis Pg. 62
Saroch Leedumrongwatthanakun, Panote Thavarungkul, Proespichaya Kanatharana and Chittanon Buranachai

A5: 5 / 15:30–15:45 hrs

Apply a GFP-based FRET apoptosis sensor in zebrafish model to study cancer metastasis and search for new anti-cancer drugs Pg. 63
Afu Fu, Weida Ngan, Yu Ming Peh and Kathy Qian Luo

A5: 6 / 15:45–16:00 hrs

Design and implementation of a calibration-free pulse oximeter Pg. 63
Harini Harinarayanan, L. S. Krithika, M. Shalini, Sirisha Swaminathan and N. Madhu Mohan

Session	B6: Pharmaceutical Science & Engineering
Date/Time	5 December 2013 / 14:30–16:00 hrs
Venue	SR-03 & 04
Chair(s)	James Kah and Feng Xu

B6: 1 / 14:30–14:45 hrs

Three-dimensional chondrosarcoma model for high throughput drug screening Pg. 64
Yu Long Han, Tian Jian Lu and Feng Xu

B6: 2 / 14:45–15:00 hrs

Effect of the polyelectrolyte hydrogel actuator network density on its mechanical behavior Pg. 64
in the DC electric field
Mikhail A. Filipovich, Tatyana F. Shklyar, Alexander P. Safronov, Sergey Yu. Sokolov
and Felix A. Blyakhman

B6: 3 / 15:00–15:15 hrs

A new anticancer agent inhibits breast cancer cell growth by reducing the expression Pg. 65
levels of ERa and HER2
Ting Yu and Kathy Qian Luo

B6: 4 / 15:15–15:30 hrs

Method development for downstream processing of therapeutic cells – high-throughput Pg. 65
process development for cell separation in aqueous two-phase systems
Sarah Nagel, Sarah Gretzinger, Stefan Oelmeier and Juergen Hubbuch

B6: 5 / 15:30–15:45 hrs

Guidelines for modelling BED in simultaneous radiotherapy Pg. 66
Jan Kubíček and Marek Penhaker

B6: 6 / 15:45–16:00 hrs

Nano protein enhancer device (NanoPED) to increase insulin production in cells Pg. 66
Yang Gao, Eugenia Yeo, Dewi Susanti and James Kah

Session	C5: Orthopaedics
Date/Time	5 December 2013 / 14:30–16:00 hrs
Venue	SR-05 & 06
Chair(s)	Kiyoshi Mabuchi and Yoshitaka Nakanishi

C5: 1 / 14:30–14:45 hrs

Effects of adduction, internal rotation, and flexion angles on disvenue for total hip Pg. 66
arthroplasty
Masaru Higa, Hiromasa Tanino, Y. Yamagami, Masayoshi Abo and Satoshi Kakunai

C5: 2 / 14:45–15:00 hrs

Bearing surface with nano-level geometry inhibits macrophage activation in joint Pg. 67
prostheses
Yoshitaka Nakanishi, Naoki Nishi, Yuuki Hikichi, Kenryo Shimazu, Yuta Nakashima,
Hirosi Mizuta, Hiromasa Miura, Yukihide Iwamoto and Hidehiko Higaki

C5: 3 / 15:00–15:15 hrs

Response of a femoral bone to stationary and continuous load from within outward
Kiyoshi Mabuchi, Taiki Ito, Kentaro Uchida, Rina Sakai and Kouji Naruse Pg. 67

C5: 4 / 15:15–15:30 hrs

Development of a robotic testing platform for investigating knee joint ligament
force contributions during various flexion extension angles Pg. 68
Ryo Takeda, Ferdinando Rodriguez y Baena and Andrew Amis

C5: 5 / 15:30–15:45 hrs

Evaluation of bone fracture and load transfer mechanisms of lower limb injuries
from under vehicle explosions Pg. 68
Angelo Karunaratne, Marit Undheim, Spyros D. Masouros and Anthony M. J. Bull

C5: 6 / 15:45–16:00 hrs

Quantification of the soft tissue artifacts of the upper limb during movements Pg. 69
Hsuan-Lun Lu, Tung-Wu Lu, Cheng-Chung Lin and Mei-Ying Kuo

Session YIA-02: Young Investigator Award II

Date/Time 5 December 2013 / 14:30–16:00 hrs

Venue SR-07 & 08

Chair(s) Peck Ha Tan

YIA-02: 1 / 14:30–14:45 hrs

A biophysically-based tissue model for optimizing gastric pacing Pg. 69
Shameer Sathar, Greg O'Grady, Mark L. Trew and Leo K. Cheng

YIA-02: 2 / 14:45–15:00 hrs

Effect of spatial arrangement of substrate topography on neuronal differentiation
of stem cells Pg. 70
Evelyn K.F. Yim, Soneela Ankam, Aung Aung Kywe Moe and Lesley Y. T. Chan

YIA-02: 3 / 15:00–15:15 hrs

Estimation of changes in mechanical bone quality by multi-scale analysis with
remodeling simulation Pg. 70
Daisuke Tawara, Ken Nagura, Tetsuya Tsujikami and Taiji Adachi

YIA-02: 4 / 15:15–15:30 hrs

Porohyperelastic analysis of single osteocyte using AFM and inverse FEA Pg. 70
Trung Dung Nguyen, Adekunle Oloyede, Sanjleena Singh and Yuantong Gu

YIA-02: 5 / 15:30–15:45 hrs

Ligament-to-bone interface tissue regeneration using a functionalized biphasic silk
fibroin scaffold Pg. 71
Thomas Kok Hiong Teh, Pujiang Shi, Xiafei Ren, James H.P. Hui, Siew-Lok Toh
and James C.H. Goh

Session	SYM-06: Reproductive Bioengineering
Date/Time	5 December 2013 / 14:30–16:15 hrs
Venue	SR-12
Chair(s)	David Elad

SYM-06: 1 / 14:30–14:45 hrs
Biomechanics of infant feeding Pg. 71
David Elad

SYM-06: 2 / 14:45–15:00 hrs
The role of fluid dynamics in the determination of the left-right asymmetry in Pg. 72
developing embryos
Oreste Piro

SYM-06: 3 / 15:00–15:15 hrs
Calaxin is a calcium sensor for turning of sperm movement Pg. 72
Kazuo Inaba

SYM-06: 4 / 15:15–15:30 hrs
Microfluidics for mammalian embryo culture Pg. 72
Séverine Le Gac

SYM-06: 5 / 15:30–15:45 hrs
Mechanical properties of the pregnant uterine cervix: can elastography provide Pg. 73
meaningful information?
Sabrina Badir, Manfred Maurer and Edoardo Mazza

SYM-06: 6 / 15:45–16:00 hrs
A novel computational approach for detecting mechanical causes of pelvic disorders Pg. 73
Manfred Maurer and Edoardo Mazza

SYM-06: 7 / 16:00–16:15 hrs
Tracking the changes in electrophysiological activity of the uterus as it approaches Pg. 74
labor using magnetomyographic technique
Eswaran Hari

16:00–16:30 **Tea Break**

Session	SYM-07: Virtual Physiological Rat Project
Date/Time	5 December 2013 / 16:30–18:00 hrs
Venue	Auditorium
Chair(s)	David Phillip Nickerson

SYM-07: 1 / 16:30–17:00 hrs
Symposium Keynote
The virtual physiological rat project: a national center for systems biology to study Pg. 74
interactions between genes, environmental factors, and physiological systems
Peter John Hunter and Daniel Andrew Beard

SYM-07: 2 / 17:00–17:15 hrs

Arterial stiffening provides sufficient explanation for primary hypertension Pg. 75
Klas H. Pettersen, Scott M. Bugenhagen, Javaid Nauman, Daniel A. Beard and Stig W. Omholt

SYM-07: 3 / 17:15–17:30 hrs

Modeling the afferent dynamics of the baroreflex control system Pg. 75
Adam Mahdi and Mette Olufsen

SYM-07: 4 / 17:30–17:45 hrs

The role of metabolic dysfunction in heart failure Pg. 75
Scott M Bugenhagen and Daniel A. Beard

SYM-07: 5 / 17:45–18:00 hrs

Modelling epithelial transport Pg. 76
David Phillip Nickerson, Kirk Lee Hamilton and Peter John Hunter

Session	A6: Medical Imaging
Date/Time	5 December 2013 / 16:30–18:15 hrs
Venue	SR-01 & 02
Chair(s)	Haoyong Yu and Sergey Yu. Sokolov

A6: 1 / 16:30–16:45 hrs

A method for automatic delineation of the left ventricle borders in echographic Pg. 76
images with use active contours model and speckle tracking technique
Sergey Yu. Sokolov and Felix A. Blyakhman

A6: 2 / 16:45–17:00 hrs

A dynamic liver phantom for ultrasound image guided biopsy Pg. 76
Cheng Li, Suan Ping Ang, Jimin Liu and Haoyong Yu

A6: 3 / 17:00–17:15 hrs

Region growing for medical image segmentation using a modified multiple-seed Pg. 77
approach on a multicore CPU computer
Agus Pratondo, Sim Heng Ong and Chee Kong Chui

A6: 4 / 17:15–17:30 hrs

CT image reconstruction algorithm to reduce metal artifact Pg. 77
Toru Kano and Michihiko Koseki

A6: 5 / 17:30–17:45 hrs

Effect of treatment using 3-dimentional disease generating model on optical coherence Pg. 78
tomography images
Ngoc Anh Huyen Nguyen, Shinji Tsuruoka, Haruhiko Takase, Hiroharu Kawanaka, Hisashi Matsubara, Hisanori Yagami and Fumio Okuyama

A6: 6 / 17:45–18:00 hrs

MRE simulation based on finite element vibration analysis of viscoelastic model Pg. 78
Sunao Tomita, Hayato Suzuki, Itsuro Kajiwara, Shigeru Tadano, Gen Nakamura and Yu Jiang

A6: 7 / 18:00–18:15 hrs

Dynamic movement of the median nerve & its relation to carpal tunnel syndrome Pg. 78
Yushan Kyryn Jo Liong, Amitabha Lahiri, Dawn Chia, Shujin Lee, Aymeric Lim,
Arijit Biswas and Heow Pueh Lee

Session	SYM-09: Pharmaceutical Science and Engineering
Date/Time	5 December 2013 / 16:30–18:00 hrs
Venue	SR-03 & 04
Chair(s)	Sierin Lim and Kathy Luo

SYM-09: 1 / 16:30–17:00 hrs

Symposium Keynote

Engineering solutions to address challenges in drug delivery Pg. 79
Samir Mitragotri

SYM-09: 2 / 17:00–17:15 hrs

The multiple uses of fluorescent proteins to visualize cancer in vivo Pg. 79
Robert M. Hoffman

SYM-09: 3 / 17:15–17:30 hrs

Nanodiamond-enabled therapy and imaging Pg. 79
Dean Ho

SYM-09: 4 / 17:30–17:45 hrs

From lab to cures to riches Pg. 80
Peng Leong

Session	C6: Computational Mechanics
Date/Time	5 December 2013 / 16:30–18:15 hrs
Venue	SR-05 & 06
Chair(s)	Siew Lok Toh

C6: 1 / 16:30–16:45 hrs

Numerical investigation of mechano-electrochemical behaviors of articular cartilage under Pg. 80
dynamic contact loading
Xian Chen, Hiroyuki Oka and Junji Ohgi

C6: 2 / 16:45–17:00 hrs

Hinge flow fields study of SJM bileaflet mechanical heart valve Pg. 81
Yee Han Kuan, Vinh-Tan Nguyen and Hwa Liang Leo

C6: 3 / 17:00–17:15 hrs

An anatomically realistic geometrical model of the intra-epidermal nerves in Pg. 81
the human foot
Muhammad Zeeshan Ul Haque, Peng D., Leo K. Cheng and Marc D. Jacobs

C6: 4 / 17:15–17:30 hrs

Blood flow analysis in patient-specific cerebral aneurysm models with realistic Pg. 81
configuration of embolized coils
Tomohiro Otani, Satoshi Ii, Toshiyuki Fujinaka, Masayuki Hirata, Junko Kuroda,
Katsuhiko Shibano and Shigeo Wada

C6: 5 / 17:30–17:45 hrs

Numerical investigation of micro-particle transport and deposition in an upper airway considering human workloads Pg. 82
Kun Hyuk Sung, Ji Tae Kim and Hong Sun Ryou

C6: 6 / 17:45–18:00 hrs

A realistic subject-specific finite element model of human head-development and experimental validation Pg. 82
Kwong Ming Tse, Long Bin Tan, Shu Jin Lee, Siak Piang Lim and Heow Pueh Lee

C6: 7 / 18:00–18:15 hrs

Local osteoporosis and its effects on anti-resorptive drug treatment: A 3-year follow-up finite-element study in risedronate-treated women Pg. 83
D. Anitha, Kim Kwang Joon, Lim Sung-Kil and Lee Taeyong

Session	E2: Assisted Technologies
Date/Time	5 December 2013 / 16:30–18:00 hrs
Venue	SR-07 & 08
Chair(s)	Alpha Agape Gopalai and Chee Kong Chui

E2: 1 / 16:30–16:45 hrs

Finger grip rehabilitation using exoskeleton with grip force feedback Pg. 83
Chee leong Chan, Suresh Gobee and Vickneswari Durairajah

E2: 2 / 16:45–17:00 hrs

Measuring human balance on an instrumented dynamic platform: a postural sway analysis Pg. 83
Darwin Gouwanda and Alpha Agape Gopalai

E2: 3 / 17:00–17:15 hrs

Integrated RT and cryo ablation of liver tumor for computer integrated surgery Pg. 84
Bin Duan, Chee Kong Chui, Kian Jon and Ernest Chua

E2: 4 / 17:15–17:30 hrs

Effects of muscle fatigue on FES assisted walking of SCI patients: A review Pg. 84
Morufu Olusola Ibitoye, Nur Azah Hamzaid and Ahmad Khairi Abdul Wahab

E2: 5 / 17:30–17:45 hrs

Energy recovery concept for collecting stochastic occurring power chunks to supply intermittent sensor measurements on prostheses or robotic limb Pg. 84
Daniel Laqua and Peter Husar

E2: 6 / 17:45–18:00 hrs

A head tracking method for improved eye motion detection in children Pg. 85
Mehrdad Sangi, Benjamin Thompson, Ehsan Vaghefi and Jason Turuwheua

Session	SYM-08: Tissue Mechanobiology: Tissue on the Move	
Date/Time	5 December 2013 / 16:30–18:00 hrs	
Venue	SR-12	
Chair(s)	Yusuke Toyama	
SYM-08: 1 / 16:30–17:00 hrs		
Symposium Keynote		
Mechano-sensitive ATP release: Critical involvement in wound healing		Pg. 85
<u>Masahiro Sokabe</u> , Hiroya Takada and Kishio Furuya		
SYM-08: 2 / 17:00–17:15 hrs		
On the role of biomechanics during embryogenesis		Pg. 86
<u>Lance A. Davidson</u>		
SYM-08: 3 / 17:15–17:30 hrs		
Forces driving epithelial wound healing		Pg. 86
<u>Vito Conte</u> , Agustí Brugués, Ester Anon, Jim H. Veldhuis, Julien Colombelli, <u>José J. Muñoz</u> , G. Wayne Brodland, Benoit Ladoux and Xavier Trepap		
SYM-08: 4 / 17:30–17:45 hrs		
Cell response on integrin-specific artificial protein biomaterials		Pg. 86
Monica Suryana Tjin, Alvin Chua, Seng Teik Lee and <u>Eileen Fong</u>		
SYM-08: 5 / 17:45–18:00 hrs		
Collective cell behavior on micropatterned substrates		Pg. 87
<u>Sriram Krishna Vedula</u> , Manchun Leong, Kevin Doxzen, Hiroaki Hirata, <u>Alexandre J. Kabla</u> , Yusuke Toyama, Benoit Ladoux and Chwee Teck Lim		
End of Day 2		

Day 3 — Friday, 6 December 2013

Session	PL6: Plenary Lecture 6
Date/Time	6 December 2013 / 09:00–09:45 hrs
Venue	Auditorium
Chair(s)	Zhiwei Huang

PL6

Advancing multi-modality clinical imaging: a challenge for the engineer and physicist Pg. 88
David W. Townsend

Session	PL7: Plenary Lecture 7
Date/Time	6 December 2013 / 09:45–10:30 hrs
Venue	Auditorium
Chair(s)	Angelo Karunaratne

PL7

Brain machine interface technology: from neurons to prostheses Pg. 88
Nitish Thakor

10:30–11:00 **Tea Break**

Session	SYM-10: Nanoparticles for Bioimaging and Targeted Therapy
Date/Time	6 December 2013 / 11:00–12:30 hrs
Venue	Auditorium
Chair(s)	Yong Zhang and James Kah

SYM-10: 1 / 11:00–11:30 hrs

Symposium Keynote

A specific surface-coating peptide for rare earth nanomaterials Pg. 88
Long-Ping Wen

SYM-10: 2 / 11:30–11:45 hrs

Selected methods of label-free magnetic resonance imaging for liver function evaluation Pg. 89
Bing Nan Li, Yi Zhuang Cheng, Xiao Bo Yao and Wei Fu Lv

SYM-10: 3 / 11:45–12:00 hrs

Upconverting fluorescent nanoparticles for theranostics Pg. 89
Yong Zhang

SYM-10: 4 / 12:00–12:15 hrs

The good side of protein corona on nanoparticles Pg. 89
James C. Y. Kah

SYM-10: 5 / 12:15–12:30 hrs

Synthesis of up-conversion fluorescent nanoparticles for photodynamic therapy of cancer cells Pg. 90
Haisheng Qian

Session	A7: Optical Imaging	
Date/Time	6 December 2013 / 11:00–12:30 hrs	
Venue	SR-01 & 02	
Chair(s)	Sergey Yu. Sokolov and Dvir Yelin	
A7: 1 / 11:00–11:15 hrs	Temporal focusing: Optically sectioned wide-field imaging for time critical biological processes	Pg. 90
	Elijah Y. S. Yew, <u>Heejin Choi</u> and Peter T. C. So	
A7: 2 / 11:15–11:30 hrs	In vivo blood microscope for patient diagnosis	Pg. 90
	<u>Dvir Yelin</u> and Lior Golan	
A7: 3 / 11:30–11:45 hrs	Distribution of Advanced glycation end-products in human dentin measured by fluorescence lifetime imaging	Pg. 91
	<u>Kantaro Nishikawa</u> , Shuichiro Fukushima, Tsutomu Araki, Mizuho Kubo, Jiro Miura and Fumio Takeshige	
A7: 4 / 11:45–12:00 hrs	An analytic method to optimize aperture design in focal modulation microscopy	Pg. 91
	<u>Yubo Duan</u> , Shakil Rehman, George Barbastathis and Nanguang Chen	
A7: 5 / 12:00–12:15 hrs	Plant intracellular PH measurement using the fluorescence intensity ratio for a study of cryopreservation technique	Pg. 92
	<u>Takako Ninagawa</u> , Akemi Eguchi, Akira Narumi, Tadashi Konishi and Yukio Kawamura	
A7: 6 / 12:15–12:30 hrs	Multimodal nonlinear optical microscopy for label-free imaging of the tooth	Pg. 92
	<u>Zi Wang</u> , Wei Zheng, Chin Ying Stephen Hsu and Zhiwei Huang	
Session	B7: Diagnostics and Therapeutics	
Date/Time	6 December 2013 / 11:00–12:45 hrs	
Venue	SR-03 & 04	
Chair(s)	Stephen E. Greenwald and Chen Hua Yeow	
B7: 1 / 11:00–11:15 hrs	Efficient intracellular delivery of polymeric MRI contrast agent for mesenchymal stem cell transplantation to myocardial infarction	Pg. 92
	Naoki Kobayashi, <u>Atsushi Mahara</u> , Jun-ichiro Enmi, Akihideo Yamamoto, Hidehiro Iida, Yoshiaki Hirano and Tetsuji Yamaoka	
B7: 2 / 11:15–11:30 hrs	Synthesizing gold nanoparticles in spherical and rod shapes for targeting cancer treatment	Pg. 93
	<u>Poh Foong Lee</u> , Guo Feng Chin, Misni Misran and Pek Yee Tang	

B7: 3 / 11:30–11:45 hrs

Gold nanoparticles cross-linked responsive polymers for a colorimetric enzyme sensor Pg. 93
Erindyah Retno Wikantyasning, Johannes Pall Magnusson, Clive J. Roberts,
Cameron Alexander and Jonathan W. Aylott

B7: 4 / 11:45–12:00 hrs

Computational diagnosis of coronary artery stenosis: experimental measurement Pg. 94
of wave propagation in soft tissue mimicking gel
H. Thomas Banks, Malcolm J. Birch, Mark P. Brewin, Stephen E. Greenwald,
Shuhua Hu, Zack R. Kenz, Carola Kruse, Dwij Mehta, Simon Shaw and
John R. Whiteman

B7: 5 / 12:00–12:15 hrs

Towards computational diagnosis of coronary artery disease Pg. 94
Simon Shaw, John R. Whiteman, Carola Kruse, Stephen E. Greenwald,
Malcolm J. Birch, Mark P. Brewin, H. Thomas Banks, Shuhua Hu and Zackary R. Kenz

B7: 6 / 12:15–12:30 hrs

Holistic cell-line metabolome profiling strategy for biomarker identification Pg. 95
Gokula Krishnan Ramachandran and Chen-Hua Yeow

B7: 7 / 12:30–12:45 hrs

A pervasive intelligent system for scoring mews and TISS-28 in intensive care Pg. 95
Filipe Portela, Manuel Filipe Santos, Álvaro Silva, José Machado, António Abelha
and Fernando Rua

Session	C7: Computational Mechanics
Date/Time	6 December 2013 / 11:00–12:30 hrs
Venue	SR-05 & 06
Chair(s)	Justin Wade Fernandez and Michihiko Koseki

C7: 1 / 11:00–11:15 hrs

Evaluating the mechanical efficacy of anabolic bone treatments using a non-destructive Pg. 96
framework
Justin Fernandez, Dharshini Sreenivasan, Maureen Watson, Raj Das, Andrew Grey
and Jillian Cornish

C7: 2 / 11:15–11:30 hrs

Individual stress analysis of bone tissue using small scale FE model with anisotropic Pg. 96
material properties
Michihiko Koseki and Takuya Hasegawa

C7: 3 / 11:30–11:45 hrs

Importance of stem orientation in total hip arthroplasty by bone remodeling simulation Pg. 96
Ji Yean Kwon, Sungjae Kim, Sungmin Kim and Masao Tanaka

C7: 4 / 11:45–12:00 hrs

Prediction of suture anchor loosening after rotator cuff repair – An investigation using Pg. 97
three-dimensional finite element method
Hirotaka Sano, Nobuyuki Yamamoto and Eiji Itoi

C7: 5 / 12:00–12:15 hrs

Predicting the line of action of forearm muscles during pronation-supination
Desney Greybe, Michael R. Boland and Kumar Mithraratne

Pg. 97

C7: 6 / 12:15–12:30 hrs

A comparative case study of a congenital dysplastic hip joint before and after a DEGA osteotomy simulation
Santiago Rendon Valencia and Diego A. Garzon Alvarado

Pg. 98

Session	DA: BES-SEC Design Awards 2013
Date/Time	6 December 2013 / 11:00–12:30 hrs
Venue	SR-07 & 08
Chair(s)	Siew Lok Toh

DA: 1 / 11:00–11:15 hrs

Design an infection screening system based on multiple vital-signs for prevention of pandemic diseases in developing countries
Guanghao Sun, Kohei Nozaki, Yosuke Nakayama, Chris Chen and Akiko Ueda
Tokyo Metropolitan University, Japan

DA: 2 / 11:15–11:30 hrs

Real time Patient monitoring system with Filter Bank and Fuzzy Classification Approach to Critical Cardiac Abnormalities Detection
Uvais Qidwai, Mohamed Shakir
Qatar University, Qatar

DA: 3 / 11:30–11:45 hrs

Low cost compact CCD microscope for vision based blood screening with microelectrophoresis system
Boon Yew Teoh
University Tunku Abdul Rahman, Malaysia

DA: 4 / 11:45–12:00 hrs

Design of a Paper-Based Micro-Viscometer for Blood Plasma
Zi Ai Chew, Brandon Bao Sheng Yew, Hsin Yao Chiu, Dorothy Shuzhen Neo
Department of Bioengineering, National University of Singapore, Singapore

DA: 5 / 12:00–12:15 hrs

Design and Implementation of a Calibration-Free Pulse Oximeter
Harini Harinarayanan, L. S. Krithika, M. Shalini, Sirisha Swaminathan
Amrita Vishwa Vidhyapeetham, India

DA: 6 / 12:15–12:30 hrs

Integrated Robotic Navigation White Cane for Visually Impaired People
Muchammad Adib, Muhammad DibaAzmi Syarif and Yuliana Cahya Nuraini
Universitas GadjahMada, Indonesia

Session	SYM-11: Biomedical Engineering in Sport Science
Date/Time	6 December 2013 / 11:00–12:30 hrs
Venue	SR-12
Chair(s)	Matthias Lochmann and Pedro Miguel Ramos Reis

SYM-11: 1 / 11:00–11:15 hrs

Biomechanical cartilage imaging patterns in professional soccer Pg. 98
Goetz Welsch, Friedrich Hennig and Matthias Lochmann

SYM-11: 2 / 11:15–11:30 hrs

Evidence based concept of insole supply Pg. 99
Gurzi Domenico, Matthias Lochmann and Fritz Bodem

SYM-11: 3 / 11:30–11:45 hrs

Heart-rate controlled E-bike-exercising Pg. 99
Holger Eckhardt and Matthias Lochmann

SYM-11: 4 / 11:45–12:00 hrs

Methodological aspects of EEG measurements during movement Pg. 99
Pedro Miguel Ramos Reis, Felix Hebenstreit and Matthias Lochmann

SYM-11: 5 / 12:00–12:15 hrs

Sensor based movement analysis Pg. 100
Bjoern M Eskofier and Dominik Schuldhaus

SYM-11: 6 / 12:15–12:30 hrs

Training 4.0 – computerized motion analysis in football training Pg. 100
Matthias Lochmann, Holger Eckhardt and Fritz Bodem

12:30–13:30 **Lunch & Poster Session**

Session	SYM-12: Emerging Developments for Regenerative and Therapeutic Medicine
Date/Time	6 December 2013 / 13:30–15:00 hrs
Venue	Auditorium
Chair(s)	Evelyn Yim and Andrew Chwee Aun Wan

SYM-12: 1 / 13:30–14:00 hrs

Symposium Keynote
Biomaterial-assisted stem cell-based therapies for intervertebral disc degeneration Pg. 101
Barbara Chan

SYM-12: 2 / 14:00–14:15 hrs

Polysaccharide hydrogels functionalized with fucoidan for tissue reconstruction Pg. 102
Catherine Le Visage

SYM-12: 3 / 14:15–14:30 hrs

Emerging therapy in corneal transplantations Pg. 102
Jodhbir Mehta

SYM-12: 4 / 14:30–14:45 hrs

Microengineered hydrogels for stem cell bioengineering and tissue regeneration Pg. 102
Ali Khademhosseini

SYM-12: 5 / 14:45–15:00 hrs

Substrate topography for gene delivery and tissue engineering applications Pg. 103
Evelyn K.F. Yim

Session	A8: Medical Imaging
Date/Time	6 December 2013 / 13:30–15:00 hrs
Venue	SR-01 & 02
Chair(s)	Chung Cheuk Wang and Jiamao Li

A8: 1 / 13:30–13:45 hrs

Efficient regularisation of temporal autocorrelation estimates in fMRI data Pg. 103
Arun Kumar and Lin Feng

A8: 2 / 13:45–14:00 hrs

A study on the high-resolution imaging system for capillary on the surface of eyeball Pg. 103
Jiamao Li and Xiaolin Zhang

A8: 3 / 14:00–14:15 hr

Measurement of undetectable walking feature by appearance based on plantar skin deformation Pg. 104
Takayuki Shiina, Akira Obara, Hiroshi Takemura and Hiroshi Mizoguchi

A8: 4 / 14:15–14:30 hrs

Novel technique to characterise corneal biomechanics *in vivo* Pg. 104
Cheuk Wang Chung, William Lim, Khai Sing Chin, Nicholas Strouthidis and Michael J.A. Girard

A8: 5 / 14:30–14:45 hrs

Development of novel endoscope with nir camera using real-time video composite method Pg. 105
Masayuki Watanabe, Hiroshi Takemura, Hiroshi Mizoguchi, Hiroshi Hyodo, Kohei Soga, Tamotsu Zako, Hidehiro Kishimoto, Masaaki Ito and Kazuhiro Kaneko

A8: 6 / 14:45–15:00 hrs

Remote photoplethysmographic imaging of dermal perfusion in a porcine animal model Pg. 105
Nikolai Blanic, Carina Barbosa Pereira, Michael Czaplík, Vladimir Blazek and Steffen Leonhardt

Session	B8: Biological Materials
Date/Time	6 December 2013 / 13:30–15:00 hrs
Venue	SR-03 & 04
Chair(s)	Alexander M. Korsunsky and Sachiro Kakinoki

B8: 1 / 13:30–14:00 hrs

Conference Keynote

Current biomaterials for tendon/ligament tissue engineering Pg. 106
Hong-Wei Ouyang

B8: 2 / 14:00–14:15 hrs

Single step peptide immobilization onto a variety of biomaterial surfaces by Tyr oxidation and its application for re-endothelialization promoting vascular stent Pg. 106
Sachiro Kakinoki, Kensuke Takasaki, Yoshiaki Hirano and Tetsuji Yamaoka

B8: 3 / 14:15–14:30 hrs

Nano-scale thermo-mechanical structure-property relationships in human dental tissues studied by nanoindentation and synchrotron X-ray scattering Pg. 106
Tan Sui, Michael A. Sandholzer, Eric Le Bourhis, Nikolaos Baimpas, Gabriel Landini and Alexander M. Korsunsky

B8: 4 / 14:30–14:45 hrs

Effect of molecular architecture of PEG-immobilized surface on plasma fibrinogen adsorption and platelet adhesion Pg. 107
Takuya Nakagoshi, Sachiro Kakinoki, Yuichi Ohya and Tetsuji Yamaoka

B8: 5 / 14:45–15:00 hrs

Synthesis and characterization of nanorod Hydroxyapatite from cockle shells Pg. 107
Nur Ain Iftitah Mohamad Razali, Belinda Pinguang-Murphy, Noor Azuan Abu Osman and Sumit Pramanik

Session	C8: Computational Mechanics
Date/Time	6 December 2013 / 13:30–15:00 hrs
Venue	SR-05 & 06
Chair(s)	Peter Hunter and Varomyalin Tipmanee

C8: 1 / 13:30–14:00 hrs

Conference Keynote
An overview of VPH/Physiome activities Pg. 108
Peter John Hunter

C8: 2 / 14:00–14:15 hrs

Application of CFD and genetic algorithms to investigation of determinants of carotid artery bifurcation shapes Pg. 108
Masako Himeno, Shigeho Noda, Kazuaki Fukasaku and Ryutaro Himeno

C8: 3 / 14:15–14:30 hrs

Simulation of Electron transfer in Cytochrome b5 reductase-Cytochrome b5: Ground study for understanding Recessive methemoglobinemia type II Pg. 108
Varomyalin Tipmanee, Thanyada Rungrotmongkol and Supot Hannongbua

C8: 4 / 14:30–14:45 hrs

Computer simulation of human respiration Pg. 109
Guangzhi Zhang, Xian Chen, Junji Ohgi, Seiryu Sugiura and Toshiaki Hisada

Session	D4: Biomedical Devices
Date/Time	6 December 2013 / 13:30–15:00 hrs
Venue	SR-07 & 08
Chair(s)	Subbaraman Ravichandran and Uvais Qidwai

D4: 1 / 13:30–14:00 hrs

Conference Keynote
Lessons learnt: Development of genomics-based diagnostics tests Pg. 109
Christopher Wong

D4: 2 / 14:00–14:15 hrs

Embedded fuzzy classifier for detection and classification of preseizure state using real EEG data Pg. 109

Uvais Qidwai, Mohamed Shakir and Aamir Malik

D4: 3 / 14:15–14:30 hrs

Qualitative studies on quartz filters used in ultraviolet sterilization system Pg. 110

Subbaraman Ravichandran and Then Tze Kang

D4: 4 / 14:30–14:45 hrs

The effect of axial variation of the plane flow rate on two-dimensional ultrasonic-measurement-integrated simulation of blood flow in a common carotid artery Pg. 110

Takuya Matsumoto, Kenichi Funamoto and Toshiyuki Hayase

D4: 5 / 14:45–15:00 hrs

Modeling of signal transmissions in nerves in vitro for the development of a renal nerve cooling device for hypertension control Pg. 111

Takuya Ito, Hidekazu Miura, Takuya Shiga, Mohamed Hashem, Kurodo Kamiya, Akihiro Yamada, Yusuke Tsuboko, Kyosuke Sano, Yasunori Taira, Yasuyuki Shiraishi, Hiroo Kumagai and Tomoyuki Yambe

Session D3: Biomedical Devices | Diagnostic Devices

Date/Time 6 December 2013 / 13:30–15:15 hrs

Venue SR-12

Chair(s) Yu Chen and Hwa Liang Leo

D3: 1 / 13:30–13:45 hrs

High sensitive detection of Ag⁺ ions in aqueous solution using silicon nanowires and silver-specific oligonucleotide Pg. 111

Yu Chen and Muhammad Hamidullah

D3: 2 / 13:45–14:00 hrs

Integration of mobile phone imaging with lateral flow assays for real-time quantitative detection of nucleic acids Pg. 112

Jie Hu, ShuQi Wang, Lin Wang, Tian Jian Lu and Feng Xu

D3: 3 / 14:00–14:15 hrs

Pressure distribution measurement of close fitting clothes on human body Pg. 112

Jan Grepl, Marek Penhaker, J Kubicek, J Prokop and L Peter

D3: 4 / 14:15–14:30 hrs

In-vitro evaluation of flow modification by covered stents for treatment of intracranial aneurysms Pg. 112

Foad Kabinejadian and Hwa Liang Leo

D3: 5 / 14:30–14:45 hrs

Gene expression of diabetic fibroblast and normal fibroblast after irradiating with light emitting diode by using Microarray Pg. 113

Pongsathorn Chotikasemsri, Boonsin Tungtrakunwanit and Surasak Sungkatat Naayutaya

D3: 6 / 14:45–15:00 hrs

Carbon nanotubes as a cradle of impulse for implantable medical devices Pg. 113
Fredrick Johnson Joseph, Karthick Madheswaran, Gopu Govindasamy and Sathiesh Kumar

D3: 7 / 15:00–15:15 hrs

Quantification and improvement of the adhesion of electrical surgical units Pg. 114
Shen-Han Chen

15:00–15:30 **Tea Break**

Session	C9: Cardiovascular Mechanics
Date/Time	6 December 2013 / 15:30–17:00 hrs
Venue	Auditorium
Chair(s)	Mohamed Omran Hashem and Jun-Mei Zhang

C9: 1 / 15:30–15:45 hrs

Effects of coronary stenosis on three-dimensional coronary blood flow: Pg. 114
implication for revascularization selection
Jun-Mei Zhang, Jinq Shya Yap, Jasmine P. L. Tham, Yunlong Huo, Min Wan, Ru San Tan and Liang Zhong

C9: 2 / 15:45–16:00 hrs

Design optimization of thoracic endovascular stent graft (EVSG) Pg. 115
Kiruthigha Shanmuga Sundaram, Johanna Rajan, Suvita Selvam, Mohan Thanikachalam, N. Viswanatha and R. K. Ramanathan

C9: 3 / 16:00–16:15 hrs

A study of mechanical behavior of an encapsulated stent design using finite Pg. 115
element analysis
Kiruthigha Shanmuga Sundaram, Davidson Jabaseelan, Rinse Jose, Ranjitha Rebecca Jeevan, Mohan Thanikachalam, George Joseph and Santhosh Joseph

C9:4 / 16:15–16:30 hrs

Comparison of hemodynamic parameters and wall condition of cerebral aneurysm Pg. 116
Daichi Suzuki, Kenichi Funamoto, Shin-ichiro Sugiyama, Toshio Nakayama, Teiji Tominaga and Toshiyuki Hayase

C9:5 / 16:30–16:45 hrs

Fatigue life enhancement of peripheral stents by an intriguing design concept Pg. 116
Ming-Ting Yin, Ling-Hsiang Chao, Li-Wei Wu, Hsiao-Nan Yang, Yu-Huan Lin and Hao-Ming Hsiao

C9: 6 / 16:45–17:00 hrs

Improvement of a shape memory alloy fibered aortic pulsation device Pg. 117
Mohamed Omran Hashem, Yasuyuki Shiraishi, Akahiro Yamada, Y. Tsuboko, Hidekazu Muira, Tomoyuki Yambe and D. Homma

Session	A9: Biosignal Processing	
Date/Time	6 December 2013 / 15:30–17:00 hrs	
Venue	SR-01 & 02	
Chair(s)	Sheng-Fu Liang	
A9: 1 / 15:30–15:45 hrs	Diagnosis of schizophrenia patients based on brain network complexity analysis of resting-state fMRI	Pg. 117
	Tsung-Hao Hsieh, Ming-Jian Sun and <u>Sheng-Fu Liang</u>	
A9: 2 / 15:45–16:00 hrs	Automated localization of seizure focus using interictal intracranial EEG	Pg. 118
	<u>Jin Jing</u> , Justin Dauwels and Sydney Cash	
A9: 3 / 16:00–16:15 hrs	Design and evaluation of a hardware-accelerator for energy efficient inertial sensor fusion on heterogeneous SoC architectures	Pg. 118
	<u>Hans-Peter Brückner</u> , Christian Spindeldreier and Holger Blume	
A9:4 / 16:15–16:30 hrs	Liver vessel segmentation using graph cuts with quick shift initialization	Pg. 118
	<u>Bichao Chen</u> , Ying Sun and Sim Heng Ong	
A9:5 / 16:30–16:45 hrs	Strategies for baseline drift compensation of DC-coupled electrooculogram measurements for human-computer-interfaces	Pg. 119
	<u>Anna Böhm</u> , Axel Uhlig and Steffen Leonhardt	
A9: 6 / 16:45–17:00 hrs	Assigning myocardial fibre orientation to a computational biventricular human heart model	Pg. 119
	<u>Arnab Palit</u> , Glen A. Turley, Sunil K. Bhudia, Richard Wellings and Mark A. Williams	
Session	B9: Biological Materials Diagnostics and Therapeutic	
Date/Time	6 December 2013 / 15:30–17:00 hrs	
Venue	SR-03 & 04	
Chair(s)	Joseph Lee Bull and Yan Wang	
B9: 1 / 15:30–15:45 hrs	Heart tissue engineering using ex vivo dynamically vascularized porcine cardiac ECM: does thickness matter?	Pg. 119
	<u>Udi Sarig</u> , Hadar Sarig, Evelyne Nguyen, Wang Yao, Gigi A. Y. C. Ting, Tomer Bronshtein, Michael Buering, Thomas Scheper, Freddy Yin Chiang Boey, Subbu S. Venkatraman and Marcelle Machluf Machluf	
B9: 2 / 15:45–16:00 hrs	Acoustic droplet vaporization for gas embolotherapy	Pg. 120
	<u>Joseph Lee Bull</u> , David S. Li, Oliver D. Kripfgans and J. Brian Fowlkes	

B9: 3 / 16:00–16:15 hrs

Evaluation of a hybrid bioartificial liver support system using CL-L cells in cynomolgus monkey models with D-galactosamine induced acute liver failure Pg. 120
Yi Gao, Zhi Zhang, Ming-Xin Pan, Yuan Cheng and Yan Wang

B9:4 / 16:15–16:30 hrs

Probing biochemical and mechanical crosstalk between EhpA2 and integrin signalling in breast cancer cells using hybrid fluid lipid bilayers and immobilized RGD patterns Pg. 121
Zhongwen Chen, Cheng-Han Yu, Kabir H Biswas, Ronen Zaidel-Bar and Jay T. Groves

B9:5 / 16:30–16:45 hrs

Hyperelastic constitutive relationship for the strain-rate dependent behavior of shoulder and other joint cartilages Pg. 121
Noyel Deegayu Thibbotuwawa, Adekunle Oloyede, Wijitha Senadeera and Yuan Tong Gu

B9: 6 / 16:45–17:00 hrs

Biopiezoelectric, bioferroelectric and subnanoscale-mechanical properties of calcified tissues Pg. 121
Tao Li and Kaiyang Zeng

Session C10: Mechanobiology

Date/Time 6 December 2013 / 15:30–16:30 hrs

Venue SR-05 & 06

Chair(s) Kazuaki Nagayama and Yusuke Toyama

C10: 1 / 15:30–15:45 hrs

On the roles of actin stress fibers on the mechanical regulation of nucleus in adherent cells Pg. 122
Kazuaki Nagayama, Yuki Yahiro, Sho Yamazaki, Mitsuhiro Ukiki and Takeo Matsumoto

C10: 2 / 15:45–16:00 hrs

Endothelial cells respond to shear stress by decreasing the lipid order of their plasma membranes Pg. 122
Kimiko Yamamoto and Joji Ando

C10: 3 / 16:00–16:15 hrs

Dimensionality and behavior of swimming Zebrafish: “The EigenFish” Pg. 123
Kiran Girdhar, Martin Gruebele and Yann Chemla

C10:4 / 16:15–16:30 hrs

Achievement of peristaltic design in the artificial esophagus based on esopha-geal characteristic analysis of goats’ specimen Pg. 123
Yasunori Taira, Kurodo Kamiya, Yasuyuki Shiraishi, Hidekazu Miura, Takuya Shiga, Mohamed Omran Hashem, Akihiro Yamada, Yusuke Tsuboko, Takuya Ito, Kyosuke Sano and Tomoyuki Yambe

Session	D5: Lab-on-Chip Micro/Nanofluidics
Date/Time	6 December 2013 / 15:30–17:15 hrs
Venue	SR-07 & 08
Chair(s)	Kathy Luo and Toshiro Ohashi

D5: 1 / 15:30–15:45 hrs

A microfluidic device for stepwise concentration generation on a microwell slide for cytotoxic assay Pg. 123
Toshiro Ohashi, Emilie Weibull, Manabu Sakai, Shunsuke Matsui and Helene Andersson-Svahn

D5: 2 / 15:45–16:00 hrs

Electrical stimulation induces enhanced myelination in a novel microfluidic platform Pg. 124
Hae Ung Lee, Nitish Thakor and In Hong Yang

D5: 3 / 16:00–16:15 hrs

A scalable method for aligning 3D micro-tissues in a microfluidic chip Pg. 124
Chukwuemeka George Anene-Nzelu, Kah Yim Peh, Azmall Fraiszudeen, Sum Huan Ng, Hwa Liang Leo, Hanry Yu and Yi Chin Toh

D5:4 / 16:15–16:30 hrs

Application of a FRET-based biosensor in studying shear stress-induced apoptosis in circulating tumor cells Pg. 125
Xiaofeng Liu, Afu Fu and Kathy Qian Luo

D5:5 / 16:30–16:45 hrs

An integrated microfluidic device for single cell encapsulation and cellular enzymatic assay Pg. 125
Tengyang Jing, Ramesh Ramji, Majid Ebrahimi Warkiani, Chia-Hung Chen, Jongyoon Han and Chwee Teck Lim

D5: 6 / 16:45–17:00 hrs

Integrated microfluidic platform for multiplexed enzymatic bioassay in ovarian cancer MMP activity study Pg. 126
Ee Xien Ng and Chia-Hung Chen

D5: 7 / 17:00–17:15 hrs

Real-time impedimetric monitoring of Poly(ethylenimine)s-mediated cytotoxicity during gene transfection Pg. 126
Claudia Caviglia, Marco Carminati, Arto Heiskanen, Giorgio Ferrari, Marco Sampietro, Thomas Lars Andresen and Jenny Emn us

Session	E3: Rehabilitation Neurotechnology
Date/Time	6 December 2013 / 15:30–17:00 hrs
Venue	SR-12
Chair(s)	Haoyong Yu and Desmond Chong

E3: 1 / 15:30–15:45 hrs

EEG-based emotion monitoring in mental task performance Pg. 127
Yisi Liu, Olga Sourina and Woon Huei Chai

E3: 2 / 15:45–16:00 hrs

A multi-level fuzzy logic system for controlling the tibialis anterior FES envelop
Negar Zakhirehdari, Hamidreza Kobravi, Mitra Masoudi and Tavakkoli Parvaneh

Pg. 127

E3: 3 / 16:00–16:15 hrs

Experimental study of FES-driven ankle joint actuator for hybrid FES walking
assistive system – I
Naosuke Yamamoto, Naoya Kurokawa, Toshiyasu Yamamoto, Yoshihiko Tagawa and
Hiroaki Kuno

Pg. 127

E3: 4 / 16:15–16:30 hrs

Experimental study of motor-driven hip joint actuator for hybrid FES walking
assistive system – II
Naoya Kurokawa, Naosuke Yamamoto, Toshiyasu Yamamoto, Yoshihiko Tagawa and
Hiroaki Kuno

Pg. 128

E3: 5 / 16:30–16:45 hrs

Development of a knee ankle robot for gait rehabilitation
Haoyong Yu, Sunan Huang and Nitish Thakor

Pg. 128

E3: 6 / 16:45–17:00 hrs

Multiobjective design optimization for a steerable needle for soft tissue surgery
Alexander Leibinger, Matthew Oldfield and Ferdinando Rodriguez y Baena

Pg. 129

18:30–21:30 **Conference Banquet (Ticketed Event)**

End of Day 3

Day 4 — Saturday, 7 December 2013

Session	A10: Biosignal Processing	
Date/Time	7 December 2013 / 09:00–10:15 hrs	
Venue	SR-01 & 02	
Chair(s)	Fook Chiong Cheong and Dharitri Goswami	
A10: 1 / 09:00–09:15 hrs		
Aging integromics: module-based markers of heart aging from multi-omics data		Pg. 130
Konstantina Dimitrakopoulou, Aristidis Vrahatis, Georgios Dimitrakopoulos and <u>Anastasios Bezerianos</u>		
A10: 2 / 09:15–09:30 hrs		
Robustness of two-pulse-synthesis model studied on toe photoplethysmograph signals		Pg. 130
<u>Dharitri Goswami</u> and Jayanta Mukhopadhyay		
A10: 3 / 09:30–09:45 hrs		
Automated parameter estimation for a nonlinear signal separation scheme		Pg. 131
<u>Yu Yao</u> , Stefan van Waasen and Michael Schiek		
A10: 4 / 09:45–10:00 hrs		
Assesment of first derivative of doppler blood flow velocity in vascular aging		Pg. 131
<u>Zulaika Hamdon</u> , Azran Azhim, Muhamad Saleh, Pouya Bagherpour, Yohsuke Kinouchi and Fatimah Ibrahim		
A10: 5 / 10:00–10:15 hrs		
Quantitative high speed tracking of bacteria motility in 3D		Pg. 131
<u>Fook Chiong Cheong</u> , Chui Ching Wong and Chwee Teck Lim		
Session	B10: Regenerative Medicine Tissue Engineering	
Date/Time	7 December 2013 / 09:00–10:30 hrs	
Venue	SR-03 & 04	
Chair(s)	Tram T. Dang and Kai Yang	
B10: 1 / 09:00–09:15 hrs		
In vivo animal model— the golden key for tissue engineering		Pg. 132
<u>Kai Yang</u>		
B10: 2 / 09:15–09:30 hrs		
Enhanced function of immuno-isolated islets in diabetes therapy by co-encapsulation with an anti-inflammatory drug		Pg. 132
<u>Tram T. Dang</u> , A. V. Thai, J. Cohen, J. E. Slosberg, K. Siniakowicz, J. C. Doloff, M. Ma, J. Hollister-Lock, K. M. Tang, Z. Gu, H. Cheng, G. C. Weir, R. Langer and D. G. Anderson		
B10: 3 / 09:30–09:45 hrs		
Preservation of left ventricular function and morphology using fibrinogen-based conjugates		Pg. 132
<u>Marian Plotkin</u> , Srirangam Ramanujam Vaibavi, Rufaihah Abdul Jalil, Venkateswaran Nithya, Jing Wang, Theodoros Kofidis and Dror Seliktar		

B10: 4 / 09:45–10:00 hrs

Infarct stabilization and cardiac repair with VEGF-loaded PEGylated fibrinogen injectable hydrogel Pg. 133

Rufaihah Abdul Jalil, Vaibavi Srirangam Ramanujam, Marian Plotkin, Nithya Venkateswaran, Jiayi Shen, Jing Wang, Dror Seliktar and Theodoros Kofidis

B10: 5 / 10:00–10:15 hrs

Towards cardiac constructs with physiologically relevant dimensions for heart regeneration Pg. 133

Evelyne Nguyen, Udi Sarig, Tomer Bronshtein, Freddy Yin Chiang Boey, Subbu S. Venkatraman and Marcelle Machluf

B10: 6 / 10:15–10:30 hrs

Development of cartilaginous tissue in chondrocyte-agarose construct cultured under traction loading Pg. 134

Keisuke Fukuda, Seiji Omata and Yoshinori Sawae

Session	D6: Biomedical Devices
Date/Time	7 December 2013 / 09:00–10:30 hrs
Venue	SR-05 & 06
Chair(s)	Daisuke Yoshino and Sheng-Fu Liang

D6: 1 / 09:00–09:15 hrs

Development of low-temperature sterilization device using atmospheric-pressure plasma Pg. 134

Kazuhiro Nakamura, Daisuke Yoshino, Tomoki Nakajima and Takehiko Sato

D6: 2 / 09:15–09:30 hrs

Micro-fabricated membranes with regular pores for efficient pathogen removal Pg. 135

Majid Ebrahimi Warkiani and Hai-Qing Gong

D6: 3 / 09:30–09:45 hrs

Development of seizure monitoring and control systems for epileptic animal models Pg. 135

Sheng-Fu Liang, Yu-Lin Wang and Fu-Zen Shaw

D6: 4 / 09:45–10:00 hrs

Challenges and trade-offs involved in designing embedded algorithms for a low-power wearable wireless monitor Pg. 135

Miguel Hernandez Silveira, Su-Shin Ang and Alison Burdett

D6: 5 / 10:00–10:15 hrs

Validation of blood vessel geometry reconstruction and of blood flow analysis system for small animals Pg. 136

by ultrasonic-measurement-integrated flow-structure interaction simulation
Sanga Sakanishi, Toshiyuki Hayase, Kenichi Funamoto and Shusaku Sone

D6: 6 / 10:15–10:30 hrs

Design of a right ventricular simulator for the evaluation of artificial pulmonary valve Pg. 136

Yusuke Tsuboko, Satoshi Matsuo, Yasuyuki Shiraishi, Hidekazu Miura, Akihiro Yamada, Mohamed Omran Hashem, Takuya Ito, Kyosuke Sano, Yasunori Taira, Toshinosuke Akutsu, Zhonggang Feng, Mitsuo Umezu, Masaaki Yamagishi, Yoshikatsu Saiki and Tomoyuki Yambe

Session	C11: Cell Mechanics	
Date/Time	7 December 2013 / 09:00–10:45 hrs	
Venue	SR-07 & 08	
Chair(s)	Chuh Khiun Chong and Taiji Adachi	
C11: 1 / 09:00–09:30 hrs		
Conference Keynote		
Title not available at time of print		Pg. 137
<u>Theodoros Kofidis</u>		
C11: 2 / 09:30–09:45 hrs		
Computer simulation of tissue morphogenesis based on multicellular dynamics		Pg. 137
<u>Taiji Adachi, Satoru Okuda and Yasuhiro Inoue</u>		
C11: 3 / 09:45–10:00 hrs		
Quantitative analysis of endothelial cell response to fluid shear stresses		Pg. 138
<u>Chuh Khiun Chong and Alexander Thomas White</u>		
C11: 4 / 10:00–10:15 hrs		
The effect of the mechanical properties of cell membrane on its passive endocytosis process		Pg. 138
<u>Xinyue Liu¹, Yunqiao Liu, Xiaobo Gong and Huaxiong Huang</u>		
C11:5 / 10:15–10:30 hrs		
Viscoelastic property and cell adhesion process of cultured fibroblasts on different self-assembled monolayers monitored by acoustic wave biosensor		Pg. 139
<u>Yuvaret Viturawong, Sukumal Chongthammakun, Nuttawee Niamsiri, Toemsak Sriksirin and Tanakorn Osotchan</u>		
C11:6 / 10:30–10:45 hrs		
Dynamic modeling of tip cell migration incorporating filopodia dynamics in degradable 3-dimensional extracellular matrix		Pg. 139
<u>Min-Cheol Kim, Peter Chen, Roger D. Kamm and H. Harry Asada</u>		
Session	E4: Bio- and Medical Robotics	
Date/Time	7 December 2013 / 09:00–10:30 hrs	
Venue	SR-12	
Chair(s)	Louis Phee	
E4: 1 / 09:00–09:30 hrs		
Conference Keynote		
Robotics in gastroenterology: bench to beside, and beyond		Pg. 140
<u>Louis Phee</u>		
E4: 2 / 09:30–09:45 hrs		
System identification of an active mechanical lung simulator in order to design a control regime		Pg. 140
<u>Tobias Laechele, Timo Zifreund, Christian Knoebel and Knut Moeller</u>		

E4: 3 / 09:45–10:00 hrs

An automatic system for batch microinjection of silkworm eggs Pg. 140
Chao Yu, Peter Chen, Daiwen Yang, Shengfeng Zhou and Hian Hian See

E4: 4 / 10:00–10:15 hrs

MR guided focused ultrasound positioning device for prostate cancer treatment Pg. 140
Christakis Damianou, Christos Yiallouras and Nicos Mylonas

E4:5 / 10:15–10:30 hrs

Modeling of bioimpedance spectroscopy measurements for the process control of an Pg. 141
orthopedic surgical milling tool
Christian Brendle, Annegret Niesche, Alexander Korff, Klaus Radermacher,
Benjamin Rein, Andrea Scholl, Berno Misgeld and Steffen Leonhardt

10:30–11:00 **Tea Break**

Session A11: Medical Imaging

Date/Time 7 December 2013 / 11:00–12:30 hrs

Venue SR-01 & 02

Chair(s) Kenichi Funamoto and Chueh Loo Poh

A11: 1 / 11:00–11:15 hrs

Finite element based tumor motion tracking based on 4D MRI thoracic data Pg. 141
Yuxin Yang, Soo Kng Teo and Chueh Loo Poh

A11: 2 / 11:15–11:30 hrs

Evaluation by high-frequency ultrasound B-mode imaging of cerebral hemorrhage in Pg. 142
mouse fetal brain resulting from ischemia/reperfusion
Kenichi Funamoto, Takuya Ito, Kiyoe Funamoto, Clarissa Velayo, Toshiyuki Hayase
and Yoshitaka Kimura

A11: 3 / 11:30–11:45 hrs

Creation of the beam hardening artifact Pg. 142
Jan Kubíček

A11: 4 / 11:45–12:00 hrs

Semi automatic segmentation of breast thermograms using variational level set method Pg. 142
S. S. Suganthi and S. Ramakrishnan

A11: 5 / 12:00–12:15 hrs

Viscoelastic properties of gel material and soft tissue measured by MRE (magnetic Pg. 143
resonance elastography) using micro MRI
Hayato Suzuki, Mikio Suga, Kazuhiro Fujisaki, Itsuro Kajiwara, Gen Nakamura,
Kogo Yoshikawa and Shigeru Tadano

A11: 6 / 12:15–12:30 hrs

Automatic cervical cell classification using patch-based fuzzy clustering and minimum Pg. 143
average correlation energy filter
Thanatip Chankong, Nipon Theera-Umpon and Sansanee Auephanwiriyaikul

Session	B11: Tissue Engineering
Date/Time	7 December 2013 / 11:00–12:30 hrs
Venue	SR-03 & 04
Chair(s)	Haseena Bashir Muhammad and Leo Hwa Liang

B11: 1 / 11:00–11:15 hrs

Design considerations for bioartificial liver devices Pg. 144
H. L. Leo, G. T. Tan, K. E. Birgersson, M. Tania, M. N. Hsu, L. Xia and Henry Yu

B11: 2 / 11:15–11:30 hrs

A physiological three-dimensional tumor construct for chemotherapeutic testing Pg. 144
Pamela H. S. Tan, Su Shin Chia, Saminathan S. Nathan, James C. H. Goh and Siew Lok Toh

B11: 3 / 11:30–11:45 hrs

Mechanical variation and proliferation behavior in hydroxyapatite based scaffolds with Pg. 145
 mesenchymal stem cells
Phanny Yos, Md Abdul Kafi and Mitsugu Todo

B11: 4 / 11:45–12:00 hrs

Immune response of implanted aortic scaffolds decellularized by sonication treatment Pg. 145
Nurul Syazwani Ahmad Sabri, Azran Azhim, Yuji Morimoto, Katsuko Furukawa and Takashi Ushida

B11: 5 / 12:00–12:15 hrs

Tissue engineering the intervertebral disc: a whole disc approach using silk-derived Pg. 145
 scaffolds and hydrogels with adipose-derived stem cells
Puay Yong Neo, Pujiang Shi, James Cho-Hong Goh and Siew Lok Toh

B11: 6 / 12:15–12:30 hrs

Development of a lab-on-a-chip system with integrated sensors for 3D tissue engineering Pg.146
 applications
Haseena Bashir Muhammad, Chiara Canali, Soumyaranjan Mohanty, Mette Hemmingsen, Maciej Skolimowski, Martin Dufva, Anders Wolff and Jenny Emnéus

Session	C13: Biomimetics Musculoskeletal Mechanics
Date/Time	7 December 2013 / 11:00–11:45 hrs
Venue	SR-05 & 06
Chair(s)	Chen-Hua Yeow

C13: 1 / 11:00–11:15 hrs

Gender differences in motion mimicry of simple tasks Pg. 146
Edwin Boon-Wee Neo, Jin-Huat Low, R. Gokula Krishnan, Luis Carlos Hernandez Barraza and Chen-Hua Yeow

C13: 2 / 11:15–11:30 hrs

Observation of filling process in injection molding for fabrication of bone biomodel Pg. 147
Masashi Ohtake, Kei Ozawa and Makoto Ohta

C13: 3 / 11:30–11:45 hrs

Accurate modelling of finger kinematics using a statistically-reduced rigid body model Pg. 147
Kumar Mithraratne and Tim Wu

Session C12: Molecular Biomechanics | Tissue Mechanics

Date/Time 6 December 2013 / 11:00–12:30 hrs

Venue SR-07 & 08

Chair(s) Olga Sourina and Masahiro Todoh

C12: 1 / 11:00–11:15 hrs

Visual haptic-based collaborative molecular docking Pg. 147
Xiyuan Hou, Olga Sourina and Stanislav Klimenko

C12: 2 / 11:15–11:30 hrs

Langevin dynamics simulation of single-stranded dna transvenue Pg. 148
through nanopore in external non-uniform electric field
Weixin Qian, Kentaro Doi and Satoyuki Kawano

C12: 3 / 11:30–11:45 hrs

Mechanical analysis of mineral and collagen phases in bone by raman spectroscopy Pg. 148
Masahiro Todoh and Shigeru Tadano

C12: 4 / 11:45–12:00 hrs.

Viscoelastic moduli of bovine cortical tissue measured by cantilever free vibrations of Pg. 148
mm-sized specimen
Yuelin Zhang, Satoshi Yamada, Masahiro Todoh and Shigeru Tadano

C12: 5 / 12:00–12:15 hrs

Assessment of tissue glycation on plantar tissue stiffness Pg. 149
Jee Chin Teoh and Taeyong Lee

C12: 6 / 12:15–12:30 hrs

Effects of the position of tongue on the sound generation of Sibilant/S/ Pg. 149
Tsukasa Yoshinaga, Kazunori Nozaki and Shigeo Wada

Session E5: Rehabilitation

Date/Time 7 December 2013 / 11:00–12:30 hrs

Venue SR-12

Chair(s) Johnny Chee and Masayuki Nambu

E5: 1 / 11:00–11:15 hrs

VASST: variable-speed sensing treadmill for gait retraining after stroke Pg. 150
Johnny Chee, Karen S.G. Chua, Wei Shin Yu, Wai Sing Ong,
Calvin C.M. Hoo, Pang Hung Lim and Wei Sheong Lim

E5: 2 / 11:15–11:30 hrs

Monitoring system for home rehabilitation using smart phone Pg. 150
Masayuki Nambu and Manabu Horiuchi

E5: 3 / 11:30–11:45 hrs

Finger and thumb rehabilitation device for stroke patients Pg. 150
Fook Rhu Ong and Boon Tat Yu

E5: 4 / 11:45–12:00 hrs

Supine gait training device for stroke rehabilitation – design of a compliant ankle orthosis Pg. 151

Fang Ming Lim, Ruyi Foong, Kay Sin Goh, Qinglin Mok, Beng Hao Tan, Soon Leng Toh and Haoyong Yu

E5: 5 / 12:00–12:15 hrs

Performance evaluation of novel ankle-foot assist device for ankle-foot rehabilitation Pg. 151

Takayuki Onodera, Ming Ding, Hiroshi Takemura and Hiroshi Mizoguchi

E5: 6 / 12:15–12:30 hrs

Prospects of mechanomyography (MMG) in muscle function assessment during FES evoked contraction: a review Pg. 152

Morufu Olusola Ibitoye, Nur Azah Hamzaid and Ahmad Khairi Abdul Wahab

12:30–13:00 **Closing & Awards Presentation @ SR-12**

End of Conference

Abstracts

Day 1 – Wednesday, 4 December 2013

Session	PL1: Plenary Lecture 1
Date/Time	4 December 2013 / 10:30–11:15 hrs
Venue	Auditorium

ID: 147 **PL1**

Biomaterials for tissue engineering

Antonios G. Mikos and F. Kurtis Kasper

Rice University, Houston, Texas, USA.

Biomaterial-based strategies for tissue engineering span a vast spectrum from the production of scaffolds tailored with appropriate mechanical properties and degradation kinetics to serve transiently as a bridge to tissue formation to the leverage of biomaterials for the controlled delivery of biological signals to regenerate tissue in specific sites in the body. For example, our laboratory has developed a variety of biodegradable polymers for the controlled delivery of bioactive agents and/or progenitor cell populations to promote regeneration of tissues such as bone and cartilage. We have also applied engineered culture of cell populations on three-dimensional scaffolds toward the development of biologically active hybrid scaffold/extracellular matrix constructs for regenerative medicine applications as well as testing of anticancer drugs. This talk will present recent examples of biomaterial-based approaches for the development of tissue engineering technologies to meet clinical needs.

Session	SYM-01: Musculoskeletal Tissue Engineering
Date/Time	4 December 2013 / 11:15–12:45 hrs
Venue	Auditorium

ID: 149 **SYM-01: 1**

Symposium Keynote: Leveraging biomaterials in translational strategies for craniofacial bone repair

Antonios G. Mikos¹, Mark E. Wong² and F. Kurtis Kasper¹

¹*Rice University, Houston, Texas, United States of America;*

²*University of Texas Health Science Center at Houston, Houston, Texas, United States of America.*

Craniofacial bone defects arising from trauma or the resection of tumors present an enormous clinical burden, given the important aesthetic and functional role of the craniofacial complex. In certain cases, immediate repair of the bone after injury or tumor resection

may not be indicated, as overlying and surrounding tissues may be compromised, necessitating a staged approach to optimize the wound site prior to a definitive repair. Consequently, a significant need exists for the development and rapid translation of novel regenerative medicine approaches for the regeneration of both soft and hard tissues to overcome the current clinical barriers to craniofacial reconstruction. The strategic leverage of existing biomaterial-based clinical products in regenerative medicine approaches may facilitate and expedite clinical translation of the associated strategies for craniofacial repair. Our laboratory has recently explored application of currently regulated non-degradable polymers for space maintenance and antibiotic release as part of an envisioned staged-strategy for craniofacial bone regeneration. This talk will present highlights of ongoing efforts to harness clinically available biomaterials as components of strategies to promote bone regeneration in an effort to accelerate clinical translation.

ID: 121 **SYM-01: 2**

Create vascularized and innervated tissue and organ from human ESC for wide applications

Tong Cao

National University of Singapore, Singapore.

Whilst simple therapies might evolve around the administration of small molecule drugs, delivery of autologous cells and replacement with prosthetics or transplants, complex diseases will more than likely require therapies to direct the regenerative and immune processes, and different vigorous cells derived from stem cells to repair and rebuild damaged tissues. As genuine pluripotent stem cells, human embryonic stem cells (ESC) serve as unlimited renewable source of genetically healthy cells potential to develop into all cell types of human body. Leading in the world, the US Congress, federal and local governments, investors and charities have been supporting 'promising' human ESC R&D through legislations, policies, guidelines and funds. US initiated the clinical trials of human ESC therapies for eye diseases and spinal cord injury since 2011.

In general, government authorities, academies, research institutes and the industries of health, drug, food, cosmetics, chemicals and environment are presently hindered by a lack of functional, healthy and standardized human platforms of cells, tissues and organs, and predominantly use costly live animal models in addition to the cells of low human relevance. Existing models of live animals or on immortalized cell lines of either animal or human

origin, often poorly reflect human physiology. Primary human cell cultures are difficult to procure in sufficient quantity and can be prone to much inter-batch variability, depending on the cell source. By contrast, self-renewable, genetically-healthy and single-sourced human embryonic stem cells (ESC) exhibit enhanced biological relevance and stable predictivity over its more expansive counterparts.

Besides various human ESC progenies, functional tissues with multiple cell lineages, unique vascularisation and innervation by autologous human ESC progenies are currently being explored. The human ESC progenies, functional tissues and organs will offer stable *in vitro* 'clinical' platforms of no-risk human test for the basic, translational studies and applications of all human health related sciences including fundamental study of health, ageing, disease, prevention, diagnosis, therapy and transplant; drug and med-tech R&D. Moreover, those standardized *in vitro* human live platforms of no-risk 'clinical' trial will be widely adopted in much more areas beyond medicine and pharmaceuticals. The major other applications will be the human function and safety evaluation of food; cosmetic; daily and general chemicals; organisms; nuclear, IT, communication, electromagnetic, radiating device and technique; environment (air, water, soil, daily living and working environment); other human-contact substance, products and techniques. The platforms of human ESC progenies, functional tissues and organs will be ethically and gradually used at reasonable and practical pace, non-clinically, pre-clinically and clinically in all human health related industries, academies and authorities.

ID: 499

SYM-01: 3

The roles of mechanics and matrix on teno-differentiation of stem cells

Xiao Chen, Zi Yin and [Hong-Wei Ouyang](#)

*Center for Stem Cell and Tissue Engineering,
School of Medicine, Zhejiang University.*

Tendons as vulnerable targets of sports injury possess poor self-repair capability. Stem cells represent a promising approach to tendon regeneration. But their teno-lineage differentiation strategy has yet to be defined. Besides of growth factors, mechanics and topography of matrix may play important roles on tendon lineage differentiation. Here, we report that force combined with the tendon-specific transcription factor scleraxis synergistically promoted commitment of hESCs to tenocyte for functional tissue regeneration. Force and scleraxis can independently induce tendon differentiation. However, force alone concomitantly activated osteogenesis, while scleraxis

alone was not sufficient to commit, but augment tendon differentiation. Scleraxis synergistically augmented the efficacy of force on teno-lineage differentiation and inhibited the osteo-lineage differentiation by antagonized BMP signaling cascade. On the other hand, tendon is a specific connective tissue composed of parallel collagen fibers. The effect of this tissue-specific matrix orientation on stem cell differentiation has been investigated. It was found that the expression of tendon-specific genes was significantly higher in hTSPCs growing on aligned nanofibers than those on randomly-oriented nanofibers in both normal and osteogenic media. In addition, alkaline phosphatase activity and alizarin red staining showed that the randomly-oriented fibrous scaffold induced osteogenesis, while the aligned scaffold hindered the process. Moreover, aligned cells expressed significantly higher levels of integrin alpha1, alpha5 and beta1 subunits, and myosin II B. In *in vivo* experiments, the aligned nanofibers induced the formation of spindle-shaped cells and tendon-like tissue. Taken together, The findings offered insights into understanding the roles of matrix, force, and transcription factors on tendon-lineage differentiation.

ID: 705

SYM-01: 4

Research strategies for optimisation of chondrogenesis for cartilage tissue engineering

[Eng Hin Lee](#)

NUS, Singapore.

It is well known that articular cartilage does not respond well to damage, often repairing with fibrocartilage at best. Orthopaedic surgeons have over the years used many different techniques to aid in or enhance the repair of damaged articular cartilage. These techniques have included drilling the subchondral bone, microfracture and transplanting autologous osteochondral cylinders (Mosaicplasty or OATS).

More recently, Brittberg *et al.* have reported on the use of autologous cultured chondrocyte implantation (ACI) to repair chondral defects, especially in the knee joint. Although the early clinical results have been promising, some reports have shown that the degeneration occurs over the long term.

The Stem Cell and Cartilage Group at the NUS Tissue Engineering Program (NUSTEP) have shown in small and large animal experiments, superior results using autologous mesenchymal stem cells (MSCs) derived from bone marrow. Controlled studies on articular cartilage healing comparing drilling, autologous chondrocyte and MSC transfers have shown that the repair tissue following MSC transfer

most closely resembles that of articular cartilage. Clinical trials comparing the use of chondrocytes (ACI) to MSCs for repair of chondral defects have shown some advantage to using MSCs in older patients.

The current challenge is to develop strategies to optimize chondrogenesis to produce the correct cartilage phenotype which has all the characteristics of native cartilage. Our group has been looking at various aspects of enhancing chondrogenesis which includes genetic, biochemical and biomechanical cues that will optimize the formation of cartilage with the typical zonal properties of the cells and the matrix components as well as the appropriate mechanical strength. Examples of these research strategies will be presented and discussed.

ID: 750

SYM-01: 5

Application of tissue engineering in spinal surgery

Hee Kit Wong

National University of Singapore, Singapore.

Back pain and spinal cord injury are two conditions that increase the health care burden significantly. Conventional treatment modalities including surgical intervention have often failed to produce satisfactory outcomes. Tissue engineering is aimed at regenerating new tissue with cells, growth factors and scaffolds. Intervertebral disc, bone fusion and spinal cord tissue engineering are being investigated in the treatment of spinal conditions.

The challenge for intervertebral disc engineering and regeneration is insufficient knowledge about disc biology and pathophysiological mechanisms responsible for intervertebral disc degeneration (IDD). Spinal fusion using bone grafts continues to be the “gold standard” treatment for back pain and IDD. In bone tissue engineering, osteobiologics such as BMP-2 have been developed to augment spinal fusion. However these new bioactive molecules could potentially induce significant adverse events like excessive swelling and bone resorption. Spinal cord tissue engineering is another big challenge as neural tissue exhibits little regenerative capacity and sparse functional recovery after injury. The combination of neurotrophin delivery, cell transplantation, and nano-structured biomaterial are being studied for their roles in spinal cord repair.

Our research focuses on developing safe and efficient delivery systems for growth factors for spinal fusion. One of the carriers is polyelectrolyte complex (PEC), which attaches BMP-2 by heparin binding and was shown to be capable of delivering the growth factor in a controlled manner. Efficient bone regeneration with reduced adverse events was observed

when very much lower but effective doses of BMP-2 were delivered by this new carrier in an *in-vivo* animal model. Another carrier – a “yolk shell”-like structure encapsulates BMP-2 into the core of nanoparticles and could also potentially increase the delivery efficiency. The delivery of novel non-BMP derived growth factors like NELL-1, and the combination with stem cells are two promising technologies for future application.

Session	A1: Medical Imaging
Date/Time	4 December 2013 11:15–12:45 hrs
Venue	SR-01 & 02

ID: 890

A1: 1

Conference Keynote: Biomedical imaging – MRI visualization of living biological systems

Ed X. Wu

University of Hong Kong, Hong Kong S.A.R., China.

With advances in engineering and computing, an extraordinary body of imaging technologies and applications has developed over the last 35 years. One of the most important applications of such technologies is study of anatomy, physiology, pathology and functions in humans and animal models of human development and diseases. Among the various *in vivo* and non-invasive imaging modalities available or under development today, magnetic resonance imaging (MRI) is the most powerful and versatile technology platform. Its unparalleled *in vivo* and quantitative capabilities offer a broad range of applications covering from noninvasive morphologic measurements, tissue microstructural characterization, hemodynamic and vascular characterization, metabolite measurements, sub-system physiologies, brain functions to monitoring of cell migrational dynamics. This presentation will illustrate these technological developments with some of the ongoing rodent brain MRI projects in my laboratory, highlighting the capacity of MRI as a platform technology to visualize biological systems *in vivo* from molecules to systems levels. They include diffusion characterization of tissue microstructure; functional imaging; monitoring of endogenous neural stem cell activities; and novel contrast agents for brain imaging.

ID: 859

A1: 2

Exploring image gradients for nuclear cataract grading

Ruchir Srivastava¹, Xinting Gao¹, Fengshou Yin¹,
Damon Wong¹, Jiang Liu¹, Carol Y. Cheung² and Tien Y. Wong²

¹Institute for Infocomm Research, Singapore; ²Singapore Eye Research Institute, Singapore.

Nuclear Cataract (NC) is the most common type of cataract and can be automatically diagnosed from slit-lamp images of the eye lens. The diagnosis can be based on two cues, 1. brightness and color of the lens, which has been used by most of the researchers and 2. visibility of parts of the lens, which has not been explored much. The main contribution of this paper is in utilizing gray level intensity gradient based features for computerized grading of NC. The idea behind the proposed system, called ACASIA-NC, is that clear visibility of landmarks in a healthy eye leads to distinct edges in the lens region. While for advanced stages of NC, the edges in this region fade, since the landmarks are vaguely visible. To capture edge information in the lens region, features related to grayscale image gradient have been extracted. Experiments performed on a large dataset of over 5000 slit lamp images show that the proposed features outperforms state-of-the-art in automatic NC grading, both in terms of speed and accuracy.

ID: 752

A1: 3

Method for determining thickness of the tongue coating by using color histogram of a tongue image

Chang Jin Jung, [Keun Ho Kim](#) and Jaeuk U. Kim

Korea Institute of Oriental Medicine, South Korea.

Color and shape features of a tongue reflect the condition of the body in traditional East Asia medicine (TEAM). In particular, the thickness of the tongue coating (TTC) is an important feature for tongue diagnosis. In this study, we proposed a feature extraction method for determining the TTC, which accords with the TEAM diagnostic method. Seventy eight tongue images were acquired by using a computerized tongue diagnosis system, and its color were linearly corrected base on CIE L*a*b* values with a color checker with 12 color samples. Subjects were classified into thin coating group (n=50) and thick coating group (n=28) by two TEAM doctors. A tongue area was segmented from an acquired image and divided into three regions along the vertical direction. In order to estimate thickness of the tongue, 2D histogram was calculated for each divided region, based on the CIE L* and a* values, and its values were normalized. Among the variables of the three 2D histograms, the valid variables, which

were significantly different between the thin and the thick coating groups, formed a color distribution matrix (CDM). Using CDM, the thick tongue coating was classified by a support vector machine and its accuracy was over 80%. It is expected to provide a quantitative standard for the tongue coating diagnosis.

ID: 767

A1: 4

A modified synthetic aperture focusing technique using beam characteristics of transducer for ultrasound image improvement

Chia-Che Ho, Yi-Hsun Lin and [Shyh-Hau Wang](#)

National Cheng Kung University, Taiwan.

The synthetic aperture focusing technique (SAFT) has been proposed to improve the lateral resolution of ultrasound image outside the focal region of the transducer. Yet, SAFT would result an unexpected artifact image at the region near the focal point of the transducer due to the use of a virtual source concept associated with limited numbers of scan lines. The artifact could be eliminated by using an appropriate time gain compensation (TGC), which however is subjective to users' settings. To further improve this issue, the present study incorporated the transducer's depth-dependency beam characteristics into SAFT-based imaging procedure. The imaging process was implemented on a graphic processing unit (GPU) platform for improving the computational efficiency.

Ultrasound images were acquired from a commercial phantom with various contrast regions using a 3.5 MHz single element transducer. The -20dB beam width of transducer as a function of axial depth were measured for better estimating the time delay of each scanning point. Two scanning intervals, 50 and 200 μm , were acquired for B-mode imaging. Subsequently, the linear interpolation was performed for correcting the error associated with the time delay estimator for the image at the focus region.

Results demonstrated that SAFT-based images implemented with virtual source correction corresponding to scanning intervals of 50 and 200 μm both displayed darker regions near the depth of 23 mm. The SAFT-based images modified with the correction of -20dB beam width of the transducer may not only improve the artifact region but also better restore the shape and contrast regions in the deeper regions of phantom. In additional, the computational efficiency is verified able to be greatly improved by the implementation with GPU platform. These results verify that current modified SAFT-based imaging may greatly enhance ultrasound image quality and be

feasible to be further applied to three-dimensional imaging.

ID: 465

A1: 5

Super resolution reconstructed 4D magnetic resonance imaging for lung cancer radiotherapy

Eric Van Reeth¹, Cher Heng Tan², Ivan W. K. Tham³ and Chueh Loo Poh¹

¹Nanyang Technological University, Singapore; ²Tan Tock Seng, Singapore; ³National University Hospital, Singapore.

Lung cancer is the leading cause of cancer-related death in men and women. High precision radiotherapy is a standard treatment for lung tumours. In radiotherapy of lung cancer patients, a major challenge to overcome is the motion of lung tumours. If the motion of the tumour can be accurately visualized and quantified, higher radiation dose could potentially be applied to the target volume while causing only minimal damage to the surrounding normal tissue. 4D (3D + time) CT is currently the standard imaging modality to assess the tumor motion during treatment planning. 4D magnetic resonance imaging because of its excellent soft tissue contrast and being free the use of ionizing radiation is an attractive alternative to 4D CT. It has been shown that fast acquisition of 3D MRI volumes over time of the thoracic region is possible. However, this is achieved at lower spatial resolution. In this presentation, we will present our recent work on improving the resolution of 4D MRI for imaging lung tumor motion through the use of a new super-resolution (SR) framework, achieving isotropic MR volumes from anisotropic volumes. Because long acquisition time is required to achieve the isotropic resolution that we have reconstructed using SR, it is currently practically impossible to acquire such resolution as the motion of the organs will blurred the images during the scan. We have performed both a phantom study and a patient study. We compared the SR reconstructed MRI images with the standard 4D CT. Our results show that the SR reconstructed images have improved sharpness, contrast and anatomical structure visualization. Quantitative evaluation also shows improved delineation of the tumor using the SR reconstructed images.

Session	B1: Regenerative Medicine
Date/Time	4 December 2013 11:15–12:45 hrs
Venue	SR-03 & 04

ID: 138

B1: 1

Conference Keynote: Nestin-expressing multipotent hair follicle stem cells for regenerative medicine

Robert M. Hoffman^{1,2}

¹AntiCancer Inc., San Diego, CA, United States of America;

²University of California, San Diego, United States of America.

Nestin-expressing hair follicle stem cells of the mouse can differentiate into neurons, glia, keratinocytes, smooth muscle cells and melanocytes *in vitro*. Nestin-expressing hair follicle stem cells enhanced the rate of nerve regeneration and the restoration of nerve function in mouse models. The nestin-expressing hair follicle stem cells transdifferentiate largely into Schwann cells when implanted in severed nerves or injured spinal cord, which may enhance neuron regrowth. The bulge area (BA) of the follicle is the source of the nestin-expressing stem cells of the hair follicle which migrate from the BA to the dermal papilla (DP) as well as into the surrounding skin tissues during wound healing. Nestin-expressing stem cells can also be readily isolated from the human scalp, thereby providing an accessible, autologous and safe source of stem cells for potential clinical use.

ID: 327

B1: 2

Directing adult human periodontal ligament-derived stem cells to retinal fate

Gary Yam¹, Li Huang², Herman S. Cheung³ and Jodhbir S. Mehta¹

¹Singapore Eye Research Institute, Singapore; ²Department of Ophthalmology & Visual Sciences, Chinese University of Hong Kong, Hong Kong; ³Department of Biomedical Engineering, University of Miami, FL, USA.

Neural crest-derived stem cells are known to reside in the postnatal periodontal ligament (PDL) in teeth. They express various markers of embryonic, neural crest and mesenchymal stem cells, and are capable to differentiate into multiple lineages. Our group investigated the retinal fate competence of human adult PDL-derived stem cells (PDLSC) through a directed differentiation mimicking mammalian retinogenesis. Human PDL tissue of the third molar was collected from healthy subjects under 35 years old and primary PDLSC were isolated by collagenase digestion. All our 25 primary cultures consistently expressed markers of neural crest cells

(including nestin, Slug, Snail1), mesenchymal stem cells (CD44, CD90) and embryonic stem cells (c-Myc, Klf4, SSEA4) by immunofluorescence and RNA analyses. To imitate retinogenesis *in vitro*, PDLSC at passage 3 were cultivated in induction media containing Noggin and Dkk-1 (antagonists of bone morphogenic protein and Wnt/b-catenin signaling, respectively). Under low attachment culture, PDLSC generated neurospheres expressing markers of neural progenitors. When plated on matrigel-coated surface, the neurospheres displayed rosette-like outgrowth. They expressed eye field transcription factors and 94% cells were Pax6^{nuclear}Rx⁺, indicative of retinal progenitors. At prolonged induction, they expressed photoreceptor markers (Nrl, rhodopsin and its kinase) and showed significant responsiveness to excitatory glutamate by fluo-4-acetoxymethyl calcium imaging assay. In conclusion, we showed that primary human PDLSC could be directed to retinal progenitors with a competence of photoreceptor differentiation. Since human neural crest-derived PDL is readily accessible, it can be an autologous and expandable source of undifferentiated cells for retinal cell regeneration.

ID: 246

B1: 3

Improvement of osteochondral repair by bi-layer electrospun nanofiber scaffold

Shufang Zhang, Longkun Chen, Yangzi Jiang, Youzhi Cai, Tong Tong, Junfeng Ji and Hong Wei Ouyang

Center for Stem Cell and Tissue Engineering,
School of Medicine, Zhejiang University, China.

An optimal scaffold is crucial for osteochondral regeneration. Collagen has been widely used for cartilage and electrospun nanofiber has shown promising for promoting osteo-lineage differentiation. This study aims to synergistically combine the advantages of collagen and electrospun nanofibers for osteochondral regeneration. We first fabricated bi-layer microporous scaffold (COL-PLA) with collagen and electrospun poly-L-lactic acid nanofibers. Mesenchymal stem cells were cultured on the bi-layer scaffold and investigated for cell adhesion, proliferation and differentiation. Moreover, osteochondral defects were created in rabbits and implanted with COL-nanofiber scaffold, cartilage and subchondral bone regeneration were evaluated at 6 and 12 weeks after surgery. Compared with COL scaffold, cells on COL-nanofiber scaffold exhibited more apparent osteogenic differentiation indicated by higher expression level of OCN and Runx2 genes as well as accumulation of calcium nodules. Subchondral bone formed more rapidly and intact, which resulted in better cartilage formation in osteochondral defects of rabbits treated with

COL-nanofiber scaffold. The results were consistent with biomechanical test and μ CT data. These findings indicate that the bi-layer microporous COL-nanofiber scaffold would be promising for the treatment of deep osteochondral defect.

ID: 182

B1: 4

Effect of biphasic calcium phosphate treated with vascular endothelial growth factor on osteogenesis and angiogenesis gene expression *in vitro*

Hamid Enezei¹, Azlina Ahmad¹, Mohd Khamis¹, Roselinda Rahman¹, Noor Hayati Abdul Razak¹, Mutum Singh² and Rani Shamsuddin³

¹School of Dental Sciences, Universiti Sains Malaysia, Health Campus, Kubang Kerian, Kelantan, Malaysia; ²School of Medical Sciences, Universiti Sains Malaysia, Health Campus, Kubang Kerian, Kelantan, Malaysia; ³College of Dentistry, University of Sharjah, Sharjah, United Arab Emirates.

Biodegradable biphasic calcium phosphate (BCP) scaffold holds tremendous potential for bone tissue engineering. It elicits response from cells such as endothelial cells (ECs) that are similar to those elicited by bone. ECs promote bone regeneration by stimulating both neovascularisation and osteogenesis. For an effective coupling of angiogenesis and osteogenesis, vascular endothelial growth factor (VEGF) is required. The aim of this work is to study the effectiveness of VEGF-added-BCP on the expression of osteogenesis and angiogenesis genes in ECs. Commercially obtained rat aortic ECs were cultured in the endothelial-cell growth medium. The cells were treated with three different modalities: BCP-only, VEGF-only, and VEGF-added-BCP. The optimal BCP and VEGF concentrations were determined. The cells were harvested at four different time intervals (day 3, day 7, day 10 and day 14) and were subjected to RNA isolation using RNA extraction kit (*analytik-jena*, Germany). This was followed by performing reverse transcriptase-PCR (RT-PCR) (Qiagen, Germany) to amplify the osteogenesis and angiogenesis-regulated genes. The RT-PCR products were then electrophoresed. The gel image was captured using Image Analyser. Suitable concentration of BCP was 10mg/ml while optimal VEGF was 15ng/ml. Angiogenesis and osteogenesis genes were clearly expressed in ECs in response to treatments. Angiogenesis gene (VEGF) was highly expressed by VEGF-only treatment but showed some changes with added BCP. Osteogenesis genes (BMP-2, ALP, OC and OPN) were shown to be positively affected by both BCP and VEGF. Some genes were expressed at an earlier time interval compared to the other genes depending on the type of treatments. BCP-only treatment induced high expression of early regulating

osteogenesis genes (BMP-2 and OPN). Mineralized gene markers (ALP and OC) were however, highly expressed with VEGF-added-BCP treatment. Combination of BCP and VEGF modality on ECs was suggested to initiate osteogenesis and angiogenesis related gene expressions earlier than the other modalities.

ID: 145

B1: 5

Induction of functional tenocyte-like cells from mesenchymal stem cells by Mohawk

Huanhuan Liu, Can Zhang, Shouan Zhu, Ping Lu, Ting Zhu, Xiao Chen and Hongwei Ouyang

Center for Stem Cell and Tissue Engineering, School of Medicine, Zhejiang University, Hangzhou, China.

Introduction: Tendons connect muscles to bone and transmit the force generated during muscle contraction to the skeleton, which are highly prone to injury. Surgical repair is common but often unsuccessful. Mohawk (Mkx) has been found as an essential transcription factor for tendon development. Here, this study illustrated whether the functional tenocyte-like cells will be induced by ectopic expression Mkx in mesenchymal stem cells (MSCs) for tendon regeneration and investigated the underlying mechanism *in vitro* and *in vivo*.

Results and Discussion: Subsequent to Mkx transduction, MSCs became smaller and thinner and had significantly reduced proliferation and clonogenicity, indicating the activation of the differentiation of MSCs. On one hand, the ability of MSC-Mkx toward osteoblasts and adipogenic differentiation were remarkably decreased. On the other hand, several tenogenic genes, especially collagen type I, scleraxis and tenascin C, were significantly up-regulated in MSC-Mkx cells. Importantly, the collagen fibril diameter of MSC-Mkx cell-sheet was obviously increased. These findings illustrated that MSC differentiated into tenocyte-like cells *in vitro* by ectopic expression Mkx. Furthermore, co-immunoprecipitation assay showed that there was a physical association of Mkx with Scx, suggesting an interaction of these two crucial transcription factors in tendon development and regeneration. In Achilles tendon defect model, the repaired tendon tissues of MSC-Mkx group showed more parallel alignment of tendon fibers and larger average collagen fibril diameter after 2 and 4 weeks implantation. Moreover, the mechanical properties of MSC-Mkx group were increased than control group.

Conclusion: The ectopic expression of Mkx remarkably reduced the osteogenesis and adipogenesis of MSCs, but to the contrary, it induced the tenogenesis

of MSCs and generated the functional tenocyte-like cells *in vivo* and *in vitro*, which provided an alternative way for restore suitable cells for tendon regeneration.

Acknowledgment: This work was supported by the National Natural Science Foundation of China (J20120101, J20110127).

Session	C1: Cardiovascular Mechanics
Date/Time	4 December 2013 11:15–12:45 hrs
Venue	SR-05 & 06

ID: 480

C1: 1

Heterogeneity in the intramural mechanical environment of the aorta: Estimation of stress applied to elastic laminae in a physiological state

Takeo Matsumoto, Yohei Uno and Kazuaki Nagayama

Nagoya Institute of Technology, Japan.

The media of elastic arteries has a concentric structure of elastic laminae (ELs). The ELs are corrugated in an unloaded state and become straight over physiological pressure range. The corrugation has a wide spatial variation. This may indicate that tension applied *in vivo* to the ELs is not uniform, but varies depending on their corrugation. To examine this hypothesis, we obtained 14- μ m-thick sections of porcine thoracic aortas perpendicular to the longitudinal direction, and stretched them circumferentially with a laboratory-made tensile tester to observe their microscopic deformation. Characteristic points on the ELs were identified under a transmitted light microscope and used as markers for their deformation. Corrugation of the ELs was evaluated with a waviness W , length of the EL along its corrugation divided by its straight length. Microscopic strain was highly heterogeneous: stretch ratio in the ELs was 1.1–2.3 at circumferential stretch ratio of 1.5. The waviness of the ELs varied widely, ranging from 1.00 to 1.35, and decreased with macroscopic stretch. Detailed observation revealed that the length of the ELs did not increase until they became almost straight, indicating that lower *in vivo* tension in the ELs with higher waviness, and was estimated to be in the range of 240–400 kPa. To check local heterogeneity in tension, the slices were then stretched by 35% and the ELs were cut by UV laser to measure the gap generated by the ablation. The gap had a significant negative correlation with the waviness. These results indicate that the microscopic mechanical environment in the artery wall is highly heterogeneous. The reason for this heterogeneity remains unclear at this stage. This may be caused by local activities of the

smooth muscle cells such as wall remodeling and cell division. Microscopic viewpoint is important to reveal the mechanism of the adaptation and remodeling of arteries.

ID: 670

C1: 2

Quantitative endothelial cell response to wall shear stress in an experimental cell-structure interaction model simulating stented coronary artery

Nii Armah Armah and Chuh Khiun Chong

The Kroto Research Institute, Department of Materials Science and Engineering, The University of Sheffield, United Kingdom.

Introduction: In-stent restenosis (ISR) remains an issue in coronary stenting procedure. Many studies use computational fluid dynamics (CFD) to predict how wall shear stress (WSS) may cause ISR. It is recognised that an experimental cell-structure interaction model would be useful in understanding how endothelial cells (ECs) in the stented region respond to the local haemodynamics and hence provides an insight on the onset/progression of ISR. The aim of this study is to establish an experimental 2D-model simulating stented coronary artery and quantify the response of ECs subjected to WSS predicted by CFD.

Methods: Computer-aided Design (CAD) was used to create the model and CFD was employed to assess the WSS under steady Newtonian flow. The CAD model was then fabricated and cultured with human umbilical vein ECs (HUVECs) to establish the 2D-experimental model and subjected to a steady flow for 24 hours (177.8 ml/min, 5% CO₂, 37°C) in our custom-designed flow-bioreactor system. HUVECs were stained, observed for migration, quantified for elongation and alignment, and mapped onto the WSS distribution. Static culture acted as a control.

Results: HUVECs migration to stent-struts was observed under the flow experiment. In the inter-strut regions where the flow had partially recovered (WSS ~ 1.5Pa), most cells were elongated with 30% aligned in the direction of flow. In the immediate regions of the struts (WSS ~ 0.3Pa), cells were less elongated and only 7% aligned to the flow direction. In the regions before the first and after the last strut (WSS ~ 2.7Pa), cells appeared mostly elongated with 67% aligned to the flow. Under static culture, cells showed no apparent orientation in all regions.

Summary: We have established a novel 2D-experimental cell-structure interaction model and demonstrated clear differential response of HUVECs to WSS distribution. It is not however clear if HUVECs would response similarly under physiological flow.

ID: 622

C1: 3

Influence of increasing oversizing and aortic neck angulation on the proximal fixation of thoracic stent-grafts

Chen Hsien Chiang¹, Ming-Long Yeh¹, Wei-Ling Chen¹ and Chung-Dann Kan²

¹*Institute of Biomedical Engineering, National Cheng Kung University, Tainan, Taiwan;* ²*Division of Cardiovascular Surgery, Department of Surgery, National Cheng Kung University Hospital, Tainan, Taiwan.*

Severe angulation and the friction fixation force developed by the stent graft design at the proximal neck are still recognized as important factors affecting for the late results of the endovascular aneurysm repair (EVAR) therapy. Severe angulation would change the sealing and attachment force between stent grafts and aortic wall in the proximal neck-landing site.

In order to have better understood for the influence of neck angulation of endovascular stent graft implantation, neck angulation condition, graft oversizing percentage, and dislodgement force were studied using two present commercial thoracic aortic aneurysm stent grafts. The *in-vitro* simulation experiment was to deploy stent grafts into designed angulated silicone aortic-neck simulating tubes in a temperature-controlled chamber. The studies of the characteristics of stent deployment were achieved via recorded video and then determined by the dislodgement force using mechanical pullout testing.

From the results of the experiment disclosed that the two commercial stent grafts (Cook Zenith TX2 and Medtronic Valiant), both stent grafts' dislodgement forces were decreased at 45 and 90 degree angulation compared to 0 degree for most of the oversizing conditions simulated. Our computed tomography images showed that stent became partly contact with the inner surface in the 90 degree simulating tube. Compared the specific stent graft performance, Valiant stent graft showed with higher dislodgement force than Cook stent graft in all angulation conditions. This might be slightly due to the higher radial force exerted from the Valiant stent graft.

Our *in-vitro* study has shown that neck angulation and stent graft oversizing really influence stent graft's proximal fixation force. Sufficient proximal fixation might improve the *in-situ* stent graft stability from stent graft migration and therefore lower the incidence of endoleak. Carefully inspect the angulation of landing zone of stent graft and calculate the oversizing ratio are really important for EVAR surgery.

ID: 244

C1: 4

Effect of wall elasticity on high and low wall shear stresses in human coronary arteries

Ashkan Javadzadegan¹, Houman Tamaddon¹, Mehrdad Behnia² and Masud Behnia¹

¹The University of Sydney, Australia; ²Georgia Health Sciences University, Georgia, USA.

High and low wall shear stresses are associated with distinct pathogenic biological pathways relevant to thrombosis and atherogenesis. It has been shown that low wall shear stress (WSS) promotes plaque development whereas high WSS is associated with plaque destabilization. The impact of wall elasticity on determining high WSS and area of low WSS regions in human coronary arteries in vivo is unclear. Computational fluid dynamics (CFD) simulations were performed on rigid and elastic three-dimensional reconstructions (3DRs) of coronary arteriograms of 25 patients. Boundary conditions for 3DR simulations were obtained by direct measurements using a pressure-temperature sensor guidewire. The results showed that rigid wall assumption overestimates the magnitude of high WSS and area of low WSS regions. For the coronary artery with %44 stenosis severity, the difference between rigid and elastic high and low WSS is %5.1 and %12, respectively; however, for the artery with %76 stenosis severity, the difference is %12 and %22. Therefore, the effect of vessel wall elasticity on hemodynamic of coronary arteries with severe stenosis is more than that of the coronary arteries with mild stenosis.

ID: 184

C1: 5

Numerical investigation of blood flow behaviour in different orders of vascular system

Houman Tamaddon¹, Ashkan Javadzadegan¹, Mehrdad Behnia² and Masud Behnia¹

¹The University of Sydney, Australia; ²Georgia Health Sciences University, Georgia, USA.

Study of the blood flow behaviour plays an important role to identify relationships between the flow patterns and the diseases that form in the vascular system. Nowadays the computational simulation is one of the most powerful tools in this area. It is evident from the in-vivo research works that the behaviour of blood flow through vessels is dependent on the diameter of the vessel. In this study, to investigate the dependency of blood flow behaviour on the vessel diameter, computational fluid dynamics (CFD) analysis has been performed to simulate three dimensional blood flow through different orders of blood vessels. Pulmonary vascular network – which

consists of wide range of vessel orders, from main pulmonary artery to the capillaries- is selected as the reference network. Geometry of vessels is reconstructed based on available data from morphometry of pulmonary vasculature. The standard k-ε turbulent model is applied because of its capability in predicting the laminar flow as well as turbulent flow with acceptable accuracy. The results for solid and elastic boundary conditions have been compared for different vessel orders in order to get better comprehension how the elastic nature of vessel wall can affect the important parameters of the flow such as blood pressure, velocity and wall shear stress. According to the literature, the blood flow behaviour in regions with shear strain rates lower than 100 (s⁻¹) is non-Newtonian. In this regard, non-Newtonian Generalised Power Law model is used to capture wall shear stress behaviour within the regions. Results show that the non-Newtonian behaviour of the blood affects flow characteristics in some vessel orders. According to the results, the general behaviour of blood flow based on Newtonian and non-Newtonian assumptions have been compared. Finally, based on the CFD results for different vessel orders, acceptable assumptions for blood flow simulation in different orders have been investigated.

Session	D1: Biomedical Devices and Biomedical Instrumentation
Date/Time	4 December 2013 11:15–12:45 hrs
Venue	SR-07 & 08

ID: 709

D1: 1

Conference Keynote: Electrochemistry and nanotechnology in biomicrosystems for point of care applications

I-Ming Hsing

Division of Biomedical Engineering and Department of Chemical and Biomolecular Engineering, Hong Kong University of Science and Technology, Hong Kong, China.

Sensing technologies in point of care testing (POCT) need to meet criteria of simple operation, compatibility for device miniaturization and cost affordability of instrument and reagent kits. Among the prospective candidate technologies, electrochemistry- and micro/nano particles-based detection methods offer promising characteristics that could rival the dominant fluorescence/optics-based counterparts. Over the years, my laboratory has developed a number of sensitive detection strategies targeting both nucleic acids and proteins, two of the most important biomolecules that provide meaningful information for diagnostics. In this talk, I will present a few electrochemistry-based

methods [1–3] and signal- amplification strategies [4–5] (e.g., utilizing polymerase and exonuclease) that could address some of the inherent deficiencies in electrochemical sensing approaches (e.g., low species specificity and high background noise). In addition, our strategies using functionalized gold nanoparticles for diagnostic applications would also be introduced.

References

- [1] Stephen S.W. Yeung, Thomas M.H. Lee, I-Ming Hsing, "Electrochemical Real-Time Polymerase Chain Reaction", *J. Am. Chem. Soc.*, 2006 **128** 13374–13375
- [2] Xiaoteng Luo, Thomas M.H. Lee, I-Ming Hsing, "Immobilization-Free Sequence-Specific Electro-chemical Detection of DNA Using Ferrocene-Labeled Peptide Nucleic Acid", *Anal. Chem.*, 2008, **80** 7341–7346
- [3] Xiaoteng Luo, Feng Xuan, I-Ming Hsing, "Real Time Electrochemical Monitoring of PCR Amplicons Using Electroactive Hydrolysis Probe", *Electrochem. Commun.*, 2011 **13** 742–745
- [4] Feng Xuan, Xiaoteng Luo, I-Ming Hsing, "Sensitive Immobilization-free Electrochemical DNA Sensor Based on Isothermal Circular Strand Displacement Polymerization Reaction", *Biosen. Bioelectron.*, 2012 **35** 230–234
- [5] Feng Xuan, Xiaoteng Luo, I-Ming Hsing, "Ultrasensitive Solution-phase Electrochemical Molecular Beacon-based DNA Detection with Signal Amplification by Exonuclease III-assisted Target Recycling", *Anal. Chem.*, 2012, **84** 5216–5220.

ID: 320

D1: 2

A bioimpedance-based sensing system for monitoring cellular dynamics in a 3D culture environment

Chiara Canali¹, Haseena Bashir Muhammad¹, Martin Dufva¹, Anders Wolff¹, Ørjan Grøttem Martinsen^{2,3}, Arto Heiskanen¹ and Jenny Emnéus¹

¹Department of Micro- and Nano-technology, Technical University of Denmark, Kgs Lyngby, Denmark; ²Department of Physics, University of Oslo, Oslo, Norway; ³Department of Biomedical and Clinical Engineering, Rikshospitalet, Oslo University Hospital, Oslo Norway.

There is currently an increasing interest in developing sensitive analytical methods for real-time monitoring of the entire process of tissue engineering, starting from a bare 3D polymer scaffold, to cell attachment, growth and differentiation, up to the formation of vascularised organ-on-a-chip systems.

Bioimpedance has shown to be a powerful tool for the study and modeling of biological systems both *in vivo* and *in vitro*, establishing a physical correlation between bioelectrical measurements and tissue growth characteristics.

In this work, a bioimpedance-based 3D culture Lab-On-A-Chip (LOC) system is presented which is designed and optimized to investigate cellular dynamics occurring under *in vitro* tissue growth conditions. The novelty of this device is to enable label-free monitoring of real cell dynamics in a more

physiological microenvironment mimicking the complex network of interactions taking place among cells and their matrix.

Since the important electrical characteristics of an electrode/tissue system are primarily determined by the electrode configuration, simplified finite element models were used to optimize electrode density and orientation within the 3D chip to enhance measurement sensitivity. Based on the simulation results, a prototype chip was developed with two opposite couples of vertical rectangular plate electrodes in a three-terminal configuration where current-carrying (CC) and pick-up (PU) electrodes could be switched between different positions to extend a positive sensitivity field to the whole bulk scaffold volume.

To demonstrate proof-of-concept, the bioimpedance-based LOC system was evaluated by growing different concentrations of mesenchymal stem cells embedded within a 3D gelatin scaffold. Preliminary results indicate that the presented device has a high potential for real-time monitoring of the entire process of tissue engineering without affecting cell viability.

Since different combinations of CC and PU electrodes can be exploited, this system will pave the way towards electrical impedance tomography applications enabling imaging of the changes occurring in 3D cell culture environments.

ID: 433

D1: 3

Diamond MEMS as new promising biochemical sensing transducers

Lionel Rousseau¹, Alexandre Bongrais², Emmanuel Scorsone², Gaëlle Lissorgues¹ and Philippe Bergonzo²

¹ESIEE-Paris, ESYCOM University Paris-EST, Cité Descartes BP99, 93162 Noisy le Grand Cedex; ²CEA LIST, Diamond Sensor Laboratory, 91191, Gif-sur-Yvette, France.

Diamond is a very promising material for future biochemical applications due to its outstanding physical and chemical properties. In particular, its remarkable mechanical features including a high Young modulus may be used advantageously for MEMS (Micro-Electro-Mechanical Systems) development. The mechanical properties of this material have never been combined to its chemical properties to develop resonating micro-cantilever MEMS-based biochemical transducers which should exhibit superior sensitivities. And the carbon terminated surface of diamond offers new options for covalent grafting of specific bio-receptors on its surface. In this study, we report on specific clean room compatible processes for diamond micro-structuring. The mechanical characterization of the cantilevers in oscillating regime was performed in order to extract the Young's

modulus E of different polycrystalline diamond structures. In the best process case, a value of E as high as 1100 GPa and very close to the Young's modulus of monocrystalline diamond (1200 GPa) was achieved. The cantilevers resonance frequency and Q -factor were on average twice higher than identical silicon structures. The measured quality factor varied from a few 100 to more than 1000 depending on the cantilever length, width and vibration mode. The maximum quality factor obtained was 1550.

This enables diamond cantilevers to be used in the dynamic regime in liquids with lower damping losses than when other conventional materials like silicon are used. Experiments on DNA grafting were then successfully explored.

Indeed, due to the carbon terminated surface of diamond, a novel one-step grafting technique. This technic consists to graft a function amine directly on diamond surface terminated hydrogen. A 24mer DNA was grafted on our diamond cantilevers.

A frequency shift of around 25 Hz was measured upon exposure to the complementary DNA. The diamond cantilevers response showed good agreement with the estimated sensitivity.

ID: 553

D1: 4

Surface-modified gold nanoparticles and porous monoliths for colorimetric immunosensing

Shao-Hsuan Chuag, Guan-Hua Chen, Yu-Chun Yen, Jun-You Chen and Chien-Fu Chen

Graduate Institute of Biomedical Engineering, National Chung Hsing University, Taichung 402, Taiwan.

Here we describe a sensitive and rapid immunoassay platform integrating polymerized monoliths and gold nanoparticles (AuNPs). The porous monoliths are photopolymerized *in situ* within a silica capillary and serve as solid supports for high mass transport and high density capture antibody immobilization to create a shorter diffusion length for antibody-antigen interactions, resulting in a rapid assay and low reagent consumption. AuNPs are modified with detection antibodies and are utilized as signals for colorimetric immunoassays without the need for enzyme, substrate, and sophisticated equipment for quantitative measurements.

Immunoassays such as enzyme-linked immunosorbent assay and nucleic acid sequence-based amplification are well-established biomolecular detection techniques that are used for drug discovery and disease diagnostics. However, the multiple incubation, washing and blocking steps that take hours to complete would limit the applications for real-time clinical diagnosis and subsequent

treatment. To increase the assay efficiency and decrease the analyte and reagent consumption, high surface-to-volume ratio materials, such as magnetic microbeads, polymer microbeads, hydrogels, porous monoliths and variety of nanomaterials were adopted to anchor larger amounts of primary antibodies. However, sophisticated laboratory infrastructure and well-trained operators are needed for the complicated fabrication processes and acquisition of assay results.

In this report, a new type of colorimetric immunoassay platform with improved temporal acquisition times and sensitivity has been demonstrated. Because the signal output is colorimetric, the assay can be performed with a desktop scanner, a smart phone or by visual inspection, thus eliminating the need for sophisticated optical equipment that is used in most conventional methods. Other colorimetric mechanisms using AuNPs for detection can also be used with this platform. The colorimetric assay mechanism can also be integrated with a microfluidic platform to provide efficient and multiplexed flow control coupled with a high sensitivity, high throughput, and low sample consumption point-of-care diagnostic system.

ID: 437

D1: 5

Diamond microelectrodes for electrochemical sensing in biofluids and record and stimulate neuronal tissue

Lionel Rousseau¹, Raphael Kiran², Myline Cottance¹, Sebastien Joucla³, Blaise Yvert³, Emmanuel Scorsone², Amel Bendali⁴, Gaëlle Lissorgues¹, Serge Picaud⁴ and Philippe Bergonzo²

¹ESIEE – ESYCOM University Paris Est, Cité Descartes, BP99, 93162 Noisy Le Grand, France.; ²CEA, LIST, Diamond Sensors Laboratory, CEA/Saclay, Gif-sur-Yvette, France; ³Université de Bordeaux, Institut des Neurosciences Cognitives et Intégratives d'Aquitaine (INICIA), UMR 5287, F-33000 Bordeaux, France ⁶Fondation Ophtalmologique Adolphe de Rothschild, Paris.; ⁴INSERM, U968, Institut de la Vision, Paris, F-75012, France.

Boron doped diamond (BDD) electrodes are extremely promising for the field of biomedical applications as they exhibit a unique combination of properties, namely: extremely wide potential window in aqueous electrolytes (>3V), corrosion stability in aggressive media, morphological and structural stability at very high current, low adsorption properties, low background current and bio-inertness.

We have developed a specific process enabling the fabrication of diamond electrodes BDD on 4 inches glass substrates as well as on pre-oxidized silicon wafers. To avoid tedious steps of RIE etching of the diamond layers, we have developed an original method. This process has been used to manufacture

strip electrodes and microelectrode array (MEA) for record and stimulating neuronal tissue.

When one tries to use such electrodes in very reactive media a biofouling affects all types of electrodes and prevents the accurate measurement of the concentration of the analytes in an electrochemical biosensor thus reducing their field of applications. On diamond however we have recently proposed a unique and simple electrochemical (EC) treatments that can be used to retrieve the loss of reactivity of the boron doped diamond (BDD) electrodes, thereby enhancing their reusability over long periods of measurements without degradation of the signal.

The technique does not require the use of a specific medium and thus can be directly performed in the probed fluid. For instance, we have successfully used it in urine, blood, milk, and red wine.

For neuronal applications, diamond planar MEAs of two matrix geometries, 8×8 and 4×15, designed for the stimulation and recording of respectively rat retina and mouse embryonic spinal cord have been fabricated. *In-vitro* electrical recordings of spontaneous activity of an embryonic mouse hind-brain-spinal cord and of a retina rat with our fabricated were successfully accomplished. Extracellular electrical neural stimulation using MEAs is the purpose of current development.

Session	E1: Assisted Technologies
Date/Time	4 December 2013 11:15–12:45 hrs
Venue	SR-12

ID: 751 **E1: 1**

**Conference Keynote:
Robots and the human**

Oussama Khatib

Stanford University, United States of America.

In the field of robotics, the motivation to emulate human movement has been driven by the desired to endow robots, humanoids in particular, with human-like movement properties. Understanding the fundamental characteristics of human motion is a challenging multifaceted problem that requires, in particular, the development of accurate models of the kinematics, dynamics, and actuation of human musculoskeletal systems. These models are essential for building full human motion simulation and for performing motion reconstruction from captured data, as well as for the analysis and characterization of human movement. Another major element in the synthesis of human motion is the control architecture needed for dealing with the highly redundant and tightly constrained nature of musculoskeletal

systems. These issues have much in common with the problems encountered in redundant articulated body systems profoundly studied in robotics. Given these shared underlying problems and given the progress and advances made in computational robotics, which has been strongly motivated by real-time needs, algorithms, methodologies, and techniques developed in robotics are being increasingly used in studies of human motion. Analytical models originated in robotics are providing much needed tools for human motion synthesis. The discussion focuses on our ongoing studies into the connection between humans and robots and on the new insights and results this exploration has produced. These developments, which are proving extremely valuable in human biomechanics, are providing new avenues for exploring human motion – with exciting prospects for novel clinical therapies, athletic training, character animation, and human performance improvement.

ID: 663 **E1: 2**

An interoperability architecture for networked medical devices and its application to neurosurgery

Stefan Bohn¹, Dirk Lindner², Stefan Franke¹, Thomas Neumuth¹ and Jürgen Meixensberger²

¹*Innovation Center Computer Assisted Surgery (ICCAS), University of Leipzig, Germany;* ²*Department of Neurosurgery, Medical Faculty, University of Leipzig, Germany.*

Background: Integration of medical devices and IT systems as well as centralized control of the integrated system in the operating room (OR) has been recognized for its potential to increase the overall surgical efficacy, ergonomics and the clinical workflow. Today, commercially available integrated OR systems are characterized by a proprietary and closed design. This work presents an OR integration infrastructure, which is based on open and standardized communication protocols and that has been clinically evaluated.

Methods: The design of the open OR integration system is based on clinical requirements and use cases that have been recorded using a structured requirements engineering approach. The integration system is based on the concept of a service-oriented device architecture and interconnects medical devices, imaging modalities, hospital information systems and systems for computer assisted surgery, e.g. navigation. The functionality of the integrated OR system is available at a control console within the sterile field. Thus, the clinical personal has centralized access to preoperative imaging data within PACS, customized display configurations, medical device functions and OR documentation close to the surgical situs. The overall system has been evaluated within neurosurgical

interventions. Functional and ergonomic aspects as well as clinical user acceptance have been recorded using questionnaires addressing 15 different aspects.

Results: The clinical evaluation study successfully showed the practical feasibility and clinical benefits of the integrated OR system. The proposed system integrates relevant information at ceiling mounted displays. This enables the surgeon to better assess the current clinical situation and increases the overall ergonomic conditions within the OR. Basic functions that formerly interrupted the surgical workflow, e.g. adjusting device parameters can be immediately accomplished by the surgeon or scrub nurse using the sterile control console. Data acquired during intervention are automatically labeled with the electronic patient context and can be seamlessly documented within PACS.

ID: 827

E1: 3

Design and development of lower limb exoskeleton for rehabilitation

Yugan Velusamy, [Suresh Gobee](#) and Vickneswari Durairajah

Asia Pacific University, Malaysia.

This project presents a simplified version of lower limb exoskeleton design. The proposed powered exoskeleton concentrates at the lower limb of the human body. The simplified design is made using aluminum. The whole system is built with the cost in mind to make it more affordable as the current exoskeleton projects required heavy funding. Inertial Measurement Units is used as sensors and the data from the sensors is collected to actuate the motors. The control is done using the Arduino microcontrollers. The right leg is assumed to be the sound limb while the left limb is considered the unsound limb. A walking algorithm has been proposed and the result has been encouraging as it can perform the walking movement. The left unsound limb managed to mimic the movement of the right sound limb. The data is also captured and transmitted wirelessly using Bluetooth technology.

ID: 111

E1: 4

Development and testing of a visuo-haptic surgical training simulator for orthognathic surgery

[Yanping Lin](#), Xiaojun Chen, Xudong Wang, Guofang Shen and Chengtao Wang

Shanghai Jiao Tong University, China.

Visuo-haptic medical training simulator offered a safe, repeatable and cost-effective alternative to

traditional surgeries in improving and assessing the surgeons' skills. In this research, we developed a visuo-haptic surgical training simulator for bone sawing procedures to provide a basically realistic training environment for bone removal processes in orthognathic surgery. The voxel-based model was constructed using computed tomography (CT) images, and the virtual tools were built through reverse engineering. The multi-point collision detection method was applied for haptic rendering to test the 3D relationship between the virtual tool and the bone voxels. By employing Omega.6 as the haptic device and Display 300 as the 3D stereo display, a surgical training simulator with haptic functions and virtual reality environment for orthognathic surgery was realized and basic bone sawing procedures were simulated. The haptic forces computed from the simulator were tested by comparing with the real machining forces obtained from the experiments on fresh human bones. Comparison indicated that the computed forces and the acquired data had the same trend for the bone-sawing procedure.

ID: 229

E1: 5

Investigating multimodal displays: reaction times to visual and tactile modality stimuli

[Jing Yu](#) and Knut Möller

Furtwangen University, Germany.

Sometimes pilots, drivers and other professional operators have to perceive and process plenty of information in visual modality simultaneously. However, excessive information may lead to distraction, confusion, and may result in overloading the user's visual sense and cognitive resources. To reduce these overload threats, the sense of touch was employed as a new information presentation scheme.

Both of the visual and tactile channels have their own merits and defects. In this paper, we focused on the reaction time to the visual and tactile modality stimuli. Our reaction time tasks are all four-choice tasks. In the visual stimuli tests, once the visual mode of a word about direction was shown, the participants pressed the corresponding arrow key with their fingers as soon as possible. In the tactile stimuli tests, the stimuli were produced through vibrators that were worn on the participants' waist or legs. Once the participants detected a vibration, they pressed the corresponding arrow key with their fingers as quickly as possible. We analyzed the influence of gender, time spent on computer, left/right finger, and tactile Venue on reaction time. The accuracy of each test was calculated.

The findings of this study provide a useful reference for engineers and designers to realize how the visual and tactile modality channels could impact the operators, and to determine the most effective modality or combination of modalities for presenting time sensitive information. Besides, the solution will be consultative for the design of tactile navigation system for visually-impaired.

Session	PL2: Plenary Lecture 2
Date/Time	4 December 2013 13:45–14:30 hrs
Venue	Auditorium

ID: 150 **PL2**

Biomechanics of arterial walls in health and disease: state of the art and challenges ahead

Gerhard A. Holzapfel

Graz University of Technology, Austria.

Mechanics regulates biological processes at the molecular, cellular, tissue, organ and organism levels. Biomechanics has the goal to better explain phenomena in bioengineering, biology, chemistry and medicine, and hence to improve, for example, diagnostic methods, therapeutic interventions, medical devices and tissue engineering.

By means of examples we will show and discuss the importance of biomechanics in quantifying the mechanical environment within arterial walls in health, disease or injury from the molecular to the organ level. We also emphasize the interdisciplinary nature of such analysis embracing bioengineering, biology, chemistry and medicine, and the importance of connecting arterial mechanics with biological processes such as growth, remodeling, adaptation and repair. Without undue detail, we discuss important mechanobiological aspects for modeling arterial walls, allude to challenges in modeling pathologies such as atherosclerosis and aneurysms, and highlight the potential clinical impact of using patient-specific modeling.

In particular, computational (multi-scale) models may lead to better understanding of the function of arteries by synthesizing medical images, powerful computers, experimental data and mechanics; they may eventually allow doctors to use computers, together with a patient's medical data, to generate and analyze "virtual arteries" and help identify the best treatment strategy.

Session	SYM-02A: Gastrointestinal Motility Symposium
Date/Time	4 December 2013 14:4–16:15 hrs
Venue	Auditorium

ID: 708 **SYM-02A: 1**

**Symposium Keynote:
Defining the mechanical states of the gut during peristalsis through the use of combined impedance/manometry catheters**

Philip Dinning^{1,2}, Lukasz Wiklendt², Taher Omari² and Marcello Costa³

¹*Dept of Gastroenterology & Surgery, Flinders Medical Centre, South Australia;* ²*Dept of Human Physiology, Flinders University, South Australia;* ³*Dept of Gastroenterology, Child, Youth & Women's Health Service, South Australia.*

Gut motility is made up of a complex interaction between myogenic and neurogenic mechanisms. Utilising measures of gut diameter (video) and intraluminal pressure (manometry) we have recently defined when and where these two mechanisms occur during peristaltic contractions in isolated sections of animal gut *in vitro* (1). For *in vivo* manometric recording video imaging of the gut is not feasible. However, as intraluminal impedance has been used to assess the cross sectional area of the lumen (internal diameter) in human clinical studies, we used a combined manometry/impedance catheter to examine whether impedance could accurately measure changes in diameter, and then when combined with manometry, map the neurogenic and myogenic states of the muscle.

Methods: Motor activity of isolated rabbit distal colon was studied. Changes in gut diameter were recorded by video and intraluminal pressure and change in internal gut diameter were measured with a combined impedance/manometry catheter. For these data we constructed combined spatiotemporal maps of; i) diameter & pressure (DPMaps); ii) diameter & impedance (DImaps); iii) pressure & impedance (PImaps). Correlation between changes in diameter and impedance were assessed with Pearson cross correlation.

Results: Data from the animal preparations showed excellent correlation between changes in impedance and diameter ($r = 0.85$). States of active and passive neurogenic activity could be identify and matched to those defined between pressure and diameter.

Conclusion: These results support the potential in vivo use of combined manometry and impedance to measure details of the mechanical state of gut during

peristaltic activity. Such strategy could provide new insights into gut motility disorders in patient populations where intestinal neuropathy is suspected.

ID: 463

SYM-02A: 2

Symposium Keynote:

Recirculating flow in the stomach during gastric mixing

Yohsuke Imai¹, Ikuma Kobayashi¹, Takuji Ishikawa¹,
Martin Buist² and Takami Yamaguchi¹

¹Tohoku University, Japan; ²National University of Singapore, Singapore.

We show the presence of recirculating flow in the stomach during gastric mixing, and that the recirculation separates the stomach into reservoir and mixing regions. It is still difficult to clearly visualize gastric flow by using medical imaging techniques. We have developed a numerical model of gastric flow based on a free-surface flow modeling and an anatomically realistic geometry of the stomach. We revealed that a J-shaped stomach generates a time-averaged recirculating flow in the antrum. Gastric content in the distal stomach is continuously transported to the distal antrum by the forward flow of antral recirculation, and it is mixed by the backward retropulsive flow. The content inside the antral recirculation is well mixed independently of initial Venue, while the content outside the recirculation is poorly mixed. We also studied the effect of posture on gastric mixing. The volume of content involved in the antral recirculation depends on posture. When the antrum lies below the fundus, corresponding to upright, prone, and right lateral positions, most of the antrum is filled with the content and the content is well mixed by antral recirculation. In contrast, when the antrum lies above the fundus, most of the content is located outside the antral recirculation, resulting in a poor mixing. If the stomach is a straight shaped organ, antral recirculation may be disappeared. Therefore, the curved, twisted shape of the stomach provides a meaningful outcome in terms of gastric mixing.

ID: 590

SYM-02A: 3

Dynamics of gastric contents during digestion – a numerical analysis

Maria J. Ferrua¹, Zhengjun Xue² and R. Paul Singh^{1,2}

¹Riddet Institute, Massey University, New Zealand; ²Department of Biological and Agricultural Engineering University of California, Davis.

Knowledge of the dynamics of gastrointestinal (GI) contents is essential to characterize the disintegration and bioavailability of nutrients and pharmaceuticals

in health and disease. While its experimental assessment has proved difficult, the increased performance and availability of computer simulation technologies have provided an alternative tool to characterize the local dynamics of GI contents under different physiological conditions.

In this work, computational modelling was used to investigate the effect of fluid rheology on the dynamics and mixing of gastric flows and their impact on the distribution of discrete food particles during digestion.

A simplified 3D model of a human stomach was developed. Gastric motility was characterized by periodic and propagating contractive waves along the distal wall (20s period, 0–60% occlusion) and tonal deformations of the proximal region. The behaviour of two Newtonian fluids (10⁻³ Pa.s, 1 Pa.s) and a shear-thinning one (0.233γ^{0.59} Pa.s) were analyzed (ANSYS-Fluent). Mixing was characterized by tracking the motion of a large number of tracers initially distributed throughout the entire gastric cavity. The dynamics of a discrete number of carrot particles (0.4 to 4mm diameter) was investigated.

The faster and more irregular motions always developed within the distal region, but large retropulsive and recirculating motions only developed for a water-like fluid. Viscosities higher than that of water decreased the overall strength of the flow by more than 50% (particularly in proximal region). Mixing efficiencies were always higher within the distal region, with viscosity having a detrimental role on its dynamics and distribution within the entire stomach. Despite slower and more ordered flow motions, the dynamics of viscous fluids increased the dispersion of carrot particles by at least 8 times (within less than 2 min). Results illustrate the complex dynamics of gastric contents and the potential of numerical modelling to advance GI research in food and health sectors.

ID: 616

SYM-02A: 4

Solid particle motion in the stomach during gastric mixing

Taimei Miyagawa, Yohsuke Imai, Takami Yamaguchi and Takuji Ishikawa

Tohoku University, Japan.

Functions of the stomach are storage, mixing and emptying of gastric contents. To understand fluid mechanics in the stomach, we have developed a numerical model of gastric flow. We revealed that time-averaged recirculating flow is generated in the distal stomach, and gastric contents are well mixed in the distal stomach. In this previous study, we only considered a simple liquid content. In the real

stomach, however, solid components are contained in the gastric contents. In this study, we clarify the motion of solid particles in the stomach.

Assuming that the viscous stress of gastric gas does not affect the motion of the gastric contents, gastric flow can be modeled by a free surface flow problem. Flow of gastric liquid is governed by the conservation laws of mass and momentum for incompressible and Newtonian fluids. The moving particle semi-implicit method was used for discretizing the governing equations. We modeled solid particles in the gastric contents as a rigid sphere which has the diameter of 6 mm and the same density with liquid. Initially, 40 solid particles were randomly distributed in the stomach. We simulated 10 cases with different initial positions of solid particles.

We studied how many particles move from the proximal/distal stomach to the distal/proximal stomach. Solid particles initially located in the distal stomach circulate in the distal stomach, and hardly move to the proximal stomach. Conversely, solid particles initially located in the proximal stomach gradually move to the distal stomach. This result indicates that the movement of the solid particles between the distal and the proximal stomach is one-way, from the proximal stomach to the distal stomach. This phenomenon results in a high concentration of solid particles in the distal stomach. Solid particles are expected to be well mixed with gastric juice, and to have a large shear stress in the distal stomach, this phenomenon would be helpful for the digestion of solid particles.

Session	A2: Biosignal Processing
Date/Time	4 December 2013 14:45–16:15 hrs
Venue	SR-01 & 02

ID: 346 **A2: 1**

An adaptable inertial sensor fusion-based approach for energy expenditure estimation

Dominik Schuldhau¹, Sabrina Dorn¹, Heike Leutheuser¹, Alexander Tallner², Jochen Klucken³ and Bjoern M. Eskofier¹

¹Digital Sports Group, Pattern Recognition Lab, Department of Computer Science, University Erlangen-Nuremberg, Germany; ²Institute of Sport Science and Sport, University Erlangen-Nuremberg, Erlangen, Germany; ³Department of Molecular Neurology, University Hospital Erlangen, Erlangen, Germany.

Using multiple inertial sensors for energy expenditure estimation provides a useful tool for the assessment of daily life activities. Due to the high variety of new upcoming sensor types and recommendations for sensor placement to assess

physiological human body function, an adaptable inertial sensor fusion-based approach is mandatory. In this paper, two inertial body sensors, consisting of a triaxial accelerometer and a triaxial gyroscope, were placed on hip and ankle. Ten subjects performed two trials of running on a treadmill under three speed levels ([3.2, 4.8, 6.4] km/h). Each sensor source was separately subjected to preprocessing, feature extraction and regression. In the final step, decision level fusion was performed by averaging the predicted results. A mean absolute error of 0.50 MET was achieved against indirect calorimetry. The system allows an easy integration of new sensors without retraining the complete system. This is an advantage over commonly used feature level fusion approaches.

ID: 733 **A2: 2**

The development of behavioral and neuronal activities of animal models with kindling-induced and spontaneous temporal lobe seizures

Yu-Lin Wang¹, Yin-Lin Chen¹, Yu-Shin Huang², Sheng-Fu Liang³ and Fu-Zen Shaw²

¹Biomedical Electronics Translational Research Center, National Chiao-Tung University, Taiwan; ²Department of Psychology, National Cheng Kung University, Tainan, Taiwan; ³Department of Computer Science and Information Engineering, National Cheng Kung University, Tainan, Taiwan.

Epilepsy, in terms of the sudden and recurrent malfunction of brain caused by abnormal discharge, is called “seizure”. The exact cause of epilepsy remains unclear, and therefore the study of epileptogenesis which occurs in epileptic brain becomes important. Experiments on animal models have successfully demonstrated the better understanding of the excitability of neuronal networks in relation to the occurrence of seizures. In this work, the developments of behavioral and neuronal activities of kindling-induced and spontaneous temporal lobe epilepsy (TLE) in rats were investigated. Daily stimulation of the right-side amygdala was delivered to Wistar rats to induce TLE. Each kindling evokes the excited neuronal activities in brain. The duration, spike density and amplitude of evoked discharges were increased during kindling procedure. With repeated 40 stimulations, the rats showed the progression from tonic seizures (stage-1,2) to generalized clonic-tonic convulsive seizures (stage-4,5). In a consequence, the daily stimulation causes the permanent brain function damage and three rats were successfully induced to have spontaneous TLE of seizure stage-2. The cortical neuronal activities exhibit high voltage rhythmic spike (HVRS) discharges oscillating in the range of 9–11 Hz and 18–21 Hz (second

harmonics). HVRS is characterized by a barrage of large spike discharge (80–400 μ V) with negative polarity. It was found that the inter-spike interval (ISI) between two negative spikes is positively correlated ($r=0.9852$) to the amplitude of former spike in a HVRS episode. A large amplitude spike was accompanied by a long ISI, while a small amplitude spike took place in group with a short ISI. The investigation on cortical epileptiform is practical to implement seizure detection algorithms in embedded systems. With integration of an electrical stimulator or drug delivery device, such a seizure warning system or a closed-loop seizure control device could enhance the patients' life quality.

ID: 640

A2: 3

Effect of mobile phone radiation on brain using wavelet energy

C. K. Smitha¹ and N. K. Narayanan²

¹College of Engineering, Vadakara, India; ²Kannur University, Kannur, India.

The usage of mobile phone is increased exponentially in last few years. So frequent exposure of human body to electromagnetic radiation is a growing concern. Most of the studies using EEG, (Electroencephalograph) concluded with contradictory results, since the signal is considered as linear. As the EEG signal is non linear, non linear methods are more suitable, so wavelet transform method is used. EEGs of 10 volunteers were recorded at rest and on exposure to radiofrequency (RF) emissions from mobile phones with different SAR by keeping phone at Cz and Auricle positions. Wavelet energy is calculated for all bands (δ , θ , α , β & γ) of EEG, using wavelet transform were used as feature parameter.

In this paper, relative wavelet energy of all bands of EEG calculated, for hundred samples of length 128 is analyzed using statistical methods. It is assumed that each band exhibit a characteristic range of wavelet energy. Relative energy is calculated as ratio of energy for each band to total energy. Data set of relative wavelet energy is analyzed using student's paired t-test. Null hypothesis is rejected with 95% confidence in all the cases. The data set of mean of normalised energy is analysed using ANOVA to verify the result. There is 100% rejection of the hypothesis. This shows that the samples behave as they are from different population. All the data of same subject were recorded in succession under same conditions, so it is evident that these changes in wavelet energy while using mobile phones demonstrates transformation in the activities of brain due to radiation.

ID: 779

A2: 4

Automatic detection of atrial fibrillation using RR interval from ECG signals

Victoria Gokana¹, Chee Teck Phua² and Gaëlle Lissorgues¹

¹ESIEE Engineering Paris, France; ²Nanyang Polytechnic, Singapore.

Atrial Fibrillation (AF) is a common arrhythmia, particularly in the elderly and those with heart disease. It can be characterized by an uncoordinated heart electrical activity leading to bad electricity propagation in the upper chambers of the heart. This anomaly can be observed on electrocardiogram (ECG) signals and different statistical methods or time-frequency domain analysis had been explored to distinguish Atrial Fibrillation from other kind of arrhythmias using RR intervals from ECG signals. Examples of such algorithms include the Root Mean Square of the Successive Differences (RMSSD), Sample Entropy and Fast Fourier transform. In this study, the MIT-BIH database such as the Normal Sinus Rhythm (NSR), AF and Arrhythmia ECGs were used. This paper applies a preprocessing algorithm based on Pan-Tompkins method to extract reliable QRS complex from ECG signals and thus accurate RR intervals. In this paper, the proposed automatic detection of AF using RR intervals extracted from ECG is based on a 3 steps approach. The first step uses the computation of the RMSSD on the RR intervals extracted from a 24 hours ECG recording to find whether an arrhythmia had occurred. The second step applies autocorrelation of the squared signal to precisely determine the start time and stop time of the arrhythmia episode within a detected arrhythmia window. The last step consists of computing the Shannon Entropy from the start to stop time extracted on the previous step to discern AF from other type of Arrhythmias. By using the developed algorithm, we were able to accurately detect AF using RR intervals extracted from 24 hours ECGs recording with up to 99.5% accuracy in time resolution.

ID: 631

A2: 5

Multiclass least-square support vector machine for myoelectric-based facial gesture recognition

Mahyar Hamed, Sheikh Hussain Shaikh Salleh, Alias Mohd Noor, Arief Ruhullah A. Harris and Norazman Abd. Majid

Universiti Teknologi Malaysia, Malaysia.

Facial gesture recognition (FGR) is considered as a state-of-the-art which has drawn the researchers' attention in numerous fields of study due to its high potential in different applications. Recognizing the gestures through bio-signals generated from facial muscle movements has been recently proposed as an accurate and reliable pathway. The performance of gesture recognition-based systems directly depends on the effectiveness of classification techniques. Besides, a reasonable trade-off between recognition accuracy and computational cost is counted as the most significant factor for designing such systems. The aim of this paper was the classification of facial gestures electromyogram (EMG) signals by means of a least square support vector machine (LS-SVM) algorithm. Ten predefined facial gestures EMGs were recorded from ten participants through three bi-polar channels. Acquired signals were preprocessed using a band-pass filter and a segmentation technique. Then, time-domain features mean absolute value (MAV) and root mean square (RMS) were extracted from each segment. In order to classify the features, LS-SVM was implemented by considering radial basis function kernel and two multiclass encoding schemes, one-versus-one (OVO) and one-versus-all (OVA). This research showed that LS-SVM was a robust method for classification of facial gestures with 97.1% classification accuracy and 1.37 seconds training time when utilizing the feature combination MAV+RMS and the encoding technique OVA. It was also concluded that LS-SVM outperformed SVM and fuzzy c-means classifiers in this field of study. The results of this paper can be used as efficient processing tools in designing reliable interfaces for FGR systems.

ID: 387

A2: 6

Hierarchical identification process of a two-parameter gas exchange model

Axel Riedlinger, Jörn Kretschmer and Knut Möller

Institute of Technical Medicine, Furtwangen University, Germany.

Using mathematical models supports clinicians in life-saving mechanical ventilation therapy by simulating gas exchange and estimating individualized

parameters that give feedback about the current patient's status. Exploiting model calculations allows suggesting appropriate ventilator settings in order to achieve a certain therapy goal, e.g. a defined partial pressure of oxygen (P_{a,O_2}) and carbon dioxide (P_{a,CO_2}).

Literature provides various gas exchange models of different number of parameters that have to be adapted to the patient's behavior. The robustness of the parameter identification process (PIP) mainly depends on the complexity of these models and on the choice of the initial parameter values.

We show how a hierarchical model structure may lead to a robust PIP of a two-parameter gas exchange model by avoiding initial value problems. Initial values for both parameters representing shunt and ventilation/perfusion-mismatch are calculated from simple and independent one-parameter models of O_2 and CO_2 respectively. The approach was evaluated using both four model-simulated plus four real patient data sets. Results show promise for a robust hierarchical PIP of the two-parameter model describing pulmonary gas exchange.

Session	B2: Regenerative Medicine Tissue Engineering
Date/Time	4 December 2013 14:45–16:15 hrs
Venue	SR-03 & 04

ID: 143

B2: 1

Conference Keynote: Application of bioimaging to tissue engineering and regenerative medicine

Kishore Bhakoo

*Singapore Bioimaging Consortium, A*STAR, Singapore.*

Stem cells are currently being evaluated for their therapeutic potential to replace cells in a number of disease or degenerative pathologies. The monitoring of cellular grafts, non-invasively, is an important aspect of the ongoing efficacy and safety assessment of cell-based therapies. Magnetic resonance imaging methods are potentially well suited for such an application, as they produce non-invasive 'images' of opaque tissues. For transplanted stem cells to be visualised and tracked by MRI, they need to be tagged so that they are 'MR visible'. We are developing and implementing a programme of Molecular Imaging in pre-clinical models that is directed towards improving our understanding of stem cell behaviour in the context of the whole organism.

In order to achieve these goals, we are engineering novel MRI contrast agents and developing specific tagging molecules to deliver efficient amounts of contrast

agents into stem cells. The intracellular contrast agents are based on either superparamagnetic nanoparticles, such as polymer-coated iron oxide, or other paramagnetic MR contrast agents.

With its ability to precisely target cell delivery, track cell migration and non-invasively evaluate living subjects over time, this technique will help in the translation and facilitate the clinical realisation and optimisation of stem cell-based therapies. Moreover, it is important that we develop additional multimodal imaging (MRI, PET, SPECT/CT and Optical) methodologies for *in vivo* monitoring of functional aspects of implanted stem cells.

ID: 204

B2: 2

Dual function of miRNA199a-HIF1-Twist1 cyclic pathway in stage-specific osteogenesis of mesenchymal stem cells

Xiao Chen¹, Shen Gu², Hongwei Ouyang¹, Tin lap Lee² and Wai Yee Chan²

¹Zhejiang University, China; ²SBS, The Chinese University of Hong Kong.

The emergence of stem cell research started a new era in clinical medicine – the era of regenerative medicine. Elucidating the molecular mechanisms that regulate osteogenesis of human mesenchymal stem cell (hMSC) is important for the development of cell therapies for bone regeneration. MSC differentiation processes involve complex pathways that are regulated at both transcriptional and posttranscriptional levels. However, the key regulator(s) of MSC differentiation has not been identified. MicroRNAs (miRNAs) are small non-coding RNAs that bind to target mRNA leading to translational arrest or mRNA degradation. Here, we show that hsa-miR-199a-5p modulates osteogenic differentiation of hMSCs.

Methods: Hsa-miR-199a expression were validated by quantitative RT-PCR during MSC osteogenesis. The function of hsa-miR-199a-5p in osteogenesis of MSC were evaluated by upregulating and inhibition of hsa-miR-199a-5p. We investigated the HIF1a-Twist1-miR-199a cyclic pathway activity during differentiation of human MSCs to find out the mechanism of hsa-miR-199a-5p on osteogenesis.

Results: Hsa-miR-199a expression were validated by quantitative RT-PCR. revealed that miR-199a was up-regulated during osteogenesis of hMSCs. Overexpression of miR-199a-5p not 3p enhance osteoblast differentiation of hMSCs *in vitro*, whereas inhibition of miR-199a-5p function by anti-miR-199a-5p reduce osteoblast-specific genes, alkaline

phosphatase (ALP) activity, and matrix mineralization. Furthermore, overexpression of miR-199a enhance ectopic bone formation *in vivo*. Target prediction analysis and experimental validation by WB confirmed HIF1a-Twist1 pathway play a key role in promoting osteoblast differentiation, as a target of miR-199a-5p. We show that HIF1a-Twist1 pathway have dual function on osteogenesis both *in vitro* and *in vivo* at least in part through miR-199a-5p. At early stage, HIF1a-Twist1 pathway activity enhance osteogenesis by upregulating miR-199a-5p while miR-199a-5p enhance osteogenesis maturation by inhibiting HIF1a-Twist1 pathway.

Conclusion: In conclusion, Our findings for the first time demonstrated that HIF-Twist1-miR-199a cyclic pathway could regulate MSC osteogenesis at different differentiation stage, which could represent a therapeutic strategy for enhancing bone formation *in vivo*.

ID: 228

B2: 3

Differential effect of biphasic calcium phosphate scaffold ratios on odontoblast cells

Sarah Talib Abdul Qader¹, Ismail Ab Rahman¹, Thirumulu Ponnuraj Kannan¹, Zuliani Mahmood¹ and Hanafi Ismail²

¹School of Dental Sciences, USM, Malaysia; ²School of Materials and Minerals Resource Engineering, USM, Malaysia.

Dentin tissue engineering is a new approach to regenerate functional new tissue using human dental pulp cells, bioactive molecules and scaffolds instead of using synthetic filling materials. Since calcium phosphate (CaP) scaffolds have been widely used with osteoblast cells for bone tissue regeneration, it is interesting to investigate the effects of these scaffolds on odontoblast cells differentiation for dentin tissue regeneration. In this study, three different hydroxyapatite (HA) to beta tricalcium phosphate (β -TCP) ratios of biphasic calcium phosphate (BCP) scaffolds, BCP20, BCP50, BCP80 of mean pore size of 300 μ m and 65% porosity were all prepared from phosphoric acid (H_2PO_4) and calcium carbonate ($CaCO_3$) sintered at 1000°C for 2 hours. The extracts of these scaffolds were assessed on the differentiation of odontoblasts. The high alkalinity, more calcium and phosphate ions release that were exhibited by BCP20 expressed high alkaline phosphatase activity compared to that cultured with BCP50 and BCP80 extracts. These results highlight the effect of different scaffold ratios on the cell microenvironment and demonstrate that BCP20 scaffold can support HDPCs differentiation for dentin tissue regeneration.

ID: 274

B2: 4

Comparison of stage specific tendon stem/progenitor cells and the inherent role during tendon development

Jialin Chen, Wei Zhang, Zeyu Liu, Ting Zhu and Hongwei Ouyang

School of Medicine, Zhejiang University, China.

Introduction: Normal mature tendon has a poor healing capacity. However, fetal tendon was demonstrated to possess extensive regenerative ability upon injury, even within an adult environment. We hypothesized that tendon stem/progenitor cells (TSPCs) at different developmental stages contributed to the different regenerative capacity. This study tried to isolate and compare TSPCs from post-natal Sprague-Dawley rats at different developmental stages, and explore the inherent molecular difference.

Results: The post-natal rat Achilles tendons experienced a striking morphological and structural alteration. From 0d to 56d, the collagen fiber structure became more and more mature. The cell morphology turned to spindle-shape compared to the initial stage's round shape. Also, the cell number decreased a lot. The diameter of collagen fibril enlarged with time, and the constitution transited from uniform small fibril to heterogeneous large fibril. The day 1, 7 and 56 post-natal were judged as three important development stages from the above results. RATSCs-1d, RATSC-7d and RATSC-56d were successfully isolated. All cells possessed cloning formation ability and RATSC-7d showed the most powerful capacity. Besides, RATSC-7d presented the strongest differentiation potential, highest proliferation rate and matrix secretion capacity. It seems RATSCs at day 7 were significant different from the other two kinds of RATSCs. DNA microarray was carried out to explore the inherent molecular difference. Several interesting genes relating to the different ability of RATSC-7d were found, and their function was demonstrated by gene over-expression and gene silencing in cell-culture model.

Conclusion: The post-natal rat Achilles tendons experienced a striking morphological and structural alteration. All TSPCs at different developmental stages possessed the ability of self-renew and multilineage differentiation. The proliferation rate and matrix secretion capacity was found highest in the RATSC-7d group, which was determined by the unique expression profile.

ID: 350

B2: 5

Stimulation of angiogenesis in tissue engineered constructs using prolyl hydroxylase inhibitors

Adeline Sham¹, Eliana C. Martinez¹, Sebastian Beyer^{1,2}, Dieter W. Trau¹ and Michael Raghunath¹

¹National University of Singapore, Singapore; ²Singapore-MIT Alliance for Research and Technology, Singapore.

Despite advances in the tissue engineering field, inadequate vascularization continues to limit clinical applications of tissue engineering mainly to thin or avascular tissues. Although growth factors such as vascular endothelial growth factor (VEGF) and basic fibroblast growth factor (bFGF) have been shown to stimulate angiogenesis, the vessels produced by the delivery of these factors alone are often leaky and have abnormal morphology.

In this study, we explore the incorporation of prolyl hydroxylase inhibitors (PHIs) into scaffolds as an alternative strategy for promoting vascularization. PHIs are a class of small molecule drugs which can stabilize hypoxia-inducible factor 1 α (HIF-1 α), an upstream regulator of angiogenesis. We conjugated pyridine-2,4-dicarboxylic acid (PDCA), an established PHI, via amide bonds to Gelfoam, a gelatin sponge. The PDCA is released when the amide bonds are cleaved by proteases from infiltrating cells.

For *in vitro* testing, fibroblasts were cultured on the scaffolds for 7 days. Results showed that PDCA-Gelfoam has low cytotoxicity (<10%) and supports cell attachment and proliferation at all dosages tested. VEGF measurements demonstrated that PDCA-Gelfoam increased VEGF secretion significantly. A HIF-1 α reporter assay was also performed, and results showed that HIF-1 α is stabilized in cells cultured on PDCA-Gelfoam.

For *in vivo* testing, PDCA-Gelfoam scaffolds were implanted into the peri-renal fat of Sprague Dawley rats for 8 days. Immunostaining of endothelial cells in explant sections showed that PDCA-Gelfoam increased vascular infiltration significantly compared to controls. In conclusion, our results indicate that the incorporation of PHIs into scaffolds is a feasible strategy for improving vascularization in tissue engineering applications.

Session	C2: Musculoskeletal Mechanics
Date/Time	4 December 2013 14:45–16:15 hrs
Venue	SR-05 & 06

ID: 576 C2: 1

Assessment of the impact of positive heels (plantarflexion) and negative heels (dorsiflexion) shoes on human walking gait

Desmond Y.R. Chong^{1,2}, Ee Xien Ng², Catriona Monkhouse³, Paul Wong³, Ganit Meyer³ and Yoav Aloni³

¹Engineering Design and Innovation Centre, National University of Singapore; ²Department of Bioengineering, National University of Singapore; ³AposTherapy Singapore Pte Ltd.

Many studies have proposed that footwear design such as shoe body, insoles, heel height and heel position can affect human walking gait. In this study, two designs namely the positive heels (PHS) and negative heels shoes (NHS) were investigated to understand its impact on gait kinematics and kinetics. Experimental results showed that different shoe designs which impose plantarflexion or dorsiflexion on the foot would lead to changes of the joint kinematics and kinetics in the sagittal plane. PHS would cause a significantly larger ankle plantarflexion, larger ankle plantarflexion moment, larger knee adduction moment and larger hip flexion moment. On the other hand, NHS did not induce large differences compared to the baseline design, only causing a significantly larger ankle dorsiflexion. This study has given an insight on how the wearing of positive heels and negative heels shoes can affect the kinematics and kinetics of the lower limb. The results can be useful for allied health professionals such as Physiotherapists and Podiatrists who are advising patients on footwear choices.

ID: 588 C2: 2

Segmental torso masses and joint torques produced by gravity in the adolescent scoliotic spine

Bethany E. Keenan¹, Maree T. Izatt^{1,2}, Geoff N. Askin², Graeme Pettet¹, Robert D. Labrom², Mark J. Pearcy¹ and Clayton J. Adam^{1,2}

¹Queensland University of Technology, Australia; ²Mater Misericordiae Health Services, Brisbane, Australia.

Introduction: Calculating segmental torso masses in Adolescent Idiopathic Scoliosis (AIS) patients allows the gravitational loading on the scoliotic spine during relaxed standing to be estimated.

Methods: Low dose CT data was used to calculate vertebral level-by-level torso masses and spinal joint

torques for 20 female AIS patients (mean age 15.0 ± 2.7 years, mean Cobb angle $53 \pm 7.1^\circ$). ImageJ software (v1.45 NIH USA) was used to threshold the T1 to L5 CT images and calculate the segmental torso volume and mass for each vertebral level. Masses for the head, neck and arms were taken from published data.¹ Intervertebral joint torques in the coronal and sagittal planes at each vertebral level were found from the position of the centroid of the segment masses relative to the joint centres (assumed to be at the centre of the intervertebral disc). The joint torque at each level was found by summing torque contributions for all segments above that joint.

Results: Segmental torso mass increased from 0.6kg at T1 to 1.5kg at L5. The coronal plane joint torques due to gravity were 5–7Nm at the apex of the curve; sagittal torques were 3–5.4Nm.

Conclusion: CT scans were in the supine position and curve magnitudes are known to be smaller than those in standing.² Hence, this study has shown that gravity produces joint torques potentially of higher than 7Nm in the coronal plane and 5Nm in the sagittal plane during relaxed standing in scoliosis patients. The magnitude of these torques may help to explain the mechanics of AIS progression and the mechanics of bracing. This new data on torso segmental mass in AIS patients will assist biomechanical models of scoliosis.

References

- 2009 Winter DA. Biomechanics and Motor Control of Human Movement, Wiley & Sons, Canada.
- 1985 Torell G. et al. *Spine* 10: 425–27.

ID: 565 C2: 3

Wheelchair propulsion torque and joint moments during manual wheelchair propulsion on a brake-type dynamometer

Youngho Kim¹, Jeseong Ryu¹, Jongsang Son¹, Seunghyeon Kim¹ and Seonhong Hwang²

¹Yonsei University, South Korea; ²University of Pittsburgh.

A brake-type wheelchair dynamometer was made for the measurement of torque and revolutions per minute (RPM) during manual wheelchair propulsion. A dynamic calibrator was also developed to calibrate the dynamometer. Calibration was performed by Korea Testing Laboratory (KTL). Torque difference between two apparatus was expressed in second-order polynomial ($R^2=0.9969$).

Using the dynamometer, experiments were performed to observe manual wheelchair propulsion torque and joint moments with various external

resistances. Seven healthy male (unskilled) and four disabled male (skilled) volunteers sat on the wheelchair mounted on the two rollers of dynamometer, and propelled the wheelchair with comfortable speed and their maximum speed. Rotational resistances were applied to the wheelchair by the powder brake with light and heavy load. The magnitude of the maximum propulsion torque (MPT) was the largest for the heavy-fast condition in both groups (unskilled: 19.21 ± 1.99 Nm vs. skilled: 15.98 ± 2.25 Nm) and was the smallest at the light-slow condition (12.47 ± 1.08 Nm vs. 9.23 ± 1.13 Nm). All MPT of the unskilled group at each condition were larger than those of the skilled group significantly ($p < 0.05$). Using inverse dynamics, joint moments were calculated for each joint. The magnitude of the maximum shoulder joint moment (MSJM) was the largest for the heavy-fast condition in both groups (unskilled: 19.12 ± 1.57 Nm vs. skilled: 21.61 ± 1.67 Nm) and was the smallest at the light-slow condition (9.21 ± 0.94 Nm vs. 5.22 ± 0.80 Nm). The variation of the MSJM was higher than that of the maximum wrist approximately four times and that of the maximum elbow about eight times.

Acknowledgement: This research was financially supported by the KHT R&D Project (HI10-C2017(A102062)) funded by the MW, Korea.

ID: 657

C2: 4

Wearable movement analysis system for children with movement disorders - lower extremities assessment system

Yu Zheng Chong¹ and Jasmy Yunus²

¹Universiti Tunku Abdul Rahman, Malaysia; ²Faculty of Biosciences and Medical Engineering, Universiti Teknologi Malaysia, Skudai, Malaysia.

This paper proposes an instrumented insole system developed to analyse Vertical Ground Reaction Forces (VGRF) of human motion. Such analysis is important in assessments of individual with movement disorders such as Cerebral Palsy or spasticities of lower extremities. The wearable system was developed utilising Force Sensing Resistors, Flex Sensors embedded in a shoe insole. In addition, the signal conditioning, and data acquisition circuitries consisting Arduino Leonardo board, and SKXBee wireless modules. A Labview-based real-time data collection software was developed to store, display, and analyse VGRF data of walking gait. The system is capable of providing kinetics parameters of movements with associated pressure distribution exerted on the foot during locomotion. Data collection were collected from 30 volunteers. Results obtained by the system

are comparable with published database that is between 1.0 – 2.0 times of body weight for walking. It is envisioned that this system will form part of a full-body wearable instrumentation system that incorporates upper-extremities movement analysis subsystem to provide overall gait analysis for individual with movement disorders. Furthermore, it is also anticipated that such movement analysis system would aid in long-term monitoring of individual with movement disorder to monitor effectiveness of various rehabilitation programs. In view of the overall development cost of this system is USD 200, it is envisioned that the developed system will be an affordable system to be owned by any caretakers of individuals with movement disorders. As such, this system will supplement the normal or conventional analyses done on analysing gait of individuals with movement disorder in gait laboratories, which is costly, and less accessible compared to continuous or long-term monitoring.

ID: 176

C2: 5

Predicting the contact of dual mobility hip implants – effect of bearing geometry and material

M. S. Uddin

University of South Australia, Australia.

This paper aims to predict contact stress with the effect of critical geometric parameters of a dual mobility implant. A three dimensional (3D) finite element (FE) model of the implant was constructed by incorporating 3D anatomical configuration, in which, the metallic shell along with the ultrahigh molecular weight polyethylene (UHMWPE) cup is orientated on the pelvic system at 45° abduction angle. Effects of radial clearance, head radius, cup thickness, shell thickness, and the interfacial friction on maximum contact pressure and von Mises stress, were investigated. Simulation results show that contact pressure and stress decrease with the decrease in radial clearance and the increase in head radius, while the cup and shell thickness reveals a negligible influence. Results were discussed with those obtained from studies available in literature, providing a guideline for biomedical engineers to further improve the design of the implants.

ID: 609

C2: 6

Influence of lower-leg muscle spindle function in irregular surface walking

Akira Obara, Takeshi Yamakoshi, Takayuki Shina, Hiroshi Takkemura and Hiroshi Mizoguchi

Tokyo University of Science, Japan.

Walking is one of basic motion of human. However, walking has risk of falling accident. Falling accident is large problem for elderly people. One of the causes of falling for elderly people is reduced sensation. The purpose of this study was to investigate difference of walking on irregular surface made from some blocks between health and reduced muscle spindle functional condition. 10 healthy young adult males (age: 21.5 ± 0.92 year) were recruited in this research. Normal and high-speed walking motion were measured on two surfaces: an even surface and an uneven surface. Healthy and reduced muscle spindle function conditions were compared. The ice immersion approach was applied on the lower-leg muscles as a method of reducing muscle spindle function. To create an irregular surface, a thin cloth carpet was modified by many blocks under the carpet. During normal walking, the step length and the rate of upper-body acceleration were significantly increased by icing and/or the uneven surface ($p < 0.01$). The step length and the rate of upper-body acceleration during high-speed walking even and uneven surface were significantly decreased compared with walking on even surface under icing ($p < 0.05$). During high-speed walking, the walking velocity was significantly decreased by icing and/or the uneven surface ($p < 0.01$). These changes in walking show that the muscle spindle function is related to walking. However, standard deviations for all walking parameters were not significantly difference between not only even and uneven surface, but also between healthy and reduced muscle spindle functional condition. The experimental results suggest that muscle spindle function is not important to walk on the irregular surface.

Session	D2: Diagnostic Devices Implantable Devices
Date/Time	4 December 2013 14:45–16:15 hrs
Venue	SR-07 & 08

ID: 165

D2: 1

Circulating tumor cell detection system on cell rolling microchip

Atsushi Mahara¹, Hao Chen¹, Carlos Agudelo¹, Kazuhiko Ishihara² and Tetsuji Yamaoka¹

¹National Cerebral and Cardiovascular Center Research Institute, Japan; ²The University of Tokyo, Japan.

Circulating tumor cells (CTCs) present in the blood of cancer patient. In the recent study, CTCs detection technology were focused on the diagnosis of the metastasis. However, a few CTCs are circulating in the blood flow, and suppression of non-specific absorption of the other cells is important for the CTCs detection. In this presentation, we have developed the CTCs detection system based on the cell rolling microchip. Cell rolling is derived from the continuous interaction of cell surface marker and the ligand, and the rolling velocity is directly correlated with the surface expression level of the marker. To immobilize the antibody, copolymers of poly[2-methacryloyloxyethyl phospho-rylcholine (MPC)-*co-n*-butyl methacrylate (*n*BMA)-*co*-N-vinylformamide (NVF)] (PMBV) were synthesized by random polymerization. Microflow pass (width: 300 μ m, depth: 100 μ m) were coated with the polymers, and anti-CD34 antibody were covalently attached by the crosslinker. KG-1a and HL-60 cells were used as CD34 positive and negative cells for the model system of CTCs detection, respectively. After the injection of the cell suspension, and the cells were stably circulated by the media flow without any non-specific adhesion on the surface. When we used the optimized condition at 0.4 μ l/min of media flow, the rolling velocity of KG-1a (CD34 positive) cells on the chip system was detected as about 40 μ m/sec. On the other hands, the velocity of the negative cells were about 55 μ m/sec. We observed the significant difference between these rolling velocities. When the media flow was increased, the significant difference of the rolling-velocity was not indicated, and the cell-moving velocity was almost same. From these results, we successfully discriminate the cell type on the microchip by the cell-rolling velocity without any non-specific absorption. This chip system would apply for the CTCs detection system based on the cell-rolling mechanisms.

ID: 301

D2: 2

Development of handheld, portable magnetic resonance relaxometry system for rapid blood screening

Weng Kung Peng¹ and Jongyoon Han^{1,2}

¹Singapore-MIT Alliance For Research and Technology, Singapore; ²Massachusetts Institute Technology.

With advances in microelectronics technology, Magnetic Resonance (MR) community sees the emergence of much more compact MR spectrometers on a highly integrated circuit platform such as field programmable gate array (FPGA), and complementary-metal oxide semiconductor (CMOS). Here, in SMART Centre, Singapore, a novel, compact-sized, and portable (250g) Magnetic Resonance Relaxometry system is designed and developed¹. The whole system consists of a coin-sized permanent magnet (0.76 Tesla), miniaturized radio-frequency microcoil probe², compact lumped-circuit duplexer, and single board 4-Watt power amplifier, in which a FPGA-based spectrometer is used for pulse excitation, signal acquisition and data processing. We show that by measuring the proton transverse relaxation rates from a large pool of natural abundance proton-nuclei presence in less than 1 μ L of red blood cells, one can indirectly deduce the relative magnetic susceptibility of the bulk cells within a few minutes of signal acquisition time. Such rapid and sensitive blood screening system can be used to monitor the fluctuation of the bulk magnetic susceptibility of the biological cells (e.g. human red blood cells), where unusual state of the bulk magnetic susceptibility is related to a number of diseases (e.g. malaria^{3,4}, genetic diseases, etc).

ID: 688

D2: 3

Research and development of the primary side frequency controlled transcutaneous energy transmission system for implantable devices

Hidekazu Miura¹, Isturo Saito², Yasuyuki Shiraishi¹ and Tomoyuki Yambe¹

¹Tohoku University, Japan; ²The University of Tokyo, Japan.

Background: Total implantable device is desirable for prevention of infection. Today, totally implantable artificial heart using a transcutaneous energy transmission system (TETS) is not available. Change of output voltage due to the coil shifting is the serious problem for TETS. However, feed-back system using a signal transmission should be avoided to make the system simple.

Methods: A primary side control method for the enhancement of the output power is under development. When the output load is heavy and the coil distance is closer than that of the optimal condition, the output power decreases drastically. From the view of primary side, the impedance changes from positive to negative, the driving frequency should be adjusted to higher so that the phase angle of the primary impedance is zero degree. This control method was examined the simplified linear circuit. This control system was realized by a phase detector, an error amplifier and a voltage controlled oscillator (VCO) with lower limit frequency set to the frequency which was chosen for the optimal condition. The error amplifier controls the VCO so that the phase angle is zero.

Results: The examination in the linear circuit showed that this control method enhanced the output power to the four times than the system with the fixed frequency. And it was found that this control system has a first order loop transfer function and showed stable response for load changes.

Discussions: The realization of the control method is simple without any signal communication. The maximum output power can be improved to meet power demand of the implantable device. Temperature raise of the device must be considered, however, the system is useful for short-term raise of the power consumption of the implantable device, such as, the motor start-up or short-term raise of friction.

ID: 536

D2: 4

Stand-alone integrated microfluidic parasite analysis system

András J. Laki^{1,3}, Gábor Zs. Nagy¹, Kristóf Iván¹, Péter Fürjes² and Pierluigi Civera³

¹Faculty of Information Technology Pázmány Péter Catholic University, Budapest, Hungary; ²MEMS Laboratory, Research Centre for Natural Sciences Hungarian Academy of Sciences, Budapest, Hungary; ³Department of Electronics and Telecommunications Polytechnic University of Turin, Turin, Italy.

A microfluidic separator device has been designed and fabricated to detect micron-size nematodes from blood samples applying a monolithic polydimethylsiloxane (PDMS) microfluidic structure. Several intravenous parasitosis can be observed by the constructed stand-alone integrated microfluidic parasite analysis system such as dirofilariasis or Lyme disease.

The developed flow-through microfluidic separator has a single inlet and one outlet. The radius of the active zone (r) is 1 mm, where the filtered

nematodes are retained after the measurement. This region consists of space-placer columns and it is surrounded by rectangular cross-section shaped microcapillaries. 48 different microfluidic devices have been designed, fabricated and tested with similar geometries but the width of the microcapillaries varies from 6.1 μm up to 83.6 μm . The channel height is 20 μm , the length of surrounding microfluidic capillaries is 100 μm . The repetition angle of the microcapillaries (α) determines the width of the channels, and also the critical diameter of filtered particles. If the diameter of in-flow particles is bigger than width of capillaries, they will be filtered out from the liquid flow. A geometrical optimization has been also made solving the time-dependent incompressible Navier-Stokes eq. The range of the predicted pressure profile is the function of width of capillaries at constant flow rate (4.8 $\mu\text{l/s}$) and it is between 13.83 Pa and 305.15 Pa.

The developed microfluidic system was tested by intravenous infected full veterinarian blood sample. An adult *Dirofilaria repens* can reach 200 mm length and 0.9 mm width, meanwhile the ovoviviparous larvae is 300 μm long and 5 μm wide.

The authors thank Éva Fok for the biological samples, Danilo Demarchi, Zoltán Fekete for their kind help. The support of the grants TÁMOP-4.2.1. B-11/2/KMR-2011-0002 and TÁMOP-4.2.2/B-10/1-2010-0014 is gratefully acknowledged.

ID: 318

D2: 5

Characterization of the role of contact surface temperature on perception of the hand-transmitted vibration

Manabu Chikai¹, Mohammad Fard² and Hitoshi Miyake¹

¹Nagaoka University of Technology, Japan; ²RMIT University, Australia.

Hand-transmitted vibrations to the human body have significant influences on perception of the vibrations, discomfort and fatigue. For instance, the transmission of the vehicle steering wheel vibrations to the driver body is a major cause of the discomfort and fatigue. However, little is known how human perceive the hand-transmitted vibrations. In this study, it is shown that the hand contact-surface temperature can significantly change the perception of the hand-transmitted vibration by human. A haptic device, which is consisted of a peltier device and a speaker, is developed. This device can therefore produce the “pseudo-sense” to the human. Twelve human volunteers (ten men and two women, age: 22.8 \pm 1.3) were instructed to put their three-finger tips on the device, and they orally answered the pre-defined haptic cognition senses. The presented

senses to the fingers were two 20°C and 40°C temperatures under different vibrations frequencies of 100Hz, 140Hz, 180Hz, 220Hz, and 260Hz generated by the device. The results show that the surface temperature can significantly change/increase the perception of the hand-transmitted vibrations by volunteers. When the contact surface of the device was 20°C, 100Hz and 260Hz were perceived only at the three surface-contacted figures of the volunteers. However, in case of warm contact surface (40°C), the vibration between 180Hz to 220Hz range were not only perceived at the three-fingers, but also at wrists, elbows, and arms of nine volunteers. The importance of the hand-transmitted vibrations between 180Hz and 220Hz and warm contact surface can be justified that the vehicle steering wheel transfers similar vibrations to the hand. Such vibrations have great potential to evoke the “pseudo-sense” of vibrations and sore feeling on the human wrist, elbow, and arm. This mechanism of the perception of the hand-transmitted vibrations may have significant influences on the ride discomfort and fatigue.

ID: 517

D2: 6

Preliminary study on contactless evaluation of peripheral perfusion during rotary blood pump support

Kyosuke Sano¹, Tomoya Kitano¹, Yasuyuki Shiraishi¹, Tomoyuki Yambe¹, A. Tanaka² and M Yoshizawa³

¹Department of Medical Engineering and Cardiology, Institute of Development, Aging and Cancer, Tohoku University; ²Fukushima University, Fukushima, Japan; ³Cyberscience Center, Tohoku University, Sendai, Japan.

Rotary blood pumps are commonly used for circulatory support in the patients with severe heart failure. We proposed a new evaluation method of peripheral perfusions by using a charge-coupled device. There is increasing case for heart rate or pulse wave detection capabilities from the record by charge-coupled devices, such as digital cameras. In this study, we performed animal experiments in goats and examined a quantitative investigation method of peripheral circulation in the organs by a noninvasive and contactless measurement using a digital high speed camera.

Measurements of peripheral blood flow in the organs were carried out in these two steps: a) the validation of the charge-coupled device detection with the laser blood flow meter in the animal experiments, and b) the examination of peripheral perfusing during a centrifugal blood pump assistance.

A simple capture of the goat's peripherals, such as the surface of kidney, lung or skins, allowed a measurement of how the RGB components were distributed within the organ peripherals. The color

components of the images were obtained with the high speed still camera (Casio, EX-F1) at 300 fps. Tissue perfusion in the vicinity of the Venue was also measured by the laser blood flow meter (Omega Flow, FLO-C1) for validation. Then a centrifugal blood pump (Evaheart, SunMedical Technology Research Corp., Japan) was employed and we examined its effects on peripheral blood flow changes.

As a result, we could obtain the pulse wave changes by the analysis of the distribution of green light histogram levels derived from the data. Therefore, it was suggested that our approach of the evaluation of peripheral blood flow distribution by a simple shot of digital cameras might achieve the evaluation of the effects of surgical treatment on peripheral organs with the rotary blood pump support.

Session	SYM-03A: Micro and Nanofluidics for Biomedical Applications
Date/Time	4 December 2013 14:45–16:15 hrs
Venue	SR-12

ID: 542 **SYM-03A: 1**

Symposium Keynote:
Measuring cell mechanics for medicine

Dino Di Carlo

University of California, Los Angeles, United States of America.

Cell deformability (i.e., the ability to change shape under an applied force) is a promising intrinsic and low-cost marker indicative of underlying structural changes associated with various disease processes and changes in cell state. We are combining precision microfluidic control of cells with automated high-speed image analysis for high-throughput cell classification based on intrinsic biomechanical properties. I will first discuss general strategies we are developing to passively manipulate particles and fluids using simple geometric modifications within microchannels. Our approaches make use of fluid inertia, generally neglected in microfluidic systems, to create well-defined directional forces and fluid deformations that can be combined in a sequential and hierarchical manner to program complex particle and fluid motions. Low complexity modular components to manipulate cells, particles, and fluid streams in which inertial fluid physics is abstracted from the designer has the capability transform biological, chemical, and materials automation in a similar fashion to how modular control of electrons and abstraction of semiconductor physics transformed computation. We apply these fundamental techniques to position cells for high-speed fluid-based

deformation and optical analysis. The “deformability cytometer” instrument shows promise in identifying cancer cells, activated white blood cells, and stem cells in mixed populations for a variety of clinical and regenerative medicine applications.

ID: 136 **SYM-03A: 2**

Integrated microfluidics for cellular functional immunophenotyping

Jianping Fu

University of Michigan, Ann Arbor, United States of America.

Rapid, accurate, and quantitative characterization of immune status of patients is of utmost importance for disease diagnosis and prognosis, evaluating efficacy of immunotherapeutics and tailoring drug treatments. Immune status of patients is often dynamic and patient-specific, and such complex heterogeneity has made accurate, real-time measurements of patient immune status challenging in the clinical setting. Recent advances in microfluidics have demonstrated promising applications of the technology for immune monitoring with minimum sample requirements and rapid functional immunophenotyping capability. In this talk, I will discuss our recent efforts in developing integrated microfluidic immunomonitoring platforms that can perform rapid, accurate, and sensitive cellular functional assays at the single-cell level on different types or subpopulations of immune cells, to provide an unprecedented level of information depth on the distribution of immune cell functionalities. Such innovative tool will allow comprehensive and systems-level immunomonitoring in the clinical setting, unlocking the potential to transform experimental clinical immunology into an information-rich science. Our microfluidics-based technology can serve as a comprehensive and standardized immune monitoring platform to define and characterize the “immunotype” of healthy individuals and patients before, during, and after targeted immunomodulation. Our research, if successful, will have a transformative long-term impact to revolutionize management of patients with immune diseases and immune system disorders.

ID: 813

SYM-03A: 3

Microfluidic *in-vitro* platform for imaging metastasis: perfusable microvascular networks and cancer cells on a microfluidic chip

Noo Li Jeon^{1,2}, Sudong Kim¹, Hyunjae Lee² and Minhwan Chung¹

¹School of Mechanical and Aerospace Engineering, Seoul National University, South Korea; ²Division of WCU Multiscale Mechanical Design, School of Mechanical and Aerospace Engineering, Seoul National University.

In-vivo imaging has provided significant insights to different mechanisms involved in cancer metastasis. An *in-vitro* experimental platform that reproduce cancer microenvironment with blood vessels, tumors, immune cells and others would allow more detailed experiments with more experimental conditions can complement the animal studies.

We describe a reproducible, *in vitro* approach to grow perfusable 3D microvascular networks on a microfluidic chip. These engineered blood vessels exhibit morphological and biochemical markers of tight junctions, apical-basal polarity, basement membrane deposition, and upregulated markers in response to inflammatory cues.

A novel microfluidic device was designed and tested for real-time imaging of various steps of cancer metastasis. Perfusable microvascular networks formed within the microfluidic device reproduce the 3D cellular niche, facilitating high-resolution live imaging of cancer cell extravasation. This approach provides a platform for developing physiologically complex but experimentally straightforward human disease models and holds potential for medical and pharmaceutical applications in drug screening and basic cancer biology.

ID: 205

SYM-03A: 4

Ultra-high throughput enrichment of viable circulating tumor cells

Majid Ebrahimi Warkiani¹, Guofeng Guan^{1,2}, Bee Luan Khoo³, Daniel Shao-Weng Tan⁵, Soo Chin Lee⁶, Chwee Teck Lim^{1,3,7}, Jongyoon Han^{1,7}, Alvin S.T. Lim⁸, Wan-Teck Lim⁴, Yoon Sim Yap⁴ and Ross A. Soo⁵

¹Singapore-MIT Alliance for Research and Technology (SMART), Singapore; ²Department of Mechanical Engineering, National University of Singapore, Singapore; ³Mechanobiology Institute, National University of Singapore, Singapore; ⁴Department of Medical Oncology, National Cancer Centre Singapore, Singapore; ⁵Departments of Hematology-Oncology and Pharmacology, National University Hospital, Singapore; ⁶Department of Bioengineering, National University of Singapore, Singapore; ⁷Department of Electrical Engineering and Computer Science, Department of Biological Engineering, Massachusetts Institute of Technology, Cambridge, Massachusetts, USA; ⁸Department of Pathology, Singapore General Hospital.

Detection, enumeration and characterization of rare circulating tumor cells (CTCs) from the peripheral blood of cancer patients potentially provide critical insights into tumor biology and is promising for cancer diagnosis and prognosis. Here, we present a novel multiplexed spiral microfluidic device for ultra-high throughput, label-free enrichment of CTCs from clinically relevant blood volumes. The fast processing time of the technique (7.5 mL blood in <5 min) and high sensitivity of the device lends itself to a broad range of potential genomic and transcriptomic applications. The method can specifically separate and preserve all fractions of blood (i.e., plasma, CTCs and PBMC) for diverse downstream analysis. CTCs were detected from 100% (10/10) of blood samples collected from patients with advanced stage metastatic breast (12-56 CTC/ml) or lung cancer (30-153 CTC/ml). Cancer cells were characterized with immunostaining and fluorescence in situ hybridization (FISH) (HER2/neu). Retrieved cells were unlabelled and hence more viable for propagation and other informative analysis such as the next generation sequencing (NGS) to guide treatment and individualized patient care.

Session	SYM-02B: Gastrointestinal Motility Symposium (cont'd)
Date/Time	4 December 2013 16:45–18:15 hrs
Venue	Auditorium

ID: 534 SYM-02B: 1

An interdisciplinary approach to understanding gastrointestinal slow wave electrophysiology

Peng Du¹ and Leo Cheng^{1,2}

¹The University of Auckland, New Zealand; ²Vanderbilt University, Nashville, TN, USA.

Propulsion of content through the digestive tract is due to the coordinated contractions and relaxations of the smooth muscles in the gut wall. The motility of the gastrointestinal tract is underpinned by an electrophysiological event called slow wave activity. Many other physiological factors, such as neural and hormonal factors, also present a significant level of regulation on both slow waves and motility. In recent years, high-resolution electrical mapping has yielded significant insight to the organization of slow wave activity *in-vivo*, both in normal as well as pathological conditions. One significant experimental finding has been the description of slow wave dysrhythmias recorded from patients with clinically significant digestive diseases such as diabetic and idiopathic gastroparesis. Accompanying these new findings regarding slow wave activity is a series of mathematical models that have been applied to perform predictive simulations capable of giving further insights to the mechanistic behaviors of slow waves under different physiological conditions. In particular, the multi-scale modeling approach has been utilized to great success to integrate experimental data from multiple recording modalities and infer the relationship between slow waves and gastrointestinal functions. Ultimately, the research efforts aim to develop a “virtual stomach” for simulation of how food is digested and how different pathological factors can influence digestive health.

ID: 563 SYM-02B: 2

A biophysically-based tissue model for optimizing gastric pacing

Shameer Sathar, Greg O’Grady, Mark L. Trew and Leo K. Cheng

Auckland Bioengineering Institute, The University of Auckland, New Zealand.

Gastric pacing has been investigated for modulating gastric motility in diseased states. However, to advance this field, new pacing protocols are needed that directly improve gastric motility while

increasing the efficiency of existing pacing devices. This study presents a mathematical tissue model for investigating slow wave entrainment during pacing, its comparison with experimental data gathered by high-resolution electrical mapping. The model was used to predict the effect anisotropic conductivities on slow wave entrainment, and the effect of gastric pacing on ectopic dysrhythmias. A diffusion based slow wave propagation model was used, with cell activity modeled as a finite-state machine. Initially, normal slow-wave antegrade propagation was modeled in accordance with experimental data. Then, these simulation parameters were applied to compare the model, in tandem with experimental studies in which an external pacing signal entrains native slow wave activity. The effect of different pacing frequencies on entrainment was demonstrated. Finally, this model was also used for simulating the effect of external stimuli for entraining a distal ectopic focal pacemaker. Two cases were studied with different fiber directions. The results showed that the pacing frequency and orientation of the fibers relative to the stimulation and ectopic site plays a critical role in gastric pacing efficacy.

ID: 600 SYM-02B: 3

A coupled model of the gastrointestinal smooth muscle cell electromechanics

Nicholas Cheng, Cheuk Wang Chung, Alberto Corrias and Martin Buist

NUS, Singapore.

Normal gastrointestinal (GI) motility, brought about by the coordinated contraction and relaxation of smooth muscle cells, is essential for good health. Impaired GI motility has been associated with diseases such as achalasia, gastroparesis, intestinal pseudo-obstruction, and irritable bowel syndrome, although the causal links to specific mechanisms are not well established. Motility is essentially the mixing and transport of ingested contents via smooth muscle contractions, and the contraction of a smooth muscle cell is underpinned by its electromechanics, being the interactions between the electrical activity of the cell and its mechanical behaviour. The electromechanical coupling within a smooth muscle cell can be divided into two phenomena: excitation-contraction coupling, and mechano-electric feedback. Excitation-contraction coupling refers to the onset of cellular contraction due to an increased intracellular calcium concentration that occurs in response to cellular depolarization, while mechano-electric feedback refers to the modulation of a cell’s electrical activity by virtue of its mechanical state. While computational models have been constructed that

describe the electrophysiology and the biomechanics of GI smooth muscle contraction individually, to date no strongly coupled model of GI cellular electromechanics has been developed which incorporates these two aspects. Here we present such an electromechanical smooth muscle cell model which is based on the underlying cellular biophysics. This represents a significant step towards providing a better understanding of GI motility and its related pathologies.

ID: 374

SYM-02B: 4

An image-based model of the interstitial cells of Cajal network in the gastrointestinal tract

Ruchi Vyas¹, Jerry Gao¹, Leo K. Cheng^{1,2} and Peng Du¹

¹University of Auckland, New Zealand; ²Department of Surgery, Vanderbilt University, Nashville, TN, USA.

Gastrointestinal (GI) electrical activity is generated by pacemaker cells called the interstitial cells of Cajal (ICC), which are located throughout the GI tract. An extended description of the variations of ICC may help improve our understanding of digestive functions. The main aim of this study is to create an image-based structural model of an extended ICC network. Feature extraction techniques were applied to dual-stained images of ICC to obtain cell distribution, fiber orientation and connectivity. In a sample image, 20 nuclei were isolated and the cell bodies were joined perpendicular to each other in a grid-like network with two principal axes orientated at approximately 20 and 80 degrees to the vertical axis. An extended virtual network model was developed to resemble the cell count and orientation. In conclusion, an extended image-based virtual ICC network was generated. This network model can be adapted to generate the ICC network structure required for large-scale GI electrical simulations and to predict the functional significance of ICC loss in diseases.

ID: 602

SYM-02B: 5

Modeling the role of pdgfr α + cells in enteric inhibitory neurotransmission

Jing Wui Yeoh, Alberto Corrias and Martin Lindsay Buist

National University of Singapore, Singapore.

Activation of enteric inhibitory motor neurons induces inhibitory junction potentials (IJPs) causing gastrointestinal (GI) muscle relaxation. The IJPs of many GI muscles are biphasic, with an initial fast hyperpolarization, due to purinergic neural input, followed by a second long-lasting hyperpolarization caused by nitrergic neurotransmission. The disruption of inhibitory neuromuscular transmission is the

key feature of several GI motility disorders, e.g., Achalasia, Gastroparesis, and Hirschsprung's disease. Impaired nitrergic neurotransmission has been implicated in the pathophysiology of many diseases. On the other hand, the pathophysiology of inhibitory purinergic neurotransmission is still poorly understood. A novel platelet-derived growth factor receptor α -positive cell (PDGFR α + cell) has recently been identified, and appears to be involved in mediating the purinergic inhibitory neural control of GI tract motility. These cells have been found to express abundant purine receptors (P2Y₁) and apamin-sensitive small conductance calcium-activated potassium channels (SK₃). The large amplitude transient outward currents generated by SK₃ channels after being activated by cytosolic Ca²⁺ may hyperpolarize the smooth muscle membrane potential via gap junctions, causing muscle relaxation. Here, we present a quantitative computational model describing a possible mechanism through which PDGFR α + cells act in the enteric purinergic inhibitory control of GI tract motility. In accordance with recent experimental recordings, this model describes how the binding of neurotransmitters from enteric motor neurons to the cell receptors triggers the increase in cytosolic Ca²⁺ concentration, and ultimately leading to the large transient outward currents through the activation of the SK₃ channels. The model has been validated by comparison with available experimental data and good agreement was found in terms of amplitude, duration, and shape under normal and pharmacologically-altered conditions. The presented model may be useful in the study of the pathophysiology of purinergic neurotransmission in the GI tract.

ID: 601

SYM-02B: 6

Potential pitfalls in the development of electrophysiological models

Martin L. Buist and Alberto Corrias

National University of Singapore, Singapore.

Our group has previously developed several models of GI cell electrophysiology, and each of these is essentially a collection of ion channel models weighted by their relative ionic conductances in the target cell type. Experimental voltage clamp data is essential for parameterizing such ion channel and cellular mathematical models, and for furthering our understanding of ion channel kinetics. However, when using data from voltage clamp experiments there are a number of confounding factors which means there is not always an obvious relationship between the specified voltage clamp protocol and the resulting cellular response. This work was motivated by an observation that some of the readily available

online tools do not properly account for these confounding factors, and therefore models developed using these tools may not provide a true representation of the underlying channel kinetics. The main source of error is that the clamp potential specified by the control software of the experimental apparatus differs from the membrane potential experienced by the cell. This can be due to several factors such as the composition of the bath and pipette solutions, and the access resistance. Interestingly, the opening and closing of ion channels, whose kinetics are the targets of such experiments, also changes the relationship between the imposed clamp potential and the cell membrane potential. In this presentation these error sources and the procedures necessary to minimize their impact when creating mathematical models will be discussed with examples from ion channels present in the GI musculature.

Session	A3: Bioelectronics
Date/Time	4 December 2013 16:45–18:15 hrs
Venue	SR-01 & 02

ID: 117 **A3: 1**

Feature analysis of myocardial ischemia based on T wave alternans

Song Jinzhong, Yan Hong, Xu Zhi, Yu Xinming and Li Yanjun

China Astronaut Research and Training Center, China.

Electrocardiogram (ECG) is an economic, non-invasive, and convenient tool in myocardial ischemia (MI) detection, whose clinical indicator is mainly exhibited by ST-T complex (namely, ST-segment and T-wave).

In this paper myocardial ischemia was analyzed based on T wave Alternans (TWA) both in time domain and in frequency domain. The characteristic in frequency domain was mainly T wave alternans ratio, whose extracted parameters from ECG signals included TWAR_{Tp}, TWAR_{Tb}, TWAR_{Te}, TWAR_{MIN}, TWAR_{MEAN}, and TWAR_{RESAMP}. Meanwhile, the characteristic (TWA magnitude) in time domain was analyzed based on correlation analysis, whose extracted parameter was ACM.

A significant difference was reached based on ACM analysis After European ST-T database (namely, MI database) and Normal ECG database verification. On the other hand, another significant difference based on ACM was reached After MIT-BIH database (namely, Arrhythmia database) verification, what's more, it was more distinguished than the one in MI analysis. Experimental results showed that the TWA features played a useful role in myocardial ischemia detection.

ID: 193 **A3: 2**

Phase detection for electric field body scanner

Ichiro Hieda¹ and Ki-Chang Nam²

¹National Institute of Advanced Industrial Science and Technology (AIST), Japan; ²Yonsei University College of Medicine, Korea.

The authors are studying a technique to measure moisture distribution inside the human body by applying weak electric field at radio frequency (RF), 1 to 60MHz. RF signal is fed to an antenna that is as small as a few centimeters square, and the same type of antenna measures electric field intensity where two antennas are located 15 to 50 cm apart from each other. A portion of the living human body located between the antennas affects the signal intensity at the measurement side. Because of the principle, the method does not provide fine resolution. However, it has such advantages as simple, safe and cost-effective so that it can be used for health care, screening of medical care, and device for handicapped and elderly.

The recent experiments gave different patterns of signal changes caused by the human body and a phantom. Unlike the phantom that consisted of a small acrylic tank filled with water, the human body connected to the earth by electrostatic induction that was caused by relatively larger dimensions of the human body compared to the water tank. Measurement of the signal phases is thought to help discriminating the losses caused by the electrostatic induction from signal increments cause by water permittivity.

The experimental system has been upgraded to measure signal phases that used to measure signal strength only. This paper introduces the new system and reports experiments where portions of the human body are measured by the system as well as water tank phantom for the comparison. Validity of the phase measurement is discussed with the results.

ID: 285 **A3: 3**

Theoretical study of non-equilibrium ionic response near electrode surface

Kentaro Doi¹, Makusu Tsutsui², Takahito Ohshiro², Masateru Taniguchi², Tomoji Kawai², Massimiliano Di Ventra³ and Satoyuki Kawano¹

¹Graduate School of Engineering Science, Osaka University, Japan; ²The Institute of Scientific and Industrial Research, Osaka University, Japan; ³University of California, San Diego, USA.

Recently, single-molecule detection using nanofluidic devices have attracted much attention, such as DNA

sequencing via biological or solid-state nanopores. However, there are some difficulties to achieve it, since single molecules are tremendously affected by surrounding environments, such as thermal fluctuations and external perturbations. In such a nano-scaled confined space, electrophoretic or electroosmotic flows become effective. Moreover, due to very weak electrical signals of a single molecule, high-resolution current measurement is also crucial. On the other hand, noise in the background current should be suppressed properly to clearly recognize signals. In order for the optimal design, the ionic flow has to be understood in more detail. Herein, focusing on ionic currents in aqueous solution, we develop a theoretical model and analyze responses of ions near a biased electrode surface. Diffusion and migration of ions in non-uniform electric fields can be expressed by coupling the Nernst-Planck equation and the Poisson equation. Solving both equations self-consistently, density distributions can be determined. In this study, transient responses of some kinds of aqueous solution are investigated. As a result, rapid increase and subsequent slow decay of ionic current can be replicated well. It is found that the response time depends on rapid screening of a strong field near the electrode surface and slow change of a diffusion layer far from the surface. This is a reason why it takes long time period until the solution gets to a steady current state.

ID: 140

A3: 4

SAR computation and channel modeling of body area networks

Zhangyong Li, Yu Pang, Jinzhao Lin, Jie Liu, Shengrong Liu and Chunyang Li

Chongqing University of Posts and Telecommunications, China.

Body Area Networks (BANs) is of importance for telemedicine and telehealth services, so cause attractiveness for engineers. Since the wireless sensor nodes adhere to the human body surface, the human body unavoidably absorbs the electromagnetic wave which may be harmful, so investigating the specific absorption rate becomes significant in exploration of BANs. Additionally, the BAN channel is different with the common wireless channel because the communication distance is very short and the electromagnetic wave propagates along the body surface. In this paper, we focus on calculating Specific absorption rate (SAR) values and exploring wireless channel in different frequencies. Firstly, we design a model approximate to human tissues including skin, fat, muscle and internal organs, then compute SAR values by placing antennas in 900MHz, 2.4GHz and 5GHz. Then we provide theoretical analysis for the

BAN channel. A model is constructed to calculate the path loss values in different distance and a power delay profile is proposed to generate frequency response of human body communication in UWB frequency.

The author gratefully acknowledges the support of K.C. Wong Education Foundation, Hong Kong.

ID: 339

A3: 5

Gastric lymph node cancer detection using multiple features support vector machine for pathology diagnosis support system

Takumi Ishikawa¹, Junko Takahashi¹, Hiroshi Takemura¹, Hiroshi Mizoguchi¹ and Takeshi Kuwata²

¹Tokyo University of Science, Japan; ²National Cancer Center Hospital East, Japan.

In this paper, an automatic cancer detection method that combines multiple features to support pathologists is presented. Cancer is the most cause of death in Japan, and patients suffering with and who die of cancer are increasing every year, while the number of pathologists is almost constant. Such issues increase the burden on the pathologists and causes service degradation for the patients. One of the ways which resolve these pathologists' issues is a double checking by pathologists and systems. The method was proposed for detecting cancer in the Pathology diagnosis support system to introduce a double checking. The proposed method combined three image features, Higher-order Local Auto-Correlation (HLAC) feature, Wavelet feature, Delaunay feature, in varying weights. At first, the features was calculated from HE stained gastric lymph node images. We connected each feature into one vector of varying combinations of the features, and discriminate cancer and no cancer by Support Vector Machine (SVM). Cancer detection rates with most combinations of more than two features were better than just one feature. In addition, by changing the scale of Delaunay in 35-order HLAC, Delaunay and Wavelet combination vector, sensitivity was improved. In the best performance, sensitivity and specificity were 95.7% and 82.1% respectively. Therefore, the proposed method can be used for a double check system.

ID: 757

A3: 6

Analysis of SELDI-TOF-MS using support vector regression for ovarian cancer identification

Isye Arieshanti and Yudhi Purwananto

Institut Teknologi Sepuluh Nopember, Indonesia.

The analysis of protein expression profile using SELDI-TOF-MS can assist early detection of ovarian cancer. The chance to save patient's life is greater when ovarian cancer is detected in early stage. However, the analysis of protein expression profile is challenging because it has very high dimensional features and noisy characteristic. In order to tackle these limitations, the Support Vector Regression model to identify ovarian cancer is proposed. We can show that the performance of the model to discriminate the protein expression profile with cancer disease from the normal ones can reach accuracy 99%, specificity 99% and sensitivity 100%. This result shows that the model is promising for SELDI-TOF-MS analysis in Ovarian Cancer identification.

Session	B3: Biological Materials
Date/Time	4 December 2013 16:45–18:15 hrs
Venue	SR-03 & 04

ID: 519

B3: 1

Nanobioactive hydrogel for myocardial therapy applications

Arghya Paul^{1,2,3}, Hamood Al Kindi⁴, MD Anwarul Hasan^{1,2}, Akhilesh Gaharwar^{1,2,3}, Mehdi Nikkha^{1,2}, Mehmet R. Dokmeci^{1,2}, Dominique Shum-Tim⁴ and Ali Khademhosseini^{1,2,3}

¹Centre for Biomedical Engineering, Brigham and Women's Hospital, Harvard Medical School; ²Harvard-MIT Division of Health Sciences and Technology, Massachusetts Institute of Technology; ³Wyss Institute for Biologically Inspired Engineering, Harvard University; ⁴Division of Cardiac Surgery and Surgical Research, McGill University.

Background: Cardiovascular disease, in particular ischemic heart disease, is one of the leading causes of death worldwide. A major limitation in treating such cardiac injuries is the failure of currently available pharmacologic therapies to address the loss of functional cardiomyocytes leading to subsequent cardiac dysfunction. Injectable hydrogel based therapeutic gene delivery to promote myocardial angiogenesis can be a potential alternative strategy to treat acute myocardial infarction (AMI). Here we have developed and characterized a new nano-graphene oxide (GO) based gene delivery system using

photo-crosslinkable low methacrylated injectable gelatin hydrogel (GelMA) for controlled delivery of pro-angiogenic vascular endothelial growth factor genes (Vegf) to the injured site. The synergistic therapeutic effects of the GO_{Vegf} and GelMA hydrogel, upon co-injection, were also investigated in a rat model with AMI.

Methods and Results: The GO nanosheets, surface functionalized with cationic branched polyethylenimine (PEI) polymer, exhibited highly efficient *in vitro* gene delivery and subsequent Vegf protein over-expression in rat cardiomyocytes, confirmed quantitatively by ELISA. *in vitro* biofunctional assays also demonstrated significant proliferation and migration effects of the released Vegf protein on vascular endothelial cells, thus confirming its strong angiogenic activities. For *in vivo* analysis, GO_{Vegf}/GelMA was intramyocardially injected to AMI rat model. Two weeks post AMI results showed increase in capillary density and reduction in ventricular scar areas ($p < 0.05$, $n=7$) in GO_{Vegf}/GelMA compared to only GelMA_{Vegf} and untreated control groups. Furthermore, the GO_{Vegf}/GelMA group showed higher cardiac performance in echocardiography compared to other groups ($p < 0.05$).

Conclusion: Take together, this data demonstrates that intramyocardial delivery of GO_{Vegf} carrying GelMA hydrogel can significantly mitigate the negative cardiac remodeling, promote local angiogenesis and attenuate ventricular dysfunction post-MI. Consequently, the results obtained in this study indicate the potential of gene activated nano-GO hydrogel for myocardial therapy and wound healing applications.

ID: 862

B3: 2

Natural patches from the heart to the infarct: functional improvements and induced vascularization towards regeneration of a scarred tissue

Hadar Sarig¹, Udi Sarig¹, Su Yin Chaw¹, Elio de Berardinis¹, Vaibavi S. Ramanujam², Rufaihah B.A. Jalil², Vu D. Thang², Dror Seliktar^{2,3}, Theodoros Kofidis², Freddy Yin Chiang Boey¹, Subbu Venkatraman¹ and Marcelle Machluf^{1,4}

¹School of Material Science Engineering (MSE), Nanyang Technological University (NTU), Singapore; ²Yong Loo Lin School of Medicine: National University of Singapore (NUS), Singapore; ³Faculty of Biomedical Engineering, Technion, Israel Institute of Technology (IIT), Israel; ⁴Faculty of Biotechnology and Food Engineering, Technion, Israel Institute of Technology (IIT), Israel.

We previously reported the isolation of porcine cardiac extracellular matrix (pcECM) exhibiting

matched myocardial bio-mechanical properties *in vitro* (Eitan, Y. et al., 2010). Here we further characterize this biomaterial as a patch treatment for acute phase myocardial infarction (MI) in rats.

Wistar rats (n=24) were divided into 3 groups: patch implantation after MI, non-treated MI (negative control) and sham operation (positive control). MI was induced by lateral artery descending ligation. Patches were sutured onto the anterior wall of the infarct site. All rats were weighed and echocardiographic and ECG parameters were recorded before and after procedures for up to 4 weeks. During sacrifice cardiac hemodynamics were recorded; carcasses and harvested hearts were histo-pathologically evaluated.

Patch treated rats displayed significant improvement (t=30 days, $p < 0.01$) in average percentage weight gain compared with the non-treated controls ($135 \pm 7\%$ and $119 \pm 2\%$, respectively), similarly to the sham group ($130 \pm 8\%$, $p > 0.05$). Concomitantly, cardiac functional parameters of treated rats (ejection fraction, EF; fractional shortening, FS; and fractional area change, FAC) were similar to the sham and significantly better ($p < 0.01$) than the negative control (EF= 88.7 ± 2.0 , 79.8 ± 6.4 and 49.5 ± 5.1 ; FAC= 86.4 ± 5.2 , 90.2 ± 7.6 and 48.0 ± 5.2 ; FS= 80.9 ± 8.2 , 135.1 ± 30 , and 26.4 ± 8.0 , respectively). Additional results of cardiac hemodynamics and histological analyses will be also presented providing further evidence for functional improvements that are associated with highly yet transiently induced vascularization of treated infarcts.

Taken together these results affirm the potential of thin acellular pcECM for the possible treatment of MI and end-stage heart failure in a patch deposition modality.

ID: 106

B3: 3

The different roles of collagenous matrices from different origin on Human Tendon Stem/Progenitor Cells fate-decision

Zi Yin, Ting Zhu, Jiajie Hu, Xiao Chen and Hongwei Ouyang

Zhejiang University, China.

Tendon stem/progenitor cells (TSPCs) may serve as an optimal seed cells to restore normal structure and function to injured tendons. However, the favorable extracellular microenvironment for directing TSPCs into tenocytes exclusively is still unclear. The hypothesis of this study was that the tendon-derived matrix may be the ideal substrate for TSPCs commitment. We examined the impact of collagenous matrices derived from different tissues (tendon, bone and dermis) on the fate decision of human tendon stem/progenitor cells (hTSPCs) and assessed the role

of the optimal matrix in forming functional engineered tendon for tendon repair. The multipotency of TSPCs toward osteogenesis, adipogenesis and chondrogenesis was confirmed. We found that all three matrices supported the adherence and proliferation of hTSPCs. We found that there was an increase in tendon specific genes expression after growing on tendon derived matrix, whereas osteogenic genes were upregulated in cells growing on demineralized bone matrix. Furthermore, we constructed an engineered tendon with TSPCs and tendon-derived matrix, and assessed the efficacy of this engineered tendon for Achilles tendon reconstruction. The histological morphology, immunohistochemistry, collagen concentration and mechanical properties of the repaired tissue were evaluated. We found that the engineered tendon showed much better structural and mechanical properties of repaired tendon than control group. In conclusion, the natural extracellular matrix derived from tendon could serve as an optimal scaffold for tendon regeneration. These findings demonstrate a practical strategy of utilizing TSPCs integrate with native tissue ECM for tendon regeneration and may assist in future treatment to tendon diseases.

ID: 821

B3: 4

Protein and cell therapeutics using polymeric hydrogel carriers

Dror Seliktar

Technion - Israel Institute of Technology, Israel.

In the near future, hydrogels are expected to play a much greater role in biomedicine, changing the way we approach issues in stem cell research, cancer biology, drug discovery, tissue engineering and biotechnology. The development of improved methods to synthesize cell-compatible biomedical hydrogels to accommodate this trend depends on a thorough understanding of the design possibilities and the limitations. While biological systems provide an exceptional source of design inspiration for creating cell-compatible hydrogels, man-made water-soluble polymers and polymer chemistry have contributed to the establishment of better control over the properties and reliability of the polymeric macromolecules, and subsequently, better control over the properties of the hydrogels they form. This presentation covers a few of the advanced design principles currently being applied to engineer cell-compatible biomedical hydrogels, with specific focus on how sophisticated new hydrogels may lead the way to new discoveries in basic science, clinical medicine and biotechnology.

ID: 473

B3: 5

Polycaprolactone fibers gellation with gelatin ground substance: engineered skin extracellular matrix aims for using as tissue engineering skin

Oraphan Chaisiri¹, N. Chanunpanich² and B. S. Hanpanich¹

¹Department of Biomedical Engineering, Faculty of Engineering, Mahidol University, Nakhon Pathom, Thailand; ²Department of Industrial Chemistry, Faculty of Applied Science, King Mongkut's Institute of Technology North Bangkok, Bangkok, Thailand.

Skin tissue regeneration was recently focused on the reconstruction and development of biomaterials to produce artificial skin for patients with skin lost defects. The research was focused on the design of an effective scaffold containing fibrous elements and ground substance mimicking the natural dermal extracellular matrix (ECM), supporting cell interaction and promoting cell growth [5]. The biomaterials selection, fabrication and modification are crucial processes for scaffold designing.

This study used Polycaprolactone (PCL) and gelatin as ECM fiber and ground substance, respectively. PCL and Gelatin was blended in tetrafluoroethanol (TFE) solvent. The mixtures were then fabricated with various electrospinning parameters. In order to enhance a material pore size supporting cell migration, and modified ground surface by using rubber pattern to obtain a proper woven fibers sheet. The efficient ground substance was then created by gellation of the gelatin fiber to insert in the sheet. Morphology observation by scanning electron microscope (SEM) showed the success of the ground substance creation and that gels infiltration between fibers of the scaffold structure had occurred. The pore size of scaffold was 40–70 micron and 98–99% of porosity. Cytotoxicity tests using primary human fibroblast cells treated with scaffold extracted solution showed that more than 90% of cells could survive. The biodegradation appeared to have an increase statistically significant with enhanced time duration of contact with media. For cellular biocompatibility tests, our engineered scaffold was co-cultured with primary human fibroblasts. The results showed that the migration and proliferation of cells can be found inside the scaffold. Our preliminary result shows that the addition of ground substance component, gelatin, can support cellular migration and attachment, which are important factors for wound healing. Further study is to co-culture dermal scaffold with primary human keratinocyte to create epidermis layer to be full-thickness skin for advanced clinical applications.

ID: 273

B3: 6

Novel scalable silicone elastomer and poly(2-hydroxyethyl methacrylate) (PHEMA) composite materials for tissue engineering and drug delivery applications

Soumyaranjan Mohanty¹, Mette Hemmingsen¹, Magdalena Wojcik², Martin Alm², Peter Thomsen², Martin Dufva¹, Jenny Emnéus¹ and Anders Wolff¹

¹Technical University of Denmark, Denmark; ²BioModics ApS, Denmark.

In recent years hydrogels have received increasing attention as potential materials for applications in regenerative medicine. They can be used for scaffold materials providing structural integrity to tissue constructs, for controlled delivery of drugs and proteins to cell and tissues, and for support materials in tissue growth. However, the real challenge is to obtain sufficiently good mechanical properties of the hydrogel. The present study shows the combination of two normally non-compatible materials, silicone elastomer and poly(2-hydroxyethyl methacrylate) (PHEMA), into a novel composite material with increased hydrophilicity in regard to virgin silicone elastomer, making it suitable as a scaffold for tissue engineering and with the concomitant possibility for delivering drug from the scaffold to the tissue.

Interpenetrating polymer networks (IPNs) of silicone elastomer and PHEMA was produced using supercritical carbon dioxide (scCO₂) as the swelling agent. By removing the scCO₂ an IPN of hydrogel and silicone elastomer was obtained, capable of absorbing water just like a traditional hydrogel, but with remarkably increased mechanical properties.

The biocompatibility of the IPN composite material was investigated using live/dead staining of hepatocytes (HepG2) growing on the polymer, showing excellent viability compared to the control polystyrene. Combinations of different types of silicone elastomers and different percentages of hydrogel were also investigated.

Finally, the model drug doxycycline (a tetracycline analogue) was loaded into the hydrogel of the IPN, and the release of the doxycycline was studied using a doxycycline regulated green fluorescent reporter gene expression assay: HeLa cells grown on the IPN composite material, previously loaded with doxycycline, were transfected with the pTRE-Tight-BI-DsRed-Express plasmid, consisting of a bidirectional tetracycline sensitive promoter. The transfected HeLa cells, expressing the Tet-On transactivator, responded nicely to the release of doxycycline from the IPN composite material by the expression of green fluorescent protein. This demonstrates the potential for combined scaffold and controlled drug delivery material.

Session	C3: Cardiovascular Mechanics Computational Mechanics
Date/Time	4 December 2013 16:45–18:15 hrs
Venue	SR-05 & 06

ID: 698

C3: 1

Effects of stent design on an emerging clinical issue of longitudinal stent compression

Chun-Ting Yeh, Chun Wang, Dian-Ru Li, Chun-Pei Chen and Hao-Ming Hsiao

National Taiwan University, Taiwan.

In recent years, interventional cardiologists have discussed over an emerging clinical issue called longitudinal stent compression (LSC), a new failure mode not previously observed and reported in coronary stents. This phenomenon occurs when the physician attempts to cross the deployed stent with other devices, such as post-dilation balloons, guide catheters, or intravascular ultrasound (IVUS) catheters, causing the stent to dramatically shorten when the two devices are accidentally entangled. If left untreated, it may increase the risk of stent thrombosis or restenosis. While this phenomenon has been observed with a number of stent designs, it seems more common with the Omega/Element stent. In this paper, a computational LSC model using finite element analysis was developed. A systematic investigation was conducted in attempts to quantify individual contribution of the stent design pattern, connector number, and connector Venue on LSC. Computational simulations were performed on two representative coronary stents resembling Omega/Element and Driver/Endeavor for comparison. Simulation results show that the connector number plays the most significant role in the development of the LSC issue. The LSC could be easily tripled or quadrupled for the same stent design simply by increasing the connector number from two to three. The design pattern plays a secondary role in LSC. The LSC could be improved by up to 30% when the design pattern changes from the offset peak-to-peak design (Omega/Element) to the peak-to-peak design (Driver/Endeavor). It was also found that the LSC could be doubled for the Omega/Element stent with two connectors simply by rearranging the connector Venue. This small design tweak could help improve the current Omega/Element LSC significantly, while still maintaining the majority of its excellent deliverability. The findings from this paper could provide great insights into this emerging clinical issue and help optimize future stent design to reduce the associated risk involved in LSC.

ID: 328

C3: 2

In-silico study of the nasal cavity's influence on the pharyngeal wall pressure in anatomically-correct airway models of patients with obstructive sleep apnea

Julien Cisonni¹, Anthony D. Lucey¹, Andrew J. C. King¹, Syed M. S. Islam^{1,2} and Mithran S. Goonewardene²

¹Curtin University, Australia; ²University of Western Australia, Australia.

Repetitive brief episodes of soft tissue collapse within the upper airway during sleep characterize obstructive sleep apnea (OSA), an extremely common and disabling disorder. Failure to maintain the patency of the airway is caused by the combination of sleep-related loss of compensatory dilator muscle activity and aerodynamic forces promoting closure. These forces are generated by negative intraluminal pressure resulting from the circulation of inspiratory airflow in anatomically predisposed airways mainly characterized by narrower lumen and increased wall compliance. The prediction of soft tissue movement in patient-specific airway 3D mechanical models is emerging as a useful contribution to clinical understanding and decision-making. Such modeling requires reliable estimations of the wall pressure forces. While nasal obstruction has been recognized as a risk factor of OSA, it is generally accepted that for most OSA patients, soft tissue collapse occurs during inspiration in the pharynx which is therefore the most common region of interest in both treatment interventions and fluid-structure interaction modeling studies. For OSA applications, the need to include the nasal cavity in airway models requires consideration, as it is most often omitted because of its complex shape. Moreover, the diversity of its components makes it difficult to obtain accurate numerical representations of this part of the airway using tomography techniques and the subsequent meshing process of the volumetric models is problematical. Thus, the present study investigates in-silico the effect of the omission of the nasal cavity on the pharyngeal airflow properties in anatomically-correct models of the airway. The hypothesis underpinning this work is that adequate boundary conditions and simple artificial geometric extensions can reproduce the essential effects of the nasal cavity as an inspiratory airflow conditioner on the pharyngeal flow field and thereby reduce the overall complexity and computational cost of accurate simulations of upper airway dynamics.

ID: 403

C3: 3

Simulation of photon propagation in multi-layered tissue for non-invasive fetal pulse oximetry

Sebastian Ley, Daniel Laqua and Peter Husar

Ilmenau University of Technology, Germany.

Monitoring the state of health from fetus and mother non-invasively is still a big challenge in prenatal diagnostics. In this contribution the photon propagation in the maternal abdomen of pregnant women was simulated in the near-infrared range. To determine the fetal oxygenation it is necessary to ensure a sufficient penetration depth. This means that the photons have to pass through the maternal layers, the amniotic fluid and finally have to reach the fetus. It is essential that the reflected signal, recorded by a photo sensor, contains information about both mother and fetus.

The penetration depth of the injected photons and their propagation inside of the tissue were analyzed by using a model of steady-state light transport which is based on the Monte Carlo method. A simplified multi-layer tissue model with maternal tissue and blood vessel, amniotic fluid, fetal tissue and blood vessel layer was implemented. The dominant reflection layer is a fetal skull layer and the fetal brain is the last considered layer of the tissue model. The dilatation of the maternal and fetal blood vessels was realized by varying the layer thickness for each of the simulation scenarios. To analyze the penetration depth inside of the tissue, a photon tracking was implemented to mark whether the photon reaches the fetus.

The simulation results show the physical photon interaction in tissue by using the Monte Carlo method. Furthermore the analysis illustrates the fundamental feasibility of the non-invasive fetal pulse oximetry. The investigations demonstrate an inversely proportional dependence between the dilatation of blood vessels and the number of reflected photons which passed the maternal and fetal tissue. This relation allows the simulation of abdominal pulse curves of pregnant women. These synthetic signals might provide basic data for the evaluation of a separation algorithm which is able to estimate the fetal oxygenation.

ID: 497

C3: 4

Improvement of thermodynamic control in the newly developed pediatric circulatory assist device for fontan circulation

Akihiro Yamada¹, Yasuyuki Shiraishi², Hidekazu Miura², Takuya Shiga³, Mohamed Omran Hashem³, Yusuke Tusboko¹, Takuya Ito¹, Kyosuke Sano¹, Yasunori Taira¹, Tomoyuki Yambe², Masaaki Yamagishi⁴ and Dai Homma⁵

¹Graduate School of Biomedical Engineering, Tohoku University, Japan; ²Institute of Development, Aging and Cancer, Tohoku University, Japan; ³Graduate School of Medicine, Tohoku University, Japan; ⁴Department of Pediatric Cardiovascular Surgery, Kyoto Prefectural University of Medicine, Japan; ⁵Toki Corporation, Japan.

Total cavopulmonary connection (TCPC) is commonly applied for the surgical treatment of congenital heart disease such as single ventricle in pediatric patients. Patients with no ventricle in pulmonary circulation are treated along with Fontan procedure, in which the systemic venous return is diverted directly to the pulmonary artery without passing through right ventricle. In order to promote the pulmonary circulation after Fontan procedure, we have been developing a pediatric pulmonary circulatory assist device using shape memory alloy fibers for Fontan circulation. The shape memory alloy fiber can contract around 7% by Joule heating. A thermography detected the increase of the surface temperature of the fiber unit at around 50 degree Celsius. In this study, we designed a thermodynamic control system for the device and examined its functions. We mounted on 16 fibered units which were connected in parallel around ePTFE graft circumferentially. In order to make the limitation of overheating and excessive loadings, we improved a contraction controller of the device based on the thermodynamic techniques. The system consisted of a thermistor, a pressure sensor, and the regulator which was controlled by adaptive thermodynamic transfer functions. We improved the systems input by digital control method using a PC with microcomputers. We calculated the sensors' response on the surface of the conduit graft. And we examined the contractile force and thermal elevation. By the application of the control based on the new feedback system, the circumferential contractile force increased by 35% with inhibiting heat generation of the device. These results suggested the effective mechanical assistance for Fontan pulmonary circulation.

ID: 507

C3: 5

Hemodynamic studies of flow modulating stent designs for aortic aneurysms

Siang Lin Yeow^{1,2}, Hwa Liang Leo¹, Tsui Ying Rachel Hong², Wee Chuan Melvin Loh² and Soo Yeng Benjamin Chua³

¹Department of Bioengineering, National University of Singapore; ²Department of Surgery, National University of Singapore; ³Department of Vascular Surgery, Singapore General Hospital, Singapore.

Aortic aneurysms are localized dilatation of 50% greater than normal diameter of the aorta. In United States alone, about 5% to 7% of people aged 60 and above have aortic aneurysm. Left untreated, the aneurysm will rupture and carries a risk of death up to 90%. Conventional treatment options available include surgical repair and graft replacement, resulted in frequent major morbidity and death. Over the years, surgical intervention has evolved with the introduction of minimally invasive endovascular repair with lower mortality and morbidity risks. Endovascular aortic repair device consists of stent graft composed of fabric or polymer material supported by a metal mesh stent. These covered stent grafts excludes the aneurysmal aorta from the blood flow thereby causing the aneurysm sac thrombosis. The shortcomings of current stent grafts of maintaining blood flow to branches and collateral vessels have lead to the development of flow modulating stent grafts. Flow modulating stent grafts preserved blood flow to the side vessels and thereby avoid risk of visceral ischemia. This study investigates the flow behavior of variety of flow modulating stent designs in treating aortic aneurysm. The study highlights the hemodynamics flow within the aneurysm as a result of the flow modulating stent designs. The hemodynamics flow study of the emerging flow-modulating stent technology in an aneurysm is analyzed using computational fluid dynamics simulation.

ID: 599

C3: 6

Influence of contact angle on the bubble transport in a rectangular bifurcating microchannel

Poornima Josyula and S. Vengadesan

Indian Institute of Technology Madras, India.

In this work, the authors present the computational fluid dynamics (CFD) studies carried out to understand the influence of contact angle on the bubble transport in a rectangular bifurcating microchannel. The bifurcating microchannel mimics a human arteriole. Blood is modeled as Newtonian fluid and a single occluding perfluorocarbon (PFC) bubble is transported through the microchannel. The static

contact angles are given as an input via the in-built module in the commercial CFD package, ANSYS® and the dynamic contact angles via an user defined function (UDF). It was found that for each of the contact angles, the bubble meniscus shape is different. The distribution of the bubble volume in the daughter channels is dependent on this meniscus shape and the pulsatile pressure imposed at the inlet. The effect of gravity was also considered to understand its influence on the bubble splitting in the daughter channels. These results will be useful when considering the transport of microbubble contrast agents or encapsulated microbubbles (containing drugs) for the purpose of drug delivery.

ID: 397

C3: 7

Three-dimensional finite element analysis of foot-ground interface to investigate different landing patterns

Jee Chin Teoh and Taeyong Lee

National University of Singapore, Singapore.

Barefoot running is believed to protect the foot from high ground impact by promoting forefoot to land before the heel strikes. This forefoot strike (FFS) pattern is different from the rearfoot strike (RFS) pattern observed in shod runners whereby the heel will land first. There is still a lack of evidence to conclude on which is the better landing strategy. Experimental assessment may be difficult due to the high discrepancy between subjects. Finite element modeling (FEM) appears to be a good alternative. The respective kinematics and kinetics and the pressure/shear stress distributions can be studied closely. The aim of this investigation is to use FEM to quantify the consequences of different landing techniques, namely FFS and RFS, on 3D stress states at interfering plantar regions and internal skeletal structure.

The three dimensional foot model is refined from our previously developed soft-tissue-skeletal foot model. The model takes into account sagittal and frontal motion at ankle and sub-talar joints respectively, enabling dorsiflexion/plantar flexion and inversion/eversion to better simulate different landing strategies.

Landing on the rigid floor with two different landing strategies, the model predicted similar order of local peak vertical pressure on plantar soft tissue. However the shear distributions are very different depending on the landing configurations. The stress distributions on foot skeletal for two different landing patterns are distinctly different. FFS exposes the forefoot structure to higher injury risk. Meanwhile, stress fracture is more likely to happen on rearfoot region when the runner lands on the heel (RFS).

This model simulates ankle and subtalar joint motion during the strike phase of two different landing techniques and provides an easy alternative to investigate the consequences of foot strike conditions. The model can also be further extended to assess the three-dimensional contact stress analysis at the foot-shoe interface.

Session	Edn: Biomedical Engineering Education Session
Date/Time	4 December 2013 16:45–18:15 hrs
Venue	SR-07 & 08

ID: 408

Edn: 1

Education of biomedical engineering in the Technical University of Ostrava

Martin Augustynek, Marek Penhaker, Martin Cerny, Jindrich Cernohorsky and Iveta Bryjova

VSB Technical University of Ostrava, Czech Republic.

This paper deals with current trends in teaching biomedical engineering at the Technical University, Technical University of Ostrava. The paper presents information about the structure of the bachelor degree – Biomedical Technology and follow-up master degree of biomedical engineering. In connection with the teaching itself is also important information about the number of graduates and their themes of final thesis. Equally important is the information about linking teaching and collaboration with practice.

ID: 681

Edn: 2

Development of biomedical engineering education in Indonesia

Cholid Badri

Graduate Program University of Indonesia, Indonesia.

Since the early 1960s, high-tech equipments have been used in several hospitals in Indonesia particularly in the major government hospitals and large private hospitals. It was largely attributable to the need of Indonesian community for better healthcare service and to fulfill the demand in higher education.

The development of biomedical engineering which is closely associated with the use of modern medical apparatus has been perceived by medical doctors and engineers in those hospitals where some of them are teaching or university hospitals.

The initiative on biomedical engineering education was pioneered by Departemen of Health who needs qualified personnel to operate, maintain and

service those medical equipments. For these reasons Ministry of Health in 1967 established a Radiology Engineering Academy, an education level for Senior High School graduates to serve as Radiology technicians.

In the later development, due to rapidly developing non – Radiology equipments, Radiology Engineering Academy was changed and expanded to Electromedical Engineering Academy. This academy was an embryonic stage in development of applied biomedical engineering education in Indonesia.

Worldwide development of science and technology has generated interest in biomedical engineering among scientists in higher education in Indonesia. This was apparent mainly among the scientists in electrical engineering as well as medical doctors in major universities and institutions.

A master program in Electrical Engineering majoring in Biomedical Engineering was established in the late 1990s in Institutue of Technology Bandung as an embryonal stage of academical Biomedical Engineering education instead of previous applied Biomedical Engineering education in Indonesia.

The interest in education on biomedical engineering also grows at the centers of other higher education such as Jakarta, Yogyakarta and Surabaya by forming Major Program or Study Program at Master Degree and subsequently at undergraduate program in Biomedical Engineering.

In Indonesia where the health and supporting industries are still in early development, biomedical engineering education through applied and academical pathways may potentially rise problems on curriculum, competency, certification and employment that should be anticipated and elaborated by the stakeholders.

ID: 839

Edn: 3

Biomedical engineering education at the University of Sheffield, UK – from biomedical engineering to bioengineering

Chuh Khiun Chong

The Kroto Research Institute, Department of Materials Science and Engineering, University of Sheffield, United Kingdom.

Biomedical Engineering (BME) education at the University of Sheffield started in 2002 with the offers of the BEng and MEng degrees. The BME programme is accredited by the Institute of Engineering and Technology (IET), and remains one of the few accredited udergraduate BME programmes in the UK. The programme is highly interdisciplinary and cross faculty, being supported by departments in the Faculty of Engineering, Faculty of Medicine, Dentistry and Health, and Faculty of Science. Since its launch, the

programme continues to evolve and transform and faces many challenges ahead. In this talk, the author will introduce the programme at the University of Sheffield, the challenges we are facing, the programme's transformation over the years and discuss what our students valued and appreciated most, what they hoped for and how we dealt with the demand from students to make the programme better. It is hoped that ideas could be shared, exchanged and best practices adopted, to develop strong BME education.

ID: 879

Edn: 4

Education of biomedical engineering in Taiwan

Kang-Ping Lin

Chung-Yuan Christian University, Taiwan.

With the booming technology development, medical devices and engineering resource applied in a hospital have increased. Biomedical engineers play an important role in medical care service in our society. The first biomedical engineering (BME) department was established in 1972; subsequently, similar education institutions increased. The latest BME department was built in 2010. Currently, there are BME programs in the universities in Taiwan including 8 undergraduate programs, 17 master's programs and 11 doctoral programs. There are about thousands people holding a BME degree including 5300 people holding a bachelor's degree, 2900 people holding a master's degree and 370 people hold a doctoral degree.

According to each institute's report of graduates in July, 2013, there are 160 full-time and 110 part-time BME lecturers in Taiwan including 21% in the field of biomedical electronics, 16% in the biomedical materials, 14% in the biomechanics, 12% in the biomedical imagine, 7% in the biomedical information and 30% in the others. The education goal of most BME departments is that students are trained to have techniques and fundamental knowledge of BME, to have practical and realistic attitude towards work, to have ability to practice interdisciplinary teamwork and to have the spirit of medical and engineering ethics and to be internationalized.

Currently, students from undergraduate programs, in about half of the universities, are required to complete a BME project in laboratory. Students are required to have internship in related institutions out of campus for 320 hours before graduating. Almost all the BME departments are certified by IEET (Institute of Engineering Education Taiwan), and met the IEET requirement in which required mathematics and fundamental engineering courses take up 25% of all courses, professional courses of engineering take up 38%, and general courses take up 20%. Modularizing the elective courses as a study package

has applied in all BME departments to develop students' specialty. After completing ~18 credits of elective courses (6~8 courses) of specialty, students will be offered a certificate of the specialty in addition to their diploma.

Around 30% students who have completed their bachelor's degree choose to pursue a higher degree in graduate schools. The other graduates, around 30~40%, may stay in the field of BME and work as an engineer (R&D, sales, service or clinical engineer) in the industrial companies or hospitals.

The Taiwanese Society of Biomedical Engineering (TSBME) provides certificates, which include Biomedical Engineer, Biomedical Equipment Technician and Clinical Engineer, for all members. They can also renew the certificate after completing 60 training credits. Over the years, 60% of applicants qualified for the certificate and 90% of them qualified to renew the certificate. Certificates issued by TSBME are certified by the Taiwan Joint Commission on Hospital Accreditation (TJCHA) as a compulsory requirement to work as a biomedical engineer in a hospital. Over the pass four years, the TSBME, BME institutes and industries have worked hard to communicate with the government to complete biomedical engineer laws.

ID: 876

Edn: 5

BME education in Hong Kong: rehabilitation engineering, biomedical engineering, medical engineering, and bioengineering

Yong-Ping Zheng

The Hong Kong Polytechnic University, Hong Kong S.A.R., China.

While research-based training in biomedical engineering (BME) in Hong Kong has been existing in different universities for a longer time, BME undergraduate education started with a BSc(Hons) programme in Prosthetics and Orthotics in the Jockey Club Rehabilitation Engineering in the Hong Kong Polytechnic University (PolyU) in 1995. This programme was restructured and named as Health Technology in 2000, and further re-named as Biomedical Engineering in 2005. The team offering this programme has a very strong track record in rehabilitation engineering, and recently it has made good achievements in the field of bioinstrumentation and biosensing. PolyU BME programme used to be in the Faculty of Health and Social Sciences. As a strategic development of the university and promote interdisciplinary research, the Interdisciplinary Division of Biomedical Engineering was established under the Faculty of Engineering as its 6th department in Apr 2013.

In addition to PolyU, currently there are other three universities offering BME undergraduate programmes. The University of Hong Kong (HKU) offers a BSc(Hons) programme in Medical Engineering, starting from 2002. The Chinese University of Hong Kong (CUHK) offers a BSc (Hons) programme in Biomedical Engineering, starting from 2010. Both BME programmes in HKU and CUHK are offered under the collaboration between their Faculty of Engineering and Faculty of Medicine. Recently, the City University of Hong Kong launched a BSc(Hons) programme in Bioengineering under the Department of Mechanical and Biomedical Engineering in 2012. Meanwhile, PolyU, CUHK, and the Hong Kong University of Science and Technology (HKUST) offer MSc programmes in biomedical or bioengineering. The undergraduate BME programmes offered by different Hong Kong universities have slightly different focused areas, well linked with the strengths of their faculty members.

With more BME graduates trained by Hong Kong universities, it becomes more important to understand the related job market. Similar to the situations in many other countries, BME graduates in Hong Kong work in variety of sectors, including further studies, hospitals, government departments, medical device industries for R&D, sales, maintenance, project managing, hospitals, etc. The medical device industries in Hong Kong grow very fast, as it needs high-value added areas like medical device to re-develop its industry. In addition, there is a great demand of high quality BME graduates from Mainland China. Therefore, it is anticipated that BME education will continue to grow in Hong Kong in coming years.

ID: 891

Edn: 6

Accreditation of the bachelor of engineering (Biomedical Engineering) program – the NUS experience

Siew Lok Toh

Department of Biomedical Engineering, National University of Singapore

The undergraduate program in biomedical engineering in the National University of Singapore started in 2002. The degree offered was the Bachelor of Engineering (Bioengineering) which was first accredited in 2008 for 5 years. The processes, policies and procedures for granting accreditation to engineering academic programs in Singapore by Institution of Engineers Singapore is administered by the Engineering Accreditation Board (EAB). In April 2013, the Bachelor of Engineering (Bioengineering)

program was again accredited for another 5 years. In this talk, the author will be sharing the EAB accreditation on the Outcome-Based Education and its challenges.

Session	SYM-03B: Micro and Nanofluidics for Biomedical Applications (cont'd)
Date/Time	4 December 2013 16:45–18:15 hrs
Venue	SR-12

ID: 796

SYM-03B: 1

Symposium Keynote:

Ultrafast image cytometry for cancer detection

Keisuke Goda

University of Tokyo, Japan.

We present an ultrafast automated single-cell image cytometer that performs blur-free image acquisition and non-stop real-time image-recording and classification of cells in high-speed flow. This method is based on a unique integration of ultrafast optical imaging, self-focusing microfluidics, and information technology. To show the system's utility, we demonstrate high-throughput image-based screening of rare breast cancer cells in blood with an unprecedented throughput of 100,000 cells/s and a record false positive rate of one in a million. This method is expected to be effective for early, noninvasive, low-cost detection of cancer metastasis and evaluation of chemotherapy.

ID: 850

SYM-03B: 2

Toward gut and pancreas on chip for pathological models

Sungsu Park

Ewha Womans University, South Korea.

3D Microfluidic cell culture device is used to grow and differentiate various cell types of cells including progenitor cells, stem cells and cancer cells because the cells in the device retain their three dimensional morphology and maintain their in-vivo like functionality. Using the 3D microfluidic cell culture platform, we have been developing 'Intestine on a chip' and 'endocrine system (intestine and pancreas) on a chip' for studying pathological models of bacterial infection and diabetes mellitus. Our results suggest that these miniaturized microfluidic cell culture system will be alternatives to existing 2D culture models for cell biologists as well as medical researchers who are interested in understanding complex cell behaviors in an *in-vivo* like condition.

ID: 880

SYM-03B: 3

Nanomechanical mapping cellular migration

Xiao Dong Chen

Nanyang Technological University, Singapore.

Due to the importance of cell migration to a diverse range of physiological and pathological processes, including angiogenesis, wound healing, and cancer metastasis, there has been enormous research interest in developing sophisticated platform that can study and control cell migration. It is now widely accepted that the mechanical interaction between cell and the extracellular matrix (ECM) can direct many important cell behaviours especially the cell migration process, but the dynamic and quantitative analysis of cell-ECM interactions are hard to achieve using the conventional microfluidics-based platforms. Hence it is valuable to fabricate a cell migration study platform in which the cell-ECM interactions can be dynamically tracked and quantified. Here, I will present our recent development in using cellular nanomechanical forces to map the cellular migration. By integrally considering the correlation between cell-ECM interactions information obtained and the biochemical signaling, we find an efficient way to regulate cell migration and may get substantial insights into the mechanism investigations of migration-related pathological processes.

crystallization, cytotoxicity screen and enzymatic assays. However, the analysis of low-abundance biomolecules directly from clinical samples in droplets is challenging because of the limitations in adding multiple chemical reagents. To fully realize its advantages, an integrated microfluidic platform combining a droplet generator, a picoinjector and droplet library was designed to offer a multiplexing bioassay in the droplets. We specifically used this droplet based microfluidic method to detect the important enzymes, Proteases Matrix metalloproteinases (MMPs) and A Disintegrin and Metalloproteinases (ADAMs) which play key roles in several physiological processes in Endometriosis. Thousands of droplets with different protease substrates were prepared to react with endometrial clinical samples. Once the clinical samples mixed with different substrates, Proteolytic Activity Matrix Analysis (PrAMA) was applied to address specific protease MMPs/AMAMs activities as the biomarkers for diagnosis. Our results revealed a significant decrease in MMP-2 activity with disease, and these observations helped explain the frequent clinical observation of isolated endometriotic cysts that did not invade the surrounding tissue.

ID: 851

SYM-03B: 4

Proteolytic activity matrix analysis for diagnosis of endometriosis using droplet based microfluidics

Chia-Hung Chen^{1,2}

¹National University of Singapore, Singapore; ²Singapore Institute of Neurotechnology.

The need for greater specificity and sensitivity in biomarker detection for diagnosis requires the amount of data to increase exponentially, resulting in complex experimental design and analysis. Existing methods, such as zymography, antibody probes, and mass-spectrometry-based methods, must balance the tradeoff between accuracy and throughput. Recently an integrated droplet based microfluidic platform was developed for high throughput bioassay. The droplet-based microfluidic technology enables the high-throughput screening of large number of biochemical reactions ($\sim 10^8$ different reactions/10hours) by using small sample amount (30mL) to facilitate the monitoring of biomolecule activity for diagnosis. Previously, droplet-based microfluidics approaches have been widely applied to improve many analytical methods in biology, such as protein

Day 2 – Thursday, 5 December 2013

Session	PL3: Plenary Lecture 3
Date/Time	5 December 2013 09:00–09:45 hrs
Venue	Auditorium

ID: 742 **PL3**

Integration of computer assisted surgical guidance and surgical robotics for robotics for minimally invasive surgery

Ichiro Sakuma

The University of Tokyo, Japan.

Minimally invasive therapy such as endoscopic surgery and catheter based intervention are being spread in many surgical intervention fields. However, surgeon's skills required for minimally invasive therapies are complicated since the surgeons have to manipulate various medical devices in a narrow surgical field with limited vision. Thus engineering assistance is important to realize safe and effective minimally invasive therapy. Computer Assisted Surgical guidance such as surgical navigation is one of key technologies. On the other hand, it is expected that application of robotic technology to minimally invasive surgery will provide the following functions:

- (1) Precise manipulation of biological tissues and surgical instruments in narrow and confined surgical field.
- (2) Precise and accurate localization of therapeutic devices using various pre and intra-operative medical information.

In the first mode of application, more compact system is required. At the same time integration with various energy devices such as ultrasonically activated scalpel, bipolar coagulator, and high intensity focused ultrasound. At the same time, intra-operative guidance utilizing various pre and intra operative information is also required.

In the second mode of application, image guided robotic system for RF ablation, laser ablation, intensity modified radiation therapy, and high intensity focused ultrasound. In this type of robot, various pre and intraoperative information including functional information is used to navigate the therapeutic devices to the target lesion.

In this presentation, several examples of surgical robotic researches as examples of the above mentioned applications. In these application, it is important to integrate computer assisted surgical

guidance and surgical robotics to improve quality and safety of minimally invasive interventions.

Session	PL4: Plenary Lecture 4
Date/Time	5 December 2013 09:45–10:30 hrs
Venue	Auditorium

ID: 179 **PL4**

Autodigestion: A missing link to inflammation and disease

Geert W. Schmid-Schönbein

University of California San Diego, United States of America.

An increasing body of clinical evidence confirms previous experimental studies, which indicates that the majority of diseases is accompanied by inflammation. Since inflammation is fundamentally a tissue repair mechanism, this evidence suggests that inflammatory markers in plasma, such as c-reactive protein, fibrinogen, cytokines and others, are synthesized as a consequence of a tissue injury. We are justified to ask the important question, what mechanism leads to tissue injury. I will discuss the case of shock and multi-organ failure, a condition with high levels of inflammatory markers and high mortality. In spite of numerous clinical trials there is currently no approved treatment for shock other than alleviation of symptoms. The intestine plays a central role in shock and multiorgan failure. In the past it has been hypothesized that bacteria in the intestine and toxins generated by them lead to inflammation and organ failure. But clinical trials in septic patients have not confirmed this hypothesis. Instead, we propose that the powerful digestive enzymes, synthesized in the pancreas and discharged into the small intestine as requirement for normal digestion, play a central role in multi-organ failure after an initial tissue insult in shock. These enzymes are relatively non-specific, highly concentrated and fully activated in the lumen of the intestine. They are normally compartmentalized in the lumen of the intestine by the mucosal barrier. But if the mucosal barrier becomes permeable, e.g. in an ischemic state or in the presence of endotoxins in the circulation, the digestive enzymes escape into the into the wall of the intestine. They digest multiple cell and tissue components in the wall of the intestine, e.g. the ectodomain of surface receptors on the epithelium and the villi, respectively, and generate small molecular weight fragments, which are cytotoxic (e.g. unbound free fatty acid), in

a process we designated as *autodigestion*. The combination of digestive enzymes and cytotoxic fragments leak into the central circulation where they compromise many cell and organ functions, and ultimately may lead to multi-organ failure. We have shown that blockade of digestive enzymes inside the lumen of the intestine at concentrations that match their high concentrations serves to reduce inflammation and improve survival in multiple models of experimental shock.

Supported by NIH Grants HL 67825 and GM 85072 and by an unrestricted gift from Leading Biosciences Inc.

Session	SYM-04: Biomechanics in Nature and Bioinspired Engineering
Date/Time	5 December 2013 11:00–12:30 hrs
Venue	Auditorium

ID: 152 SYM-04: 1

Symposium Keynote:
Bio-inspired mechanical systems and biomimetics in bio-flights

Hao Liu

Chiba University, Japan.

Aerodynamics, structural dynamics, and flight dynamics of small birds and insects, as well as micro air vehicles (MAVs), with the maximum dimension of O(10) centimeters or smaller, and weight of O(10) grams or lighter, intersect with some of the richest problems in the interdisciplinary community including biology, mathematics and computer science, mechanical and aerospace engineering, and so forth. The agility and spectacular flight performance of natural flyers, thanks to their flexible, deformable wing structures as well as outstanding wing, tail, and body coordination, is of particular interest, both from the perspectives of those engaged in fundamental engineering science and in the development of flight vehicles. Aiming at unveiling key mechanisms in bio-flight as well as providing guidelines for bio-inspired MAV design, we have proposed a computational framework, which integrates aerodynamics, flight dynamics, vehicle stability and maneuverability. This framework is proven to be capable to support systematic analyses of bio-and bio-inspired mechanical systems in bioflights. Here we highlight the results of rigid-and flexible-wing aerodynamics of hovering hawkmoth, aerodynamics and flight dynamics of butterfly undergoing take-off, and maneuvering stability of hovering fruitfly as well as of the

flexible wing-based aerodynamic performance of a bio-inspired flapping MAV.

ID: 153

SYM-04: 2

Mechanobio-materials: design of elastically-micropatterned gels to control cell mechanotaxis and motility-related functions

Satoru Kidoaki

Kyushu University, Japan.

In general, cell adhesion mechanics onto the substrate surface critically affect not only its static shaping behaviors but also the dynamic changes in the cell morphology, i.e., regulation of cell motility. Such the substrate-mechanics-induced directional cell movement, so-called “mechanotaxis”, is one of the new categories of cell thigmotaxis behaviors. Recently, we have clarified the essential condition to induce mechanotaxis by utilizing the originally-developed photolithographic elasticity micropatterning for cell adhesive hydrogels: introduction of the elasticity boundary with enough high elasticity jump and narrower boundary width than adhesion area for a single cell. It was found that mechanotaxis cannot be induced on the diffuse elasticity gradient field but induced on the sharp elasticity boundary. To make clear this principle, the precise mechanical engineering of gel surface based on the nano/micro-technology was essentially required, suggesting that nano/micro mechanical engineering of soft materials provides novel key platform for the investigation of cell mechanobiology. We call such the platform materials that enable to regulate and to systematically investigate the mechanobiological behaviors of cells as “mechanobio-materials”. In this presentation, I will introduce our recent approaches for the sophisticated design of mechanobio-materials and discuss some expected direction of its engineering application to share the new possibility of material engineering for the study on cell biology issue.

ID: 882

SYM-04: 3

Bio-inspired aquatic omnidirectional multi-link propulsion mechanism

Shunichi Kobayashi

Shinshu University, Japan.

Observing view of organisms that swim in water by bending movement, there is a difference in propulsion direction between organisms having slick body surfaces such as nematodes and those having protrusions (parapodia) such as polychaetes. For slick

surface, propulsion is generated in the direction opposite to the wave propagation, while for a surface with protrusions, propulsion is generated in the same direction as the wave propagation. This can be explained by the resistive force of fluid to the bending body: A slick-surfaced organism has resistive force in normal direction of the bending body to fluid that is greater than resistive force of the tangential direction. An organism with projecting protrusions, however, has resistive force in tangential direction of the bending body to fluid that is greater than resistive force in normal direction. Inspired by this, we thought omnidirectional fluid-propulsion on the assumption that freely changing the resistance relationship between normal and tangential resistive force components, and developed the bio-inspired aquatic omni-directional bending movement mechanism by changing the angle of fins corresponding to projecting protrusions.

ID: 155

SYM-04: 4

Tunable optical diffuser based on deformable wrinkles

Takuya Ohzono, Kosuke Suzuki, Tomohiko Yamaguchi, Nobuko Fukuda

National Institute of Advanced Industrial Science and Technology, Japan.

We study the optical diffusion of transmitted or reflected light via a deformable wrinkled surface with a periodicity in the range of hundreds of micrometers. Without strain, the sample shows no wrinkles and no optical diffusion. With uniaxial strain, the surface shows aligned wrinkles and anisotropically diffuses incident light in a manner that depends on the degree of applied strain. The relationship between the sinusoidal microstructure and the diffused state is successfully explained in the regime of geometric optics. The present system can be used as a mechanically tunable optical diffuser.

ID: 156

SYM-04: 5

Biomimetic adhesive superhydrophobic surface for water droplet manipulation

Daisuke Ishii

Nagoya Institute of Technology, Japan.

“Biomimetic materials” have now attracted worldwide attentions because of their unique surface properties, e.g. anti-fouling, anti-reflectance, drag reduction, superhydrophobicity, etc. These surface properties will provide many kinds of environmentally conscious materials. Self-assembly and self-organization are other key words of the eco-

friendly manufacturing procedures. We fabricated adhesive superhydrophobic surfaces composed of metal-polymer hybrid structures in mimicry of surfaces of gecko feet and lose petals by using self-organization process and simple metal plating and showed strong adhesive force to water droplet on the hybrid surface. The adhesive superhydrophobic surface consists of two independent microstructures, hydrophobic polymer pillar array and hydrophilic metal microdomes. Density of the metal microdomes in the hybrid films was precisely changed from 0 to 30% by temperatures of the catalytic solution in the preparation processes. Adhesion property of the hybrid film to water droplets was adjusted by density of the metal domes. It was demonstrated that water droplet transfer between superhydrophobic surfaces by using the hybrid surface possessing different adhesion properties. This is the first example of the water droplet transfer from a superhydrophobic surface to a superhydrophobic surface. In addition, we fabricate the adhesive gradient superhydrophobic surfaces having concentration gradient of the metal domes. The adhesive gradient superhydrophobic surface shows that characteristic water droplet sliding behaviours such as invisible gates. Control of the adhesion of water droplets will be applied to microfluidics devices, open-air lab-on-a-chip, and the other functional superhydrophobic surfaces. Droplet manipulation by control of wettability is important for further understanding of superhydrophobic surfaces and application in microfluidic devices.

Acknowledgement: This research was partly supported by Grant-in-Aid for Scientific Research on Innovative Areas “Engineering Neo-Biomimetics” (No. 24120004) of The Ministry of Education, Culture, Sports, Science, and Technology (MEXT), Japan.

Session	A4: Biosignal Processing
Date/Time	5 December 2013 11:00–12:30 hrs
Venue	SR-01 & 02

ID: 818

A4: 1

Classification of EEG signals from imagined writing for treating writing disorder

Azlee Zabidi, Wahidah Mansor and Khuan Y. Lee

Universiti Teknologi Mara, Malaysia.

The occurrence of imagined writing event can be recognised from Electroencephalogram (EEG) when the signal is passed through several processes including feature extraction and classification. The imagined writing process may be useful for treating

writing disorder if the activity is repeated several times. A technique called Autoregressive (AR) is able to model the EEG signal with imagined writing activity and produce coefficients that can be used as input feature for Multi Layer Perceptron (MLP). This study investigates the optimum AR order combined with MLP in classifying EEG signals from imagined writing letters that dyslexic children often get confused. Result shows that there is distinct pattern in EEG dataset during imagined writing which can be discriminated between different tasks. The best AR order for classifying EEG signals from imagined writing activity is between 16 to 20 orders.

ID: 516

A4: 2

Acoustic cochlear implant models incorporating electrical field interaction between neighboring electrodes

Charles T. M. Choi¹, Shang-Yi Huang¹ and Yi-Hsuan Lee²

¹National Chiao Tung University, Taiwan; ²National Taichung University of Education, Taiwan.

Cochlear implant (CI), which has been a commercial device for nearly thirty years, can provide opportunities for patients with severe to profound hearing impairment to regain hearing. Sound processed in the CI can be modeled by acoustic CI models on specific stimulating strategies. Speech processed by acoustic CI models was used to test normal hearing test subjects and can be a basis to evaluate the performance of various stimulating strategies. Unfortunately, there is still a significant performance difference between hearing test result based on acoustic CI model with normal hearing test subjects with hearing tests from CI patients. There are a number of explanations for this, but one important factor is that traditional acoustic models do not account for the electric field interaction between electrodes. For CI users, the electrical field interaction or current spread between electrodes distorts the speech and introduce noises. In order to model the electrical field interaction in the acoustic model, we proposed a new SPREAD model which is created by the activating function profile generated from a finite element model we developed. In previous SPREAD model, the current spread was fixed at a certain decay rate. In the proposed model, activating function and finite element model of a CI is introduced to improve the SPREAD matrix. The performance of the proposed SPREAD matrix with the acoustic CI model significantly improves its match with clinical CI data. This shows the acoustic CI model with the proposed SPREAD matrix can be a more accurate model to evaluate the performance of CI stimulating strategies.

ID: 795

A4: 3

A study on the effect of subliminal priming on subjective perception of images: a machine learning approach

Justin Dauwels¹, Parmod Kumar², Faisal Mahmood³, Ken Wong⁴, Abhishek Agrawal¹, Mohamed Elgendi⁵, Srinivasan Kannan¹, Dhanya Menoth Mohan¹, Rohit Shukla⁶ and Alice H. D. Chan¹

¹Nanyang Technological University, Singapore; ²INRIA Sophia Antipolis – Méditerranée; ³Okinawa Institute of Science and Technology, Okinawa, Japan; ⁴Temasek Laboratories, National University of Singapore, Singapore; ⁵University of Alberta Edmonton, AB, Canada; ⁶University of Wisconsin-Madison, Madison, Wisconsin.

The term 'priming' refers to increased sensitivity to certain stimuli resulting from prior exposure to related visual/audio messages. This effect is extensively documented over the past few decades. In our present study, we investigate the influence of subliminal prime words on peoples' judgment about an image, through questionnaires and electroencephalograms (EEGs). We use statistical analysis tools to analyze the effect of priming on behavior and machine learning techniques to infer the primes from EEGs. We access Positive Affect and Negative Affect Score, Mindfulness Attention Awareness Score, Need for Cognition test score, and Singelis' Self Construal test to analyze how personality is correlated with behavioral responses and event-related potentials (ERPs).

Forty English-speaking university students (26 males; mean age: 22.3 years) participated in this experiment. The participants were instructed to rate the images on a 7-point Likert scale, after being subliminally exposed to a masked prime word. Simultaneously, 32-channel EEG was recorded at 250Hz. Each participant performed 100 trials of rating task for each set of positive, negative and neutral prime words.

The responses on 7-point Likert scale were analyzed by means of one-way repeated measure ANOVA for three priming conditions. This test yielded strongly significant results, indicating strong priming effects on the behavior of participants, in particular, on subjective perception of images.

The ERPs extracted from EEGs were analyzed using one-way repeated measure ANOVA after pre-processing. Interestingly, a significant difference between 3 priming conditions, at different latencies of ERPs was observed.

We designed support vector machines in wavelet domain that are able to infer the prime types from average ERPs with a classification rate of 70%. This finding emphasizes that the ERPs encode information about the different kinds of primes. Overall, our

study provides results to support the strong effect of subliminal priming in human cognition.

ID: 393

A4: 4

Unobtrusive, mobile ECG monitoring and arrhythmia detection using mobile phones

Heike Leutheuser¹, Patrick Kugler¹, Stefan Gradl¹, Dominik Schuldhaus¹, Stephan Achenbach² and Bjoern M. Eskofier¹

¹Digital Sports Group, Pattern Recognition Lab, Department of Computer Science, Friedrich-Alexander-University Erlangen-Nuremberg, Erlangen, Germany; ²Division of Cardiology and Angiography, Department of Internal Medicine II, University Hospital Erlangen, Germany.

Cardiovascular diseases are the leading cause of death worldwide. Common cardiovascular diseases are for example caused by myocardial infarctions. In this case, fast and professional help is needed to prevent further damage to the heart. To detect indicators of a myocardial infarction accurately and to react immediately is difficult for untrained individuals. An ECG monitoring application for mobile devices (smartphones, tablets) that gives indications for a doctor's visit could decrease the high number of deaths caused by myocardial infarction.

We implemented a Pan-Tompkins algorithm for real-time detection of QRS complexes and heart rate on a mobile device. We further implemented an automated, intervention free heart beat classification that can differentiate between 'normal' and 'abnormal' beats.

For the determination of heart rate, we detected single QRS complexes with a Pan-Tompkins algorithm. The R-peaks were detected with threshold-based methods from the output of the Pan-Tompkins algorithm.

For the classification of the heartbeats into 'normal' and 'abnormal', we calculated time and frequency domain features to train a Support Vector Machine (SVM). We used, additionally to a generic feature set (mean, standard deviation, variance, kurtosis, skewness, minimum, maximum, energy, and median), the QRS duration and the RR interval. Evaluation was based on the MIT-BIH Arrhythmia database and the MIT-BIH Supraventricular database using leave-one-subject-out cross-validation.

The classification accuracy of the SVM outperformed a previously presented tree classifier. Especially, the number of false positive beats was reduced.

This application has the potential to be an unobtrusive ECG monitoring tool that can easily be integrated in daily life. Especially in developing countries, where medical experts are scarce but

mobile devices become abundant, such an application can have a tremendous impact.

ID: 361

A4: 5

SVM for semi-automatic selection of ICA components of electromyogenic artifacts in EEG data

Florian Gabsteiger¹, Heike Leutheuser¹, Pedro Reis², Matthias Lochmann² and Bjoern M. Eskofier¹

¹Digital Sports Group, Pattern Recognition Lab, Department of Computer Science, Friedrich-Alexander-University Erlangen-Nuremberg, Erlangen, Germany; ²Institute of Sport Science and Sport, Friedrich-Alexander-University Erlangen-Nuremberg, Erlangen, Germany.

Traditionally, electroencephalography (EEG) that is recorded during movement has been considered too noise prone to allow for sophisticated analysis. Superimposed electromyogenic activity interferes and masks the EEG signal. Presently, computational techniques such as Independent Component Analysis (ICA) allow reduction of these artifacts.

However, to date, it relies on the user to select the artifact-contaminated components to reject. This process is tedious and its effectiveness is highly dependent on the user's expertise.

To automate this process and to reduce user dependent factors, we trained a support vector machine (SVM) to assist the user in choosing the independent components (ICs) most influenced by electromyogenic artifacts. We designed and conducted a study with specific neck and body movement exercises and collected data from five human participants (35 datasets total). After preprocessing, we decomposed the data by applying the Adaptive Mixture of Independent Component Analysis (AMICA) algorithm. An expert labeled the ICs found in the EEG recordings after decomposition as either 'myogenic activity' or 'non-myogenic activity'. For each of these components 255 wavelet-packet features were extracted and used to train a SVM. The classifier is available as a plugin for the EEGLab toolbox.

Afterwards, the classifier was evaluated on the dataset of one participant, whose data were not used in the training phase, and obtained 93% sensitivity and 96% specificity.

Our study was designed to cover a diverse selection of exercises that stimulate the musculature that most interferes in EEG recordings during movement. This selection should produce similar artifact patterns as seen in most exercises or movements. Although unfamiliar exercises could result in worse classification performance, the results are expected to be equivalent to ours.

Our study showed that this tool can help EEG analysis by reliably and efficiently choosing electromyogenic artifact contaminated components after AMICA decomposition, ultimately increasing the speed of data processing.

ID: 624

A4: 6

Measurements and data processing in home care telemetry systems

Marek Penhaker and Hoang Tran Minh

VSB - Technical University of Ostrava, FECS, K450, Czech Republic.

This paper describes the design, implementation telemetry system for data collection and processing in Home Care applications. The system measures and evaluates the temperature, humidity, atmospheric pressure and ambient lighting. The data collection system is solved using digital sensors downstream wireless Bluetooth technology provides. Processing includes evaluation to eliminate the number of sensors and prediction of the situation.

Session	B5: Controlled Drug Delivery
Date/Time	5 December 2013 11:00–12:30 hrs
Venue	SR-03 & 04

ID: 202

B5: 1

Evaluation of particle deposition efficiency in human oral passage: A CFD study

Jianhua Zhu¹, Hong Siang How¹, De Yun Wang², Shu Jin Lee³ and Heow Pueh Lee¹

¹Department of Mechanical Engineering, National University of Singapore, Singapore; ²Department of Otolaryngology, National University of Singapore, Singapore; ³Department of Surgery, National University of Singapore, Singapore.

Targeted drug-aerosol delivery in human respiratory airway has become a popular method for specific disease treatment with costly and/or aggressive medicine, and a standard procedure for treating quite a few respiratory diseases. However, the efficiency of targeted drug-aerosol delivery is still a problematic issue due to the complex geometry of human upper airways. In this study, CT scans of a male subject were obtained to reconstruct a 3D model of human oral passage. The airway was extended to a hemisphere region representing for zero gauge pressure boundary condition. Velocity magnitude was applied at the hypopharynx. Sinusoidal variation of velocity corresponding to ventilation rate of both 7.5 and 15 L/min was simulated. Particles with diameters of 1,

8, 15, 22 and 31 μm were released near the mouth. These particles were released in three directions: parallel to the oral airway, 30 degree above the oral airway and 30 degree below the oral airway. And the particles were released at three different initial speeds, 0, 2.5 and 5 m/s. For each of the above categories, 10,000 particles were released. The deposition efficiency (DE) was found to generally increase with particle sizes. In most of the cases, the DE increased with initial released velocity. With release angles of 30 and -30 degree, the DE increased greatly for initial velocity magnitudes from 0m/s to 2.5m/s but would increase at a slower rate for initial velocity magnitudes from 2.5m/s to 5m/s. Compared to higher global airflow rate (15 L/min), at 7.5 L/min the DE is generally larger for particle size below 15 μm , but smaller for particle size above.

ID: 543

B5: 2

Near-Infrared photothermal activation of microgels incorporating polypyrrole nanotransducers through droplet microfluidics

Rong-Cong Luo and Chia-Hung Chen

Department of Bioengineering, National University of Singapore, Singapore.

Photo responsive microgels were colloidal particles whose properties changed when irradiated with light of appropriate wavelengths. Light stimulation offered advantages including the ability of remote activation, point-specific controllability, and tunable intensity of the irradiated light. Ultraviolet (UV), visible (VIS) and near-infrared (NIR) light had been applied as stimuli for photo responsive microgels. NIR light (700–1100nm) controls were of particular interest for in vivo applications, as it is above the light absorption of most biological molecules so that could penetrate tissue with relatively mild tissue damage.

Various approaches, such as template-guided synthesis and precipitation polymerization had been developed to synthesize the NIR light responsive composite microgels. However, the resultant microgels from the bulk chemical synthetic methods reached the limitations in controlling size, structure, and encapsulation efficiency. Moreover, current NIR light responsive composite microgels are mostly synthesized by using gold nanorods that were reported to have low photostability, thus limiting their applications in long term utility.

In this study, Poly (N-isopropylacrylamide) (pNIPAM) composite microgels incorporating polypyrrole (PPy) nanoparticles were made using droplet microfluidics. The high controllability of droplet microfluidics enabled an effective way for

designing monodisperse composite microgels with tunable sizes, structures and encapsulation efficiency. The photo responsive pNIPAM microgels incorporating organic PPy nanoparticles as the photothermal transducers were synthesized through droplet microfluidics. PPy nanoparticles absorbed the irradiated NIR light to generate heat locally, enabling the site-specific swelling/de-swelling controls of the composite microgels. In addition, the FITC-albumin release profiles of the composite microgels were characterized by applying periodic NIR light stimulations to demonstrate the programmable drug release. In conclusion, the composite microgels would be advantageous for delivery systems that required local release of the active ingredients. Furthermore, the promising photostability of PPy nanoparticles provided the opportunities for the long term *in vivo* drug delivery, robust implanted devices and reliable fluidic regulations.

ID: 203

B5: 3

Objective assessment of the effects of long-duration wearing of N95 and surgical facemasks on upper airway functions

Jian Hua Zhu¹, Heow Pueh Lee¹, Shu Jin Lee² and De Yun Wang³

¹Department of Mechanical Engineering, National University of Singapore, Singapore; ²Department of Reconstructive Surgery, National University Hospital, Singapore; ³Department of Otolaryngology, National University of Singapore, Singapore.

Background: Although many reported studies were done on the effectiveness of various facemasks in filtering out airborne pathogens, there is still a lack of reported studies on how the long duration wearing of N95 respirators or surgical facemasks affects the upper airway functions.

Materials and Methods: In the current study, 100 healthy subjects will be recruited, and 16 have been completed. All the subjects go through 2 sessions, one for N95 mask (S1), and the other for surgical mask (S2). In the first 20 minutes of the session, the participants are informed with details of the experiments, adapt to the room environment and take the nasal function tests as benchmark. The participants would then wear the mask for 3 hours. In the subsequent 1.5 hours, nasal function tests are done every half an hour till the end of the study.

Results and Discussion: During S1 wearing N95, the inspiratory flow resistance increased once the participant put off the mask, peaked 1 hour later and then decreased at the end of the study; and the expiratory flow resistance increased to the maximum at 3.5

hours after putting on the mask, then slightly decreased. In S2, both the inspiratory and expiratory nasal resistances significantly increased once putting off the surgical mask, decreased half an hour later, and increased till the end. The average respiratory nasal resistance did not recover to the initial condition at the end of both S1 and S2. The average scores of smell test before and after wearing masks, in both the two sessions are all around 33.

Conclusions: Based upon the current 16 healthy subjects, long duration of wearing both N95 and Surgical masks increased nasal resistance even 1.5 hours after putting off the masks. Minimal influence of wearing N95 and Surgical masks on smell function was found.

ID: 846

B5: 4

Quantifying *in vivo* resorption and integration of hydrogel scaffolds using bimodal imaging

Sasha Berdichevski¹, Haneen Simaan Yameen¹, Hagit Dafni², Michal Neeman² and Dror Seliktar¹

¹Technion, Israel; ²Weizmann Institute, Israel.

Scaffold geometry may affect the successful integration of the implant in the host by influencing the transport properties to and within an implant. Especially in cell therapy, where strategies are constantly being developed to create vascularized networks to help overcome diffusion limitations. Another big challenge is finding a quantitative and non-invasive methodology to document the *in situ* integration of the implanted scaffold. PEG-fibrinogen (PF) hydrogel precursor was labelled with gadolinium (Gd) and Cy5.5 to document and to compare the integration of biodegradable hydrogels with various geometries. Cylindrical plugs, spherical micro-beads, and *in situ* cross-linked PF were implanted subcutaneously (SC) in rats, and degradation kinetics, as well as the resorption of the degradation products were estimated using bimodal fluorescence/MRI imaging. Further, the effect of hydrogel geometry on VEGF release was investigated by calculating the number and total area of capillaries in the area of hydrogels implantation.

MRI demonstrated the slowest degradation of plugs, while *in situ* cross-linked PF degraded in a fastest manner. Fluorescence signal showed a biphasic temporal pattern of implant degradation and resorption: its increase correlated with the release of degradation products from the hydrogel implant and had a diffusive pattern, while its decline was associated with the resorption of the degradation products. The *in situ* cross-linked PF was most rapidly disassembled, but the degradation products were not

resorbed faster than the other configurations. Microbeads degraded and released degradation products much faster than bulky plugs. Further research was focused on implementation of these findings in tissue regeneration strategies: the induction of angiogenesis by slow release of VEGF. The *in situ* polymerized hydrogel contributed to enhanced angiogenesis, compared to the untreated, VEGF alone-treated and plug-treated SC tissues. Moreover, the micro-carriers-treated SC tissue was significantly more vascularized, as compared to all other groups.

The ability to predict spatial and temporal patterns of biomaterial degradation *in vivo* is crucial to the design of engineered cell scaffolds and matrices. We were able to demonstrate significant differences in implant integration parameters and angiogenic potential of three types of implants – underscoring the importance of implant geometry and implantation strategy.

ID: 707

B5: 5

Biodegradable nano-conjugates for non invasive insulin delivery

Pooja Hurkat and Sanjay K. Jain

Dr. H.S Gour Central University, India.

Oral peptide and protein delivery has been a constant challenge, in which oral insulin delivery for diabetes management has been unendingly pursued in the past. In present work, Concanavalin A conjugated PLGA nanoparticles (ConA NPs) have been developed as carrier for insulin delivery due to its M cell targeting potential. NPs were prepared using double emulsion solvent evaporation method and later conjugated with Con A employing carbodiimide chemistry. The conjugation was verified by FTIR. Further, they were characterized for particle size, shape (SEM/TEM), polydispersity index, zeta potential, conjugation efficiency, entrapment efficiency and *in vitro* drug release. Stability of entrapped insulin in the developed formulation was confirmed by SDS PAGE, DSC, XRD and CD spectrum. *Ex-vivo* (Histopathological study and Intestinal transport study) and *in-vivo* studies (Blood glucose monitoring) were done using streptozotocin-induced diabetic albino rats (Wistar strain), which indicated that Con A NPs were localised at Peyer's patches and also reduced blood glucose level effectively within 4 h of its oral administration, respectively. Convincingly, ConA NPs bearing insulin exhibited sustained release profile, and better absorption and stability.

ID: 208

B5: 6

Controlled release system of antisense molecule from atelocollagen porous gel for hyperlipemia treatment

Genki Mihara^{1,2}, Joeng-Hung Kang¹, Takahiko Nakaoki², Hidetaka Torigoe³, Mariko Harada-Shiba¹, Satoshi Obika⁴ and Tetsuji Yamaoka¹

¹National Cerebral and Cardiovascular Center Research Institute, Japan; ²Innovative Materials and Processing Research Center, Ryukoku University, Japan; ³Faculty of Science, Tokyo University of Science, Japan; ⁴Graduate School of Pharmaceutical Sciences, Osaka University, Japan.

Introduction: When formulation was injected into the body by single injection, pharmacological effect did not maintain continually. The controlled release of therapeutic agents is very important medical treatment to maintain their pharmacological effect for a long time, and to reduce dose and frequency of administration. We have developed an antisense molecules targeting for proprotein convertase subtilisin/kexin type 9 (PCSK9) to lower the serum low-density lipoprotein, and atelocollagen gel-based release system to maintain long term pharmacological effect of PCSK9 antisense molecules.

Materials and Methods: Atelocollagen (type I) was used as a controlled release carrier. An atelocollagen solution was mixed with antisense molecules and lyophilized. The mixture was extruded through 18G nozzle to make a rod and cut into lengths of 10 mm. This gel was named atelocollagen porous gel. We evaluated controlled release mechanism of antisense molecules from atelocollagen porous gel by using *in vivo* imaging. The PCSK9 mRNA level in the liver was analyzed by RT-PCR at day 3, 7, and 14 after implantation.

Results and Discussion: From *in vivo* imaging data, we found that controlled release of antisense molecules depends on the formulation. Next, we evaluated the therapeutic effect by the injection of antisense molecules alone or the controlled release of antisense molecules by porous gel. Injection of antisense molecules alone downregulated PCSK9 mRNA up to 50% at day 3, but PCSK9 mRNA was recovered to the normal level at day 7. In contrast, when atelocollagen porous gel was implanted into mice, the downregulation of PCSK9 mRNA was downregulated about 40% in the liver at day 14. These results suggest that the atelocollagen porous gel-based release system of antisense molecules is useful to maintain the long term pharmacological effect.

ID: 383

B5: 7

Fabrication of spherical multi-shells with discrete porosity differences via organic phase polymer-hydrogel assemblies

Houwen Matthew Pan¹ and Dieter Trau^{1,2}

¹Department of Bioengineering, National University of Singapore, Singapore; ²Department of Chemical and Biomolecular Engineering, National University of Singapore, Singapore.

The fabrication of well-defined, multi-porous striated shells within a spherical scaffold is reported. Multi-compartmentalized microcapsules are attractive as materials in biosensors, advanced drug delivery and tissue engineering. They are next generation carriers with sophisticated structures and functionalities. However, a method capable of producing multi-shells with discrete porosity differences within a single compartment remains unreported. By the alternating deposition of polyallylamine (PA) and polystyrenesulfonic acid (PSS) in 1-butanol, at equal mass ratios, multiple levels of porosity are generated within an agarose microsphere. Each level of porosity is represented by a well-defined, concentric shell of interweaving PA and PSS layers. The number, thickness, and porosity of the striated shells can be easily controlled by varying the number of PA/PSS bilayers and the polymer concentration, respectively. The feasibility of utilizing this morphology for the assembly of a multi-shell porous spherical scaffold is validated by trapping different molecular weight dextrans within different regions of porosity. The unique interaction of polyacids and/or polyamines in hydrogels represents a facile and inexpensive approach to the development of complex multi-porous morphologies. By further incorporating different shells with distinct functionalities and properties, we could vastly expand on the range of techniques available for separation and delivery of different biomolecules.

Session	C4: Musculoskeletal Mechanics
Date/Time	5 December 2013 11:00–12:30 hrs
Venue	SR-05 & 06

ID: 710

C4: 1

**Conference Keynote:
Development, validation of a degenerated intervertebral disc model and its application in disc research**

Jaw-Lin Wang

National Taiwan University, Taiwan.

Low back pain is a common symptom in adults and mainly resulted from the intervertebral disc

degeneration. Intervertebral disc is the largest avascular organ in human body. Intervertebral disc is a viscoelastic organ composed of collagen fibers, proteoglycan and water. The major mechanical functions of discs are to resist external loading and absorb shock energy. Declination of disc function makes discs vulnerable to external stress, which in turn accelerates disc degeneration.

The nutrient supply of intervertebral disc is complicated. One of the primary causes of disc degeneration is the failure of the nutrient supply to disc cells. The calcification of cartilaginous endplate leads to the block of nutrient transportation pathway and insufficient oxygen concentration in the aging process. The disc cells then undergoes the anaerobic metabolism with the more accumulation of lactic acid, hence causes an acidic pH environment. The dead disc cells and degradation of proteoglycan and extracellular matrix aggravate the disc degeneration.

The aging and excessive fatigue loading are recognized as major triggers of disc degeneration. Two major methods, i.e. the enzymatic denaturation and mechanical fatigue loading, are used to create disc degeneration models. The hydrolysis enzymes, such as trypsin, ChABC and collagenase and glycation, are activated to cleave collagen fibers and proteoglycan in the aging process. Disc functions can be quantitatively represented by disc viscoelastic properties. Understanding the alteration of disc viscoelastic properties of injured discs improves the knowledge on degeneration etiology and mechanism of treatment.

In this study, we showed the results of several methods to create a degenerated disc model, and validated with the biological, biomechanical, microstructure behavior. Examples of effect of treatment, i.e., the spinal traction and PRP, is presented to show their efficacy in recovering the disc structure and functions.

ID: 195

C4: 2

Computational study on the effect of the ligaments in knee joint during quasi-static stand-to-sit motion

Chunhui Chung¹ and Bing-Shiang Yang²

¹National Taiwan University of Science and Technology, Taiwan; ²National Chiao Tung University, Taiwan.

Musculoskeletal simulation is the powerful tool to analyze the human motion and provide related information such as muscle activities and reaction force in the joints. It has been successfully applied to the fields of surgery, rehabilitation, and ergonomics. However, most of the models assume the articulations as the standard mechanical joints such as spherical and revolute joints. Although these joints

can provide good approximation of the articulations, they cannot exactly simulate the motions of the articulations and provide correct data such as slippage and reactions among femur, tibia and patella in the knee articulation. In addition, the effects of ligaments are totally ignored. The cruciate ligaments are very important to stabilize the knee. Injury on cruciate ligaments, especially anterior cruciate ligament, happens very often on athletes who play intense sports, and it is almost impossible to recover to its original state. In order to study the effect of ligaments in knee articulation, both conditions of force and moment equilibrium and contact engagement analysis are utilized in the planar model presented in this paper. The motion of quasi-static stand-to-sit is studied based on the method. The results also show the consistent with previous studies. In addition to the effect of ligaments, this method also provides a computational method for the contact conditions among femur, tibia, and patellar. This problem was studied by comparing the distance of discrete points on the femoral condyle surfaces. Therefore, it costs a lot of computing time. With the method of contact analysis, which was developed in gear theory, solutions can be obtained faster and more accurate.

ID: 276

C4: 3

Investigation of determinants of atypical femoral fractures using multiscale computational modeling

Peter Pivonka¹, Saulo Martelli² and Peter R. Ebeling¹

¹Northwest Academic Centre, The University of Melbourne, Australia; ²Department of Mechanical Engineering, The University of Melbourne, Australia.

Atypical femoral fractures (AFF) are predominantly transverse stress fractures from the lateral aspect of the subtrochanteric and diaphyseal region for which long-term bisphosphonate treatment have been suggested an important determinants. However, the physiological loading environment triggering AFFs in typical femoral regions remain largely unexplored. The aim of this study was to test the hypothesis that typical AFFs onset Venue is associated with high daily cyclic tensile strains. The study was based on body- and organ-level models from a single donor (female, 81-years-old) and motion data recorded from a body-matched volunteer (female, 25 years-old). Models were the donor's lower-limb musculoskeletal model validated against published measurements of the hip reaction force and the finite-element model of the donor's right femur validated against measurements of cortical strains. Motion data including skin marker trajectories and ground reaction forces were recorded from the volunteer during

walking, which is the most frequent daily activity. The muscle and hip forces were calculated using the musculoskeletal model and applied to the finite-element model to calculate the cortical tensile and compressive strains in two extreme sections of the femoral diaphysis. The anterior, medial, posterior and lateral femoral aspects were assumed at 0°, 90°, 180°, and 270° respectively. In the sub-trochanteric section the peak tensile strain during stance was 1300-2287 me constantly located laterally (270°-300°) and the peak compressive strain was 1433-2730 me constantly located medially (90°). In the distal diaphysis the peak tensile strain varied from 1714 me to 4171 me located antero-laterally at 300°-330° and the peak compressive strain varied from 1813 me to 4674 me located postero-medially (90°-150°). We conclude that high cyclic tensile strains determine the typical AFFs onset Venue whereas more research is necessary to understand how different activities and the individual anatomy affect the femur's physiological tensile loads.

ID: 386

C4: 4

Muscle force prediction during knee flexion/extension using EMG-driven model

Saran Keeratihattayakorn¹ and Shigeru Tadano²

¹Division of Human Mechanical Systems and Design, Graduate School of Engineering, Hokkaido University; ²Division of Human Mechanical Systems and Design, Faculty of Engineering, Hokkaido University, Japan.

Predicting muscle force during joint movement is important to gain a better understanding of musculoskeletal system. In this study, an EMG-driven model for predicting the muscle force in lower limb during knee flexion-extension is presented and the rate-effect on muscle model parameters is investigated. The model was based on Hill-type muscle model to describe the contraction mechanism of muscle. Surface electrodes were attached to the subject's leg to detect the EMG signals and the knee joint angle was measured by an electrogoniometer. The subjects performed a series of knee flexion-extension with various movement frequencies. Muscle fiber length, velocity and activation during the movement were used as inputs in the muscle model to predict the muscle force. To study the rate-effect on muscle model parameters, optimization processes were performed to obtain muscle model parameters at various movement frequencies. The external forces calculated from the predicted muscle forces were compared with measured forces from load cell to validate the accuracy of the model. The results showed that the muscle model parameters changed with respect to the movement frequency. In order to

improve the accuracy of Hill-type muscle model, various muscle model parameters which change with movement frequency were suggested. Development in muscle model is very useful in studying the musculoskeletal system leads to improvement in diagnostic tool, planning effective exercise training programs and development of rehabilitation procedure.

ID: 394

C4: 5

Differences in soccer kick kinematics for left-side and right-side targets

Luis Carlos Hernandez Barraza and Chen-Hua Yeow

National University of Singapore, Singapore.

Soccer is one of the most popular sports played around the world and typically requires good eye-muscle coordination during soccer kick. For this study, the soccer kick was divided in three phases: Initiation, Kick and Recovery. The aim is to investigate soccer kick kinematics in relation to the target position that the subjects are required to hit. Two recreational players were recruited (weight 61 ± 10 Kg, height 172 ± 5 cm, age 23 old). Both of the subjects were right-footed kickers. Kinematic data were collected using an eight camera motion capture system at 100-Hz sampling rate. A standard soccer ball was used in the trials and the subject wore the same Adidas F50 shoes. A total of five targets were positioned on a white board (2m x 1.5 m), one in each corner and one in the center. Each subject performed a total of fifteen trials, three trials for each target. The kinematic of each trial was analyzed and the results were compared to determine if there was a difference when the subject tried to hit the targets located on the right side of the board versus the left side. Interestingly, we found that- for the sagittal and frontal planes, the right hip, knee and ankle joints angles were generally higher during the Kick phase when the subject tried to hit the targets located on the left side than the right side. This difference in joint angles could be because the target on the left side would require the subject to achieve greater ranges of motion for the right limb joints in order to kick off the ball from the right foot to hit the left-side targets.

ID: 304

C4: 6

Biomechanics of artificial elbow joints

Norio Inou², Michael Surjawidjaja¹, Katsuyuki Kobayashi², Taisuke Osanai², Ren Kadowaki², Hitoshi Kimura², Jun Ikeda³ and Katsunoki Inagaki³

¹National University of Singapore, Singapore; ²Tokyo Institute of Technology; ³Showa University.

This paper evaluates biomechanical characteristics of artificial elbow joints. To enhance the durability of the joint components, it is important to evaluate the mechanical condition at the bone-joint interface. In this report, we examined the effect of torque produced by the biceps with a three-dimensional model instead of the two-dimensional model used by our previous study. This paper proposes a three-dimensional mathematical model which includes the minimum number of muscles to maintain a balanced arm posture. Calculation of the reaction forces and torque at the elbow joint was done with a 10N load applied at the hand. Stress analysis was then performed using a finite element model composed of the ulna and radius for the lower arm. This study focuses on the stress produced inside the bony tissue around the joint component at the ulna side. The result shows the lateral force of biceps has positive relation to the stress value.

Session	YIA-01: Young Investigator Award I
Date/Time	5 December 2013 11:00–12:30 hrs
Venue	SR-07 & 08

ID: 190

YIA-01: 1

Synchrotron nano-mechanical imaging techniques to understand how altered bone quality increases fracture risk in secondary osteoporosis

Angelo Karunaratne^{1,2}, Alan Boyde³, Chris T. Esapa^{4,5}, Nick Terrill⁶, Graham R. Davis³, Steve DM Brown⁵, Roger D. Cox⁵, Liz Bentley⁵, Rajesh V. Thakker⁴ and Himadri S. Gupta²

¹Royal British Legion, Centre for Blast Injury Studies, Department of Bioengineering, Imperial College London, UK; ²Queen Mary University of London, School of Engineering and Material Sciences, UK; ³Queen Mary University of London, Barts and the London School of Medicine and Dentistry, Institute of Dentistry; ⁴Academic Endocrine Unit, Nuffield Department of Clinical Medicine, Oxford Centre for Diabetes, Endocrinology and Metabolism, University of Oxford, Churchill Hospital, UK; ⁵MRC Mammalian Genetics Unit and Mary Lyon Centre, UK; ⁶Diamond Light Source Ltd., Diamond House, Harwell, UK.

Bone diseases such as osteoporosis and rickets cause significant reduction in bone quantity and quality, leading to mechanical abnormalities. While the reduction of bone quantity can be assessed using existing clinical tools like DXA and pQCT, there is little quantitative knowledge of how altered bone quality in diseased bone increases fracture risk. For an example patients suffering with glucocorticoid induced osteoporosis (GIOP) have a higher fracture risk at a similar bone mineral density (BMD) level measured by DXA compared with non-users. This indicates that bone quantity, as currently assessed by BMD, is not the overriding, or sole, factor in fracture risk. There is a clear need to develop high-resolution diagnostic techniques to close the gap between onset of fracture relevant changes and diagnosis. Here, a functional imaging technique (*in-situ* synchrotron X-ray imaging with micromechanics) was developed to measure alterations in fibrillar deformation mechanisms in GIOP. During applied loading, percentage shifts in Bragg peak positions arising from the meridional collagen stagger, measured from the small angle X-ray scattering (SAXS) patterns, give fibrillar level strain as a function of applied stress in real time. To link nanostructural changes to altered fracture risk and deformability, well defined mouse model with an *N*-ethyl-*N*-nitrosourea (ENU)-induced corticotrophin releasing hormone promoter mutation that developed secondary osteoporosis was used. The fibril modulus, maximum fibril strain and fibril-to-tissue strain ratio were determined, complemented by quantitative backscattered scanning electron microscopy and microcomputed tomography to measure microscale mineralisation. A significant reduction of fibril modulus and enhancement of maximum fibril strain was found in GIOP mice. A significantly larger fibril strain/tissue strain ratio was found in GIOP mice compared to wild-type mice, indicative of a lowered mechanical competence at the bone matrix level. These results demonstrate the ability of synchrotron-based *in-situ* X-ray nanomechanical imaging to identify functional alterations in nanoscale bone quality in metabolic bone diseases.

ID: 219

YIA-01: 2

Design and actuation of a snake-like robot for minimally invasive surgeries

Zeqi Tan and Hongliang Ren

National University of Singapore, Singapore.

Endoscopic minimally invasive surgeries (MIS) are being more common procedures in hospitals. Instead of a single large opening, only several small incisions are needed to be opened through the patient to

perform the surgery. As such, MIS has better recovery rate and efficiency than convention surgeries. However, the access ports of such surgeries constrain conventional MIS instruments made of straight rigid bodies to limited degrees-of-freedom (DOFs) and distal dexterity. Also, tight and irregular spaces within the human body restrict and complicate the surgery procedure due to the maneuverability of the instruments.

To address these challenges and achieve more flexible manipulations inside human body, a new snake-like robotic system was developed combining the usage of springs and support structures and the concept of parallel manipulators using push-pull wire actuation. Such robotic systems are needed due to the limited space of the small access ports opened through the human body during minimally invasive surgeries.

Instead of using a central backbone and the multiple plates of the distal dexterity units, a spring was used as the supporting structure of the robot. The characteristics of a spring are exploited in this design to enable the robot to orientate and position with increased maneuverability. A simple support structure is then inserted into the spring to allow for wire actuation.

Key design considerations and features are discussed. The prototype of the robotic system is able to achieve five degree of freedoms through the actuation control and show the feasibility of active steering intracorporeal endoscopes.

ID: 340

YIA-01: 3

Relationship between pathology and hemodynamics of human unruptured cerebral aneurysms

Yasutaka Tobe¹, Takanobu Yagi¹, Yuki Iwabuchi¹, Momoko Yamanashi¹, Kenji Takamura¹, Takuma Sugiura¹, Mitsuo Umezu¹, Yoshifumi Hayashi², Hiroataka Yoshida², Atsushi Nakajima², Kazutoshi Nishitani², Yoshifumi Okada², Michihito Sugawara², Shin Hiraguchi², Toshiro Kubo² and Shigemi Kitahara²

¹Waseda University, Japan; ²Kitahara International Hospital, Japan.

This research compared the intraoperative appearance, computational fluid dynamic (CFD) analysis, and scanning electron microscope (SEM) observation of endothelial cells (EC) of seven human cerebral aneurysms in an effort to find the relationship between hemodynamic patterns and wall-thinning of aneurysms.

Aneurysm walls were categorized into blister-like appearance as *thinning*, similar appearance to the parental artery or white thickened part as *thickening*, and areas similar to arteriosclerosis as *calcifying*

region. Seven aneurysms were dissected after clipping operation with markings to confirm the orientation of specimens. Specimens were rinsed in PBS, immersed into 2% glutaraldehyde, 1% osmium solution, graded series of ethanol and tertiary-butyl alcohol, and freeze-dried to observe under SEM. For CFD analysis, 3 dimensional vascular models were constructed and meshed using tetra and prism mesh. The inlet boundary condition used an average flow rate of 350 ml/min. The outlet boundary conditions were set to flow rates based on literature data and for regions with unknown flow rates were set to static pressure. Vascular models were analyzed using CFX 13.0 (ANSYS).

Aneurysms contained four thinning, six thickening, and four calcifying regions. SEM analysis showed variations of endothelial cell patterns over aneurysms. Missing EC was only found at thinning regions and all thickening and calcifying regions confirmed damaged or normal EC. CFD analysis showed impinging flow at the thinning region. Impingement was defined by the direction of wall shear stress (WSS) vector and rise of pressure at wall. The impinging flow was only found at the thinning region. The WSS magnitude did not confirm any relationship between wall characteristics or EC patterns. These results suggested that the impinging flow may cause wall thinning of aneurysm.

ID: 307

YIA-01: 4

Optimal intra-articular injection of parathyroid hormone-related protein effectively promotes osteochondral defects repair

Wei Zhang^{1,2}, Jialin Chen^{1,2}, Jiadong Tao^{1,2}, Changchang Hu^{1,2}, Junfeng Ji^{1,2} and Hongwei Ouyang^{1,2}

¹Center for Stem Cell and Tissue Engineering, School of Medicine, Zhejiang University, Hangzhou, China; ²Zhejiang Provincial Key Laboratory of Tissue Engineering and Regenerative Medicine, Hangzhou, China.

Terminal differentiation often occurs in the repair progress of osteochondral defects. It is reported that parathyroid hormone-related protein (PTHrP) could inhibit terminal differentiation but may elicit adverse effects on chondrogenesis when administrated at improper time. Here we apply PTHrP by optimal intra-articular injection together with implantation of a collagen-silk scaffold to treat osteochondral defect. The injection schedule was set at three different time windows: 4–6, 7–9 and 10–12 weeks post-operatively. Samples were obtained and evaluated macroscopically, histologically and immunohistochemically at 16 weeks post-injury. *In vivo* delivery of PTHrP at 4-6 weeks exhibited better repairing effects and less terminal differentiation compared with other time

windows. These results showed that PTHrP would invoke best repair effects for osteochondral defects when intra-articularly injected at 4–6 weeks post-injury, which not only prevented terminal differentiation but also promoted cartilage regeneration in rabbit model. The findings offer insight into understanding the mechanisms involved and pave the way for clinical application of PTHrP for osteochondral defects repair.

ID: 254

YIA-01: 5

Correlation between facial trauma and brain injury – a finite element study

Kwong Ming Tse¹, Long Bin Tan¹, Shu Jin Lee², Siak Piang Lim^{1,3} and Heow Pueh Lee^{1,3}

¹Department of Mechanical Engineering, National University of Singapore, Singapore; ²Division of Plastic, Reconstructive and Aesthetic Surgery, National University Hospital, Singapore; ³National University of Singapore (Suzhou) Research Institute, China.

The objective of this study is to determine the relationship between facial and brain injuries, using a subject-specific finite element (FE) model of human head. Nine common impact scenarios of facial injuries are simulated. Both extracranial and intracranial injuries are evaluated based on the tolerance limits of the biomechanical parameters. General trend of maximum intracranial biomechanical parameters occurring in nasal bone and zygomaticomaxillary bone impacts indicates that severity of brain injury is highly associated with the proximity of Venue of impact to the brain. It is hypothesized that the midface is capable of absorbing considerable energy and protecting the brain from impact. We also propose that the nasal cartilages dissipate the impact energy in the form of large scale deformation and fracture, with the vomer-ethmoid diverging stress to the “crumpling zone” of air-filled sphenoid and ethmoidal sinuses; in its most natural manner, the face protects the brain. This numerical study hopes to provide surgeons some insight in what possible brain injuries to be expected in various scenarios of facial trauma and to help in better diagnosis of unsuspected brain injury, thereby resulting in decreasing the morbidity and mortality associated with facial trauma.

ID: 299

YIA-01: 6

Understanding nanotopography induced stem cell differentiation: a focus on focal adhesion kinase

Benjamin Kim Kiat Teo^{1,2}, Sum Thai Wong^{1,3}, Choon Kiat Lim², Terrence Kung², Chong Hao Yap², Yamini Ramgopal², Lewis H. Romer⁴ and Evelyn Yim^{1,2,5}

¹Department of Bioengineering, National University of Singapore; ²Mechanobiology Institute Singapore, National University of Singapore; ³Institute of High Performance Computing, A*STAR, Singapore; ⁴Department of Anesthesiology and Critical Care Medicine, Cell Biology, Biomedical Engineering, Pediatrics and Center for Cell Dynamics, Johns Hopkins University School of Medicine; ⁵Department of Surgery, National University of Singapore.

Biophysical cues, such as nanotopography, have been shown to be integral for tissue regeneration and embryogenesis in the stem cell niche. Tissue homeostasis involves the interaction of multipotent cells with nanoscaled topographical features in their ECM to regulate aspects of cell behavior. Synthetic nanostructures can drive specific cell differentiation, but the sensing mechanisms for nanocues remain poorly understood. Here, we report that nanotopography-induced human mesenchymal stem cell (hMSC) differentiation through cell mechanotransduction is modulated by the integrin-activated focal adhesion kinase (FAK). On nanogratings with 250 nm line width on polydimethylsiloxane, hMSCs developed aligned stress fibers and showed an upregulation of neurogenic and myogenic differentiation markers. The observed cellular focal adhesions within these cells were also significantly smaller and more elongated on the nanogratings compared to microgratings or unpatterned control. In addition, our mechanistic study confirmed that this regulation was dependent upon actomyosin contractility, suggesting a direct force-dependent mechanism. The topography-induced differentiation was observed on different ECM compositions but the response was not indicative of a direct ECM-induced hMSC differentiation pathway. FAK phosphorylation was required for topography-induced hMSC differentiation while FAK overexpression overruled the topographical cues in determining cell lineage bias. The results indicated that FAK activity had a direct impact on topography-induced gene expression, and that this effect of FAK was independent of cell shape. These findings suggest that hMSC sense and transduce nanotopographical signals through focal adhesions and actomyosin cytoskeleton contractility to induce differential gene expression.

Session	B4: Tissue Engineering
Date/Time	5 December 2013 11:00–12:30 hrs
Venue	SR-12

ID: 113

B4: 1

Conference Keynote: Drug delivery technology for tissue regeneration therapy

Yasuhiko Tabata

Institute for Frontier Medical Sciences, Kyoto University, Japan.

The basic idea of tissue regeneration therapy is to promote the natural-healing potential of body itself for tissue regeneration and repairing. The body potential is based on the cell ability of proliferation and differentiation. To realize this cell-based tissue regeneration, there are two approaches of cell transplantation and tissue engineering. Key cells of healing potential are transplanted to naturally induce tissue regeneration. In tissue engineering, a local environment to enhance the cell ability for tissue regeneration is designed and artificially created by making use of biomaterial technology or methodology. For example, if a key growth factor is supplied to cells in the right place at the right time period or concentration, the cells are activated to naturally induce cell-based tissue regeneration. The biological functions of in vivo in-stable molecules can be augmented with the drug delivery system (DDS) of biomaterial technology.

Biodegradable hydrogels have been designed for the controlled release of growth factor to experimentally and clinically succeed in the factor-induced regeneration and repairing of various tissues with or without cell scaffold. The hydrogel system is also available for the dual release of growth factors to augment the tissue regeneration. This release technology is combined with cell transplantation to significantly enhance the therapeutic efficacy in tissue regeneration.

In this paper, several applications of drug delivery technology to cell-based tissue regeneration are introduced to emphasize significance and necessity of biomaterials in tissue regeneration medicine.

ID: 207

B4: 2

Fibroblast growth factor-immobilized polyethylene porous scaffolds via mussel adhesive peptide and heparin for inducing angiogenesis

Yusuke Sakai^{1,2}, Sachiro Kakinoki¹, Taro Takemura³, Nobutaka Hanagata³, Thosia Fujisato² and Tetsuji Yamaoka¹

¹National Cerebral and Cardiovascular Center Research Institute, Japan; ²Osaka Institute of Technology, Japan; ³National Institute for Materials Science, Japan.

The ultimate goal of tissue engineering is to repair and construct 3D tissues and organs. Porous materials have been investigated as a temporary extracellular matrix in regenerative medicine, but even a simple tissue has not been well reconstructed yet. The most crucial problem is the difficulty in inducing vascular network into scaffolds. In this study, we developed the easy method for immobilizing fibroblast growth factor (FGF) on polyethylene porous scaffold (PEPS) using mussel adhesive peptide and heparin, and evaluated the angiogenesis within scaffolds *in vivo*.

FGF was immobilized on PEPS with the pore size of 30 or 150 μm by just immersing in three kinds of solutions. First, PEPS was immersed in the aqueous solution of peptide having oligo-lysine and mussel adhesive sequence (Pep-PEPS) to make a positively-charged surface. Then, heparin was electrostatically adsorbed on Pep-PEPS by dipping in heparin solution (Hep-PEPS). Finally, FGF was immobilized on Hep-PEPS via the heparin-FGF specific interaction by immersing in FGF solution. Two types of FGF-treated PEPS were prepared: unwashed (FGF-PEPS-uw) and washed to remove the unreacted FGF (FGF-PEPS-w). The surface of modified-PEPSs was analyzed by X-ray photoelectron spectroscopy (XPS). Modified-PEPSs were subcutaneously implanted in mice and the infiltration of cells and angiogenesis were histologically evaluated.

FGF immobilization was confirmed by XPS N1s peak assigned to peptide on FGF-PEPS-w. Angiogenesis was induced in FGF-PEPS-w, but not in PEG-PEPS-uw. In the case of FGF-PEPS-uw, encapsulation was formed quickly and the infiltration of cells was inhibited. Interestingly, the neovascular vessel appeared in FGF-PEPS-w after 7 and 14 days of implantation in pore size of 150 and 30 μm , respectively, suggesting that the neovascularization behavior is affected by the pore size of PEPS.

These results demonstrated that the FGF immobilization is very important to induce the neovascularization within 3D scaffolds.

ID: 583

B4: 3

In situ non-invasive cellular assays in microfabricated well arrays using scanning electrochemical microscopy (SECM)

Adithya Sridhar, Hans L. de Boer, Albert van den Berg and Séverine Le Gac

University of Twente, The Netherlands.

We report a non-invasive approach for monitoring microtissue activity in microstamped well arrays using scanning electrochemical microscopy. This approach is illustrated for drug testing and cellular differentiation assays.

Conventional cellular assays rely on the use of fluorescent stains. While fluorescent assays are virtually applicable to the detection of any marker, they are highly invasive, and not suitable for time-lapse imaging. In that context, SECM is highly attractive, and it is suitable for both extra- and intracellular recordings, and the detection of different markers in a direct or indirect way.

Microtissues are produced in a microstamped Petri-dish including a microwell array (200- μm depth; 400- μm diameter), which is compatible with fluorescence microscopy and scanning probe techniques. Microtissues from various cell lines or even co-cultures (3T3/B16) spontaneously form in the wells.

For drug testing, microtissues (e.g., HepG2 or HeLa) are exposed to drugs, and their respiratory activity is monitored by measuring variations in the oxygen concentration in their vicinity using SECM. At 100 μm above the tissues, a 10% decrease is observed in the oxygen reduction current for viable tissues, while no change is detected after drug exposure.

For differentiation assays, C2C12 muscle microtissues are exposed to BMP-2 (bone morphogenic protein) to induce their differentiation into bone. ALP (alkaline phosphatase), which is expressed by osteoblasts is a differentiation marker, and it is indirectly detected using enzymatic assays. For SECM measurements, PAPP (4-aminophenyl-phosphate) is added to the solution; it is enzymatically degraded into PAP (4-aminophenyl), which is subsequently oxidized at the microelectrode. Subsequently, by measuring the PAP oxidation current, ALP can be detected, and thereby tissue differentiation monitored. Control microtissues don't give rise to any oxidation current, while after ~2 days of BMP-2 treatment, ALP formation is electrochemically detected.

We will present live/dead and differentiation assays on microtissues using SECM in our custom platform.

ID: 718

B4: 4

Proliferation behavior of mesenchymal stem cells in peptide functionalized chitosan scaffolds

Md. Abdul Kafi, Phanny Yos, Nakamuta Yusuke and Mitsugu Todo

Kyushu University, Japan.

Fabrications of biodegradable polymer materials are of much significance in establishing living cells on artificial surfaces for tissue engineering applications. Chitosan derived by de-acetylation of chitin may be one of the important candidates for this purpose. In the present study, porous chitosan scaffolds were fabricated using freezing (-20°C to -80°C) and lyophilization (overnight) method. We established a nano-scale thin film of RGD (Arg - Gly - Asp) peptide using self-assembly (SA) technique to make mechanical link between the cell and the scaffolds surface to improve its cell adhesion efficiency. The fabricated porous scaffolds were characterized by scanning electron microscopy (SEM) as well as tensile testing. The pore diameter was found to be varied with different freezing temperature and the scaffold with larger pore size shows lower tensile strength. The scaffolds with pore diameter of 150 and 100 (achieved by freezing at -20°C and -80°C, respectively) were subjected to cell functions study using hMSC. The scaffold with 100 µm pore diameters, found to be suitable for hMSC adhesion, spreading and proliferations. Furthermore, the improved adhesion, spreading and proliferation efficiencies were reported from RGD functionalized scaffolds compared with non-functionalized one. From this study, it was concluded that the RGD functionalized chitosan scaffolds with 100 pore diameters established strong attachment of cells as well as mimic functions of living cells. So, the fabricated scaffold can be potentially useful tool of *in vitro* cellomics for tissue engineering applications.

ID: 535

B4: 5

Decellularised organs – a tool to enable neovascularisation in tissue-engineered skin

Lindsey Dew, Sheila MacNeil and Chuh Khiun Chong

Kroto Research Institute, Department of Materials Science and Engineering, University of Sheffield, UK.

Introduction: Delayed neovascularisation following transplantation of tissue-engineered (TE) skin is a major problem in getting such grafts to survive on a patient's wound bed. To tackle this problem, we aim to induce neovascularisation in 'pre-vascularised' TE skin model, obtained by incorporating TE skin with a re-endothelialised biological vascular network, using

a bioreactor. This present work discusses the decellularisation of rat liver and jejunum to establish bioscaffolds that retain their native vascular networks and some preliminary recellularisation results.

Methods: Rat liver and jejunum were harvested from fresh cadavers. Their main vessels were cannulated and flushed with heparin solution and distilled water before treatment of 1% Triton-X 100. Residual detergent was removed by circulating distilled water. The matrices were sterilised using 0.1% peracetic acid. To assess the vascular networks, blue dye injection, low magnification and confocal microscopies along with microCT imaging were performed. Matrix compositions were analysed using histochemical and DAPI staining.

To recellularise, dermal fibroblasts were injected into the decellularised liver and subsequently perfused continuously with cell culture medium for 5 days at 37°C. Samples were taken at days 1, 3 and 5 for histological analysis. Similarly, the jejunum was injected with CellTracker red stained oral fibroblasts. Samples were taken at days 1 and 3 for histological analysis, fluorescence microscopy and cell viability tests using MTT assay.

Results: In both matrices, well-defined vascular trees with multiple branching were obtained. Histochemical analysis showed proteinous ECM but no evidence of cells. For both repopulated matrices, histochemical analysis showed that cells were attached to the vascular networks whilst MTT analysis showed the presence of viable cells.

Discussion: The decellularisation procedure appears effective in removing most cellular matter whilst preserving the matrices with vascular networks. Preliminary recellularisation results demonstrate that the vascular networks could be revived, suggesting its potential in establishing a "pre-vascularised" tissue model.

Session PL5: Plenary Lecture 5

Date/Time 5 December 2013 | 13:30–14:15 hrs

Venue Auditorium

ID: 144

PL5

Biomedical micro and nanotechnology: from lab-on-chip to building systems with cells

Rashid Bashir

University of Illinois, United States of America.

Biomedical applications of micro and nanotechnology hold tremendous promise in diagnostics,

therapeutic, and tissue engineering. Lab on chip devices can be used for the rapid and sensitive detection of biological entities including cells, bacteria, proteins and DNA. These microfluidic devices can provide for the sensitive and selective detection of CD4+ T cells for detection of HIV/AIDs for global health at point of care. Significant opportunities exist for rapid point-of-care detection of nucleic acid molecules from bacterial or viral agents of infection, for food borne pathogens. To date, many of such devices or systems are constructed with silicon, PDMS, or other polymers. However, the fabrication of milli and micro scale systems and machines, with living cells as the building blocks, can represent a new frontier for BioMEMS. Tremendous opportunities exists in the 3-dimensiononal bio-fabrication of such cell-based bioactuators, autonomous biological micro robots, and cellular machines for a wide range of applications. This talk will present an overview of our efforts in these exciting areas at the intersection of biology and engineering at the micro and nanoscale.

Session	SYM-05: Supramolecular and Nano-Biomaterials
Date/Time	5 December 2013 14:30–16:00 hrs
Venue	Auditorium

ID: 726 SYM-05: 1

Symposium Keynote:
Translational nanomedicine from self-assembling prodrugs

Youqing Shen

Zhejiang Univ, China.

To achieve efficient drug delivery from the *iv* injection site to the target in the tumor cells and thereby high therapeutic efficacy and few side effects, an nanocarrier must be capable of *simultaneously* satisfying the opposite *2R2SP* requirements at the right places, that is, “drug Retention in blood circulation vs. Release in tumor cells (*2R*)” and “Stealthy in blood vs. Sticky in tumor (*2S*)”. While the *2R2SP* capability of a nanocarrier may render its resulting nanomedicine efficacy and safety potential for translation, there are other two elements indispensable for a nanomedicine truly translatable from the benchtop to the bedside, i.e., the feasibility of the nanocarrier materials to be proved for use as excipients (material excipientability) and the ability to establish scaling up production processes for good manufacture processes (GMP) for the nanocarrier and its formulation with drug (nanomedicine) (process scale-up ability). Thus, when we design a nanocarrier towards translation, the *CES* (capability, excipientability and

scale-up ability) elements must be considered carefully(1). Herein, we review our understandings and approaches addressing nanocarrier’s CES including self-assembling prodrugs(2,3), aimed at promoting the developments of truly translatable nanomedicine for cancer drug delivery.

ID: 723 SYM-05: 2

Sliding graft copolymers – supramolecular derivatives equipping promising potentials

Jun Araki

Shinshu University, Japan.

Among a wide variety of supramolecules, polyrotaxanes and their derivatives are the most investigated and most promising candidates from the viewpoint of materials chemistry. One category of such derivatives involves a series of molecules, in which many side chains are grafted to the ring moieties of the polyrotaxane backbone, yielding a novel type of graft copolymer with freely sliding/rotating side chains. These types of copolymers, which were very recently synthesized and named as “sliding graft copolymers” (SGC), indicates numbers of peculiar properties, which were not observed for conventional covalent graft copolymers. In the present article, recent results on synthesis, characterizations and properties of various types of SGC molecules are briefly overviewed.

ID: 538 SYM-05: 3

Mesoporous polymer materials through solvent nano-crystallization

Sadaki Samitsu and Izumi Ichinose

National Institute for Materials Science, Japan.

Phase separation of polymer solutions has been used as a main route in industry to fabricate porous polymer materials (membranes and absorbents). Despite the long-term history (over 50 years), direct fabrication of mesopores without block-copolymer is still challenging. Here we propose a novel mechanism of phase separation in polymer solutions, which is related to crystallization of solvent molecules. Dispersed polymer chains significantly disturb the crystallization of the solvent molecules and therefore reduce the crystal size of the solvent molecules to be down to ten nanometers or so. Based on this concept, we have successfully fabricated mesoporous polymers consisting of three-dimensional network of ultrafine polymer nanofibers. We have also revealed physico-chemical properties of polymer surfaces using SEM, TEM tomography, MDSC, solid-state NMR, and gas/vapor sorption measurements. The

potential application of the mesoporous material in separation technology will be presented.

ID: 438

SYM-05: 4

Pillararenes: easy-to-make and versatile receptors for supramolecular chemistry

Tomoki Ogoshi

Kanazawa University, Japan.

In 2008, we reported a new class of macrocyclic hosts named “pillararenes”. Pillararenes have repeating units connected by methylene bridges at the para-position, and thus they have a unique symmetrical pillar architecture differing from the basket-shaped structure of meta-bridged calixarenes. Synthesis of pillararenes is easy-to-make. They can be synthesized in high yield by reacting commercially available reagents. The reaction was completed in 3 minutes. Pillararenes also show versatile functionality similar to cyclodextrins. Based on the various synthetic approaches, position-selective mono-, di-, tetra-, penta- and per-functionalization of pillararenes can be achieved. Pillararene can capture electron accepting guest molecules within their cavity similarly to cucurbiturils. Because of their unique pillar-shaped architectures, high yield synthesis, outstanding host-guest properties, planar chirality and functionality, pillararenes are useful platform to construct various supramolecules including rotaxanes, catenanes, supramolecular polymers and sensors.

ID: 888

SYM-05: 5

Bioreducible stimuli-responsive cyclodextrin-based star polymer for efficient gene delivery

Yuting Wen

National University of Singapore, Singapore.

Establishing polymeric gene delivery carriers to release DNA at the optimal time and appropriate subcellular compartment is desired for efficient gene delivery. In this study, we develop a reduction-sensitive system comprising beta-cyclodextrin (beta-CD) based core with poly(2-dimethylamino)ethyl methacrylate (pDMAEMA) arms and disulfide linkages for responsive gene delivery. The star pDMAEMA with a beta-CD core and disulfide linkages named CDSSpDMAEMA is synthesized via Cu(I)-mediated ATRP from the disulfide bonds contained macroinitiator α -bromoisobutyric amidoethyl disulfanylethylcarbamoyl beta-CD (CDSSBr). CDSSpDMAEMA demonstrates good capacity to condense DNA into compact nanoparticles, which are stable in PBS. Upon interaction with reducing

reagent DTT, particles undergo dissociation and pDNA release, which are verified by DLS detection and PicoGreen assay. The real-time intracellular degradation of disulfide bonds in MCF7 cells is observed by confocal microscope, using FITC-labeled polymer and rhodamine-labeled pDNA. The amount of pDNA release inside the cell is further quantitatively measured, 83% of the pDNA are released from polyplexes at 6 h, which is significantly higher than that of the analogue lacking disulfide moieties (CDpDMAEMA). In addition, the bio-responsive polymer CDSSpDMAEMA exhibits improved cytotoxicity profile and higher luciferase protein expression level compared to the nondegradable control polymer CDpDMAEMA. Conclusively, disulfide-contained system CDSSpDMAEMA is sensitive to reduction intracellular environment and would facilitate rapid pDNA release in cytosol, which is beneficial to improve gene transfection and reduce cytotoxicity.

Session	A5: Biosignal Processing
Date/Time	5 December 2013 14:30–16:00 hrs
Venue	SR-01 & 02

ID: 475

A5: 1

NniLSM: A unified level set model for medical image segmentation

Bing Nan Li¹, Fang Chen¹, Yi Zhuang Cheng², Jing Qin³ and Ning An¹

¹Hefei University of Technology, China; ²Anhui Provincial Hospital, China; ³Chinese Academy of Sciences, China.

Level set methods (LSMs) have been extensively investigated for medical image segmentation. However, there are a few inherent drawbacks in common level set formulations using image variation or region competition. For example, edge-based LSMs are susceptible to weak or broken boundaries, while region-based ones are often dominated by suboptimal solutions. By incorporating the functional of fuzzy controlling, we propose a unified level set model – UniLSM – in this paper to combine the merits of edge-based and region-based LSMs while overcoming their drawbacks. UniLSM also provides a convenient framework to integrate prior information or knowledge for medical image segmentation. Its performance has been preliminarily verified for medical images of computed tomography (CT) and magnetic resonance imaging (MRI).

ID: 614

A5: 2

3-D lung visualization using electrical impedance tomography combined with body plethysmography

Stefanie Heizmann, Moritz Baumgärtner, Sabine Krüger-Ziolek, Zhanqi Zhao and Knut Möller

Furtwangen University, Germany.

Electrical impedance tomography (EIT) is a noninvasive, radiation-free imaging technique that can be used at the bedside for monitoring the regional lung ventilation and tidal volume distribution. EIT measures the electrical potentials at the chest wall surface based on the phenomenon that changes in regional air content and regional blood flow modify the electrical impedance of lung tissue. Up to now, EIT data are reconstructed to 2-dimensional images. In this paper, the time-resolved visualisation of 3-dimensional lung EIT data is presented.

An EIT electrode belt, which carries 16 electrodes with a width of 40mm, was placed around the thorax of one healthy volunteer. Series of measurements were recorded at 5 consecutive planes, started at the level of axilla towards caudal. The volunteer was asked to breathe at similar ventilation level during the measurements. Tidal volume (V_T) and functional residual capacity (FRC) were measured at the same time with our modified body plethysmograph. The lengths of ventral-to-dorsal and left-to-right of the chest wall surface were measured at the corresponding measurement planes. An ellipse with corresponding transverse and conjugate diameter was used to approximate the thorax contour. EIT images were transformed to adapt the ellipse contour.

Three dimensional transient imaging of lung contour, airflow trace and volume distribution was implemented by numerical conversion of 2-D relative impedance data from EIT measurement. The movement of the lungs during tidal breathing was visualized in 3-D. Ventilation levels of the volunteer among different measurements were similar confirmed by our body plethysmograph (FRC_{pleth} : 3.68 ± 0.09 L, V_T : 0.93 ± 0.12 L; mean \pm SD).

Concluded, we presented first steps to visualize the lung ventilation distribution in 3-D measured by EIT. This novel fast supporting method may provide better insight into lung disease and its progression as well as the acceleration of clinical acceptance of EIT.

ID: 838

A5: 3

ELM based classification and analysis of spirometric pulmonary function data

A Mythili¹, C. M. Sujatha² and S. Srinivasan¹

¹MIT Campus, Anna University, India; ²CEG Campus, Anna University, India.

Spirometric pulmonary function test plays a critical role in the diagnosis of respiratory diseases and its clinical utility depends on the accuracy of the measured values. Classification of human respiratory functions experimentally recorded with spirometric pulmonary function test is analyzed using Extreme Learning Machines (ELM). In this study, data (N=300) are obtained using gold standard Spirolab II spirometer under controlled protocol from normal, obstructive and restrictive subjects. The considered parameters include Forced Expiratory Volume in first second (FEV_1), forced expiratory volume in sixth second, forced vital capacity and peak expiratory flow. The demographic parameters are also considered. These data are analyzed using extreme learning machines with five different basis functions which include sigmoid, sine, hard limit, triangular basis and radial basis functions. Results show that ELM is able to differentiate normal and abnormal subjects. The accuracy, sensitivity and specificity of ELM are found to be high for ELM with sine basis function. The clinical useful index FEV_1 is further validated by correlating it with the performance measures of ELM classifier. The methodology, results and discussion are also presented in this study. As automated analysis of spirometric data is significant for classification of prognosis of respiratory diseases, this study seems to be clinical relevant.

ID: 604

A5: 4

Signal quality improvement in time domain optical coherence tomography (TD-OCT) and Doppler optical coherence tomography (DOCT) using wavelet analysis

Saroch Leedumrongwatthanakun¹, Panote Thavarungkul^{1,3}, Proespichaya Kanatharana^{2,3} and Chittanon Buranachai^{1,3}

¹Department of Physics, Faculty of Science, Prince of Songkla University, Thailand; ²Department of Chemistry, Faculty of Science, Prince of Songkla University, Thailand; ³Trace Analysis and Biosensor Research Center, Prince of Songkla University, Thailand.

Optical Coherence Tomography (OCT) is a versatile non-invasive imaging technique capable of producing morphology images and velocity profiles. However, usually the image quality is compromised by noises. In this work one-dimensional wavelet denoising is proposed to improve the quality of both

morphology image and velocity profile simultaneously by doing the analysis on short-time Fourier transform domain of raw scattering signal prior to constructing the images. The parameters of wavelet denoising process are optimized based on the Figure of Merit (FOM) value of morphology images and maximum velocity and R-square value of velocity profiles. Our technique can improve image quality markedly and the optimal cases contain the detail coefficients from decomposition level 1–3, Universal thresholding, sln-rescaling and soft and hard transformation.

ID: 235

A5: 5

Apply a GFP-based FRET apoptosis sensor in zebrafish model to study cancer metastasis and search for new anti-cancer drugs

Afu Fu, Weida Ngan, Yu Ming Peh and Kathy Qian Luo

Division of Bioengineering, School of Chemical and Biomedical Engineering, Nanyang Technological University, Singapore.

Resistance to apoptosis is an important hallmark of malignant cancer cells and may contribute to their chemoresistance. Thus a better understanding on how cancer cells acquire this resistance to apoptosis during metastasis is needed for developing new strategies to treat metastatic cancer. To achieve this goal, a novel model for visualizing cell apoptosis *in vivo* during cancer metastasis and cancer therapy is urgently needed. We have developed a new cancer xenograft model in zebrafish embryos by transplanting cancer cell lines stably expressing a FRET based caspase-3 sensor. This sensor was constructed by fusing a CFP and YFP with a specialized linker containing caspase-3 cleavage sequence DEVD. When a cancer cell undergoes apoptosis in zebrafish, the linker will be cut to separate YFP from CFP; consequently, the cell will change its color from green to blue. After injected into zebrafish blood circulation, malignant MDA-MB-231 cells showed higher resistance to apoptosis and extravasation from blood vessel than non-metastatic MCF7 cells. This difference was found to correlate with their different antioxidant capacities. By using reactive oxygen species (ROS) detection reagent CM-H₂DCFDA, we found that blood flow could promote ROS generation in circulating cancer cells through activation of NADPH oxidase on cell membrane. Pretreating MDA-MB-231 cells with inhibitors of PI3K, ROCK and FAK before injecting into zebrafish blood circulation significantly reduced their resistance to apoptosis and prevented their metastatic action-extravasation. These results suggest that hemodynamic shear stress in the bloodstream can destroy circulating cancer cells by ROS generated by NADPH

oxidase. For cancer cells to become malignant they need to gain resistance to oxidative stress-induced apoptosis by increasing cell survival, deformation and adhesion. Finally, in zebrafish xenograft tumors, PI3K inhibitor was found to increase apoptosis and reduce tumor growth of B16F10 cells suggesting PI3K-activated survival pathway is also critical for cancer cell proliferation.

ID: 281

A5: 6

Design and implementation of a calibration-free pulse oximeter

Harini Harinarayanan, L. S. Krithika, M. Shalini, Sirisha Swaminathan and N. Madhu Mohan

Amrita Vishwa Vidyapeetham, India.

Oxygen saturation in human beings is measured as the ratio of the amount of oxygen carried by hemoglobin to the maximum amount it could carry. A pulse oximeter is a device which measures this saturated oxygen content using the technique of photoplethysmography. Generally, the device consists of two LEDs (Red and IR) as light sources, and a photo diode as the detector. Depending on the intensity of light transmitted or reflected to the detector, oxygen saturation is computed. Commercially available pulse oximeters require calibration, since the device is dependent on sensor and patient-dependent parameters like skin color and thickness of the digit. This is normally done by acquiring data from volunteers, after which the necessary coefficients are extracted, for computing the saturated oxygen content. Such a calibration technique is dependent on the sample population, and hence is undesirable. The work presented here, makes use of a calibration-free algorithm published earlier, incorporating it into a micro-controller, leading to a compact, power-efficient, pulse oximeter. Moreover, present day pulse oximeters do not give access to the raw PPG data, which could be used for extracting important cardiovascular parameters. The preliminary design presented here provides a serial port interface in order to acquire and communicate the PPG signal to a PC, for further offline analysis.

Session	B6: Pharmaceutical Science & Engineering
Date/Time	5 December 2013 14:30–16:00 hrs
Venue	SR-03 & 04

ID: 233 **B6: 1**

Three-dimensional chondrosarcoma model for high throughput drug screening

Yu Long Han^{1,2}, Tian Jian Lu² and Feng Xu^{1,2}

¹The Key Laboratory of Biomedical Information Engineering of Ministry of Education, Xi'an Jiaotong University School of Life Science and Technology, Xi'an, China; ²Bioinspired Engineering and Biomechanics Center, Xi'an Jiaotong University, Xi'an, China.

Chondrosarcoma is a common bone cancer that affects thousands of people worldwide. Although chondrosarcoma has been recognized for a long time, little breakthrough has been achieved in the treatment due to the poor understanding on cancer-treatment interactions, which depends on the availability of clinically relevant *in vitro* models. Muticellular spheroid (MCS) is one of the most promising *in vitro* cancer models as a replacement of monolayer cells for anti-cancer drug text and therapy screening. This because MCS partly recapitulate cell-cell and cell-ECM interactions compared with monolayer cells, representing by a more likely gene expression profiles compared with cancer *in vivo* than that of monolayer cells. Thus, various technologies have been developed to generate MCS recent years such as hanging drop methods, substrate with unadherent treatment, and spinner flask. Such methods always suffer from time-consuming, labor intensity, and a wide range of size distribution. Here we fabricate a polythene plate with hollow well to realize hanging drop culture on conventional 96 well-plate. In this system, we control the drop volume and geometry by surface tension to adjust the microenvironments of cell in drop. Besides, large volume of drop permit long time culture without periodic replenishment, which is one of the most notable challenge in conventional hanging drop methods. Based on this system, we establish the first *in vitro* 3D chondrosarcoma model which has great potential in therapy screening and drug text.

ID: 236 **B6: 2**

Effect of the polyelectrolyte hydrogel actuator network density on its mechanical behavior in the DC electric field

Mikhail A. Filipovich¹, Tatyana F. Shklyar^{1,2}, Alexander P. Safronov¹, Sergey Yu. Sokolov^{1,2} and Felix A. Blyakhman^{1,2}

¹Ural Federal University, Russian Federation; ²Ural State Medical Academy, Russian Federation.

This work addresses the mechanics of biocompatible actuators made of polyelectrolyte gels. Polyacrylic acid gels with sodium counterions were synthesized by free-radical polymerization in aqueous solution, and N,N'-methylene-diacrylamide was used as a cross-linker. In order to make gels with varying network density, cross-linker to monomer concentration was set at 1:25, 1:50, 1:100, and 1:200. The DC current initiated periodic bending of gel rectangular actuators (10 mm length and 1x1 mm in cross-section) placed in the bath with 0.8 mM CaCl₂ was observed. One end of the gel strip was attached to the wall of the bath while the other remained free. When the DC electric field with intensity 1.0 V/mm was applied across the actuator's longer axis, the free end of gel first bent to cathode, then more substantially to anode, then to cathode again and so on with damping amplitude. With the use of the optical system and the original software for the frame-by-frame actuator's borders tracing, the angle of gel's free end displacement (θ) from reference position was determined. We found that the increase of gel network density resulted in: a) the decrease of the number of successive bending; b) the decrease of θ for all actuator's oscillations and c) the decrease of actuator's free end displacement velocity (θ/t). Close correlations between the gel cross-linking and the θ and θ/t were determined for second and third oscillations of actuators. Thus, obtained results may help for the controlled optimization of actuators' mechanics for the application in different areas.

The study is supplied by Russian Foundation for Basic Research (grants ##13-08-01050a and 12-08-00789a).

ID: 206

B6: 3

A new anticancer agent inhibits breast cancer cell growth by reducing the expression levels of ER α and HER2

Ting Yu and Kathy Qian Luo*

Division of Bioengineering, School of Chemical and Biomedical Engineering, Nanyang Technological University, Singapore.

Breast cancer is the second leading cause of cancer death in women with 460,000 casualties worldwide in 2008. The most common type of breast cancer is the one overexpresses estrogen receptor (ER) and progesterone receptor (PR) which counts for near 70% of breast cancer cases. Hormone therapies using tamoxifen and aromatase inhibitors are standard treatment for ER positive breast cancer. However, breast cancer patients usually develop drug resistance to hormone therapy, especially from patients who overexpress human epidermal growth factor receptor 2 (HER2). Thus there is a need to develop new drug candidates that can target ER positive and HER2 overexpressing breast cancers. Recently we have found a new agent, acetyltanshinone IIA (ATA), which is a small molecular weight compound chemically modified from tanshinone IIA, a major compound isolated from a medicinal plant, *Salvia miltiorrhiza*, also known as Danshen. In our previous study, it was found that ATA almost completely inhibited the growth of xenografted tumor from human melanoma cells in nude mice. Recently, ATA was found to have potent growth inhibition effects on breast cancer cells that are either ER positive or HER2 overexpression. The results of mechanistic study suggest that ATA may inhibit ER positive cell growth by reducing ER α gene expression and promoting ER α degradation. As ER α is a transcription activator, the reduced ER α level was found to further reduce ER α -responsible gene expression, thus inhibiting the proliferation of ER positive breast cancer cells. More importantly, ATA also reduced the HER2 protein level and inhibited HER2 positive cell proliferation. So far no anticancer drugs have been reported with this dual effect on ER α and HER2 which are the most important therapeutic targets of breast cancer. Thus, ATA can be used to treat ER α and HER2 positive breast cancers which are resistant to the current hormonal and anti-HER2 therapies.

ID: 354

B6: 4

Method development for downstream processing of therapeutic cells – high-throughput process development for cell separation in aqueous two-phase systems

Sarah Nagel, Sarah Gretzinger, Stefan Oelmeier and Juergen Hubbuch

Karlsruhe Institute of Technology, Germany.

Preparative cell separation is a crucial step in therapeutic applications and is gaining increasing importance as cell therapies enter the market. In the past years, it has e.g. become feasible that insulin-producing beta-cells can be derived from human embryonic stem cells by specific differentiation. However, to date obstacles exist in the development of methods for large-scale cell separation, and a broader transfer of cell therapeutics to clinical applications remains challenging. Current methods use cell surface antigens for affinity purification. However, the extremely high costs due to large amounts of clinical-grade antibodies required for cell purification, interferes with the feasibility of those methods for clinical applications. Consequently, new label-free and cost-effective separation technologies will be required in order to purify therapeutic cells for clinical applications.

The present work focuses on the establishment of cell separation methods using aqueous two-phase systems (ATPS). The use of aqueous systems consisting of two immiscible polymer solutions offers a gentle, cost-effective, and scalable method for cell separation. Using ATPS, cells can be separated according to their physicochemical properties, thus, without antibody-labeling. In the present work, a high-throughput screening method using a Tecan Liquid handling station was developed for cell partitioning in ATPS, including cell quantification and analysis. The ATPS screening process was evaluated in regards to reproducibility and cell viability and optimal process parameters were determined. Subsequently, the high throughput screening method was applied to the partitioning of different differentiation states of a model cell line. The influence of polymer and salt types and concentrations, as well as the pH was evaluated, and separation conditions were optimized. Finally, it was shown that differential partitioning of different differentiation stages using ATPS is possible. The here developed high throughput screening method enables the fast and directed design of purification protocols for therapeutic cells.

ID: 650

B6: 5

Guidelines for modelling BED in simultaneous radiotherapy

Jan Kubiček and Marek Penhaker

VŠB - TU Ostrava, Czech Republic.

The paper deals with deduction and description of mathematical models which are used for assessment of radiotherapy efficiency and extent of damage to surrounding healthy tissue. Real historic data of 300 patients have been processed within the analyses. The first model is the Biological Equivalent Dose (BED) which has been composed for simultaneous radiation of two volumes: tpv_1 and tpv_2 . The mathematical formula for the BED model contains variables which represent the character of the tissue under radiation.

No fixed values exist there – only estimated intervals are used for the variables. The analysis results in optimum values of the parameters. They are obtained on the basis of the mathematical optimising process and calculation of BED values which forecast damage to the health tissue and radiotherapy effects. The mathematical model makes it possible to extend the BED model, as it takes into account two doses which are applied simultaneously. The other significant advantage of the model is that it comprises the values of the tumour volumes under radiation.

The second model (TCP) describes efficiency of the radiotherapy with respect to tissues under radiation. The patients were divided, for purposes of that analysis, into three groups, depending on efficiency of radiotherapy. An important role is also played by the total time of radiation and biological parameters of the tissue which is exposed to radiation. These parameters have been mathematically optimised. The result of the TCP model is the rate of success of the radiation and a correlation function within the patient's aVenue and result in the TCP model. This model is used to forecast whether the radiotherapy will success or fail and it an important part of the radiotherapy planning process.

ID: 734

B6: 6

Nano protein enhancer device (NanoPED) to increase insulin production in cells

Yang Gao¹, Eugenia Yeo¹, Dewi Susanti² and James Kah¹

¹Department of Bioengineering, National University of Singapore; ²Department of Biological Science, National University of Singapore.

Type 1 diabetes arises from the body's deficiency in production of insulin which is crucial in regulating carbohydrate and fat metabolism and may lead to

fatality is left untreated. Conventional strategies using subcutaneous injection of insulin and insulin pumps do not provide insulin independence to patients. Other strategies including transplantation, stem cells treatment and genetic manipulation in cells are either limited by allogenic rejection or complex cellular procedures with limited control to regulate insulin level. We aim to develop NanoPED with an interface to the cellular protein translation machinery that can serve to enhance insulin production in cells. This was done by conjugating DNA with appropriate sequence to gold nanoparticles (GNP) that allowed NanoPED to interact with human insulin DNA. The present study examines the different factors that affect insulin production *in vitro*. These include varying the size of GNP from 10 to 20nm, designing different human insulin DNA oligos to be conjugated onto the GNPs, and changing DNA:GNP ratios for conjugation. DNA-GNP conjugates were then evaluated in cell lysate to quantify the enhancement of insulin production. Results have shown that the larger the GNP size, and the higher the DNA:GNP ratio, the greater the enhancement. This is due to the fact that with larger GNP size and higher DNA:GNP ratio, more mRNA can be recruited for translation thus more insulin is produced. However, enhancement saturates at DNA:GNP ratio of 80:1. DNA oligos that were chosen to be complimentary to the 5' end of insulin mRNA results in greater enhancement in production compared to those complimentary to the 3' end. We conclude that human insulin production can be enhanced *in vitro* using NanoPED, which can potentially be used to treat insulin deficient cells in diabetic conditions.

Session	C5: Orthopaedics
Date/Time	5 December 2013 14:30–16:00 hrs
Venue	SR-05 & 06

ID: 262

C5: 1

Effects of adduction, internal rotation, and flexion angles on disVenue for total hip arthroplasty

Masaru Higa¹, Hiromasa Tanino², Y. Yamagami¹, Masayoshi Abo¹ and Satoshi Kakunai¹

¹University of Hyogo, Japan; ²Asahikawa Medical University, Japan.

Passive muscle tension around the hip joint following total hip arthroplasty (THA) plays an important role in post-surgery disVenue mechanisms, especially posterior disVenue. To analyze disVenue objectively and to clarify the distinction between implant-to-implant impingement and disVenue, three-dimensional finite element (FE) models of hybrid

THA components were generated. An acetabular component was implanted into the acetabulum in 20 degrees of anteversion and 45 degrees of inclination. The bearing surface had 26 mm hemispherical plus 1 mm flat depth and a chamfered edge. In this study, posterior disVene-prone movements such as flexion, adduction, internal rotation, and their combinations were analyzed, starting with the femoral component oriented in a manner corresponding to the hip being flexed to impingement with 0°, 10°, 20°, and 30° of internal rotation and 0°, 10°, 20°, and 30° of adduction. The nonlinear explicit FE simulations were driven by inputting a series of incremental flexion moments and hip joint forces concurrently. The angles of internal rotation and adduction affected both impingement and disVene angles of flexion. The flexion angles both at impingement and disVene decreased by increasing the internal rotation angles. Although the peak flexion moment to make the hip joint dislocate increased by increasing the internal rotation angle, it didn't always increase with an increase in the adduction angle. The highest value of the peak flexion moment to disVene was observed at 30° of internal rotation. Conversely, the lowest value of the peak flexion moment was observed at 10° of adduction. This lowest value means that the hip joint is easy to dislocate at this adduction angle.

ID: 269

C5: 2

Bearing surface with nano-level geometry inhibits macrophage activation in joint prostheses

Yoshitaka Nakanishi¹, Naoki Nishi¹, Yuuki Hikichi¹, Kenryo Shimazu¹, Yuta Nakashima¹, Hiroshi Mizuta¹, Hiromasa Miura², Yukihide Iwamoto³ and Hidehiko Higaki⁴

¹Kumamoto University, Japan; ²Ehime University, Japan; ³Kyushu University, Japan; ⁴Kyushu Sangyo University, Japan.

An ultra-high molecular weight polyethylene (UHMWPE) is widely used as bearing material in artificial joints, however, UHMWPE wear particles are considered to be a major factor in long-term osteolysis and loosening of implants. To minimize the amount of wear of UHMWPE and to enlarge the size of UHMWPE wear particle, a bearing surface with nano-level geometry, textured on Co-Cr-Mo alloy, was invented. Although the generally-used surface for a conventional artificial joint has 10 nm roughness, the textured surface with nano-level geometry has a superfine surface of 1 nm with 3% of groove and dimples against the bearing area. The depths of groove and dimples are less than 50nm. Pin-on-disc wear tester was used, UHMWPE pin with an average molecular weight of 6.0 million was placed in contact with the disc and the contact pressure was 6.0 MPa.

The textured surface reduced the amount of UHMWPE wear, this would ensure the long-term durability of artificial joint. Morphological aspects of the wear particles isolated from lubricating liquid were investigated. No significant difference was found in the distributions of aspect ratios. However, the distributions of the size were increased by using the textured surface. These results suggest that the textured surface does not change the morphological aspect of UHMWPE particle but enlarges the size of UHMWPE particle. Cells (RAW264.7, blood, Mouse) were cultured with the particles in supplemented Dulbecco's modified Eagle's medium for 24 h in an atmosphere of 5% CO₂ in air at 37 degrees C, and the quantitative PCR was performed for genetic expression of IL-6. The wear debris generated on the textured surface inhibited the genetic expression of IL-6, which does not induce the tissue reaction and joint loosening.

ID: 334

C5: 3

Response of a femoral bone to stationary and continuous load from within outward

Kiyoshi Mabuchi, Taiki Ito, Kentaro Uchida, Rina Sakai and Kouji Naruse

Kitasato University, Japan.

An experimental method was designed to exert a stationary load from the inside femur of a rat by inserting a loop spring made from a super elastic wire of titanium alloy. The stationary load generated the bone resorption with the migration of the spring wire into cortical bone if the severity is strong enough.

Stress in bone tissue can be remained after the press-fit-fixation of joint prostheses. The effect of residual stress has not been sufficiently discussed, yet, because the stress is stationary, which is unlike physiological conditions of fluctuation.

The response of bone tissues on mechanical stimuli has been already discussed by many investigators [1]. Major investigation composed the mechanical stimulation natural reaction force within the animal motions [2]. Therefore, the load on bone cannot be precisely estimated. Few studies have discussed the effects of stationary loads [3]. Quantitative study is scarcely performed by either clinical or animal experiments.

In the present study, we designed an experimental method to exert a stationary load from the inside femur of a rat by inserting a loop spring made from a super elastic wire of titanium alloy. The assessment of bone morphology around the implanted loop spring was performed by soft X-ray and micro-CT imaging 12 weeks after implantation. Each response on

various intensity of the stationary load was estimated respectively.

ID: 506

C5: 4

Development of a robotic testing platform for investigating knee joint ligament force contributions during various flexion extension angles

Ryo Takeda¹, Ferdinando Rodriguez y Baena² and Andrew Amis²

¹Hokkaido University, Japan; ²Imperial College London, United Kingdom.

A robotic testing platform for investigating the force contribution of the knee joint cruciate ligaments during various flexion and extension angles was developed. The system consisted of a 6 DoF industrial robotic manipulator (TX90, Stäubli Ltd) with a 6 axis load/torque sensor (Gamma, ATI Industrial Automation) attached to the end-effector. The developed platform was capable of measuring the force/torque and 3-dimensional position data at the end effector at a sampling rate of 250Hz. Experiments were conducted on ex-vivo ovine stifle (knee) joints with the femur part of an knee joint specimen attached to the end effector of the robot, while the tibia part was securely fixed to the ground. The center of rotation changes according to the flexion extension angle of the knee joint. Therefore a position control based strategy to implement a flexion extension rotation on a knee joint will result in damaging the specimen due to excessive internal force. In this work, an admittance control strategy to drive the robot which enables force adaptive trajectories around the knee was developed. The control was setup to neutralize five of the six DoFs (three translational and two rotational DoFs) during a flexion extension motion implemented by the robot. The knee joint specimen, with the cruciate ligaments intact, was moved from full extension (0 degree) to 90 degrees flexion and the end effector position was recorded onto a log file. Afterwards the cruciate ligament was surgically cut and the robot was operated under position control to repeat the motion of the log file, thus duplicating the motion of the intact knee. The developed robotic testing platform allowed for the exact comparison of load contribution of intact and severed cruciate ligament states during various flexion extension angles. As a result the platform can be used for evaluating new artificial ligaments.

ID: 348

C5: 5

Evaluation of bone fracture and load transfer mechanisms of lower limb injuries from under vehicle explosions

Angelo Karunaratne, Marit Undheim, Spyros D. Masouros and Anthony M. J. Bull

Royal British Legion, Centre for Blast Injury Studies, Department of Bioengineering, Imperial College London, UK.

Enhanced personal protection and advances in resuscitative techniques in recent years have resulted in an increase of survivors from explosions with complex musculo-skeletal injuries. Under-vehicle explosions result in axial loading of the lower extremity of the occupants with foot and ankle fractures commonly arising. There is no structural analysis of the effect of the transmitted load proximal to the zone of fracture, where no gross skeletal failure is observed. Potential alterations in microstructure may result in reduction in fracture toughness, thereby making bone more prone to secondary failure and unable to support potential surgical fixation. The aim of this study was to characterize the mechanical integrity of human tibiae loaded axially at high loading rates. We have previously tested lower limbs using our traumatic injury simulator that replicates the reponse of the vehicle floorpan that has been attacked by a mine. Different occupant postures tested resulted in diverse injury severities, all concentrated at the hind foot, without gross failure of the tibia. We harvested samples of cortical bone from the mid-diaphysis and the metaphysis of these tibiae, tested them to failure under three-point bending, and compared their reponse to unimpacted tibiae. There was a significant spatial variation ($p < 0.001$) in the work of fracture of cortical bone along the unimpacted tibiae. Samples from the proximal tibia (48.1 ± 7.3 Nmm) were significantly tougher ($p < 0.01$) than those of the distal (18.9 ± 9.5 Nmm) and mid-diaphysis (30.8 ± 8.9 Nmm) regions in control specimens and in specimens that did not sustain any fracture at the foot when tested in the simulator. This spatial variation was not observed in the tibiae of specimens that had sustained calcaneal fractures when tested in the simulator, suggesting that a stress pulse transmitted through long bones weakens their mechanical competence which concomitant clinical sequelae.

ID: 654

C5: 6

Quantification of the soft tissue artifacts of the upper limb during movements

Hsuan-Lun Lu¹, Tung-Wu Lu^{1,2}, Cheng-Chung Lin¹ and Mei-Ying Kuo³

¹Institute of Biomedical Engineering, National Taiwan University, Taiwan; ²Department of Orthopedic Surgery, School of Medicine, National Taiwan University, Taiwan; ³School of Physical Therapy, China Medical University, Taiwan.

Introduction: The upper limbs are essential for daily activities, and their functional performances are often evaluated using skin marker-based motion analysis. The measured kinematics of the upper limb is often affected by errors associated with the marker movements relative to the underlying bone, called soft tissue artifacts (STA), which are difficult to eliminate noninvasively. Quantification the STA of the upper limb during activities will be helpful for better choice of marker placement and for development of mathematical methods in reducing STA, which was the purpose of the current study.

Methods: Six healthy adults were attached with 24 retro-reflective markers on the upper arm (9 technical markers: UA1-UA9; humerus epicondyles: LE, ME), and forearm (9 technical markers: FA1-FA9; olecranon: OLE; radius head: RH; radial styloid: RS; ulnar styloid: US). Each subject performed whole ranges of elbow flexion/extension (F/E) and forearm pronation/supination (P/S) under the simultaneous surveillance of a motion capture system and a fluoroscopy system. The subjects also received CT scans so that the motions of the humerus, radius and ulna were accurately determined using a novel fluoroscopy-to-CT registration approach. The STA of the markers were then calculated as the marker movement relative to the underlying bone.

Results and Discussion: During F/E, markers around the elbow showed the largest STA (RH: 15.5, LE: 21.1, ME: 26.2, unit: mm) while markers away from the elbow showed the smallest STA (UA1: 8.0, RS: 4.6, US: 4.8, unit: mm). During P/S, upper arm markers near the elbow and forearm markers away from the elbow showed the smallest STA (UA3: 9.7, UA9: 9.7, US: 8.0, RS: 9.0, unit: mm) while the largest STA were found at FA1 (29.9) and FA7 (30.3). The current results indicate the marker positions with less STA for future kinematic measurements of the upper limbs during activities.

Session	YIA-02: Young Investigator Award II
Date/Time	5 December 2013 14:30–16:00 hrs
Venue	SR-07 & 08

ID: 453

YIA-02: 1

A biophysically-based tissue model for optimizing gastric pacing

Shameer Sathar, Greg O'Grady, Mark L. Trew and Leo K. Cheng
Auckland Bioengineering Institute, New Zealand.

Gastric pacing has been investigated for modulating gastric motility in diseased states. However, to advance this field, new pacing protocols are needed that directly improve gastric motility while increasing the efficiency of existing pacing devices. This study presents a mathematical tissue model for investigating slow wave entrainment during pacing, its comparison with experimental data gathered by high-resolution electrical mapping. The model was used to predict the effect anisotropic conductivities on slow wave entrainment, and the effect of gastric pacing on ectopic dysrhythmias. A diffusion based slow wave propagation model was used, with cell activity modeled as a finite-state machine. Initially, normal slow-wave antegrade propagation was modeled in accordance with experimental data. Then, these simulation parameters were applied to compare the model, in tandem with experimental studies in which an external pacing signal entrains native slow wave activity. The effect of different pacing frequencies on entrainment was demonstrated. Finally, this model was also used for simulating the effect of external stimuli for entraining a distal ectopic focal pacemaker. Two cases were studied with different fiber directions. The results showed that the pacing frequency and orientation of the fibers relative to the stimulation and ectopic site plays a critical role in gastric pacing efficacy.

ID: 000

YIA-02: 2

Effect of spatial arrangement of substrate topography on neuronal differentiation of stem cells

Evelyn K.F. Yim^{1,2,3}, Soneela Ankam^{1,4}, Aung Aung Kywe Moe⁴ and Lesley Y. T. Chan^{5,6}

¹Department of Bioengineering, National University of Singapore, Singapore; ²Department of Surgery, National University of Singapore, Singapore; ³Mechanobiology Institute, Singapore, National University of Singapore, Singapore; ⁴Duke-NUS Graduate Medical School, National University of Singapore, Singapore; ⁵NUS Graduate School for Integrative Sciences and Engineering, National University of Singapore, Singapore; ⁶Bioprocessing Technology Institute, Singapore.

Tissue engineered substrates can be modified to provide suitable mechanical cues for efficient manipulation of stem cell responses in the *in vitro* stem cell niche. Recent studies have shown that physical forces from the topography play a role in stem cell fate determination. We are interested in studying the response of human embryonic stem cells (hESCs) and murine neural progenitor cells (mNPCs) to substrate topography in the presence of neural differentiation media. A Multi ARChitectural (MARC) chip containing fields of various geometries and size was developed to investigate the influence of topography spatial arrangement on differentiation. The hESCs and mNPCs were differentiated on the MARC with minimal neuronal supplements for seven days and 14 days, respectively. The gene and protein expression analysis of neuronal markers β Tubulin III (Tuj1) and microtubule associated protein 2 (MAP2), and the glial marker, glial fibrillary acidic protein (GFAP) indicated an interesting trend on the anisotropic patterns versus the isotropic patterns. Human ESCs and mNPC grown on anisotropic patterns expressed significantly higher percentage of Tuj1 and MAP2 positive cells and lower percentage of GFAP positive cells, thereby supporting neuronal differentiation. The percentage of GFAP positive cells were significantly higher than the neuronal cells when hESCs or mNPCs were grown on the isotropic patterns, thus supporting glial differentiation. This study showed that optimal combination of topography and biochemical cues could shorten the differentiation period and allowed derivation of neurons bearing longer neurites that were aligned along the grating axis. Our results also showed that the topography contact during the differentiation period was necessary for topography induced differentiation. The MARC chip platform would enable high-throughput screening of topographical substrates that could maximize the efficiency of neuronal differentiation from stem cells.

ID: 420

YIA-02: 3

Estimation of changes in mechanical bone quality by multi-scale analysis with remodeling simulation

Daisuke Tawara¹, Ken Nagura², Tetsuya Tsujikami¹ and Taiji Adachi³

¹Department of Mechanical and Systems Engineering, Ryukoku University, Japan; ²Graduate School of Science and Technology, Ryukoku University, Japan; ³Department of Biomechanics, Research Center for Nano Medical Engineering, Institute for Frontier Medical Sciences, Kyoto University, Japan.

Mechanical bone quality and its related load-supporting function at the macro-scale is a result of adaptation, which is achieved by trabecular bone remodeling at the micro-scale. The increase in fracture risk in patients with osteoporosis is a clear example of this structure/function relationship, where decreased bone mass as a result of structural changes during remodeling leads to changes in the stress distribution of trabecular bone. This stress distribution is closely associated with the morphology and orientation of the nano-scale biological apatite (BAP) crystallite – the main factor determining bone quality. It is therefore important to evaluate both the changes in mechanical bone quality and bone mass when predicting fracture risk. We propose a computational model of remodeling and multi-scale stress analysis of trabecular bone based on homogenization techniques, considering the mechanical properties of the BAP crystallite orientation to be anisotropic. We first identified morphological changes in healthy and osteoporotic cases, and then performed a multi-scale stress analysis for the remodeled osteoporotic trabecular bone to elucidate changes in mechanical bone quality leading to fracture risk. Our results demonstrate that the load-supporting function of remodeled bone correlates with mechanical adaptability to external loads through remodeling, despite a progressive decrease in bone mass. These findings suggest the potential to use changes in mechanical bone quality as a predictor of fracture risk. The availability of these simulation methods for bone quality evaluation is discussed.

ID: 618

YIA-02: 4

Porohyperelastic analysis of single osteocyte using AFM and inverse FEA

Trung Dung Nguyen, Adekunle Oloyede, Sanjleena Singh and Yuantong Gu

Queensland University of Technology, Australia.

Osteocytes are the mature cells in bone and perform as the mechanosensors within the bone. The mechanical property of osteocytes plays an important role to

fulfill these functions. However, little researches have been done to investigate the mechanical deformation properties of single osteocytes. Atomic Force Microscopy (AFM) is a state-of-art experimental facility for high resolution imaging of tissues, cells and any surfaces as well as for probing mechanical properties of the samples both qualitatively and quantitatively. In this paper, the experimental study based on AFM is firstly used to obtain force-indentation curves of single round osteocytes. The porohyperelastic (PHE) model of a single osteocyte is then developed by using the inverse finite element analysis (FEA) to identify and extract mechanical properties from the experiment results. It has been found that the PHE model is a good candidature for biomechanics studies of osteocytes.

ID: 861

YIA-02: 5

Ligament-to-bone interface tissue regeneration using a functionalized biphasic silk fibroin scaffold

Thomas Kok Hiong Teh¹, Pujiang Shi¹, Xiafei Ren², James H.P. Hui², Siew-Lok Toh^{1,3} and James C.H. Goh^{1,2}

¹Department of Bioengineering, National University of Singapore, Singapore; ²Department of Orthopedic Surgery, National University of Singapore, Singapore; ³Department of Mechanical Engineering, National University of Singapore, Singapore.

The emergence of the tissue engineering approach has shown to be a game changer in ligament reconstruction, making it possible to create multi-phasic scaffold structures for multi-specific tissue regeneration. To regenerate the bone-ligament-bone tissue, mimicking hard to soft tissue transition, we propose the use of a functionalized biphasic silk scaffold. Hydroxyapatite nanoparticles (nHA) and bone morphogenetic protein 2 (BMP2) were loaded in the ends of Bombyx mori silk fibroin (SF) scaffold system to enhance entheses regeneration and bone tunnel healing, while the central one-third supported ligament regeneration. Two groups of biphasic scaffolds, distinguished by the different ends' additive, were fabricated: nHA only (Ctrl) and n-HA/BMP2 (Exp). A series of bench work, small animal study and large animal preclinical trial was performed using MSC-seeded constructs for the reconstruction of excised ACL. The bioactivity of BMP2 was ascertained and shown to be eluting with an initial burst, followed by a lowered sustained release. Osteogenic genes were upregulated in both groups compared to pure SF. By 24 weeks *in vivo*, the ACL was regenerated and bone tunnel narrowing was observed with histological evidences indicating new bone and entheses regeneration in Exp. Better graft to bone integration was observed in Exp compared to Ctrl. From this

study, it was demonstrated that the BMP2 eluting biphasic silk scaffold is promising as an advanced tissue engineering treatment modality for complete bone-ligament-bone reconstruction.

This study was supported by A*STAR, Singapore.

Session	SYM-06: Reproductive Bioengineering
Date/Time	5 December 2013 14:30–16:00 hrs
Venue	SR-12

ID: 344

SYM-06: 1

Biomechanics of infant feeding

David Elad

Tel Aviv University, Israel.

Breastfeeding is a dynamic process, which requires coupling between periodic motions of the infant's jaws, rhythmic pulsation of the surface of the tongue, and the breast milk ejection reflex. In preparation to breastfeeding the infant latches on to the breast and the nipple so that the nipple, the areola and the underlying mammary tissue and vessels are drawn far into the infant's mouth. During breastfeeding the infant moves its mandible up and down, compressing the nipple and areola in concomitant with sucking and spontaneous undulating motions of the tongue which channel the extracted milk towards the back of the oral cavity for swallowing into the esophagus.

In this study we developed a dynamic procedure for analysis of the contours of the tongue and upper palate in submental ultrasound (US) video recordings in order to explore the dynamics of tongue movement with respect to the palate during infant bottle and breast-feeding. In addition, we also developed a fluid-structure interaction (FSI) model of the breast and lactiferous tubes in order to explore the biomechanics of breastfeeding.

Analysis of US images during breastfeeding from 8 infants revealed that the anterior tongues moves as a rigid body while the posterior section of the tongue undulates in a pattern similar to a propagating peristaltic wave, which is essential for the human swallowing process. Applying an FFT algorithm to the contours representing tongue motility revealed dominant frequencies in the vicinity of 1.5 Hz. The simulations of the FSE computational model of breastfeeding revealed that latch-on and milk extraction during breastfeeding required sub-atmospheric pressures within the infant's oral cavity.

The present study may solve a century long dispute regarding the actual mechanisms performed by

infants in order to extract milk during breastfeeding. Moreover, the dynamic analysis of this study can also demonstrate the differences between bottle- and breast-feeding, as well as the advantage of performing the frenotomy in infants born with a tied tongue.

ID: 342

SYM-06: 2

The role of fluid dynamics in the determination of the left-right asymmetry in developing embryos

Oreste Piro

University of Balearic Islands, Spain.

The mechanism by which the flow within the Hensen's node determines the breaking of left-right symmetry during the development of embryos, is a beautiful example of the application of fluid dynamics to developmental biology. Detailed understanding of this crucial developmental process has greatly advanced by the transfer of ideas between these two disciplines. In this talk, we review our and others' work on applying fluid dynamics and dynamical systems to the problem of left-right symmetry breaking in vertebrates.

ID: 558

SYM-06: 3

Calaxin is a calcium sensor for turning of sperm movement

Kazuo Inaba

Shimoda Marine Research Center, University of Tsukuba, Japan.

Sperm chemotaxis is widely seen both in animals and plants and is considered to be necessary for efficient success of fertilization. Although intracellular Ca^{2+} is known to play important roles in sperm chemotaxis, the molecular mechanism how it causes the change in flagellar waveform that drives sperm directed toward the egg is still unclear. Several Ca^{2+} -binding proteins, especially calmodulin, have been discussed as an important regulator of the molecular motor dynein in flagellar motility during chemotactic movement of sperm. However there has been no experimental evidence to show the binding of calmodulin to dyneins. Recently we found a novel Ca^{2+} -binding protein, termed calaxin, in the axonemes of sperm flagella in the ascidian *Ciona intestinalis*. Calaxin binds to the outer arm dynein in a Ca^{2+} -dependent manner and suppresses its activity to glide microtubules at high Ca^{2+} concentration. Inhibition of calaxin results in significant loss of chemotactic behavior of sperm, indicating that calaxin is essential for sperm chemotaxis. In this paper, we describe the finding history, molecular

nature and the roles in sperm chemotaxis of calaxin, as well as its phylogenetic consideration.

ID: 341

SYM-06: 4

Microfluidics for mammalian embryo culture

S  verine Le Gac

University of Twente, The Netherlands.

Lab on a chip technology (LOC) or microfluidics has reached a mature state and is currently very popular in the field of life sciences, due to the numerous advantages it offers. Microfluidic devices enable faster, more sensitive and reproducible analysis using lower amounts of reagents or less energy. Furthermore, microfluidics lends itself well to the realization of complex platforms that integrate a series of independent but identical devices or a succession of operations. Originally, the development of LOC devices has been driven by the field of bioanalysis. However, their application has recently been diversified and extended to cellular investigations, field for which LOC present additional advantages: *in vivo*-like and tunable microenvironment, dynamic culture, and capability to couple cell culture, treatment and analysis on one single device. Lastly, sensors can be integrated for *in situ* monitoring of the cell status and its environment.

Here, we focus on one clinical application of LOC for assisted reproductive technologies (ART). ART comprise all techniques employed in the clinics to help sub-fertile couples founding a family. The field of ART is relatively young since the first test-tube baby was born in 1978, but it is growing at a high pace (5–10%/year) as a result of the increasing number of sub-fertile couples (~10% worldwide). At the same time, the ART success rate remains low (<30% clinical pregnancies), which can be partly attributed to the lack of maturity of the *in vitro* techniques employed. Those techniques are entirely manual and have known little change since their introduction. We will first briefly introduce the field of ART and highlight its current limitations, and explain why LOC technology can remedy the current situation. Following this, we will present our research on the culture and characterization of pre-implantation mammalian embryo in microfluidic devices.

ID: 335

SYM-06: 5

Mechanical properties of the pregnant uterine cervix: can elastography provide meaningful information?

Sabrina Badir, Manfred Maurer and Edoardo Mazza

ETH, Zürich, Switzerland.

Transvaginal ultrasound imaging is clinically used to evaluate the morphology of the cervix. Measurement of the cervical length is the golden standard to determine the risk of preterm delivery. The pregnant uterine cervix undergoes a progressive softening from early pregnancy to time of delivery. Palpation is the most common diagnostic tool in obstetrics to evaluate changes in consistency of the pregnant cervix. This method is subjective and provides only qualitative data about the state of the cervix. Recently, several groups used the ultrasound imaging technique called “quasi-static elastography” to characterize the mechanical properties of the uterine cervix in gestation. This technique aims at quantifying tissue consistency (in a similar way as palpation). The investigator applies a compressive force by the vaginal ultrasound probe on the anterior lip of the cervix and deforms the underlying tissue. The generated deformation field is directly proportional to the applied force and inversely proportional to tissue stiffness. Commercially available elastography machines compare successive images during the compression cycle to extract displacement and calculate strain fields. The outcome is an image which indicates differences between soft and hard regions within the deformed organ. The essential point of this elastography procedure is the lack of information about the applied force because ultrasound probes are not equipped with a force sensor.

An alternative ultrasound based method uses B-mode images to visualize the deformation of the cervix and increases the compressive force until no further deformation of the anterior-posterior distance is visible. Maximum deformation is the criterion for this measurement and the outcome is the deformability of the cervix as difference in diameter between compressed and uncompressed cervix. These procedures are discussed based on corresponding FE simulations and experiments with ultrasound phantoms. The results of clinical studies using ultrasound procedures are compared with our recent aspiration measurements.

ID: 338

SYM-06: 6

A novel computational approach for detecting mechanical causes of pelvic disorders

Manfred Maurer and Edoardo Mazza

ETH, Zürich, Switzerland.

Pelvic disorders, including urinary and fecal incontinence up to severe cases of pelvic organ prolapse (POP), occur in more than 30% of women in all age groups, posing a great restriction in quality of life for affected patients. Current treatments for POP include operative reconstruction of the anatomy of prolapsed organs and tissues. However, the recurrence rate for such operations is high (30–50%). Also due to the mechanical complexity of the female pelvic system, the mechanical causes for POP still remain largely unknown. A better understanding of the biomechanical context might lead to better treatments and therapies specifically targeting affected anatomical regions.

In this approach, a finite element model of the pelvic floor muscles is generated from MRI or CT data sets. In order to reduce the complexity of the modeled system, other pelvic organs and structural elements important for the kinematics and interconnectivity in the pelvic region (e.g. ligaments, fascias and connective tissues) are idealized and replaced by specific “regions of interaction” (ROI). These regions influence the kinematics of the pelvic system, being important connection points of the pelvic floor muscles to bones, ligaments or surrounding organs.

The proposed approach is based on (i) the application of kinematic boundary conditions (i.e. displacement fields) extracted from dynamic imaging during a valsalva maneuver in the ROI, thus prescribing their deformation and (ii) the optimization of material properties of all muscle groups to match the observed displacement field of the whole pelvic muscular system during the simulation of the same maneuver. This procedure allows to draw conclusions on the mechanical integrity of muscles and/or suspension and support structures of the pelvic floor.

We show a proof of concept of this approach, laying the basis for further advancement in understanding the mechanical complexity of the pelvic region, including patient specific models and predictions.

ID: 866

SYM-06: 7

Tracking the changes in electrophysiological activity of the uterus as it approaches labor using magnetomyographic technique

Eswaran Hari

University of Arkansas for Medical Sciences, United States of America.

Early and reliable diagnosis is essential to the development of successful interventions to prevent preterm delivery and improve outcome. In terms of physiology, the uterus is a complex organ and the underlying mechanism of labor is only partially understood. The complexity in understanding the uterine activity arises from the fact that each myometrial cell, unlike cardiac cells, can act as a pacemaker or as a pacerfollower. In order to better understand the uterine physiological mechanism, we have studied for the past few years, the use of a non-invasive, spatial-temporal device that uses SQUID (superconducting quantum interference device) sensors to record biomagnetic fields (Magnetomyography-MMG) corresponding to the electrical activity of the uterine smooth muscle. This instrument, called SARA (SQUID Array for Reproductive Assessment), is a maternal-fetal physiograph and has a broad range of applications specific to the improvement of the maternal-fetal health. We analyzed uterine magnetomyographic (MMG) signals recorded serially over time to determine if electrophysiological changes occur in signal characteristics of the uterus as it nears onset of active labor. Using a 151 sensor array system spread across the maternal abdomen, we serially record signals from pregnant women between the gestational ages of 36 and 40 weeks. Data is collected for a period of 20 minutes and band-pass-filtered between 0.35 and 0.8 Hz. Spatial-temporal mapping of uterine MMG data was achieved and applied to study the evolution of uterine electrophysiological activity as the uterus approaches active labor. Synchronization analysis shows that close to the onset of labor there is increase in synchronization across different areas of the uterus indicating that the uterus goes through a preparatory phase.

Session SYM-07: Virtual Physiological

Rat Project

Date/Time 5 December 2013 | 16:30–18:00 hrs

Venue Auditorium

ID: 739

SYM-07: 1

Symposium Keynote:

The virtual physiological rat project: a national center for systems biology to study interactions between genes, environmental factors, and physiological systems

Peter John Hunter¹ and Daniel Andrew Beard²

¹Auckland Bioengineering Institute, The University of Auckland, New Zealand; ²Department of Physiology, Medical College of Wisconsin, Milwaukee, WI, USA.

It is increasingly recognized that multifactorial diseases arise from interaction between genetic and environmental factors, and physiological systems. Examples of particular relevance to human health include the major health burdens that we face: cardiovascular disease and heart failure; metabolic syndrome and type 2 diabetes; and cancer. In all of these examples, acute and chronic (mal) adaptations of specific molecular mechanism and pathways in disease states occur against a background of physiological regulation. Since processes involved in complex disease operate in the context of physiological regulatory mechanisms, an understanding of a disease process builds upon an understanding of the associated physiological systems.

This talk will introduce the Virtual Physiological Rat (VPR) project, which aims to simulate the integrated cardiovascular function of the rat, and to build validated computer models that account for genetic variation across rat strains and physiological response to environment (i.e., diet). Specifically, examples from cardiac, renal, and cellular physiology will be used to illustrate three principles of the VPR: (1) Progress in physiology depends on application of computational modeling; (2) Complex diseases manifest on the background of physiological control; and (3) Computational physiology is a vehicle for genotype-to-phenotype mapping. In summary, Following the great successes in molecular genetics of the past decades, the challenge for integrative biology now is to “put Humpty Dumpty back together again” [1]. Our approach puts Humpty Dumpty together using computational modeling as the engine to integrate knowledge of interacting systems (often operating at different time and space scales), to analyze systems-level data, to formulate and test quantitative hypotheses, and to explore how function may emerge from the integration of interacting components in biological system.

Reference

1. Noble, D., *The music of life: biology beyond the genome.* 2006, Oxford; New York: Oxford University Press. xiii, 153 p.

ID: 367

SYM-07: 2

Arterial stiffening provides sufficient explanation for primary hypertension

Klas H. Pettersen¹, Scott M. Bugenhagen², Javaid Nauman³, Daniel A. Beard² and Stig W. Omholt³

¹Norwegian University of Life Sciences - UMB, Norway;
²Medical College of Wisconsin, USA; ³NTNU Norwegian University of Science and Technology, Norway.

Hypertension is one of the most common age-related chronic diseases and by predisposing individuals for heart failure, stroke and kidney disease, it is a major source of morbidity and mortality. Its etiology remains enigmatic despite intense research efforts over many decades. By use of empirically well-constrained computer models describing the coupled function of the baroreceptor reflex and mechanics of the circulatory system, we demonstrate quantitatively that arterial stiffening seems sufficient to explain age-related emergence of hypertension. Specifically, the empirically observed chronic changes in pulse pressure with age, and the impaired capacity of hypertensive individuals to regulate short-term changes in blood pressure, arise as emergent properties of the integrated system. Results are consistent with available experimental data from chemical and surgical manipulation of the cardiovascular system. In contrast to widely held opinions, the results suggest that primary hypertension can be attributed to a mechanogenic etiology without challenging current conceptions of renal and sympathetic nervous system function. The results support the view that a major target for treating chronic hypertension in the elderly is the reestablishment of a proper baroreflex response.

ID: 621

SYM-07: 3

Modeling the afferent dynamics of the baroreflex control system

Adam Mahdi and Mette Olufsen

North Carolina State University, United States of America.

Understanding the cardiovascular control system is crucial for gaining more insight into the physiology not only for the healthy individual, but also to detect pathologies. The main role of the cardiovascular system is to maintain adequate oxygenation of all tissues. This is achieved by maintaining blood flow and pressure at homeostasis. To accomplish the transport, a number of control mechanisms are imposed regulating vascular resistance, compliance, and frequency. An important contributor to the cardiovascular control is the baroreflex (or baroreceptor

reflex), which uses specialized neurons, called baroreceptors, that are activated using mechano-sensitive sensors located mainly in the aortic arch and carotid sinuses. These neurons are stimulated by changes in blood pressure and contribute to short-term regulation of vascular efferents including: heart rate, cardiac contractility, and vascular tone.

In this talk we will discuss how to develop a flexible and useful modeling framework for predicting baroreceptor firing rate as a function of blood pressure. We show how to use this framework in combination with parameter estimation to test and compare models. As a result, we propose a “generic baroreceptor model” and demonstrate that it can exhibit all known qualitative features of the pressure-response curve, as well as fit well quantitative data.

ID: 714

SYM-07: 4

The role of metabolic dysfunction in heart failure

Scott M Bugenhagen and Daniel A. Beard

Medical College of Wisconsin, United States of America.

Heart failure is known to be associated with changes in substrate pools for ATP synthesis, and modeling studies have revealed that such changes result in a loss in the available free energy for ATP hydrolysis [*Proc. Natl. Acad. Sci. U S A.* 2009 Apr 28;106(17):7143-8]. Since a variety of cellular processes in the heart depend critically on ATP (including cross-bridge cycling and Ca²⁺ sequestration into the sarcoplasmic reticulum), it is conceivable that alterations in ATP hydrolysis potential could result in mechanical dysfunction at the level of the cardiac myocyte resulting in impaired contractile performance of the heart and, ultimately, heart failure. In order to investigate the effects of cardiac energy failure on mechanical function independently of any effects of structural remodeling, a multiscale computational modeling approach is adopted integrating cardiac energetics with cell and organ level models of cardiac mechanics along with models of whole-body cardiovascular dynamics. Simulations reveal a possible role of metabolic dysfunction in the etiology of heart failure.

ID: 716

SYM-07: 5

Modelling epithelial transport

David Phillip Nickerson¹, Kirk Lee Hamilton² and Peter John Hunter¹

¹Auckland Bioengineering Institute, The University of Auckland, New Zealand; ²Department of Physiology, University of Otago, New Zealand.

We present an epithelial modeling tool facilitating the development and validation of models of individual transport processes and whole cell transport. Making use of established standards in computational physiology, our tool enables the user to assemble epithelial cell models from a library of reusable transport process descriptions, starting from either a blank canvas or pre-existing templates and models from the library. Our modeling tool uses CellML (<http://cellml.org/>) to encode the mathematical models. The CellML models are annotated with specific biological information, such as Venue within a cell membrane and identification of the ions being transported, and we make use of these annotations to automate the model building process. In a similar manner, existing template models in the library can be annotated to make it easier for the user to determine a suitable starting point for their work – an epithelial cell from the ascending limb in a renal nephron or a sodium transporter from the basolateral membrane of a proximal tubule cell, for example. We make use of SED-ML (<http://sed-ml.org/>) to associate experimental protocols with the mathematical models, allowing the user to compare their work against existing simulation and experimental data. Users are able to contribute new models, data, and protocols to the library for easy dissemination to, and reuse by, the community.

Supported by the Virtual Physiological Rat Project, National Institutes of Health grant [P50-GM094503].

Session	A6: Medical Imaging
Date/Time	5 December 2013 16:30–18:00 hrs
Venue	SR-01 & 02

ID: 187

A6: 1

A method for automatic delineation of the left ventricle borders in echographic images with use active contours model and speckle tracking technique

Sergey Yu. Sokolov^{1,2} and Felix A. Blyakhman^{1,2}

¹Ural State Medical Academy, Russian Federation; ²Ural Federal University, Russian Federation.

At present, an ultrasound imaging of the heart is widely used method for heart disease diagnostics.

The main object of ultrasound cardiac examination is the left ventricle (LV) – the most powerful chamber of the heart. In order to evaluate the necessary functional parameters of the LV, we need to delineate inner (and sometimes outer too) borders of the LV in ultrasound image. Manual borders tracing is very time-consuming procedure and it can produce subjective errors. Therefore, it is a vital problem to develop automatic (or semi-automatic) method for LV border delineation in echographic images. For solving this problem, we used as a base the active contours model (snake) - one of the most frequently used method for objects delineation in images. As the mitral valve should not be included in the analysis, in the first frame of the image sequence the user should annotate two points (so called anchor points) – one on each side of the mitral valve, and the third anchor point on the apex of the LV. Then the modified method of speckle tracking with prediction is used for automatically detection these points in the rest frames. Using these three anchor points, an initialization of inner contour of LV border as ellipse is performed. To reduce the time-consuming and increase method's convergence, we applied multi-scaling technique. As the ultrasound images often suffer from the effects of noise, the preliminary image filtering is carried out.

We tested proposed technique with images obtained during clinical cardiac ultrasound examination. The method showed good results of LV border delineation in images with high and middle quality.

The study is supplied by Russian Foundation for Basic Research (grants ## 12-08-00789a, 13-08-01050a).

ID: 439

A6: 2

A dynamic liver phantom for ultrasound image guided biopsy

Cheng Li¹, Suan Ping Ang¹, Jimin Liu² and Haoyong Yu¹

¹National University of Singapore, Singapore; ²Singapore Bioimaging Consortium (SBIC), Singapore.

Ultrasound image-guided liver biopsy has been widely applied in hospitals all over the world. However, tracking the target point on the liver surface is difficult due to motion induced by respiration. There is a strong need for phantoms that can simulate dynamic motion of the tissue for development and validation of accurate imaging tracking algorithms and biopsy system. To date, most commercialized phantoms or those reported in the literature are static ones that can't simulate the dynamic motion of the liver tissue. We propose a novel dynamic liver phantom for ultrasound liver biopsy. The phantom consists of a linear servo actuator for respiratory

motion generation and an ultrasound compatible compartment that can hold either gelatin liver models or porcine livers for testing. The performances of the phantom are tested on porcine livers with an ultrasound tracking system. The results show that the phantom can provide stable and repeatable movement cycles to simulate the human respirations. It has proven to be a very suitable dynamic phantom for ultrasound liver biopsy system development.

ID: 321

A6: 3

Region growing for medical image segmentation using a modified multiple-seed approach on a multicore CPU computer

Agus Pratondo¹, Sim Heng Ong^{1,3} and Chee Kong Chui²

¹Dept. of Electrical and Computer Engineering; ²Dept. of Mechanical Engineering; ³Dept. of Bioengineering.

Region growing is known as a simple and fast algorithm to segment an image. Many papers on medical image segmentation have reported the use of this algorithm in a variety of applications, for example, to detect cardiac disease and breast cancer and to delineate tumor volumes. One approach compares the initial seed pixels with the unassigned pixels. Another approach compares the outermost pixels with their unassigned neighbor pixels at each iteration. The first leads to consistent segmented areas but is very sensitive to noise. The second may result in inaccurate segmentations especially in cases where the pixel attributes change gradually, but it is robust to noise. In this paper we propose a method which is based on the modification of the multiple-seed approach by combining the above two approaches to obtain the advantages of each method. We consider the speed of segmentation for user convenience in segmenting the images from a DICOM file. A fast segmentation will make the application more user-friendly in displaying a series of images. This is achieved by using parallel programming on the multi-core computers that are commonly available. For hardware compatibility, an application program interface (API), openMP, is used to parallelize the program. Each outermost pixel can be expanded in a parallel manner. In our method, a global threshold is defined based on the initial seed, and the region is expanded by comparing the neighborhood pixel intensity with the global threshold, instead of using statistical region calculation. The evaluation of the performance is measured based on the time required to segment an image.

ID: 392

A6: 4

CT image reconstruction algorithm to reduce metal artifact

Toru Kano and Michihiko Koseki

Shinshu University, Japan.

X-ray CT reconstructs cross-sectional image of an object using projection data collected from many different directions. This technology has spread rapidly in the field of diagnostic medicine as a low-invasive inspection. X-ray CT has been brought great benefit to us, however, it is still facing some technical issues. In particular, metal artifact is a significant problem in CT imaging. Metal artifact is a strong streak noise caused by a discrepancy of projection data, and makes it difficult to diagnose patients with metal implants in his/her body. Even though various studies to reduce metal artifacts were conducted, the problem is not resolved yet.

In this study, we propose a reconstruction algorithm to reduce metal artifacts. The algorithm is based on the nature of sinogram which is also known as the Radon transform in rectangular coordinates. The sinogram is a data that is arranged projection data from many different directions. By this definition, sinograms consists of piles of sine curves and our algorithm utilizes this feature to resolve the discrepancy of the sinogram.

The proposed algorithm is divided into three processes. Firstly, sine curves of the metal region are extracted from sinograms by pattern matching, and the sliced image of the metallic object is reconstructed. Secondly, metal region on sinograms are interpolated along non-metal sine curves, and the filtered back projection is performed in order to reconstruct non-metal region. Finally, the two images are synthesized. The algorithm is able to reduce metal artifacts because it is not sensitive to the discrepancy.

We developed the CT simulation software in order to verify effects of complex situations assuming actual medical diagnoses. As a result, metal artifacts were effectively reduced either.

ID: 253

A6: 5

Effect of treatment using 3-dimensional disease generating model on optical coherence tomography images

Ngoc Anh Huyen Nguyen¹, Shinji Tsuruoka², Haruhiko Takase¹, Hiroharu Kawanaka¹, Hisashi Matsubara³, Hisanori Yagami⁴ and Fumio Okuyama⁵

¹Faculty of Engineering, Mie University, Japan; ²Graduate School of Regional Innovation Studies, Mie University, Japan; ³Faculty of Medicine, Mie University, Japan; ⁴Community University Research Cooperation Center, Mie University, Japan; ⁵Faculty of Health Science, Suzuka University of Medical Science, Japan.

Automatic extraction of retinal border lines for optical coherence tomography (OCT) images is important for assisting ophthalmologists in clinical decision making in terms of both diagnosis and treatment. 3D-OCT consists of 128 2D-OCT images representing cross-sectional structure. OCT has proven clinically useful for diagnosing a variety of retinal diseases. Some ophthalmologists desire the automatic measurement of a retinal thickness and its quantitative evaluation. Previously, the automatic measurement methods of the retinal thickness have been reported for retinal OCT images. However, the methods extracted the retinal border lines intermittently for OCT images, but they cannot measure the effect of treatment for an abnormal area automatically. And it's difficult in evaluating the effectiveness of laser treatment or medication.

In this paper, we propose a new three dimensional (3D) disease generating model to display the effect of treatment. To extract the change of the abnormal area, we applied the automatic measurement method of a retinal thickness in OCT image, which is the dynamic contour model ("One Directional Active Net (ODAN)") proposed by our research group to extract two retinal border lines, which are Inner Limiting Membrane (ILM) and Retinal Pigment Epithelium (RPE). The proposed generating model generates the border line of disease based on ILM, and employs the temporal subtraction technique to detect the effect of treatment. We confirmed the usefulness of the proposed model using the generated disease OCT images from normal retinal OCT images. We are considering that the proposed method is useful as the visual evaluation for the effect of treatment for retinal disease.

ID: 603

A6: 6

MRE simulation based on finite element vibration analysis of viscoelastic model

Sunao Tomita¹, Hayato Suzuki¹, Itsuro Kajiwara¹, Shigeru Tadano¹, Gen Nakamura² and Yu Jiang³

¹Division of Human Mechanical Systems and Design, Graduate School of Engineering, Hokkaido University, Sapporo, Japan; ²Department of Mathematics, Inha University, Incheon, Korea; ³Department of Applied Mathematics, Shanghai University of Finance and Economics, Shanghai, China.

Elastogram of magnetic resonance elastography (MRE) is a technique to identify the viscoelastic parameters of biological tissue by solving inverse problem from the displacement fields inside the tissue measured by the hardware of MRE. Finite element analysis (FEA) is effective to support developing elastogram. In this study, as the forward problem of elastogram three-dimensional numerical simulation of MRE measurement is conducted by applying FEA to a viscoelastic model of tissue. Then the inverse problem of elastogram is solved by applying the modified integral method to FEA results. The accuracy of numerical simulation is verified by comparing calculated results to real data measured by MRE.

ID: 189

A6: 7

Dynamic movement of the median nerve & its relation to carpal tunnel syndrome

Yushan Kyrin Jo Liong¹, Amitabha Lahiri², Dawn Chia³, Shujin Lee⁴, Aymeric Lim², Arijit Biswas³ and Heow Pueh Lee¹

¹Department of Mechanical Engineering, National University of Singapore; ²Department of Hand & Reconstructive Microsurgery, National University Hospital; ³Department of Obstetrics & Gynecology, National University Hospital; ⁴Division of Plastic, Reconstructive & Aesthetic Surgery, National University Hospital, Singapore.

Carpal tunnel syndrome (CTS) is one of the most common nerve neuropathies, affecting a significant portion of the population. However, the exact etiology of CTS remains unknown. We utilized dynamic ultrasound (US) to study the transverse median nerve displacement in 12 normal and 12 mild CTS candidates while they performed a fist action, and thumb, index finger (IF) and middle finger (MF) flexion actions. Fist action elicited the greatest nerve displacement, followed by MF, IF and thumb flexion, for all candidates. In all motions, median nerve displacements in normal candidates were significantly greater than that quantified in mild CTS candidates. A majority of candidates displayed an ulnar-volar movement of structures and the compression of the

nerve against the flexor retinaculum. In fist action, particularly, normal candidates displayed an extended-arc movement of the nerve, where it initially moves in a volar-ulnar direction, followed by a dorsal-ulnar direction, thereby subjecting the normal nerve to less pressure. In CTS candidates, however, the displacement arc is relatively linear, with the nerve becoming fully compressed against the flexor retinaculum. We also identified that maximum nerve deformation occurs mid-motion, as opposed to the previously assumed final position. In addition, in quantifying the percentage change in the aspect ratio of the nerve throughout each motion, we found that normal candidates displayed a greater deformation than their symptomatic counterparts, indicating the inherent malleability of a normal nerve. These findings suggest that in addition to increased carpal tunnel contents, a stiffer nerve and a decrease in nerve gliding movement may lead to CTS symptomatology. Our study also suggests the use of median nerve displacement during a fist action as a more easily observed and convenient discriminatory characteristic during US diagnosis of CTS.

Session	SYM-09: Pharmaceutical Science and Engineering
Date/Time	5 December 2013 16:30–18:00 hrs
Venue	SR-03 & 04

ID: 784 SYM-09: 1

**Symposium Keynote:
Engineering solutions to address challenges in drug delivery**

Samir Mitragotri

University of California, Santa Barbara, United States of America.

Targeted delivery of therapeutics in a patient-compliant manner is a critical technological and societal challenge in today's healthcare. Our laboratory is addressing this challenge by focusing on two critical needs; development of non-invasive alternatives to needle-based injections and development of strategies to target drugs to diseased sites. We have engineered approaches to deliver macromolecules across the skin using various tools including ultrasound, chemical enhancers, liquid microjets and peptide transporters. We have also extended these approaches to oral delivery to enable oral administration of proteins.

My talk will primarily focus on the strategies developed by our laboratory for targeted delivery of drugs to diseased sites by encapsulating them in polymeric particles. Particle properties have a significant impact on their therapeutic performance

including circulation half-life, drug release rates and toxicity. Our studies have shown that particle morphology plays a significant role in determining the biological and therapeutic outcome of nanoparticles. We have devised methods to generate particles of several distinct morphologies and studied their impact on key processes in drug delivery including phagocytosis, circulation, adhesion of vascular walls, and targeting. Based on this understanding, we have designed novel nanoparticles that demonstrate enhanced targeting towards cancer and cardiovascular disease sites.

My talk will present an overview of the engineering principles that lay the foundation of our research in drug delivery, applications of these principles to address critical needs in drug delivery and translation of these solutions to clinical practice.

ID: 135 SYM-09: 2

The multiple uses of fluorescent proteins to visualize cancer *in vivo*

Robert M. Hoffman^{1,2}

¹*AntiCancer Inc., San Diego, CA, United States of America;*
²*University of California, San Diego, United States of America.*

Naturally fluorescent proteins have revolutionized biology by enabling what was formerly invisible to be seen clearly. These proteins have allowed us to visualize, in real time, important aspects of cancer in living animals, including tumor cell mobility, invasion, metastasis and angiogenesis. These multi-colored proteins have allowed the color-coding of cancer cells growing *in vivo* and enabled the distinction of host from tumor with single-cell resolution. Visualization of many aspects of cancer initiation and progression *in vivo* should be possible with fluorescent proteins.

ID: 699 SYM-09: 3

Nanodiamond-enabled therapy and imaging

Dean Ho^{1,2,3}

¹*Oral Biology and Medicine, and Bioengineering;* ²*The Jane and Jerry Weintraub Center for Reconstructive Biotechnology;*
³*Jonsson Comprehensive Cancer Center and California NanoSystems Institute.*

Nanodiamonds have emerged as promising candidates for therapeutic delivery and imaging due to their uniquely faceted surface properties. Nanodiamond-anthracycline compounds have mediated marked improvements to drug delivery efficacy and safety. Most recently, NDX, a nanodiamond-doxorubicin agent, significantly enhanced the

pre-clinical efficacy of multiple drug-resistant tumor models with no apparent myelosuppression, demonstrating potent drug binding and the absence of early drug release [1]. Nanodiamonds bound to gadolinium have also resulted in contrast agents that are 12 times more efficient than clinical standards with among the highest ever reported per-gadolinium relaxivity values which may potentially markedly decrease patient gadolinium dosing. This lecture will highlight recent advancements in the use of nanodiamond-anthracycline complexes towards the treatment of multiple hard to address drug resistant models through clinically relevant administration modalities. In addition, diamond-based multimodal imaging/therapy approaches will be explored as potential clinically-relevant platforms [2]. The combination of these pre-clinical advancements in diamond-based nanomedicine and promising nanodiamond surface properties serves as a foundation for its translational roadmap which will also be discussed [3].

References

- [1] E.K. Chow, *et al.* *Science Translational Medicine*, 73ra21, 2011.
- [2] L.K. Moore, *et al.* *Advanced Materials*, doi: 10.1002/adma.201300343, 2013.
- [3] V. Mochalin, *et al.* *Nature Nanotechnology*, 7, 2012.

ID: 887

SYM-09: 4

From lab to cures to riches

Peng Leong

Merck Pte. Ltd, Singapore.

The world as we know it is changing. The population in developed and many emerging countries is aging. With the aging population comes more heart disease, diabetes, obesity, and cancer. The increasing prevalence of these diseases creates enormous opportunities for medical researchers to make a difference and to make a lot of money! As researchers in one of the leading biomedical centers in the world, you should ask yourself, how can your work fundamentally change the treatment paradigm and improve health and quality of life for everyone. Many of the scientists who invented the basic medical technologies behind our medicines today have also profited from their discoveries. The top 20 universities by royalty income earned \$1.3 billion USD in 2012 from sales of pharmaceuticals. Their inventions included the technologies for producing monoclonal antibodies in mammalian cells, methods for humanizing antibodies so they be used as therapeutics for humans, and stem cells. Many of the inventions were related to biotech as discoveries in biotech fundamentally changed medicine of the last 20 years. Do you know what is next after biotech? If you can

figure it out, you can be the one to take it out of the lab and in the process help patients and change your own life.

Session	C6: Computational Mechanics
Date/Time	5 December 2013 16:30–18:00 hrs
Venue	SR-05 & 06

ID: 613

C6: 1

Numerical investigation of mechano-electrochemical behaviors of articular cartilage under dynamic contact loading

Xian Chen¹, Hiroyuki Oka² and Junji Ohgi¹

¹*Yamaguchi University, Japan;* ²*The University of Tokyo, Japan.*

Articular cartilages are mainly composed of extracellular matrix, interstitial water and negatively charged proteoglycan aggregates. For modeling such material, triphasic theory has been proposed by assuming the tissue as a mixture composed of solid matrix phase, interstitial fluid phase and ionic phase, and taking into account the interaction between the phases. Extra mechanical stresses resulting from electro-chemical swelling have been revealed to be important in the functional load support of articular cartilages.

On the other hand, contact phenomenon as a mechanical characteristic distinguishes articular cartilages from other soft tissues such as intervertebral disks, since the diarthrodial joint functions as a load transfer mechanism by contact between cartilage surfaces. Considering that contact analysis of mechano-electrochemical coupling behavior appears an indispensable tool in investigations of joint disease since the destruction of the extracellular matrix and chondrocyte death may be caused by excessive contact load, the authors have developed a mechano-electrochemical coupling contact analysis algorithm for large deformation problems.

Another important feature is that the articular cartilages have anisotropic and inhomogeneous structure which contains three zones with different collagen content and fibrils orientation. The superficial tangential zone has been shown to play a major role to resist shear stresses due to the collagen fibrils orientation parallel to the joint surface.

In this work, the anisotropic and inhomogeneous structure of the articular cartilages was introduced into the mechano-electrochemical coupling contact analysis algorithm. By taking into account the distribution of the collagen fibrils orientation in the cartilage layer, the sliding contact analysis was carried out to obtain the cartilage deformation, flow of interstitial fluid, ionic fluxes, distributions of stress, strain,

hydrostatic pressure and osmotic pressure and thus to investigate the effects of dynamic contact load on the mechano-electrochemical behaviors of articular cartilages.

This work was supported by JSPS KAKENHI Grant Number 23560087.

ID: 447

C6: 2

Hinge flow fields study of SJM bileaflet mechanical heart valve

Yee Han Kuan¹, Vinh-Tan Nguyen² and Hwa Liang Leo¹

¹NUS, Singapore; ²A*STAR Institute of High Performance Computing, Singapore.

The complexity of the hinge flow fields results in potential thromboembolic complications in bileaflet mechanical heart valves (BMHV) and has been shown in earlier numerical simulations. By looking into the flow fields in the hinge regions, we can characterize and identify the regions of high wall shear stress and back flow leakage. The geometry of the hinge regions of BMHVs plays a crucial role in minimizing complications. In earlier simulation models, there is a lack of study on the resultant flow field due to the angle of implantation of BMHV. In this study, we aimed to look at the effect of different angle of implantation BMHV with respect to the anatomical three aortic sinuses chamber on the flow fields in the hinge regions. We looked at several angle of implantation at 0, 30, 60, and 90 degree of an anatomical three aortic sinuses model. A 29mm St Jude Medical Bileaflet Mechanical Heart Valve with all its four hinges were modeled. The simulations are performed during the systolic and diastolic phases. Physiological flow with inlet velocity and outlet pressure is set as the boundary conditions. A complex flow leakage was observed in the simulation results during early diastole, whose intensity decreases towards late diastole. Also, elevated wall shear stresses were observed in the ventricular regions of the hinge recess. The simulation results showed that numerical tools are important in observing the physical viscous stresses experienced by the blood elements and complex flow fields. They can also provide high spatial resolution and details that would be hard to achieve experimentally.

ID: 478 C6: 3

An anatomically realistic geometrical model of the intra-epidermal nerves in the human foot

Muhammad Zeeshan Ul Haque, Peng D., Leo K. Cheng and Marc D. Jacobs

The University of Auckland, New Zealand.

The intra-epidermal nerve fibre (IENF) network in the skin of the foot generates the sensory nerve action potentials (SNAP). Variations in the conduction velocity (CV) of the SNAP can be recorded to identify diabetic neuropathies. A computational model of the IENF network of the foot may provide a suitable platform to investigate small fibre neuropathy by determining SNAP and CV at different stages of disease and in different regions of the foot. In this work, we demonstrate the development of an anatomically realistic model of the IENF network in the skin of the whole foot and also an IENF network with localized neuropathy. A Monte Carlo algorithm was used to generate the bifurcated IENF network tree based on IENF density (IENFD). In addition, this model demonstrates an initial perturbed IENF network at the lateral region just above the little toe of the foot based on IENFD at this region, to simulate small fibre neuropathy. This generated model will be used in forthcoming studies to integrate the structural and functional consequences of small fibre neuropathy.

ID: 336

C6: 4

Blood flow analysis in patient-specific cerebral aneurysm models with realistic configuration of embolized coils

Tomohiro Otani, Satoshi Ii, Toshiyuki Fujinaka, Masayuki Hirata, Junko Kuroda, Katsuhiko Shibano and Shigeo Wada

Osaka University, Japan.

In this study, we simulate the blood flow in 3D patient-specific model of the cerebral aneurysm embolized with coils. The patient-specific model of the cerebral aneurysm was constructed from clinical CT images. To represent a realistic configuration of embolized coils in the aneurysm, a virtual coil model was employed constructed by means of a coil insertion simulation based on the minimum energy principle. The packing density of embolized coils was approximately 30% which was higher than required values in clinical practice. A blood flow analysis was done by solving the N.S. and continuity equations numerically with the finite volume method under rigid wall assumption. The blood flow simulation revealed that the flow shear rate was locally increased near the coil surface imposing no-slip velocity, especially around the entrance of the

aneurysm, and the increase/decrease of the overall shear rate in the aneurysm was determined by the coil configuration embolized in the aneurysm. The present simulation also revealed a difference of coil-insertion condition exhibited various geometric configuration of the embolized coil and it sometimes gave a unique case, in which the coils were mainly distributed in the deep region in the aneurysms, in other words the local packing density of the entrance region was low, resulting in the strong shear flow as compared before the coil embolization.

ID: 771

C6: 5

Numerical investigation of micro-particle transport and deposition in an upper airway considering human workloads

Kun Hyuk Sung, Ji Tae Kim and Hong Sun Ryou

Mechanical Engineering, Chung-Ang University, South Korea.

During a respiration, the process of transport /deposition of inhaled particles is influenced by the morphological characteristics of airway and respiratory conditions related to the human workload. Especially in a heavy workload or a panic state, the flow rate and the breath frequency remarkably increase with compared to a normal state, and then the particle transport and the flow characteristics change dramatically in the airway. In this study, the flow characteristics and micro-particle deposition patterns were numerically investigated in a representative human upper airway model using the real respiratory waveform considering workloads. Also, the mean Stokes number for particles is in the equivalent range of $0.00015 < St_{mean} < 0.03377$ at each workload. In the results, the deposition fraction (DF) steeply declines with a decrease in the mean Stokes number at the upper region from the oral cavity to the pharynx, while the change in the DF is relatively small at the lower region from the larynx to the trachea in all workloads. This is because the mechanism of the transport/deposition process is diffusion dominant due to turbulent dispersions at the lower region, whereas at the upper region is impaction dominant. Also, compared with the light workload, the total DF increases in whole mean Stokes numbers at the heavy workload, while the dominant region where particles deposited differs with the workload. These implies that the human workload as well as the particle size are important to investigate the optimal drug aerosol targeting and the effect of the inhaled toxic materials in the human airway.

ID: 256

C6: 6

A realistic subject-specific finite element model of human head-development and experimental validation

Kwong Ming Tse¹, Long Bin Tan¹, Shu Jin Lee², Siak Piang Lim^{1,3} and Heow Pueh Lee^{1,3}

¹Department of Mechanical Engineering, Faculty of Engineering, National University of Singapore, Singapore; ²Division of Plastic, Reconstructive and Aesthetic Surgery, National University Hospital, Singapore; ³National University of Singapore (Suzhou) Research Institute Suzhou Industrial Park, Jiang Su, China.

Head injury, being one of the main causes of death or permanent disability, continues to remain as a major health problem with significant socioeconomic costs. Therefore, there is a need for biomechanical studies of head injury. To assess the biomechanics of head injury mechanism, many finite element head models (FEHMs) had been built. However, in order to reduce the computation efforts, most of these FEHMs were simplified and details of complex head anatomical features are often ignored in modeling. The main purpose of the present work is to build and validate a detailed finite element model of human head in order to better predict the mechanical responses of the human head during head injury. Geometrical information of a human head is obtained from medical images of computed tomography (CT) and magnetic resonance imaging (MRI) with the use of image-processing software, for segmentation and reconstruction of a comprehensive FEHM. The head model is then validated against both intracranial pressure (ICP) data of the two experimental cadaver tests. General shape trends, magnitudes and duration of the pressure pulses in the simulation agree well with the experimental pressure pulse. Overall, there is a good correlation between the simulations and the experiments. Once being validated, this representative FEHM can be used in the assessment of the injurious effects of different loading conditions and enable the development of enhanced head injury and protection equipments through the reconstruction of the available real-world accidents information.

ID: 313

C6: 7

Local osteoporosis and its effects on anti-resorptive drug treatment: A 3-year follow-up finite-element study in risedronate-treated women

D. Anitha¹, Kim Kwang Joon², Lim Sung-Kil² and Lee Taeyong¹

¹National University of Singapore, Singapore; ²Division of Endocrinology and Metabolism, Yonsei University Health System, Korea.

Osteoporosis remains a prevalent problem amongst the elderly. Its prevalence is known to vary from 10-20% in patients aged 50 years and older, depending on race and assessment methods. Currently, bone mineral density (BMD) obtained from dual X-ray absorptiometry (DXA) is the golden standard in diagnosing osteopenia ($-1.0 < t < -2.5$) and osteoporosis ($t > -2.5$). However, following osteoporosis therapy, increases in BMD can be deceptive. Although hip fracture risk can be reduced with the aid of drugs, treated patients still face considerable risk as most people who sustain hip fracture do not have generalised osteoporosis. This necessitates a study of the local distribution of bone mass which contributes to the geometry and consequently the bone strength. By identifying the respective regions in the femoral neck, the geometric changes were localized and differed between each patient, leading to the conclusion that drug treatment elicits local changes in R_{mean} and CT_{mean} . This is further validated by finite element analysis where critical strain regions were predicted at similar zones and this is coherent with the fact that reduced thickness of the cortical bone has been related to increased risk of fracture initiation. Hence, from individual radar plots, we can determine if the effect of drugs had outweighed the effect of aging and thus propose a course of treatment drug better suited for the patient in the clinical scenario. Clinically, little conclusion can be drawn from just the BMD in osteopenic/osteoporotic patients. This emphasizes the necessity of using geometry and structure to predict fracture risk. Thus, we believe that focusing on a patient specific analysis for clinical diagnosis will improve diagnosis of osteoporosis and ultimately fracture prediction.

Session	E2: Assisted Technologies
Date/Time	5 December 2013 16:30–18:00 hrs
Venue	SR-07 & 08

ID: 828

E2: 1

Finger grip rehabilitation using exoskeleton with grip force feedback

Chee leong Chan, Suresh Gobee and Vickneswari Durairajah

Asia Pacific University, Malaysia.

This paper introduces a pair of exoskeleton hand for finger rehabilitation. There is slave and master exoskeleton was designed to have force feedback system on gripping force. The exoskeleton system construction is divided to three parts. First is the hybrid conductive silicone construction is shown and the best way to use as force sensor is presented. Followed by Labview configuration with force feedback system is presented. Third is the mechanical designed principle of exoskeleton is explained in this paper. Finally the response of the system is presented.

ID: 557

E2: 2

Measuring human balance on an instrumented dynamic platform: a postural sway analysis

Darwin Gouwanda¹ and Alpha Agape Gopalai²

¹Monash University Sunway campus, Malaysia;

²Curtin University Sarawak, Malaysia.

A system to monitor the trajectory and distribution of Center of Pressure (CoP) oscillations in real-time was designed. The system used a custom built force plate that measured sway area and sway velocity based on the measured CoP. A stable posture is reflected by a controlled CoP oscillation, where the oscillation lies within the limits of stability. Large magnitudes of CoP oscillations (large sway area) indicate weak proprioception strength and a heightened risk of falls. Experiments carried out involved self-induced perturbations that destabilized postural control among volunteers with active and inactive lifestyles. The observed results from the experiment indicate that individuals with active lifestyle have better postural control than individuals with inactive lifestyle. Subjects with active lifestyles demonstrated greater sway velocities, while maintaining a small sway area.

ID: 575

E2: 3

Integrated RT and cryo ablation of liver tumor for computer integrated surgery

Bin Duan, Chee Kong Chui, Kian Jon and Ernest Chua

NUS, Singapore.

Recent research shows combining Radiofrequency (RF) and Cryosurgery could improve the outcome of tumor treatments. Reasons for combining RF and Cryo includes: (1) producing maximal destruction while maintaining hemostatic control; (2) reinforcing the tissue destruction; (3) inducing anti-tumor immune response. For large liver tumor treatment, multiple insertions of electrodes are always required and computer planning is needed to achieve optimally planned ablation. This study investigates the effectiveness of combined RF and Cryo ablation in computer planning of large tumor ablation.

ID: 226

E2: 4

Effects of muscle fatigue on FES assisted walking of SCI patients: A review

Morufu Olusola Ibitoye, Nur Azah Hamzaid and Ahmad Khairi Abdul Wahab

University of Malaya, Malaysia.

Sequel to spinal cord injury (SCI), functional impairment is sustained and the SCI individuals are often confined to wheelchair usage. Current trends of walking rehabilitation adopted is functional electrical stimulation (FES) assisted gait with partial body weight support. However, lack of lower limb proprioception, inability to control complex joint trajectory, rapid energy consumption, unstable and insufficient muscle force due to motor unit recruitment strategy often lead to fatigue thus constituting major limitation. Substantial literatures document significant effect of FES assisted rehabilitation of SCI individuals with highlights on functional gait and characteristics. Advances in neuroscience have also improved FES assisted gait but limiting effect of muscle fatigue consistently remains a considerable challenge. It is also evident from reviewed articles that rate of fatigue during FES elicited contraction is generally higher than voluntary contractions. By implication, optimized functional recovery of people with SCI by FES could significantly improve once muscle fatigue is addressed. This review constitutes a unique attempt to assess available evidence of effects and extents of muscle fatigue in FES assisted walking of SCI patients. It highlights state of the art procedures to minimize fatigue and looking forward to approaches that could further reduce the effect of fatigue on FES evoked contraction for patient enhanced beneficial

gait to avoid secondary illness due to physical inability. The outcome of this study is relevant in clinical optimization of effects of FES rehabilitation on individuals with SCI.

ID: 391

E2: 5

Energy recovery concept for collecting stochastic occurring power chunks to supply intermittent sensor measurements on prostheses or robotic limb

Daniel Laqua and Peter Husar

Ilmenau University of Technology, Germany.

Finite energy sources like batteries have to be recharged or exchanged. Replacing them by autonomous power supply concepts could prevent running out of energy and expand the durability enormously. A potential field of application is energy harvesting on prosthesis or robotic limb using unexploited mechanical energy. The restriction of this approach is the inconsistent and non-continuous energy supply. Conventional energy harvesting systems need an almost continuous power input and merely brief interrupts are allowed or could be bridged. This contribution presents a system, which is able to handle input signals regardless of their signal characteristics to supply a sensor circuit, as such as a force sensor.

The mechanical energy is transformed into electrical energy by using energy harvesting devices like a piezoelectric cantilever or a stepping motor if part of the prosthesis or robotic limb. Predicting the occurrence of power chunks during the operation of a prosthesis or robotic limb is not reliable. Hence it is a preferable approach to collect them first until there is enough power to supply a sensor circuit. The developed energy recovery system uses a passive energy measurement without any active sensors to minimize the power consumption. The major source of error and thus also the limiting factor of this procedure are the complex electrical parameters of the real parts. If sufficient energy is gathered, the system awakes from sleep mode. A switching converter stabilizes the voltage to the required level for the connected load.

The presented energy recovery system was evaluated using several synthetic signals and different power inputs. Further experiments with a piezoelectric cantilever as power source were successfully realized.

This investigation has revealed that interval-wise sensor measurements with undetermined idle times are possible. Our investigations demonstrate the feasibility of the presented energy harvesting concept applied to prostheses or robotic limb.

ID: 740

E2: 6

A head tracking method for improved eye motion detection in children

Mehrdad Sangi¹, Benjamin Thompson², Ehsan Vaghefi^{1,2} and Jason Turuwhenua^{1,2}

¹Auckland Bioengineering Institute, University of Auckland, New Zealand; ²Department of Optometry and Vision Science, University of Auckland, New Zealand.

The presence of untreated visual disorders in early childhood can result in abnormal visual cortex development (amblyopia). However, accurate clinical assessment of visual function in young children is highly challenging. Reflexive eye movements may allow for precise measurement of visual functions such as resolution acuity in young children if age appropriate, clinically acceptable, quantitative eye tracking techniques can be developed. Children do not tolerate chin-rests or head mounted eye-tracking equipment, therefore we have developed a method to measure and compensate for unrestrained head motion that may facilitate detection of eye movements. We implemented an automatic feature-based algorithm to track features on the face in pre-recorded videos. These data were used to “lock” the head to its initial position. Secondly, we implemented a single un-calibrated camera method to estimate the 3D movements of the head. The method was tested using video footage from five children who observed visual stimuli designed to induce horizontal optokinetic nystagmus (a reflexive sawtooth motion of the eye consisting of pursuit and saccadic eye movements). The children’s heads were unrestrained, thereby exhibiting natural movement within the video. Markers placed on participants’ faces were manually segmented to yield ground truth data. The standard deviation of head movement improved from (18.6676, 8.9088) to (1.8828, 1.4282) pixels after stabilization. The average mean square error (MSE) between the manual and automatic stabilization methods was 7.7494 pixels. The percentage error for 3D pose estimation was 0.2428%. Stabilization of the eyes (relative to the head) was achieved. In conclusion, our initial results suggest that head movement stabilization is possible as a post processing step which could significantly facilitate the monitoring of eye movements in children. Furthermore automated methods could improve the monitoring of neuro-developmental disorders that manifest through head movement.

Session	SYM-08: Tissue Mechanobiology: Tissue on the Move
Date/Time	5 December 2013 16:30–18:00 hrs
Venue	SR-12

ID: 373

SYM-08: 1

Symposium Keynote: Mechano-sensitive ATP release: Critical involvement in wound healing

Masahiro Sokabe^{1,2}, Hiroya Takada^{1,3} and Kishio Furuya¹

¹Nagoya University Graduate School of Medicine, Japan; ²Mechanobiology Institute, National University of Singapore; ³Pixy Corporation, Japan.

ATP is not only an energy currency in cells but also an extracellular signal that activates purinergic receptors in autocrine and paracrine ways, resulting in an increase in the intracellular Ca^{2+} level ($[Ca^{2+}]_{cyt}$). Interestingly, ATP is often released from cells subjected to a variety of mechanical stimuli such as stretch and flow, suggesting that ATP mediates intercellular communications in tissues under mechanical stress. Wound healing may be a good model to test this hypothesis. The leading cells facing the scar migrate into vacant region with dragging the following cells adhered to them. Our previous result that stretching an endothelial cell sheet facilitated wound healing supports the idea that mechanical force is a crucial factor to regulate wound healing.

In this study, we used a keratinocyte (HaCaT cell) monolayer with a linear scar (200 μ m width) cultured on an elastic silicone chamber coated with collagen, by which we could apply stretch to the cell sheet. ATP releases and $[Ca^{2+}]_{cyt}$ were live imaged using luciferin-luciferase luminescence and fluo-8 fluorescence, respectively.

When the HaCaT cell monolayer was stretched (20%, 1 sec), which significantly facilitated wound healing, a transient ATP release followed by a $[Ca^{2+}]_{cyt}$ transient was observed only in the leading cells facing the scar. Associated with ATP diffusion, Ca^{2+} wave propagated across the following cell layer in several minutes. Treating the cells with apyrase an ATP hydrolytic enzyme or suramin a purinergic receptor blocker significantly inhibited the ATP release and $[Ca^{2+}]_{cyt}$ transient as well as wound healing. Pharmacology suggested that the $[Ca^{2+}]_{cyt}$ increases were mediated by Ca^{2+} influx through TRPC6 activated via P2Y2 receptors. Importantly, pharmacology to inhibit these signals was perfectly in line with that to inhibit wound healing even in non-stretched cells, indicating that mechanosensitive ATP- Ca^{2+} signaling is a crucial factor to mediate normal wound healing.

ID: 530

SYM-08: 2

On the role of biomechanics during embryogenesis

Lance A. Davidson

University of Pittsburgh, United States of America.

Morphogenesis during embryonic development requires the coordinated movement of large numbers of cells. This coordinated tissue movements requires force production integrated with the mechanical properties of the tissues involved. Our group has developed both the experimental tools and a conceptual framework needed to understand how forces and material properties are integrated during tissue and self-assembly. This talk will survey recent findings on global regulation of tissue tension and the local coordination of cell traction during the gastrulation.

ID: 711

SYM-08: 3

Forces driving epithelial wound healing

Vito Conte¹, Agustí Brugués¹, Ester Anon^{1,2}, Jim H. Veldhuis³, Julien Colombelli⁴, José J. Muñoz⁵, G. Wayne Brodland³, Benoit Ladoux^{2,6} and Xavier Trepât^{1,7,8}

¹Institute for Bioengineering of Catalonia, Spain; ²Institut Jacques Monod (IJM), Université Paris Diderot, France; ³Department of Civil and Environmental Engineering, University of Waterloo, Canada; ⁴Institute for Research in Biomedicine (IRB Barcelona), Spain; ⁵Laboratori de Càlcul Numèric, Department of Applied Mathematics III, Universitat Politècnica de Catalunya, Spain; ⁶Mechanobiology Institute (MBI), National University of Singapore, Singapore; ⁷Institució Catalana de Recerca i Estudis Avançats (ICREA), Spain; ⁸Unitat de Biofísica i Bioenginyeria, Facultat de Medicina, Universitat de Barcelona, and CIBERES, Spain.

A fundamental feature of multicellular organisms is their ability to self-repair wounds through the movement of epithelial cells into the damaged area^{1,2}. This collective cellular movement is commonly attributed to a combination of cell crawling and "purse-string" contraction of a supracellular actomyosin ring³⁻⁴. Here we show by direct experimental measurement that these two mechanisms are insufficient to explain force patterns observed during wound closure. Contrary to common assumptions, we found that actin and myosin accumulate at the leading edge in a heterogeneous mechanical structure that transmits part of its tension to the underlying substrate through focal adhesions. The orientation of these adhesions and the traction forces they transmit are mainly parallel to the wound edge and thus perpendicular to the direction of cell motion. This structural and mechanical organization provides cells with an

unanticipated mechanism to close the wound by cooperatively compressing the underlying substrate.

References

1. Cordeiro, J. O. V. & Jacinto, A. N. The role of transcription-independent damage signals in the initiation of epithelial wound healing. *Nature Reviews Molecular Cell Biology* **14**, 249–262 (2013).
2. Sonnemann, K. J. & Bement, W. M. Wound Repair: Toward Understanding and Integration of Single-Cell and Multicellular Wound Responses. *Annual Review of Cell and Developmental Biology* **27**, 237–263 (2011).
3. Anon, E. *et al.* Cell crawling mediates collective cell migration to close undamaged epithelial gaps. *Proceedings of the National Academy of Sciences of the United States of America* **109**, 10891–10896 (2012).
4. Abreu-Blanco, M. T., Verboon, J. M., Liu, R., Watts, J. J. & Parkhurst, S. M. *Drosophila* embryos close epithelial wounds using a combination of cellular protrusions and an actomyosin purse string. *Journal of Cell Science* **125**, 5984–5997 (2012).

ID: 303

SYM-08: 4

Cell response on integrin-specific artificial protein biomaterials

Monica Suryana Tjin¹, Alvin Chua², Seng Teik Lee³ and Eileen Fong¹

¹School of Materials Science and Engineering, Nanyang Technological University, Singapore; ²Skin Bank Unit, Singapore General Hospital, Singapore; ³Department of Plastic Reconstructive & Aesthetic Surgery, Singapore General Hospital, Singapore.

Cell-matrix interactions play a critical role in regulating cellular behavior in wound repair and regeneration of the human skin. In particular, human skin keratinocytes express several key integrins for binding to the extracellular matrix (ECM) present in the basement membrane in uninjured skin. To mimic these key integrin-ECM interactions, we prepared artificial ECM (aECM) proteins containing functional domains derived from laminin 5, type IV collagen, fibronectin and elastin. We showed that human skin keratinocyte cell response on each aECM protein was specific to the cell-binding domain present in each construct. Keratinocyte attachment to the aECM protein substrates was also mediated by specific integrin-material interactions. In addition, the aECM proteins were able to support the proliferation of keratinocyte stem cells, demonstrating their potential for use in skin tissue engineering.

Collective cell behavior on micropatterned substrates

Sriram Krishna Vedula¹, Manchun Leong¹, Kevin Doxzen¹,
Hiroaki Hirata¹, Alexandre J. Kabla³, Yusuke Toyama¹,
Benoit Ladoux^{1,2} and Chwee Teck Lim¹

¹*Mechanobiology Institute, Singapore;* ²*Institut Jacques Monod (IJM), CNRS;* ³*Cambridge University.*

Collective cell migration plays an important role in various physiological (e.g. gastrulation and wound healing) and pathological processes (e.g. cancer metastasis). Both chemical (chemotaxis and haptotaxis) and physical cues (e.g. confinement, substrate stiffness etc.) within the extracellular environment have been shown to play a crucial role in regulating the social behaviour of cell sheets. While the role of extracellular matrix (ECM) geometry in regulating cell migration has been extensively investigated in the context of single cells, few studies have focused on how migrating epithelial monolayers respond to such challenges. Combining microfabrication tools with live cell imaging, we have developed a novel *in vitro* migration assay to study how epithelial monolayers respond to various micromechanical cues. In particular, we show that geometrical constraints imposed by ECM proteins can strongly influence collective cell migration.

Day 3 – Friday, 6 December 2013

Session	PL6: Plenary Lecture 6
Date/Time	6 December 2013 09:00–09:45 hrs
Venue	Auditorium

ID: 151 **PL6**

Advancing multi-modality clinical imaging: a challenge for the engineer and physicist

David W. Townsend

*A*STAR-NUS Clinical Imaging Research Centre, Singapore.*

Throughout the development of instrumentation for medical imaging, both engineer and physicist have played a critical role. The quest to provide instruments offering high spatial resolution, excellent signal-to-noise and short acquisition times has led, over the years, to the introduction of new and advanced technologies. The development of better scintillator materials, higher performance detectors, faster acquisition electronics, efficient reconstruction algorithms, and in the last decade, dual-modality devices, have provided the clinician with unique tools to image human disease. Increasingly detailed medical questions from referring physicians have challenged the performance of the technology and the interpretation of the images. Since the introduction of hybrid instrumentation, each new generation of technology has revealed greater internal anatomical and functional detail of disease, often necessitating some level of physician retraining to ensure accurate interpretation. Focusing primarily on instrumentation for positron emission tomography (PET), this presentation will explore the challenges faced by engineers and physicists over the past two or three decades, and the pioneering and ground-breaking work that now gives the physician access to imaging tools of unparalleled performance, allowing the visualisation of disease processes that were once invisible.

Session	PL7: Plenary Lecture 7
Date/Time	6 December 2013 09:45–10:30 hrs
Venue	Auditorium

ID: 148 **PL7**

Brain machine interface technology: from neurons to prostheses

Nitish Thakor^{1,2}

¹*SiNAPSE, Singapore;* ²*Johns Hopkins School of Medicine, USA.*

The Brain Machine Interface is best seen in the form of Neural Prosthesis has lately captured a great deal of interest and imagination. For example, we have demonstrated that brain signals can be used to control advanced dexterous, anthropomorphic prosthetic arm. However, interfacing to neurons individually or the entire brain both pose significant challenges that are both technological and experimental. Neural interface utilizes microtechnologies and very large scale integrated circuits developed for *in vitro* or *in vivo* recording and stimulation of neurons, while analysis for this neural activities requires advanced signal processing and decoding of neural signatures. The experimental challenges are to create the reliable biological interface, from neurons to electrodes and electronics, and restoring neural function from myelination, synapse formation and neuromuscular junction. This talk will review the Brain Machine Interface and Neural Prosthesis technologies and lay out major challenges towards building chronic implantable neural interfaces and prostheses.

Session	SYM-10: Nanoparticles for Bioimaging and Targeted Therapy
Date/Time	6 December 2013 11:00–12:30 hrs
Venue	Auditorium

ID: 731 **SYM-10: 1**

Symposium Keynote: A specific surface-coating peptide for rare earth nanomaterials

Long-Ping Wen

University of Science & Technology of China, China.

The induction of autophagy on exposure of cells to a variety of nanoparticles represents both a safety

concern and an application niche for engineered nanomaterials. Using phage display, we have discovered an 11-amino acid peptide that binds to rare earth nanomaterials with high affinity and forms a stable coating layer on the surface of the nanocrystals. The peptide efficiently reduces sedimentation of the nanocrystals and the interaction of nanocrystals with cells and surfaces, while the addition of a homing peptide enhances the interaction of nanocrystals with the target cells and organs. In this presentation I will present the latest development on utilizing this novel peptide to enable biomedical applications for rare earth nanomaterials.

ID: 696

SYM-10: 2

Selected methods of label-free magnetic resonance imaging for liver function evaluation

Bing Nan Li^{1,2}, Yi Zhuang Cheng³, Xiao Bo Yao³ and Wei Fu Lv³

¹Hefei University of Technology, China; ²National University of Singapore, Singapore; ³Anhui Provincial Hospital, Hefei, China.

Conventional imaging modalities are good at anatomical or structural anomalies, but are less sensitive to functional deficiencies or physiological alterations. The latter are more significant for early intervention and treatment; hence nuclear medicine including PET and SPECT receives more and more attention in clinics for functional imaging. Nevertheless, the performance of nuclear medicine is subjected to radioactive labels, where safety and toxicity are always a big concern. Magnetic resonance imaging (MRI) is advantageous in this regard. We have investigated several label-free MRI protocols, such as blood oxygen level dependent contrast (BOLD), liver acquisition with volume acquisition (LAVA), diffusion weighted imaging (DWI) and magnetic resonance elastography (MRE), for liver function evaluation. The underlying mechanisms, strengths and weaknesses are detailed with illustration of clinical MRI scans. In this presentation we also pay attention to nonradioactive contrast agents as well as the hints of developing new MRI contrast materials for liver function evaluation.

ID: 732

SYM-10: 3

Upconverting fluorescent nanoparticles for theranostics

Yong Zhang

National University of Singapore, Singapore.

Upconverting nanoparticles (UCNs) present a new technology for optical imaging/detection which is a growing field with both diagnostic and drug discovery uses. Currently, fluorophores including

fluorescent dyes/proteins and quantum dots (QDs) are used for fluorescence-based imaging and detection. These are based on 'downconversion fluorescence', emitting low energy fluorescence when excited by high energy light (such as UV or short wavelength visible light). Fluorophores in current use have several drawbacks: photobleaching, autofluorescence, short tissue penetration depth and tissue photo-damage. UCNs emit detectable photons of higher energy in the visible range upon irradiation with near-infrared (NIR) light based on a process termed 'upconversion'. UCNs show absolute photostability, negligible autofluorescence, high penetration depth and minimum photodamage to biological tissues. They can be used for ultrasensitive interference-free biodetection because most biomolecules do not have upconversion properties. UCNs are also useful for light based therapy with enhanced efficiency, for example, photodynamic therapy (PDT) of cancer. UCNs are used for enhanced PDT in deep tissues, because NIR light can go much deeper in tissues than visible light. They are used not only as a light converter but also a carrier for photosensitive drugs.

ID: 735

SYM-10: 4

The good side of protein corona on nanoparticles

James C. Y. Kah

National University of Singapore, Singapore.

It is now widely known that when nanoparticles are placed in biological media, they interact with biomolecules such as proteins through a combination of electrostatic interaction and high affinity co-ordinate bond with thiol or amine groups present in proteins to result in the spontaneous formation of a protein corona. The protein corona is considered by many to be undesirable as they form the root of many downstream issues plaguing the nanomedicine community including the loss of physical properties, unwanted immune responses, poor targeting efficacy and undesirable clearance. In this talk, we show how we can embrace the spontaneous formation of protein corona and turn them into useful functionalities in at least three specific examples: (1) to enhance efficiency of protein translation *in vitro*; (2) to enable loading and trigger release of drugs by exploiting the non-specific adsorption of protein corona formed around nanoparticles; and (3) to turn non-specific adsorption of proteins on nanoparticles into a cost-effective and instantaneous protein assay. The results of these studies demonstrate how we can adopt innovative approaches to relook at certain physical phenomena from an opportunist perspective instead of considering them as undesirable side effects.

ID: 459

SYM-10: 5

Synthesis of up-conversion fluorescent nanoparticles for photodynamic therapy of cancer cells

Haisheng Qian

Hefei University of Technology, China.

Photodynamic therapy (PDT) is considered to be both minimally invasive and toxic; these advantages alone make PDT an attractive alternative. Up-conversion nanoparticles (UCNs) are nanoparticles that are excited in the near infrared (NIR) region with emission in the visible or NIR regions. This makes these particles attractive for use in biological imaging, in-depth imaging and photodynamic therapy (PDT) of cancer cells as the NIR light can penetrate the tissue better with minimal absorption/scattering.

This presentation will summarize our research work on the synthesis of up-conversion nanoparticles for PDT. Much efforts has been made to synthesize lanthanide ions doped NaYF₄ (NIR-Vis) upconversion fluorescent nanocrystals of with controlled size and nanostructures. In particular, the system of mesoporous silica coated NaYF₄ up-converting nanoparticles with a large surface area has been established to use as nanotransducers for photodynamic therapy of cancer cells. Upon excitation by a NIR laser, the nanocrystals convert NIR light to visible light, which further activates the photosensitizer incorporated into the mesoporous layers to release reactive singlet oxygen to kill cancer cells.

Session	A7: Optical Imaging
Date/Time	6 December 2013 11:00–12:30 hrs
Venue	SR-01 & 02

ID: 250

A7: 1

Temporal focusing: Optically sectioned wide-field imaging for time critical biological processes

Elijah Y. S. Yew¹, Heejin Choi² and Peter T. C. So^{1,2}

¹Singapore MIT Alliance for Research and Technology, Singapore; ²Department of Mechanical Engineering and Biological Engineering, Massachusetts Institute of Technology, Cambridge, Massachusetts, USA.

Current 3D imaging with high transverse and axial resolution is often limited to raster scanning methods such as confocal or multi-photon microscopy. This method often generates signal from a point on the object and detected with a single detector. This limits the usefulness of optical imaging in cases of observing important biological processes that occur within a large 3D distribution and also in real-time because

the time it takes to excite and record a signal and also transverse to another Venue far away means that any image formed suffers a time delay between any two pixels. This delay becomes more severe when the dwell time per pixel increases. An example is that of observing phosphorescence/fluorescence lifetimes (P/FLIM) of oxygen content. Because of the long decay lifetime a raster scanned approach to P/FLIM means a 2D image takes a prohibitively long time to be recorded. Wide-field techniques may be applied but they lack the optical sectioning that a confocal or multi-photon microscope has. A new technique developed is that of temporal focusing. In this technique, a wide-field yet optically sectioned image may be formed using multi-photon excitation. The advantage of this method is that it generates a confined plane of excitation by taking advantage of the spectral spread of ultrafast lasers to focus a plane in time to generate excitation that is confined axially. In this presentation, we cover some of our work on temporal focusing and the improvement of the optical sectioning properties through structured illumination methods. We also look at other promising methods of improving the optical sectioning as put forth by theory.

ID: 823

A7: 2

In vivo blood microscope for patient diagnosis

Dvir Yelin and Lior Golan

Technion - Israel Institute of Technology, Israel.

In vivo imaging of blood cells provides a unique opportunity for researchers to visualize the morphology and dynamics of circulating cells, but is often limited by imaging speed, resolution and by the need for exogenous labeling of the cells. We present a label-free approach for *in vivo* flow cytometry of blood using a compact probe that could be adapted for imaging of patients in clinical settings, and demonstrate subcellular-resolution imaging of red and white blood cells flowing in the oral mucosa of a human volunteer. By analyzing the large data sets obtained by the system, valuable blood parameters could be extracted and used for direct, reliable assessment of patient physiology.

ID: 464

A7: 3

Distribution of Advanced glycation end-products in human dentin measured by fluorescence lifetime imaging

Kantaro Nishikawa¹, Shuichiro Fukushima¹, Tsutomu Araki¹, Mizuho Kubo², Jiro Miura² and Fumio Takeshige²

¹Osaka University, Graduate School of Engineering Science, Japan; ²Osaka University, Dental Hospital.

Aging is an irreversible and physiological phenomenon in human being. Among various processes in human aging, glycation of body protein namely Maillard reaction is one of the most interesting process. By the Maillard reaction, Advanced Glycation End-products (AGEs) are produced and they cause cross-linking of collagen, resulting in change of mechanical property of collagen tissue such as decrease of elasticity of skin and the fragility of bones. We assume that glycation occurs also in dentinal collagen, resulting in accumulation of AGEs in dentin by aging, because older dentin becomes fragile clinically. AGEs fluoresces blue light under excitation with UV light. Therefore the fluorescence measurement is attractive to determine an existence AGEs in dentin. However, stationary fluorescence measurement gives limited information with respect to localization of AGEs in dentin, because there is no appreciable difference between the fluorescence spectra of AGEs and that of dentinal collagen.

Then we applied measurement of fluorescence lifetime of demineralized dentin. Fluorescence lifetime of AGEs is shorter than that of collagen. Therefore fluorescence of AGE-rich portion shows faster decay comparing with that of less AGE portion. In this study, we achieved both mechanical compression test and fluorescence lifetime measurement to young and old person's dentin. To obtain the fluorescence lifetime images, time-correlated single photon counting method was employed. From these measurements, we found that hardness and fluorescence lifetime of the old dentin are harder and shorter, respectively, than those of the young one.

To obtain detailed information about AGEs' accumulation in dentin, we observed fluorescence lifetime images around dental tubules. Resultant lifetime images show that AGEs accumulate around dental tubules. This result was consistent with immuno-staining images obtained with an anti-AGEs antibody. These studies demonstrate the potential of fluorescence lifetime imaging for probing some kinds of phenomenon caused by AGEs.

ID: 500

A7: 4

An analytic method to optimize aperture design in focal modulation microscopy

Yubo Duan^{1,2}, Shakil Rehman^{1,2}, George Barbastathis^{1,3} and Nanguang Chen^{1,2}

¹National University of Singapore, Singapore; ²Singapore-MIT Alliance for Research and Technology (SMART), Singapore; ³Massachusetts Institute of Technology, USA.

Focal Modulation Microscopy (FMM) was recently developed as a novel method for in-vivo imaging of thick biological tissues. FMM introduces a spatial phase modulator into the illumination beam path to modulate part of the beam, which results in temporal oscillation of the interference pattern in the focal volume; whereas no oscillatory emission occurs in the out-of-focus region because of spatial separation between the modulated and unmodulated beams. Only the modulated emission light from the focal volume is retrieved to form FMM images, so FMM can achieve improved imaging depth compared to conventional confocal microscopy.

Modulation depth is an essential parameter in designing FMM aperture because it determines the signal-to-noise ratio and the efficiency of FMM signal generation. Large modulation depth not only improves penetration depth, it also reduces the threshold of excitation power, which is important for avoiding photobleaching. We employed genetic algorithm (GA) in the design of annular aperture to maximize modulation depth for given conditions e.g. numerical aperture, light polarization and pinhole size. However, GA method is time consuming, especially for designing an aperture with many sub-zones. Here, we propose an analytic method to design annular apertures for FMM with the benefit of pupil-moment. The pupil-moment method is very simple to implement, since only solving a set of equations is needed. Furthermore, this aperture optimization method can also be applied to the cases of high numerical aperture imaging using vector diffraction theory for both linearly polarized incident beam and radially polarized incident beam. The modulation depth from the pupil-moment method is very close to the optimal results from GA design. Several annular apertures with simple configurations and large modulation depth are proposed and demonstrated.

ID: 194

A7: 5

Plant intracellular PH measurement using the fluorescence intensity ratio for a study of cryopreservation technique

Takako Ninagawa¹, Akemi Eguchi², Akira Narumi³, Tadashi Konishi⁴ and Yukio Kawamura⁵

¹Graduate Student, Kanagawa Institute of Technology, Japan; ²Toyo Engineering Works, Ltd., Japan; ³Dept. of Mechanical Engineering, Kanagawa Institute of Technology, Japan; ⁴Dept. of Mechanical Engineering, Oita National College of Technology, Japan; ⁵Faculty of Agriculture Cryobiofrontier Research Center, Japan.

Intracellular pH (hereafter pHi) is used as one of indicators of cell activity in the cryopreservation study. Fluorescence measurement is frequently used as one of available methods because of the advantages of non-contact, real-time and two-dimensional distribution. However, fluorescence measurement is very tough to obtain the accurate result since fluorescence itself is extremely weak light intensity and has the characteristics that light intensity fades spontaneously. For the improvement of measuring error, fluorescence pH ratiometry was proposed and used. This method determines pH by calculating the ratio of fluorescence intensity at each excitation wavelengths having the highest and isosbestic pH dependence. BCECF-AM was used as pHi indicator in this research. However, in same use as open protocol on web, pHi values are scattered more significantly than expected. The value varied widely even in same cell in even the calibration of the relationship between intensity ratio and pHi. This research was carried out to establish the practical procedure for obtaining more accurate result. Jerusalem Artichoke and Allium cepa were used as plant tissue. The fluorescence intensity was measured using the cryomicroscopy having cooled CCD camera. First, to determine the conditions for obtaining the good image enough to analyse, we performed many experiments with varying reagent concentration, incubation-time and pH concentration. Next, using the images obtained in this way, the scattering of value was examined in detail from the distributions of fluorescence intensity and intensity ratio at each pixel. Then, the difference in pHi value between at cell nucleus and at cytoplasm was also examined. The value at each pixel was compared with average value at 20x20 pixels. Through these results, we discussed the procedure to acquire the higher accurate value using fluorescence pH ratiometry. As a result, we could find out the procedure to minimize the scatter of data.

ID: 786

A7: 6

Multimodal nonlinear optical microscopy for label-free imaging of the tooth

Zi Wang, Wei Zheng, Chin Ying Stephen Hsu and Zhiwei Huang

Optical Bioimaging Laboratory, Department of Bioengineering, Faculty of Engineering, National University of Singapore, Singapore.

We report the development of a multimodal nonlinear microscopy technique including second-harmonic generation (SHG), third-harmonic generation (THG), two-photon excitation fluorescence (TPEF), and coherent anti-Stokes Raman scattering (CARS) for label-free imaging of the tooth. A picosecond tunable laser together with an OPO system (wavelengths of 700–990 nm, 1150–2300 nm; repetition rate of 75 MHz with a pulse width of 7 ps) is used as an excitation source for simultaneously multimodal imaging. Specifically, SHG imaging clearly shows the structures of collagen fibrils that only exist in the primary dentin region; THG reveals the interface information of dentinal micro-tubules in the dentin as well as the rodlike structure of hydroxyapatite crystal in enamel; both TPEF and coherent anti-stokes Raman scattering (CARS) imaging can provide the morphological structures of dentin and enamel in the tooth. CARS imaging gives a much better optical sectioning ability with no photodamage effects compared to TPEF imaging. The co-registration of different nonlinear optical imaging modalities provides new insight into the understanding of morphological structures and biochemical/biomolecular distributions in the dentine and enamel of the tooth without the need of labeling, paving the way for early diagnosis and characterization of tooth disease in dentistry at the submicron level.

Session	B7: Diagnostics and Therapeutics
Date/Time	6 December 2013 11:00–12:30 hrs
Venue	SR-03 & 04

ID: 261

B7: 1

Efficient intracellular delivery of polymeric MRI contrast agent for mesenchymal stem cell transplantation to myocardial infarction

Naoki Kobayashi^{1,2}, Atsushi Mahara¹, Jun-ichiro Enmi¹, Akihide Yamamoto¹, Hidehiro Iida¹, Yoshiaki Hirano² and Tetsuji Yamaoka¹

¹National Cerebral and Cardiovascular Center Research Institute, Japan; ²Kansai University, Japan.

Introduction: Noninvasive tracking of transplanted cells is attracting a great deal of attention to reveal the

mechanism of stem cell therapies. We have recently developed a polymeric MRI contrast agent by conjugating Gd-chelate with dextran (Gd-Dextran) which enables the stem cell labeling. Cells were labeled with the contrast agent by electroporation but the labeling was not homogeneous, and only 11% of the cell was labeled. In addition amount of Gd-Dextran was not large enough to track for long term period. In this study, sonoporation was used for homogenous cell labeling with the contrast agent. Mesenchymal stem cells (MSCs) derived from porcine bone marrow cells and fibroblastic cells were labeled with Gd-Dextran, and the labeling efficiency and cell-sheet imaging were investigated.

Experimental: Polystyrene tube containing NIH/3T3 cells, FITC-labeled dextran (F-Dextran) and microbubbles was placed at a distance of 8 cm from ultrasound transducer in water bath at 37°C. The cell suspension was stirred gently and exposed to ultrasound for 120 seconds. The number of microbubbles was varied from 1.0×10^7 to 1.0×10^8 and exposed power was varied from 0.1 to 5.0 W/cm², and the cell-labeling efficiency was measured by the flow cytometry. Porcine MSCs sheet labeled with Gd-Dextran under optimum conditions was embedded in agarose gel and observed with the clinical 3T MRI.

Results: When 1.0×10^6 NIH/3T3 cells were treated with 5×10^7 microbubbles at 1.5W/cm², 67% of cells were labeled with F-Dextran. Moreover, mean fluorescent intensity value was increased to 9.8-fold as compared with the electroporation methods. The labeled cells were grown on thermoresponsive cell-culture dish to confluency as well as non-labeled cells, and MSCs sheets were prepared. The cell-sheet of 6.0×10^5 MSCs was clearly observed under the clinical 3T MRI.

ID: 396

B7: 2

Synthesizing gold nanoparticles in spherical and rod shapes for targeting cancer treatment

Poh Foong Lee¹, Guo Feng Chin¹, Misni Misran² and Pek Yee Tang¹

¹University Tunku Abdul Rahman, Malaysia; ²University Malaya, Malaysia.

Gold nanoparticles (GNP) and its relevant studies have been giving promising applications in the biomedical area recent years such as the drug carrier in aiding drug delivery, and the multi-functional platform in cancer diagnostic and treatment due to its uniqueness in non-radiative relaxation in local heat transfer, and the strong enhanced optical properties associated with the localized surface plasmon reso-

nance (LSPR). However, the most native shape of the synthesized gold nanoparticles, which is spherical in shape, will give the LSPR similar to the intrinsic chromophores in human native tissues, that is ± 520 nm. This phenomenon has caused a disadvantage in the utilization of gold nanosphere (GNS) in some of the applications that utilized LSPR such as the plasmonic photothermal therapy (PPTT) in cancer treatment because of the interference of the human native tissues and the efficacy of such treatment will be much reduced. To solve this issue, alternative such as shifting the LSPR of the synthesized gold nanoparticles to the near infra-red (NIR) spectra, which range from 700nm to 1000nm, that is able to avoid the overlapping of the LSPR of spherical gold nanoparticles and the human tissues. To achieve this, rod shape gold nanoparticles, or gold nanorod (GNR) were synthesized. This study focused on the investigation of the synthesis methods of the GNS and GNR, together with the characterization of both synthesized gold nanoparticles via zetasizer, spectrophotometer and transmission electron microscope (TEM).

ID: 788

B7: 3

Gold nanoparticles cross-linked responsive polymers for a colorimetric enzyme sensor

Erindyah Retno Wikantyasning¹, Johannes Pall Magnusson², Clive J. Roberts², Cameron Alexander² and Jonathan W. Aylott²

¹Muhammadiyah University of Surakarta, Indonesia;

²The University of Nottingham, UK.

The use of enzymes as a sensor target is promising because of their high selectivity in the reactions they catalyze; they operate in aqueous media between the pH range 5 to 8 and body temperature (37°C); they play an important role in healthy and diseased biological pathways. Thermoresponsive polymers and gold nanoparticles (AuNPs) have been explored for their potential use as colorimetric sensors. The shrinking and swelling behaviour of thermoresponsive polymers cross-linked by AuNPs induces a colour change around the LCST (Lower Critical Solution Temperature) that can be visualized by naked eye. The principle of the colorimetric sensor was applied for detection of an enzyme. A peptide is introduced to a thermoresponsive polymer and the peptide conjugated responsive polymer is cross-linked with AuNPs.

AuNPs was synthesized by Turkevich method (~18 nm) and was characterized using TEM, AFM and disc centrifuge. A thermoresponsive polymer, Poly-(N-isopropylacrylamide)-Poly-(aminopropyl methacrylamide) (PNIPAM-PAPMA) was prepared by RAFT polymerization using a bifunctional RAFT

agent and characterized by NMR. The turbidity profile of the responsive polymers was determined using UV-Vis spectrophotometer. Synthetic peptides (Pro-Ala-Ala-Ala) were then conjugated to the PNIPAM-PAPMA polymers and the polymers were cross-linked with AuNPs. The colour transition was observed by naked eye and the correlated UV-Vis spectra were recorded.

The response of the AuNPs-crosslinked PNIPAM-PAPMA-peptide to the enzyme was observed by the colour change from red to blue, due to the shrinking of the polymer when the peptide was cleaved by elastase. The peptide cleavage causes changes to the responsive polymer hydrophobicity which leads to the phase transition of the responsive polymer, so that a colour transition from red to blue can be observed as a result of aggregation of the AuNPs.

ID: 137

B7: 4

Computational diagnosis of coronary artery stenosis: experimental measurement of wave propagation in soft tissue mimicking gel

H. Thomas Banks⁴, Malcolm J. Birch², Mark P. Brewin¹, Stephen E. Greenwald¹, Shuhua Hu⁴, Zack R. Kenz⁴, Carola Kruse³, Dwij Mehta¹, Simon Shaw³ and John R. Whiteman³

¹Barts & The London School of Medicine & Dentistry, United Kingdom; ²Clinical Physics, Barts Health NHS Trust, London, United Kingdom; ³Department of Mathematics, North Carolina State University, Raleigh NC, USA; ⁴Institute of Computational Mathematics, Brunel University, UK.

Background & Methods: Plaque developing in a coronary artery produces turbulent flow downstream and wall shear stresses varying at frequencies up to 1kHz. These give rise to low amplitude acoustic shear waves which propagate through the chest and can be detected by skin sensors. This acoustic surface signature may provide a cheap non-invasive means of diagnosing arterial disease. We report measurements of the propagation of 1-D free oscillations induced in cylindrical tissue-mimicking-gel specimens following the sudden release of shear or compressive stresses and the results of two sets of preliminary experiments. Firstly, 2-D oscillations were induced in the gel by an electro mechanical vibrator at frequencies between 250 and 1000 Hz and amplitude between 10 and 50 mm. Secondly, by passing fluid through a partially occluded tube embedded in rectangular gel specimens, turbulence was induced downstream of the occlusion.

Results: On releasing the load, free damped oscillations were seen with a characteristic frequency of

70Hz and $t_{1/2}$ of around 0.05s. Forced oscillations parallel to the long axis of the gel produced movement at its surface predominantly in the same direction, of the same frequency and of reduced amplitude. Amplitude modulation at around 40Hz, probably due to resonance in the gel, was also observed.

Turbulent flow within the gel induced oscillations in the frequency range 100 to 800 Hz, of an amplitude that increased with flow rate and with a peak frequency which depended inversely on the dynamic viscosity of the fluid.

Conclusions: The methods described above provide internally consistent and repeatable data, forming a reliable experimental basis for the computational arm of the project (described in a companion presentation) in which the computational results will be compared with the experimental observations presented here.

Acknowledgement: This work is supported by the Engineering and Physical Sciences Research Council. Grant: EP/H011072/1 & EP/H011285/1.

ID: 116

B7: 5

Towards computational diagnosis of coronary artery disease

Simon Shaw¹, John R. Whiteman¹, Carola Kruse¹, Stephen E. Greenwald², Malcolm J. Birch³, Mark P. Brewin², H. Thomas Banks⁴, Shuhua Hu⁴ and Zackary R. Kenz⁴

¹Brunel University, UK; ²Queen Mary, University of London, UK; ³Barts Health National Health Service trust, UK; ⁴North Carolina State University, USA.

Blood turbulence in the wake of plaque build-up in an atherosclerotic coronary artery induces wall shear stresses which travel through the thorax and produce an audible 'bruit' at the chest wall. Detection and identification of this (very weak) signal has the potential to provide a low-cost and non-invasive diagnostic technology.

This presentation will describe an early stage proof-of-concept investigation into the use of computational mechanics to perform this diagnosis. We describe an in-vitro rig of tissue mimicking agarose gel through which a simulated stenosis signal (at 250–1000 Hz) is transmitted to the chest wall under reproducible conditions (further details will be given in a companion presentation).

We explain how we obtained the viscoelastic bulk and shear properties of the gel, and also explain how these are now deployed in a computational forward-inverse solver loop. A novel high-order bespoke space-time finite element dynamics code has

been developed to run on a high performance GPU computing platform, and this is used to predict the chest-wall signal given the input of the stenosis signal. This code is coupled to an inverse solver that compares the measured-to-computed signal in order to better estimate the presence, Venue and nature of the stenosis. All of these steps will be described and the results of our computations will be outlined.

At present, we are working with a scaled down axi-symmetric homogeneous 'virtual chest' in order to confirm whether this procedure is feasible under these simplistic lab conditions. We will offer an evaluation of the progress to date and speculate on the future potential of this methodology.

This work was supported in the UK by the Engineering and Physical Sciences Research Council under grants: EP/H011072/1 & EP/H011285/1.

ID: 450

B7: 6

Holistic cell-line metabolome profiling strategy for biomarker identification

Gokula Krishnan Ramachandran and Chen-Hua Yeow

National University of Singapore, Singapore.

Metabolomic profiles are important in identification of the cell type and the physiological and pathological state of the cell type. There are various modalities available for the deciphering the metabolic signature of the tissue types. Here we come with a methodology for profiling the metabolic signature of cell lines holistically. Any cell type can have metabolites in four compartments as follows: (1) the volatile metabolites emitted from the cells, (2) the metabolites secreted by the cells into the culture medium, (3) the metabolites on the surface of the cells and (4) the metabolites present inside the cells. Holistic metabolic profile represents the metabolites present in these four compartments. We employed Solid Phase Micro-Extraction for deciphering the volatile metabolites, High Performance Liquid Chromatography – Mass Spectrometry for identifying the metabolites of the secreted metabolites and the metabolites present inside the cell and finally Nuclear Magnetic Resonance for analyzing the surface metabolites. We used Human Renal Proximal Tubule Epithelial cells as the pilot model cell line to evaluate the efficiency of this methodology. In the NMR analysis we could able to identify major peaks matching with lipids and nucleotides this enable as to identify novel surface biomarkers. We further expanded this methodology towards deciphering the novel biomarkers for cancer by comparing the metabolic profiles between normal and diseased cell lines. For the second part of this study, we used skin cell lines as the model cell type. As this holistic strategy will provide a complete

metabolomic profile, important biomarkers may be possibly identified which will enable us to develop prospective treatments to target these biomolecules for disease diagnosis and treatment.

ID: 730

B7: 7

A pervasive intelligent system for scoring mews and TISS-28 in intensive care

Filipe Portela¹, Manuel Filipe Santos¹, Álvaro Silva³, José Machado², António Abelha³ and Fernando Rua²

¹Algoritmi Centre, University of Minho, Portugal; ²CCTC, University of Minho, Portugal; ³Serviço de Cuidados Intensivos, Centro Hospitalar do Porto, Hospital Santo António, Portugal.

Usually intensive care medicine practice is highly supported on scores as SOFA, SAPS and Glasgow. More recently, two new scores have been considered: MEWS and TISS-28.

This paper presents how the Scoring System (SS) of the Intensive Care Unit (ICU) of Centro Hospitalar do Porto, evolved in order to accommodate the new scores.

SS can automatically, in real-time and using online learning, provide a set of scores with a minimum human effort. SS is integrated in the Electronic Nursing Record (ENR) used for better comprehension of the patient condition through a set of information available: vital signs graphs, therapeutic plans, interventions, laboratory results and others. Those systems are supported by a pervasive platform for monitoring patient data anywhere and anytime. In order to improve the information available a set of scores were added.

SS calculates the TISS-28 Score per day and turn and the MEWS per minute, hour and day. These two new scores improve the understanding of the real condition of the patients. SS allows for obtaining automatically and in real-time the following scores: SAPS II, SAPS III, SOFA, GLASGOW, TISS28 and Mews anywhere and anytime. The development of SS only was possible due to a continuous and real-time execution of the data acquisition and data processing phases of the ETL process.

The work presented in this paper shows how can be introduced, in real-time, two new scores as daily ICU measures: MEWS and TISS-28. These new measures were requested by the ICU nurses and brought some benefits at level of the decision process because allow to have a better comprehension of the patient condition evolution and their workload. The introduction of the SS present some benefits to the patient and to the ICU management process.

Future work includes the improvement of SS and the induction of predictive data mining models based on these scores.

Session	C7: Computational Mechanics
Date/Time	6 December 2013 11:00–12:30 hrs
Venue	SR-05 & 06

ID: 192 **C7: 1**

Evaluating the mechanical efficacy of anabolic bone treatments using a non-destructive framework

Justin Fernandez¹, Dharshini Sreenivasan¹, Maureen Watson², Raj Das³, Andrew Grey² and Jillian Cornish²

¹Auckland Bioengineering Institute, The University of Auckland, New Zealand; ²School of Medicine, The University of Auckland, New Zealand; ³Department of Mechanical Engineering, The University of Auckland, New Zealand.

Osteoporosis is characterised by low bone mass, deterioration of bone micro-architecture, enhanced bone fragility and increased fracture risk. There is an increasing interest in using anabolic treatments that proliferate bone formation. Measurement outcomes include bone mineral density (BMD), micro CT indices and 2D histology. In this study an additional computational assessment is integrated to mechanically evaluate bone quality in a virtual environment by loading bones in compression, torsion and shear. The anabolic effects on mechanical strength from bone architecture, bone type (cortical and trabecular), and remodelled material properties are then evaluated. Following this the micro CT indices are assessed for their ability to estimate bone strength. A validation of this method is performed using a 3D printed version of the biopsy compressed using an Instron machine.

This framework is presented in the context of two anabolic treatments; (i) a human clinical trial into the effects of low-dose fluoride treatment; and (ii) a murine trial into the effects of the milk derived anabolic Lactoferrin. In both trials there was a placebo and 2–3 different treatment levels with BMD and micro CT indices collected. Virtual 3D models of each specimen (or biopsy) were computationally assessed using damage criteria. This study showed that treatment with low-dose fluoride led to a non-significant linear decline in strength with increase in fluoride dose, consistent with previous studies. Treatment with Lactoferrin produced no effect in cortical bone with variable effects in trabecular bone. Percentage bone volume was shown to be a strong surrogate measure for mechanical strength. Trabecular thickness and bone surface density were moderately correlated to bone strength. This framework may be used to inform clinical trials about anabolic treatment effects on bone architecture, material strength and highlight which micro CT indices are good surrogate measures for mechanical strength.

ID: 382 **C7: 2**

Individual stress analysis of bone tissue using small scale FE model with anisotropic material properties

Michihiko Koseki and Takuya Hasegawa

Shinshu University, Japan.

Patient-specific simulation with Finite Element (FE) method is a significant technique to examine biomechanical characteristics of bones. For this reason, many researchers have contributed individual FE analyses based on X-ray Computed Tomography (CT) images. These studies computed the material properties of the model according to the CT values in the images, because a configuration of proper material properties is one of the most important procedures to obtain reliable analytical results. However almost of the conventional FE models contained only isotropic material properties in each element despite of anisotropic characteristics of bone tissue. This may degrade reliability of the analytical results especially in the case of small scale FE models.

In order to improve the analytical performance, we have studied an individual FE analysis method with a consideration of structural anisotropy of bone tissue. This paper mainly focuses on the anisotropy in a cortical bone. Firstly we extract the structural anisotropy of cortical bone from microfocus X-ray CT images. The extracted image clearly illustrates Haversian and Volkmann's canals that causes the structural anisotropy of the cortical bones. Next we compute anisotropy factors based on the images. The factors indicate three dimensional stiffness distributions. Finally we perform FE analyses using the anisotropic material properties based on the factors. The analytical results suggest the importance of the material anisotropy in stress analyses of bone tissue.

ID: 646 **C7: 3**

Importance of stem orientation in total hip arthroplasty by bone remodeling simulation

Ji Yean Kwon¹, Sungjae Kim¹, Sungmin Kim¹ and Masao Tanaka²

¹Dongguk University, South Korea; ²Osaka University, Japan.

A correct positioning of the stem of a hip prosthesis is major important factor for the long-term stability of THA. To ensure accurate execution of pre-operative planning, methods for computer assisted surgery have been used commonly. The aim of this study is to evaluate the effect of small changes in orientation of the stem on successfulness of the THA procedure using bone remodeling simulation. Ultimately, we want to develop the index to predict

the biomechanical behavior of bone surrounding the stem based on the stem orientation.

In this study we examined 6 different CT datasets. One post-operative scan was performed where the stem was oriented as pre-planned by a qualified orthopedic surgeon and five artificially made datasets were derived from this scan with increasing rotational deviation of the stem in the transversal plane (1–5°). All datasets were analyzed by a bone remodeling simulation which was modeled local equivalent strain in the bone surrounding the stem. The equivalent strain distribution in the different Gruen zones have corresponded to the characteristic change of bone structures.

ID: 573

C7: 4

Prediction of suture anchor loosening after rotator cuff repair – An investigation using three-dimensional finite element method

Hiroataka Sano, Nobuyuki Yamamoto and Eiji Itoi

Tohoku University School of Medicine, Japan.

Introduction: Suture anchor loosening constitutes one of the major causes of re-tearing after rotator cuff repair. The purpose of the present study was to clarify whether the early postoperative anchor loosening could be predicted using three-dimensional finite element (3D-FE) method or not.

Methods: Twenty rotator cuff tear patients (mean age: 63, range: 52–75) who underwent arthroscopic repair with suture anchors were included in the present study. There were 9 females and 11 males. In 5 patients, loosening of the inserted anchor occurred immediately after the repair (4 females and 1 male, loosening group). On the other hand, the anchors were intact in the rest 15 patients (5 females and 10 males, intact repair group). A 3D-FE model of the lateral part of the humeral head was developed for each patient based on the CT-DICOM data. A virtual TwinFix anchor was inserted into 6 different sites of the greater tuberosity. A tensile force (400N) was applied to each anchor and the analysis was performed with 80 incremental steps. The failure load of inserted anchor was compared between the loosening group and the intact repair group.

Results: The mean failure load of inserted anchor (standard deviation: SD) was 70.3 N (25.6) in the loosening group and 119.0 N (28.3) in the intact repair group. A statistically significant difference was found between these 2 groups ($p < 0.0001$). The optimum cutoff value for the failure load of inserted anchor was determined as 75.4 N according to the ROC analysis (sensitivity: 80%, specificity: 100%).

Discussion: Failure of inserted anchors can be predicted using 3D-FE method. According to the results of ROC analysis, it might be better for surgeons not to use suture anchors in the patients whose mean failure load was less than 75.4 N with this method to avoid the early postoperative anchor loosening.

ID: 424

C7: 5

Predicting the line of action of forearm muscles during pronation-supination

Desney Greybe¹, Michael R. Boland^{1,2} and Kumar Mithraratne¹

¹*Auckland Bioengineering Institute, The University of Auckland, New Zealand;* ²*Department of Surgery, The University of Auckland, New Zealand.*

The forearm is a complex part of the body, where its movement involves many degrees of freedom and 22 muscles. At present, the way in which the muscles of the forearm produce pronation and supination is not well understood. Most of the muscles involved cross more than one joint, and have other primary functions. Knowledge of their lines of action is valuable in understanding how they influence forearm rotation. However, a muscle's line of action will change during pronation and supination. As a result, predicting its line of action throughout the range of motion is important.

This study presents a computational model which consists of anatomically accurate finite element (FE) meshes of the brachioradialis (BRAR) muscle and the humerus, ulna and radius bones derived from MRI data. The forearm of a subject was scanned in seven positions of forearm rotation using a 3T MRI scanner. The humerus, ulna and radius bones were segmented in each scan, and FE meshes of the bones were created in each position of forearm rotation. A similar procedure was adopted to create a FE model of the BRAR muscle using the segmented data in neutral position. The muscle's points of insertion were defined with respect to the bone meshes, and their spatial Venue in each position of forearm rotation formed the boundary conditions for the computational model. The deformation that the muscle underwent as the forearm rotated away from a neutral position was predicted by solving the equations governing theory of finite elasticity. The results were validated against its line of action determined from the MRI scans in the other positions of forearm rotation.

This method can be used to evaluate the varying lines of action of other muscles of the forearm, which is particularly important in understanding their relationship to forearm rotation.

ID: 816

C7: 6

A comparative case study of a congenital dysplastic hip joint before and after a DEGA osteotomy simulation

Santiago Rendon Valencia^{1,3} and Diego A. Garzon Alvarado^{2,3}

¹Biomedical Engineering Program, Faculty of Medicine, National University of Colombia; ²Department of Mechanical Engineering and Mechatronics, National University of Colombia.; ³Modelling and Numerical Methods in Engineering Research Group GNUM, National University of Colombia.

Congenital hip dysplasia is a condition that if it is not treated on time, it is necessary to perform a surgery to prevent its development; this kind of surgery can affect normal stresses on the femoral head and on the acetabulum. Surgeries that change the acetabulum shape as DEGA osteotomy, can affect the contact surface between the acetabulum and the femoral head in specific areas. This study compares the stresses on a hip with congenital dysplasia before and after a surgery simulation with normal loads reported in the literature.

The medical data were obtained from a computerized axial tomography, these data were the base to create a three-dimensional model of the hip by image segmentation processing. Then it was performed a simulated DEGA osteotomy over a copy of the main model. A finite element analysis was developed to both the main model and the DEGA model, using ANSYS software; results were compared with normal hip stresses. In a dysplastic hip model it was found small contact areas with high stresses; while in the model with DEGA osteotomy, the stresses were localized mainly in large areas in the upper femoral head.

Although a DEGA surgery is applied to prevent the progression of hip dysplasia, this may affect the load distribution through modification of the acetabulum shape, which could be a cause of early arthrosis and therefore a new surgery in young adult people.

Session	SYM-11: Biomedical Engineering in Sport Science
Date/Time	6 December 2013 11:00–12:30 hrs
Venue	SR-12

ID: 725

SYM-11: 1

Biomechanical cartilage imaging patterns in professional soccer

Goetz Welsch, Friedrich Hennig and Matthias Lochmann

University of Erlangen, Germany, Germany.

Introduction: The high demands to the knee joints in professional soccer may lead to repetitive trauma and

possibly early cartilage injuries. Aim of this study was to assess biomechanical loading and unloading parameters in the knee joints of adolescent professional soccer players by means of T2 Mapping analysis.

Material and Methods: In this prospective study we analyzed the knee of the supporting leg of 45 healthy volunteers (17.1±1.0years) of the junior section of a professional soccer team (all playing in the first national league in their respective junior team). Exclusion criteria were history of surgery or any traumatic knee lesion. Biochemical T2 mapping of the femoro-tibial joint was performed at 3-Tesla MRI using a zonal (superficial and deep) analysis.

T2 mapping was performed immediately after loading and 30 minutes after unloading. This imaging pattern was shown to provide valuable information on cartilage biomechanics and load distribution in previous studies.

Region-of-Interest analysis was performed by two observers followed by statistical Analysis-of-Variance to assess differences in between loaded and unloaded cartilage with respect to the different anatomical zones.

Results: The reproducibility was very high in all knee compartments (ICC>0.9). T2 values (ms) showed to be different in between the anatomical zones, most obvious in between the femoral condyles and the tibial cartilage (p<0.05).

When comparing loading to unloading, a clearly significant increase of the T2 values was present in the superficial cartilage zones of the anterior (loading: 52.8±10.6ms; unloading: 55.3±11.6ms; p=0.016) and central (loading: 63.8±11.9ms; unloading: 67.1±12.9ms; p=0.005) femoral condyle. The underlying deep cartilage zone (anterior (loading: 38.6±11.4ms; unloading: 39.9±11.7ms; p=0.217) and central (loading: 43.4±10.0ms; unloading: 44.6±11.0ms; p=0.214)) of the weight-bearing aspect of the femoral condyle, as well as all other cartilage areas (Tibial anterior (sup./deep): loading: 43.2±8.8/30.8±7.3ms, unloading: 44.2±9.8/31.1±6.9; p=0.276 and 0.678); (Tibial central (sup./deep): loading: 47.2±8.5/31.1±6.3, unloading: 47.8±10.0/31.3±7.1; p=0.463 and 0.693); (as well as femoral posterior (sup./deep): loading: 58.8±13.1/46.6±10.1, unloading: 58.3±12.7/45.3±9.2; p=0.695 and 0.144) did not reveal a significant difference of the T2 values.

Conclusion: This prospective analysis is the first available approach to understand cartilage kinematics in young professional soccer players and to prevent cartilage injuries. The increase of the T2-values during unloading takes place in the area were

traumatic and osteochondral cartilage lesions usually appear. The presented approach may help to monitor soccer players at high risk for cartilage injuries.

ID: 310

SYM-11: 2

Evidence based concept of insole supply

Gurzi Domenico¹, Matthias Lochmann² and Fritz Bodem²

¹Corpusconsult GmbH & Co. KG; ²Friedrich-Alexander University Erlangen-Nuremberg, Germany.

Most insole supply systems worldwide use standardised modules which, in their construction, are commonly based on static foot measurement techniques. This ignores the fact that an insole will mainly be used in dynamic situations. A second problem of common insole supply chains is that they are not closed. This means that there does not exist any sufficient evidence based analysis of the effect the insole supply actually takes after the delivery to the sportsmen or patient. With special regard to these two problems we have designed an evidence based concept of insole supply which consists of the following 6 steps: (1) orthopaedic consultation, (2) dynamic baropedographical analysis, (3) dynamic spine analysis, (4) CAD modeling and construction of the insole, (5) ensemble average based biomechanical effect analysis, (6) orthopaedic feedback consultation. The innovative element in this supply chain is especially located in step 5, i.e. the biomechanical effect analysis. For this analysis we use a state of the art gait analysis motion lab with the following components: (a) 8 camera system (Qualisys) for marker based object tracking using infrared light. (b) dual running belt instrumented with two force plates (Bertec). (c) 8 channel wireless EMG (Noraxon). For the analysis of an insole supply we use special Matlab routines. With these routines we compare more than 60 biomechanical variables in real time using a special ensemble average procedure. This procedure allows to compare with statistical validation two different experimental conditions within a measuring time of two minutes each. 100 data points of the gait cycle averaged over nearly 60 cycles are synchronously compared. In the graphical display of this analysis each variable is highlighted in those parts of the gait cycle, where a statistically significant difference has been observed. With the approach described here it is possible to evaluate and optimize in an evidence based manner the CAD insole model derived from a dynamic baropedographic measurement.

ID: 377

SYM-11: 3

Heart-rate controlled E-bike-exercising

Holger Eckhardt and Matthias Lochmann

Institute of Sport Science and Sport, Friedrich-Alexander-University Erlangen-Nuremberg, Germany.

The following pilot study was supposed to review in what way a heart rate controlled e-bike can allow for specific exercising within a certain intensity zone, regardless of the heart's physiologically delayed heart beat adaptation at variable external demands for performance (incline, headwind). Eight untrained test subjects (age: 63 ± 6 years, weight: 91 ± 8 kg, height: 174 ± 10 cm, BMI: 30 ± 3 kg/m², VO_{2max}: 25.3 ± 2.7 ml/kg · min⁻¹) took a test ride with their respective, previously determined heart rate (HR_{target}) cycling at 50 Watts. Test rides took place on a standardized route with incline (max. 12%), decline and various ground surfaces (blacktop, gravel, forest soil). Permanently, the heart rate was sent to the engine timing via heart rate sensor, which was strapped to the chest and at the same time recorded using a smartphone. The average heart rate recorded, ranged from 99.4 ± 9.4 bpm. The average heart rate HR_{target} was 101.4 ± 10.5 bpm. Consequently, average deviation was 2.0 bpm. This slight difference between the recorded heart rate during test ride and HR_{target} proves that the combination between hardware and software with this e-bike is capable of compensating the heart's physiologically delayed heart beat adaptation to sudden external demands for performance. To improve validity of these results, 17 more test subjects are being included.

ID: 167

SYM-11: 4

Methodological aspects of EEG measurements during movement

Pedro Miguel Ramos Reis¹, Felix Hebenstreit^{1,2,3} and Matthias Lochmann¹

¹Institute of Sport Science and Sport, Friedrich-Alexander-University Erlangen-Nuremberg, Erlangen, Germany; ²Digital Sports Group, Pattern Recognition Lab, Department of Computer Science, Friedrich-Alexander-University Erlangen-Nuremberg, Erlangen, Germany; ³Department of Trauma and Orthopaedic Surgery, University Hospital Erlangen, Erlangen, Germany.

Electroencephalography (EEG) is a classic method for brain activity exploration. EEG involves recording, analysis, and interpretation of voltages recorded on the human scalp originated from the brain gray matter. In 1924 Hans Berger recorded the first human electroencephalogram. Since that time, it has been one of the favorite methods to study and understand

processes that underlie behavior, mostly because in opposition to other methods, EEG is relatively cheap, easy to wear, light weight and has high temporal resolution. In terms of behavior, this encompasses actions that are performed by beings in response to their environment, and these include movement. However, is difficult to record EEG during movement situations and hence most studies about the human brain examine subjects in static conditions. The problem is that until recently the methodology was not developed enough, and therefore EEG signals were extremely artifact sensitive to allow analysis of brain dynamics during movement. Artifacts such as electromyographic activity (EMG) have traditionally greatly impaired the use of EEG during movement. In this paper we will discuss methods for allowing more mobile EEG measurements. We will present solutions for static EEG systems recording and for analysis of movement related brain activity. These solutions cover suggestions of how to avoid motion artifacts, the use of custom designed accessories for EEG recording in movement, determination of real/custom electrode positions, EEG electrodes types, use of different EEG recording systems, powerful algorithms for signal decomposition and EMG noise reduction. An overview of how to record and analyze EEG during movement tasks will be presented. In the end we will conclude that it is possible and no longer only an aspiration, to record and analyze EEG from movement or exercise tasks.

ID: 131

SYM-11: 5

Sensor based movement analysis

Bjoern M Eskofier and Dominik Schuldhaus

Digital Sports Group, Friedrich-Alexander-University
Erlangen-Nuremberg, Germany.

Wearable computing systems that allow sensor based movement analysis play an increasingly important role in sports. Those systems comprise of two parts. Firstly, sensors embedded into clothes and equipment are used for biomechanical (accelerometer, gyroscope, magnetometer, GPS, ...) data recording. Secondly, embedded microprocessors are used for the analysis of the recorded data. Together, these systems provide support, real-time feedback and coaching advice to sportsmen of all performance levels as well as their coaches.

Our group works on four of the most prevalent challenges that have to be addressed in order to implement wearable computing systems:

integration: sensors and microprocessors have to be embedded unobtrusively and have to record a variety of signals;

communication: sensors and microprocessors have to communicate in body-area-networks in a secure, safe and energy-saving manner;

interpretation: physiological and biomechanical data have to be interpreted using signal processing and pattern recognition methods;

usability: interaction with the systems is provided by human-machine-interfaces (HMIs) that have to be intuitive and adapted to several use cases.

The talk presents the named challenges and technological solutions to overcome them. Motivated with the help of real-world examples, the opportunities that such systems offer for work fields such as performance enhancement, injury prevention, activity monitoring and health promotion will be presented. Subsequent to the overview of these aspects, the talk will conclude with an outlook with respect to important future challenges in the presented research field.

ID: 183

SYM-11: 6

Training 4.0 – computerized motion analysis in football training

Matthias Lochmann, Holger Eckhardt and Fritz Bodem

Institute of Sport Science and Sport, Friedrich-Alexander-University Erlangen-Nuremberg, Germany.

Traditional football training does; at the present time, not take full advantage of the modern technology readily available for a dedicated optimization of its efficiency. Due to the availability of fast measuring data processing power by inexpensive computer systems, high resolution and high speed position tracking technology, and large screen optical display techniques, however, it is possible to design complex systems for real time motion diagnosis and training suitable for all kinds of ball playing. The world of actual physical training may thus be completed by a cyber world created by and resulting from its computerized real time analysis. The position tracking technology developed in the past for all sorts of motion analysis can be used to determine with high spatial accuracy and high sampling rates the ball position and spin as well as the trajectories of suitably chosen anatomical landmarks on the football players body. The placement of special position measuring devices in a player's headband can be used for the real time analysis of his head position and movement and his viewing direction. The thus obtained position measurement data can be used to calculate objective information on the technical skills of a player with regard to the velocity and the spin of the ball. The calculated results can be displayed on 4 large screens surrounding the training environment thus continuously displaying in an easy to visualize manner features like ball control, dribble, pass

dynamics and pass accuracy. The individual playing skills and the interaction between different players and the ball can thus serve as an immediate feedback to the football players and their coach. Additional sensors can be fixed to the player's body to record and display biosignals like heartrate and body temperature. Under these circumstances a technical training can be interlaced with a tactical and a physical training. On the basis of the diagnosis elaborated in the training sessions an objective strength-weakness profile of every player can be created. In a continuous long term training process these profiles can be permanently adapted to the ongoing changes of the players' performance observed. We believe that a computer controlled training system of this type has the potential to strongly and sustainably increase football training efficiency. Furthermore, the principles of this approach are, in principle, applicable to different ball sports, ice hockey and games like tennis or squash. The computerized training system outlined here has been named "Training 4.0", its principles being in accordance with the "Industry 4.0" hightech strategy initiative promoted by the German government.

Session	SYM-12: Emerging Developments for Regenerative and Therapeutic Medicine
Date/Time	6 December 2013 13:30–15:00 hrs
Venue	Auditorium

ID: 852 SYM-12: 1

**Symposium Keynote:
Biomaterial-assisted stem cell-based therapies for intervertebral disc degeneration**

Barbara Chan

The University of Hong Kong, China.

Degenerative disc disease (DDD) poses an increasing threat to our quality of life as we age. Existing treatments have limitations. New treatment modalities using biological rather than surgical approach are appealing. Mesenchymal stem cells (MSC)-based therapy hold great potential in treating disc degeneration. Numerous studies in mouse, rat, rabbit, porcine and bovine models showed encouraging results with survival, proliferation and differentiation of MSCs, enhanced matrix accumulation, and improved disc height and hydration level. However, during intra-discal injection, the vast majority of cells leaked out even in the presence of hydrogel carrier. Recent evidence even suggests that annulus puncture is associated with cell leakage and contributes to osteophyte formation, an undesirable side-effect.

This suggests the significance of developing appropriate cell carriers and effective approaches to prevent leakage and associated osteophyte formation before MSC-based therapies can be applied in a clinical setting.

Using a collagen microencapsulation platform, solid yet porous microspheres entrapping MSCs, and supporting their survival, proliferation, differentiation and matrix remodeling, were fabricated. We hypothesize that intra-discal injection of MSCs in collagen microspheres will outperform MSCs in saline in improving functional outcomes and reducing side effect osteophyte formation. Using a well-established disc degeneration model in rabbits, autologous MSCs, either packaged within collagen microspheres or directly suspended in saline, were intra-discally injected into different disc levels. Comparing with MSC in saline, MSC in collagen microspheres showed slight advantages in disc height maintenance, dynamic mechanical behavior and GAG:HYP ratio. More importantly, delivering MSC in collagen microspheres significantly reduced the risk of osteophyte formation. This work demonstrates the significance of cell carriers during intra-discal injection of MSCs in treating disc degeneration. Nevertheless, osteophyte formation cannot be completely eliminated by using microsphere carriers.

Using a patented photochemical crosslinking technology, an injectable collagen-based annulus plug was fabricated to block the injection portal during intra-discal delivery. A custom-made delivery device was also developed to deliver the plug intra-discally following delivery of MSCs in collagen microsphere carriers. Ex vivo studies showed that the plug survived physiologically relevant loadings and significantly reduced leakage and enhanced retention of the injected materials. *In vivo* study in the same rabbit model showed encouraging results. Microcomputed tomography imaging and histology revealed that the plug significantly reduced osteophyte formation. This work suggests the potential of the annulus plug as an adjunct or annulus closure device for intra-disc delivery of cells and materials.

Many questions remain to be answered before successful translation of stem cell based therapies for disc degeneration. A discussion on these topics such as better understanding of the niche factors inducing differentiation of MSCs towards nucleus pulposus-like lineages will also be included, depending on the time allocation.

ID: 783

SYM-12: 2

Polysaccharide hydrogels functionalized with fucoidan for tissue reconstruction

Catherine Le Visage

Inserm U698, Cardiovascular Bioengineering, France.

To date, bone loss is conventionally repaired by allogenic and autologous bone grafts and bone tissue engineering research is focused on the development of biomaterials that can stimulate bone healing. To this end, we have developed chemically cross-linked polysaccharide hydrogels based on pullulan and dextran, both being composed of glucose units linked by glycosidic bonds. Porous hydrogels supplemented with nanocrystalline hydroxyapatite particles (2.8% w/w) were investigated in ectopic sites, i.e. subcutaneously in mice and intramuscularly in goat. Micro-CT images revealed high degree of mineralization, beginning at day 15 and increasing significantly over time, as shown after quantification of mineral content and mineral density. In addition, excellent abilities for mineralization and formation of a dense mineral collagenous tissue in critical-sized orthotopic defects in small (femoral condyle of rats) and large animals (transversal mandibular defect in goat, tibial osteotomy model in goat) were demonstrated.

Thus, these porous composite scaffolds are promising substrates for bone tissue engineering due to their ability to mimic the natural nanostructure of the bone tissue. However, we observed that in all animal experiments vascularization was limited. We then functionalized these porous scaffolds with natural non-animal sulfated polysaccharide fucoidans in order to allow for delivery of vascular endothelial growth factor (VEGF) and to potentiate its angiogenic activity. Exogenous fucoidan, a natural sulfated L-fucose extracted from marine brown seaweed, has a heparin-like structure, with a low anticoagulant activity and is devoid of direct anti-thrombin effect. Interestingly, soluble fucoidans, partly owing to their ionic structure, can act as a reservoir for proangiogenic factors, influence the balance between storage and release of these factors and induce an increased endothelial cell migration. *in vitro*, fucoidan (medium molecular weight fucoidan MMWF) promoted endothelial progenitor cells proliferation inside the functionalized porous scaffolds. Surface plasmon resonance experiments confirmed a direct interaction between MMWF and VEGF₁₆₅, characterized by an affinity K_D (K_d/K_a) of 1×10^{-9} M. In a subcutaneous angiogenesis model in mice, fucoidan functionalized scaffolds showed a more intense vascularization response than control groups. Expression of isolectin-B4 and α -smooth muscle actin, as well as confinement of erythrocytes, demonstrated the neoformed blood vessels functionality. There was a

significant difference in neovessel area and neovessel density between control groups and MMWF scaffolds or MMWF+VEGF₁₆₅ scaffolds ($p < 0.001$ for all cases).

Hence we demonstrated that fucoidan sequesters VEGF₁₆₅, protecting it from degradation, and thus delivers biological cues promoting angiogenesis. We also provide the evidence that functionalized scaffolds loaded with VEGF₁₆₅ increase vascular network formation in a mice subcutaneous model of angiogenesis. In a future work, we will investigate whether hydrogels functionalized with both hydroxyapatite and fucoidan could direct the formation of mature vasculature through a local release of VEGF₁₆₅ and be a useful tool to guide therapeutic angiogenesis during bone regeneration.

ID: 860

SYM-12: 3

Emerging therapy in corneal transplantations

Jodhbir Mehta

Singapore Eye Research Institute, Singapore.

Corneal transplants are the commonest transplantation procedures performed. Outcomes have improved due to the use of selective tissue transplantation techniques. The most common selective tissue technique is endothelial keratoplasty. This may be improved further with tissue engineering. The aim of the talk is to review the improvement in surgical engineering outcomes with current endothelial keratoplasty techniques. It will also cover new emerging therapy in the treatment of endothelial keratoplasty with respect to tissue engineering and also the direction of future work in this area. The ultimate goal will be to use an autologous source or a non corneal donor tissue source.

ID: 875

SYM-12: 4

Microengineered hydrogels for stem cell bioengineering and tissue regeneration

Ali Khademhosseini

Harvard Medical School, United States of America.

Micro- and nanoscale technologies are emerging as powerful tools for controlling the interaction between cells and their surroundings for biological studies, tissue engineering, and cell-based screening. In addition, hydrogel biomaterials have been increasingly used in various tissue engineering applications since they provide cells with a hydrated 3D microenvironment that mimics the native extracellular matrix. In our lab we have developed various approaches to merge microscale techniques with

hydrogel biomaterials for directing stem cell differentiation and generating complex 3D tissues. In this talk, I will outline our work in controlling the cell-microenvironment interactions by using patterned hydrogels to direct the differentiation of stem cells. In addition, I will describe the fabrication and the use of microscale hydrogels for tissue engineering by using a 'bottom-up' and a 'top-down' approach. Top-down approaches for fabricating complex engineered tissues involve the use of miniaturization techniques to control cell-cell interactions or to recreate biomimetic microvascular networks. Our group has also pioneered bottom-up approaches to generate tissues by the assembly of shape-controlled cell-laden microgels (i.e. tissue building blocks), that resemble functional tissue units. In this approach, microgels were fabricated and induced to self assemble to generate 3D tissue structures with controlled microarchitecture and cell-cell interactions.

ID: 886

SYM-12: 5

Substrate topography for gene delivery and tissue engineering applications

Evelyn K.F. Yim

National University of Singapore, Singapore.

In the *in vivo* natural microenvironment, cells are surrounded by various biochemical and biomechanical cues, including micro- and nanotopography. An ideal scaffold for tissue engineering application should mimic the microenvironment for natural tissue development and present the appropriate biochemical and topographical cues in a spatially controlled manner. Recent findings demonstrated mammalian cells respond to nanoscale features on synthetic polymeric substrate. Our research group is interested in studying the interactions of adult and embryonic stem cells with nanotopography, the mechanism of the topography-induced cell behaviour and how to apply this knowledge to direct stem cell differentiation for tissue engineering applications. We have showed that nanotopography can significantly influence cellular behaviours ranging from attachment to proliferation and differentiation. In this presentation, nanotopography-regulation on adult and embryonic stem cells will be presented as examples of applying nanotopography in tissue engineering. The nanotopography-modulation on drug and gene delivery will also be discussed.

Session	A8: Medical Imaging
Date/Time	6 December 2013 13:30–15:00 hrs
Venue	SR-01 & 02

ID: 220

A8: 1

Efficient regularisation of temporal autocorrelation estimates in fMRI data

Arun Kumar^{1,2} and Lin Feng²

¹School of EEE, Singapore Polytechnic, Singapore; ²School of Computer Engineering, Nanyang Technological University, Singapore.

Temporal autocorrelation present in functional magnetic resonance (fMR) images affects their statistical analysis. Pre-whitening is thus performed on fMRI data, generally with a first order autoregressive, i.e., AR(1) model implemented to estimate the temporal autocorrelations. Spatial smoothing filter is then normally applied to regularize these autocorrelation estimates, in order to reduce their variance, before using them in an REML process to perform pre-whitening. Some researchers have found that smoothing these autocorrelation estimates with spatial smoothing filters prevents the successful modeling of negatively correlated and approximately white spectra. Smoothing was also found to result in underestimation of positive correlations when weakly correlated or white spectral residuals bordered these positively correlated residuals. In our proposed method, we apply random field analysis based regularization, with a modified conditional random field, rather than a smoothing filter. It provides the necessary reduction in variance of AR(1) coefficients by taking into account the neighborhood autocorrelation estimates and at the same time preserves the borders between the positive, negative and white spectral residuals.

ID: 632

A8: 2

A study on the high-resolution imaging system for capillary on the surface of eyeball

Jiamao Li¹ and Xiaolin Zhang²

¹Chinese Academy of Sciences, China; ²Tokyo Institute of Technology, Japan.

A number of studies have shown that information of state of peripheral vessels and their blood flow may be helpful in the early diagnosis of various diseases such as diabetes, myocardial infarction, and cerebral infarction. Currently, most optical techniques for monitoring blood flow in both research and clinical settings use either the Doppler effect or the temporal statistics of time-varying laser speckles. These types

of blood flow meters are non-invasive, but they cannot be used to acquire additional information, such as blood vessel width. A novel device for non-invasively observing peripheral blood vessels and their blood flow using high-speed photography of the surface of the sclera was developed in our laboratory. The peripheral vasculature of the sclera was directly observed using our device. Fixational eye movements refer to the continual movement of the eyes while the gaze remains fixed on an object. Utilising phase-only correlation to detect the displacement of blood vessels, we eliminated the effects of fixational eye movements to stabilise the sclera images. Morphological operations were then applied to segment the data locally and to extract the shape of the blood vessels. High-speed optical flow generation with the steepest descent method was used to detect the velocity of the red cells flowing in the blood vessels. A variety of experiments verified the validity of our novel method for observing capillary blood flow.

ID: 337

A8: 3

Measurement of undetectable walking feature by appearance based on plantar skin deformation

Takayuki Shiina, Akira Obara, Hiroshi Takemura and Hiroshi Mizoguchi

Tokyo University of Science, Japan.

Walk is fundamental motion in daily life. Everyday life isn't without walk. However, walk always involves risk of falling. This study was focused on a plantar skin deformation which was undetectable part by appearance during a walk. This research investigated the plantar skin deformation and variability in elder and young. The changes of plantar skin contact area, slipped contact area and non-slipped contact area were measured and compared during the stance phase. A total of 30 (10 normal young males (22±2 years) and 20 normal elders (73±5 years) human subjects were recruited in this research. Subjects were asked throughout the experiment to walk at a comfortable speed on a walkway four times per one trial. Feature points of plantar skin were calculated by using Harris corner image processing method. Changes of plantar skin contact area were calculated by using binarization images. As results, the changes of plantar skin contact area in the elder were significantly higher than the young group during Initial grounding ($p<0.05$). The standard deviation of the changes of plantar skin contact area in elder group were significantly higher than in young group during initial grounding and front swing phase ($p<0.05$). The results suggested that the elder have more risk of falling than young during

initial grounding and front swing phase ($p<0.05$). The changes amount of plantar skin slipped area in the elder group were significantly higher than the young group during the plantar skin contact ($p<0.05$). This phenomenon suggested that the elder group tend to slide feet during the stance phase. In conclusion, the plantar skin deformation measurement can potential to calculate of undetectable walking feature by appearance and screen people who has potential risk of falling.

ID: 756

A8: 4

Novel technique to characterise corneal biomechanics *in vivo*

Cheuk Wang Chung¹, William Lim¹, Khai Sing Chin¹, Nicholas Strouthidis^{2,3} and Michael J.A. Girard^{1,2}

¹Department of Bioengineering, National University of Singapore, Singapore; ²Singapore Eye Research Institute, Singapore; ³Moorfields Eye Hospital, London, United Kingdom.

Glaucoma is a sight-threatening disease which affects over 60 million people worldwide. Recent published evidence suggesting that the disorder is instigated by an increased intraocular pressure (IOP), which distorts the optic nerve head (ONH) and induces optic neuropathy. Many patients are unaware of their pathological conditions until they experience deteriorating vision at the later stage of the disease.

Early detection of glaucoma is essential for timely treatment. Although ONH deformation could serve as an indicator of disease severity, direct measurements remain challenging. An alternative method is to assess the mechanics of the cornea, which could become a surrogate for ONH mechanics and thus glaucoma susceptibility.

A new technique was developed to characterise corneal biomechanics *in vivo*, and was tested here in *ex-vivo* porcine eyes. It involves applying deformation to the cornea with the process being captured by optical coherence tomography (OCT). A specialised in-house software is developed to process the images. To test the feasibility of the novel technique, an eye holder was connected to an IOP control system and an OCT camera. Porcine corneas were deformed through two different approaches. In the first method, a static pressure control system was used to apply a suction pressure on the cornea. OCT images of the contorted cornea volume were captured at different IOP and suction pressure magnitudes. In the second method, only IOP was raised incrementally with a column of saline from 10 to 60 mmHg. Cross-sectional OCT images of the cornea were captured during the deformation processes.

The result shows that there is a correlation between corneal deformation and IOP. Our software

can perform image segmentation, three-dimensional tracking of sample points on cornea and calculate their displacements during deformation. The new technique has the potential to become a reliable minimally-invasive diagnostic tool for glaucoma.

ID: 351

A8: 5

Development of novel endoscope with NIR camera using real-time video composite method

Masayuki Watanabe¹, Hiroshi Takemura¹, Hiroshi Mizoguchi¹, Hiroshi Hyodo¹, Kohei Soga¹, Tamotsu Zako², Hidehiro Kishimoto³, Masaaki Ito⁴ and Kazuhiro Kaneko⁴

¹Tokyo University of Science, Japan; ²RIKEN, Japan; ³University of the Ryukyus, Japan; ⁴National Cancer Center Hospital East, Japan.

Recently, a near-infrared (NIR) Fluorescence Biomedical Imaging (FBI) attracts increasing attention from many researchers. The light of wavelength region in 1000 nm to 1700 nm has been known to be a "biological window" where the both tails of scattering and infrared absorption decrease to form a valley in optical loss spectra of biological objects. The inside of biological objects which cannot be usually seen in a normal endoscopy can be seen because of NIR light can penetrate in biological objects, and the further development of medical equipment is expected by using NIR camera. We are experimenting towards the realization of a NIR laparoscope which composes of a NIR camera and a visible light camera. The visible light camera can observe the surface in biological objects, and the NIR camera can observe the inside of biological objects. The NIR laparoscope has a potential of the helpful in the early detection of tumor. In our current system, the images captured by a NIR laparoscope and a normal laparoscope are shown on the separate screens simultaneously. The operator need to more experience to use the system. It was difficult to figure out the clinical usefulness of the NIR laparoscope with a visible light camera. We proposed the image composite method using a projection transform and a distance correction. The proposed method, compared to existing methods, is simple and fast. The proposed composite method of the two video images from a NIR camera and a visible light camera can facilitate the diagnosis and the surgery. The proposed system can reduce not only operator's burden but also patient one's. We are applying the proposed method to a viscous endoscope and conducting the evaluation experiment of the proposed method.

ID: 238

A8: 6

Remote photoplethysmographic imaging of dermal perfusion in a porcine animal model

Nikolai Blanic, Carina Barbosa Pereira, Michael Czaplik, Vladimir Blazek and Steffen Leonhardt

RWTH Aachen University, Germany.

Introduction: Photoplethysmography Imaging (PPGI) is a camera-based diagnostic tool developed at RWTH Aachen University, Aachen, Germany, for remote analysis of heart rate, respiration rate and their variability by detecting skin brightness behaviour as a function of dermal perfusion. A PPGI feasibility study was performed in anesthetized pigs with Acute Respiratory Distress Syndrome (ARDS) as extension of an ongoing study (approved by the North Rhine-Westphalia State Regional Office for Nature, Environment and Consumer Protection: 84-02.04.2012.A173).

Methodology: The basic principle of PPGI is similar to classical photoplethysmography (PPG), but instead of a skin-attached optoelectronic sensor, a high sensitive CCD camera has been used (AVT, Pike 210B). For illumination, the environmental light sources of the surgical theatre are sufficient.

During the experiments, the pigs were placed in supine position on the surgical table. From 1–2 meter distance, PPGI sequences were recorded with duration of approximately 30 seconds. The displayed details include the region from the pig's snout to its abdomen. The video sequences were stored on the controlling PC and analysed off-line.

Therefore, the progress in time of the gray value of every single pixel or alternatively the mean gray value of pixels inside a region of interest are considered as single PPG signals. For their further assessment, the same algorithms than for classic PPG were used.

Preliminary results and conclusion: Up to now, the perfusion of five different animals was analysed at minimum five different points in times. Comparing the vital parameters achieved by PPGI with standardized monitoring devices, the extracted heart and respiration rate could be confirmed in more than 90% in contactless manner. This demonstrates that PPGI is a promising alternative for monitoring of vital signs in animal and also human observations.

Session	B8: Biological Materials
Date/Time	6 December 2013 13:30–15:00 hrs
Venue	SR-03 & 04

ID: 545 B8: 1

Conference Keynote:
Current biomaterials for tendon/ligament tissue engineering

Hong-Wei Ouyang

Zhejiang University, China.

Tendons and ligaments function as transmission force from muscle to bone or bone to bone, so they are often targets of sports injury. Recent advancement of biomaterials provides new devices of augmentation for tendon/ligament repair and tissue engineering. This talk systematically reviews the current tendon/ligament researches of biomaterials. The choice of materials, macro-structure, microstructure and incorporation of bioactive molecules are highlighted and discussed. The limitation, questions and directions for future tendon/ligament research are also suggested.

ID: 163 B8: 2

Single step peptide immobilization onto a variety of biomaterial surfaces by Tyr oxidation and its application for re-endothelialization promoting vascular stent

Sachiro Kakinoki¹, Kensuke Takasaki^{1,2}, Yoshiaki Hirano² and Tetsuji Yamaoka¹

¹National Cerebral and Cardiovascular Center Research Institute, Japan; ²Kansai University, Japan.

A variety of materials including metals and polymers were used as substrates of biomedical devices. Since these materials do not possess biological activity like cellular adhesiveness, immobilization of bioactive peptides onto their surfaces is useful. However, there is no simple procedure for peptide immobilization which is available for a variety of materials. In this study, we developed a novel peptide immobilization technique onto metallic and polymeric substrates by single-step oxidation of Tyr residue, and applied this technique to the vascular stent for promoting re-endothelialization. Polystyrene, polyethylene, poly(vinyl chloride), expanded poly(tetrafluoroethylene), polyester (Cell Desk), poly (L-lactic acid) (Mw=160,000), stainless steel (SUS316L) were chosen as substrates. Fibronectin-derived cell adhesive peptide, Arg-Glu-Asp-Val with Tyr residue (Ac-YG₃REDV) was immobilized on the substrates by just immersing into an aqueous solution of Ac-YG₃REDV with CuCl₂ and H₂O₂ used as catalyst and oxidant,

respectively. Adhesion behavior of human umbilical endothelial cells (HUVEC) onto REDV-immobilized substrates was evaluated *in vitro*. REDV-immobilized Cr-Co stent was also prepared by this technique and placed into the rabbit abdominal aorta.

Immobilization of REDV-peptide by Tyr oxidation was confirmed by XPS spectra. Briefly, nitrogen peak assigned to peptide was detected on all substrates after Tyr oxidation, but this peak did not appear after immersion in peptide solution without CuCl₂ and H₂O₂. This result demonstrated that CuCl₂ and H₂O₂ are required for REDV immobilization. HUVEC adhesion was improved on REDV-immobilized surfaces. In addition, re-endothelialization was observed at the most part of strut inside REDV-immobilized stent without thrombosis formation in a week of stenting. We successfully immobilized REDV peptide onto a variety of substrates by Tyr oxidation with CuCl₂ and H₂O₂, and demonstrated the promoted re-endothelialization in REDV-immobilized stent. This technique is very useful for the surface functionalization of medical devices constructed with various substrates because of high reactivity and biocompatibility of Tyr residue.

ID: 263 B8: 3

Nano-scale thermo-mechanical structure-property relationships in human dental tissues studied by nanoindentation and synchrotron X-ray scattering

Tan Sui¹, Michael A. Sandholzer², Eric Le Bourhis³, Nikolaos Baimpas¹, Gabriel Landini² and Alexander M. Korsunsky¹

¹University of Oxford, United Kingdom; ²University of Birmingham, United Kingdom; ³Universite Poitiers, France.

Human teeth are hierarchical mineralized structures consisting of collagen fibres decorated with hydroxyapatite (HAp) crystallites at nano-scale. Teeth are composed of two major calcified tissues: harder outer enamel layer and softer dentine core. These tissues are joined by an interface known as the dentine-enamel junction (DEJ). The knowledge of the mechanical properties related to the hierarchical structure of dentine, enamel and the DEJ is essential for understanding and predicting the effects of microstructural alterations due to disease, treatment, or environmental or thermal exposure on the performance of dental tissues and their artificial replacements. So far, few studies have focused on the nano-scale mechanical properties of human teeth, in particular the response to thermal treatment that is thought to be strongly affected by the evolution of the mineral crystallite size, their spatial arrangement and orientation. In this study, small and wide angle synchrotron X-ray scattering (SAXS/WAXS) was

used to investigate the structural alterations at the nano-scale, while nanoindentation was introduced to map the nano-mechanical properties variation in thermally treated dental tissues. The thermo-mechanical structure-property relationships in human dental tissues were analysed. This property alteration is likely to occur due to changes in the size and orientation of HAP crystallites, but is also strongly affected by the presence of the organic phase (collagen). The results are likely to be broadly useful in understanding the mechanical property correlations in hierarchical biomaterials in the context of forensic and archaeological investigations.

ID: 191

B8: 4

Effect of molecular architecture of PEG-immobilized surface on plasma fibrinogen adsorption and platelet adhesion

Takuya Nakagoshi^{1,2}, Sachiro Kakinoki¹, Yuichi Ohya² and Tetsuji Yamaoka¹

¹National Cerebral and Cardiovascular Center Research Institute, Japan; ²Department of Chemistry and Materials Engineering, Faculty of Chemistry, Materials and Bioengineering, Kansai University, Japan.

Introduction: To prevent protein adsorption and platelet adhesion onto the surface is important for the biomaterials design. It is well-known that the hydrophilic surface with polyethylene glycol (PEG) chain immobilized through one terminal inhibits protein adsorption and platelet adhesion. On the other hand, segmented polyurethane (SPU) containing PEG units has been reported that adhesion and spreading of platelets slightly occurred on its surface.

We hypothesize that platelet adhesion might be influenced by the molecular architecture of interfacial PEG chains, because PEG chain forms graft and loop structures on the PEG-immobilized substrate and SPU surfaces, respectively.

In the present study, PEG was immobilized on the gold substrate through its one or both terminals to construct the well-defined surfaces with different molecular architectures, PEG-graft and PEG-loop, and the behavior of protein adsorption were evaluated.

Materials & Methods: The PEG surfaces with graft or loop structure were prepared using OMe-PEG-SH or SH-PEG-SH (Mw of PEG: 2000, 5000, 10000) via Au-SH bond. Water-in-air contact angle of PEG-immobilized surfaces were measured. The mobility factor of interfacial PEG chains and the amount of adsorbed human plasma fibrinogen (HPF) were determined by the resonance frequency and the energy dissipation quantified by Quartz Crystal Microbalance with dissipation monitoring (QCM-D).

Results & Discussion: Water contact angle of both PEG-graft and PEG-loop was about 30°. The mobility factor of PEG-graft was twice higher than that of PEG-loop. HPF adsorption was suppressed on PEG-graft in comparison with PEG-loop. These results demonstrated that high molecular mobility of PEG chains is important for preventing HPF adsorption.

ID: 581

B8: 5

Synthesis and characterization of nanorod hydroxyapatite from cockle shells

Nur Ain Iftitah Mohamad Razali, Belinda Pinguan-Murphy, Noor Azuan Abu Osman and Sumit Pramanik

University of Malaya, Malaysia.

Hydroxyapatite (HAp) is widely known to have a similar structure to human bones. Synthetic HAp is mainly synthesized from calcium and phosphorus precursors. Many studies report the efficient use of using HAp, namely in bone fillers, bone grafts and implant coatings in orthopedics. Natural biocompatibility makes HAp reliable as a human bone replacement biomaterial. Several studies report the synthesis of HAp using organic materials as calcium sources, including seashells, hard clams and coral. Such organic materials have been shown to consist of 97–98% wt/wt calcium. Nanoscale particles are currently important because they provide a higher surface area and porosity to a bioceramic. Recently, the potential of sintered cockle shells to be used directly as bioceramics was reported. The present study reports synthesis of pure HAp from cockle shells as calcium precursor and diammonium hydrogen phosphate $(\text{NH}_4)_2\text{HPO}_4$ as phosphorus precursor. The sol-gel technique was selected to obtain a crystalline HAp structure. Cockle shells were sintered at 450°C (CS450) and 800°C (CS800) to obtain a calcite calcium carbonate, CaCO_3 structure. Cockle shells were mixed with $(\text{NH}_4)_2\text{HPO}_4$ and water before being heated and stirred continuously. The addition of ammonium hydroxide drop wise kept the pH at 10.5. The slurry obtained was washed and dried to form powder. Characterization of the powder was performed using Field Emission Scanning Electron Microscopy (FESEM), X-Ray Diffraction (XRD) and Fourier Transform Infrared (FTIR) analyses. Results from XRD and FTIR analyses showed that pure HAp was produced by CS800 and mix of CaCO_3 and HAp produced by CS450. Rod-shaped particles were captured from FESEM analysis. Average diameter of the particles was 25nm for CS450 and 15nm for CS800. Highly crystalline nanorod HAp was successfully synthesized from raw cockle shells via a low temperature sol-gel technique. Further studies related to mechanical properties are

required to determine the various applications of this bioceramic.

Session	C8: Computational Mechanics
Date/Time	6 December 2013 13:30–15:00 hrs
Venue	SR-05 & 06

ID: 746

C8: 1

**Conference Keynote:
An overview of VPH/Physiome activities**

Peter John Hunter

The University of Auckland, New Zealand.

Multi-scale models of organs and organ systems, based on model encoding standards, are being developed under the umbrella of the IUPS Physiome Project and the Virtual Physiological Human (VPH) project funded by the European Commission. These computational physiology models deal with multiple physical processes (coupled tissue mechanics, electrical activity, fluid flow, etc) and multiple spatial and temporal scales. They are intended both to help understand physiological function and to provide a basis for diagnosing and treating pathologies in a clinical setting. A long term goal of the project is to use computational modelling to analyze integrative biological function in terms of underlying structure and molecular mechanisms. Web-accessible databases, based on the standards (which include SBML, CellML and FieldML), have been established for models and model-related data at the cell, tissue, organ and organ system levels. This talk will discuss recent developments in the VPH/Physiome Project and the application of these multi-scale modelling approaches to several physiological systems including the cardiovascular system, the respiratory system, the musculo-skeletal system and the digestive system.

ID: 118

C8: 2

Application of CFD and genetic algorithms to investigation of determinants of carotid artery bifurcation shapes

Masako Himeno, Shigeo Noda, Kazuaki Fukasaku and Ryutaro Himeno

RIKEN, Japan.

We studied which factors play an important role to determine the artery shapes by performing multi-objective optimization with computational fluid dynamics (CFD) and genetic algorithms (GA). We took the following approach. First, multi-objective optimization of arterial radius and center line that set

objectives as assumed factors was performed to obtain optimized shapes in the base of an actual shape. Next, the actual artery shape was compared with the results of the optimized one. By applying this process to other several shapes, common factors displaying actual shapes were selected. We assumed five factors: a) to minimize the maximum time-averaged wall shear stress (max WSS), which means the artery is created not to have an excessively high degree of time-averaged WSS, b) to maximize the minimum time-averaged WSS (min WSS), c) to minimize the maximum wall shear stress gradient (WSSG), d) to minimize the maximum wall shear stress temporary gradient (WSSTG), e) to minimize the summation of the artery radius measured by the inner surface area (area). We picked up 7 shapes of carotid artery bifurcation as actual shapes whose ages lay between the 20s and the 80s. We performed a multi-objective optimization with six kinds of combinations of two-objectives; (max WSS, area), (max WSS, min WSS), (WSSG, area), (WSSG, min WSS), (WSSTG, area) and (WSSTG, min WSS). As a result, in the case of minimizing both the max WSS and surface area, all actual shapes were optimized ones. This combination was the best in the six tested combinations. It became clear that the combination of minimizing local time-averaged WSS and minimizing the artery radius plays a more important role to determine normal artery shapes than the other tested combinations. We confirmed that performing multi-objective optimization with CFD and GA is very useful to examine the determinants of artery shapes.

ID: 161

C8: 3

Simulation of electron transfer in Cytochrome b5 reductase-Cytochrome b5: Ground study for understanding recessive methemoglobinemia type II

Varomyalin Tipmanee¹, Thanyada Rungrotmongkol² and Supot Hannongbua³

¹Department of Biomedical Sciences, Faculty of Medicine, Prince of Songkla University, Thailand; ²Department of Biochemistry, Faculty of Science, Chulalongkorn University, Thailand; ³Department of Chemistry, Faculty of Science, Chulalongkorn University, Thailand.

NADH-Cytochrome b5 reductase deficiency leads to recessive methemoglobinemia(RCM) type II, blood disease due to too high level of methemoglobin in human blood, and able to cause cyanosis and eventually death. NADH-Cytochrome b5 reductase (Cb5R) plays a crucial role in methemoglobin control via catalytic electron transfer(ET), through the complex between the enzyme and cytochrome b5(Cb5). The catalytic deficiency, as a result of various types of structural mutation, is hypothetically elucidated by

the electron transfer rate constant. Yet, no apparent consensus on electron transfer of mutant enzyme has been concluded. Prior to investigation of mutant Cb5R catalytic efficiency, the simulations of ET reaction in enzyme complex between wild type Cb5R and Cb5 at given NaCl concentration (100, 150, 200 or 300 mM), corresponding to osmotic pressure ranges in red blood cell, have been carried out to establish a standard protocol for advanced study. In Moser-Dutton ruler, an electron transfer rate constant directly depends on driving force, distance between ET reactive cofactors, and reorganization energy. The main focus of interest is quantitative prediction of ET reorganization energy and inter-cofactor distance so as to form an implication of catalytic affinity through ET rate. Therefore, the electron transfer reactions in Cb5R-Cb5 complex were simulated and the reorganization energies were computed, using Molecular dynamic simulation combined with DFT calculation. The four resulting reorganization energies, within a range of 1.4 to 1.6 eV, were in good agreement with an experiment. In addition, combining the computed reorganization energy and inter-cofactor distance along with an experimental driving force yielded the rate constant on the microsecond timescale, comparable to one for biological electron transfer. The overall results reflect the protocol validity for further atomistic investigation of how mutation contributes towards ET and leads to RCM type II occurrence. Some of mutant enzyme systems are ongoing.

ID: 196

C8: 4

Computer simulation of human respiration

Guangzhi Zhang¹, Xian Chen¹, Junji Ohgi¹, Seiryu Sugiura² and Toshiaki Hisada²

¹Applied Medical Engineering Science, Yamaguchi University, Japan; ²The University of Tokyo, Japan.

Revealing the mechanism of respiration by modern computational methods will contribute to pneumology and the study on thoracic diseases. Also, it will lead to not only the reproduction of its rational mechanical boundary conditions for heart simulators, but also the application to cardiopulmonary resuscitation (CPR) and commotio cordis. Towards such a goal, the present work aims to establish a computational model for simulating human respiration. A finite element chest model was constructed including sternal, rib, vertebral bones and intercostal muscles, diaphragm, and furthermore, heart and lung. Transversely isotropic hyperelastic muscle model of Hill-type was adopted as the constitutive relation of intercostal muscles and diaphragm. Heart and lung were modeled as hyperelastic and porous hyperelastic materials, respectively. The contraction of intercostal muscles and diaphragm

reproduced the chest respiratory movement. The results show that the contraction of intercostal muscle generates the moment about costovertebral joint and thus the direction of the muscle fiber on the chest movement is influential. By introducing the experimental data on the fiber directions (Loring, 1992), the chest deformation modes were obtained compatible with the conventional inference. The intrathoracic and intrapulmonary pressures were obtained consistent with clinical observation. Although the effectiveness of the proposed computational model was demonstrated, further improvement is scheduled to introduce lung airway system. This research is granted by the Japan Society for the Promotion of Science (JSPS) through the "Funding Program for World-Leading Innovative R&D on Science and Technology (FIRST Program)," initiated by the Council for Science and Technology Policy (CSTP).

Session D4: Biomedical Devices

Date/Time 6 December 2013 | 13:30–15:00 hrs

Venue SR-07 & 08

ID: 889

D4: 1

Conference Keynote: Lessons learnt: Development of genomics-based diagnostics tests

Christopher Wong

Genome Institute of Singapore, Singapore.

In the past decade, I have been involved in the development of genomics-based diagnostics and prognostics tests for cancer and infectious diseases. These tests have made it into different stages of commercialization, but aside from a simple SARS PCR diagnostic, no other products have received regulatory approval for clinical use. I will highlight some of these non-scientific challenges and issues that scientists need to be aware of, and be prepared to overcome in order to get their product to market.

ID: 210

D4: 2

Embedded fuzzy classifier for detection and classification of pre-seizure state using real EEG data

Uvais Qidwai¹, Mohamed Shakir² and Aamir Malik²

¹Qatar University, Qatar; ²Universiti Teknologi PETRONAS, Tronoh, Perak, Malaysia.

This paper presents a classification technique using Fuzzy Logic Inference System to identify and predict the partial seizure from the epileptic EEG data. The presented work covers the initial findings related to

some of the brain conditions in different scenarios so that the detection system can produce warning signals for epileptic seizure. Electroencephalography (EEG) plays an important role, especially EEG based health diagnosis of brain disorder. However, the common clinical approaches fall short when attempting to design an automated system to detect and predict partial seizure for epileptic patients. The situation becomes even more difficult when the detection system is being designed for a ubiquitous application in which the patient is not confined to the hospital and the device is attached to him/her externally while the person is involved in daily chores. Therefore, the work presented here includes embedded hardware system that works with classification algorithm on real EEG signals, in a ubiquitous setting. The performance of the system is shown under various conditions of daily activities. In order to make all this in a ubiquitous form factor, the algorithm for classification and detection of the pre-seizure conditions should be tremendously simple for processing the signal in a low cost ubiquitous microcontroller. This has been achieved in this work through the use of Fuzzy Classifiers based on the lookup table to empower system simplicity. The algorithm also utilizes certain statistical features from the EEG signal that are used as features to the classifier logic. While the clinical testing of the device is still awaited, various scenarios have been implemented using a custom-built hardware simulator based on empirical modeling of the real EEG signals. By using this type of fuzzy logic classifier, we were able to get over 90% accurate classification for the partial seizure.

ID: 126

D4: 3

Qualitative studies on quartz filters used in ultraviolet sterilization system

Subbaraman Ravichandran¹ and Then Tze Kang²

¹Temasek Polytechnic, Singapore; ²National University of Singapore, Singapore.

In this paper, we have summarized our findings on the use of suitable filters and the methods of configuring them for effective transmission of ultraviolet (UV) rays with the known wavelength of 253.7nm. Ultraviolet rays of this wavelength are known as UVC and the radiation dose of UVC energy is measured in microwatts per centimeter square. We have investigated the design of filters and reflectors for an ultraviolet sterilization unit developed to work in conjunction with a fluid dispenser for dispensing fluids in measured quantities periodically. Absorption of UV energy by DNA in the nuclei is a primary lethal mechanism for the destruction of microorganisms. It

is well known that the germicidal mechanism of UVC light has the ability to damage deoxyribonucleic acid (DNA) nucleotide, which in turn, disrupts the organism's ability to replicate. Contamination of fluids in these dispensers are common problems which we always encountered and we have investigated to qualitatively document the requirements of the system to overcome the contaminations using UVC energy. One of the problems encountered in designing the system was in the selection of suitable filters as common filters made of glass do not allow ultraviolet rays to pass through them. We have conducted our studies on selection of different filters specially designed for the chamber and these studies have provided a clear understanding on the advantages and the limitations of various filters. Thus it was possible to qualitatively analyze each sample for documenting antimicrobial effect. To conclude, this study gives a good understanding on the requirements of the filters and reflectors incorporated in the system for providing an optimum antimicrobial environment for dispensing fluids used in biological applications.

ID: 353

D4: 4

The effect of axial variation of the plane flow rate on two-dimensional ultrasonic-measurement-integrated simulation of blood flow in a common carotid artery

Takuya Matsumoto, Kenichi Funamoto and Toshiyuki Hayase
Tohoku University, Japan.

Circulatory diseases are closely related to hemodynamics. However, it is difficult to obtain detailed information on hemodynamics with conventional clinical measurement equipment. As a new method to obtain hemodynamic information in a carotid artery, we have developed the two-dimensional ultrasonic-measurement-integrated (2D-UMI) simulation system, which performs blood flow simulation with a feedback signal from ultrasonic measurement. In our previous report, we presented the potential of the 2D-UMI simulation for distinguishing healthy carotid arteries from diseased ones. However, the validity of the 2D-UMI simulation for a three-dimensional (3D) blood flow has not yet been clarified. Especially, it is essential to investigate the effect of axial variation of the flow rate on a measured cross-section plane, or plane flow rate, of real blood flow, which is inherently constant in the 2D-UMI simulation. As a preliminary study, as reported here in, we investigated the accuracy of the 2D-UMI simulation for a steady blood flow in a common carotid artery. A 3D computational result for the blood flow in a realistic common carotid artery was obtained for a model of real flow, that is, a standard solution. Assuming synthetic ultrasonic measurement for the standard

solution, the cross-sectional shape of a blood vessel and the velocity field on the longitudinal two-dimensional plane were extracted. Then, the 2D-UMI simulation was performed based on the synthetic measurement data, and the computational results were compared with those of the standard solution. The plane flow rate of the standard solution varied 13% in the axial direction. The error of the velocity vector of the 2D-UMI simulation over the standard solution decreased, particularly in the region where the plane flow rate was close to that of the standard solution, indicating that the 2D-UMI simulation properly reproduced hemodynamics of the targeted flow locally by setting the corresponding plane flow rate.

ID: 524

D4: 5

Modeling of signal transmissions in nerves *in vitro* for the development of a renal nerve cooling device for hypertension control

Takuya Ito¹, Hidekazu Miura², Takuya Shiga³, Mohamed Hashem³, Kurodo Kamiya³, Akihiro Yamada¹, Yusuke Tsuboko¹, Kyosuke Sano¹, Yasunori Taira¹, Yasuyuki Shiraiishi², Hiroo Kumagai⁴ and Tomoyuki Yambe^{1,2}

¹Graduate School of Biomedical Engineering, Tohoku University, Sendai, Japan; ²Department of Medical Engineering and Cardiology, Institute of Development, Aging and Cancer, Tohoku University, Sendai, Japan; ³Graduate School of Medicine, Tohoku University, Sendai, Japan; ⁴National Defense Medical College, Japan.

Hyperactivity of the central nervous system may increase feedback gains in the hemodynamic system. We have been developing a totally implantable renal nerve cooling system which is capable of changing the hyperactive renal nerve function; in particular, those that reversibly eliminate excess signal-gains by using Peltier effects. In this study, we examined the effect of cooling on neurotransmission *in vivo* and *in vitro*. Then we evaluated functional characteristics of signal transmission by the change in thermal implication on the nerve to perform thermal sedation of nervous activity. After the animal experimental procedures, we examined the electrical signal transmission in the nerves extracted from the goats. Using the neurogram amplifier and the functional signal generator, we tested the signal transmission characteristics through the nerves and evaluated their filtering functions by regional nerve cooling. In order to examine of natural renal neurotransmission, the renal nerves were dissected from the left kidney in goats under the normal anesthesia using 2.5% of isoflurane. Aortic pressure and the neurogram were measured, and we applied the low-temperature exposure of the nerve. The electric signals exhibited

filtered-transmission through the nerve by the cooling *in vitro*. In the goat's experiment, the amplitude of the signal which was obtained at the renal nerve decreased when we decreased the nerve surface temperature by -15 degrees. Then we could evaluate these transmission functions of the renal nerve with the interactive changes of the temperature which was to be controlled by the cooling device. We examined characteristics of the signal transmission in the renal nerve in goats by cooling. And we could evaluate these changes in the functional transmission model with the thermal interactions.

Session	D3: Biomedical Devices Diagnostic Devices
Date/Time	6 December 2013 13:30–15:00 hrs
Venue	SR-12

ID: 243

D3: 1

High sensitive detection of Ag⁺ ions in aqueous solution using silicon nanowires and silver-specific oligonucleotide

Yu Chen and Muhammad Hamidullah

Institute of Microelectronics, A*STAR (Agency for Science, Technology and Research), Singapore.

We report the development of a novel label free Ag⁺ sensor in aqueous solution based on silicon nanowire field effect transistor (FET) sensor and silver specific oligonucleotide (SSO). Cytosine-rich SSO which contains C-C mismatched base pairs can selective bind to Ag⁺ ions. C-Ag⁺-C will help to convert the single stranded oligonucleotide to duplex structure. This conformation change will introduce the charge density change on the silicon nanowire which can be detected through the field effect. The fabrication process of this high sensitive device is full CMOS compatible and the operational method is simple without any fluorescence label or complicated instrumentation.

ID: 294

D3: 2

Integration of mobile phone imaging with lateral flow assays for real-time quantitative detection of nucleic acids

Jie Hu^{1,2}, ShuQi Wang³, Lin Wang^{1,2}, Tian Jian Lu² and Feng Xu^{1,2}

¹The Key Laboratory of Biomedical Information Engineering of Ministry of Education, School of Life Science and Technology, Xi'an Jiaotong University, Xi'an, China; ²Bioinspired Engineering and Biomechanics Center, Xi'an Jiaotong University, Xi'an, China; ³Brigham and Women's Hospital, Harvard Medical School, Boston, USA.

Nucleic acids, as essential biomolecules encoding and regulating the expression of hereditary information, exist in all the living organisms, such as viruses, bacterium, parasites. The detection of nucleic acids thus promises accurate, sensitive and specific analysis of infectious diseases, food safety and environmental pollution. However, commercial technologies for nucleic acid detection, such as electrophoresis, spectrophotometry and real-time polymerase chain reaction (qPCR), are time-consuming, labor-intensive, or costly. Recently, lateral flow assays (LFAs) have been developed as a cost-effective platform for detection of nucleic acids. Although the specificity and sensitivity of LFAs can be assured through probe design, its accuracy of quantification remains a big challenge. Currently, two strategies have been developed to provide semi-quantitative or quantitative analyses for LFAs. One strategy is to employ a standard chart like pH indicator cards. However, this strategy is affected by different environment and end-users. The other strategy is to adopt a reader for colorimetric measurement. However, this strategy increases the cost and decreases the portability of LFAs. In this study, we modified conventional lateral flow test strips with dispensing multiple test lines to grade nucleic acid targets. The developed lateral flow test strips gave different amount of targets by different number of test lines. Further, we used a camera mobile phone for real-time record of the assay procedure in order to quantify the assay result in real time. The developed strategy for LFAs improved the accuracy of nucleic acid detection, which holds a great potential in rapid tests and telemedicine.

ID: 416

D3: 3

Pressure distribution measurement of close fitting clothes on human body

Jan Grep¹, Marek Penhaker², J Kubicek², J Prokop³ and L Peter²

¹VSB – Technical University Ostrava, Faculty of Mechanical Engineering, Department of Mechanics/IT4Innovations, Ostrava, Czech Republic; ²VSB – Technical University Ostrava, Faculty of Electrical Engineering and Computer Science, Department of Cybernetics and Biomedical Engineering, Ostrava, Czech Republic; ³Faculty Hospital, Clinic of Surgery, Ostrava, Czech Republic.

The article introduces research of noninvasive techniques used for measuring of pressure distribution on human skin by the wearing very tight and close fitting clothes. This fact may lead to significant health complications, because long-term constricting of tissue restricts fluid movement around tissue cells which may cause creation of tumors. Especially occurrence of tumor in the women breast is diagnosed with ascending tendency. From these reasons was performed research in the area of possible techniques for noninvasive measurement of forces and corresponding pressures on a human skin. Our goal in this part of research was in the idea, how is possible to measure pressure distribution between clothes and human skin. Through results comparison from different devices leded to evaluation of used techniques and to possibilities their potential upcoming application in the future experiments. Also we pointed on weaknesses and disadvantages of these techniques used for measurement.

ID: 251

D3: 4

In-vitro evaluation of flow modification by covered stents for treatment of intracranial aneurysms

Foad Kabinejadian and Hwa Liang Leo

National University of Singapore (NUS), Singapore.

Intracranial aneurysms cause a weakened arterial wall segment which can lead to initiation, growth, and eventually rupture of the aneurysm. Recently, there has been considerable interest in the use of stents as endovascular flow diverters for the treatment of intracranial aneurysms. We have recently designed and developed a novel covered stent for treatment of carotid artery bifurcation stenotic disease and prevention of late embolic stroke which is capable of preserving the side-branch flow. In this study, we evaluated the applicability of this novel carotid covered stent in the treatment of cerebral aneurysms by *in-vitro* investigation of different flow parameters. For this purpose, a clear silicon replica of

a cerebral aneurysm has been fabricated and the flow velocity field in the internal carotid artery and within the aneurysm has been measured under physiological flow conditions, utilizing particle image velocimetry (PIV) technique. Subsequently, the effects of this covered stent on the vorticity and inflow to the aneurysm have been investigated by deriving their quantitative values using the PIV measurement results. Furthermore, the mean, peak systolic, and pulse pressures within the aneurysm and the internal carotid artery have been measured both before and after the stent deployment to investigate the effects of the covered stent on the pressure. The results showed that this novel covered stent design is capable of providing desired conditions for the embolization of the aneurysm while preserving the side-branch flows.

ID: 128

D3: 5

Gene expression of diabetic fibroblast and normal fibroblast after irradiating with light emitting diode by using Microarray

Pongsathorn Chotikasemsri¹, Boonsin Tungtrakunwanit² and Surasak Sungkatat Naayutaya³

¹Institute of Biomedical Engineering, Faculty of Medicine, Prince of Songkhla University, Thailand; ²Department of Orthopedic, Faculty of Medicine, Prince of Songkhla University, Thailand; ³Department of Surgery, Faculty of Medicine, Prince of Songkhla University, Thailand.

Diabetes mellitus is a major cause of impaired tissue repair. Patients with this disease tend to have difficulty healing those wounds where the fibroblast cells reside. Simple wounds often become chronic and infectious wound. Unfortunately, the amputation rate for diabetics is much higher than for the non-diabetic population. Absorption of photons from LED by molecules leads to electronically excited states and consequently can lead to acceleration of electron transfer reactions at cytochrome c oxidase molecule. Cytochrome C oxidase is an important component of electron transport chain in cellular respiration which is directly related to ATP production. The more electron transport reaction increase, the more increased ATP production. However, no one have understood how the whole genome respond to the LED light in a particular amount of energy. Therefore, this research is trying to reveal some amazing benefits of using LED light to treat Diabetic wounds. We found that at a particular amount of LED light energy, which had irradiated to the cells, can provide a better healing response in specific purposes. For example, if a diabetic wound shows a sign of infection, 2 watts of LED light will be daily administered for four days. Then, all infamatory genes will dramatically express which

can facilitate wound healing process. if a diabetic wound shows a sign of Ischemic, 1 watts of LED light will be daily administered for only two days. Then, all vascular growth factors and angiogenesis genes will suddenly soar which help more oxygen flow to the wound area. Therefore, these results can provide a new approach for diabetic wound healing treatment in details that directly reflect to the cellular response in gene level.

ID: 792

D3: 6

Carbon nanotubes as a cradle of impulse for implantable medical devices

Fredrick Johnson Joseph¹, Karthick Madheswaran¹, Gopu Govindasamy¹ and Sathiesh Kumar²

¹Department of Biomedical Engineering Sri Ramakrishna Engineering College, Coimbatore TamilNadu India; ²Department of Nanotechnology Sri Ramakrishna Engineering College Coimbatore , Tamil Nadu India.

The Most thought-provoking part of Nano Technology is using the CNT (Carbon Nano Tubes) as a cradle for converting Fluid Dynamic Energy (FDE) into Electrical Energy (EE).The ability of the CNT to entertain as a semiconductor or a metal impressively depends on the diameter on which it is rolled and its chirality. The flow of a liquid on CNT bundle induces a voltage in the sample along the direction of flow which is a very novel effect. The Columbic interaction between the ions in the liquid and the charge carriers in the nanotube plays a key role in electrical generation that obeys the Bernoulli's principle and Seeback effect. The magnitude of Voltage depends significantly on the Ionic strength of the flowing liquid. The Expected Potential Drop will be a minimum of 30mv to 60mv.The flow induced current on the surface of CNT thin films are prominently dependent on the angular velocity, concentration, properties and temperature of the liquid. The CNTs will be fabricated on Si (Silicon) substrate by Chemical Vapor Deposition (CVD). The CNT are placed in an Fabricated Substrate surrounded by the insulating material. The Electrodes on the either side of CNT picks up the Electrical Drift in the custom of Potential gradient. CNT on Interaction with Bio Fluids generates a Potential which can be amplified and Transmitted through the Nanowires that would serve for driving the Implantable Medical Devices. Biocompatibility, environmental impacts and other Biological Factors of CNT in the Human Body is to be studied by the results of implementation into the Animals and from further research; this New Technology can be deliberated as one of the most fascinating invention. Consequently this approach

overlooks the Patient Hiking to the Operation Theatre (OT) Intermittently.

ID: 701

D3: 7

Quantification and improvement of the adhesion of electrical surgical units

Shen-Han Chen

National Cheng Kung University, Taiwan.

Electrical surgical unit (ESU) becomes more popular in regular surgery and minimally invasive surgery (MIS) to diathermy. Yet, during tissue removal, the formation of tissue adhesion on the tips and smoke remains a major problem during MIS.

This study tries to build an *ex vivo* tissue adhesion evaluation system of ESU based on the adhesion volume, adhesion strength and weight and histology.

In this study, four types of monopolar electrical surgical unit materials including commercial stainless steel (SS) (Control), polished SS, polytetrafluoroethylene (PTFE) coated SS and polyethylene glycol (PEG) coated polished SS were investigated. Pork liver was used as tissue for cauterization. The blade was linked to the Valley lab™ ESU and the operating mode was set at “pure cutting” with power at 40 watts. Four different diathermy times (the contact duration of blade and tissue) of 0.5s, 1s, 2s and 4s were investigated. Each blade was connected to Instron™ materials testing system and given an entire cyclic stroke 10 mm beneath the liver surface. The force was recorded for each test, and after every five tests, then the tip of each blade was put on a balance to measure the adhesion weights. The damage was recorded by a digital camera and was quantitated by the software Image J. Single liver was tested by 4 blades 5 times and each blade was tested on 6 livers for each cauterizing time.

The tip modified with PEG shows significant less contact angle comparing to all other 3 types of tips. The corresponding maximum volume of damage was about 143.34 mm³ (PTFE) and adhesion weights were assessed at around 20.27 mg (PEG). No significant difference in adhesion weight and damaged volume. The maximum adhesion force was occurred at 1 second cauterization, and PEG tip has the smallest adhesion force followed by polished, PTFE and regular SS tip. It is interesting to find the adhesion strengths for 2 and 4 seconds cauterization were less than those for 0.5 and 1 seconds.

This novel *ex vivo* model allows standardized, objective and quantitative assessment of tissue-ESU-induced adhesion effects and damage in porcine liver tissue.

Session	C9: Cardiovascular Mechanics
Date/Time	6 December 2013 15:30–17:00 hrs
Venue	Auditorium

ID: 289

C9: 1

Effects of coronary stenosis on three-dimensional coronary blood flow: implication for revascularization selection

Jun-Mei Zhang¹, Jinq Shya Yap², Jasmine P. L. Tham², Yunlong Huo³, Min Wan¹, Ru San Tan^{1,4} and Liang Zhong^{1,4}

¹National Heart Center Singapore, Singapore; ²SIM University, Singapore; ³Peking University, China; ⁴Duke-NUS Graduate Medical School Singapore, Singapore.

Background and Objectives: Coronary artery disease (CAD) is the most common cardiovascular disease, which is caused by the build-up of plaques on the endothelial walls. In clinical practice, the anatomic and functional significance of coronary stenoses is evaluated by diameter stenosis and fractional flow reserve (FFR) separately. The decision to perform revascularization is based on the latter (i.e., FFR≤0.80). In addition to diameter stenosis, the severity of coronary stenosis may also depend on the Venue and length of the stenosis. This study aims to study the effect of diameter stenosis, stenosis length and Venue (proximal to distal) on FFR.

Methods: A porcine left anterior descending (LAD) model reconstructed from computed tomography angiography (CTA) was studied as the baseline model. With ANSYS workbench 13.0, a series of models were created by adding an idealized stenosis (with diameter stenosis from 45% to 75%, stenosis length from 5mm to 20mm and at 4 Venues separately). With a total of around 0.5 million cells and resistance outflow boundary conditions, blood flow and pressure distributions were computed with FLUENT.

Results: For the baseline model, FFR is close to 1 at 0.96 due to negligible viscous force. For the model with stenosis, FFR decreased: a) from 0.94 to 0.65 with increase of diameter stenosis from 45% to 75% (at a fixed stenosis length of 4mm); c) from 0.94 to 0.65 with the change of stenosis Venue from distal to proximal segments of the LAD (at fixed diameter stenosis of 75% and stenosis length of 4mm); c) from 0.82 to 0.80 with increase of stenosis length from 5mm to 20mm (at a fixed diameter stenosis of 60%).

Conclusion: Diameter stenosis and stenotic Venue change the pressure drop more than the stenosis length. For a coronary lesion located proximally with diameter stenosis more than 65%, revascularization is recommended.

ID: 402

C9: 2

Design optimization of thoracic endovascular stent graft (EVSG)

Kiruthiga Shanmuga Sundaram¹, Johanna Rajan¹,
Suvi Selvam¹, Mohan Thanikachalam^{1,3}, N. Viswanatha² and
R. K. Ramanathan¹

¹Agada Medical Technologies, Chennai, India; ²Tata Consultancy Services, Bangalore, India; ³Tufts University School of Medicine, USA.

Aim: EVSG, a tube composed of biocompatible fabric supported by a stent, is inserted percutaneously using a catheter to treat thoracic aortic aneurysm. The aim of study was to improve the mechanical performance of EVSG by design optimization using Finite Element Analysis (FEA).

Methods: A 36 mm tubular device composed of ePTFE (Elastic modulus = 45Mpa, and Poisson's ratio = 0.49) and supported by nitinol rings (Elastic modulus = 27Gpa, and Poisson's ratio = 0.3, maximum super elastic strain = 0.08) was modeled. The parameters used to define the EVSG geometry included the number of struts, height, thickness and spacing of the nitinol rings and the thickness of the ePTFE. The analysis was performed using ANSYS 12.0. The determination of radial force was done by compressing the stent radially to 9 mm and measuring the hoop forces at different diameters during re-expansion. The load that initiates longitudinal buckling and crippling was determined through Eigen Buckling Analysis. The durability of the EVSG was evaluated by simulating 400 million cycles of minimum (50 mmHg) and the maximum (150 mmHg) blood pressure loading.

Results: Based on the analysis of various nitinol ring configurations, a ring with thickness of 0.35mm, 8 struts and 7.5mm height provided for adequate radial force of 0.9N and 1.75N when deployed in 34mm and 32mm arteries, respectively. The graft thickness, when compared to the spacing of the rings, was the major determinant of the buckling load. A 0.25mm ePTFE with 10 mm spacing between the rings provided for adequate buckling strength and tolerated 200mmHg blood pressure load. The 36 mm tubular ePTFE graft supported by nitinol rings demonstrated adequate durability at 400 million cycles.

Conclusion: Thoracic EVSG with optimal properties could be designed and validated using FEA. Further *in-vitro* testing and animal trials would help validate this analytical study.

ID: 617

C9: 3

A study of mechanical behavior of an encapsulated stent design using finite element analysis

Kiruthiga Shanmuga Sundaram¹, Davidson Jabaseelan²,
Rinse Jose², Ranjitha Rebecca Jeevan¹,
Mohan Thanikachalam^{1,5}, George Joseph³ and
Santhosh Joseph⁴

¹Agada Medical Technologies, Chennai, India; ²VIT University, Chennai Campus, Chennai, India; ³Dept of Cardiology, Christian Medical College & Hospital, Vellore, India; ⁴Dept of Radiology, Sri Ramachandra Medical College, Chennai, India; ⁵Tufts University School of Medicine, Boston, USA.

Aim: Peripheral vasculature of the human body includes the blood vessels that supply the extremities and the major vessels that supply the brain. Major peripheral vascular pathologies that affect the peripheral vasculature are arterial occlusive disease or stenosis (vessel narrowing), aneurysms (vessel enlargement) and various types of trauma. The aim of this study was to develop a peripheral vascular endovascular stent-graft for the treatment of various pathologies that affect peripheral vasculature, in particular, femeropopliteal arterial disease. The stent graft is composed of a nitinol framework covered by a polymeric tube.

Methods: The present work explores an innovative device design which includes separate nitinol rings encased between layers of ePTFE. The vessel remodeling is studied by considering various vessel diameters and the efficacy of the device is studied by varying the nitinol wire diameter (0.1 to 0.25mm), the number of struts in the ring (6 to 10) and the height of the struts (1 and 2mm). Finite element studies were done to understand the best design for the changing vessel morphology by studying the crimping pattern and the radial stiffness of a single ring. A single ring is modeled as an axisymmetry FE-3D model. An 8-node hexahedral element SOLID185 was used for this study. The nodes of the symmetric model were constrained and the radial displacement was given to the model. The boundary conditions were the same for crimping and deployment.

Results: The results of the FEA analyses show 1 mm height ring with 0.15mm thickness and 8 struts combination provides the ideal crimped profile of 1.7mm and radial force of 0.996N/mm when deployed in a 6mm vessel diameter.

Conclusion: The finite element analysis results show that the radial force and crimping analysis perform a vital role in determining the device design and geometry.

ID: 428

C9: 4

Comparison of hemodynamic parameters and wall condition of cerebral aneurysm

Daichi Suzuki, [Kenichi Funamoto](#), Shin-ichiro Sugiyama, Toshio Nakayama, Teiji Tominaga and Toshiyuki Hayase

Tohoku University, Japan.

A major cause of subarachnoid hemorrhage, a type of stroke, is the rupture of a cerebral aneurysm. The initiation, growth and rupture of a cerebral aneurysm have been revealed to be related to hemodynamics in cellular and animal experiments and by computational fluid dynamics. However, the detailed mechanisms underlying the pathologic events are not completely understood and there are two conflicting hypotheses: an aneurysmal rupture is triggered by physical stimuli of high or by low wall shear stresses (WSS). During surgery, it is observed that cerebral aneurysms have either or both reddish thin walls and yellowish white thickened walls. The thicken wall of the aneurysm is unlikely to rupture, while the thin wall is at high risk of rupture. Clarification of the relationship between hemodynamics and the wall conditions of aneurysms would facilitate evaluation of the risk of cerebral aneurysm ruptures with reference to hemodynamic information obtained by blood flow simulation. In this study, hemodynamic parameters related to the thinning and thickening of the cerebral aneurysmal wall were investigated by blood flow simulations in three cerebral aneurysms. Three-dimensional blood vessel configurations of the cerebral aneurysms were reconstructed with MRI slice images, and unsteady blood flow simulations were performed by applying patient-specific pulsatile blood flow rates. Hemodynamic parameters were then calculated and evaluated in comparison with clinical images of cerebral aneurysms to investigate the effect of hemodynamics on the rupture and stabilization of the cerebral aneurysm. As a result, at the sites of thickening walls, the time-averaged WSS was small and the relative residence time (RRT), an indicator of blood retention, was relatively high. In contrast, the opposite tendency was observed at the sites of thinning walls. The finding in the present study should be verified by more cases of blood flow simulation and clinical observation of cerebral aneurysms.

ID: 695

C9: 5

Fatigue life enhancement of peripheral stents by an intriguing design concept

Ming-Ting Yin, [Ling-Hsiang Chao](#), Li-Wei Wu, Hsiao-Nan Yang, Yu-Huan Lin and Hao-Ming Hsiao

National Taiwan University, Taiwan.

Intravascular stenting has emerged as the primary treatment for intravascular diseases and has received great attention from the medical society since its introduction two decades ago. The endovascular self-expanding stent is used to treat peripheral artery diseases; however, once implanted, these peripheral stents suffer from various cyclic motions caused by pulsatile blood pressure and daily body activities. Due to this challenging environment, stent fatigue performance has become a critical issue for stent design. In current industrial practice, the stent fatigue resistance could be improved by several design options. Two of the most commonly-used tactics are crown enlargement and strut lengthening. With these two approaches, high stresses/strains near the crown can be alleviated to allow a better survival rate to fatigue failure, but with significant prices to pay. Crown enlargement increases the overall stent profile and strut lengthening reduces the stent scaffolding capability; however, both stent profile and scaffolding are important clinical attributes and cannot be easily compromised. Therefore, it is necessary to find design alternatives to resolve this trade-off dilemma. In this paper, a simple yet novel concept of stent design aimed at enhancing stent fatigue life is proposed. The concept of this design is to shift the highly concentrated stresses/strains away from the crown and re-distribute them along the stress-free bar arm by varying its strut width. Finite element models were developed to evaluate the mechanical integrity and fatigue resistance of the stent to various loading conditions consistent with the current practice. Simulation results show that the fatigue safety factor jumped to almost 2.5 times that of the counterpart stent with constant strut width. This is astonishing considering that the stent profile and scaffolding were not compromised. The findings of this paper provide an excellent approach to the optimization of future stent design to greatly improve stent fatigue performance.

ID: 668

C9: 6

Improvement of a shape memory alloy fibered aortic pulsation device

Mohamed Omran Hashem¹, Yasuyuki Shiraishi², Akahiro Yamada³, Y. Tsuboko⁴, Hidekazu Muira⁵, Tomoyuki Yambe⁶ and D. Homma⁷

¹Department of Medical Engineering and Cardiology, Graduate School of Medicine, Tohoku University, Japan; ²Department of Medical Engineering and Cardiology, Tohoku University, Japan; ³Department of Medical Engineering and Cardiology, Graduate School of Biomedical Engineering, Tohoku University, Japan; ⁴Department of Medical Engineering and Cardiology, Graduate School of Biomedical Engineering, Tohoku University, Japan; ⁵Department of Medical Engineering and Cardiology, Tohoku University, Japan; ⁶Department of Medical Engineering and Cardiology, Tohoku University, Japan; ⁷Toki Corporations, Tokyo, Japan.

Aim: We have been developing a new aortic blood flow support device using shape memory alloy (SMA) fibers as an actuator. The special features of the device were as follows: a) totally implantable design, b) small and foldable structure with actuators. The system could represent similar function of the aortomyoplasty and the extra aortic balloon pump at the ascending or descending installation. The purpose of this study was to improve the device as a non-blood contacting pulsation system, aiming at the application for the physiologically effective assistance in the artery.

Material & Methods: We have designed the prototype by using covalent-type Ni-Ti SMA fibers which is capable of contracting around the aorta circumferentially. In this study, we developed a new structural design with oblique fiber orientations. The device consisted of rubber silicone wall plates, serially connected for radial contraction by the SMA fibers. We reduced the diameter of the contraction by the device. Then we tested the new structural design in the mock system, and examined its functional changes to optimize the mechanical structural design with SMA fibers. We demonstrated the radial deformation effect by using 150 micron Ni-Ti SMA fibers in a multiple circumferential oblique patterns. The orientation and length of the fibers were evaluated by the changes in oblique angles against the longitudinal axis. The fibers were secured circumferentially by using a pair of plastic grooved chambers, where the changes and contractile function was examined for each fiber.

Result: We could sandwich the aortic tubing of which the diameter was smaller than 30mm, under the constant pressure condition of the aortic tubing at 100mmHg.

Conclusion: We successfully achieved the improvement of the contraction effects of the SMA fibered device for aortic compression for smaller diameter vessels by the circumferential alignment by oblique angle of fibers.

Session	A9: Biosignal Processing
Date/Time	6 December 2013 15:30–17:00 hrs
Venue	SR-01 & 02

ID: 738

A9: 1

Diagnosis of schizophrenia patients based on brain network complexity analysis of resting-state fMRI

Tsung-Hao Hsieh, Ming-Jian Sun and Sheng-Fu Liang
National Cheng Kung University, Taiwan.

Schizophrenia is a chronic, severe, and disabling brain disorder, about 1% of Americans have this illness. It typically occurred in young adulthood (15–45 year). Generally, schizophrenia patients usually could not identify reality and hallucination and it would make social and occupational dysfunctions. Until now, diagnosis of schizophrenia is based on observed behavior and the patient's reported experiences (Diagnostic and Statistical Manual of Mental Disorders, DSM-V). The aim of this study is to evaluate the feasibility of classifying schizophrenia and healthy people by analyzing physiological information. In this paper, resting-state fMRI data from 69 schizophrenia patients and 72 healthy people were studied. Comparing to task-related fMRI, patients are not required to perform any task during the resting-state fMRI experiment so that it reduces the difficulty of data collection. We estimated the correlation matrix of 116 regions of interesting (ROI) from automated anatomical labeling (AAL). Then the resultant correlation matrix is converted to the binary graph. The network complexity analysis is applied to the binary graph by estimating the largest connected components (LCC) and their coordinate information to differentiate abnormal brain regions of patients from normal brains of healthy people. Finally, the extract features were fed to the linear SVM for classification. Accuracy of the proposed method can reach 71.63% through leave-one-out cross validation. Experimental results demonstrate the feasibility of schizophrenia diagnosis based on the brain network complexity of the resting-state fMRI.

ID: 790

A9: 2

Automated localization of seizure focus using interictal intracranial EEG

Jin Jing¹, Justin Dauwels¹ and Sydney Cash²

¹Nanyang Technological University, School of Electrical and Electronic Engineering, Singapore; ²Massachusetts General Hospital and Harvard Medical School, USA.

For approximately 30% of epilepsy patients, seizures are poorly controlled with medications alone. Those patients may be successfully treated by surgically removing the brain area(s) where the seizures originate. It is crucial to accurately localize the seizure foci, which often resorts to semi-chronic invasive recordings of cortical activity, as non-invasive methods are frequently inconclusive. Neurologists rely heavily on seizures to determine the foci. The invasive recordings usually continue for days or weeks until enough seizures are captured, as seizures are infrequent in nature. The procedure is costly, uncomfortable, and risky of side effects.

Our long-term objective is to drastically shorten the hospitalization of epilepsy patients, from weeks to a few days: We hope to localize the seizure foci from short invasive recordings made in the operating room, before the resection surgery. The goal of the proposed project is to explore the feasibility of this idea, building upon our promising preliminary results. Our hypothesis is that, even at rest, the seizure focus is characterized by seizure measures such as interictal spikes, high frequency oscillations (HFOs), slowing and synchrony. Our novelty is to exploit combinations of all measures in a machine-learning framework to localize the seizure foci. We have proposed methods for detecting spikes and HFOs respectively. We have applied signal processing techniques to invasive semi-chronic recordings between seizures, in order to extract signatures of the seizure foci. We have designed statistical decision algorithms that leverage those signatures to determine the seizure foci in an automated fashion. In future work, we will apply those algorithms to short invasive recordings made in the operating room.

The proposed procedure may have enormous impact on clinical practice of epilepsy, and would substantially reduce treatment costs. Moreover, our novel automated approach to medical decision making is not only relevant for neurosurgery but many other medical disciplines.

ID: 826

A9: 3

Design and evaluation of a hardware-accelerator for energy efficient inertial sensor fusion on heterogeneous SoC architectures

Hans-Peter Brückner, Christian Spindeldreier and Holger Blume
Leibniz Universität Hannover, Germany.

Real-time orientation estimation based on mobile, low-power hardware platforms requires customized processor cores or dedicated hardware accelerators to achieve the throughput requirements demanded by applications like monitoring training sessions in sports or medical rehabilitation. In this paper, instruction-set extensions for a basic ASIP core and a dedicated hardware accelerator for sensor fusion of inertial measurement unit RAW data are presented. The results show the minimization of the execution time due to the instruction-set extensions and the dedicated hardware accelerator. The use of an optimized ASIP increases the throughput up to a factor of 1.7. Compared to the base core, the hardware accelerator achieves an increase by a factor of 2.5. Utilizing the hardware accelerator increases energy efficiency by a factor of 17.0.

ID: 633

A9: 4

Liver vessel segmentation using graph cuts with quick shift initialization

Bichao Chen, Ying Sun and Sim Heng Ong

National University of Singapore, Singapore.

Accurate liver vasculature segmentation can provide guidance for doctors to do surgical planning for liver tumor resection. Due to the low contrast level between small vessels boundary and background tissues, complete extraction of liver vessel structures has become a challenging task. In this paper, we propose a method to achieve small vessel extraction by an iterative regional updating process. The gradient vector flow field is first calculated. The vector field has large magnitudes around vessel boundaries with the vectors pointing towards the center of the vessel. By calculating the divergence of the vector field, vessel structures can be identified as the vector field's sinks. Quick shift clustering is then applied to group image voxels with similar intensities into patches. The divergence feature is combined with the clustering result to obtain seed regions that are parts of vessel structures. Next, the seed regions are used as initialization of the graph cuts segmentation. In order to perform segmentation using local intensity information to deal with intensity inhomogeneity, quick shift clustering is applied a second time to group spatially neighboring voxels into local regions. Graph

cuts is then applied based on regional intensity distribution. The final result is obtained by iteratively performing regional graph cuts until the change between consecutive binary masks drops below a threshold. The proposed method is compared with global graph cuts, demonstrating the capability of segmenting the complete vessel network. The comparison with manual segmentation shows that the proposed method can also extract small vessel structures that are not available in the manual result.

ID: 418

A9: 5

Strategies for baseline drift compensation of DC-coupled electrooculogram measurements for human-computer-interfaces

Anna Böhm, Axel Uhlig and Steffen Leonhardt

RWTH Aachen University, Germany.

Human computer interfaces (HCI) can be created with electrooculograms (EOG). By analysis of an acquired vertical and horizontal EOG, mouse interaction on a computer is controlled. We used a measurement setup with four EOG channels for vertical and horizontal EOG with a DC-coupled amplifier. One of the biggest challenges for such EOG-controlled HCI systems is baseline drift.

ID: 412

A9: 6

Assigning myocardial fibre orientation to a computational biventricular human heart model

Arnab Palit¹, Glen A. Turley¹, Sunil K. Bhudia², Richard Wellings² and Mark A. Williams¹

¹WMG, The University of Warwick, United Kingdom; ²University Hospitals Coventry and Warwickshire, United Kingdom.

Finite element based surgical simulation has the potential to be used as a surgical planning tool for the repairing of ventricular aneurysm, a substantial cause for heart failure. However, in order to be effective, this simulation requires the geometrical accuracy of the ventricle. In addition, fibre orientation is indispensable to define heart muscle's material anisotropy but creation of a smooth fibre map for biomechanical analysis is still a challenge. In this paper, an innovative procedure has been developed to create 3D geometry in order to minimise the error occurs in the volume assessment of ventricle due to the large slice thickness of cardiac magnetic resonance imaging. Also, the procedure is used to investigate the effect of increasing slice thickness of the image data on the accuracy of the created 3D geometry. Furthermore, a novel Laplace-Dirichlet-Region growing-Finite element based algorithm has

been developed to create a fibre map based on the histological data. This algorithm is capable of generating smooth fibre orientations quickly, efficiently and robustly on the created 3D geometry. Thereafter, the fibre map can be imported easily to any finite element solver to define material anisotropy to simulate surgical treatments.

Session	B9: Biological Materials Diagnostics and Therapeutic
Date/Time	6 December 2013 15:30–17:00 hrs
Venue	SR-03 & 04

ID: 863

B9: 1

Heart tissue engineering using ex vivo dynamically vascularized porcine cardiac ECM: does thickness matter?

Udi Sarig¹, Hadar Sarig¹, Evelyne Nguyen^{1,2}, Wang Yao^{1,2}, Gigi A. Y. C. Ting^{1,2}, Tomer Bronshtein², Michael Buering³, Thomas Scheper³, Freddy Yin Chiang Boey¹, Subbu S. Venkatraman¹ and Marcelle Machluf^{1,2}

¹School of Material Science Engineering (MSE), Nanyang Technological University (NTU), Singapore; ²Faculty of Biotechnology and Food Engineering, Technion, Israel Institute of Technology (IIT), Israel; ³Institute of Technical Chemistry, Leibniz University of Hanover, Hanover, Germany.

Functional vascularization is a requisite to cardiac tissue engineering of physiological thicknesses. We previously isolated thin and thick porcine cardiac extracellular matrix (pcECM) with myocardial matched bio-mechanical properties. The thick pcECM retained its main vascular conduits, hypothesized to provide possible support for thick construct tissue engineering. Here we tested this hypothesis using a custom designed bioreactor system.

Decellularized thick (~15mm) pcECM scaffolds were mounted on a custom made bioreactor system. To evaluate cell support under static and dynamic cultures, human mesenchymal stem cells (hMSCs) and human umbilical vein endothelial cells (HUVEC) were reseeded and co-cultured within bulk pcECM scaffold cavities and the inherent vasculature, respectively. Cell growth and morphological localization were monitored through time. Functional vascularization of 1.6 mm thick constructs was observed, whereby newly formed blood vessel structures, in various maturation stages, were sprouting from re-endothelialized conduits. This is to our best knowledge the first time such a completely *in vitro* system was able to mature and functionally support relatively thick constructs which may have clinical applicability. In addition, we will also present a robust methodology recently developed in our lab to assess

the pcECM cell capacity, resembling physiological densities, which may also benefit rapid biological characterization of other biomaterials.

ID: 419

B9: 2

Acoustic droplet vaporization for gas embolotherapy

Joseph Lee Bull, David S. Li, Oliver D. Kripfgans and J. Brian Fowlkes

University of Michigan, United States of America.

We are currently developing gas embolotherapy as a potential method of treating cancer by occlusion of blood flow to the tumor via selectively formed gas bubbles, with or without drug delivery. The droplet originate from encapsulated liquid dodecafluoropentane (DDFP, C₅F₁₂) microdroplets that may be injected intravenously and circulate until activated by ultrasound. The DDFP is maintained in droplets via an albumin or lipid shell despite its boiling point of 29°C at atmospheric pressure being lower than body temperature. Acoustic droplet vaporization (ADV) is the process in which super-heated liquid microdroplets are selectively vaporized using focused ultrasound generating larger gas bubbles. In other recent studies, we have shown that ADV can induce bioeffects in endothelial cells and bioeffects resulting from ADV can lead to extravasation, suggesting potential for drug delivery to surrounding tissue. Previously, the mechanism underlying the onset of ADV has not been elucidated. The onset of the ADV process with nucleation site formation was imaged at sub-microsecond time resolution using an ultra-high speed camera. In this process, the vaporization begins from a nucleation site, and bubble(s) within the droplet vaporize, consuming the liquid DDFP while the droplet/bubble expands. A computational model was used to model the acoustic field within and surrounding DDFP microdroplet. The Venue of the initial nucleation site was observed to be dependent on droplet diameter. Comparison of experimental and computational results elucidated the role of acoustic refocusing inside the droplet in the initiation of ADV.

This research has been funded by NIH grant R01EB006476.

ID: 803

B9: 3

Evaluation of a hybrid bioartificial liver support system using CL-L cells in cynomolgus monkey models with D-galactosamine induced acute liver failure

Yi Gao^{1,2}, Zhi Zhang¹, Ming-Xin Pan¹, Yuan Cheng¹ and Yan Wang^{1,2}

¹Department of Hepatobiliary Surgery, Southern Medical University Zhujiang Hospital, China; ²Institute of Regenerative Medicine, Southern Medical University Zhujiang Hospital, China.

Acute liver failure (ALF) is a critical clinical condition, featured with intensive, rapid progress and ominous prognosis. To evaluate the safety and efficacy of a Hybrid Bioartificial Liver Support System (HBALSS) in primate model of ALF to assess its feasibility for future clinical application, an ALF model was established with 0.3g/kg of D-galactosamine (D-gal) in Cynomolgus monkeys; CL-1 cells, a human hepatic cell line, were loaded into a perfusion bioreactor to carry out HBALSS treatment. Forty-eight hours after D-gal injection, Cynomolgus monkeys in treatment group received HBALSS supportive care, while the ones in control ALF group did not. Clinical manifestations, survival time, liver and kidney functions, and serum biochemical changes were recorded of all animals. On-line detection of the cell number, viability and function of CL-1 in HBALSS were also performed. It was found that serum biochemical levels in monkey models were significantly increased at 48 hours after injection of D-gal ($P < 0.05$), while albumin levels and Fischer index were reduced. The serum biochemical levels was significantly different between HBALSS treatment and control groups ($P < 0.05$). In the HBALSS treatment group, five Cynomolgus monkeys survived, and the remaining five died; the duration of survival was 128 ± 3 h. In control group, all animals died; the survival duration was 112 ± 2 h. Cell number, viability and function of CL-1 maintained at a relatively high level during the treatment. In conclusion, Cynomolgus monkey model of ALF was successfully established in our study; the present HBALSS could significantly reduce serum biochemical level and extend survival time in the primate model, which indicates its therapeutic potential for ALF.

ID: 822

B9: 4

Probing biochemical and mechanical crosstalk between EhpA2 and integrin signalling in breast cancer cells using hybrid fluid lipid bilayers and immobilized RGD patterns

Zhongwen Chen¹, Cheng-Han Yu¹, Kabir H Biswas¹, Ronen Zaidel-Bar¹ and Jay T. Groves^{1,2,3}

¹Mechanobiology Institute, Singapore; ²Howard Hughes Medical Institute; ³Department of Chemistry, UC Berkeley.

During normal development and in disease, cells undergo both cell-cell and cell-matrix interactions continuously to affect tissue behaviours, including organogenesis, cell migration and/or tumor invasions. While myriad studies have been done to address either cell-cell or cell-matrix interactions, few have combined them to investigate their integrated effect *in vitro*, largely because of the limitations in presenting cells with the proper environment.

EphA2, for example, which binds ephrin-A1 on an apposed cell membrane, is overexpressed in over 40% of all breast cancers. Supported lipid bilayers provide a useful way to study EphrinA1-EphA2 clustering and lateral movement, which gives insight into tumor metastasis. However, how EphA2 receptors will react in a more physiological condition, for example, in the context of integrin adhesions is still unknown.

Here, we developed a subcellular hybrid pattern of fluid lipid bilayers and immobilized RGD to simultaneously mimic both cell membrane and extracellular matrix environments. The scale and shape of the patterns is tuneable with photomasks, and can be made as low as 2 μm -wide stripes or 2 μm -diameter circles. EphrinA1 was conjugated onto lipid bilayers specifically through metal chelating. Fluorescence recovery after photobleaching showed that the lateral diffusion of EphrinA1 was not affected by the presence of RGD patterns. Live cell experiments revealed that cells can form focal adhesions on these patterns as well as EphrinA1-EphA2 complexes. In all, this hybrid pattern provides a promising method to study cell-cell and cell-matrix signaling crosstalk.

ID: 290

B9: 5

Hyperelastic constitutive relationship for the strain-rate dependent behavior of shoulder and other joint cartilages

Noyel Deegayu Thibbotuwawa, Adekunle Oloyede, Wijitha Senadeera and Yuan Tong Gu

Queensland University of Technology, Australia.

Non-linear finite deformations of articular cartilages under physiological loading conditions can be

attributed to hyperelastic behavior. This paper contains experimental results of indentation tests in finite deformation and proposes an empirical based new generalized hyperelastic constitutive model to account for strain-rate dependency for humeral head cartilage tissues. The generalized model is based on existing hyperelastic constitutive relationships that are extensively used to represent biological tissues in biomechanical literature. The experimental results were obtained for three loading velocities, corresponding to low ($1 \times 10^{-3} \text{ s}^{-1}$), moderate and high strain-rates ($1 \times 10^{-1} \text{ s}^{-1}$), which represent physiological loading rates that are experienced in daily activities such as lifting, holding objects and sporting activities. Hyperelastic material parameters were identified by non-linear curve fitting procedure. Analysis demonstrated that the material behavior of cartilage can be effectively decoupled into strain-rate independent (elastic) and dependent parts. Further, experiments conducted using different indenters indicated that the parameters obtained are significantly affected by the indenter size, potentially due to structural inhomogeneity of the tissue. The hyperelastic constitutive model developed in this paper opens a new avenue for the exploration of material properties of cartilage tissues.

ID: 579

B9: 6

Biopiezoelectric, bioferroelectric and subnanoscale-mechanical properties of calcified tissues

Tao Li and Kaiyang Zeng

National University of Singapore, Singapore.

Calcified tissues, mainly including mollusk shell, teeth, and bone, play important roles in living systems, for instance, protection and mechanical support. To develop new synthetic materials or to understand tissue behaviors, it is necessary to have comprehensive studies of tissue properties and their working mechanisms.

In this presentation, the studies on biopiezoelectricity and bioferroelectricity of calcified tissues will be presented. These properties are now believed as one of the important reasons for proper functioning of biological systems, for instance, cell movement and proliferation, neuron signal transmission, and enzyme production. For calcified tissues, these properties may also contribute to their superior mechanical properties and self-healing behaviors. To characterize these properties, Piezoresponse Force Microscopy (PFM) and Switching Spectroscopy-PFM (SS-PFM), which are the sub-modes of SPM techniques particularly for electromechanical coupling studies, is used as the primary characterization tool.

In addition, the sub-nanoscale elastic modulus and loss tangent mappings of calcified tissues will also be presented. All of the mappings are observed by the Contact Resonance-Force Microscopy, which is an advanced non-destructive SPM technique to quantify elastic modulus on the true nanoscale.

Session	C10: Mechanobiology
Date/Time	6 December 2013 15:30–17:00 hrs
Venue	SR-05 & 06

ID: 212 **C10: 1**

On the roles of actin stress fibers on the mechanical regulation of nucleus in adherent cells

Kazuaki Nagayama, Yuki Yahiro, Sho Yamazaki, Mitsuhiro Ukiki and Takeo Matsumoto

Nagoya Institute of Technology, Japan.

Actin stress fibers (SFs) play important roles in cellular mechanotransduction and regulation of various cellular functions. SFs generate internal tension and contribute to physical interactions between cells and extracellular matrices. It has been suggested that cytoskeletons have the potential to interact with the nuclei via nuclear membrane proteins. However, it remains unclear at this stage whether SFs are involved in a mechanical interaction with the nucleus, and their internal forces are transmitted directly to the nucleus and influence the intranuclear DNA.

Here we investigated the roles of SFs on the mechanical regulation of the nucleus in adherent vascular smooth muscle cells (SMCs) using a laboratory-made UV laser nanoscissor. We cut an apical SF over the nucleus at a point adjacent to the nucleus by the laser to release its pretension, and observed their movement and deformation. SFs shortened immediately after dissection. Nuclei also moved and showed marked local deformation. The displacement direction of the nucleus had a strong positive correlation with the direction of the SF shortening. These results indicate that SFs over the nucleus stabilize the position of the nucleus, and that the internal tension of SFs significantly affects nuclear movement. A line-like concentration of intranuclear DNA along SFs was often observed near the upper surface of the nucleus. These line-like structures of DNA disappeared and changed markedly following the dissection and shortening of SFs. Interestingly, the dissected SFs reorganized near their original Venue in several tens of minutes following SF dissection in some cases. Intranuclear DNA also aggregated along the reorganized SFs and aligned in the direction of the fibers. These dynamic

realignments of DNA along the reorganized SFs may be due to interactions between SFs and perinuclear DNA. This interaction may play a role in the stabilization and positional memory of DNA in the nucleus.

ID: 209 **C10: 2**

Endothelial cells respond to shear stress by decreasing the lipid order of their plasma membranes

Kimiko Yamamoto¹ and Joji Ando²

¹The University of Tokyo, Japan; ²Dokkyo Medical University.

Endothelial cells (ECs) sense shear stress and transduce blood flow information into functional responses that play important roles in vascular homeostasis and pathophysiology. A unique feature of shear-stress-sensing is the involvement of many different types of membrane-bound molecules, including receptors, ion channels, and adhesion proteins, but the mechanisms remain unknown. Because cell membrane properties affect the activities of membrane-bound proteins, shear stress may activate various membrane-bound molecules by altering the physical properties of EC membranes. To determine how shear stress influences the cell membrane, cultured ECs were exposed to shear stress and examined for changes in membrane lipid order and fluidity by Laurdan two-photon imaging and FRAP measurements. Upon shear stress stimulation, the lipid order of EC membranes rapidly decreased in an intensity-dependent manner, and caveolar membrane domains changed from the liquid-ordered state to the liquid-disordered state. Notably, a similar decrease in lipid order occurred when the artificial membranes of giant unilamellar vesicles were exposed to shear stress, suggesting that this is a physical phenomenon. Membrane fluidity increased over the entire EC membranes in response to shear stress. Addition of cholesterol to ECs abolished the effects of shear stress on membrane lipid order and fluidity and markedly suppressed ATP release, which is a well-known EC response to shear stress and is involved in shear-stress Ca²⁺ signaling. These findings indicate that EC membranes directly respond to shear stress by rapidly decreasing their lipid phase order and increasing their fluidity; these changes may be linked to shear-stress-sensing and response mechanisms.

ID: 787

C10: 3

Dimensionality and behavior of swimming Zebrafish: “The EigenFish”

Kiran Girdhar¹, Martin Gruebele² and Yann Chemla³

¹University of Illinois Urbana Champaign, United States of America; ²University of Illinois Urbana Champaign, United States of America; ³University of Illinois Urbana Champaign, United States of America.

How simple is the underlying control mechanism for the complex locomotion of vertebrates? To answer this question, we study the swimming behavior of zebrafish larvae. A dimensionality reduction method (singular value decomposition), in analogy to previous studies of worms, is used to analyze swimming movies of fish. That way, the animals can directly provide us with a minimal set of shapes to describe their motion, rather than us imposing arbitrary coordinates. We show that two low dimensional attractors (an ellipse and a distorted ellipse) embedded in a three-dimensional space of motion coordinates are sufficient to describe 95% of the locomotion. We also show that scoots and R-turns, previously thought to be independent behaviors based on qualitative studies, are in fact just extremes of a continuous family of motions bounded by the two attractors. We did the similar analysis on neuro-kinematic model of fish. We have optimized parameters like synaptic weights, neural signal & stiffness function of simulated fish to obtain the eigenfish gaits like scoots and routine turns.

ID: 493

C10: 4

Achievement of peristaltic design in the artificial esophagus based on esophageal characteristic analysis of goats' specimen

Yasunori Taira¹, Kurodo Kamiya², Yasuyuki Shiraishi³, Hidekazu Miura³, Takuya Shiga⁴, Mohamed Omran Hashem⁵, Akihiro Yamada¹, Yusuke Tsuboko¹, Takuya Ito¹, Kyosuke Sano¹ and Tomoyuki Yambe³

¹Graduate School of Biomedical Engineering, Tohoku University, Japan; ²Advanced Surgical Science and Technology, Graduate School of Medicine, Tohoku University, Japan; ³Medical Engineering and Cardiology, Institute of Development, Aging and Cancer, Tohoku University, Japan; ⁴Anesthesiology and Perioperative Medicine, Graduate School of Medicine, Tohoku University, Japan; ⁵Medical Engineering and Cardiology, Graduate School of Medicine, Tohoku University, Japan.

In order to promote activity of daily life of patients with severe esophageal diseases, supporting peristalsis motion at the esophagus might be efficient. So we have been developing an artificial esophagus (AE)

which has peristalsis motion function, and we have achieved the AE by using Ni-Ti shape memory alloy fibers.

We extracted the esophagus from the epiglottis to the cardia portion from goats, which weighed 48.6 ± 16.3 kg (n=4), after the animal experiment procedures. Prior to the measurement of characteristics of natural esophagus, we defined 5 segments in each extracted esophagus. Then we set the specimen in the static characteristic test apparatus in which we could measure segmental pressure-volume relations. Pressure and volume were measured simultaneously. All these measurement were performed within 3 hours from the extraction.

Average length of each esophagus was 63 ± 7 cm. Because of the proximal segment of the specimen exhibited that the steeper increase of pressure than the distal portion near the cardia, we characterized that the distal esophagus is firmer than proximal. The proximal segment exhibited 55% bigger increase in pressure than the distal portion near the gastric cardiac part. Therefore it was suggested that compliance at the proximal portion could be lower at the small amount of internal volume. On the other hands, the extensibility of distal esophagus might be bigger than that at proximal segment.

Consequently it was indicated that a new mechanical structure could be applied for the development of AE which could reproduce peristaltic motions.

Session	D5: Lab-on-Chip Micro/Nanofluidics
Date/Time	6 December 2013 15:30–17:00 hrs
Venue	SR-07 & 08

ID: 482

D5: 1

A microfluidic device for stepwise concentration generation on a microwell slide for cytotoxic assay

Toshiro Ohashi¹, Emilie Weibull², Manabu Sakai¹, Shunsuke Matsui¹ and Helene Andersson-Svahn²

¹Hokkaido University, Japan; ²Royal Institute of Technology, Sweden.

In this study, a microfluidic stepwise concentration generator that adds substantial utility to the high-throughput nature of a microwell slide that we have previously established is proposed. Using microfluidic dynamics, we have designed microchannels to deliver a reagent and its dilutant with precisely controlled flow volumes, generating 8 discrete steps of reagent concentration in designated microwells. In the generator, PDMS-made microfluidic components consist of three layers: a microchannel layer, a mixing

chamber/drain layer and a gasket layer. The experimental reagent and its dilutant are introduced from each individual inlet and delivered to 8 mixing chambers. The reagent and dilutant concentration in the mixing chamber is dependent on the width and the length of the flow channels, resulting in a 8 steps reagent concentration, ranging from $\times 1$ (input concentration) to $\times 0.01$. To validate the device, a solution of FITC-labelled dextran in water at 0.6 mM and dextran-free water were injected using a syringe pump. Fluorescence intensity in the mixing chamber was measured using an inverted fluorescent microscope and compared to a theoretical result. In a cell experiment, cultured bovine endothelial cells were exposed to Saponin solution and a live/dead assay was performed on the cells with 5 μM Calcein AM and 5 μM Ethidium Homodimer solution. It was confirmed that a 8 step concentration of the FITC-dextran solution was created, spanning three orders of magnitude. In the experiment with Saponin treatment, the amount of dead cells increased with the concentration of Saponin, while live cells deceased. These results show the ability of the present microfluidic device to create designated concentration steps of a reagent, and suggest that the newly developed microfluidic components add a substantial utility to the microwell slide.

ID: 164

D5: 2

Electrical stimulation induces enhanced myelination in a novel microfluidic platform

Hae Ung Lee¹, Nitish Thakor^{1,2} and In Hong Yang^{1,2}

¹Singapore Institute for Neurotechnology, National University of Singapore, Singapore; ²Dept of Biomedical Engineering Johns Hopkins University, Baltimore, USA.

A demyelinating disease in the nervous system is associated with the degeneration of myelin sheath of axons resulting in the reduction of conduction of nerve signals causing deficiencies in sensation, movement, cognition, and other functions. However, therapeutic approaches to treat these demyelinating diseases are still not well developed. Electrical stimulation has shown a great potential for therapeutic effect in various neurological diseases including spinal cord injuries and brain injuries. Thus, electrical stimulation for demyelinating disease will be one of the plausible therapeutic approaches. In addition, previous reports indicated that electrically stimulated neuron promoted oligodendrocytes proliferation, differentiation, and myelination *in vitro*. In order to identify the role of electrical stimulation in the myelination, we have developed a novel microfluidic platform to stimulate sub-cellular parts of neuron electrically in a fluidically-isolated manner.

Focally applied electrical stimulation showed the enhanced proliferation of oligodendrocyte and myelination of axon. The novel microfluidic electrical stimulation platform will allow us to examine the effect of electrical stimulation for myelination in development and demyelinating conditions. These chambers separated neurons into 3 parts: cell soma, axon and axonal terminal. Our system was able to stimulate axons focally: the point between cell soma and axon or the point between axon and axonal terminal. We successfully have developed novel microfluidic system to identify the role of electrical stimulation for myelination. Our microfluidic system will provide the mechanisms for electrical stimulation in the treatment of demyelinating diseases.

ID: 794

D5: 3

A scalable method for aligning 3D micro-tissues in a microfluidic chip

Chukwuemeka George Anene-Nzelu¹, Kah Yim Peh¹, Azmall Fraiszudeen¹, Sum Huan Ng², Hwa Liang Leo¹, Harry Yu^{1,3} and Yi Chin Toh¹

¹National University of Singapore, Singapore; ²Singapore institute of Manufacturing Technology; ³Institute of Bioengineering and Nanotechnology, Singapore.

In recent years, microfluidic technology has gained traction for biological applications, such as drug screening and stem cell differentiation, due to its miniaturization capability and the inclusion of flow parameters. Nonetheless, harnessing useful biological data from these devices will require tailoring the microfluidic environment for specific cell types to maintain their physiological phenotypes and functions. While there have been considerable efforts to engineer 3D microfluidic environments to enhance cellular performance over conventional 2D cultures, there are few reports on the inclusion of cell-specific topographical microenvironments. *in vitro* topographical cues, such as micro/nano-grooves, have been shown to be beneficial for cell types of cardiac, skeletal and neuronal lineages, where they experience anisotropic topography from the extracellular matrix *in vivo*. Here, we developed a cheap and scalable method to incorporate micro-topographical cues into microfluidic chips to induce cell alignment. Using commercially available optical grating sheets as molds for replica molding, large surface areas of polydimethylsiloxane (PDMS) micro-groove substrates can be produced and be plasma bonded to multiple microfluidic chips. Besides aligning a 2D monolayer culture, we demonstrated that the micro-groove substrate was also capable to aligning a 3D micro-tissue on chip. C2C12 mouse myoblasts that were seeded into a previously developed 3D

microfluidic chip incorporating the PDMS micro-groove substrate remodeled into an aligned micro-tissue, where the actin cytoskeleton and nuclei were preferentially oriented along the micro-grooves. We observed that cells within the micro-tissue can align without being in direct contact with the micro-grooves, and there was synergism between topography and fluid shear stress. We also showed that this alignment enhances the maturation of C2C12 into skeletal muscles. The transcriptional expressions of skeletal muscle markers were higher in an aligned 3D C2C12 micro-tissue as compared to a randomly aligned one. This novel method enables the routine inclusion of micro-topographical cues into 2D or 3D microfluidic cultures of other cells that require alignment for proper functioning so as to generate more physiological models for studying tissue morphogenesis and drug screening applications.

ID: 242

D5: 4

Application of a FRET-based biosensor in studying shear stress-induced apoptosis in circulating tumor cells

Xiaofeng Liu, Afu Fu and Kathy Qian Luo

School of Chemical and Biomedical Engineering, Nanyang Technological University, Singapore.

The migration of cancer cells from the primary tumor to other parts of the body, a process known as metastasis, is responsible for more than 90% of all cancer-related deaths. During metastasis, cancer cells leave the tumor and enter the circulatory system. So far, few studies have attempted to investigate the apoptotic effect of shear flow on circulating tumor cells (CTC) with different metastatic capacities.

In this study, we compared the apoptotic effect of fluid shear stress on two types of breast cancer cells: non-metastatic MCF7 and metastatic MDA-MB-231 cells. The plasmid DNA encoding a FRET-based caspase sensor (C3) was transfected into the cells to generate two stable cell lines of MCF7-C3 and 231-C3. The sensor C3 was constructed by fusing the genes encoding a cyan fluorescent protein (CFP) with a yellow fluorescent protein (YFP) and a caspase-3 cleavage sequence DEVD. This sensor can detect caspase activation based on the principle of FRET. The sensor will emit more green light if cells are alive and more blue light when cells are killed via apoptosis. We can easily determine cell apoptosis by visualizing FRET images generated by merging the images of YFP and CFP. Sensor cells were circulated in a microfluidic system under a pulsatile shear stress of 15 dyn/cm² for 0–48 h. Real-time analysis of ~200 cells at each time point showed that non-metastatic MCF7-C3 cells had significantly higher apoptotic

rates than metastatic 231-C3 cells. The differences were more prominent at 12, 18 and 36 h.

By investigating the fluid shear stresses-induced CTC apoptosis, our results indicate that the ability for 231-C3 cells to survive the shear stress-induced apoptosis increased their metastatic potential. This study provides a new method of real-time detection and selection of metastatic CTC and an approach of investigating the mechanisms of cancer cell metastasis during circulation.

ID: 432

D5: 5

An integrated microfluidic device for single cell encapsulation and cellular enzymatic assay

Tengyang Jing^{1,2}, Ramesh Ramji¹, Majid Ebrahimi Warkiani², Chia-Hung Chen^{1,3}, Jongyoon Han^{2,4,5} and Chwee Teck Lim^{1,2,6}

¹Department of Bioengineering, National University of Singapore, Singapore; ²Singapore-MIT Alliance for Research and Technology (SMART) Centre, Singapore; ³Singapore Institute for Neurotechnology (SiNAPSE), Singapore;

⁴Department of Electrical Engineering & Computer Science, Massachusetts Institute of Technology, USA; ⁵Department of Biological Engineering, Massachusetts Institute of Technology, USA; ⁶Department of Mechanical Engineering, National University of Singapore, Singapore.

Direct biochemical assay on individual cells of patient sample is becoming increasingly important in disease diagnosis, treatment monitoring and drug screening. Conventional bulk measurement methods appear to be insufficient as many critical cell signals are masked by the response from a pool of heterogeneous cell population. Hence, there is a strong need for a cost-effective and high-throughput cell assay technology to obtain accurate analysis on heterogeneous cell samples at single cell level. Here we present an integrated microfluidic device capable of encapsulating individual cells into aqueous picoliter droplets and instantaneously sorting these droplets out from empty ones. Single cell encapsulation is achieved using jetting mechanism in a two-phase flow focus junction. The flowrate is carefully controlled so that droplets with cell encapsulated inside are generally 5 to 10 μm larger in diameter than empty ones. Size-based sorting is realized using deterministic lateral displacement (DLD) design. Encapsulation and sorting are operated at more than 5,000 droplets per second continuously with at least 70% separation efficiency. Comparing with other single cell assay technologies, our device can produce single cell compartment inside simple emulsion without relying on any other external power sources for active sorting or valve control. Moreover, it can be operated independent of cell concentration restriction. Therefore, it can encapsulate primary patient

samples in most scenarios. From the individual droplets, we demonstrated intercellular enzymatic assays at the single cell scale. Both time lapse and end-point studies demonstrated the heterogeneity of cell metabolism even under the same culture conditions. This may enable deeper understanding of single cell activity and categorize a batch of cells into different subpopulations for further downstream clinical analysis.

ID: 697

D5: 6

Integrated microfluidic platform for multiplexed enzymatic bioassay in ovarian cancer MMP activity study

Ee Xien Ng and Chia-Hung Chen

National University of Singapore, Singapore.

The performance of enzymatic assay relies on the tools available to study them. Current conventional devices such as Enzyme-linked immunosorbent assay (ELISA) and microtiter well plate reader are limited by their physical ability to produce results with their throughput and accuracy by using limited clinical samples offered. Here we proposed an integrated microfluidic platform for multiplexed enzymatic assay by combining a droplet library and a picoinjector. The droplets generated by the droplet generators were used as micro-size test tubes with pico-liter volume capacity for compartmentalization of chemical reagents, and clinical samples were injected by picoinjector for enzymatic bioassay in a high throughput manner (~4000 droplets/s). We used this integrated microfluidic platform to study protease signatures along the epithelial-mesenchymal transition (EMT) spectrum during tumor progression by analyzing an important enzymatic biomarkers – matrix metalloproteinases (MMPs) and study their reaction activities. Epithelial-mesenchymal transition (EMT) is a highly conserved and fundamental process that governs morphogenesis in multicellular organisms and they might be involved in the dedifferentiation programme that leads to malignant carcinoma. The importance of studying MMPs arises as they act as critical mediators of these processes, degrading and remodeling ECM, stimulating cell proliferation and apoptosis, and inducing cell migration and cell morphological alterations.

ID: 678

D5: 7

Real-time impedimetric monitoring of Poly(ethylenimine)s-mediated cytotoxicity during gene transfection

Claudia Caviglia¹, Marco Carminati², Arto Heiskanen¹, Giorgio Ferrari², Marco Sampietro², Thomas Lars Andresen¹ and Jenny Emnèus¹

¹Technical University of Denmark, Denmark; ²Politecnico di Milano, Italy.

Poly(ethylenimine)s (PEIs) are able to condense DNA and RNA into stable toroidal and globular nanostructures (polyplexes) and are among the most efficient and promising synthetic transfectants, but they induce severe cytotoxicity. The mechanisms of PEI-mediated cytotoxicity have not been fully delineated but PEI toxicity appears to predominantly depend on membrane perturbing effects in cellular compartments in which they accumulate. Electrochemical Impedance Spectroscopy (EIS) is used as a non-invasive biophysical approach for the investigation of the electrical properties of biological materials according to their physiological and morphological changes. In this work, EIS has been used to evaluate impedance changes due to the polycation perturbations on a cell population. HeLa cells have been cultured on laminin-coated gold interdigitated electrode arrays integrated into a tailor-made microfluidic cell culture platform. Multiplexed EIS data from each sensor element were acquired using a 24-channel miniaturized potentiostat (30 points between 100 Hz and 100k-Hz). Two alternative sensing configuration approaches (the standard “vertical” configuration (a single working electrode (WE) versus a large, distant counter electrode (CE)), and the interdigitated configuration (WEa comb versus WEb comb)) have been used and compared on the same cell population, providing optimal detection conditions. The experiments have been performed by initially seeding about 10³ cells into each chamber, continuously perfused with fresh culture medium. The platform was incubated in a humidified atmosphere. After 24 hours, different concentrations of PEIs have been introduced in the culture medium and the incubation continued for other 24 hours. Cell adhesion, growth and PEI-cytotoxicity have been detected in real-time by following impedance changes. Microscopic imaging and MTS assays have been combined to the electrochemical detection. Complementary ongoing experiments aim to monitor in real-time gene transfection in order to detect the cytotoxic effects (apoptosis and necrosis) induced by different cationic polyplexes. This approach can contribute to a clearer and detailed mechanistic understanding of polycation-modulated cellular functions and cell death and could initiate

rational approaches for design and engineering of safer vectors for nucleic acid transfection.

Session	E3: Rehabilitation Neurotechnology
Date/Time	6 December 2013 15:30–17:00 hrs
Venue	SR-12

ID: 415

E3: 1

EEG-based emotion monitoring in mental task performance

Yisi Liu, [Olga Sourina](#) and Woon Huei Chai

Nanyang Technological University, Singapore.

Emotional engagement during mental tasks performance when the difficulty level of mental tasks increases is studied using Electroencephalogram (EEG) recorded by Emotiv Epoch device. A real-time EEG-based emotion recognition algorithm using Valence-Arousal-Dominance emotion model is applied. An experiment with 5 levels of workload is proposed and carried out with 7 subjects. The mental tasks are given to the participants to solve addition problems of increasing complexity. For each task, 3 min is given to complete additions with 2 min rest between the tasks sessions. Performance score for each participant is recorded as well. Emotions are recognized from the EEG during each task using the subject-dependent emotion recognition algorithm. The algorithm consists from feature extraction and classification parts. The classifier is trained for each participant using short calibration session with emotion induction before the experiment. The combined features obtained from the training session are used to train a SVM classifier. The following hypotheses are confirmed. Participants have mostly negative, high arousal, low dominance emotions during the mental tasks performance under the stress since high arousal can speed up the mental process and enhance information retrieval, and as the limited time is given to perform the tasks, the feeling of losing control is dominated in the participants that corresponds to low dominance on the scale of Valence-Arousal-Dominance emotion model. At the same time it is found that when the difficulty level of mental tasks increases under the stress, people tend to be more negative and more aroused.

ID: 215

E3: 2

A multi-level fuzzy logic system for controlling the tibialis anterior FES envelop

Negar Zakhirehdari, [Hamidreza Kobravi](#), Mitra Masoudi and Tavakkoli Parvaneh

Islamic Azad University, Mashhad branch, Iran.

In this paper, a predictive two-level hierarchical fuzzy model is applied to control the FES envelop of disabled tibialis anterior (TA) muscle in patients with unilateral drop foot. The proposed control methodology is based on EMG signal of Rectus Femoris (RF) muscle of ipsilateral leg. Its control structure consists of an upper level fuzzy controller and a lower level direct fuzzy controller. The appropriate fuzzy if-then rules of lower level fuzzy logic system are extracted to model the existing muscle coordination pattern between activities of ankle dorsiflexor muscle and ipsilateral knee extensor muscle of unimpaired side. Then the adjusted fuzzy logic system forecasted the TA muscle activity of one foot using rectus femoris muscle activity of ipsilateral foot during the over-ground walking. The results show quite promising and impressive performance of presented control scheme.

ID: 844

E3: 3

Experimental study of FES-driven ankle joint actuator for hybrid FES walking assistive system - I

[Naosuke Yamamoto](#)¹, Naoya Kurokawa², Toshiyasu Yamamoto², Yoshihiko Tagawa¹ and Hiroaki Kuno²

¹*Kyushu Institute of Technology, Japan;* ²*Okayama University of Science, Japan.*

Human waking consists of adjusting large numbers of the activated muscles, and quasi-passive walking is efficiently used by activating the calf muscle. The activation of the two-joint muscle (gastrocnemius muscle) can assist the knee flexion at the initial swing phase. However, FES (functional electrical stimulation)-activated walking is artificially rebuilt by fewer muscles.

In this study, we have developed a new hybrid FES walking assistive system for body weight support treadmill training.

In the experimental system, joint angles and torques are online-estimated by the 3 dimensional motion analysis system with 2 sets of force plates

Quasi-passive walking is mainly accomplished by push-off motion of the FES-driven ankle joint torque. In walking, the motor-driven hip joint motion usually adjust a stride length for assisting walking speed, as shown in the accompanying paper.

Here we mainly explain the FES-activated quasi-passive walking by a push off driving forces by stimulating the muscles; gastrocnemius, soleus, and tibialis anterior.

The ankle joint driving torque is estimated and adjusted by the angular pattern of hip joint, based on the quasi-passive walking model. Here the angular pattern of hip joint is also controlled by cycle-to-cycle control theme, whose feedback gain is scheduled.

The muscular outputs (muscular forces) of the stimulated muscles are optimally estimated by the revised musculoskeletal system. The electrical responses of the stimulated muscles are feedback to make a stable condition of the muscular outputs.

In this paper, we lastly examined relation between hip and ankle joint torques for searching a better control theme of the driving forces.

ID: 841

E3: 4

Experimental study of motor-driven hip joint actuator for hybrid FES walking assistive system - II

Naoya Kurokawa¹, Naosuke Yamamoto², Toshiyasu Yamamoto¹, Yoshihiko Tagawa² and Hiroaki Kuno¹

¹Okayama University of Science, Japan; ²Kyushu Institute of Technology, Japan.

In recent years, several robotic assistive systems has been developed for walking rehabilitation exercise. However, these are usually large and expensive, such as Lokomat. In this study, we have developed the hybrid FES walking assisted system, which has combined the motor-driven hip joint actuator with ankle joint actuator by the functional electrical stimulation (FES). Ankle actuation FES system is mainly driven by the quasi-passive walking theme, as shown in the accompanying paper.

Here the motor-driven hip joint actuator is mainly explained. This system was fabricated by the pelvis-thigh plastic orthosis, supported by the waist, which is actuated by the DC driven-AC servo motor (weight = about 1 kg for each).

Firstly, each side of hip joint torques was estimated from a strain gauge attached to the thigh brace. In the pretest, torque feedback control gain was adjusted to be zero during walking, with cycle-to-cycle control by walking stride (detected by the foot switch). Secondly, from the hip joint angle pattern during walking which is measured and estimated by the 3 dimensional motion analysis apparatus, a set of reference pattern was created for the hip joint angle patterns. Next, gain-scheduled angular feedback control was applied during walking, cooperated with the ankle FES driven this pattern, whose system were designed to create a stable walk. We also tried to elucidate a physiological

relation between hip and ankle joint. These results will be useful to apply for the stroke walking training in the body weight support treadmill training.

ID: 694

E3: 5

Development of a knee ankle robot for gait rehabilitation

Haoyong Yu, Sunan Huang and Nitish Thakor

National University of Singapore, Singapore.

Gait disorders are common for patients post stroke and in most cases cannot be treated medically or surgically. Therefore, treatment often relies on rehabilitation service. Rehabilitation robotics has shown promise in providing patients with intensive therapy leading to functional gains. This involves the use of a robotic exoskeleton device or end-effector device to help the patient retrain motor function by performing gait movement. The purpose of an exoskeleton as an assistance device is to amplify the moment generated by the human muscles. Here, we are developing a wearable knee ankle robot for gait rehabilitation based on a novel actuator design (most existing devices are hip-knee type robot). The robot system consists of an ankle foot module and a knee module. Each module is driven with the same compact compliant force controllable actuator. The reason for using compliant actuator is that traditional stiff actuators are not safe in robots interacting with humans for rehabilitation purpose. Pratt and Williamson have pointed out that since the spring deforms a significant amount, the fidelity compared to traditional strain gauges for force control is much higher. The proposed rehabilitation robot can implement two basic functions for human-robot interaction control: one is human-in-charge mode where the robot should be able to follow the walking human, not to hinder human motion; the other is robot-in-charge mode where the robot is able to realize the desired walking pattern. The description of the controllers and experimental results with the robot are presented in the paper, especially for several healthy subjects. In future, the rehabilitation robot will be used on stroke patients.

ID: 217

E3: 6

Multiobjective design optimization for a steerable needle for soft tissue surgery

Alexander Leibinger, Matthew Oldfield and Ferdinando Rodriguez y Baena

Imperial College, United Kingdom.

A novel steerable probe is being developed to access deep seated targets within the brain, with the aim of improving the accuracy of minimally invasive percutaneous needle insertions. Consisting of multiple axially interlocked segments that independently slide along each other, miniaturisation of the design is required in order for the needle to be used in neurosurgery. Within this study, a design optimization procedure based on finite element models of the needle geometry is presented, where a set of parameters is identified, which minimizes the risk of both buckling and separation. Four significant design variables are defined for a genetic multiobjective optimization algorithm. Loads and interactions between the four parts due to paths taken inside the soft tissue are modelled using generalized plane strain elements. The performance of the optimization and the resulting set of non-dominated solutions are analysed. By applying a decision-making process based on the value path method, the non-dominated solutions are then compared across the four objectives. Trade-off relationships between sliding performance and interlock strength are identified and the most feasible design solution is selected. It is found that smaller and less pronounced interlock features reduce the resulting contact forces and improve the sliding performance between needle segments. The outcome is a new optimized design for the needle, which will be manufactured and tested with a suitable controller both *in vitro* and *ex vivo*.

Day 4 – Saturday, 7 December 2013

Session	A10: Biosignal Processing
Date/Time	7 December 2013 09:00–10:30 hrs
Venue	SR-01 & 02

ID: 283 **A10: 1**

Aging integromics: module-based markers of heart aging from multi-omics data

Konstantina Dimitrakopoulou¹, Aristidis Vrahatis¹,
Georgios Dimitrakopoulos¹ and [Anastasios Bezerianos](#)²

¹University of Patras, Greece; ²University of Patras, Greece and
SINAPSE Institute, Center of Life Sciences, National University
of Singapore, Singapore.

In the emerging Systems Medicine field, the study of aging is re-evaluated and contextualized through the combination of 'omics' investigations (i.e. transcriptomic, proteomic, metabolomics, fluxomic). In particular, heart aging is a highly complex process in terms of molecular changes and the role of microRNAs (miRNAs) as key gene regulators has recently arisen.

Towards this orientation, we describe a three-step methodological framework for designating markers of heart aging at the level of modules by integrating proteome and heart-specific transcriptome information in the mouse model. First, a Multi-layer Large Scale Omics Network (MLSON) is constructed integrating two types of nodes (mRNAs and miRNAs) and three types of relations (mRNA-mRNA, miRNA-mRNA and miRNA-miRNA). Secondly, two adapted weighting schemes were designed and applied on MLSON, based either on mRNA or miRNA expression profiles, with the scope to pinpoint the significantly altered relations due to aging factor. Finally, an efficient module-detecting algorithm, namely Detect Module from Seed Protein (DMSP), is recruited so as to identify multi-layer modular markers discriminative of the two states (young/old).

Our large scale integromics approach is an enabling step towards elucidating heart longevity mechanisms at multiple levels. The identified modules provide novel biological evidence for the interference and synergistic effect of miRNAs in heart aging process.

ID: 115 **A10: 2**

Robustness of two-pulse-synthesis model studied on toe photoplethysmograph signals

[Dharitri Goswami](#) and Jayanta Mukhopadhyay

IIT Kharagpur, India.

Photoplethysmography (PPG) is a low-cost, non-invasive method for assessing the cardiovascular health of an individual using infrared optical sensor-detector pair. Recent research has established that PPG signal may be useful for providing vital clinical information related to cardiac and arterial systems. The pulsatile component of the PPG is a composite signal that contains vital information. Information about the cardiac activity and blood flow of an individual can be available from this pulsatile AC component after careful processing and interpretation.

Recently, a Two-Pulse Synthesis (TPS) model based on the digital volume pulse signal obtained by noninvasive photoplethysmography has been suggested as a simple and low-cost, technology to assess arterial degeneration in various disease conditions. Extensive results of investigations, obtained using the TPS model on sizeable groups of volunteers in typical disease conditions such as hypertension, diabetes mellitus, end stage renal diseases and coronary artery diseases have also been interpreted and presented in our earlier work and publications.

In this paper, we present results of studies based on TPS model applied to toe PPG signals. When various TPS model parameters obtained from finger and toe PPG signals are compared for both healthy and diseased subjects, strong positive correlations are found between most of the parameters of clinical interest which is not possible by conventional or second order derivative method. In TPS model it is possible to deal with two distinct waves and two distinguishably separate peaks for the forward and reflected waves. This study brings out the robustness and preciseness of the TPS model in describing vascular health parameters of a subject.

ID: 211

A10: 3

Automated parameter estimation for a nonlinear signal separation scheme

Yu Yao, Stefan van Waasen and Michael Schiek

Research Center Jülich, ZEA-2 Electronic Systems, Jülich, Germany.

The current trend towards telemedicine has sparked a renewed interest in Ballistocardiography (BCG), a method for measuring mechanical cardiac activity. Due to its unobtrusive nature it is considered as a promising approach for home monitoring systems. However, BCG recordings are often contaminated by respiratory baseline variations, which have to be separated from the cardiac component before analysis. Performing this separation with linear filters can be difficult, since the spectra of the cardiac and respiratory components overlap. A recently proposed nonlinear separation method circumvents the problem of spectral overlap by performing the signal separation in delay space. However, finding the correct parameters for the new method is difficult and had to be performed manually. In this paper an automated parameter estimation algorithm is proposed, which is able to estimate suitable parameters for the nonlinear signal separation method.

ID: 114

A10: 4

Assesment of first derivative of doppler blood flow velocity in vascular aging

Zulaika Hamdon¹, Azran Azhim^{1,2}, Muhamad Saleh¹, Pouya Bagherpour¹, Yohsuke Kinouchi³ and Fatimah Ibrahim⁴

¹Malaysia - Japan International Institute of Technology, Universiti Teknologi Malaysia, Malaysia; ²IJN-UTM Cardiovascular Engineering Center, University of Technology, Johor, Malaysia; ³Dept. of Electrical and Electronic Engineering, Faculty of Engineering, The University of Tokushima, Japan; ⁴Department of Biomedical Engineering, Faculty of Engineering Building, University of Malaya, Malaysia.

The aim of this study is determine first derivative of blood flow velocity (FDBFV) in common carotid artery (CCA) in order to evaluate cardiovascular functions. The extracted derivative features suggest the acceleration waves which able to provide aging index (AGI) in the cardiovascular system. In the study, acceleration wave derived from FDBFV consist of a,b,c,d,e and f waves which represent the initial positive, early negative, re-increasing, late re-decreasing, diastolic positive waves and diastolic negative waves, respectively. The FDBFV waveforms of 227 healthy volunteers are statistically analyzed in the study. Pearson's correlation analysis was used to determine the relationship between all variables and

factors on the selected hemodynamic data. As a result, AGI in FDBFV ($r=0.727$, $p<0.0001$) shows strong correlation and consistency as compared to the other previous study. In particular, there are significant correlations between systolic blood pressure, gender and heart rate in f waves. We found that there are sensitive to blood pressure and unknown wave features in CCA. In conclusion, FDBFV in CCA is an effective method to evaluate the vascular aging.

Acknowledgement: The authors are grateful to the Japanese Ministry of Education, Culture, Sport, Science and Technology (MEXT) for its finance support through a Strategic Research Foundation Grant for Private Universities. We also thank to Malaysia - Japan International Institute of Technology (MJIT).

ID: 589

A10: 5

Quantitative high speed tracking of bacteria motility in 3D

Fook Chiong Cheong¹, Chui Ching Wong¹ and Chwee Teck Lim^{1,2}

¹Mechanobiology Institute, Singapore; ²National University of Singapore, Department of Bioengineering, Singapore.

Quantitative measurement of planktonic bacteria in 3D can be extremely challenging with current optical techniques. We introduce a high-speed holographic video microscopy technique that is capable of capturing 3D dynamics of fast moving microorganisms. This microscopy technique makes use of optical scattering properties of cells to infer the 3D position and physical characteristic of individual bacteria. Using this optical approach, subtle motility dynamics of multiple bacteria in 3D, such as speed and turn angles, can be obtained within minutes. We demonstrated the efficiency of this technique by tracking 3D behavior of pathogens, like *Pseudomonas aeruginosa* and *Escherichia coli* bacteria.

Session	B10: Regenerative Medicine Tissue Engineering
Date/Time	7 December 2013 09:00–10:30 hrs
Venue	SR-03 & 04

ID: 598

B10: 1

***In vivo* animal model— the golden key for tissue engineering**

Kai Yang

SG Med International Pte Ltd, Singapore.

In this talk, the concept, evolution and significance of *in vivo* animal models in biomedical science will be described. The principle and classification of *in vivo* animal models will also be discussed. The basic requirement of FDA for preclinical animal study for medical product registration is certainly a most important part in this presentation. The legal and ethical issues involved in animal study in a Singapore context will also be touched on in the talk. In the last portion of the presentation, the commonly used *in vivo* animal models and their applications, including bone fracture, neuropathic pain, spine instability, myocardium infarction and etc., will be illustrated for the audience to have a better understating of the indispensable role of *in vivo* animal models in tissue engineering.

ID: 869

B10: 2

Enhanced function of immuno-isolated islets in diabetes therapy by co-encapsulation with an anti-inflammatory drug

Tram T. Dang^{1,2}, A. V. Thai^{2,4}, J. Cohen³, J. E. Slosberg^{2,4}, K. Siniakowicz³, J. C. Doloff^{2,4}, M. Ma^{2,4}, J. Hollister-Lock³, K. M. Tang^{2,4}, Z. Gu^{2,4}, H. Cheng^{1,2}, G. C. Weir³, R. Langer^{1,2} and D. G. Anderson^{1,2}

¹Department of Chemical Engineering, Massachusetts Institute of Technology, USA; ²David H. Koch Institute for Integrative Cancer Research, Massachusetts Institute of Technology, USA; ³Joslin Diabetes Center, Harvard Medical School, USA; ⁴Department of Anesthesiology, Children's Hospital Boston, USA.

Immuno-isolation of islets has the potential to enable the replacement of pancreatic function in diabetic patients. However, host response to the encapsulated islets frequently leads to fibrotic overgrowth with subsequent impairment of the transplanted grafts. This study identified anti-inflammatory agents to be incorporated into islet-containing microcapsules to address this challenge. Using parallel non-invasive fluorescent and bioluminescent imaging, we performed *in vivo* subcutaneous screening of 16 small

molecule anti-inflammatory drugs to select promising compounds that could minimize the formation of fibrotic cell layers. We identified dexamethasone and curcumin as the most effective drugs in inhibiting the activities of inflammatory proteases and reactive oxygen species in the host response to subcutaneously injected biomaterials. Next, we further demonstrated that co-encapsulating curcumin with pancreatic rat islets in alginate microcapsules reduced fibrotic overgrowth and improved glycemic control in a mouse model of chemically-induced type I diabetes. These results showed that localized administration of anti-inflammatory drug can improve the longevity of encapsulated islets and may facilitate the translation of this technology toward a long-term cure for type I diabetes.

ID: 835

B10: 3

Preservation of left ventricular function and morphology using fibrinogen-based conjugates

Marian Plotkin¹, Srirangam Ramanujam Vaibavi¹, Rufaihah Abdul Jalil², Venkateswaran Nithya², Jing Wang², Theodoros Kofidis^{2,4} and Dror Seliktar^{1,3}

¹Nanoscience and Nanotechnology Initiative, National University of Singapore, Singapore.; ²Dept of Surgery, Yong Loo Lin School of Medicine, National University of Singapore, Singapore.; ³Faculty of Biomedical Engineering, Technion-Israel Institute of Technology, Haifa, Israel.; ⁴Dept of Cardiac, Thoracic & Vascular Surgery, National University Heart Centre Singapore, National University Health System, Singapore.

Myocardial infarction (MI) occurs when the coronary arteries blood flow is interrupted. The resulted ischemia causes necrosis of the affected myocardium tissue. In our study, we have synthesized and tested the effectiveness of UV-Crosslinked hydrogels on the post-MI Left ventricle (LV) remodelling process in a rodent model. With this aim in mind, we have synthesized two types of Fibrinogen-based conjugates: Fibrinogen-PEG (PF) and Fibrinogen-Tetronic (TF). Each hydrogel type was further subdivided into two groups, each with different storage modulus properties. This was accomplished by adding additional 1% or 2% (W/V) of Poly (ethylene glycol) diacrylate (PEG-DA) to the PF hydrogel and by adding additional 1% or 2% (W/V) of T1307 tetraacrylate to the TF hydrogel. MI was created by ligating the left anterior descending coronary artery in a rodent model. Hydrogel was injected into four sides of the infarcted zone and exposed with UV light for the polymerization process to occur. The four test groups were compared to control and sham groups. Control animals underwent MI and treated with saline. Sham animals underwent thoracotomy and pericardiotomy, but not LAD ligation. Analysis of the Left

ventricular morphology and histology revealed that all hydrogel treated groups exhibited increase in wall thickness and increased survival of viable tissue. Echocardiography showed that treatment resulted in improvement in heart function. Ejection fraction (%) was $37.3 \pm 5.8\%$ in control group, $64.1 \pm 2.8\%$ in PF 1% group, $74.2 \pm 4.3\%$ in PF 2% group, $74.1 \pm 10.4\%$ in TF 1% group, $73.6 \pm 10.4\%$ in TF 2% group and $87.6 \pm 8.2\%$ in Sham group. Arterial density analysis, using alpha-smooth muscle actin (alpha-SMA) staining, showed a twofold increase in arterial density in PF groups compared to control group. We have demonstrated that Fibrinogen-based conjugates show significant heart function rescue and serve as promising candidates for treatment of MI.

ID: 830

B10: 4

Infarct stabilization and cardiac repair with VEGF-loaded PEGylated fibrinogen injectable hydrogel

Rufaihah Abdul Jalil¹, Vaibavi Srirangam Ramanujam², Marian Plotkin², Nithya Venkateswaran¹, Jiayi Shen¹, Jing Wang¹, Dror Seliktar³ and Theodoros Kofidis^{1,4}

¹Department of Surgery, National University of Singapore, Singapore; ²NUS Nanoscience and Nanotechnology Institute, Singapore; ³Faculty of Biomedical Engineering, Technion-Israel Institute of Technology, Haifa, Israel; ⁴National University Heart Centre Singapore, National University Health System, Singapore.

Objective: Angiogenesis relies on the interplay of growth factors, including vascular endothelial growth factor (VEGF). However, direct bolus VEGF delivery into ischemic tissues has limited therapeutic potential due to lack of sustainable release. To effectively deliver VEGF to target site with spatial and temporal adequacy, we utilized a biosynthetic scaffold comprising of fibrinogen backbone crosslinked with polyethylene glycol (PEG). We explored the hydrogel's potential as a delivery matrix for VEGF and its effectiveness in inducing neovascularization in myocardial infarction model.

Methods: PEG-fibrinogen (PF) hydrogels were synthesized with their properties analyzed. VEGF was incorporated and the kinetics of VEGF release was studied. Acute myocardial infarction was generated in rodent models and the animals were randomly assigned to 3 groups; saline, PF and PF-VEGF (n=10 each group). A total volume of 150ml of either saline or hydrogel was injected in infarct and peri-infarct areas of the myocardium. The animals were monitored for 4 weeks and myocardial function was assessed using echocardiography. Myocardial tissue samples were harvested for Hematoxylin & Eosin, Masson Trichrome and a-smooth muscle actin stain-

ing to assess the extent of fibrotic scar and arteriogenesis.

Results: PF-VEGF hydrogels showed a sustained slow release over 30 days. Highest degree of cardiac muscle preservation was observed in PF-VEGF-treated animals. PF-VEGF-treated animals showed the best improvement in ejection fraction (PF-VEGF= $74.68\% \pm 4.23$, PF= $64.15\% \pm 2.64$, saline= $41.86\% \pm 7.32$), left ventricular internal dimensions, end-systolic and end-diastolic volumes. Higher degree of arteriogenesis was seen in animals treated with PF-VEGF hydrogels (Infarct area: PF-VEGF= 33.3 ± 6.75 , PF= 18.1 ± 3.80 , saline= 8.29 ± 2.87 ; Periffinfarct area: PF-VEGF= 10.8 ± 2.78 , PF= 8.2 ± 1.91 , saline= 3.83 ± 1.27 blood vessels/200x magnification field, $p < 0.05$).

Conclusion: This study demonstrated that PF hydrogel is a suitable and efficient matrix for VEGF delivery in restoring the ischemic myocardium. In addition to providing mechanical support, PF-VEGF provided a sustained and controlled release of VEGF in the ischemic tissue resulting in improved neovascularization and cardiac function.

ID: 864

B10: 5

Towards cardiac constructs with physiologically relevant dimensions for heart regeneration

Evelyn Nguyen^{1,2}, Udi Sarig¹, Tomer Bronshtein², Freddy Yin Chiang Boey¹, Subbu S. Venkatraman¹ and Marcelle Machluf^{1,2}

¹School of Materials Science and Engineering, Nanyang Technological University Singapore; ²Faculty for Biotechnology and Food engineering, Technion, Haifa, Israel.

Cardiac Tissue Engineering receives much attention as an important approach for heart regeneration. Previous studies demonstrated the use of thin scaffolds (<1 mm) to patch the infarcted area, with limited clinical applicability. We recently reported the isolation of thick (> 10 mm) porcine cardiac extracellular matrix (pcECM) having clinically relevant dimensions and resembling the native tissue with its inherent vasculature. This study focuses on reproducing optimal cell environments for pcECM re-cellularization leading to physiologically relevant cardiac constructs.

Mesenchymal stem cells (MSCs) were shown to better attach and grow on decellularized pcECM treated with nitrocellulose compared to other biochemical treatments. Dynamic culturing was shown to support not only cell survival but also cell growth for up to 14 days which also led to a much deeper cell infiltration into the tissue bulk (>0.8 mm) compared

with static culturing (<0.1 mm). Most reseeded MSCs retained lineage integrity as evident by their constitutive expression of typical MSC markers: CD73, CD90, CD44, CD105 and CD29. Surprisingly, ~30% of reseeded MSCs have shown positive expression of CD31, an endothelial positive marker suggesting ECM induced MSC-to-endothelial transition.

Taken together, those preliminary results support the feasibility of obtaining physiologically relevant cardiac constructs by combining reseeded thick pcECM with preserved vasculature, growth factors and our customized bioreactor system for deeper cell infiltration. The results also present cues towards MSC-endothelial trans-differentiation, which may have been triggered by the pcECM composition.

ID: 460

B10: 6

Development of cartilaginous tissue in chondrocyte-agarose construct cultured under traction loading

Keisuke Fukuda¹, Seiji Omata² and Yoshinori Sawae³

¹Graduate school of Engineering, Kyushu University, Japan;

²Research Center for Advanced Biomechanics, Kyushu University, Japan; ³Faculty of Engineering, Kyushu University, Japan.

In this study, chondrocytes isolated from bovine cartilage tissue were seeded in agarose gel and resultant chondrocyte-agarose constructs, a well-established experimental model to examine the effect of mechanical loadings on the chondrocyte metabolism, were cultured with a traction loading on the construct surface to examine its effect on the regeneration of the cartilaginous tissue by chondrocytes. Custom-designed mechanical loading equipment was developed to apply the traction loading on the upper surface of constructs being cultured in the CO₂ incubator. After 2 or 3 weeks culture, quantities of glycosaminoglycan (GAG) molecules that proteoglycan, and type II collagen were determined, and immunofluorescent staining of keratin sulfate, a type of GAG, and type II collagen was performed to verify the chondrocyte biosynthesis of extra cellular matrix (ECM) and characterize the structure of elaborated cartilaginous tissue by confocal laser scanning microscopy (CLSM). Results indicated that the traction loading enhance ECM biosynthesis in the surface region of constructs and collagen rich layer covered with GAG rich superficial layer was formed in the articulation surface. Results of quantification for ECM molecules indicated that the production of type II collagen and GAG was more significant outside the slide track compared with inside the slide track.

Session	D6: Biomedical Devices
Date/Time	7 December 2013 09:00–10:30 hrs
Venue	SR-05 & 06

ID: 322

D6: 1

Development of low-temperature sterilization device using atmospheric-pressure plasma

Kazuhiro Nakamura², Daisuke Yoshino¹, Tomoki Nakajima¹ and Takehiko Sato¹

¹Institute of Fluid Science, Tohoku University, Japan; ²Graduate School of Engineering, Tohoku University, Japan.

Medical instruments are generally sterilized by using high pressure steam, ethylene oxide gas (EOG) or gamma radiation. However, the method of high pressure steam which becomes more than 121°C and 2 atm is not suitable for products using a low-heat resistant polymer. The EOG method can be handled at low temperature less than 60°C, but problems are its longer sterilization and aeration time, and the residual gas in the products. In addition, the method of gamma radiation is high in cost. Therefore, development of sterilization method with safety, low temperature and lower cost is expected. Plasma sterilization method has high potential as an alternative sterilization method of the conventional method. Using the atmospheric-pressure air plasma, we can easily generate effective chemical species for sterilization at low temperature. In this study, we developed a plasma sterilization device using circulating air flow, and verified the sterilization performance of the device. The sterilization verification was performed using the bio-indicators which use spores of *Geobacillus stearothermophilus* (ATCC 7953) and *Bacillus atrophaeus* (ATCC 9372), and this method guarantees 5 log reduction of the spores. The *G. stearothermophilus* and *B. atrophaeus* were sterilized in 25 and 35 min at room temperature, respectively. In the condition of atmospheric-pressure air plasma, the generated chemical species were mainly NO₂, and we revealed that there was a sterilization effect of the Ar gas that NO₂ was mixed beforehand. We also succeeded in reducing the generated NO₂ to less than several ten ppm using an air bubbling method.

ID: 222

D6: 2

Micro-fabricated membranes with regular pores for efficient pathogen removal

Majid Ebrahimi Warkiani^{1,2} and Hai-Qing Gong¹

¹Singapore-MIT Alliance for Research and Technology (SMART), Singapore; ²School of Mechanical and Aerospace Engineering, Nanyang Technological University, Singapore.

Rapid and accurate detection of pathogenic bacteria in drinking-water systems is a challenging problem. Numerous attempts are underway to develop new methods to isolate and recover waterborne pathogens such as *Cryptosporidium parvum* oocysts and *Giardia* cysts efficiently. Filtration based concentration techniques have been widely used for isolation and recovery of *C. parvum* oocysts into small volumes for downstream analysis. Negative features of commercial filters like rough surface, tortuous pore path and low pore density are the major factors which compromise their efficiency, lower their throughput and prolonged processing time in microfiltration process. Micro-fabricated membranes that contain pores with the same size and shape can overcome these micro-structural defects. The fabrication process allows enough flexibility to control the porosity and pore geometry according to desired application in order to have higher flow rate, lower clogging ratio, better recovery and enough reliability. An isoporous polymeric microfilter was fabricated and validated for concentration and recovery of *C. parvum* and *Giardia* (oo)cysts from tap-water according to the EPA standard protocol. Microfiltration results of the isoporous polymeric microfilter revealed that using a simple back-flushing procedure, more than 90% of the *C. parvum* and *Giardia* (oo)cysts spiked in the tap-water samples can be recovered, indication greater performance than available commercial microfilters. This research demonstrated the potential application of micro-fabricated filters with regular pores for large-scale filtration and monitoring of *C. parvum* and *Giardia* (oo)cysts contamination in drinking-water distribution systems.

ID: 744

D6: 3

Development of seizure monitoring and control systems for epileptic animal models

Sheng-Fu Liang¹, Yu-Lin Wang² and Fu-Zen Shaw³

¹Department of Computer Science and Information Engineering, National Cheng Kung University, Taiwan; ²Biomedical Electronics Translational Research Center, National Chiao Tung University, Taiwan; ³Department of Psychology, National Cheng Kung University, Taiwan.

The worldwide prevalence of epilepsy is approximately 1%, and 25% of epilepsy patients cannot be treated sufficiently by any available therapy. Recently, alternative techniques, such as vagus nerve stimulation and deep brain stimulation have been proposed for open-loop seizure control. However, the efficacy of intermittent stimulation may decrease due to neuron acclimation. A closed-loop device is more likely to achieve seizure control than an open-loop seizure controller. The objectives of this study are first to develop various epileptic rat models, second to develop a portable wireless closed-loop seizure controller including on-line seizure detection and real-time electrical stimulation for seizure elimination, and third to apply the developed seizure controller to the animal models to perform on-line seizure elimination. Three epileptic rat models including Long-Evans rats with spontaneous absence epilepsy, pentylentetrazol (PTZ)-induced convulsive seizure, and temporal lobe epilepsy (TLE) induced by amygdala kindling were successfully developed. A wireless brain-behavior monitoring system that can acquire EEG and accelerometer signals simultaneously was designed and it demonstrates successful observation of kindling process and reduces the wire artifacts of EEG signals during convulsions. A portable seizure controller consists of neural interface with EEG acquisition and electrical stimulation, and on-chip seizure detection was developed. All of the components have been further integrated in the chip-on-board and system-on-chip platform.

ID: 216

D6: 4

Challenges and trade-offs involved in designing embedded algorithms for a low-power wearable wireless monitor

Miguel Hernandez Silveira¹, Su-Shin Ang² and Alison Burdett³

¹Toumaz Healthcare Ltd, United Kingdom; ²Toumaz Healthcare Ltd, United Kingdom; ³Toumaz Microsystems Ltd, United Kingdom.

Patient monitoring is an important part of healthcare workflow in hospitals. In the general ward, nurses typically check on patients three times a day by manually measuring and taking note of vital signs every eight hours. Sometimes this results in misdetection of adverse physiological events, which in turn may lead to severe and irreversible conditions. Although conventional bedside monitors could be used in general wards, they are expensive and impractical for ambulatory patient monitoring (bulky size and wires restricting patients' mobility).

Based on our Sensium[®] system-on-chip Toumaz has recently developed wearable, low cost technologies

for healthcare ambulatory monitoring. The SensiumVitals® is an end to end system that incorporates a new and alternative concept in wireless monitoring – the digital patch. This wireless, unobtrusive, lightweight and disposable body-worn device is capable of continuously acquiring and processing vital signs information from patients (temperature, heart rate and respiration rate) in real-time. To achieve this, the digital patch runs a number of embedded algorithms, and then wirelessly transmits every two minutes the data to bridges and servers for interpretation and display. This enables continuous monitoring of patients and early detection of physiological adverse events; thus alerting clinical staff about potential patient deterioration that may cause irreversible damage and in some cases fatal consequences if untreated.

Unfortunately, one major issue of healthcare ambulatory monitoring technologies is the negative impact of body movement on the quality of the physiological data. Motion artifacts (MAs) often distort the ECG signals and compromise the reliability of vital signs computation. Furthermore, MA and heart contaminants are responsible for inaccurate results when processing respiration rates from impedance pneumography signals.

In this paper we briefly describe of our system and embedded algorithms, including how we dealt with different disturbances affecting the quality of the signals. Finally, we present preliminary results of the evaluation of our SensiumVitals® in terms of accuracy and performance of our algorithms when compared with a validated/clinical vital signs monitor.

ID: 388

D6: 5

Validation of blood vessel geometry reconstruction and of blood flow analysis by ultrasonic-measurement-integrated flow-structure interaction simulation system for small animals

Sanga Sakanishi, Toshiyuki Hayase, Kenichi Funamoto and Shusaku Sone

Tohoku University, Japan.

Circulatory diseases account for about 25% of all deaths in the world. As revealed by many studies, including animal experiments, the development and progression of circulatory diseases are closely related to hemodynamics. As a new methodology to analyze hemodynamics in small animals, we have developed an ultrasonic-measurement-integrated flow-structure interaction (UMI-FSI) simulation system, in which ultrasonic measurement on blood flow and vessel geometry is fed back to the fluid-structure interaction simulation. In previous studies using this system, we

obtained unsteady three-dimensional (3D) hemodynamics of a mouse carotid artery and validated the accuracy of Doppler velocity measurement. However, the accuracy of the reconstructed 3D blood vessel configuration and that of the analysis results of hemodynamics obtained by the system had not yet been verified. Validation of the system is necessary for its use in animal experiments. In the present study, we investigated the accuracy of the reconstruction of the blood vessel configuration and of computation of hemodynamics by the UMI-FSI simulation system. As a preliminary study, we analyzed a fully developed steady flow in a straight ultrasound flow phantom to evaluate the reconstructed vessel configuration and the analyzed flow field, and improved the system as necessary. We then analyzed blood flow in a mouse carotid artery using the improved system and compared the results with the former ones. The image processing of the B-mode image of the present ultrasonic equipment was found to result in a vessel shape with an 11% smaller diameter in the ultrasound beam direction. With modification of the method for extraction of the vessel configuration, the UMI-FSI simulation accurately reproduced both the vessel geometry and the theoretical velocity distribution of the developed laminar flow. The result of hemodynamics in a mouse carotid artery showed increased blood vessel diameter and blood flow rate in comparison with the former result.

ID: 504

D6: 6

Design of a right ventricular simulator for the evaluation of artificial pulmonary valve

Yusuke Tsuboko¹, Satoshi Matsuo², Yasuyuki Shiraishi³, Hidekazu Miura³, Akihiro Yamada¹, Mohamed Omran Hashem⁴, Takuya Ito¹, Kyosuke Sano¹, Yasunori Taira¹, Toshinosuke Akutsu⁵, Zhonggang Feng⁶, Mitsuo Umezu⁷, Masaaki Yamagishi⁸, Yoshikatsu Saiki² and Tomoyuki Yambe^{1,3,4}

¹Graduate School of Biomedical Engineering, Tohoku University, Japan; ²Department of Cardiovascular Surgery, Graduate School of Medicine, Tohoku University, Japan; ³Department of Medical Engineering, Institute of Development, Aging and Cancer, Tohoku University, Sendai, Japan; ⁴Department of Medical Engineering and Cardiology, Graduate School of Medicine, Tohoku University, Japan; ⁵Department of Mechanical Engineering, Kanto Gakuin University, Japan; ⁶Graduate School of Science and Engineering, Yamagata University, Japan; ⁷TWIns, Waseda University, Japan; ⁸Department of Pediatric Cardiovascular Surgery, Children's Research Hospital, Kyoto Prefectural University of Medicine, Japan.

Prosthetic materials are used for right ventricular outflow tract (RVOT) reconstruction in cases of congenital heart defects with right ventricular outflow hypoplasia or atresia and for pulmonary valve

replacement in the Ross procedure. This procedure is to replace the stenotic pulmonary heart valve such as hypoplastic RVOT by the artificial valved conduit in infants.

The authors have been developing a mechanical mock circulatory system for the evaluation of RVOT reconstruction. Improving the inflow characteristics of the right ventricular function and pulmonary circulatory hemodynamics was essentially necessary for more precise evaluation of newly designed heart valves. We developed an original pediatric pulmonary mechanical circulatory system, which was capable of simulating normal pulmonary hemodynamics in children. The system consists of a pneumatic-driven silicone right ventricle, a pneumatic-driven right atrium with a bileaflet polymer valve, a pulmonary valve chamber with a visualization port, a pulmonary arterial compliance tubing, a pulmonary peripheral resistance unit, and a venous reservoir. The mechanical interaction between the right atrium and ventricle was pneumatically controlled by the originally developed microcomputer. Transvalvular pressure waveforms were measured by the pressure transducers and the pulmonary flow was obtained at the outflow portion of right ventricle by the electromagnetic blood flow probe.

As a result, Hemodynamic waveforms of either the right ventricle or atrium were obtained at the revised pulmonary mock circulatory system. The characteristics with atrial kick were well simulated as the natural hemodynamics. Moreover we could examine the effects of the bulging sinus structure on the valve leaflet motion in the vicinity of the leaflet as well as the atrial contraction.

In this study, we simulated natural hemodynamics in our pulmonary circulatory system. We concluded that the simulation of right atrial contraction was inevitable in the quantitative examination of right heart prosthetic valves for congenital heart failure.

Session	C11: Cell Mechanics
Date/Time	7 December 2013 09:00–10:30 hrs
Venue	SR-07 & 08

ID: 885 **C11: 1**

Conference Keynote:
Title not available at time of print

Theodoros Kofidis

National University Heart Centre, Singapore.

Not available at time of print.

ID: 488

C11: 2

Computer simulation of tissue morphogenesis based on multicellular dynamics

Taiji Adachi¹, Satoru Okuda² and Yasuhiro Inoue¹

¹Kyoto University, Japan; ²RIKEN, Japan.

During tissue morphogenesis, mechanical forces are coordinated and integrated by multicellular dynamics, leading to self-organizing phenomena controlled by orchestrated mechanical and biochemical signaling. Particularly, mechanical interactions among cells, which dynamically vary during the wide time range of developmental process, produce a variety of large-scale tissue shape and structure. Therefore, understanding such complicated tissue morphogenesis requires revealing the effects of mechanical actions at subcellular level on the multicellular dynamics. In this study, we propose a new mathematical framework that describes multicellular dynamics based on mechanical interactions among cells, and perform computational biomechanics analyses of tissue morphogenesis. The proposed model is based on a three-dimensional (3D) vertex model, in which each cell shape is expressed by a polyhedron and a shape of cell aggregate by a network composed by edges and vertices of the polyhedrons. In addition, cell configurations can be rearranged by reconnecting topological patterns of the network. By improving a reversibility of the network reconnections, we found that the proposed model, the reversible network reconnection model, can be applied for simulating 3D complicated deformations with large deformation during dynamic tissue morphogenesis. Furthermore, by modeling cell proliferation, the proposed model can also be applied for simulating mechanical effects of cell division and growth on tissue morphogenesis. Case studies have been conducted to demonstrate basic features of the proposed framework, showing that computer simulations using the proposed model enable us to predict a dynamics in tissue morphogenesis that is useful in discussing a cause-and-effect relationship in multicellular dynamics. This work was partially supported by the Funding Program for Next Generation World-Leading Researchers (NEXT Program: LR017) from the Japan Society for Promotion Science (JSPS).

ID: 690

C11: 3

Quantitative analysis of endothelial cell response to fluid shear stresses

Chuh Khiun Chong and Alexander Thomas White

The Kroto Research Institute, Department of Materials Science and Engineering, The University of Sheffield, United Kingdom.

Introduction: Endothelial Cells (ECs) are known to be sensitive to fluid shear stresses. Abnormal level of stresses caused by disturbed flow *in vivo* is believed to be important in the development of vascular disease. Different fluid shear parameters e.g. wall shear stress (WSS), spatial and temporal WSS gradient (S/TWSSG) have been proposed, but how they affect the ECs are not fully understood. Further, it is difficult to differentiate their individual effects as they are often co-localised *in vivo*. This study aims to demonstrate the capabilities of a versatile flow-bioreactor system (F-BS) we recently developed by quantifying EC response to shear stresses.

Methods: Human umbilical vein ECs (HUVECs) were cultured in either a parallel plate or a converging flow chamber and subjected to physiologically-relevant time-averaged WSS, TWSSG, and SWSSG, by either imposing a steady or left coronary artery flow for 24 hrs in the F-BS. The WSS distribution was predicted computationally and mapped onto the morphology of HUVECs (alignment, elongation), quantified using our in-house developed image processing programme. Static cultures were used as controls.

Results: The F-BS shows good control over the flow (and therefore SS) waveforms. HUVECs showed clear alignment in the direction of the applied WSS for both pulsatile and steady flows that applied the same average magnitude of WSS. The alignment and elongation appeared to be slightly stronger for the steady than pulsatile WSS. Early results suggested that SWSSG produced a similar alignment response as WSS, and it appeared to depend primarily on the magnitude of WSS. Interestingly, the alignment and elongation of HUVECs correlated inversely with cell density, for all WSS conditions.

Summary: Quantitative response of HUVECs to shear stresses was demonstrated using our F-BS. WSS magnitude appears to exert a stronger influence on endothelial morphological changes than WSSG and this is dependent on the cell density.

ID: 429

C11: 4

The effect of the mechanical properties of cell membrane on its passive endocytosis process

Xinyue Liu^{1,2}, Yunqiao Liu², Xiaobo Gong² and Huaxiong Huang³

¹National University of Singapore, Singapore; ²Shanghai Jiao Tong University, China; ³York University, Canada.

Endocytosis is an energy-consumption process. Lipid bilayer of cell membrane (CM) and Nano-partical (NP) undergo elastic and bending deformation during endocytosis. To complete a passive endocytosis, the total deformation energy is assumed to be less than the receptor-ligand binding energy.

In the present work, a Quasi-static process of a NP endocytosis was studied. Helfrich-Skalak energy function was adopted to model the deformation of CM and NP as a system in 2D. At the initial conditions, a cylindrical NP on a CM flat which size is much bigger than the radius of the NP was assumed. The overall energy of the system was modeled and the equation was discretized for using mathematical optimization to find the minimum value under constraints: (1) volume conservation of NP, (2) tangent angle continuing and force balance at the edge points of CM and NP adhesion area, and (3) symmetric assumptions from NP axis to the infinity.

Different bending and elastic properties of cell membrane were studied and quantitative results showed that stiffer cells have larger energy barrier to finish a passive endocytosis. The internal forces and external loads of the system as well as the adhesion force were analyzed. It is found that an internal force jump appears at the separation point representing a concentrated load between the CM and NP. The concentrated load approaches its maximum value when the arc length of wrapping area is around one-quarter of the perimeter of NP, which may lead to rupture of receptor-ligand bonds. It is concluded that an additional constrain for a successful passive endocytosis is required for the interaction force between CM and NP has to be less than the receptor-ligand rupture force.

ID: 268

C11: 5

Viscoelastic property and cell adhesion process of cultured fibroblasts on different self-assembled monolayers monitored by acoustic wave biosensor

Yuvaret Viturawong¹, Sukumal Chongthammakun², Nuttawee Niamsiri³, Toemsak Sriksirin^{1,4} and Tanakorn Osotchan^{1,4}

¹Materials Science and Engineering Program, Faculty of Science, Mahidol University, Thailand; ²Department of Anatomy, Faculty of Science, Mahidol University, Thailand; ³Department of Biotechnology, Faculty of Science, Mahidol University, Thailand; ⁴Department of Physics, Faculty of Science, Mahidol University, Thailand.

A quartz crystal microbalance (QCM) technique was used to reveal the effect of alkanethiol self-assembled monolayers (SAMs) on the viscoelastic properties and cell adhesion process of cultured fibroblasts (L929), by measuring the change in frequency (Δf) and resistance (ΔR). Four types of SAMs having different functional groups including hydroxyl (OH), carboxylic acid (COOH), amine (NH₂) and methyl (CH₃) were used in this study. The QCM measurements during cell adhesion showed that floating cells were rapidly adsorbed on all functionalized surfaces as a soft cell monolayer which their stiffness was increased by cell spreading process. Initially, the Δf and ΔR were both positive shifts for COOH and NH₂ surfaces indicated fluid-like behavior of adherent cells. A multi-step decreasing of Δf and an increasing of ΔR were observed in case of COOH and OH surfaces represented solid-like behavior of cell spreading. The CH₃ surface was used as a control because no cell adhesion occurs. QCM responses and morphological changes during cell adhesion process were resulted from viscoelastic nature of mammalian cells. The changes of cell morphology and viscoelastic property during cell adhesion process strongly depend on the surface functionality which can be observed by QCM technique.

Acknowledgement: This research is partially supported by NANOTEC Center of Excellence at Mahidol University.

ID: 292

C11: 6

Dynamic modeling of tip cell migration incorporating filopodia dynamics in degradable 3-dimensional extracellular matrix

Min-Cheol Kim¹, Peter Chen^{1,4}, Roger D. Kamm^{1,2,3} and H. Harry Asada^{1,2}

¹BioSyM IRG, Singapore MIT Alliance for Research Technology, Singapore; ²Department of Mechanical Engineering, Massachusetts Institute of Technology, Cambridge; ³Department of Biological Engineering, Massachusetts Institute of Technology, Cambridge; ⁴Department of Mechanical Engineering, National University of Singapore.

Several prior works have incorporated reaction-diffusion systems in their 2-D or 3-D cell migratory models. These works, however, have considered only the secretion of MMPs from the cell body rather than phase change of the degraded ECM due to the secretion of MMPs, which is a moving boundary problem between the degraded ECM (solid phase) and cell culture medium (fluid phase) during sprout elongation. We have extensively developed an integrative tip cell migration model incorporating filopodia dynamics, focal adhesion (FA) dynamics, and cytoskeleton and nuclear remodeling in a computational cell model, as well as a computational reaction-diffusion model involving tip cell localized expression of soluble matrix metalloproteinases (MMPs) during sprout elongation in angiogenesis. This work is motivated by two experimental works: one shows traction dynamics of filopodia in compliant substrates, and the other shows that sprouting vessel diameters are inversely correlated with their elongation rates. These works suggest 1) two distinct regimes of traction dynamics of filopodia: "frictional slippage," with fast retrograde flow and low traction forces on stiff substrates and oscillatory "load-and-fail" dynamics, with slower retrograde flow and higher traction forces on soft substrates and 2) that MMP2 produced/activated at the tip cell may be a dominant mediator of matrix proteolysis and sprout diameter. The integrative tip cell migration model of this paper successfully incorporated two functions of filopodia, such as 1) environmental sensing and 2) force generation along filopodial-oriented actin bundles, reproduced these experimental results, and suggests the mechanism of tip cell migration in angiogenesis.

Session	E4: Bio- and Medical Robotics
Date/Time	7 December 2013 09:00–10:30 hrs
Venue	SR-12

ID: 858 **E4: 1**

Conference Keynote:
Robotics in gastroenterology: bench to beside, and beyond

Louis Phee

Nanyang Technological University, Singapore.

The combination of robotics and flexible endoscopy gives rise to significant benefits for patients and clinicians. The increased accessibility means more of the gastrointestinal (GI) tract could be inspected less invasively. Robotics also offers higher dexterity and manoeuvrability of the end effectors. Together with the minimally invasive nature of flexible endoscopy, more therapeutic procedures could be performed without unnecessary damage to healthy tissues. Robotics has been successfully introduced to improve colonoscopy, inspection of the small bowel and removal of GI cancers. In the near future, more GI procedures would be performed robotically. The GI tract could also serve as a good access point for robotic manipulators to reach other organs to deliver minimally invasive therapeutic procedures.

ID: 677 **E4: 2**

System identification of an active mechanical lung simulator in order to design a control regime

Tobias Laechele, Timo Zifreund, Christian Knoebel and Knut Moeller

Furtwangen University, Institute of Technical Medicine, Villingen-Schwenningen.

In modern medicine simplified mechanical or mathematical substitute models of the human body has become an effective method for analyzing processes, estimating parameters for diagnostic purposes and performing simulations. Active mechanical models of respiratory systems are consulted to train clinicians and medical staff as well as to optimize ventilator soft- and hardware. To provide a realistic scenario it is important to create a system that behaves as similar as possible to the physiological respiratory tract.

Therefore a novel concept for active mechanical lung simulation was developed. The design is based on a cylinder-piston-system employing an electromagnetic linear motor. Roll membranes are used for sealing allowing for smooth movement with low inner friction. For such a new system it is necessary to analyze the transfer behavior in order to develop an

appropriate control system. To determine the transfer function of the system, the frequency response for different motor positions was used.

For calculating amplitude and phase responses, the measured sinusoidal signals were approximated using a least-squares approach. Based on the calculated values, Bode diagrams were derived. As the Bode diagrams for all measured positions were comparable, it can be assumed that the transfer behavior over the whole piston travel range is constant.

Hence, one transfer function was determined by means of system identification that can now be used as a basis for designing the control regime.

This method represents an effective procedure to design a precise regime and makes it possible to design this new type of a realistic lung simulator.

ID: 172 **E4: 3**

An automatic system for batch microinjection of silkworm eggs

Chao Yu, Peter Chen, Daiwen Yang, Shengfeng Zhou and Hian Hian See

National University of Singapore, Singapore.

In this paper, we report the development of a novel prototype micromanipulation system for automatic batch microinjection of silkworm (*Bombyx mori*) eggs. The automatic batch process is made possible by (i) incorporating vision feedback in the system to determine whether the penetration point is appropriate, (ii) exploiting the force trajectory associated with the microinjection process by integrating force sensing capability into the system to ascertain the success of piercing the silkworm eggshell, (iii) designing a unique microinjection procedure to improve the efficiency of the automatic batch process, and (iv) synthesizing a visual-servo control. The effectiveness of the prototype micromanipulation system has been demonstrated and quantified through a set of experiments that yielded statistically meaningful results. These results show that the proposed prototype system provides a potential practical engineering solution for high throughput microinjection.

ID: 104 **E4: 4**

MR guided focused ultrasound positioning device for prostate cancer treatment

Christakis Damianou¹, Christos Yiallouras¹ and Nicos Mylonas²

¹*MEDSONIC LTD, Cyprus;* ²*Frederick University Cyprus.*

Object: A prototype magnetic resonance imaging (MRI)-compatible positioning device that navigates a high intensity focused ultrasound (HIFU) transducer

is presented. The positioning device has 2 user-controlled degrees of freedom (linear and angular).
Materials and Methods The positioning device was designed and fabricated using construction materials selected for compatibility with high magnetic fields and fast switching magnetic field gradients encountered inside MRI scanners. The positioning device incorporates only MRI compatible materials such as piezoelectric motors, and ABS plastic. The HIFU/MRI system includes the multiple subsystems: a) HIFU system, b) MR imaging, c) Positioning device (robot) and associate drivers, and d) Software. The system includes MRI compatible optical encoders.

Results: The MRI compatibility of the system was successfully demonstrated in a clinical high-field MRI scanner. The robot has the ability to accurately move the transducer thus creating discrete and overlapping lesions in biological tissue was tested successfully.

Conclusion: A simple, cost effective, portable positioning device has been developed which can be used in virtually any clinical MRI scanner since it can be sited on the scanner's table. The proposed system can be used in the future for clinical trials for prostate cancer treatment using HIFU.

ID: 188

E4: 5

Modeling of bioimpedance spectroscopy measurements for the process control of an orthopedic surgical milling tool

Christian Brendle¹, Annegret Niesche², Alexander Korff², Klaus Radermacher², Benjamin Rein¹, Andrea Scholl¹, Berno Misgeld¹ and Steffen Leonhardt¹

¹Philips Chair for Medical Information Technology (MedIT), RWTH Aachen University, Germany; ²Chair of Medical Engineering, RWTH Aachen University, Germany.

Surgical standard procedures such as the total hip replacement are essential to maintain individual mobility and life quality in aging industrial societies. As a consequence the number of these surgeries increases, but the used instruments do not guarantee the desired precision and application security in all cases. Due to this fact the integration of medical measurement methods like the Bioimpedance Spectroscopy (BIS), which is cheap, fast, accurate and unobtrusive, into surgical instruments for online process control and fault detection is suggested to solve this drawback. For example during the necessary bone cement (BC) removal at the revision of cemented artificial hip joints, for which in standard procedures hammers and chisels are employed man-

ually, unintended harming of the surrounding tissue has to be accepted. To improve this we developed an Impedance Controlled Surgical Instrument (ICOS), which enables BIS measurements during the BC removal by milling over the fast rotating milling head as active electrode.

To establish BIS as a measured variable for the control setup of surgical tools the dependency of the impedance on the specific process quantity is modeled. Besides we predicted the BIS values for our ICOS in finite elements method (FEM) simulations of the physiological operation scenario. Based on this an experimental *in vitro* set-up is designed, with Agar-Agar gel as tissue substitute and polymethylmethacrylate as BC substitute, and validated with FEM simulations to enable the reproducible trail and analysis of additional influencing variables. Thereby we model the BC removal with a variable capacitive impedance in dependence of the residual BC thickness and a constant serial impedance offset for the surrounding tissue. Based on the experimentally parameterized model a sensitivity analysis and first results of the feedback control will be given.

Session	A11: Medical Imaging
Date/Time	7 December 2013 11:00–12:30 hrs
Venue	SR-01 & 02

ID: 466

A11: 1

Finite element based tumor motion tracking based on 4D MRI thoracic data

Yuxin Yang¹, Soo Kng Teo² and Chueh Loo Poh¹

¹Nanyang Technological University, Singapore; ²Institute of High Performance Computing, Singapore.

Radiation therapy (RT) is one of the important and standard methods for the treatment of lung cancer. However, respiration motion poses a major challenge for optimal radiation delivery to the tumor in current RT as the tumor motion is not accounted for during the RT planning. Consequently, four-dimensional (3D + time) RT that involves the use of 4D imaging modalities is developed to address this problem by tracking the tumor motion during the entire respiratory cycle. In this study, we present the results of tumor tracking using a patient specific finite element (FE) lung model constructed using 4D-MRI. A series of 3D-MRI volume image of the lung were first acquired during free breathing to produce the 4D-MRI dataset. These volumes were then sorted into different respiratory phases. The volume at full exhale phase was chosen to be the reference volume and deformable image registrations were performed to align the subsequent volumes at other respiratory

phases to this reference volume. The surface displacement fields generated from registration were used as boundary conditions to deform the FE model constructed from the reference volume to the other respiratory phases. The tumor motion in the lung interior is then given by the FE model. Results shows that the predicted tumor motion from our FE model is in reasonable agreement with that computed from the original 4D-MRI images. The tumor trajectory follows a highly non-linear path during the respiratory cycle, which further strengthens the need for accurate tracking of the tumor as its motion is time-dependent. The advantage in our approach is that the material properties of the lung and tumor in the FE model can be optimized for individual patient to minimize error between the predicted motion and the actual tumor motion during the RT planning phase.

ID: 427

A11: 2

Evaluation by high-frequency ultrasound B-mode imaging of cerebral hemorrhage in mouse fetal brain resulting from ischemia/reperfusion

Kenichi Funamoto, Takuya Ito, Kiyoe Funamoto, Clarissa Velayo, Toshiyuki Hayase and Yoshitaka Kimura

Tohoku University, Japan.

Cerebral hemorrhage induced by hypoxic-ischemic events, such as intrapartum asphyxia, is a major cause of neonatal injury. Maternal nutrition during pregnancy is considered to be a significant preventive factor for cerebral hemorrhage; however, the exact mechanism has not yet been elucidated. Using a nutrient controlled mouse model, both areas susceptible to bleeding and the timing of cerebral hemorrhage were investigated during ischemia/reperfusion treatment with high-frequency ultrasonic equipment. Pregnant female mice in the undernutrition group were given a low protein diet, while those in the control group were given a normal diet. On day 17.5 of gestation, pregnant mice were anesthetized, and both uterine horns were exposed. At one horn, ischemia and reperfusion were induced by occluding and opening the uterine and ovarian arteries every five minutes. This sequential process was repeated three times for a total of 30 minutes. Before and throughout the treatments, coronal sections of the fetal brain were observed by high-frequency ultrasound B-mode imaging. Sequential ultrasound B-mode images of the same coronal cross section were successfully obtained during the whole ischemia/reperfusion treatment as well. Circular regions of interest (ROI), 0.35 mm in diameter, were selected to quantify the blood flow at the septal branch of the anterior cerebral artery (ACA), the

upper side of the third ventricle (3V), and the peripheral outer portions of both lateral ventricles (LVs). The relative intensities in all the ROIs of the normal fetal brain without hemorrhage (N = 5) slightly increased. In contrast, those of the undernourished fetal brains (N = 5) gradually decreased in the ACA and 3V ROIs, but increased in the LV ROIs with a large variation. This result implied that hemorrhage mostly occurred in the outer peripheral portion of the LVs during the second reperfusion.

ID: 651

A11: 3

Creation of the beam hardening artifact

Jan Kubiček

VŠB – TU Ostrava, Czech Republic.

This paper focuses on description, implementation and simulation of a specific artifact - Beam hardening - which occurs in CT examinations. The theoretical part of this paper describes background for formation of this undesirable phenomenon which influences considerably quality of final images. The practical part deals with simulation and viewing of the images with the Beam hardening artifact.

ID: 832

A11: 4

Semi automatic segmentation of breast thermograms using variational level set method

S. S. Suganthi¹ and S. Ramakrishnan²

¹Indian Institute of Technology Madras, India; ²Indian Institute of Technology Madras, India.

In this work, an attempt has been made to delineate the breast tissue from breast thermograms. Breast thermograms used for this experimentation and validation were taken from public database PROENG. Firstly, a spatially adaptive wavelet based denoising method was used to improve signal to noise ratio. Secondly, contrast-limited adaptive histogram equalization method was used to improve the contrast. Finally, an active contour based level set method using variational formulation without re-initialization was adopted to segment the region of interest. The segmented results were validated and evaluated against the ground truth taken from the database by calculating few overlap measures considering pixels in the region of interest. Further, the segmented results of preprocessed image were compared with the results obtained on raw images. The results demonstrated the accurate segmentation of region of interest using variational level set method. Better edges were observed by improving signal to noise ratio and contrast of the image. Consequently,

subjective and experimental analysis shows that the removal of noise and improvement in contrast led to precise segmentation of region of interest.

ID: 483

A11: 5

Viscoelastic properties of gel material and soft tissue measured by MRE (magnetic resonance elastography) using micro MRI

Hayato Suzuki¹, Mikio Suga², Kazuhiro Fujisaki³, Itsuro Kajiwara⁴, Gen Nakamura⁵, Kogo Yoshikawa⁶ and Shigeru Tadano⁴

¹Division of Human Mechanical Systems and Design, Graduate School of Engineering, Hokkaido University, Sapporo, Japan; ²Department of Medical System Engineering, Faculty of Engineering, Chiba University, Chiba, Japan; ³Department of Intelligent Machines and System Engineering, Faculty of Science and Technology, Hirosaki University, Hirosaki, Japan; ⁴Division of Human Mechanical Systems and Design, Faculty of Engineering, Hokkaido University, Sapporo, Japan; ⁵Department of Mathematics, Inha University, Incheon, Korea; ⁶Department of Mathematics, Faculty of Science, Hokkaido University, Sapporo, Japan.

Magnetic resonance elastography (MRE) was developed for detecting the region and the stage of disease by changing in the hardness of human tissue or organ. The MRE technology requires an external excitation system for generating transverse waves to the subject in the gantry of MRI. Stiffness of the organ is quantitatively calculated from the wave patterns through a mathematical model. Techniques to measure viscoelastic property of soft materials have been developed. For example, rheometer and ultrasound elastography has been generally used for gel materials and soft tissues. For example, rheometer and ultrasound elastography has been generally used for gel materials and soft tissues. Magnetic resonance elastography have an important role to measure a distribution of quantitative viscoelastic property under a keeping shape of soft material objects and an influence of frequency. In this study, we focused the viscoelastic property of gel material and soft tissue measured by the MRE based on the micro MRI (0.3 T) designed from a high-power vibration generator and a bar-type vibration transmitter. The MRE represent the viscoelastic property at a complex modulus $G^* = G' + iG''$. The storage shear G' and the loss shear modulus G'' shows elasticity and viscosity, respectively. Specimens made by gelatin gel and bovine liver and muscle. We report about influence of excitation frequency that is used 62.5 to 500 Hz and specimen boundary condition that fix each plane of the specimen. The G' of gelatin gel increase with the frequency. We will discuss about the boundary condition of the specimen and the soft tissue.

ID: 570

A11: 6

Automatic cervical cell classification using patch-based fuzzy clustering and minimum average correlation energy filter

Thanatip Chankong¹, Nipon Theera-Umpon^{1,2} and Sansanee Auephanwiryakul^{2,3}

¹Department of Electrical Engineering, Faculty of Engineering, Chiang Mai University, Thailand; ²Biomedical Engineering Center, Chiang Mai University, Thailand; ³Department of Computer Engineering, Faculty of Engineering, Chiang Mai University, Thailand.

Cell segmentation and cell classification are important steps in an automatic cervical cell detection system. In this paper, we propose a method to automatically segment and classify cervical cells. A nucleus is segmented using the patch-based fuzzy c-means (FCM) algorithm. Each segmented nucleus is classified as normal or abnormal using the minimum average correlation energy (MACE) filter. Low-frequency components of the MACE filter are discarded in order to reduce the complexity of computation. The accuracy of segmentation by the patch-based FCM is compared to the segmentation by the active contour model (ACM). The segmentation performance is evaluated by the probability of error and the Hausdorff distance comparing to the manual segmentation by an expert. The nucleus segmentation by using the patch-based FCM clustering method corresponds well with the expert's opinion and yields better results than the ACM. The overall segmentation error by the patch-based FCM is approximately 6%. Four-fold cross validation is performed to test the efficiency of the proposed MACE filter on both ACM- and FCM-based segmented images. Using the patch-based FCM segmentation together with the compact MACE filter yields a good classification rate of about 85% which is higher than that using ACM-based segmentation. The proposed segmentation and classification methods yield promising results for further development in an automatic cervical cell detection system.

Session	B11: Tissue Engineering
Date/Time	7 December 2013 11:00–12:30 hrs
Venue	SR-03 & 04

ID: 247 **B11: 1**

Design considerations for bioartificial liver devices

H. L. Leo, G. T. Tan, K. E. Birgersson, M. Tania, M. N. Hsu, L. Xia and Harry Yu

National University of Singapore, Singapore.

Even though liver transplantation remains the main curative option for patients suffering from fulminant hepatic failure (FHF), it is still plagued by problems of cost, donor scarcity and donor compatibility. The developments of bioartificial liver assist devices (BLADs) technology in recent years have traction in applications for the treatment of FHF. These BLA-type devices can serve as an extracorporeal support for liver failure patients, either allowing the patient's liver to regenerate, or to act as a bridge for liver transplantation. Numerical simulations have been routinely employed by tissue engineers as one of the important tools for the optimization of the bioreactor design physical parameters such as flow shear stress and mass transport of nutrient to the cell surface. In this presentation, we will share our experiences in the design and development of BLADs, reviewing the different techniques (sandwich culture, 3D spheroids). Important considerations include the perfusion of culture medium and the resultant fluid-induced shear stresses that act on the cell surfaces. Our earlier experimental data showed that the hepatocytes culture was sensitive to low wall shear stress of the order ~ 0.002 Pa. Flow rate exceeding ~ 10 ml/min could have detrimental effect on the cell culture as a result of elevated flow shear stress level, and lead to non-uniform distribution of mass transport across the cell surface. Our experimental and computational studies have shown that the mass transport of nutrients and gases need to be carefully calibrated and controlled for different BLADs designs. The interaction of among various metabolites such as albumin, urea need to be carefully considered in the design of BLADs since an effective removal of these metabolites can directly impact the overall performance of these devices.

ID: 857 **B11: 2**

A physiological three-dimensional tumor construct for chemotherapeutic testing

Pamela H. S. Tan¹, Su Shin Chia¹, Saminathan S. Nathan², James C. H. Goh^{1,2} and Siew Lok Toh¹

¹Department of Bioengineering, National University of Singapore, Singapore; ²Department of Orthopaedic Surgery, National University of Singapore, Singapore.

Progress in anticancer drug discovery has been hampered by the lack of good preclinical models. Standard preclinical protocols require the growth of cells in high throughput two-dimensional (2D) culture systems. Such *in vitro* drug testing methods yield drug efficacy results that differ greatly from animal models. Conversely, it is much more difficult and expensive to use xenograft models for large-scale molecular biology research. It is conceivable that three-dimensional (3D) growth may be responsible for some of these changes and that such growth may form a reproducible and more representative step in tumoricidal validation prior to animal implantation. It is hypothesized that 3D tissue engineered osteosarcoma solid tumor constructs are able to approximate *in vivo* cell physiology and chemosensitivity. The role of 3D culture on angiogenic potential and tumor growth was studied and there was an upregulation in the expression of angiogenic factors VEGF-A and IL-8 under 3D culture, as compared to 2D culture systems. 3D co-culture with immortalized fibroblasts resulted in a further increase in angiogenic potential, as observed from the upregulation in angiogenic factor expression and subsequent increase in endothelial cell migration towards the tumor construct. Although treatment targeting VEGF-A has been established for the inhibition of angiogenesis, the use of a monoclonal anti-IL-8 antibody was found to be more effective than anti-VEGF-A treatment in inhibiting endothelial cell migration. 3D culture also caused G1 cell cycle arrest, resulting in a significant decrease in susceptibility to doxorubicin, a cell cycle specific cytotoxic drug. Cytotoxicity results using the 3D tumor constructs were similar to *in vivo* xenograft mouse tumors. Finally, the tumor constructs were cultured in a bioreactor with replicated interstitial fluid pressure, and these constructs were found to closely approximate the subcutaneous tumors in SCID mice, with almost identical angiogenic factor expression profiles.

ID: 719

B11: 3

Mechanical variation and proliferation behavior in hydroxyapatite based scaffolds with mesenchymal stem cells

Phanny Yos, Md Abdul Kafi and Mitsugu Todo

Kyushu University, Japan.

Calcium phosphate bioceramics such as hydroxyapatite (HA) have widely been applied as scaffolds in bone tissue engineering because of high osteo-conductivity and biocompatibility. In the present study, continuous porous HA scaffold was fabricated using the template method. Human mesenchymal stem cells (hMSC) were then seeded into the HA scaffold up to four weeks to observe the proliferation behavior and variation of the compressive mechanical properties. The scaffold with hMSCs was also characterized by scanning electron microscopy (SEM). It was found that the compressive strength and elastic modulus tend to increase with increasing culture time due to proliferation and attachment of the cells. The HA scaffold was also found to be suitable for hMSC adhesion, spreading and proliferation. Moreover, improvement of cellular adhesion was achieved by introducing RGD (Arg-Gly-Asp) peptide into the HA scaffold. We can conclude that the HA scaffold provides good environmental conditions for hMSCs as an artificial extracellular matrix. It is also important to note that the cellular adhesion can be effectively improved by RGD.

ID: 703

B11: 4

Immune response of implanted aortic scaffolds decellularized by sonication treatment

Nurul Syazwani Ahmad Sabri¹, Azran Azhim^{1,2,5}, Yuji Morimoto³, Katsuko Furukawa⁴ and Takashi Ushida⁵

¹Malaysia-Japan International Institute of Technology, University of Technology Malaysia, Malaysia; ²IJN-UTM Cardiovascular Engineering Centre, UTM, Johor, Malaysia; ³Dept. of Int. Physiol. Bio-Nano Medicine, National Defense Medical College, Tokorozawa, Japan.; ⁴Dept. of Mechanical Engineering, The University of Tokyo, Hongo, Japan.; ⁵The Center for Disease Biology and Integrative Medicine, Faculty of Medicine, The University of Tokyo, Hongo.

Sonication treatment is used in the preparation of scaffold that was able to elicit minimal immune response following implantation. The aim of this study is to investigate the immunologic response of sonicatedly decellularized aortic scaffolds after 7 days of implantation in rat's subcutaneous tissue. In this study, aorta samples are sonicatedly decellularized at frequency of 170 kHz in the solution of 0.1% and 2% SDS detergents. It was followed by washing

process with PBS solution for 5 days. The treated samples are then evaluated histologically by Hematoxylin Eosin (HE) staining. The samples are subcutaneously implanted on the lower right thoracic cavity of Wistar rats. The implants are explanted and evaluated by HE staining. From the histological results, the implanted samples after sonicatedly decellularized with 2% SDS shows minimal immune response, compared to that decellularized with 0.1% SDS detergents. Hence, treated scaffolds that are sonicatedly decellularized with 2% SDS showed great potential as biomedical implants due to its ability in reducing the immune response to a minimal level.

ID: 856

B11: 5

Tissue engineering the intervertebral disc: a whole disc approach using silk-derived scaffolds and hydrogels with adipose-derived stem cells

Puay Yong Neo¹, Puijiang Shi¹, James Cho-Hong Goh^{1,2} and Siew Lok Toh^{1,3}

¹Department of Bioengineering, Faculty of Engineering, National University of Singapore; ²Department of Orthopaedic Surgery, Yong Lin Loo School of Medicine, National University of Singapore; ³Department of Mechanical Engineering, Faculty of Engineering, National University of Singapore.

The intervertebral disc (IVD) is a complex organ consisting of two main regions: the inner gelatinous nucleus pulposus (NP) and the outer fibrous annulus fibrosus (AF). A strategy that aims to regenerate the IVD as a whole is important for eventual clinical success. The objective of this study is to regenerate the IVD using an easily available stem cell source (ASCs) and combining it with silk-derived biomaterials to recreate both regions.

Silk fibroin was first doped with Polyvinyl Alcohol (PVA) hydrogels to form NP replicas. Characterization of its physical properties, namely swelling capability, degradation profile and porosity was carried out. ASCs isolated from New Zealand white rabbits were then seeded into the Silk-PVA hydrogels to study the ASCs hosting ability of the hybrid hydrogels. The tissue engineered AF component consists of knitted lamellae of silk scaffolds electrospun with a thin layer of nanofiber silk mat. To mimic the architecture of the native AF, a custom-made jig was fabricated to align the silk electrospun fibres across two rotating collector rods before being integrated with the knitted lamellae. ASCs were also seeded onto electrospun silk mats to study the compatibility of the mats with the ASCs.

Results showed that Silk-PVA hybrid hydrogels have better rehydration capability, swelling capacity, porosity and cell hosting abilities than pure PVA hydrogels. Alamar blue assay results indicate that

ASCs and ASCs cell-sheets seeded onto the electrospun mats remain healthy and viable for up to 28 days.

During loading/unloading in a native IVD, the NP swells and distributes its hydraulic pressure to the AF that is restraining it. It is difficult to achieve high mechanical strength properties in a newly tissue engineered AF, and hence a semi-rigid and yet cell compatible gel was fabricated as the NP, while allowing the tissue-engineered AF to strengthen with time.

ID: 369

B11: 6

Development of a lab-on-a-chip system with integrated sensors for 3D tissue engineering applications

Haseena Bashir Muhammad, Chiara Canali, Soumyaranjan Mohanty, Mette Hemmingsen, Maciej Skolimowski, Martin Dufva, Anders Wolff and Jenny Emnéus

Department of Micro- and Nanotechnology, Technical University of Denmark, Kgs Lyngby, Denmark.

Organ transplantation is often the primary life-saving medical approach for treatment of several diseases. However limitations in this procedure such as shortage of donor organs and tissue rejection have motivated research into the development of bioartificial organs as an alternative approach. In this work, the development of a novel, modular, microfluidic lab-on-a-chip system is presented, which is designed to engineer liver tissue in an *in vivo* mimicking environment. The system incorporates smart bioreactors, designed to support a 3D porous scaffold with embedded cells and integrated sensors for monitoring the development of the tissue. Each bioreactor is designed to accommodate a microporous scaffold having dimensions of $5 \times 5 \times 5 \text{ mm}^3$ and includes spatially distributed bioimpedance based sensors which penetrate the scaffold for real time monitoring of the distribution, proliferation and viability of cells under continuous perfusion conditions. To enable delivery of nutrients and removal of tissue culture waste products, the system also incorporates peristaltic pumps, motors and reservoirs. An array of eight bioreactors are included, to enable parallel tissue culture experiments for optimisation of parameters such as flow rate, and to allow screening of various stem cell differentiation factors.

The system components are fabricated using a combination of 3D rapid prototyping and microfabrication techniques. Proof of principle is demonstrated by culturing liver cancer cell line (HepG2 cells) in porous scaffolds based on polymers such as gelatin and polylactic acid.

The robust and versatile microfluidic platform presented in this work has a huge potential for 3D

tissue engineering applications. The novelty of the device is in the employment of combined micro sensing and polymer scaffold engineering approaches for 3D organ engineering. The use of integrated non-invasive sensing strategies, overcome limitations in traditionally adopted optical techniques, and enable monitoring of tissue development within otherwise inaccessible areas of a 3D tissue construct.

Session	C13: Biomimetics Musculoskeletal Mechanics
Date/Time	7 December 2013 11:00–12:30 hrs
Venue	SR-05 & 06

ID: 305

C13: 1

Gender differences in motion mimicry of simple tasks

Edwin Boon-Wee Neo, Jin-Huat Low, R. Gokula Krishnan, Luis Carlos Hernandez Barraza and Chen-Hua Yeow

National University of Singapore, Singapore.

Motion mimicry is an evolutionary ability that has persisted for millions of years from early hominids to modern humans. Early hominids needed this ability to share drawing, food-hunting and combat skills necessary for their communications and survival. The modern-day humans require this ability to share skills in activities like sports and surgery. Moreover, males are generally labeled as aggressive, initiating and assertive while females are sighted as gentle, dependent and observant. Therefore, this preliminary study sought to investigate and compare the motion mimicking ability between males and females during simple tasks. One female and one male instructor subjects were recruited, together with seven female and seven male copier subjects. For each gender, the instructor was asked to perform simple arm-raising and squatting tasks, while the copier was asked to copy the actions of the instructor. Female copiers were asked to mimic the actions of the female instructor while male copiers were asked to mimic the actions of the male instructor. Their motions were recorded using a motion capture system for at least three trials per task. In general, we found that copiers were comparatively better in mimicking the instructor's actions in the sagittal plane than in the frontal plane, suggesting that visual perspective of the instructor may play an important role in human motion mimicry. Interestingly, we also observed strong correlations between female instructor kinematics and female copier kinematics in the sagittal plane for the simple arm-raising and squatting tasks. On the other hand, relatively weaker correlations were noted between the male instructor kinematics and male frontal plane during the complex

task, indicating that gender could be a contributing factor towards human motion mimicry. Future works will look into brain imaging to identify gender differences in brain activation areas during motion mimicry.

ID: 264

C13: 2

Observation of filling process in injection molding for fabrication of bone biomodel

Masashi Ohtake¹, Kei Ozawa² and Makoto Ohta³

¹Graduate School of Engineering, Tohoku University, Sendai, Japan; ²Graduate School of Biomedical Engineering, Tohoku University, Sendai, Japan; ³Institute of Fluid Science, Tohoku University, Sendai.

The injection molding is one of the major process methods for fabricating specially for composite materials. This method is useful for fabricating complex shape and advanced properties of materials such as bone model, recycled plastics or building materials. A bone biomodeling requires a realistic mechanical properties and the geometry as use of mechanical tests of medical devices such as bone screw or drill. The development of bone biomodel also requires the composite materials and the method of an injection molding to produce a unified model for the tests. The mechanical properties of bone biomodeling, specially the strength or the fracture toughness have a strong relation not only to the compound condition, but also to the filling process under injection molding, because the geometry of bone has a large volume and the flow in the injection is not stable. Therefore, visualization of flow of materials in the molding is important to grasp the filling process and microstructure of the model. However, the observation of flow during the molding is hard because the molding system is, in general, not to be transparent. Ozawa et al. carried out the observation of flow behavior with tungsten fiber using micro-CT. The orientation and distribution of fibers shows the flow direction. However, the image of micro-CT scanning shows only "a result of the filling process of materials in injection". To reveal the filling process, we develop a visible system of injection by using Poly (vinyl alcohol) (PVA) solution with good transparency and capability of changing its viscosity. Then, PVA solution can be detected by using a camera for analyzing visualization process such as particle image velocimetry (PIV). We found PVA solution is useful for investigation of relationship between flow behavior and viscosity of the material in the injection molding.

ID: 227

C13: 3

Accurate modelling of finger kinematics using a statistically-reduced rigid body model

Kumar Mithraratne and Tim Wu

Auckland Bioengineering Institute, The University of Auckland, New Zealand.

This article presents a framework for modelling finger kinematics accurately with an optimal number of degrees of freedoms (DoFs). High temporal resolution motion data were acquired on the middle finger using a six-camera optical motion capture system with reflective skin mounted markers. A constrained multi-link rigid body kinematic model consisting of 13-degrees of freedom (two rotations and three translations for the metacarpophalangeal joint, and one rotation and three translations for each of the interphalangeal joints) was created. The model was then fitted to the acquired motion data to estimate the unknown rotational and translational DoFs. Furthermore, a nonlinear statistical relationship was defined between the joints' rotations and translations using partial least squares regression (PLSR) method reducing the number of DoFs to four rotations. Using this statistically reduced kinematic model, dexterous finger movements can be accurately and efficiently reproduced. A significant improvement was observed when compared to the conventional 4-DoF rotations-only model demonstrating the potential and practicality of the statistically reduced model. Moreover, the modeled relationship can be extended with statistical extrapolation to simulate gestures that are difficult to measure dynamically.

Session	C12: Molecular Biomechanics Tissue Mechanics
Date/Time	6 December 2013 11:00–12:30 hrs
Venue	SR-07 & 08

ID: 404

C12: 1

Visual haptic-based collaborative molecular docking

Xiyuan Hou¹, Olga Sourina¹ and Stanislav Klimenko²

¹Nanyang Technological University; ²Moscow Institute of Physics and Technology.

In this paper, we propose a novel approach to search for protein-protein complementary pairs in collaborative virtual environment. This method employs visual and force feedback tools to search for the optimal interaction between proteins. The search is manual with force feedback consisting of a repulsion or attraction force. We developed a prototype system

that allows real-time interactive visualization and manipulation of molecules with force feedback in virtual collaborative environment. In our system, we implemented haptic interface to facilitate the exploration and analysis of molecular docking. Haptic device enables both users to manipulate the molecules and feel its interaction during the docking process in collaborative virtual experiment on computer. In future, these techniques could help the user to understand molecular interactions, and could be used both in research and e-learning.

ID: 288

C12: 2

Langevin dynamics simulation of single-stranded dna transvenue through nanopore in external non-uniform electric field

Weixin Qian, Kentaro Doi and Satoyuki Kawano

Graduate School of Engineering Science, Osaka University, Japan.

Nanopore sequencers for deoxyribonucleic acid (DNA) have attracted significant attention to achieve high speed analysis with lower cost. TransVenue mechanisms of DNA through a nanopore are not only essential in polymer physics but also critical in single-molecule detection. We address the electrokinetic transport of single-stranded DNA (ssDNA) through a nanopore in the presence of external non-uniform electric fields. Herein, a long-chain DNA molecule is represented by a coarse-grained bead-spring model consisting of 400 beads connected with harmonic springs. Langevin dynamics simulations are performed to investigate the electrokinetic transport dynamics in solution. In the whole structure of a nanofluidic device consisting of microchannel, nanochannel, and nanopore, non-uniform electric fields are numerically analyzed by using the finite element method. Conformation changes of the DNA chain during the transVenue process is analyzed and we can predict a waiting time of ssDNA at the entrance of nanochannel before entering a nanopore, which is of great interest but difficult to observe in experiments. Our simulation results are expected to provide useful information to design an advanced nanopore devices for DNA sequencing.

ID: 370

C12: 3

Mechanical analysis of mineral and collagen phases in bone by raman spectroscopy

Masahiro Todoh and Shigeru Tadano

Hokkaido University, Japan.

Bone is often regarded as a composite of mineral particles of apatite crystals and organic matrix of Type I collagen in microscopic scale. The mechanical properties of bone tissues at macroscopic scale depend on the structural organization and each and both properties of constituents in the microscopic scale. Raman spectroscopy is known as useful tool for the analysis of material at ultra-structural level. The aim of this study are to observe the mechanical behaviors of mineral and collagen phases in bone tissues by using Raman spectroscopy, and to investigate the effects of mechanical properties related to bone ageing.

Cortical bone specimens of bovine femoral diaphyses (Age: 23 months and 9 years old) were prepared with a size of 10.0(L)x1.0(W)x0.5(T) mm, where the longer edges of specimens were aligned to the parallel or perpendicular to the femoral axis. Raman microscope system was used for the analysis of mechanical response of bone tissue under tensile loading by the micro-tensile device. The relationship between the Raman shift and applied stress were investigated by analyzing the Raman spectrum of bone tissues.

From all experiments, the Raman shifts of mineral and collagen phases to lower wave numbers were observed with increase of applied tensile stress. The changes in Raman shifts under femoral axial stress were relatively larger than that under circumferential stress. Also, the changes in the collagen shifts of 9-year old bone tissue significantly increased compared with 23-month old one. From these results, the Raman shifts of mineral and collagen phases in bone tissues were well related to the applied tensile stress. In addition, those relationships were dependent to the mechanical properties related to structural anisotropy or degree of ageing. It was confirmed that the mechanical analysis by Raman spectroscopy was sufficiently useful for the bone quality assessment for bone degeneration as osteoporosis.

ID: 512

C12: 4

Viscoelastic moduli of bovine cortical tissue measured by cantilever free vibrations of mm-sized specimen

Yuelin Zhang, Satoshi Yamada, Masahiro Todoh and Shigeru Tadano

Hokkaido University, Japan.

Not only elasticity but also viscosity of bone tissue is important mechanical properties for evaluating bone health condition and bone fracture risk. The aim of this study is to propose a method for measuring both elastic and viscous moduli of tissue level in cortical bone by using cantilever free vibration experiment of a small mm-sized specimen. The bending vibration

characteristics were formulated by a parallel model of a spring and a dashpot element.

The strip specimens of 15.0 mm in length 2.0 mm in width 1.0 mm in thickness were taken from the femoral cortical bone of a 23-month-old bovine in bone axial and circumferential direction. An initial displacement (0.20 ± 0.02 mm) was applied at the free end of the specimen for free vibration. The elastic and viscous moduli were calculated from a vibration wave measured by a laser extensometer.

As results, the elastic modulus of the specimens was 19.9 ± 1.2 GPa in the bone axial direction and 16.7 ± 0.6 GPa in the circumferential direction. The viscous modulus of the specimens was 26.4 ± 1.1 kPa's in the bone axial direction and 33.3 ± 4.3 kPa's in the circumferential direction. Therefore, this method had a possibility to quantitatively evaluate the viscoelastic moduli of tissue level in the cortical bone.

ID: 398

C12: 5

Assessment of tissue glycation on plantar tissue stiffness

Jee Chin Teoh and Taeyong Lee

National University of Singapore, Singapore.

Core pathological changes among diabetics occur at cellular level. Reactions between reducing sugars and cellular proteins leads to the formation of multiple compounds collectively referred to as advanced glycation end products. Accumulation of glycation end products accelerates age-related changes in the tissue, decreasing elasticity and stiffening the tissues. It is therefore postulated that plantar tissue stiffness serves as an indirect measure of tissue glycation, and in turn a reflection of the body's overall glycemic control.

There are several existing tools used by clinicians to assess ulcer risk in diabetic patients like monofilament, tuning forks, biothesiometers, neurothesiometers etc. However, these measure subjective sensing ability which only indirectly indicates foot ulceration risk. A prototype of a diagnostic tool which measures objective and direct plantar soft tissue properties was developed. The tester can directly probe the mechanical response of plantar soft tissue by inducing rate-controlled tissue deformation, similar to that experienced in walking. 35 normal and 5 diabetic subjects of similar physical attributes participated. During testing, indenter tip probed the plantar soft tissue to obtain localized mechanical response underneath the 2nd metatarsal head pad, hallux and heel. Maximum tissue deformation was set at 5.6mm (close to literature data).

The objective of this study is to investigate the relationship between plantar tissue stiffness and tis-

sue glycation due to diabetes mellitus. Eventually it is aimed to provide a preventive method to identify patients at a higher risk for diabetes related foot complications as well as suggesting a screening measure for patient's overall glycemic control. Preliminary data on a small sample of non-diabetic subjects and diabetic patients has been obtained. Notably based on the study conducted on the limited samples, tissue glycation resulted in stiffer tissue property. This study successfully demonstrated the positive relationship between tissue glycation and plantar soft tissue stiffness in a realistic manner.

ID: 452

C12: 6

Effects of the position of tongue on the sound generation of Sibilant/S/

Tsukasa Yoshinaga¹, Kazunori Nozaki² and Shigeo Wada¹

¹Graduate School of Engineering Science, Osaka University;

²Dental Hospital, Osaka University, Japan.

The sibilant /s/ is one of the fricative sounds produced by raising the tongue against the frontal palate of the mouth to form a constriction of the airflow. Thus, the movement of the tongue plays important roles in the sound generation of sibilant /s/. In this study, we investigated the effect of the tongue positions on the airflow and generation of the sibilant /s/ using an *in vitro* vocal tract model implementing a movable tongue. A replica model of vocal tract was produced by a 3D printer from the CT images of a subject who pronounced sibilant /s/. Steady airflow was given to the vocal tract model by compressor and the sound generated was measured with a microphone. The time variations of airflow velocity in the vocal tract were also measured with a hot wire anemometer. Our results showed that the power spectrum density of the sound generated by the vocal tract model quantitatively agreed with that of the sibilant /s/ from the subject by adjusting the position of the tongue. The flow measurements revealed that the flow fluctuation increased in the vicinity of the incisors rather than the constriction where the flow velocity was the highest. We found that the sound source of sibilant /s/ was produced by turbulence enhanced by the impingement of the airstream emerging from the constriction on the downstream incisors.

Session	E5: Rehabilitation
Date/Time	7 December 2013 11:00–12:30 hrs
Venue	SR-12

ID: 357 **E5: 1**

VASST: variable-speed sensing treadmill for gait retraining after stroke

Johnny Chee¹, Karen S.G. Chua², Wei Shin Yu¹, Wai Sing Ong¹, Calvin C.M. Hoo¹, Pang Hung Lim² and Wei Sheong Lim²

¹*Ngee Ann Polytechnic, Singapore;* ²*Department of Rehabilitation Medicine, Tan Tock Seng Hospital, Singapore.*

World Health Statistics indicate 15 million people worldwide will suffer stroke every year. In Singapore, there are 10,000 stroke patients annually (nearly 1 every hour!), and this is increasing rapidly as her population rapidly ages. Locally, stroke is a leading cause of disability. Despite advances in stroke management and rehabilitation, the prevalence remains stable and it is estimated that there are now 200,000 people living with the consequences of stroke in our community. For younger patients who form a minority of the population with stroke, they live with more remaining years of disability.

Approximately 45% of stroke survivors have residual impairments following stroke and 50% are unable to regain premorbid walking abilities and capacity, leading to reduced physical fitness, reduced mobility, osteoporosis risk and reduced quality of life and life expectancy. Furthermore, gait and balance impairments may increase the risks of falls, fractures, further disability and even death.

To retrain for proper walking, we collaborated with clinicians to develop a special treadmill (VASST) with multiple sensors, and a suspension harness to reduce fall risk during training. VASST overcomes the limitations and risks of standard treadmills used to train hemiplegic stroke survivors as VASST automatically adapts to the demonstrated ability of the trainee. This allows the therapist to individually customise gait re-training to each stroke patient so as to maximise recovery.

VASST was researched and developed over a period of about one and half years with funding of \$360,000 grant from the Singapore Ministry of Education. Our clinical collaborators from the Department of Rehabilitation Medicine, Tan Tock Seng Hospital, recently completed a successful pilot clinical trial for sub-acute stroke patients with moderate residual walking disabilities with promising results! This paper will present the key features of the treadmill and discuss the key findings of the clinical trial.

ID: 368 **E5: 2**

Monitoring system for home rehabilitation using smart phone

Masayuki Nambu¹ and Manabu Horiuchi²

¹*Osaka Electro-Communication University, Japan;* ²*Graduate School of Osaka Electro-Communication University, Japan.*

Monitoring systems of biomedical information is necessary for the home rehabilitation. We proposed some monitoring system using mobile phone. However, sensory system and communication system are independent. Therefore, it was difficult to use the system by elderly people. In this time, we developed the monitoring system of health conditions using smart phone. Several sensors such a accelerometer, gyro sensor, or temperature sensor are implemented to the usual smart phones. In addition we developed electrocardiogram (ECG) monitor using audio input. This system needs only a commercial electrode and a simple amplifier. We succeeded to acquire the ECG signal easily, using this simple ECG monitor. Since the consumption current of external circuit was 10 mA or less, it was able to drive for 24 hours or more, using a coin type lithium battery. As a result, we also confirmed that an electrocardiogram could be acquired continuously, as long as the smart phone could communicate.

By the way, when using this system for support of rehabilitation, data of subject must be able to be monitored from two or more places. We built the system which can monitor data by making a smart phone into a server using the framework of WWW. However, the IP address of a smart phone is not fixed, but whenever a user moves, an IP address will be changed. In order to solve this problem, we used the system which exchanges e-mail whenever an IP address changes at first. However, since a time lag occurred and it was an obstacle of continuous monitoring, we proposed another method. We installed the server which manages change of an IP address, and we call this server as match making server. Using this system, we tried to simultaneous access from five places, and we confirmed that monitoring of data was possible.

ID: 684 **E5: 3**

Finger and thumb rehabilitation device for stroke patients

Fook Rhu Ong and Boon Tat Yu

Singapore Polytechnic, Singapore.

Stroke is the leading cause of adult neurological disability in many countries, which include

Singapore, Australia and the US. There are more than 10,000 new cases of stroke in Singapore every year, and it is reported that more than half of the surviving stroke patients will require specialised rehabilitation to recover specific impaired motor function sufficiently to perform activities of daily living. Studies have shown that repetitive movement in a task oriented rehabilitation programme can support and enhance the overall recovery of the motor function.

One of the affected motor functions is the hand grasp and release in a timely manner. The objective was to design and build a rehabilitation device that can provide repetitive training to the fingers and thumb with feedback for performance monitoring and assessment.

The design uses a pin-jointed link mechanism which forms a closed-chain to allow stroke patients to exercise the combination of grasp and release actions. A servo motor is used to drive the link mechanisms for all the digits through a crankshaft to convert rotary motion to linear motion. The driving links are connected to the fingers and thumb through attachments to the fingers and thumb.

Bi-direction forces exerted on or by the fingers and thumb and their displacements are measured using custom-made force and displacement sensors respectively. The force measurement is not just for monitoring the rehabilitation performance, but also serves as a safety mechanism to stop the operation when an allowable rehabilitation force is exceeded. An additional safety feature is also incorporated to prevent excessive force being exerted on the thumb and fingers by disengaging the driving mechanism mechanically to release the finger and thumb attachments. A control program has been developed but requires further development for better interactive environment and rehabilitation monitoring and assessment.

ID: 807

E5: 4

Supine gait training device for stroke rehabilitation – design of a compliant ankle orthosis

Fang Ming Lim, Ruyi Foong, Kay Sin Goh, Qinglin Mok, Beng Hao Tan, Soon Leng Toh and [Haoyong Yu](#)

National University of Singapore, Singapore.

Stroke is the leading cause of chronic physical disability, including locomotion. Patients not only suffer the primary deficits of stroke which include impaired walking, paralysis and poor motor control, but also secondary implications due to lowered cardiovascular performance and musculoskeletal consequences. After the trauma, the Central Nervous System (CNS) undergoes continuous remodelling

through cerebral reorganization starting from the acute phase, in response to physical activity of the subject.

A Supine Gait Training Device is developed to enable patients to undergo gait training while lying in bed, thus allowing the early re-education of the CNS immediately after the trauma. Part of this device is the ankle orthosis. It encompasses the metatarsophalangeal (MTP) and tibiotalar (TBT) joints, which according to principles of neuroplasticity, must be activated in meaningful ways for effective rehabilitation. This paper will focus on the mechanical design of the ankle orthosis and its features of compliance and adjustability.

ID: 471

E5: 5

Performance evaluation of novel ankle-foot assist device for ankle-foot rehabilitation

[Takayuki Onodera](#)¹, [Ming Ding](#)², [Hiroshi Takemura](#)¹ and [Hiroshi Mizoguchi](#)¹

¹Tokyo University of Science/Japan; ²RIKEN-TRI Collaboration Center for Human-Interactive Robot Research, Advanced Science Institute, RIKEN, Japan.

In this research, we propose a novel ankle-foot assist device for rehabilitation. The developed device applies a Stewart platform mechanism to measure and assist the movements of a human ankle joint in six DOF. The Stewart platform mechanism adapts to the displacement of the rotation axis of a human ankle joint during the movement of a human foot. In this study, we investigate the accuracy of the performance of motion control of the developed device by conducting motion reproduction experiments. The developed device can follow frequency of 2 [Hz] and has sufficient speed for rehabilitation. The mean reproducibility of all subjects was 0.98. These experimental results show the validity of the proposed assist device, and the developed 6 degrees of freedom assist device could be used during ankle-foot rehabilitation.

ID: 847

E5: 6

Prospects of mechanomyography (MMG) in muscle function assessment during FES evoked contraction: a review

Morufu Olusola Ibitoye, Nur Azah Hamzaid and Ahmad Khairi Abdul Wahab

University of Malaya, Malaysia.

Significant number of research attempts are noticed lately on validation of efficacy of alternative paradigm for muscle function assessment such as MMG after exhaustive trials on voluntary and evoked EMG with limited clinical and experimental impacts. Enhanced performance of conventional FES application for the SCI patients remains elusive partly due to lack of precise prediction of muscle force and fatigue. Quantification of muscle performance by processing MMG parameters is increasingly reported due to availability of inexpensive, non-invasive and sensitive sensors. Substantially, analysis of isometric and dynamic muscle actions using MMG signal during FES evoked contractions are being documented. However, the literature base to holistically address the signal's applications to assess muscle performance with highlights on experimental and clinical practices could benefit from further validation. Sequel to a systematic literature survey, it is evident that MMG possesses certain salient potentials and further exploration and evaluation studies is suggested especially during evoked dynamic muscle action to further optimize the performance of FES system.

Poster Abstracts

Day 1 – Wednesday, 4 December 2013

Session Poster Session 01 (PO-01)

Date / Time Wednesday, 4 December 2013 / 11:00–17:00 hrs

ID : 124

PO-01 : 01

A forward-backward subsequence smoothing approach to designing clutter filter in color flow image

Zhiyuan Shen^{1,2}, Naizhang Feng¹, Yi Shen¹ and Chin-Hui Lee²

¹Department of Control Science and Engineering, Harbin Institute of Technology, China; ²School of Electrical and Computer Engineering, Georgia Institute of Technology, USA.

In color flow image (CFI), the prevalent clutter filters fail to accurately separate blood flow signal from the demodulated ultrasound echo signal containing undesired clutter with single-ensemble (S-E) samples of small pulse size. A novel clutter filter design framework based on forward-backward subsequence smoothing (FBSS) as an extension to the prevalent eigen-based method is proposed. The proposed FBSS algorithm simulates the multi-ensemble behaviors with only single-ensemble (S-E) samples such that a fixed-length segment of each S-E sample is considered as a short conventional S-E vector. By moving forward and backward one sample, many vectors of the same-length can be created. This process can be repeated until all sample points in the original S-E sequence is exhausted and the collection of these vectors are considered as a simulated M-E ensemble. The pulse size needed to guarantees a nonsingular property of autocorrelation matrix in the FBSS framework is usually three-quarter of those used in the Hankel framework. As a consequence, FBSS leads to a good discrimination between the clutter and blood flow components for the low-velocity blood flow signals. Based on the results obtained from a series of simulations, the proposed FBSS eigen-based filter is shown to achieve a superior performance to the state-of-the-art regression and Hankel-SVD filters in estimating the blood flow velocities.

ID : 139

PO-01 : 02

Validation of algorithm with noise tolerance methods to detect R-wave

Won Kyu Lee¹, Hong Ji Lee¹, Jeong Su Lee¹, Hee Nam Yoon¹, Soo Young Sim¹, Yong Gyu Lim³ and Kwang Suk Park^{1,2}

¹Interdisciplinary Program for Bioengineering, Graduate School, Seoul National University, Seoul, Korea; ²Department of Oriental Biomedical Engineering, College of Health Science, Sangji University, Gangwon-do, Korea; ³Department of Biomedical Engineering, Seoul National University College of Medicine, Seoul, Korea.

Long-term monitoring of electrocardiogram (ECG) is one of the basic measurement in healthcare and provides decisive information regarding cardiovascular system status. In all ECG applications, the R-wave detection is important. However, it is difficult to detect R-wave automatically because signals obtained in daily life frequently include noise from various sources. Daily life monitoring ECG signal is particularly measured over cloth during walking and sleeping states by using non-invasive sensor, so that it usually presents higher noise level. To improve detection accuracy under noisy condition, we developed algorithm which has some noise tolerance techniques that analyze characteristics of R-wave. The proposed algorithm was evaluated by using the records of the MIT-BIH Polysomnographic database and the data from non-intrusive vital sign monitoring system previously developed in our laboratory. Algorithm reliability was assessed by detection error rate (De), sensitivity (Se) and positive predictivity (P+). The result shows average De of 2.62%, average Se of 98.29% and average P+ of 99.03%. We suggest that our R-wave detection method is useful in the presence of noisy signals.

ID : 168

PO-01 : 03

Realization of rehabilitation device using MFER and wireless bio-signal transport

Hojong Chang^{1,2}, Song Jae Lee² and Sang Hyun Park¹

¹Bio Medical Team, Institute for Information Technology Convergence, KAIST; ²Electronics Engineering Department, Chungnam National University.

Most of current rehabilitation devices usually depend on pre-programmed processes provided by manufacturers. However, the pre-programmed processes in general can provide only standard treatments even when the needs for particular patients may be widely different. It is believed that the demand for devices that can be optimized individually to patients would increase rapidly. Thus we propose a smart rehabilitation device, in which movements of various parts are intimately linked to patient's bio-signal. The rehabilitation device proposed consists of transmission unit and reception (or processing) unit. In order to achieve real-time transmission of patient's bio-signal, the

transmission unit is implemented by adopting ZigBee technology that is based on based on IEEE 802.15.4, a low-power wireless network. The analogue bio-signal is converted to digital form by using the STM32F103RB chip, which is an MCU from the ARM Cortex M3 series. The digital form of the signal is then transmitted through CC2520, RF chip of IEEE 802.11.5. It is noted that the patient's bio-signal is encoded with MFER (Medical waveform Format Encoding Rules) that has been established by JAHIS (Japanese Association of Healthcare Information systems Industry), and thus it is compatible to other medical devices. Patient's respiration rate can be extracted by processing the signal received at the reception (processing) unit. The respiration rate is then converted into Control Signal(PWM wave) to subsequently control the motor that regulates the rate of reciprocating movement of the device. In this way, we have implemented a system in which both the intercommunication and real-time feedback between device and operation unit are achieved. With the movement of the device synchronized to the patient's respiration rate, patients become quickly stabilized mentally. We expect that the above concept would contribute to development of personalized rehabilitation device, which ensure the scalability and versatility of the patient's demands and bio-signals.

ID : 169

PO-01 : 04

Brainwave sub-band power spectral density characteristics for human brain balanced via three dimensional electroencephalographic model

Norfaiza Fuad^{1,2}, M. N. Taib², A. H. Jahidin², R. Mohd Isa² and M. E. Marwan³

¹Universiti Tun Hussein Onn Malaysia, Malaysia; ²Faculty of Electrical Engineering, University Teknologi MARA, 40450 Shah Alam, Selangor, Malaysia; ³Kolej Poly-Tech MARA Batu Pahat, 83000 Johor, Malaysia.

This paper discusses on the brainwave sub-band characteristics for different brain balancing index groups based on electroencephalogram (EEG) power spectral density. The EEG datasets have been collected from 51 healthy. There are three groups of brain balancing index; index 3 (moderately balanced), index 4 (balanced) and index 5 (highly balanced). The raw EEG data have done using pre-processing techniques, two dimensional (2D) EEG image development methods and then three dimensional (3D) EEG model development methods. Maximum power spectral density (PSD) was extracted from 3D EEG model. Some analyses done such as Shapiro-Wilk to test normality data, Z score

to observe data skewness and Pearson correlation to observe the relationship between sub-band for right and left side. The results show that by implementing maximum PSD, the pattern of brain balancing groups (index 3 to 5) can be clearly observed. The correlation of sub-band for left-right frontal increase when number of index increment. This indicates that the maximum PSD can discriminate the characteristic of brainwaves for brain balancing application.

ID : 174

PO-01 : 05

Controlling of backbone rehabilitation machine using real-time bio-signal feedback system

Hojong Chang^{1,2} and Song Jae Lee²

¹Bio Medical Team, Institute for Information Technology Convergence, KAIST; ²Electronics Engineering Department, Chungnam National University.

Recently, the number of people having severe spinal pains due to bad posture is increasing rapidly. The spinal diseases suffered by approximately 10% of the whole population are known to be chronic one. In addition, the demand for equipment of personalized medical care is increasing as a result of development of the e-health care system. Especially, conventional rehabilitation machines that provide some physical stimulation on the patient back have become popular as one of home health machines. We propose a rehabilitation machine that has been customized individually based on patient's bio-signals. The most important feature of the machine is its intelligence. Firstly, the back-stimulation is achieved by combination of the movement of the whole bed back and forth and the rolling of the bars underneath the patient's back. To achieve both stimulation and therapeutic effect improved, the machine is designed to use patient's own weight to tilt reversely the bed by an appropriate angle. The rolling bars would provide relaxing effect to patient's back muscles. Secondly, the sliding motion of the bed is synchronized with the patient's respiration rate. The rate of reciprocating movement is controlled by using feedback system, which is in turn synchronized to the patient's bio-signal (PPG, SpO₂, etc.). The new approach of utilizing the real-time bio-signals in designing customized rehabilitation machine may be applied to design other therapeutic machines. In the future, therapeutic machines that has been customized to patients may become established as home appliances.

ID : 185

PO-01 : 06

The research of high-speed data caching algorithm in the CCD/DR system

Jie Liu, [Zhangyong Li](#), Lifang Zhang and Chunyang Li

Chongqing University of Posts and Telecommunications, China.

Research using asynchronous FIFO and SDRAM to realize high-speed data caching algorithm in the CCD/DR system. According to the requirements of the imaging time of CCD/DR system, Using asynchronous FIFO as data buffer between CCD and ARM, FIFO in table tennis response mode, to realize the seamless data cache. When ARM sending and receiving data, using a pair of SDRAM to data cache, to realize the high speed data transmission. This scheme is efficient, stable, occupy less resources, very suitable for special application environment of CCD/DR system.

The author gratefully acknowledges the support of K. C. Wong Education Foundation, Hong Kong.

ID : 221

PO-01 : 07

Analysis of scalp electroencephalogram used in BCI

[Minoru Kuroiwa](#) and Kazushige Magatani

Tokai University, Japan.

In late years, a study of BCI (Brain Computer Interface) which can perform the apparatus control of the computer by using a signal occurring with the activity of the brain is performed flourishingly. It is expected that BCI technique will make possible to support of communication with general-paralysis patients. There are two types of BCI. One is an invasive type which can gain in high quality and stable brain signals, and the other is a non-invasive type which uses EEG (Electroencephalogram) measured from scalp. However, invasive type BCI requires a surgery which becomes cause of patient's burden. Therefore, the objective of this study is a development of a BCI system using EEG which is non-invasively measured from a scalp.

The EEG measurement system for BCI was experimentally developed and assessed. In order to find features of EEG, the EEG which was measured when a subject held his/her hand and the EEG which was measured when a subject imagined holding his/her hand were analyzed by the system. As a result, we could confirm the differences between right hand holding and left hand holding. And we also found that wide area of the brain tended to be activated when a subject held not the dominant hand. A similar tendency was found when a subject imagined holding his/her hand. Furthermore, the

tendency for frequency band of μ -wave to decay was observed in around motor cortex. From these results, we think that the development of the BCI system which uses these experimental results is possible in the near future.

ID : 224

PO-01 : 08

Ambient-noise effects on oscillatory neural activity during cognitive activation

[Kazuo Kato](#)¹, Satoshi Yasukawa¹, Kazunori Suzuki² and Atsuo Ishikawa²

¹Tohoku Gakuin University, Japan; ²Takekana Research and Development, Japan.

Few studies have examined how ambient noise affects intellectual activity performance in everyday environments. The purpose of the present study was to characterize the changes in oscillatory neural activity recorded in subjects who performed intellectual activities as they were exposed to amplitude-modulated Brownian noises that were similar to typical environmental noises.

Nine healthy men between the ages of 21–23 years participated in the study. Subjects performed a verbal and spatial task that used an N-back task paradigm to study working memory. During the task, subjects were presented with the following 4 auditory stimuli: (1) a sound with frequencies similar to Brownian noise (no modulation); (2) a sound with an amplitude modulated between 0.05 and 1 Hz, and with frequencies similar to white noise (slope of power spectral density, $1/f^0$); (3) pink noise ($1/f$); and (4) Brownian noise ($1/f^2$). Electroencephalographic data were recorded, and the event-related synchronization and desynchronization for each visual stimulus were analyzed on the basis of their inter-trial variances of wavelet coefficients for theta band (4–8 Hz) activity.

In all conditions, we observed theta-band event-related synchronizations near the central area at latencies between 240 and 340 ms. During the verbal task, the variance in theta activity in the left-frontal area at F_5 increased as the low-spatial-frequency component increased when the sounds changed between white and Brownian noise. The opposite frequency-dependent response was observed during the spatial task. The differences in variance observed between white and Brownian noise presentations were significant between the tasks. We conclude that these frequency-dependent activities may reflect the neural activity that processes amplitude-modulated sounds during working memory tasks.

ID : 225

PO-01 : 09

A study on the closed loop robot arm control system using SEMG

Yuma Hiramatsu and Kazushige Magatani

Tokai University, Japan.

In this study, we use SEMG (Surface EMG) that can be derived from the skin surface in order to develop the system which can operate an artificial hand like as a human hand. The previous developed system used a pull solenoid to display grip power to the user. Using this display, the system could feed back grip power to the user. However, from results of experiments it was apparent that more precise resolution of the display is necessary. From these reasons the new grip power display which uses a manchette in order to display the grip power by air pressure has been experimentally developed. A manchette is an air bag which is used at a blood pressure meter in order to put pressure on the upper arm. We thought that new system can display grip power easier than previous system.

In our new system, SEMG of 48 channels are measured from forearm by using a multi-channel electrode. Measured SEMGs are amplified 4000 times, and converted to digital value in a personal computer. In a PC, user's hand motion is estimated by using measured SEMGs. If the estimated result is "grip", user's grip power is calculated using amplitude of measured SEMGs. The grip force of a robot hand (or an artificial hand) is controlled based on a calculating result. A force sensor is set on a robot hand and the output of the sensor is analyzed in a one-chip microprocessor. And then based on analyzed result our new grip power display presents grip power of a robot hand as the air pressure of a manchette. In this paper, we will describe about our new developed system and the results of experiments using our new system.

ID : 231

PO-01 : 10

Long-range correlations of stride time, stride length and stride velocity during feedback-controlled treadmill walking

Jin Seung Choi, Dong Won Kang, Jae Hyuk Bae, Yoon Ho Shin, Joo Hack Lee and Gye Rae Tack

Konkuk University, South Korea.

The gait fractal dynamics during between conventional treadmill (CTM) and feedback-controlled treadmill (FTM) walking were compared in this study. Seven healthy male subjects performed for 5 min walking with each treadmill condition. FTM can be tuned its belt speed to walker's speed, which controls

belt speed by walker's anterior-posterior location by using installed-loadcell under treadmill floor. Each subject's preferred walking speed was determined by FTM walking, and those were used for a belt speed of CTM. 3D motion analysis system was used for acquiring motion data of the toe and heel markers. To compare gait fractal dynamics in both treadmill conditions, a of detrended fluctuation analysis (DFA) was calculated. In general, α represents that it has persistence of long-range correlation or not ($\alpha > 0.5$: persistence, $\alpha \leq 0.5$, no persistence). The result showed that there was no significant difference in α of stride time between CTM and FTM while there were significant differences in α of stride length and stride velocity between both conditions. Especially, the long-range correlation of stride velocity was not persisted when they walked on the CTM while there is persistence in the FTM. It reveal that FTM walking, compared with CTM walking, was more similar to overground walking from fractal dynamics perspective. It is possible to apply for various walking studies by using FTM.

ID : 258

PO-01 : 11

A study of the influence which MP3 formatted sound gives EEG of the human

Daiki Yamaguchi and Kazushige Magatani

Tokai University, Japan.

Currently, many types of no-reversible compressed sound source, represented by MP3 (MPEG Audio Layer-3) are popular in the world and they are widely used to make the music file size smaller. The sound data created in this way has less information as compared to pre-compressed data. The objective of this study is by analyzing EEG to determine if people can recognize such difference as differences in sound. Measurement systems that can measure and analyze EEG when a subject listens to music were experimentally developed. And ten subjects were studied with this system. In this experiment, a WAVE formatted music data and a MP3 compressed music data that is made from the WAVE formatted data were prepared. Each subject was made to hear these music sources at the same volume. From the results of this experiment, clear differences were confirmed between two sound sources.

ID: 282

PO-01: 12

Feature evaluation of flow limitation in obstructive sleep apnea cases

Kang Ping Lin^{1,2}, Po-Chung Shih¹, Keng Hung Lin¹,
Wen Chen Lin², Ching Liang Yu³, Yun Yueh Liu³, Ya Ting Shih³,
Sheng Cheng Huang¹ and Yu Ju Chiang¹

¹Chung Yuan Christian University, Taiwan; ²Holistic Medical
Device Research and Development Center; ³APEX MEDICAL
CORP.; kplin@cycu.edu.tw

Purpose: Obstructive Sleep Apnea (OSA) is an airway obstructed during sleep, due to intermittent respiratory arrest disease. Flow limitation is an important symptom of OSA, but the method of detecting flow limitation was not clear now. Materials: Signal source record of clinical patients with Polysomnography (PSG), Capture identified as RERA respiratory flow different categories 47 cases respiratory flow signal, 10 cases marked normal, 37 cases marked flow limitation.

Method: Use 3 methods to Detect. (1) Flattening index (F.I) feature: Accepted standards for the majority of studies, the mean deviation of the inspiratory wave from the reference amplitude, for a middle portion of the wave are calculated. Weight F.I by F.I is based on the weighted improvements. (2) Value Weight: Weighted above average of inspiratory waveform data. (3) Time Weight: Weighted after the middle of inspiratory waveform data.

Results: Comparison 4 different detection methods analysis 47 cases of respiratory flow signal. The results of measurement, F.I could correctly distinguish the 41 cases, the error rate is about 12%. Value Weight could correctly distinguish the 42 cases, the error rate is about 10%. Time Weight could correctly distinguish the 41 cases, the error rate is about 12%.

Conclusions: Use described above 4 methods detection can be achieved correct rate of 80% or more. The value weight has the lowest error rate, Can clearly distinguishing severe and mild obstructive, is the best detection of 4 methods. The ability of F.I to distinguish mild and severe slightly inferior to Value Weight, but enhanced slightly discernment. The time weight is particularly suitable for distinguishing M shaped or square shaped respiratory patters indicative of partially obstructed airways.

ID: 296

PO-01: 13

Automatic registration of bone surface models with biplanar fluoroscopic images for 3D kinematic analysis of human foot

Kohta Ito¹, Naomichi Ogihara¹, Koh Hosoda², Kenichi Narioka²,
Shinnosuke Kume², Takeo Nagura³, Toshiyasu Nakamura³,
Nobuaki Imanishi³, Sadakazu Aiso³ and Masahiro Jinzaki³

¹Department of Mechanical Engineering, Keio University,
Yokohama, Japan; ²Graduate School of Information Science and
Technology, Osaka University, Suita, Japan; ³School of Medicine,
Keio University, Tokyo, Japan

Quantifying skeletal movement of the human foot is crucial for understanding biomechanical function of the complex foot musculoskeletal systems that mechanically interact with the ground. Recently, X-ray fluoroscopy is used to quantify the 3D skeletal movements. In this study, we aimed to develop an automatic reconstruction method of the 3D foot skeletal movement using biplanar fluoroscopic images for 3D kinematic analysis of human foot.

We firstly developed a biplanar dynamic X-ray fluoroscopic system with Shimadzu Corporation, Kyoto, Japan for cadaveric studies of human foot. The system consists of two sets of x-ray sources and flat panels with a resolution of 2688 x 2208 pixels. We recorded biplanar X-ray videos of foot skeletal movement at 15 frames per second using the system. For 3D kinematic analysis of the foot bones, we developed an automatic method to register bone surface models with the two fluoroscopic images. Specifically, the 3D surface models of the foot bones were generated based on the computed tomography (CT), and a similarity measure between occluding contours of the bone surface models with the edge-enhanced fluoroscopic images was evaluated to reconstruct the position and orientation of each bone model in a 3D space. Collisions among the reconstructed bones were also evaluated to avoid penetration.

Using the biplanar X-ray fluoroscopic images and the proposed reconstruction methodology based on CT, we reconstructed 3D kinematics of the calcaneus with respect to the talus when a human cadaveric foot was in contact with the ground. The surface models of the two bones were successfully matched with the corresponding fluoroscopic images and the subtalar joint movement was quantified automatically. The present methodology must be undergone further evaluation, but the proposed framework may serve as an effective tool for understanding the morphofunctional relationships of the human foot.

ID: 308

PO-01: 14

The autonomic nervous system functions in integrated circuit design company employees during different working time

Chih Yuan Chuang, Cheng Nan Tsai, Ming Tsan Kao and Sen H. Huang

Pixart Imaging Inc., Taiwan

The purpose of this study was to investigate the autonomic nervous system functions in integrated circuit design company employees during different working time by analyzing heart rate variability (HRV).

The participants were twenty-six company employees aged between 23 and 44 years (mean: 34 years) that divided into two groups. The morning group was measured two minutes photoplethysmography (PPG) between eight thirty to nine thirty A.M.. The afternoon group was measured PPG between five thirty to six thirty P.M.. The peak-to-peak interval of heart pulse signals were analyzed using power spectral analysis to quantify the time and frequency domain properties of heart rate variability. Comparisons the HRV indices of two groups were performed with the Mann-Whitney U-test.

There was no significant difference between the mean age of two groups. Comparison of the quantitative heart rate variability measures of two groups revealed that the high frequency power (HFP), low frequency power (LFP), total power (TP) and standard deviation of normal intervals (SDNN) were significantly lower in afternoon group, compared with morning group ($p < 0.05$).

HRV analysis showed that both cardiovascular sympathetic (LFP) and parasympathetic (HFP) nervous system had decreased significantly by eight hours working. The TP and SDNN of heart rate variability is well known to be representative of the entire autonomic nervous system (ANS) activity of the heart, and hence our results suggest that the entire ANS function will withdrawal after hard working. Reduced ANS activity may be a consequence of work stress and fatigue. There are a lot of link from the condition of reduced HRV to cardiovascular disease. Therefore, these findings suggest that the HRV analysis should be used to assess the ANS function and the risk of cardiovascular disease in the employees of long-term working on computer.

ID: 314

PO-01: 15

Statics and positioning control of an underactuated wire-driven flexible robot arm

Zheng Li¹, Hongliang Ren² and Haoyong Yu²

¹The Chinese University of Hong Kong, Hong Kong S.A.R. (China); ²National University of Singapore, Singapore

In this paper, an underactuated wire-driven flexible robot arm is introduced. It is composed of a serpentine flexible backbone and a set of controlling wires. The backbone has ten vertebrae which are articulated by spherical joints and an elastic tube. Two pairs of orthogonally distributed wires control the joints' rotation. Static model of the robot arm is developed using the Newton-Euler method. In the model, forces acting on the backbone are divided into internal actuation and external loads. The loads can be various, including distributed force, lumped force, and moment. The actuation is equivalent to a lumped force and a moment at the distal end. Combined with the inverse kinematic model, wire motion needed to drive the backbone distal end to a given position and actuation needed to maintain the position are derived. In the meantime, the deformed backbone curve is obtained from the static model. The results are compared with experiment results.

ID: 316

PO-01: 16

Highly integrated, low cost, palm-top sized magnetic resonance relaxometry system for rapid blood screening

Nguyen Vo¹, Lan Chen¹, Weng Kung Peng¹, Yi Ming Zhou¹, Jongyoon Han^{1,2} and Xuening Liu¹

¹BioSystems & Micromechanics IRG (BioSyM), and Infectious Diseases IRG (ID), Singapore-MIT Alliance for Research and Technology (SMART) Centre, 1 Create Way, #04-13 Enterprise Wing, Singapore 138602; ²Department of Electrical Engineering and Computer Science, and Department of Biological Engineering, Massachusetts Institute of Technology, 38-841, 77 Massachusetts Avenue, Cambridge, MA 02139.

A highly integrated, palm-top sized radio-frequency Magnetic Resonance Relaxometry System (19cm x 16cm x 5cm, weigh 250g) is developed. In this work, we show strategy on how to integrate all the modules into a single mother board which consists of coin-sized permanent magnet, miniaturized radio-frequency microcoil probe, compact lumped-circuit duplexer, and single board 4-Watt power amplifier, in which a FPGA-based spectrometer is used for pulse excitation, signal acquisition and data processing. We demonstrated that by measuring the proton transverse relaxation rates from a large pool of natural abundance proton-nuclei presence in less than 1 μ L of red blood cells, one can indirectly deduce the relative

magnetic susceptibility of the bulk cells within a few minutes of signal acquisition time.

ID: 325

PO-01: 17

3D structured models of multi-cellular cancer spheroids

Reiko Minamikawa-Tachino¹, Ayane Itoh², Katsuya Nagayama²
and Kiyoshi Ogura¹

¹Tokyo Metropolitan Institute of Medical Science, Japan;

²Kyushu Institute of Technology, Japan.

Three-dimensional (3D) culture is a culture method to form three-dimensional multi-cellular cell spheroid. Cell morphology is different compared to conventional culture method using two-dimensional (2D) culture (monolayer culture). Multi-cellular spheroids are known to have closer characteristics to *in vivo* compared to monolayer cultured cells. The 3D culture enables to enhance *in vitro* tests for basic biological research as well as for therapeutics development.

The morphology of the spheroids is observed as 2D images by the optical microscope and may be often observed as their surface topography with the scanning electron microscope. The measurement procedure of the spheroids is still insufficient. The size of a spheroid is measured as its diameter of the region corresponding to the spheroid in the 2D image.

Therefore, we simulated the growth of multi-cellular cancer spheroids and formed 3D structured models of the spheroids *in silico* in order to improve the measurement procedure. The spheroid is defined as a cluster of spherical cells as particles. The number of cells is estimated based on their packing density. A particle model has been introduced to describe the interaction between particles and to track them. The force between the particles maintains the distance between them and their packing density. Nutrients are transported based on the diffusion equation. A cancer growth model is designed to give a cell cycle based on the interaction of nutrition and cell density, because cancer cells are known to form tumors due to unchecked growth arising from defects in cell cycle control.

In the obtained 3D structured models of spheroids, it was confirmed that growth activity was at a peak in the surface, slowing down toward the center. We will improve this work so that the simulation method enables to promote the effective test *in vitro* for cancer therapeutics development.

ID: 329

PO-01: 18

Effects of massage therapy intervention on autonomic nervous system promotion in integrated circuit design company employees

Chih Yuan Chuang, Cheng Nan Tsai, Ming Tsan Kao and Sen H. Huang

Pixart Imaging Inc., Taiwan

Massage is accepted as a universal means to help people to regain physical health. The purpose of this study was to investigate the autonomic nervous system function in integrated circuit design company employees who treated with massage by analyzing heart rate variability (HRV).

The participants were fifteen company employees aged between 28 and 45 years (mean: 37.5 years) treated with back, shoulder and waist massage. The treatment period was approximately 20 minutes. Measurement of photoplethysmography was obtained during 2 minutes before massage therapy as pretest and after massage therapy as posttest. The peak-to-peak interval of heart pulse signals were analyzed using power spectral analysis to quantify the time domain and frequency domain properties of heart rate variability. Comparisons the heart rate variability indices of pretest and posttest were performed with the Wilcoxon Sign-Rank Test. Comparison of the quantitative heart rate variability measures at pretest and posttest revealed that the heart rate (HR) was significantly lower and standard deviation of normal intervals (SDNN) was significantly higher in posttest, compared with pretest ($p < 0.05$).

Heart rate variability analysis showed that HR was decreased and SDNN was increased significantly by 20 minutes massage treatment. The decreased HR is related to physical or mental relaxation. The SDNN is well known to be representative of the entire autonomic nervous system of the heart. The results of this research suggest that entire autonomic nervous system and physical or mental state can be promoted with massage. Therefore, the massage therapy may be used to promote health in the employees with autonomic nervous system function withdrawal which was induced by working stress and fatigue.

ID: 330

PO-01: 19

Research of operation method of accessibility equipment for severely handicapped based on voluntary eye blink

Tetsuya Ohya¹, Yohei Nomoto², Hironori Koyama¹ and Masashi Kawasumi¹

¹Tokyo Denki University, Japan; ²University of Niigata Prefecture, Japan.

Serious disabled persons with motor disabilities such as amyotrophic lateral sclerosis and progressive speech impairment necessitates the use of an assistive communication aid. However, the disabled also need accessibility equipment to use the aids. This paper describes the research of the input method for the operation of the accessibility equipment which is used by the serious disabled. The input method is based on electro-oculo-gram (EOG) that is controlled by the disabled. EOG is a technique for recording eye movements and eye blinks through electrodes placed around the eye. If the disabled can create several patterns of EOG waveforms, multi-input method is realized using these differences. We previously reported the technique to identify voluntary eye blink appeared on the EOG. Because voluntary eye blink is simple operation, we investigate the possibilities of utilization of consecutive blinks and gaze.

- 1) We examined the influences of the consecutive voluntary eye blinks by changing the blink intervals. We revealed that the blinks in interval at <300ms generate a unique waveform of EOG.
- 2) Because it is possible to specify the point of gaze with rough accuracy by EOG, we also investigated if specifying approximate gaze positions could make different EOG.

The gaze positions results showed that the blink-evoked EOG waveforms were extracted at a reliability >95% when incorporating upward gaze and forward gaze. The results suggest that the incorporation of upward gaze and forward gaze has possibilities of realization of multi-input method.

ID: 332

PO-01: 20

Study of touch display in surrounding environmental information acquisition system for deaf-blind persons

Yoji Naganuma, Yuya Onishi, Tetsuya Ohya, Hironori Koyama and Masashi Kawasumi

Tokyo Denki University, Japan.

Surrounding environmental information on the approach of the person etc. is transmitted to deaf-blind person by the interpreter and caregiver. However, when the interpreter and caregiver leave the side, the deaf-blind person comes not to be able to

understand surrounding environmental information and feels insecurity. It is considered that the uneasiness can be reduced by presenting the distance and direction of the others from the deaf-blind person. To reduce this uneasiness, the surrounding environmental information acquisition system is developed in the study. This system is assuming use at home, since deaf-blind person spends a lot of time at home. The system is useful to understand the distance and direction of the others when the interpreter and caregiver are away from the side of deaf-blind person. The information are the direction and the distance from deaf-blind person to the others. The system can present the horizontal directions and the three distances, less than 1m, 1m to 2m, and 2m or more. Deaf-blind person can obtain the information via vibration of solenoid built in the touch display. In this paper, the appropriate shape of display and arrangement of presentation devices in the acquisition system for surrounding environment information for use were examined.

ID: 360

PO-01: 21

Classification of evoked potentials associated with error observation using artificial neural networks

Pantelis Asvestas¹, Errikos Ventouras¹, George Matsopoulos² and Irene Karanasiou³

¹Technological Education Institution of Athens, Greece;

²Institute of Communications and Computer Systems, School of Electrical and Computer Engineering, National Technical University of Athens; ³Institute of Communications and Computer Systems, National Technical University of Athens.

Observation plays an important role in learning processes. Human development takes place through observation. Observational learning studies indicate that the processes through which observation contributes to learning resemble mechanisms contributing to self-action learning. Scalp-recorded Evoked Potentials (EPs) reflect brain electrical activity related to processing of stimuli and preparation of responses. An EP waveform is recorded when an incorrect action is committed by a person called Error-Related Negativity (ERN). ERN is also recorded, with a longer latency and reduced amplitude, when errors are not committed but observed by the person whose EPs are recorded. In the present work the performance of a classifier that discriminates between EPs that are produced by observation of correct or incorrect actions is investigated. Initially, first-order statistical features (mean value, standard deviation, kurtosis, skewness, energy, entropy) from the histogram of each EP recording are calculated. Then, the most significant features are selected using the Sequential Floating Forward Selection (SFFS)

algorithm. The Artificial Neural Network (ANN) algorithm combined with the leave-one-out technique is used for the classification task. The overall accuracy for the two classes to be differentiated is above 85%. The successful implementation of systems based on the proposed classifier might enable the improvement of the performance of brain-computer interfaces (BCI) that base their action, among other parameters, on the brain signals that the user emits when he/she detects an undesired response of the BCI.

ID: 365

PO-01: 22

Recognition of Korean monosyllabic speech using 3D facial motion data

Dongwon Kang¹, Jinseung Choi¹, Yoonho Shin¹, Joohack Lee¹, Jaebong Choi², Gyeræ Tack¹ and J. H. Bae¹

¹Konkuk University, South Korea; ²Hansung University, South Korea.

The purpose of this study was to extract accurate parameters of facial movement features using 3D motion capture system. Facial movement was measured for 50 Korean monosyllable vocalizations, and parameters changed by each subject's oral structure were presented. Fifteen subjects all in 20s of age were asked to vocalize 50 Korean vowel monosyllables twice with 18 reflective markers on their lower faces. Facial movement data were then calculated into 8 parameters (the lip width, lip height, lip depth, lip angle, lip protrusion, lip-nose length, cheek area, and the angle of temporomandibular joints) and presented as a pattern for each monosyllable vocalization. Learning and recognizing process for each monosyllable was performed through speech recognition routine with Hidden Markov Model and Viterbi algorithm. The accuracy rate of all 50 monosyllables recognition was about 93.6%. Through this result, it was suggested that the possibility of speech recognition of the Korean language through quantitative facial movements using 3D motion capture system and it is believed that this be a basic research in developing speech recognition algorithms that can perform more sophisticated speeches.

ID: 372

PO-01: 23

A hierarchical model family of human gas exchange for the use in medical decision support

Jörn Kretschmer^{1,2}, Axel Riedlinger¹ and Knut Möller¹

¹Furtwangen University, Institute of Technical Medicine, Germany; ²Faculty of Medicine Carl Gustav Carus, Dresden University of Technology, Dresden, Germany.

Mechanical ventilation is a life-saving procedure providing the patient with oxygen and allowing sufficient carbon dioxide removal. Although being a routine therapy, finding optimal settings for each patient remains a complex task for the clinician. Mathematical models are a widely accepted tool to simulate physiological processes in the human body, thus being able to predict patient response towards changes in the therapy regime. Such predictions might be exploited to provide medical decision support for the clinician with the goal of finding optimal settings for an individual patient. To allow for suitable reproduction of patient physiology in all clinical situations, rather complex models would be necessary. However, such all-embracing models require an extensive amount of measurements for robust parameter identification without providing further insight into the patient's disease state. We are therefore proposing to employ multiple model versions each specialized in a different simulation focus and of varying complexity. A medical decision support system might choose from this family of models depending on the patient's disease state and the physiological parameters that need to be predicted. The proposed model family is hierarchically ordered, i.e. each model is linked to its neighbours. This enables employing model parameters that are identified using simple models to be exploited as initial values for parameter identification in complex models.

Results show, that a simple model of three compartments containing lung and body gas exchange as well as a shunt compartment is suitable for prediction of blood oxygenation for various FiO₂ settings. Prediction of carbon dioxide levels at different levels of minute ventilation was achieved with a four compartment model including ventilation/perfusion mismatch that might be extended further by a dead space compartment to simulate tidal breathing. The proposed model family thus demonstrates the practical applicability of hierarchical modelling in clinical practice.

ID: 379

PO-01: 24

Monitoring step length and foot clearance during walking in outdoor environment using wearable sensors

Naoki Kitagawa, Shumpei Maeda and Naomichi Ogihara

Keio University, Japan.

In order to establish a supportive technology to reduce the risk of falling in older people, it is essential to clarify how falls actually occur in daily activities. In this study, we developed a system to monitor human gait in outdoor environment using a wearable sensor unit consisting of a tri-axial acceleration and tri-axial gyro sensor, and a global positioning system (GPS). Step-by-step step length and foot clearance were estimated from the sensor unit mounted on the dorsum of the shoe. Specifically, step length and foot clearance were calculated by integrating the translational acceleration over time during swing phase. However, the measured acceleration vector contains not only the translational acceleration but also the gravitational acceleration. Therefore, the latter must be separated and removed for correct calculation of displacement. For this, the change in the spatial orientation of the sensor unit with respect to the global coordinate system was estimated based on the data from the tri-axial gyro sensor (angular velocity vector). The gravitational acceleration vector was then subtracted for integration. The GPS data is used to understand how the gait parameters change by location. Walking of three healthy participants was measured using the proposed system and a conventional motion capture system simultaneously for comparisons. The results demonstrated that the swing phase trajectory of the sensor unit mounted on the foot was successfully reconstructed using the proposed system. This system will serve as a useful tool to monitor human walking in daily activities.

ID: 000

PO-01: 25

Multiple classifier system applied to the control of bioprosthetic hand based on recognition of multimodal biosignals

Marek Kurzynski and A. Wolczowski

Wroclaw University of Technology, Poland.

The paper presents an advanced method of recognition of patient's intention to move of multijoint hand prosthesis during the grasping and manipulation of objects in a dexterous manner. The proposed method is based on two multiple classifier (MC) systems dedicated to EMG and MMG biosignals working in two-level structure. At the first level, both MC systems use a dynamic ensemble selection (DES) scheme

with probabilistic measures of competence and diversity. These measures are calculated on the base of the original concept of randomized reference classifier (RRC). RRC acts – on average – as classifier evaluated and hence its probability of correct classification can be considered as the competence of that classifier and probability of misclassification can be used for construction of measure of ensemble diversity. At the second level the weighted majority voting fusion scheme with the continuous-valued outputs is applied.

The performance of MC system with proposed competence and diversity measures was experimentally compared against three benchmark MC systems using real data concerning the recognition of six types of grasping movements (tripoid, pinch, power, hook, column and mouse grip). Biosignals were registered using 3 EMG electrodes and 3 MMG microphones located on a forearm. The dataset consisted of 400 measurements, i.e. pairs "EMG and MMG signals segment/movement class". The values from STFT product corresponding to the $k = 3, 4, 5$ most representative time slices were considered as feature vector. The system developed achieved the highest classification accuracies demonstrating the potential of MC systems with multimodal biosignals for the control of bioprosthetic hand.

ID: 390

PO-01: 26

A fundamental study on an input operation of the communication aids by eyeblink using image analysis methods – change of the feature of an eyeblink waveforms resulting from attributed to conscious actions accompanying voluntary eyeblink –

Yuya Onishi¹, Tetsuya Ohya², Yohei Nomoto³ and Masashi Kawasumi¹

¹Information, Communication and Media Design Engineering, Graduate School of Advanced Science and Technology, Tokyo Denki University, Japan; ²Department of Information Systems and Multimedia Design, School of Science and Technology for Future Life, Tokyo Denki University, Japan; ³Department of International Studies and Regional Development, Faculty of International Studies and Regional Development, University of Niigata Prefecture, Japan.

The input devices for the operation of communication aids and the switches that enable multiple value input are required for disabled at the terminal stage of Amyotrophic Lateral Sclerosis (ALS). We considered the utilization of eyeblink that is relatively less associated with ALS at the terminal stage for the switches. It is known that eyeblink waveforms are different in between voluntary eyeblink and spontaneous eyeblink. Eyeblink waveforms are one-dimensional waveforms obtained by sampling

palpebral fissure widths of eye blinking at a constant time interval and by plotting them on a temporal axis. The purpose of this study is to investigate the possibility of categorizing eyeblink data into multiple spaces. We focused on the variations in the shape of eyeblink waveforms attributed to conscious actions accompanying voluntary eyeblink. There was a significant difference in shape feature parameters obtained from eyeblink waveforms between normal voluntary eyeblink and voluntary eyeblink accompanying conscious actions. The results suggest that eyeblink data could be differentiating into five values. The palpebral fissure widths at the time of eyeblink were recorded by the image analysis method, which is a non-contact measurement with fewer burdens. A high-speed video camera with the temporal resolution equivalent to that of EOG is used for the measurements. From the obtained eyeblink waveforms, we extracted six feature points including the starting points of eyelid closure and eyelid opening, shape feature parameters such as eyelid closure time and the mean eyelid opener speed based on these feature points. We made a comparison examination of shape feature parameters of eyeblink waveforms obtained from not only normal voluntary eyeblink but also the following three conscious actions: voluntary eyeblink firmly, lightly; voluntary eyeblink after opening eyes wide; and the combination of the two conscious actions.

ID: 405

PO-01: 27

Improved algorithm of adaptive DR image denoising based on fast curvelet transform and anisotropic median-diffusion filtering

Lifang Zhang, Zhangyong Li, Jie Liu and Chunyang Li

Chongqing University of Posts and Telecommunications, China.

In the direct digital X-ray (DR) imaging process, there are wide variety of complex noises which are due to various causes, such as a CCD camera, the imaging screen, X-ray scatter, control circuit and so on. Therefore, this paper, according to characteristics of the CCD/DR image noise, and combined with adaptive threshold method, research a improved algorithm of adaptive DR image denoising based on fast curvelet transform and anisotropic median-diffusion filtering. This algorithm is simple, direct, more comprehensive and targeted. It is well preserved and enhanced DR image detail and edge information while better denoising to prepare for the post-processing.

The author gratefully acknowledges the support of K.C.Wong Education Foundation, Hong Kong

ID: 421

PO-01: 28

Scalability tower multi-scale DR image enhancement algorithm based on human visual characteristics

Lifang Zhang, Zhangyong Li, Jie Liu and Chunyang Li

Chongqing University of Posts and Telecommunications, China.

Direct digital X-ray (DR) images, which is high resolution, wide dynamic range and rich in a lot of human tissues information, are enhanced to extract a wealth of clinical diagnostic information for early lesions found to provide a good basis for the diagnosis. Therefore, this paper, according to the system for the CCD-DR imaging features, studies a scalability tower multi-scale DR image enhancement algorithm based on human visual characteristics. Method: Firstly, the algorithm uses an improved Laplace Pyramid structure in image decomposition processing. Secondly, the high frequency part can be enhanced by the local nonlinear adaptive contrast enhancement method, the low frequency part of the improved method of histogram equalization combined with human visual characteristics. Lastly, original image will be reconstructed through the repeated extension of image and the results. Conclusion: In this paper, the image enhancement algorithm extends the DR image useful information, highlights the image detail and speeds up image processing speed, while it limits noise amplification and local contrast over enhanced so as to facilitate medical diagnosis and operation.

The author gratefully acknowledges the support of K.C.Wong Education Foundation, Hong Kong

ID: 426

PO-01: 29

Investigation of significant attributes based on image feature and texture analysis for automatic noise reduction in MRI

Yu-Ju Lin and Herng-Hua Chang

National Taiwan University, Taiwan.

In MR image analysis, noise is one of the main sources of quality deterioration not only for visual inspection but also in computerized processing such as tissue classification, segmentation and registration. Consequently, noise removal in MR images is important and essential for a wide variety of subsequent processing applications. In the literature, abundant denoising algorithms have been proposed, most of which require laborious tuning of parameters that are often sensitive to specific image features and textures. Automation of these parameters through artificial intelligence techniques will be highly beneficial. However, this will induce another problem of seeking appropriate meaningful attributes among a

huge number of image characteristics for the automation process. This paper is in an attempt to systematically investigate significant attributes from image features and textures to facilitate subsequent automation process. In our approach, a total number of 60 image attributes are considered that are based on three categories: 1) Image statistics. 2) Gray-level co-occurrence matrix (GLCM). 3) 2-D discrete wavelet transform (DWT). To obtain the most significant attributes, a t-test is applied to each individual image features computed in every image. The evaluation is based on the distinguishing ability between noise levels, intensity distributions, and anatomical geometries. We have adopted the BrainWeb image data with various levels of noise and intensity non-uniformity to evaluate our methods. Finally, we report the most significant attributes in ascending order based on the p-value and suggest the use of these features for the automation process.

ID: 430

PO-01: 30

Evaluation of floor slipperiness during walking – Measuring dynamic friction coefficient under incremental vertical load

Hiroshi Matsuura and Toshiaki Kaneeda

Okayama University of Science, Japan.

In this study, a new evaluation method has been proposed for the floor slipperiness using dynamic friction coefficient instead of static one. More than ten thousand people died caused fatal accidents in houses every year in Japan. Among them a number of the aged people died in falling down to the flat floor even though without any steps. The floor slipperiness is usually identified as static friction coefficient at the slips in toe-off during last half of gait cycle. However, it is said that the slips are also occurred at heel down to the floor during first half of gait cycle. In order to evaluate the floor slipperiness at the heel down, it is necessary to measure the dynamic friction coefficient between footwear and floor under incremental vertical load during the heel down. In the new tester, natural rubber sole attached to the artificial foot was pressed against the moving floor at a speed of 0.20–0.25m/s, and then the friction force and vertical load were measured by strain gauge-type load cells. A wooden-made plate, cushion sheet and P-tile were selected as the floor in dry, wet or oily surface conditions. The experimental results suggested that: in dry condition, the vertical load as well as the friction force reached the maximum values less than 0.1s from the beginning of the heel down. The dynamic friction coefficients in dry condition were calculated to be 0.5–0.8. On the other hand, in wet and oily conditions, the coefficients were lower than

the former. The static friction coefficient in wet was higher than that in dry. Difference between static and dynamic coefficient is caused by squeezing liquid film. This suggested that floor slipperiness should be used by dynamic friction coefficient under incremental vertical load.

ID: 440

PO-01: 31

Consideration for the brain waves analysis for BMI system constitution using the EEG.

Hiroki Okayasu, Kazushige Magatani and Minoru Kuroiwa

Tokai-University, Japan.

In our research, the development of a BMI (Brain Machine Interface) system using EEG (Electroencephalogram) which can be measured safely and easily is the objective. If this system can be established, QOL of the people who has disability will improve by using this system. In order to realize our BCI system, we are developing an EEG amplifier, a hardware system which can analyze measured EEG and can control support equipment like as robot, and software which estimate user's intention from measured EEG. Our developing BCI system consists of electrodes, which derive EEG from user's scalp, the EEG amplifier which amplify measured EEG, and a personal computer which identify use's intention. In our system, EEGs from around motor cortex are measured, because one of our objectives is the understanding about user's motor intention. Therefore, 16 electrodes were set on a subject's scalp where is positioned around motor cortex. In order to find features of EEG when a subject did some action was measured and analyzed. From this experiment, average power of μ -band of EEG changed with subject's motion notably. where, μ -band means from 7 to 12 Hz of EEG frequency band. In our experiment, average power of μ -band was decreased just before action and increased just after action. In this paper, we will describe about our experimentally developed system and the results of our experiments.

ID: 443

PO-01: 32

Computer-aided technique for the design and manufacturing of auricular prostheses

Takeshi Murayama¹, Masamine Ogasawara¹, Toru Eguchi¹, Yuji Morishita² and Mitsuhiro Tamamoto¹

¹Hiroshima University, Japan; ²Aichi Medical University Hospital, Japan.

Custom-made esthetic auricular prostheses, which are used for rehabilitation of patients with missing or impaired auricles, have been fabricated manually.

However, such fabrication is time-consuming and requires manual skill. This paper proposes a computer-aided technique for fabricating auricular prostheses to save time and allow fabrications that do not require considerable manual skill. In this technique, the shape of a patient's healthy auricle, which is contralateral to the impaired auricle, is first scanned using a laser scanner to make a 3D model of the healthy auricle. Because the 3D model obtained by laser scanning has the surface abnormalities and gaps, we apply morphing technology to make the 3D model complete. The morphing technology is originally for changing (or morphing) one image to another through a seamless transition. In this study, the morphing technology is used to change the 3D model of standard auricle by referring to the 3D model obtained by laser scanning, and consequently we obtain a 3D model that resembles a patient's healthy auricle. An auricular prosthesis for the patient is designed by mirroring the 3D model obtained by morphing. Based on the 3D model, a mold is designed, using the 3D modeling tools and computer-aided design system. The resulting mold is then fabricated using a 3D printer. An auricular prosthesis is fabricated by pouring silicone resin into the mold. An auricular prosthesis for a volunteer was experimentally fabricated according to the proposed technique.

ID: 444

PO-01: 33

Brain extraction based on an improved charged fluid model in MRI

Yu-Sheng Chen and Herng-Hua Chang

National Taiwan University, Taiwan.

Brain extraction is an important preprocessing step in many research and clinical applications. It aims to remove non-brain tissues (e.g., skull, scalp, and dura) and retain brain parenchyma in MR images. Among a number of brain extraction methods, deformable models are gaining attention as they provide robust abilities to deform contours under the guidance of geometric properties and image information to fit salient edges in images. In particular, the charged fluid model has been shown less critical than many existing deformable models in segmenting objects with sharp corners and cusps. This paper proposes a new brain extraction algorithm based on the charged fluid model. To improve the segmentation accuracy, a new image stopping force of using the local intensity difference along the normal line of the evolving curve is introduced. For brain extraction, this new stopping force is then incorporated into the governing equation weighted by a global intensity difference between the interior and exterior of the evolving con-

tour. We have adopted the BrainWeb image data with various levels of noise and intensity non-uniformity to evaluate this new algorithm. Preliminary results indicated that our method successfully stopped the leakage comparing to the traditional charged fluid model and produced high segmentation accuracy across a number of brain MR images.

ID: 456

PO-01: 34

Development of biofeedback equipment for toes weight-bearing exercise in a standing position

Ayako Hisari^{1,2}, Masaki Sekine¹ and Masaki Yoshida¹

¹*Osaka Electro-Communication University, Japan;*

²*Osaka Kawasaki Rehabilitation University.*

To use their toes to support their body weight is one of the ways for people to improve standing balance. Some people undergoing this training (toes weight-bearing exercise) do not know how to use their toes to support their body weight.

In the present study, biofeedback equipment was developed to help understand how to use the toes to support the body weight, and the effects of biofeedback were examined.

As the results, ratios of mean toe to whole plantar load values (toe-loading rates) increased about 10% of body weight as the effects of biofeedback.

ID: 457

PO-01: 35

Measurement of the orientation of 2D ultrasound probe for medical diagnosis of left ventricular motion

Yuma Inui¹, Hitoshi Kimura¹, Norio Inou¹, Konomi Sakata² and Yasuhiro Nakajima³

¹*Tokyo Institute of Technology, Japan;* ²*Kyorin University School of Medicine;* ³*YD, Ltd.*

To make an accurate diagnosis of a certain heart disease, the three-dimensional movement of the left ventricle (LV) is important. Although direct 3D motion observation is possible with 3D echocardiography, the limited viewing angle and frame rate hinders its efficiency. On the other hand, 2D echocardiography (2D echo) has advantages in the both points, and is widely used. Clinicians take 2D echographic images following a guideline crafted by the American Society of Echocardiography (ASE), and imagine 3D LV motion from those images. In order to accurately visualize 3D LV motion, the orientation of the 2D echo probe must be measured. This paper examines the efficacy of a sensor device to objectively measure the orientation of a 2D echocardiogram probe.

A commercial 6-axis sensor, consisting of a 3-axis accelerometer and a 3-axis gyro sensor, was attached to a 2D echocardiogram probe. Using the output of the gyro sensor, the orientation of the echocardiogram probe was estimated. Then, necessary corrections to the orientation at steady state were made using the direction of gravitational acceleration from the accelerometer. To further improve accuracy, calibration of the echo probe against a datum plane was done before and after the measurement. This method enabled us to determine the position of the probe to within ten degrees during a seven minutes echocardiogram session.

Experiments to measure orientation of 2D echo probe were performed with two healthy subjects. The estimated orientation of 2D showed quite a difference from the ASE guideline. We reconstructed 3D image of LV motion with 8 different cross-sectional images by synchronizing the heartbeat of each data. The 3D image clearly demonstrates LV motion and shows existence of a part that has insufficient information even with 8 echo data following the guideline of ASE.

ID: 462

PO-01: 36

Application of list mode image reconstruction to fine DOI-PET scanner using position-sensitive CdTe semiconductor detector unit

Yohei Kikuchi and Abdella Ahmed

Graduate School of Engineering, Tohoku University, Japan.

We report the effects of implementing the list mode image reconstruction method (LMR) in a new brain scanner based on positron emission tomography. The benefits of LMR include reduced load in imaging processes and conservation of fine spatial data-sampling, the latter of which may be lost by data binning in histogram mode image reconstruction (HMR). In our project, we aim to build a high-spatial-resolution scanner that employs three-dimensional position-sensitive CdTe semiconductor detector units. We experimentally confirmed that the unit could measure the detected positions of annihilation photons with a position resolution of 1 mm³ full width at half maximum (FWHM). Therefore, the scanner can potentially minimize the parallax-induced decrease in the spatial resolution of off-center positions in the field of view (FOV), thereby providing high resolution throughout the FOV because it obtains accurate depth of interaction (DOI) information at a sampling pitch ~1 mm finer than that of conventional DOI technologies (~4 mm). We simulated the proposed scanner using the GEANT4 Application for Tomographic Emission. Reconstructed images were obtained by LMR or HMR based on the maximum likelihood-expectation maximization (ML-EM) algo-

rithm. The system matrix for ML-EM reconstruction was calculated by Siddon's ray-driven method to fully exploit accurate detection positions. The spatial resolution at the center of the FOV acquired by LMR is 0.6 mm FWHM, which is superior to that acquired by HMR (1 mm FWHM). We confirmed that the resolutions of both methods are maintained at off-center positions, and the resolutions acquired by LMR at these positions are superior to those acquired by HMR. Furthermore, we simulated Hoffman-brain-phantom imaging to evaluate the image quality of the scanner and LMR in human brain studies.

ID: 468

PO-01: 37

Study on movement assistance with robot suit HAL

Rie Kasai¹, Hitoshi Kawasaki², Hiroto Kamikura², Ryota Yamanaka², Masaru Ueno², Shunsuke Yoshida², Koichi Ohnaka² and Sunao Takeda³

¹Tokyo University of Technology School of Health Science Dept. of Physical Therapy; ²Medical corp. HAKUZJINKAI Shimuraomiya Hospital Ibaraki Northwest General Rehabilitation Center; ³Tokyo University of Technology School of Health Science Dept. of Clinical Engineering.

Robot suit Hybrid Assistive Limb (HAL) is a wearable robot that assists human movement. Recently, many Japanese medical institutions have introduced the HAL. The preset study aimed to assess the support functions of the HAL by performing postural evaluation. A subject in his 50s with right hemiparesis (Brunnstrom stage III) participated in the study. Supervision and a handrail were needed when the subject stood-up. This study was approved by the ethics committee of Tokyo University of Technology and informed consent was obtained before commencing the study. A Single-leg HAL was attached to the subject's right lower limb and 2 accelerometers were attached at the C7 and L3 level. Postural changes during standing-up with or without HAL were assessed using the accelerometers. For comparison, the same assessment was performed in a healthy subject in his 20s. In the patient, the time taken to stand up increased from approximately 2 s to 4 s with the HAL. This finding suggests that the patient's movement was changed from quick to smooth because of the assistance provided by the HAL. This was not observed in the healthy subject. The accelerometer attached at L3 demonstrated that without the HAL, the patient could not extend his trunk after lifting his buttock off the treatment bed, and his trunk remained forward-bent after completely standing-up. However, with the HAL, the patient could extend his trunk, which contributed to the stability of his standing posture. Additionally, in both the patient and the healthy subject, the trunk

tilted to the side opposite to the HAL when the buttocks were lifted. This tendency was also observed in the cervical posture of the patient. These results suggest that the HAL may be effective for making the patient's movement pattern more similar to a normal movement pattern.

ID: 476

PO-01: 38

Subcortical shapes distinguished mild cognitive impairment and Alzheimer's disease from normal aging

Mingzhen Tan and Anqi Qiu

National University of Singapore, Singapore.

Brain atrophy is a recognized pathology of the prodromal stage in Alzheimer's disease (AD). While volumetric assessments of the brain can provide insights into atrophy for specific regions-of-interests (ROIs), anatomical shape patterns characterizing both regional abnormalities and their precise localizations are often overlooked. We aimed to discriminate mild cognitive impairment (MCI) and AD from normal aging using anatomical shapes. For this, large deformation diffeomorphic metric mapping (LDDMM) was employed to characterize shapes of the subcortical structures (hippocampus, amygdala, caudate, globus pallidus, putamen, thalamus) and lateral ventricles in an infinite-dimensional manifold. ISOMAP was subsequently employed to embed the shapes into a low-dimensional space, which was in turn, applied as features in a soft margin Support Vector Machine (SVM) to produce a unique decision function/classifier. Our results showed that classification rates vary 70–84% to distinguish MCI and AD from normal aging. Hence, subcortical shapes can be potentially used for the discrimination of MCI and AD from normal aging.

ID: 484

PO-01: 39

A Study of low frequency acoustic information for cochlear implant users with background noise

Yi-Hsuan Lee¹, Bo-Cheng Huang¹ and Charles T. M. Choi²

¹National Taichung University of Education, Taiwan; ²National Chiao Tung University, Taiwan.

Recent studies have reported speech intelligibility in noisy environment from cochlear implant (CI) users was reduced because the spectral resolution is not high enough. For the user who had only implanted one CI in unilateral ear, combined a hearing aid (HA) in contralateral ear, known as bimodal hearing, can improve the speech perception. This is partly true due to the residual low frequency acoustic information provided from HA can help CI users to segregate

the target speech from noise. In this study, a vocoder was conducted to evaluate the effect of low frequency information, especially the fundamental frequency (F0), in recognizing Taiwanese Mandarin for bimodal CI users. The result showed that F0 was the main factor in low frequency acoustic information, and bimodal apparently enhance the performance of speech recognition in noise in Taiwanese Mandarin.

ID: 486

PO-01: 40

A measurement technique on CSEP and SSEP for an SCI measure

Naotoshi Orij, Motohiro Kuriyagawa, Masaki Kyoso and Yuichi Shimatani

Tokyo City University, Japan.

It had been said that an injured spinal cord (SC) would never be recovered. A patient who has spinal cord injury (SCI) suffers from disorders on motor and sensory function because SC is an important part of CNS (central nervous system). However, a hope for recovery from SCI came out with thanks to advanced technology of regenerative medicine (e.g. iPS cell and ES cell). In Japan it was announced that clinical study of regenerative medicine on SCI would be started by 2016. Detailed evaluation on recovery process from SCI would be required, however, there is few quantitative evaluation technique.

In this research, we have proposed to use event-related evoked potentials to monitor SC functions. Particularly we focused on ascending evoked potentials, CSEP (Cortical Somatosensory Evoked Potentials) and SSEP (Spinal Somatosensory Evoked Potentials). Analysis on many signals many points on CNS must give precise information on SCI. In this report, we have done some experiments to show an effectiveness of our idea.

CSEP was evoked by right hind paw stimulation and recorded from cerebral sensory cortex with implanted electrodes. SSEP was evoked by right hind paw stimulation and recorded from T6 on the SC with rod electrode. For the first step of the evaluation, we used matured rats without SCI. CSEP and SSEP were successfully detected in sufficient amplitude for the next analysis on SC function. CSEP and SSEP peak latencies were found around 20ms and 4ms respectively. From these results, it was shown that we succeeded in measuring response of both CSEP and SSEP to analyze conduction functions at many points on somatosensory pathway. We are currently improving the experimental methods and techniques for chronic monitoring. For the next step, we will prepare SCI model rats with contusion injuries for detailed analysis on SCI.

ID: 508

PO-01: 41

Effect of transmitter and receiver electrodes configurations on the capacitive intrabody communication channel from 100 kHz to 100 MHz

Zeljka Lucev Vasic¹, Yueming Gao², Siohang Pun³, PunUn Mak³, Mangl Vai³, Igor Krois¹ and Mario Cifrek¹

¹University of Zagreb, Croatia; ²Fuzhou University, China;

³University of Macau, China.

In the intrabody communication (IBC) the human body behaves as a medium that connects transmitter and receiver, which are placed directly on the skin, or are in its close proximity. The signal transmission path is closed through the human body, and the return signal path is closed capacitively through the environment. Hence, the received signal level is affected by the orientation of the transmitter with respect to the receiver, the number of ground electrodes connected to the body, the size of the receiver ground plane, and the surrounding environment. Both a transmitter and a receiver have a signal and a ground electrode, which can be connected to the human body in two ways: predominantly resistive and predominantly capacitive. In a predominantly resistive configuration, signal and ground electrodes are in a direct contact to the skin. The contact is obtained using standard Ag/AgCl electrodes, placed 2 cm apart. In a predominantly capacitive configuration, signal electrode is connected to the skin using standard Ag/AgCl electrode, and the ground electrode is a bare copper electrode placed on a plastic housing, 2 cm above the signal electrode. In this paper we measured transmission characteristics of the intrabody communication system in a frequency range from 100 kHz to 100 MHz using battery-powered network analyzer, for all four transmitter-receiver electrode configurations (resistive-resistive, capacitive-resistive, resistive-capacitive, and capacitive-capacitive), at five different distances along the arms (namely, 4 cm, 16 cm, 28 cm, 36 cm, and 120 cm). We proved that intrabody communication channel was reciprocal. The highest transmission gain was measured for capacitive-capacitive configuration, regardless of the distance between the transmitter and receiver.

ID: 550

PO-01: 42

Performance analysis of EM, SVD and SVM classifiers in classification of carcinogenic regions of medical images

Vinothkumar Bojan and Harikumar Rajaguru

Bannari Amman Institute of Technology, India.

In this paper, the performance analysis of classifiers for classification of carcinogenic regions from various

medical images is carried out. Expectation Maximization (EM), Singular Value Decomposition (SVD) and Support Vector Machines (SVM) are well thought-out for analysis. EM classifier performs as the optimizer and SVD classifier performs as the dual class classifier. SVM classifier is used as both optimizer and classifier for multiclass classification procedure and for wide stage cancer detection procedures. The performance analysis of all the three classifiers are analyzed for a group of cancer patients based on the benchmark parameter such as perfect classification, sensitivity, specificity, false positive rate, false negative rate and missed classification. From the experimental results it is evident, that the SVM classifier significantly outperforms other classifiers in the classification of carcinogenic regions of medical images.

ID: 567

PO-01: 43

Fluctuation of heart rate in neonates

Muneaki Mizote and Miyoko Kume

Teikyo Heisei University, Japan.

In 15 normal full-term neonates (weighed more than 2,500 g) delivered normally (Apgar scores: 8–10), ECG and respiratory movement were measured for about 15 min each, at 30 min, 1 hr, 3 hrs and 5 hrs after birth. In all cases, informed consent of the mothers was obtained prior to the measurements. The neonates were quiet and awake during the measurements. An ECG measurement tool developed with the aim of easing the discomfort of the subjects during the measurements was employed. A rubber sheet (300 × 300mm) on which three plate-type silver electrodes (20 × 35mm) were mounted, was put in a neonate basket. A damp saline cotton cloth was laid over the sheet, and neonates were laid on the cloth. Two electrodes, fitted around shoulders of a neonate, were used as bipolar electrodes for ECG recording. In one hour after birth, dispersion of joint interval histogram was focused at one spot. Slope of f-n fluctuation of intervals was close to a horizontal line. In the LF band (0.04–0.15 Hz) and HF band (>0.15 Hz) of power spectral densities at one hour after birth, mean value of PSD was decreased compared with that in 30 min ($p < 0.01$ in LF and $p < 0.05$ in HF). And mean values of PSD in LF and in HF band were increased two hours later. Rise time of respiration movement at one hour after birth was shorter ($p < 0.05$) than those of other periods. Relation among heart rate, respiration movement, intercostal muscles and neuronal network will be reported.

ID: 577

PO-01: 44

Eye torsion determination using optical flow

Waldemar Krzok and Uwe Schönfeld

Charite Medical school, ENT Department, Germany.

Torsional image registration is of crucial importance for a wide variety of medical applications especially in the field of ophthalmology and refractive surgery.

We would like to underline particularly the relevance for refractive surgery where, beside the translational, also the torsional motion of the eye has to be known exactly in order to guide the tissue ablating laser beam towards the intended location on the anterior corneal surface to achieve the desired shape. So-called eye trackers, nowadays mostly video based, are used to determine the eye position accurately. Those systems compare the current image with a reference image (e.g. taken at the beginning of the operation or from a diagnostic device) to derive the torsional component of the eye motion relative to that reference.

A further array of application with growing significance are implantations of toric Intraocular lenses (IOL) after cataract surgery. In such an operation an artificial plastic lens is used to replace the crystalline lens. Due to the fact that toric IOLs are not rotationally symmetrical they have to be properly aligned with respect to the visual axis of the eye in order to achieve the optimum visual outcome. A video based system that during implantation keeps track of the torsional orientation of the eye can be used to assist the surgeon to place the toric lens into the right angular orientation.

In this paper we propose a novel approach for finding the torsional displacement between two eye images – mostly this pair will consist of a reference image and the current camera image. Our technique makes use of optical flow methods, which are well known and widely used.

ID: 594

PO-01: 45

Microwave ablation system design to study the effects of coaxial antenna on in vitro animal tissues

Montree Chaichanyut, Polsart Lertprasert and Supan Tungjitkusolmun

King Mongkut's Institute of Technology Ladkrabang, Bangkok, Department of Electronics, Faculty of Engineering, Thailand.

This paper presents a novel low cost microwave ablation system design to study the effects of coaxial antenna on In Vitro animal tissues. The system utilizes a high-voltage power supply so that the magnetron can generate a microwave field continuously, and its output power can be adjusted from

10–80 W at frequency of 2.45GHz. We control output microwave power level by using control the magnetron power supply, which it is an important part of a microwave heating system. Power control of the magnetron's power supply is desired for microwave heating to enhance performance and to provide system flexibility. The high frequency switching technique in the power supply control is costly and complicated. In another way, pulsing the output power of the magnetron can be simply realized with TRIAC, but in that case the magnetron does not operate continuously. The proposed circuit is a simple one with TRIAC. The power control is achieved by controlling the triggering events at appropriate phase angle of the household 220V. Experimental protocol was composed by a radiation system and a thermometry system. Coaxial antenna works at 2.45 GHz, power apply during experiments was 10W × 8min; 20W × 4min; 40W × 2min and 80W × 1min. Thermal sensors were placed next to the antenna at 1mm., a large number of experiments on porcine liver are carried out, the temperature distribution within the liver are measured and illustrated, for cases of different injected microwave power and ablation time. In addition, the ablation areas in cases of different input microwave powers are measured also. All these results indicate the potential validity of this system on medical treatment of liver cancer of human body.

ID: 595

PO-01: 46

Effects of anti-depressant treatment and chronic mild stress on trabecular architecture parameters of adult female rats over a 14-week period using micro-computed tomography

Boon Horng Kam¹, Roger Ho², Weifen Ong³, Clifford Chen³ and Ramruttun Amit Kumarsing⁴

¹School of Applied Science, Republic Polytechnic, Singapore; ²Dept of Psychological Medicine, Yong Loo Lin School of Medicine, National University of Singapore, Singapore; ³School of Science and Technology, SIM University, Singapore; ⁴Dept of Orthopedic Surgery, National University of Singapore, Singapore.

Introduction: Depression drugs may increase or decrease bone mass and can be referred to studies with administration of depression drugs in mice i.e. Battaglini *et al.* (2007) showed 6 weeks of administration of fluoxetine leads to increase bone mass. On the other hand, Bonnet *et al.* (2007) showed 4-weeks of administration of fluoxetine resulted in lower bone stiffness and Young's modulus. The objective of this project is to study the trabeculae parameters of adult female rats that undergone anti-depressant treatment and chronic mild stress over a 14-week period utilizing micro-computed-tomography (micro-XCT, Xradia Inc).

Materials-and-Methods: A total of 31 left and right femoral bones from adult female rats which were divided into chronic-mild-stress (CMS) + anti-depressant treatment (Fluoxetine) [CMS+FN], CMS, Control [C] and Fluoxetine [FN] (10mg/kg) over 14-week period were micro-CT scanned using micro-XCT (100KV x-ray source with a focal spot size of 5 μ m). The scans consisted of 1024 slices with 10 μ m spanning a 10.24mm of each bone. Micro-XCT and GE Microview bioimaging-softwares were used to analyse the bone-volume-fraction (BVF) and trabeculae-thickness (TbTh). Statistical-analysis of T-test for independent-samples-design was carried out on lateral and medial condyles.

Results-and-Discussion: FN has higher BVF compared to C and CMS+FN significantly medially-laterally (T-values: 2.467^a, 2.839^b, 1.391^a, 1.452^b) (T-Table-values ^aT_{0.20,9} = 1.383, ^bT_{0.20,13} = 1.350, ^cT_{0.20,14} = 1.345, ^dT_{0.20,18} = 1.330). CMS has significantly higher BVF compared to CMS+FN medially-laterally (T-values: 2.316^d, 1.557^d). CMS has significantly higher BVF compared to C medially (T-value: 2.379^c). FN has significantly higher TbTh compared to C, CMS and CMS+FN laterally (T-values: 2.196^a, 3.031^b, 4.894^b). FN has higher TbTh compared to C and CMS and significantly higher compared to CMS+FN medially (T-values: 1.104^a, 0.771^b, 2.270^b). CMS has higher TbTh compared to C and significantly higher compared to CMS+FN medially-laterally (T-values: 0.349^c, 1.861^d, 0.150^c, 3.566^d). CMS+FN has significantly lower TbTh compared to C medially-laterally (T-values: 1.355^c, 2.477^c).

Conclusion: This concludes just the administration of Fluoxetine or CMS itself cause significant increase in the TbTh and BVF over CMS+FN with the fact that the effects of just the administration of Fluoxetine on trabecular architecture parameters has the highest significance over CMS or CMS+FN evidently.

ID: 596

PO-01: 47

The modeling techniques for analyses of electromagnetic distributions and reflection coefficients for microwave ablation

Montree Chaichanyut, Polsart Lertprasert and Supan Tungjitkusolmun

King Mongkut's Institute of Technology Ladkrabang, Bangkok, Department of Electronics, Faculty of Engineering, Thailand.

Many advantages of microwave ablation over the other ablative therapies in the field of liver tumor ablation have driven researchers to develop innovative interstitial microwave antennas to effectively treat deep seated, nonresectable hepatic tumors. A

new coaxial antenna for microwave ablation therapies has been proposed in this research paper. Three dimensional Finite Element Method (FEM) has been used to design the results of the proposed antenna. Objective metrics for assessing the characteristics of helix antennas for microwave ablation by analyzing the electromagnetic field distributions and reflection coefficients for efficiency of antenna has been specified and verified for the proposed antenna, at frequency of 2.45GHz. Our simulation results, Relative permittivity at 2.45GHz during thermal ablation. Accumulated ablation times noted on each figure to identify temporal variations. Values tended to drop quickly in all cases when temperatures reached 100 °C and continued to drop as temperature was maintained and the tissue became more dehydrated. Changes were irreversible as tissue returned to baseline temperatures. We designs the antenna matching obtained at 2.45 GHz. During thermal ablation, the reflection coefficients it can be noted that the antenna resonance shifts toward higher frequencies and the electric field distribution at the near field region changing follow the temperature variations in tumor tissue.

ID: 620

PO-01: 48

Synchronized medical image viewer for remote consultation

Pasan Manura Karunaratne, Praveen Nisal Jayasuriya, Hasith Ruchiran Karunasekera, Rajith Delanka Karunaratne and Nuwan Dayananda Nanayakkara

University of Moratuwa, Sri Lanka.

The collaborative analysis between radiologists and surgeons of digitized medical images in the surgical planning phase is a critical step in the process of patient treatment. The shortage of radiologists who are qualified to carry out this task has proven detrimental to patient care. The proposed solution is a tool for collaboration where a radiologist and a surgeon are able to analyze scans while being in geographically disparate locations.

Though a superficial examination of the options currently available would suggest the use of an off-the-shelf desktop sharing software solution, these fall well short of the performance and quality requirements of such an application which is to be used in a medical setting.

We propose a novel approach, based on low-level command capturing that enables near-real-time synchronization with zero loss of information or distortion of the images. We discuss the underlying technology of our implementation of the synchronization solution as well as present the manifest performance gains of our solution in comparison

with the highly popular commercial desktop sharing solution TeamViewer.

ID: 625

PO-01: 49

Principles of design, implementation and testing of external pacemakers

Tomáš Klinkovský and Marek Penhaker

VSB-Technical University of Ostrava, Czech Republic.

This paper describes the design of a bipolar external pacemaker for temporary pacing, including important practice implementation. The prototype pacemaker was designed for analogue sensing and stimulation by microprocessor control with the lowest possible amount of power consumption (20 days from one 9V battery). The pacemaker meets the latest requirements of CSN, EN, IEC and ANSI. It was successfully tested under clinical conditions.

ID: 634

PO-01: 50

A volume-preserving free-form deformation technique for customising a face model to another configuration

Tim Wu and Kumar Mithraratne

Auckland Bioengineering Institute, The University of Auckland, New Zealand.

This article presents a volume-preserving free-form deformation technique that can be used to customise a face model generated from magnetic resonance (MR) images into another configuration using only the surface (skin) data. This customisation process is useful when comparing anatomical measurements between datasets that may have undergone a different mode deformation. For example, gravity and other body forces were often neglected in most biomechanical simulations, and as a result, a supine face model generated from MR images is not suitable for analysis of activities performed in upright posture (i.e. expression detection for human computer interaction). To address this problem, the supine model can be fitted to the scanned skin data of an upright posture, in which conventional biomechanical simulations can be applied. Volume-preservation is an important characteristic of soft tissue deformation due to the high water content, and therefore is essential to produce realistic results, especially when only surface information is available. Validation studies presented in this article showed good agreement between the actual deformations and the predictions by the proposed method.

ID: 636

PO-01: 51

Development of a stand-alone physiological monitoring system for noncontact heart and respiration rate measurements on real-time linux platform

Guanghai Sun¹, Shinji Gotoh² and Takemi Matsui¹

¹Tokyo Metropolitan University, Japan; ²Tau Giken, Japan.

We developed a stand-alone physiological monitoring system without any constraints on its users for daily life healthcare. The system measures tiny movements on a body surface induced by heartbeat and respiration in a noncontact manner using a 24-GHz microwave radar. To extract the related signals from the radar output, an analog band pass filter was designed and integrated into a printed circuit board. The software was developed on an embedded Linux platform for a stand-alone and modular design. To assess the performance of noncontact physiological monitoring, we conducted a laboratory test on eight healthy male subjects (ages: 22.0 ± 1.25 years). The heart and respiration rates determined by the proposed system correlated significantly with those measured by the contact-type electrocardiogram ($r = 0.83$, $p < 0.01$) and respiratory effort belt ($r = 0.90$, $p < 0.01$). The results showed that the respiration and heartbeat were accurately detected by the proposed system, which appears promising for monitoring physiological condition in daily life.

ID: 658

PO-01: 52

Quantification of soft tissue artifacts on the thigh and shank during cycling exercises using a novel CT-to-fluoroscopy registration method

Tung-Wu Lu^{1,2}, Cheng-Chung Lin¹, Jia-Da Li¹, Yu-Huan Wu¹ and Mei-Ying Kuo³

¹Institute of Biomedical Engineering, National Taiwan University, Taiwan; ²Department of Orthopaedic Surgery, School of Medicine, National Taiwan University, Taiwan; ³School of Physical Therapy, China Medical University, Taiwan.

Introduction: Cycling plays an important role in transportation, recreation, and sport in our daily lives but cycling-related overuse injuries are not uncommon. Skin marker-based motion analysis has been used to assess the functional performance of cycling exercises and potential injury risks. However, the associated soft tissue artifacts (STA) of the markers affected the accuracy of calculated mechanical variables. Therefore, knowledge of STA will be helpful for a better interpretation of the results obtained and further development of STA-compensation methods. The aims of the study were to quantify the STA of selected markers on the thigh and shank during cycling exercises using a novel technique.

Methods: Seven healthy adults wearing skin markers on the medial and lateral femoral epicondyles (MFC and LFC), thigh (THIL, THIC, THIM), tibial tuberosity (TT), fibular head (FIB), shank (SHA), and medial and lateral malleoli (MA) performed cycling movement under simultaneous surveillance of a motion capture system and a fluoroscopy system. They also received a CT scan so that their femoral and tibial bone poses could be obtained using a fluoroscopy-to-CT registration method. The STA of the skin markers were then calculated as the marker movement relative to the underlying bone.

Results and Discussion: Considerable STA's were found during cycling exercises with greater STA on the thigh. MFC and LFC were displaced posteriorly from their true positions with knee flexion, and moved anteriorly with knee extension. THIC had greater STA among the technical markers on the thigh and moved mainly along the proximal/distal direction. TT moved within a small range throughout the cycling movement, while FIB moved mainly along the proximal/distal direction. The STA around the knee joint during the cycling movement were quantified for the first time in the literature, which will be helpful for developing guidelines for using skin markers and STA-compensation methods.

ID: 660

PO-01: 53

Compensation of soft tissue artifacts on the calculated angles and moments at the knee during cycling using global optimization method

Jia-Da Li¹, Tung-Wu Lu^{1,2}, Cheng-Chung Lin¹, Yu-Huan Wu¹ and Mei-Ying Kuo³

¹Institute of Biomedical Engineering, National Taiwan University, Taipei, Taiwan; ²Department of Orthopaedic Surgery, School of Medicine, National Taiwan University, Taiwan; ³School of Physical Therapy, China Medical University, Taiwan.

Introduction: Soft tissue artifacts (STA) are a major source of errors in human motion analysis, affecting the calculated joint angles and moments. The Global Optimization Method (GOM) is effective in compensating STA during gait but its performance for activities involving large range of motion such as cycling has not been reported, mainly owing to the difficulty in obtaining accurate skeletal motion non-invasively. This study evaluated the GOM using the skeletal motions of the knee measured by a 3D fluoroscopy technique during cycling.

Method: Five young adults wearing 14 skin markers on the right lower limb performed cycling exercises on an ergometer while the pedal reaction forces were measured with an instrumented pedal and the trajec-

tories by a motion capture system. The skeletal motions of the right knee were measured using a CT-to-biplane fluoroscopy registration technique and then taken as the gold standard. A 3-link model composed of the pelvis, thigh and shank was used to calculate the angles and moments at the knee from the skin markers, without considering STA and with GOM to compensate for STA. The root-mean-squared errors (RMSE) of the calculated variables were then obtained with respect to the gold standard.

Results & Discussion: The RMSE's of the angles in the sagittal, transverse and frontal planes using GOM were 2.9, 3.8 and 9.3 degrees, respectively, compared to 9.1, 7.8 and 10.8 degrees without considering STA. The corresponding values for joint moments were 1.5, 0.6 and 2.3 Nm for GOM, and 2.4, 1.1 and 3.3 Nm without considering STA. The results showed that the GOM was effective in compensating the STA of the markers for the calculation of the angles and moments at the knee during cycling movement, which will be useful for future study of knee biomechanics during cycling using skin marker-based motion analysis.

ID: 661

PO-01: 54

Chaotic analysis of epileptic EEG signals

Kannathal Natarajan¹, Johnny Chee¹, Kenneth Zi Jian Er¹, Karen Lim² and Hian Tat Ong²

¹NgeeAnn Polytechnic, Singapore; ²National University Health System (NUHS), Singapore.

Electroencephalogram (EEG) is the recording of the electrical activity of the brain. One of the major fields of application of this relatively cheap and non-invasive diagnostic technique is epilepsy, which affects almost 1% of the world's population. Automatic seizure detection is very important in clinical practice and has to be achieved by analyzing the EEG signals. Inter-ictal spikes and sharp waves in human EEG are characteristic signatures of epilepsy. These potentials originate as a result of synchronous, pathological discharge of many neurons. The reliable detection of such potentials has been the long standing problem in EEG analysis, especially after long-term monitoring became common in investigation of epileptic patients. In this paper, a comprehensive chaotic analysis of the normal, ictal and inter-ictal segments in EEG signals is studied using nonlinear dynamical parameters such as correlation dimension, fractal dimension exponent and entropies. These measures show distinct difference for normal, ictal and inter-ictal segments in the EEG recordings. The results are further supported by ANOVA test which gives a p-value of less than 0.01 with 95% confidence. The

results of the study done for two age groups of paediatric subjects, demonstrated the potential of these chaotic measures in quantifying and automatically detecting the presence of any seizure activity in the EEG recordings with high statistical significance.

ID: 667

PO-01: 55

Channel modeling and simulation for galvanic coupling intra-body communication

Yueming Gao¹, Xiuxiang Li¹, Željka Lučev Vasić², Siohang Pun³, PengUn Mak³, Igor Krois², Mario Cifrek² and Mangl Vai³

¹College of Physics and Information Engineering, Fuzhou University, Fuzhou, China; ²University of Zagreb, Faculty of Electrical Engineering and Computing, Zagreb, Croatia; ³Department of Electrical and Computer Engineering, University of Macau, Macau, China.

Intra-body communication (IBC) utilizes the human body as the data channel to ensure the signal transmits through the on-body and implanted sensors. It offers a low power, low radiation and high transmission quality method for currently fast developing Body Area Network (BAN). In our previous work, the theory model and simulation of the physical model have been researched. In order to design and implement the IBC system, the channel model should be investigated. In this paper, a channel model of the IBC was constituted, including the signal generator, modulator-demodulator, human channel with AWGN noise and equalizer module. The communication theory related to different types of modulation methods, data rate, SNR (signal noise rate) and BER (bit error rate) based on this model was analyzed. Then, in order to attain the attenuation properties of the human channel, the in vivo experiments with 7 volunteers were carried out through the signal analyzer with trace generator and the differential probe. Due to the frequency-dependent of human channel attenuation, the equalizer was designed to compensate frequency distortion. The effect of the equalizer was approximated to the amplifier, filter and reshape in the communication system. At last the constellations diagrams of PSK, BER versus SNR of intra-body communication system were investigated. The results showed that the human body has a stable propagation characteristic in the frequency range from 10 kHz to 500 kHz with different volunteers. The constellation diagrams with the equalizer were much better than the situations without the equalizer. It indicated that the ISI (inter-symbol interference) induced by the frequency distortion of human channel was effectively reduced by the equalizer. FSK can achieve the lowest BER versus SNR and it was the best modulation for communication system. QPSK

and BPSK had the similar BER with SNR. Yet the 8PSK was the worst collection.

ID: 676

PO-01: 56

Indirect-contact surface electrocardiography measurements by capacitive electrodes

Michal Gála¹, Branko Babušiák², Marek Penhaker¹, Martin Černý¹ and J. Kraus²

¹VSB-TU Ostrava, Czech Republic; ²ZU Žilina, Slovak Republic.

This article describes electrocardiography measurements using capacitively coupled electrodes. The advantage of this measurement type lies in an indirect-contact between the electrode surface and skin and movement artifact protection. The measurement is easier and more comfortable since capacitively coupled electrodes eliminate the need for conductive gel and direct skin contact with the electrodes. The indirect-contact measurement is also suitable for long-term measurements, where in conductive gel desiccation resulted in loss of contact between the electrode and skin. There is also discussed the electrical design of the indirect-contact ECG prototype mentioned above and the accompanying electrodes along with practical measurements in sitting and lying position with various artifact types. This article serves as a preliminary study of indirect-contact ECG with future intention to implement this system within textile products for sophisticated, comfortable and non-obtrusive ECG measurements.

ID: 675

PO-01: 57

Pacemaker battery state checking by stimulation pulse width detection

Michal Gála¹, Ivana Vajdíková², Branko Babušiák², Marek Penhaker¹, Martin Černý¹ and Martin Augustynek¹

¹VSB-TU Ostrava, Czech Republic; ²ZU Žilina, Slovak Republic.

Pacemaker therapy has indispensable role in therapy of many cardiac diseases. Lifetime of implantable pacemakers is several years. The time of right guaranteed functionality is limited by battery lifetime. The pacemaker battery state verifying is realizable by programmer of the concrete producer. This solution is costly. The other method of pacemaker battery state checking is analysis of patient's electrocardiogram. The paper deals with possibilities and methods of pacemaker battery state verifying and propose a motion for suitable system creation. The final system will provide the information about battery state. It will be embedded system with small size which will be used by general physicians and by patient at home as well.

ID: 715

PO-01: 58

Discrimination of Parkinsonian tremor from essential tremor using the nonlinear analysis of wrist muscle EMG signals

Parvaneh Tavakkoli¹, Hamid reza Kobravi¹, Ali Shoeibi² and Negar Zakhirehdari¹

¹Department of Biomedical Engineering, Islamic Azad University, Mashhad Branch, Mashhad, Iran; ²Department of Neurology, School of Medicine, Mashhad University of Medical Sciences, Mashhad, Iran.

Discrimination of Parkinsonian tremor from Essential tremor is a controversial diagnostic category. Similar clinical traits, usually results in incorrect diagnosis, and degrade the performance of clinical diagnostic methods. In this paper, a new methodology is presented to discriminate the patients suffering from Parkinsonian tremor and the patients suffering from Essential tremor through the analysis of wrist muscle surface EMG signals recorded in rest and a postural position. Twenty patients with Parkinson disease and twenty patients with Essential tremor participated in the experimental studies. Some frequency and time features were extracted from EMG signals and were fed to nonlinear classifiers. The MLP neural network and SVM were used as the classifiers. According to the results, using the EMG signals recorded in rest position, the SVM classifier reached the performance of 89% accuracy and MLP classifier reached the performance of 92.25% accuracy. In addition, using the EMG signals recorded in a postural position, the SVM classifier reached the performance of 90.25% accuracy and MLP classifier reached the performance of 95.75% accuracy.

ID: 729

PO-01: 59

The role of talin in governing the molecular architecture of focal adhesions

Jaron Zhongliang Liu, Honzhen Goh, Yilin Wang and Pakorn Kanchanawong

National University of Singapore, Singapore.

Integrin-based focal adhesions (FA) are multifunctional organelles that mediate cell-ECM adhesion, force transmission, cytoskeletal regulation, and eventual cell migration. These dynamic structures consist several different proteins, and defining clearly the molecular architecture will allow us to understand how mechanical force may be essential for FA formation and maintenance. Recently, Kanchanawong and colleagues [1] were able to map the nanoscale protein organization in FA using interferometric photoactivated localization microscopy (iPALM), revealing

that integrins and actin are vertically separated by a ~40-nm FA core region consisting of multiple protein-specific strata containing proteins such as focal adhesion kinases (FAK), paxillin, talin, vinculin, zyxin, and α -actinin. However, it remains unclear what regulates this nanoscale stratification in these molecularly crowded structures. Interestingly, Talin, a large protein implicated in integrin-mediated adhesion and force transmission, is observed to orient in a unidirectional manner spanning this gap. As talin has multiple binding sites for FA proteins, we hypothesize that this large protein might form a vertical scaffold across the integrin-actin gap, and thus talin may effectively serve as a molecular ruler that controls FA molecular architecture. To test this hypothesis, we aim to investigate whether the alteration of talin's length affects the molecular architecture of FA. We reconstituted engineered minimal talins (in lieu of endogenous talin) in siRNA-mediated talin-depleted HUVECs, and found that several constructs provided the phenotype rescue in the same way as wild-type full-length talin. Next, we want to utilize iPALM to directly observe the apparent integrin-actin gap and the resulting FA architecture.

ID: 743

PO-01: 60

Comparative study of water-logged meat and fresh meat using micro-CT

Amirinnisa Dyah Atrisandi¹, Saumi Zikriani Ramdhani², Nugroho Budi Wicaksono¹, Eko Arianto¹, Tati L. R. Mengko¹ and Fourier D. E. Latief³

¹Biomedical Engineering Research Group, SEEI-ITB, Indonesia; ²Medical Physics Research Group, FMNS-ITB, Indonesia; ³Rock Physics Laboratory, Physics of Complex Systems, FMNS-ITB, Indonesia.

Water-logged meat (or Glonggongan meat) can be found widely in the Indonesian local market to meet market demands, especially on holiday sessions. Its microstructure and content are barely distinguishable with the Fresh Meat. In this project, the detection and comparative analysis between fresh and glonggongan meat using MicroCT is proposed to differentiate both of those meat samples. The methods are by acquiring and reconstructing meat images using MicroCT, and then the reconstructed images are analyzed using MATLAB and CTan software. The results of this project are the fresh meat has less closed pores volume than the water-logged meat which shows that the number of fibers in the glonggongan meat sample is less than the fresh one.

ID: 763

PO-01: 61

Evaluation of electrohysterogram feature extraction to classify the preterm and term delivery groups

Soo Young Sim¹, Ho Suk Ryou¹, Han Byul Kim¹, Jung Min Han¹ and Kwang Suk Park²

¹Interdisciplinary program of Bioengineering, College of Engineering, Seoul National University, Republic of Korea;

²Department of Biomedical Engineering, College of Medicine, Seoul National University, Republic of Korea.

The prediction of preterm delivery is very important for investigating risk factors for preterm birth and initiating risk specific treatment but still remains a challenge for obstetricians. Based on the fact that the characteristics of uterine muscle activities change as pregnancy progresses, many researchers have tried to use noninvasive Electrohysterogram (EHG) for separating the preterm and term delivery. To investigate novel and useful features to classify the preterm and term delivery groups, we randomly selected 40 records from Physionet EHG database. The records were classified into four groups depending on the time of recording (before or after the 26th week of gestation) and the length of gestation (term delivery: ≥ 37 weeks of pregnancy duration or preterm delivery: < 37 weeks of pregnancy duration). 40 records were composed of 10 records from each group. 26 features including 18 time domain features and 8 frequency domain features were applied to each record to find out the difference in characteristics of the uterine muscle activities between term and preterm delivery. As a result, Frequency Ratio (FR) and Mean Absolute Value Slope1 (MAVSLP1) indicated a significant difference between term and preterm delivery records recorded before 26th week. And Willison amplitude (WAMP), Slope Sign Change (SSC), and 3rd Spectral Moments (SM3) had significant difference between preterm and term delivery data recorded during the later period of gestation. Also, Slope Sign Change (SSC) and Frequency Ratio (FR) showed a significant difference between all term and all preterm delivery records.

ID: 766

PO-01: 62

Diaphysis fracture on tibia and fibula detection based on digital image processing and scanline algorithm

Yunendah Nur Fuadah¹, Achmad Rizal² and Yuli Sun Hariyani²

¹ITB, Indonesia; ²ITTelkom, Indonesia.

The X-Ray images of tibia and fibula are the important aiding for clinical diagnosis of fracture because detection fracture performed by medical practice based on it. Under conditions of tired eyes, some medical practice miss fracture cases. There are many

previous research developed various methods to process X-Ray images and make system that can detect fracture automatically.

In this paper, we proposed the simple system that can detect fracture on the tibia and fibula in two stages. The first stage image pre-processing using image enhancement, edge detection, filtering to remove noises and results the edge of image perfectly. The second stage is feature extraction using scanline algorithm that find the maximum value of difference distance to the nearest pixels from the right and left border margin of image. The maximum value of scanline is used as a threshold to classify fracture cases and normal cases.

Accuracy system is calculated based on images were tested right for all images tested. Total images that used are 70 images, 30 normal images and 40 fracture images. Accuracy in this simulation reach 100% for normal images and 90% for fracture images, with time computation about 2.33 seconds.

ID: 819

PO-01: 63

Brain behavior in learning and memory recall process: a high-resolution EEG analysis

Hafeez Ullah Amin¹, Aamir Saeed Malik¹, Nasreen Badruddin¹ and Weng-Tink Chooi²

¹Universiti Teknologi PETRONAS, Malaysia; ²Universiti Sains Malaysia.

Learning is a cognitive process, which leads to create new memory. Today, multimedia contents are commonly used in classroom for learning. This study investigated brain physiological behavior during learning and memory process using multimedia contents and Electroencephalogram (EEG) method. Fifteen healthy subjects voluntarily participated and performed three experimental tasks: i) Intelligence task, ii) learning task, and iii) recall task. EEG was recorded duration learning and memory recall task using 128 channels Hydro Cel Geodesic Net system (EGI Inc., USA) with recommended specifications. EEG source localization showed that deep brain medial temporal region was highly activated during learning task. EEG theta band in frontal and parietal regions and gamma band at left posterior temporal and frontal regions differentiated successful memory recall. This study provide additional understanding of successful memory recall that complements earlier brain mapping studies.

ID: 829

PO-01: 64

Detection of insomnia from EEG and ECG

Haslaile Abdullah^{1,2}, Dean Cvetkovic² and T Penzel³

¹Razak School of Engineering and Advanced Technology, Universiti Teknologi Malaysia, Kuala Lumpur, Malaysia; ²School of Electrical and Computer Engineering, RMIT University, Melbourne, Australia; ³Sleep Medicine Center, Department for Cardiology, Charité Universitätsmedizin Berlin, Charitéplatz 1, Berlin, Germany.

Insomnia is a sleep disorder that causes disturbance in a normal sleep pattern resulting from the difficulties to fall asleep or to stay asleep. Biosignals of human body if measured are also affected due to these abnormal conditions. A current practise in diagnosing insomnia is through clinical interview by the physician which is subjective and suffers from human error judgement. Therefore, a more reliable and accurate diagnostic tools are needed to help physician in making decision. The objective of this study is to classify healthy and insomnia by implementing advanced classification technique based on Artificial Neural Network (ANN).

In this study, sleep EEG and ECG signals of 10 insomnia patients and 10 healthy subjects are analysed. Several linear and nonlinear features are extracted from the denoised signals: linear features (power spectral of EEG frequency bands, brain rate, Hjorth parameters, heart rate variability) and nonlinear features (Largest Lyapunov Exponent (LLE), Sample Entropy and Correlation Dimension (CD)).

For classification purpose, a Feedforward Neural Network (FNN) is implemented to classify the two groups. Half of the data is used for training and the other half is used for testing the classifier. The Levenberg Marquardt backpropagation algorithm is used as a training function. Several numbers of hidden layers are tested in order to achieve optimum classification accuracy. A classification accuracy of 81.3 % is obtained for 3 hidden layers This result shows that the combination of features extracted from EEG and ECG signals during sleep and FNN are useful to be adopted as a biomarker and classifier in identifying insomnia of FNN.

ID: 833

PO-01: 65

Diffusion tensor based Alzheimer image analysis using region specific volume features and random forest classifier

Ranjan Piyush¹ and S. Ramakrishnan²

¹Indian Institute of Technology Madras, India; ²Indian Institute of Technology Madras, India.

In this work a method to utilize volume information as an independent feature for diagnosis of Alzheimer's disease (AD) using Diffusion Tensor Images (DTI) is proposed. For this study the DTI were obtained from ADNI, an international repository for current Alzheimer's study. Equal number of AD and normal control subjects were used for the study. The volume of six regions namely, Fornix/Stria Terminalis Left, Fornix/Stria Terminalis Right, Fornix, Corpus Callosum, Cerebral Peduncle and Anterior Corona Radiata, reported to be prominently responsible for AD were extracted. Volume features corresponding to the above said feature set was used to classify AD and controls using random forest classifier. The data was also used for classification with significant components extracted using principle component analysis. The classification accuracy of 71.4% was achieved for full dataset which further improved to 85.7% on application of principle components as the feature. An enhancement in precision was observed which increased from 72.7% for full dataset to 88.9% for principle components. The sensitivity was observed to be 88.9%. The results demonstrate that volume can be used as a feature for differentiating AD from normal controls. The volume feature can be used independently for initial screening tests. This can be used for automated identification of AD using DTI.

ID: 842

PO-01: 66

Electrophysiological signal segmentation for EEG frequency bands and heart rate variability analysis

Haslaile Abdullah^{1,2} and Dean Cvetkovic²

¹Universiti Teknologi Malaysia, Malaysia; ²RMIT University, Australia.

Biological signals like Electroencephalography (EEG) and Electrocardiography (ECG) provide very useful information related to brain and heart condition. Spectral analysis of EEG frequency bands and analysis of Heart Rate Variability (HRV) of ECG signal are largely used as a biomarker in studying various pathological conditions. However, the studies on EEG and HRV frequency bands analysis have shown inconsistency in the size of segment length used to extract the features. In the power spectral analysis, the trade-off between time and frequency resolution remain unsolved issue. To increase a frequency resolution and reduced a spectral leakage, a long segment of input data is necessary. However, for a stationary consideration a short segment data is needed. Therefore, in this study we examine the effect of segmentation time window and overlapping in spectral analysis of EEG frequency bands and HRV. The EEG and ECG signals used in this study are collected from

the healthy and sleep apnea patients. Five features (delta, theta, alpha, sigma and beta) are extracted from EEG frequency bands and three (LFnu, HFnu, LF/HF) from the HRV by using spectral analysis at various window size and overlapping percentage. The results show the optimum window size for EEG is achieved at 10 sec and 120 sec for HRV analysis.

system and shorter processing time than method A were realized by method B while keeping purity.

ID: 260

PO-01: 67

System improvements for exhaled breath measurement system

Saki Kanou¹, Shinjiro Iitsuka¹, Takashi Nagaoka³,
Naofumi Kobayashi⁴, Muneshige Kurahashi⁴, Sunao Takeda⁵,
Takuya Aoki², Chizuko Tsuji², Tetsuya Urano², Tadashi Abe²
and Kazushige Magatani¹

¹Tokai University, Japan; ²Tokai University School of Medicine;
³Waseda Research Institute for Science and Engineering; ⁴Nihon
Kohden Corporation; ⁵Department of Clinical Engineering.

As many as 200 kinds of volatile organic compounds (VOCs) are included in human exhaled breath. Many papers using VOCs as a biomarker of chronic respiratory diseases have been reported. However, it is very difficult to measure very low concentration of VOCs in exhaled breath with high precision. Moreover, it is also difficult to distinguish VOCs in exhaled breath and VOCs in atmosphere. Therefore, measurement of VOCs is rarely used in a clinical field because complicated and large-sized system is required for measure VOCs in exhaled breath. We are developing exhaled breath measurement system which overcame these problems. Our system analyzes exhaled breath discharged from living body by inhaling atmosphere from which VOCs were removed. In this paper, results of system improvements are reported. At first, we adopted a cold trap method with dry ice as a method of purifying atmosphere (method A). Method A needs complicated device and long-time processing. Next, we changed the method into solid absorbent from method A (method B). We verified purity of purified air by standard gas. 10 kinds of VOCs contained in both exhaled breath and atmosphere were adopted as VOCs contained in the standard gas. Its contents are as follows: benzene, cyclohexane, ethylbenzene, heptanes, hexane, isoprene, nonane, octane, toluene and xylene. The concentration of each VOC in standard gas was 10 ppb. The standard gas was purified by the method A and B. Concentrations of VOCs contained in the purified air were measured by gas chromatography. As a result of measurement, VOCs were not detected in the purified air created by both methods. Furthermore, time to create purified air was reduced from 70 minutes to 10 minutes. Simplification of the

Day 2 – Thursday, 5 December 2013

Session Poster Session 02 (PO-02)

Date / Time Thursday, 5 December 2013 / 11:00–17:00 hrs

ID: 120

PO-02: 01

The multi-physics simulation of prototype designs for channel mixing structures in microfluidic device

Bernardino Jerez Buenaobra and Romel G Bacabac

Medical Biophysics Laboratory, Department of Physics, University of San Carlos, Philippines.

This work highlights the computer simulation performance of two designs of microfluidic structures using computational fluid dynamics (CFD) software. Under simulated conditions of a forced steady and unsteady flow scheme, the possibility of detection for potential mixing in the channels that can be brought about by changes in velocity profile and nodal pressure along the fluid path is investigated. The solid geometry model were extracted and derived from experimental fabrication work, where no physical model for them has existed yet. The two dimensional (2D) relative coordinates were obtained where from actual prototype structures that were successfully fabricated, done much earlier before this effort began at the Medical Biophysics Laboratory at the Department of Physics in the University of San Carlos. At the time of this writing the technologies used were all based on PDMS (Polydimethylsiloxane) in tape and mold process all at the early stages of development; that work employed image processing techniques from digital camera captures for quantifying perceived effects of mixing from laminar flow. In contrast with the focus of this report, the simulation results shows that at points and areas where there are changes of channel width from wide to narrow and its reversed order as well noted where there are bends and curves that occurred along the fluid path it indicates a rise in Reynold's number from a laminar value to a close turbulent flow demonstrating a potential to non-Newtonian flow in the microfluidics domain. These observed effects demonstrated in software animations could indicate an introduction of small but accumulated change along the way in the entire length of the channels which could lead to a mixing action. This geometry that brought about these changes has implications on the function of merit for the design of practical devices for medical bioengineering applications.

ID: 127

PO-02: 02

Development of pneumatic wheeze generator for analysis of wheeze in biomedical applications

Subbaraman Ravichandran¹, Ng Wan Ern Shirlynn¹, Muthayya Hamsan¹, Ng Jun Wen Javie¹, Ng Chuan Fang Favian¹, Lin Shanshan¹ and Then Tze Kang²

¹*Temasek Polytechnic, Singapore;* ²*National University of Singapore, Singapore.*

This paper discusses the design and development of pneumatic wheeze generator that has been developed for the first time to provide wheeze signal for calibrating biomedical tools for analyzing wheeze without the participation of patients. The wheeze generator essentially consisted of vibrating columns which are energized by an airway generator providing inspiratory and expiratory flow patterns. These vibrating columns have been designed to customize the frequency and the pitch of the tones. Wheezes are usually defined as high-pitched continuous tones with a dominant frequency of 400Hz or more. In some patients, they may be audible at some distance from the patient. The transmission of wheezing sounds through airways is better than transmission through the lung to the surface of the chest wall. The higher frequency sounds are more clearly detected over the trachea than at the chest. The high frequency components of breath sounds are absorbed mainly by the lung parenchyma. The peaks at 480 and 650Hz were seen over both locations, but their relative magnitudes were reversed as a result of the low-pass filtering effect of the lung. Wheezing may result from localized or diffused airway narrowing or obstruction from the level of the larynx to the small bronchi. The airway narrowing may be caused by bronchoconstriction, mucosal edema, external compression, or partial obstruction or by tenacious secretions. The mechanisms underlying wheeze production appear to involve an interaction between the airway wall and the gas moving through the airway. Their mechanisms of production have been compared with musical wind instruments. To conclude, the newly developed pneumatic wheeze generator has expanded the scope to perform simulated conditions to fine tune analytical packages for greater accuracies.

ID: 142

PO-02: 03

Study on the safety improvement of double filtration plasmapheresis circuit

Aya Morisaki¹, Masakuni Iwahashi², Yukiko Nkahara¹, Hiroyuku Nakayama¹ and Shingo Takezawa³

¹Junshi Gakuen University, Japan; ²Tokai University, Kumamoto, Japan; ³Kyushu University of Health and Welfare, Nobeoka, Japan.

Purpose: A cassette type circuit of double filtration plasmapheresis was reported previously. The operating time and operational errors for setting up the circuit were investigated by means of a questionnaire survey. This paper is intended as an investigation of improving the safety of the circuit.

Method: According to the results of questionnaire survey, some currently in used circuit samples that had accident happened was extracted. The problems of safety on operation of setting up circuits were examined. Furthermore, a more secure circuit was simulated. The operation time in setting up circuit and the priming volume were compared between a cassette type circuit and a currently used circuit. A modified circuit was simulated.

Results: It was understood that the currently being used circuit was complexity and the operational errors for setting it up were occurred easily even by a skilled clinical engineer' operation. However, it was clear that the operating time was shorter in setting up a modified circuit than in a currently used circuit. The priming volume was also reduced in the modified circuit.

ID: 159

PO-02: 04

Synthesis and characterization of novel self-assembly and pH-sensitive anticancer drug carriers: (PAMAM-AP)-modified PEG loading with DOX

Kung-Chin Chang, Pei-Shan Wu, Jui-Ming Yeh and Ming-Fa Hsieh

Chung-Yuan Christian University, Taiwan;
kimi681016@cycu.edu.tw

A self-assembly and pH-sensitive drug release system that is based on aniline pentamer (AP) as a shell conjugated to polyethylene glycol (PEG)-modified dendrimers (PAMAM) with doxorubicin (DOX) (DOX-PEG-PAMAM-AP) has been constructed and characterized. First of all, the higher generations (G = 5) are demonstrated to self-assemble into bilayer vesicles owing to the strong tendency of the AP to form PAMAM-AP G5. Subsequently, PAMAM-AP G5 modified hydrophilic and biocompatibility segment

PEG synthesis of PEG-PAMAM-AP G5. Finally, load with the anticancer drug (DOX) to synthesis DOX-PEG-PAMAM-AP G5. The use of amphiphilic characteristics form these aggregations as new drug carrier to explore the ability to cytotoxicity of human breast cancer cells, and compare the drug release efficiency.

Identification part of the ¹H-NMR structural analysis and UV-vis measurements of the absorption values of DOX into the calibration curve to calculate the rate of drug loading content (DLC) and drug loading efficiency (DLE) and the microscope to observe cell growth circumstances. The results show that the novel anticancer drug carriers (DOX-PEG-PAMAM-AP G5) could effectively enhance the DLE and drug cumulative release at pH = 4.0 compared with DOX-PEG-PAMAM G5. The cancer cell cytotoxicity of DOX-PEG-PAMAM-AP G5 is similar to DOX.

Acknowledgements

We gratefully acknowledge the financial support of the Ministry of Education (MOE), Taiwan, R.O.C., NSC 101-2632-M-033-001-MY1, the Center for Nanotechnology and Institute of Biomedical Technology at CYCU.

ID: 175

PO-02: 05

On the optimization of cutting parameters for the manufacture of metallic femoral heads

M. S. Uddin

University of South Australia, Australia.

This paper presents an optimization of cutting parameters in turning of metallic femoral heads. Three important machining variables – cutting speed, feedrate, and depth of cut, were considered for optimization where the objective was to minimize surface roughness and sphericity. A factorial design of experiments was planned to capture the effect of machining variables on the output variables. A series of single-pass finish turning tests was conducted on a 28 mm femoral head made of biomedical grade stainless steel AISI 316L by using tungsten carbide inserts. We used a statistical analysis using ANOVA (analysis of variance) to elucidate the influence of dominant parameters, which led to derive a regression model and response surface to estimate the desired outcome. Feedrate and depth of cut were found to impact the overall result. Using a desirability function criteria, both single-response and multi-response optimizations were performed to select the optimum combination of machining parameters. The objective was to maximise the desirability under the given range of parameters. Optimization results show that cutting speed of 280 m/min, feedrate of 0.1 mm/rev, and depth of cut of 0.2 mm are the optimum set

which is expected to provide minimum roughness and sphericity.

ID: 198

PO-02: 06

Development of a non-invasive system to estimate ankle brachial index

Xin Ji Alan Tan, Kok Poo Chua and Jong Yong Abdiel Foo

Ngee Ann Polytechnic, Singapore.

Peripheral arterial disease (PAD) occurs when plaque builds up in the artery walls and limits the blood flow in the legs which may subsequently cause muscle pains. It is a highly prevalent medical condition among diabetic patients and in severe cases; it can lead to limbs amputation. PAD affects 4.3% of the Singapore population, mainly those aged above 60 years. Ankle brachial index (ABI) is used to assess the presence or severity of PAD of the lower extremity. The current method uses blood pressure cuffs and a Doppler ultrasound. One of its limitations is the discomfort caused from the inflation of the four pressure cuffs during the measurement, especially when repeated measurements are required. This study describes a surrogate method to screen the ABI value using the pulse transit time (PTT) approach and to reduce the stated discomfort. The developed system is portable and standalone which consists of a combination of electrocardiogram (ECG) and photoplethysmography (PPG) circuitry. In this study, PTT readings from 8 healthy subjects (5 male, 20–64 years) were acquired in the sitting posture. The developed system was able to estimate PTT readings from the 4 limbs simultaneously and by using a ratio based approach, it shows potential to indirectly compute the corresponding ABI value.

ID: 199

PO-02: 07

Changes in the water content of the corneal layer of newborn infants using a corneometer

Kiyoko Shirai¹ and Yoshitake Yamamoto²

¹Okayama University, Okayama, Japan; ²Himeji Dokkyo University, Himeji, Japan.

This study measured serial changes in the water content of newborn infants to investigate the characteristics of newborn skin and obtain basic information to provide effective cleansing care and create the perfect environment to promote the formation of the corneal layer of newborn infants.

The subjects were 73 term infants who had an appropriate-for-date (AFD) birth weight ($\geq 2,500$ g) consisting of 39 infants born between October and December 2007 (fall) and 34 infants born between

April and March 2011 (spring). The water content of the corneal layer of the epidermis was measured using a corneometer (CM825: Courage + Khazaka, Germany). Using this corneometer, the water content of the skin from the skin surface to areas 30–40mm below is measured by the electrostatic capacity method, and measurement values are expressed as values from 0 to 120 that are proportional to the skin water content. before bathing from the 1st to 5th day after birth in the following 6 areas of the body: (1) between the eyebrows, (2) left corner of the mouth, (3) the middle of the left forearm, (4) left area of the abdomen (between the anterior superior iliac spine and navel), (5) infrascapular area (at the nipple level), and (6) the lateral side of the thigh (2 fingerbreadths above the knee joint).

The water content of newborn skin was the lowest on the 1st day after birth, and increased with days. The water content of the skin differed among the areas of the body, being highest in the corner of the mouth and lowest on the forearms. The temperature and humidity of the neonatal intensive care unit was higher in the spring than fall, and the water content on the 1st day after birth was higher in infants born in the spring than those born in the fall.

ID: 200

PO-02: 08

Construction of skin impedance model for evaluation of skin barrier functions in case wet-type electrode

Yoshitake Yamamoto¹, Kiyoko Shirai², Toshimasa Kusuohara² and Takao Nakamura²

¹Himeji Dokkyo University, Himeji, Japan; ²Okayama University, Okayama, Japan.

Skin has barrier functions which prevent injection of bacteria and perspiration of water. In the field of clinic, there are many situation of failure in barrier functions by stimuli of apply and remove in tape in dialysis patient, by exchange of artificial anal (ostomate), and frequent disinfection. Then, simple evaluating method barrier function of skin is expected non-invasive and quantitatively. So, skin impedance model was proposed in order to develop the evaluation method of barrier functions. Various levels of skin barrier function were prepared artificially by cellulose adhesive tape stripping of forearm stratum corneum. The stripping was performed up to 32 times. Skin impedances were measured with applying PEG liquid wet concentric electrode by impedance meter (Agilent model E4980A) over the frequency 20Hz–2MHz. Frequency characteristics of skin impedance satisfy Cole-Cole arc's law. It is characterized by four parameters Z_0 , f_m , C_0 , and β estimated in impedance loci. Skin impedance varies over 1000 times in magnitude and decrease rapidly

with increase of striping time. It is cleared that the relationship between magnitude of skin impedance and barrier function. Then, skin impedances were divided to six groups from magnitude in logarithmic scale. The standard values of arc's parameters to each group were determined. One of parameter Z0 in this model is 1M, 260k, 35k, 6k, 1.2k, 0.65kohms. They are, that is, skin impedance models for evaluation of barrier functions. From the consideration of fundamental characteristic in four parameters, when the skin barrier function is failure, Z0 is lower, fm is higher, C0 is bigger, and beta is smaller. Because these agree with experimental results, skin impedance models are useful to evaluation of barrier functions. If a skin impedance measurement result on subject is compared with these models, the barrier function in its site could be determined easily.

ID: 237

PO-02: 09

Native tapioca starch-based plasma expander: preliminary investigation

Surapong Chatpun^{1,2}, Jirut Meesane^{1,2} and Pairaya Rujirojindakul³

¹Institute of Biomedical Engineering, Faculty of Medicine, Prince of Songkla University, Thailand; ²Biological Materials for Medicine Research Unit, Faculty of Medicine, Prince of Songkla University, Thailand; ³Department of Pathology, Faculty of Medicine, Prince of Songkla University, Thailand.

Volume replacement is a conventional treatment when blood loss from the body to maintain cellular oxygenation activities. Commercial plasma expanders (PEs) are widely used in the volume replacement such as hydroxyethyl starch which is modified corn starch-based PE. In Thailand, the plantation and production of tapioca are numerous and can be exported worldwide in the top level. This work aimed to preliminary study the possibility of using native tapioca starch as a component for plasma expander. The formulations of mixture between modified tapioca starch and 0.9% sodium chloride solution were prepared and characterized in order to obtain the proper rheological properties. Viscosity, colloid osmotic pressure and red blood cell morphology were determined and investigated. An acute hemodilution by 40% of blood volume was carried out in male golden Syrian hamsters (n=7) for each group. There were two groups involved in this study: 1) control group hemodiluted with Voluven and 2) test group hemodiluted with native tapioca starch-based plasma expander. Vital signs such as mean arterial pressure and heart rate were periodically monitored after hemodilution. The results showed that native tapioca starch-based PE had very high turbidity and viscosity compared to Voluven. There was no observation

about shape deformity of red blood cells when blood was mixed with native tapioca starch-based PE. In vivo study demonstrated that animals hemodiluted with native tapioca starch-based PE could maintain mean arterial blood pressure similar to Voluven. However, heart rate, colloid osmotic pressure of plasma and plasma viscosity in animals hemodiluted with native tapioca starch-based PE were lower compared to those in animals hemodiluted with Voluven. Although the in vivo study reported positive results of using native tapioca starch-based PE, it is necessary to modify native tapioca starch to improve some properties for the purpose of the use as a composition in plasma expander.

ID: 265

PO-02: 10

Electrical read-out label-free bio/chemical sensor

Junfeng Song^{1,2}, Xianshu Luo¹, Jack Sheng Kee¹, Kyungsup Han^{1,3}, Chao Li¹, Mi Kyoung Park¹, Xiaoguang Tu¹, Huijuan Zhang¹, Qing Fang¹, Lianxi Jia¹, Yong-Jin Yoon³, Tsung-Yang Liow¹, Mingbin Yu¹ and Guoqiang Lo¹

¹Institute of Microelectronics, A*STAR (Agency for Science, Technology and Research), 11 Science Park Road, Science Park II, Singapore 117685; ²State Key Laboratory on Integrated opto-electronics, College of Electronic Science and Engineering Jilin University, Changchun, People's Republic of China, 130012; ³School of Mechanical & Aerospace Engineering, Nanyang Technological University 50 Nanyang Avenue, Singapore 639789.

We propose and demonstrate a tracing-assisted dual-microring resonator-based optical sensor system in silicon-on-insulator substrate. The system comprises grating coupler, one microring resonator-based sensing element, another microring resonator-based tracing element integrated with electrical controller, and a Germanium photodetector. The grating coupler is used to vertically couple the light into silicon nanowaveguides. The sensing microring is opened and will contact with object directly. Different object will cause different resonance wavelength shift of the sensing ring. Tracing ring is an add/drop microring system. The resonance wavelength is tunable by thermo-optical efficiency and working as a tunable filter. Ge photodetector is for a direct electrical readout. Different from the conventional wavelength-scanning method, we adopt low-cost broadband ASE light source, together with the on-chip tunable filter to generate sliced light source. The effective refractive index change of the sensing microring induced by the sensing target is traced by scanning the supplied electrical power applied onto the tracing microring, and the detected electrical signal is read out by the Ge photodetector. Such optical sensing system eliminates the traditional wavelength-scanning method

thus provide a cost effective sensing scheme. Therefore, it is suitable for point-of-care applications.

Acknowledgment: This work was supported by the Agency for Science, Technology and Research (A*STAR) Joint Council Office (JCO) Development Programme Grant (1234e00018), Singapore.

ID: 271

PO-02: 11

The biomechanic quality of dura mater correlating histology 3D-findings

Jan Hemza

Faculty Hospital at Saint Ann, Czech Republic.

The work goals are determination of the dural quality of the skull base area under localisation and there are into anterior skull base fossa, which the most connected with paranasal spaces, the study of the most sensitivity area - lamina cribrosa. The method of histology of dural sheats into 3 mutually perpendicular coordinate axis, finding out their biomechanic characteristics. In literature there is only one study of biomechanic quality of dura mater – Melvin, 1970. Melvin described the technic of study in different plane, but in paper published only one number of biomechanic duality. In the different part of intracranium the dura mater analyses different biomechanical characteristic. On the convexity and anterior fossa the dura mater have different biomechanical characteristics in coronal and sagittal way. The cribriform plate and middle part of skull base – clival and apical pyramidal dura mater is very thin and have low biomechanical characteristics. The best biomechanical characteristic have convexital dura mater, posterior fossa, falx and tentorium. In the study we have in sagittal and coronal plane on convexity and anterior skull base 2 different biomechanical quality – statistically important. This biomechanical study is in correlation of histological study of space collagen distribution. The dura on convexity is the strongest and the most stiff, firm cover of brain, to the skull base way comes to this thin, is finner-grained, less strong and less stiff. On convexity there is dura 2time strong, less elastic then on skull base. The different quality are into coronary nad sagittally plane in convexity (it is statistically significant diference) and to in anterior skull base fossa. Sagittally is dury stronger, less elastic, less drawable on convexity and anterior skull base fossa. The comparison of 3D histology findings and biomechanic characteristics of dura are very narrow related and correlated.

ID: 279

PO-02: 12

A systemic approach to peripheral temperature monitoring and its biomedical applications

Richeek Dey, Lalith Nag Sharan, Goutam Thakur and Dhruv Mohan

Manipal Institute of Technology, India.

Temperature is a crucial diagnostic tool in the assessment of metabolic needs of the body. In this paper peripheral temperature monitoring using a strap-on device is done, the above obtained data including field settings is then assessed in the laboratory. The device consists of an SHT15 temperature module controlled using a low-power micro-controller connected to an OLED/LCD display. Most devices are constricted by the memory data requiring another system to interpret the data or to be connected with the sensor rendering it non-portable. To achieve mobility in these sensors progress has been made through the introduction of bluetooth and RFID but by limiting the power it has made impact on the accuracy. This has been overcome in this paper with the use of micro SD card which also time-stamps the data for further analysis and through the OLED display immediate run-time data can be provided. Thus the requirement of an all time present system and immediate interpretation of the data is overcome without a sacrifice in the accuracy. The indigenous device in this paper is calibrated to sample temperatures at a rate of 1 sample per 8 seconds with a resolution of $0.1\pm C$.

ID: 287

PO-02: 13

A continuous model for the embedment of osteocytes in bone matrix

Pascal Renato Buenzli

Monash University, Australia.

The formation of new bone involves both the deposition of bone matrix and the formation of a network of cells embedded within it, called osteocytes. Osteocytes are essential to the detection of micro-damage and to the control of bone renewal. Osteocytes derive from osteoblasts (bone matrix-laying cells) that become trapped in the matrix during the deposition. In turn, osteocytes control osteoblast activity through their interconnected cell processes. In this contribution, a spatiotemporal continuous model is proposed to investigate the osteoblast-to-osteocyte transition. The model elucidates the interplays between speed of new bone formation, rate of entrapment, and curvature of the bone substrate in determining the density of osteocytes in the new bone matrix.

ID: 291

PO-02: 14

Injectable and thermosensitive PEG-PLGA-PEG hydrogels containing hydroxyapatite: In-vitro and In-vivo characteristics

Mei-Chun Lai, Jui-Ming Yeh and Ming-Fa Hsieh

Chung-Yuan Christian University, Taiwan.

The propose of this study was to design and characterization of injectable and thermosensitive hydrogel composites comprised of poly (ethylene glycol)-poly (lactic acid-co-glycolic acid)-poly (ethylene glycol) (PEG-PLGA-PEG) containing hydroxyapatite (HA) for the delivery of bone morphological protein 2 (BMP-2). PEG-PLGA-PEG was synthesized using ring opening polymerization technique whereas HA was synthesized in a chemical co-precipitation method. In the part of chemical synthesis of PEG-PLGA-PEG, the structure was determined by ¹H nuclear magnetic resonance spectrophotometer and Fourier-transform infrared spectrum. The thermosensitivity and in-vitro degradation of PEG-PLGA-PEG and PEG-PLGA-PEG/HA composite hydrogels were studied by following the rheological measurement and in-vitro degradation test, respectively. On the other hand, the crystal structure of HA was measured by powder X-ray diffraction, scanning electron microscopy and transmission emission microscopy, respectively. The results revealed the PEG-PLGA-PEG/HA composite presented good biocompatibility in the ICR mice subcutis at 8 weeks. In conclusion, PEG-PLGA-PEG/HA composite is believed to be promising for injectable orthopedic tissue engineering due to its good thermosensitivity and injectability.

Acknowledgement

We gratefully acknowledge the financial support of the Ministry of Education (MOE), Taiwan, R.O.C., NSC 101-2632-M-033-001-MY1, the Center for Nanotechnology and Institute of Biomedical Technology at CYCU.

ID: 302

PO-02: 15

Enhancement of cytotoxic effects of bleomycin with permeabilization of plasma membrane by photofrin®-mediated photodynamic therapy in vitro

Daisuke Nishikiori^{1,2} and Yuichi Miyamoto¹

¹Saitama Medical University, Japan; ²Higashi-Yamato Hospital, Japan.

Photodynamic therapy (PDT) is a treatment for malignant tumor employing the interaction of a photosensitizer with light of the appropriate wavelength in the presence of molecular oxygen. We previously

reported that the hematoporphyrin derivative mediated PDT would promote to delivery macromolecules into cytoplasm. Thus, it is considered that the PDT also has an enhancing effect of the anticancer drugs which most likely unable to diffuse across plasma membrane such as bleomycin. In the present study, we examined whether or not Photofrin®-mediated PDT possessing no remarkable cell injury can enhance the cytotoxic effects of the bleomycin for the HeLa cells.

HeLa cells were seeded into a 96-well flat-bottom culture plate at a cell density of 4.2×10^4 cells/well and incubated at 37°C overnight. The medium in each well was replaced with 10 µg/mL Photofrin®-containing PBS(-) and incubated for 15 minutes, then replaced to bleomycin (BLM)-containing medium (BLM: 0.5 µM–100 µM). The cells were irradiated in the medium using a pulsed or continuous wave laser. The wavelength of the lasers was around 630 nm. The irradiation of the laser was carried out with an average fluence rate of 5–50 mW/cm² at light doses 1–3 J/cm². The cytotoxic effects of the PDT alone, the BLM alone and BLM combined with PDT (BLM/PDT) were estimated by XTT viability assay.

There were no remarkable cytotoxic effects without BLM in above PDT conditions. The viability value of the BLM/PDT group at 10 µM BLM concentration was about 20% lower than that of the BLM alone group ($p < 0.0001$). These findings suggest that the cytotoxicity of the BLM is enhanced by the PDT which does not have sufficient cytotoxic effects. This work was supported by JSPS KAKENHI Grant Number 24650268.

ID: 311

PO-02: 16

Frictional properties of polyvinyl alcohol hydrogel mixed with water as an artificial articular cartilage

Koji Morimoto¹, Yoshihiro Kimura², Noriyasu Hirokawa¹, Tadashi Shibue¹ and Takashi Hayami¹

¹Kinki University, Japan; ²JAPAN VAM & POVAL CO., LTD., Japan.

We have investigated the use of polyvinyl alcohol (PVA) hydrogels for hemiarthroplasty. The PVA-hydrogels were prepared in two different solvents using a low-temperature crystallization method. The first was a conventional mixture of water and dimethyl sulfoxide (DMSO), and the second comprised water only. The hardness and wear resistance of the PVA-hydrogel mixed in water (PVA-H/Water) were compared with that of PVA-hydrogel mixed in a DMSO aqueous solution (PVA-H/DMSO). The results indicated no significant difference in the indentation hardness between PVA-H/DMSO and PVA-H/Water. However, the frictional coefficients of PVA-H/DMSO were larger than those of

PVA-H/Water. Fewer wear tracks were observed in PVA-H/Water than in PVA-H/DMSO.

ID: 324

PO-02: 17

Neural stem cells homing to glioma

Sihua Huang^{1,2}, Roger Kamm¹ and Jerry Chan²

¹Singapore-MIT Alliance of Research and Technology, Singapore;
²National University of Singapore.

Glioma is a type of brain tumor that derives from glial cells. The average life expectancy of patients diagnosed with glioma is less than 2 years in spite of surgical resection, radiation and chemotherapy. Glioma cannot be completely removed surgically because of its wild dissemination into surrounding tissue. Neural stem cells (NSCs) have recently been found to home to glioma. Researchers have been using them to carry gene therapies to kill brain tumor and this approach has been reported to reduce 80% to 90% of tumor volume. However the mechanism of NSC tropism to glioma is still poorly understood.

We have shown that NSCs migrate much more extensively to glioma-conditioned media than control in vitro. Various pathways have been suggested to contribute to NSC glioma tropism and we hope to investigate whether there is a major receptor-ligand interaction. We have carried RT-PCR on U87 glioma cells and they are found to genetically express SDF1, HGF, VEGF, uPA, SCF etc. These are cytokines associated with NSC glioma tropism. We will further compare the expression of these cytokines to see which are mostly upregulated in U87 cells comparing to normal astrocytes. Those cytokines will be selected for transwell migration assay and further for NSC migration in microfluidic devices. Microfluidic devices allow movement of NSCs in a 3D gel matrix under a stable cytokine gradient established by flow. We have demonstrated that the gradient can maintain for at least 6 hours under which NSC migration can be studied. In vivo studies will also be carried out to study the effects of selected cytokine on the migration of NSCs. Normal and si-RNA deleted NSCs will be injected into mouse models bearing glioma and their migration efficiency will be examined in parallel.

This study will help us better use NSCs as therapeutic agents to kill glioma.

ID: 331

PO-02: 18

Possible contribution of mesenchymal stem cells in basement membrane reconstruction through extracellular matrix secretion and organization

Priscilla Peh, Casey Chan and Michael Raghunath

National University of Singapore, Singapore.

Mesenchymal stem cells (MSCs) improve wound healing through multiple mechanisms. Recent literature reported that allogenic MSCs helped restore type VII collagen (ColVII) deficit in the dermal-epidermal junction (DEJ) of dystrophic epidermolysis bullosa patients. The efficacious dose was much lower than in fibroblast cell therapy, suggesting that MSCs might have a greater potential in regenerating the DEJ. We compared MSCs with human dermal fibroblasts (HDF) for their matrix deposition properties when co-cultured with a human keratinocyte cell line, HaCaT.

Immunostaining for matrix proteins such as type I, IV and VII collagen (ColI, ColIV, ColVII) and laminin 3,3,2 showed deposition more specifically at the boundaries between HaCaTs and MSCs. A clear border of extracellular matrix protein was formed between the two cell types. No defined borders were identified in the co-cultures with HDFs however, despite increased deposition of matrix proteins around the boundaries. Interestingly, ColVII expression in co-cultures without ascorbic acid appeared restricted to the HaCaT population. When ascorbic acid was added to facilitate collagen secretion, ColVII staining was strong in the MSC/HDF region and appeared to co-localized with ColI.

Our current data suggest that MSCs may be responsible for the secretion and organization of extracellular matrices in a wound healing situation. We are repeating the experiment with primary keratinocytes and investigations are on-going in hope to reveal how MSCs may facilitate wound healing and basement membrane formation through matrix deposition.

ID: 347

PO-02: 19

Modified siRNA as a therapeutic tool for obesity

Jui-Wen Huang¹, Yen-Ju Lin¹, Wei-Chen Hsieh²,
Huan-Yuan Chen², Fu-Tong Liu² and Chung-Wai Shiao³

¹Biomedical Technology and Device Research Laboratories,
Industrial Technology Research Institute, Hsin-Chu, Taiwan;

²Institute of Biomedical Sciences, Academia Sinica, NanKang,

Taipei, Taiwan; ³Institute of Biopharmaceutical Sciences, National Yang-Ming University, Taipei, Taiwan.

Obesity is a growing global health problem. It leads to reduced life expectancy and increases the risk of

various diseases, such as heart disease, type 2 diabetes, and osteoarthritis. Currently, the main prescription weight-loss drugs either try to block the digestion and absorption of fat or help to reduce appetite by affecting the central nervous system. Both medications may cause significant side effects. We develop a superior therapeutic method by applying a modified b-galactoside-binding lectin siRNA as a therapeutic tool. This member of b-galactoside-binding lectins is preferentially expressed by adipocytes and negatively regulates lipolysis in mice. The designed siRNAs showed good activities to knock down the expression of this specific b-galactoside-binding lectin in adipocytes which was differentiated from human mesenchymal stem cells (hMSCs). Compared to the unmodified siRNA that were fully degraded within 1 hour in 50% fetal bovine serum at 37°C, the modified one showed slightly degradation even at 48 hours. The further in vivo b-galactoside-binding lectin inhibitory efficacy of the modified siRNA is under investigation.

ID: 362

PO-02: 20

A novel surgeon-assistant device applicable for pedicle detecting in open spine surgery

Reyhane Moradiahghighat¹, Mostafa Rostami¹ and Mohammad Ali Ghasemi²

¹Faculty of Biomedical Engineering, Amirkabir University of Technology, Tehran, Iran; ²Kian Hospital, Tehran, Iran.

Spinal instrumentations, particularly pedicle screws placement are widely used to combine two or more vertebrae during a surgical procedure. The most important concern in spinal fusion is locating the instrumentations precisely. Since any misplacement may cause postoperative pain, serious injuries to the patient such as spinal canal violation, etc. To insert the pedicle screws accurately, "Free-hand" technique of pedicle instrumentation is frequently used. In this technique, the surgeon implements the pre-operative imaging of patient, visible anatomic landmarks and the geometrical relation to place the pedicle screw. However, this technique depends on the surgeon's skill, and also, multiple redirections and intraoperative imaging might be required.

In this regard, a novel surgeon-assistant device has been presented in this paper. The designed device is capable of finding the exact position and orientation of pedicle screw placement during open spine surgery by using artificial tactile sensing method and pre-operative planning.

The proposed device has five degrees of freedom to be moved easily in the space by the surgeon and be located on the anatomic landmarks. Whenever the device end-effector touches the anatomic landmarks

the coordination of the mentioned points would be measured, using sensors embedded in the device joints. The entry point location is formulated and defined for the device program before surgery according to the existing geometrical relation between anatomic landmarks and entry point. Additionally, the insertion orientation of instrumentation obtained from the anatomical consideration would be saved in the device program. So, the exact entry point would be calculated according to the pre-operative defined program and the measured coordination. At the last step, the accurate entry point and insertion orientation would be accessible for the surgeon to create the guide hole in order to place pedicle screw. Consequently, the risk of damages would be decreased impressively by accurate creation of guide hole.

ID: 376

PO-02: 21

Cell culture device for mesenchymal stem cells and control of differentiation to regenerate an interface of two tissues in a single-phase hydrogel

Shogo Miyata and Toshifumi Ohi

Keio University, Japan.

The recent research about cartilage tissue engineering has reported the development of osteochondral construct using bone-derived mesenchymal stem cells (bMSC). However, the regeneration of osteochondral construct requires a long time to differentiate MSC firstly into chondrocyte and then into osteoblast by chondrogenic and osteogenic cytokines. The objective of this study was to develop a differentiation control device to create the interface of these two kinds of tissues in a single-phase gel. Our novel differentiation control device consisted of syringe pump and culture chamber to induce two kinds of culture medium. The MSC-seeded agarose gels were cultured in this device using basal medium and osteogenic medium. As the results, there was a significant difference in the calcium content between the part subjected to basal medium and osteogenic medium in the single-phase gel. This result indicated that our control device could regenerate the interface of two kinds of tissues in a single-phase hydrogel.

ID: 378

PO-02: 22

Combined effect of compression and electrical stimuli simulating *in vivo* condition on material properties of tissue-engineered cartilage

Shogo Miyata and Yuya Okuda

Keio University, Japan.

Recently, tissue engineering therapy, culturing chondrocyte *in vitro* to create three dimensional tissue and implanting the tissue to replace damaged tissue, has been developed. Native articular cartilage has superior material properties; A high load tolerance, viscoelasticity, and material anisotropy to bear physiological loading *in vivo*. However, mechanical properties of the engineered tissue are not sufficient compared to native one. In this study, we focus on the combined effect of compressive loading and electrical stimuli on cartilaginous tissue regeneration. It is well known that streaming potential in articular cartilage is closely related to both compression and electric stimuli. In this study, chondrocyte-seeded agarose gel was cultured under cyclic compression and electric stimuli to generate the streaming potential. Moreover, the combined effect of compression and electrical stimuli on the tissue regeneration was investigated.

ID: 385

PO-02: 23

The performance photodynamic therapy as an alien-like apparatus for wound healing

Pongsathorn Chotikasemsri

Institute of Biomedical Engineering, Prince of Songkhla University, Thailand.

Some of you may have seen a Sci-Fi movie about an alien using a flashlight-like tool to treat their alien friends' skins after an accident. Then, next 5 minutes, their skins become completely normal and leave happily again. This presentation would like to show some possible and astonishing ideas how we can make one of that tool on earth. Actually, this tool could be made in the near future by using new modern whole gene expression microarray, knowledge of functional medicine, genomic pathway and gene interaction databases, and LED light technology. This tool will be revealed its features in this presentation.

ID: 399

PO-02: 24

The simple setting of microfluidic system with microelectrophoresis setup for surface charge measurement

Foong Poh Lee, Boon Yew Teoh and Yong Sheng Fong

University Tunku Abdul Rahman, Malaysia.

We present a microfluidic system with microelectrophoretic setup that equipped by a compact modified CCD camera for acquiring image of the target and a special design chambers with 2 poles when electric applied to measure the surface charge particles. It is built for characterizing surface charge of different strains of cancer cells or cancer cell conjugation with other substances. The setup was employed with real time image acquiring system, a series of lens was placed in between the sample and the CCD sensor. For calibration purposes, polystyrene bead (10 μ m) was used in this system. The beads were placed in a chamber with two copper electrode located at both ends, it was then supplied with power supply to create the electric field at the chamber to move the charge particles. Meanwhile, image was captured by using the CCD camera which the image was then being processed and produces data on size, morphology and enables the calculation of velocity to the particles. The velocity enables the calculation of electrophoretic mobility (EPM) for particle surface charge estimation. In this investigation, sample of yeast cells were utilized and measured with a magnification of 125 times. Report shows that the EPM of yeast was -10 μ m cm/Vs and the surface charge polystyrene beads obtained was -0.0370 mm²/Vs. The morphology of the yeast and polystyrene bead was also reported. With its simplicity, low production cost and high efficiency, this new device configuration would be useful as medical instrument for diagnostic purposes.

ID: 400

PO-02: 25

Pressure dominated PTT calculation and its relation with BP

Yibin Li, Yangyu Gao, Shenlong Li, Hongyang Li, Yang Zhang and Ning Deng

Tsinghua University, China.

Pulse transit time (PTT) which can be obtained from the peaks of R-wave of Electrocardiogram (ECG) and pulse wave, is promising for non-invasive continuous blood pressure measurement. However, there are different kinds of waves can be employed in this method, namely pressure pulse wave (PPW), photoplethysmography (PPG) and modulated magnetic signature of blood (MMSB). It is critical to clarify the

relationship between those three kinds of pulse waves for practical applications. In this paper, the relationship between blood pressure (BP) and three different types of pulse wave is investigated experimentally. It is found that the MMSB and the PPW measured at the same position have a fixed phase difference. This means that we have to establish different models for MMSB and PPW to obtain accurate blood pressure. We calculate blood pressure based on PPG and PPW, respectively. We find that both PPG and PPW shows high dependency on systolic blood pressure, while only PPW appears to be reasonable correlated with diastolic blood pressure (DBP). This implies that PPG may be not a good signature for blood pressure measurement. Finally, a model on the relationship between those three pulse waves is proposed. The different relationships between three pulse waves and BP are explained based on that model.

ID: 409

PO-02: 26

Label-free detection of meca-mediated Methicillin-Resistant Staphylococcus Aureus (MRSA) using surface plasmon resonance spectroscopy

Kawin Nawattanapaiboon¹, Toemsak Srihirin¹, Boonsong Sutapun², Wansika Kiatpathomchai³, Pitak Santanirund⁴ and Apirom Wongsakulyanon⁴

¹Materials science and Engineering programme, Faculty of Science, Mahidol University, Bangkok, Thailand; ²Department of Electronic Engineering, Faculty of Engineering, Suranaree University of Technology, Nakhon Ratchasima, Thailand; ³National Center for Genetic Engineering and Biotechnology (BIOTEC), National Science and Technology Development Agency, Pathumthani, Thailand; ⁴Department of Pathology, Faculty of Medicine Ramathibodi Hospital, Mahidol University, Bangkok, Thailand.

The DNA hybridization of methicillin-resistant staphylococcus aureus (MRSA) was investigated based on surface plasmon resonance (SPR) technique. 3 dimensional (3D) surface, carboxymethyl dextran hydrogel, were used as the sensor surface. The surfaces were functionalized with streptavidin where the biotinylated DNA probe can be specifically bound. Loop-mediated isothermal amplification (LAMP) products of MRSA were hybridized with the biotinylated probe and were followed by SPR. The SPR spectroscopy was achieved to monitor the hybridization signal in real-time measurement of unlabeled mecA Lamplicons. In this work, The optimal condition of probe density was 0.1 μM that gave high specific SPR signal with the limit of detection for MRSA at 0.2 ng/ μl and non-specific absorption was not observed.

ID: 410

PO-02: 27

Infusion technology – risk analysis from the perspective of biomedical engineering

Josef Cihak, [Martin Augustynek](#) and Marek Penhaker

VSB Technical University of Ostrava, Czech Republic.

The content of this work is the definition of the basic requirements of infusion techniques and their application parameters. The infusion technique is highly effective and safe combination of equipment and special supplies which allows clinically effective therapy, consisting of a precise dose of high drug concentrations or large volumes of solutions which is necessary for the health care. Therefore it is important to highlight the risks associated with this combination of equipment and supplies as well as the closely related procedures and optimization processes that are intended to reduce potential risks, stability and performance. This topic is very important in education especially for biomedical technicians/engineers and others who are troubled with this very often.

ID: 436

PO-02: 28

Design, fabrication, experimental study, and test electrochemical detector with ewod for chemical analysis

Kessarat Ugsornrat¹, Thitima Maturros², Tawee Pogfai³ and Adisorn Tuantranont⁴

¹King Mungkut's University Technology North Bangkok, Thailand; ²Nanoelectronics and MEMS Laboratory, National Electronics and Computer Technology Center; ³Nanoelectronics and MEMS Laboratory, National Electronics and Computer Technology Center; ⁴Nanoelectronics and MEMS Laboratory, National Electronics and Computer Technology Center.

In this research, an electrochemical detector with electrowetting on dielectric (EWOD) digital microfluidic biochip is designed, fabricated, and experimental studied for chemical analysis. For the design, the biochip consists of T-junction EWOD microchip for merging buffer reagent and analyte droplets and three internal electrochemical detectors at the end of T-junction. Three electrodes consist of Au working, Au reference, and Au auxiliary for rapid chemical analysis with minimal reagent consumption. In experiment, the electrochemical with EWOD microchip is fabricated by thin film deposition and tested to study possibility of moving (merging and transporting) droplet on the microchip by digital operation.

ID: 470

PO-02: 29

DNA inserts in alginate gels enhance elastic properties

Mary Ann Agosto Ruelan, Verdad Canila Agulto,
Amos Monterroyo Santoya and Rommel Gaud Bacabac

Medical Biophysics Group, Department of Physics, University of San Carlos, Philippines.

Alginate is a naturally occurring biocompatible material that has been used in various pharmaceutical and medical applications (e.g., as scaffolds for tissue engineering and microencapsulation for drug delivery). It has been shown that the mechanical environment of cells influence biological function. Furthermore, to implement dose-controlled drug release, the permeability of microencapsulating polymer network has to be controllable. Thus, the wide spectrum of applications of alginate gels demands tunable mechanical versatility in order to have predictable outcomes. A seemingly straightforward protocol for tuning biopolymer network mechanics is by inserting materials of known elastic behavior. Hence, this study investigated the bulk mechanical properties of composites consisting of an alginate network with helical inserts modeled using double-stranded deoxyribonucleic acid (DNA). The rheological properties of the alginate-DNA composites were characterized using passive microrheology by videomicroscopy, extracting viscoelasticity signatures based on the thermal fluctuations of embedded tracers. We found an increase in both the viscous and elastic moduli of the composite compared to that of alginate gels without inserts. Based on recent theoretical work, the helical inserts seemingly acted like rod inclusions enhancing both elastic and viscous properties. This demonstrates that the bulk mechanical properties of alginate gels are tunable without applying active cross-linkers. Our results imply that alginate-DNA composites have great potential for high precision tuning by compounding the viscoelastic-enhancement effect of helical insertion with cross-linker based stiffening.

ID: 491

PO-02: 30

Mechanical tuning of dilute DNA solutions is length scale dependent

John Philip Taroma Billones¹, Florencio Salono Bustamante¹,
May Noren Dugang Nanud¹, Paul John Legaspi Geraldino² and
Rommel Gaud Bacabac¹

¹Medical Biophysics Group, Department of Physics, University of San Carlos, Cebu City, Philippines; ²Department of Biology, University of San Carlos, Cebu City, Philippines.

The deoxyribonucleic acid (DNA) is a highly extensible molecule with unique mechanical properties.

These properties enable DNA to tolerate or resist various deformation modes that include bending, stretching, and twisting, high order coiling, along with more complex shear forces encountered while interacting with other macromolecules at pertinent cell cycles. Thus, the viscoelastic properties of dilute DNA solutions was investigated by quantifying the complex shear modulus of whole genomic DNA preparations and solutions with varying DNA lengths at constant concentration. We found that the elastic modulus is DNA length dependent, observing that DNA length anti-correlated with elastic modulus while the viscous modulus remained length independent. This implies that DNA length tunes the elastic component but not the viscous component of the complex shear modulus. Length-dependent mechanical tuning is however more enhanced as DNA approaches its persistence length suggesting that bending modes dominate at dilute solutions. However, we found that both the elastic and viscous moduli are concentration dependent in preparations using whole genomic DNA, which is much longer than the persistence length. This implies that the mechanical behavior of dilute DNA solutions favor elastic enhancement only at regimes where the DNA molecule is at scales close to the persistence length. Furthermore, cross-over frequencies, where the viscous and elastic moduli coincide, occurred at low frequency regimes (<15Hz). The crossover frequency increased as the DNA concentration increased, suggesting that for concentrated DNA solutions, the liquid-like property of the solution will dominate only at much higher frequencies (> 10³ kHz). These results provide further insights on the dynamics of helical biopolymers, modelled using DNA.

ID: 492

PO-02: 31

Characterisation of tissue-engineered corneal graft materials using cultivated human corneal endothelial cells

Hengpei Ang¹, Gary S. L. Peh¹, Khadijah Adnan¹, Andri K. Riau¹,
Xin-Yi Seah¹ and Jodhbir S. Mehta^{1,2,3}

¹Singapore Eye Research Institute, Singapore; ²Singapore National Eye Centre; ³Duke Medical School of Medicine, National University of Singapore, Singapore.

Introduction: Reversible corneal blindness resulting from the dysfunctional corneal endothelium can be restored by the replacement of the diseased endothelial layer with a healthy donor endothelium through a corneal transplant. However due to the global donor cornea shortage, there has been increasing interest in developing suitable graft substitute through tissue-engineering using expanded primary

human corneal endothelial cells (CECs) grown on suitable scaffold carriers.

Experiments: We have developed a strategy for the successful propagation of human CECs isolated from paired donors using a dual media system, where robust expansion of human CECs to the third passage is achievable. For the transfer of cultivated CECs to recipient, a scaffold carrier is required. In this study, we describe the use of both synthetic and biological constructs as carriers on which CECs were seeded at a density of 3000 cells/mm². The CECs morphology were analysed by scanning and transmission electron microscopy. They were also characterized for the expression of function-associated markers, pump protein NA⁺K⁺/ATPase and tight junction protein ZO-1.

Results: Preliminary results showed that human CECs seeded at high density on each of the carriers formed stable monolayers. Ultra-structural analysis showed well-integrated cell-layer consisting of cells with overlapping cellular borders. Corneal endothelial cell counts on these constructs maintained above 2,500 cells/mm², and retained their expression of markers indicative of the corneal endothelium.

Conclusion: The various substrates presented in this study makes good carriers for cultivated human CECs. These can be potentially developed into transplantable cell-tissue engineered graft alternatives where one donor cornea could be used to treat multiple patients. Future work will involve comparative functional validation of the tissue-engineered constructs.

ID: 498

PO-02: 32

A preliminary experimental study on the sound generation by flow impingement in branching airway

Gabriel Pramudita Saputra¹, Kazunori Nozaki², Satoshi Ii¹ and Shigeo Wada¹

¹Graduate School of Engineering Science, Osaka University, Japan; ²Division of Dental Informatics, Osaka University Dental Hospital, Japan.

Auscultation method used for diagnosing the respiratory conditions has been conducted since a long time ago. Nevertheless, lack understanding of the formation and propagation of the sound made auscultation remained a perfunctory method. To understand the sound generation mechanisms, we constructed one-generation T-branch model and a straight tube model to study the importance of flow impingement. All models were prepared in 7 mm and 10 mm major diameter to observe the influence of diameter change. Air of Reynolds numbers between 1,000 and 5,000 calculated at the inlet of the

parent tube was flown through the models, and the emitted sounds were recorded. Flow in the upstream region was then disturbed by introducing constriction of 25%, 50% and 75% diameter changes in the parent tube. As results, for the no-constriction case, small increase of the overall sound pressure level (OASPL) for increase of Reynolds number in 7 mm and 10 mm models (straight tube and T-branch models) was observed, however, one-generation T-branch model produced higher sound level compared to the straight tube model. When a constriction was introduced in the parent tube of the models, the OASPL increased in a non-linear relationship for all models. The sound level slightly increase as the increase of Reynolds number in all models particularly when the constriction had reached 50%. Small models (7 mm diameter) generates higher sound pressure level when the constriction was less than 50%, but when the constriction reached 75%, large models (10 mm diameter) generate higher sound level. These results indicate that flow impingement play important role in both condition, constricted and not constricted airways. In addition, combination of diameter and constriction percentage would determine the dominant sound source of the models which could be an indicator of the lung condition.

ID: 522

PO-02: 33

Design sensor chip for repelling the non-specific binding for its application in biomedical sensor

Thidarat Wangkam¹ and Toemsak Sriksirin²

¹Department of Industrial Physics and Medical Instrumentation, Faculty of Applied Science, King Mongkut's University of Technology north Bangkok, Thailand; ²Department of Physics, Faculty of Science, Mahidol University, Thailand.

The important parameter for the application in biomedical sensor is specificity on the specimen. However, there is the limitation in a low detection signal in real sample applications. The measurement cannot avoid contaminant from some biomolecules, components in patient samples such as blood or serum, which are effect on low detection or error diagnostic. Thus, to decrease this non-specific binding from some contaminants, we designed the sensor chips which are capability on repelling the non-specific binding in order to increase the efficiency of specificity. The ultra thin film and polymeric film were chosen for design. The atomic force microscope (AFM) was used for monitoring behavior of the adsorption of the non-specific binding on the designed chip. The results were found that the ultra thin film can repel some components of samples better than polymeric chip by observation the topography of the sensor chip via AFM. It was found that

the area of the covered biomolecules was shown the inhomogeneous and higher roughness in the polymeric thin film than the ultra thin film. It means that there is more residual contaminant from serum on the polymeric chip and less efficiency repelling the contaminant than the results from the ultra thin film. This result was also correlated to measurement the non-specific binding of patients' serum via surface Plasmon resonance technique.

ID: 546

PO-02: 34

Single cell kinase assay using droplet microfluidics

Ramesh Ramji¹, Chwee Teck Lim^{1,2} and Chia Hung Chen^{1,3}

¹National University of Singapore, Singapore; ²Mechanobiology Institute, Singapore; ³SINAPSE, Singapore.

Recent advances in droplet microfluidics have shown potential for high throughput single cell assays through individual cell encapsulations in water-in-oil emulsions. This compartmentalization allows us to carry out various enzymatic assays which quantify intra and extra-cellular proteins. Kinase is an important class of enzymes which trigger cellular signaling cascades to regulate essential biological mechanisms including cell proliferation, differentiation, growth and metabolism. An abnormal increase or reduction in the activity of kinases often results in a diseased state such as cancer. Hence there is an utmost need to develop and screen potential drugs that can modulate the kinase activity. Current methods follow an ensemble approach to determine the activity thereby ruling out the differences in expression among individual cells, which could be misleading due to the averaging of the signal from a subpopulation.

Here using droplet microfluidics, we demonstrated a dynamic enzymatic assay to measure the activity of intracellular kinases triggered by cell surface biomolecular binding at the single cell level. Epidermoid carcinoma cells (A431) and lung cancer cells (PC9) were encapsulated in droplets along with a specific tyrosine kinase substrate, with and without a specific modulator (Epidermal growth factor, EGF). The binding of EGF to its receptor, EGFR, triggers a cascade of signaling events among cancer cells. In the absence of EGF molecules, the substrate peptide was phosphorylated and reached saturation rapidly with a peak emission at 485nm. Addition of EGF to the droplet triggers EGFR signaling thus phosphorylating peptides resulting in an increase in fluorescence with time. Such assays would not only help one determine the functional effects of biomolecular binding but also would allow one to screen the modulatory effects of drugs at the single cell level.

ID: 555

PO-02: 35

Point-of-care colorimetric-based Tb diagnosis using unmodified-AuNPs on paper substrates

Tsung-Ting Tsai¹, Shu-Wei Shen², Chao-Min Cheng³ and Chien-Fu Chen²

¹Department of Orthopaedic Surgery, Chang Gung Memorial Hospital, Taipei 105, Taiwan; ²Graduate Institute of Biomedical Engineering, National Chung Hsing University, Taichung 402, Taiwan; ³Institute of Nanoengineering and MicroSystems, National Tsing Hua University, Hsinchu 300, Taiwan.

This paper describes a colorimetric sensing strategy employing unmodified gold nanoparticles (AuNPs) and microfluidic paper-based analytical devices (μ PAD) for tuberculosis (TB) diagnosis.

TB, mainly caused by *Mycobacterium tuberculosis* (MTB), is a common and often lethal infectious disease caused by various strains of mycobacteria. Skeletal tuberculosis may account for 35% of extra-pulmonary cases, and TB is often more likely to attack the spine. Diagnosing spinal TB is hard to distinguish between TB infection, other bacterial infections and spinal tumor from X-rays, CT and MRI assessments. Current TB detection methods employ smear microscopy, bacilli culture and molecular species diagnostics. However, these identification methods either have a low sensitivity and additional diagnostic methods need to be used for the confirmation, or require hours to weeks to complete. In addition, the requirement of sophisticated infrastructure and trained personnel limit their feasibility in the developing countries. AuNPs have been adopted to provide alternative schemes than conventional detection methods for TB diagnosis. However, the preparation time for the formation of thiol-modified ssDNA linked AuNPs probes takes hours to complete.

Here, a colorimetric sensing strategy employing unmodified gold nanoparticles and paper assay platform is developed for tuberculosis diagnosis. Unmodified gold nanoparticles and detection single-stranded oligonucleotides are used to achieve rapid diagnosis without complicated and time consuming surface modified probe preparation processes. After hybridizing with extracted DNA sequences from tuberculosis patients and health controls, the existence of free single-stranded detection oligonucleotides would affect the surface charges of gold nanoparticles in test complex and results in the color of gold nanoparticles colloid changes associated with the interparticle distance. Furthermore, the color variance of multiple detection results were simultaneously collected and concentrated on cellulose paper with the data readout via a smart phone transmitting for cloud computing. The proposed platform possesses the potential for ASSURED diagnostic applications.

ID: 561

PO-02: 36

Cardiac output measurement using ballistocardiogram

Ganesan Marimuthu, Rohit Suresh, Bharath Kurumaddali,
Syam BS, Vyshak Suresh and Mayur Venkatesh S

Amrita School of Engineering, India.

Ballistocardiogram (BCG) is a non-invasive technique to measure cardiac parameters. It was popularized by Dr. Isaac Staar in 1940. The Ballistocardiogram signal is generated due to the vibrational activity of the heart. BCG was considered as a promising technique but was replaced by Electrocardiogram due to the difficulty involved in detecting and analysing the BCG waveforms. With the increase in processing power and better signal processing techniques over the last few decades, BCG has regained its prominence and is being considered to be used as a continuous patient monitoring system. The usability of BCG was limited in the earlier days due to the large size of the equipment and the lack of signal processing systems to analyse this complicated signal. Cardiac output is defined as the amount of blood pumped out by the heart in a minute. This parameter can be utilized to determine the state of the heart. One method to determine the cardiac output from BCG waveform has been discussed in section II of this paper. The sensor used for our experiment is a lightweight and flexible sheet type electromechanical film which is placed on the seat of the chair. The setup used has a two-stage amplifier which is connected to a data acquisition card which is in turn connected to a laptop. The signal processing is done using NI's software LabView. The BCG setup was made and the signal was successfully validated with ECG. The R-J interval, which is the interval between the R peak of the ECG signal and J peak of the BCG signal, was determined. Echocardiogram, another cardiac measurement instrument, was kept as a standard basis for determining the cardiac output from the BCG signal. Recording of 14 different subjects have been taken and the cardiac output has been determined for each case.

ID: 569

PO-02: 37

Deformation analysis of balloon expanded stent during and after its expansion considering viscoplasticity and vessel pulsation

Achmad Syaifudin, Katsuhiko Sasaki and Ryo Takeda

Hokkaido University, Japan.

Stent is widely used for medical treatments of such as angiostenosis due to arterial sclerosis. Most of medical treatments using stents are conducted for

narrowing of coronary arteries. However, stent is expected to be used for narrowing of arteria carotis which is much narrower than coronary. To use stents for arteria carotis, therefore, precise control of deformation of stents during expansion and understanding effects of vessel pulsation on the stent is required. In this paper, finite element analyses (FEM) of a balloon expanded stents made of Type 316 stainless steel are conducted during its expansion to understand how the blood vessel is damaged. The FEM model of the stent consists of both balloon and blood vessel having a plaque. The viscoplastic deformation of stents is considered for the analysis to clarify the aging effect of the expanded stent, which is a cause of loosening of the stent. The effect of vessel pulsation on the boundary between the stent and the vessel wall is also clarified by the FEM analysis. For the analysis, the pressure due to the vessel pulsation is detected by a simple experiment using silicon tubes and fluids pressured by a pump. The detected pressure of the vessel is used for the deformation analysis of the blood vessel located the stents. The analysis clarifies the stress and strain distributions of both the stent and vessel after the expansion of the stent, and the stress and strain relaxation due to the aging of the stent caused by the viscoplastic deformation. The change in the stress and stress distributions due to the vessel pulsation is revealed and the effect of the vessel pulsation on the boundary between the stent and vessel wall is clarified.

ID: 580

PO-02: 38

Development and characterization of CNT/biopolymer electrodes for bio-fuel cell

Mitsugu Todo¹, Kentaro Yamauchi¹ and Takaaki Arahira²

¹*Kyushu University, Japan;* ²*Fukuoka Dental Collage, Japan.*

CNT/biopolymer composite materials having continuous porous structure were developed as the electrode materials for bio-fuel cell. Biodegradable polymer, PLLA, and natural biopolymer, collagen, were utilized as the polymer matrix of the composite materials. Enzymes were also distributed in the composites. Microstructures of the composites were observed using a field-emission scanning electron microscope. A simple experimental set-ups of bio-fuel cell were also constructed using the composite materials as the electrodes. Fundamental electric property such as electrification was then examined using the systems.

ID: 585

PO-02: 39

Influence of gamma-linoleic acid on the ageing process in wistar rat

Rangaswamy Raja¹ and A. V. Natarajan²

¹Department of BIE, Temasek Polytechnic, Singapore; ²Professor formerly with Division of BIE, Erode Arts College, Tamil Nadu, India.

Essential fatty acids (EFAs) are required components of all membranes within the body, conferring on them properties of fluidity, flexibility and selective permeability. Further they have a role as precursors of biologically very active metabolites like prostaglandins, leukotrienes, etc. Gamma – linoleic acid (GLA) one of the essential fatty acids of interest has been studied in wistar rat spanning over a period of two years. The study has established that deficiency of GLA has a profound influence on ageing process. One major reason for deficiency of GLA could be the blockage of the metabolic pathway involving a deficiency of δ - 6 desaturase. Others include Zinc deficiency, deficiency of pyridoxine, magnesium, biotin and calcium, excessive intake of trans linoleic acid (refined oils). Ability to 6-saturation in the present investigation has been shown to decline considerably with ageing resulting in a significant fall in the levels of plasma DGLA. The study has clearly established that the fall in 6-desaturation in old animals can be bypassed by administering GLA directly. Extrapolating the results, there is therefore a reasonable biochemical case for providing supplement to GLA for elderly humans. Earlier studies in human have shown that the normal endogenous production is of the order of 200–1000mg/day. With a loss of 50 to 60% of this by age 60 it is reasonable to consider nutritional supplementation in the range of 150–500 mg/day to bring the supply of GLA available to the body to normalcy. GLA as a normal intermediate of human metabolism is unlikely to be inherently toxic. Clinical significance of the finding is discussed in relation to human health care.

ID: 591

PO-02: 40

Development and characterization of bioceramic/polymer composite scaffold with drug release function for bone tissue engineering

Mitsugu Todo¹, Naoki Yamada¹, Takaaki Arahira², Yasunori Ayukawa¹ and Kiyoshi Koyano¹

¹Kyushu University, Japan; ²Fukuoka Dental College, Japan.

Hydroxyapatite porous material was coated by bioabsorbable polymers such as PCL or PLGA containing statin which is a commercial drug known to

enhance bone formation in vivo condition. The compressive mechanical properties of the composite scaffolds were evaluated to assess the effects of polymer coating. Drug release tests were also performed to assess the effects of coating polymer and coating method on the drug release rate. It is concluded that the stain/PLGA(PCL)/HA scaffolds can be one of the potential candidates for bone tissue engineering.

ID: 615

PO-02: 41

Microfluidic device for monitoring and evaluation of intracellular mechanostress responses

Yuta Nakashima^{1,2}, Yin Yang² and Kazuyuki Minami²

¹Kumamoto University, Japan; ²Yamaguchi University, Japan.

This paper presents a microfluidic device for monitoring and evaluating real-time cellular responses to compression stimuli. The device was produced by a three-dimensional micro structure fabrication process using multiple exposures to the photoresist. The presented device consists of cell inlet ports, a pressure inlet port, a gasket, microchannels, culture chambers, and a diaphragm on the culture chamber for applying compressive pressure to cells. Compression stimuli applied to the cells can be controlled by regulating the expansion of the diaphragm via a pressure control. The device permits the observation of cellular responses to compressive pressure in real time because it is made of transparent materials and stimulates the cells without deforming the cell culture surface, when observed by optical microscope. We observed the cellular deformation and response behavior using a fabricated microdevice in real time. The changes of intracellular calcium concentration before and after compressive stimuli were observed by the fabricated device. Also, the intracellular maximum strain part and strain distribution of a cell that received compression stimulus were clarified by FEM analysis. Moreover, threshold level of cell deformation amount and strain amount which a cell detects was evaluated by combination of the cell compression test and FEM analysis. These results indicate the device is expected to clarify the cellular mechanoreceptor mechanisms and signal transduction pathways and facilitate the control of stem cell differentiation by a combination of the experimental results and FEM analysis results.

ID: 639

PO-02: 42

Polymer microneedle array integrated with CNT nanofilter for selective drug delivery review decision

Hao Wang¹, Zhuolin Xiang¹, Chih-Fan Hu², Aakanksha Pant¹, Weileun Fang², Giorgia Pastorin¹ and Chengkuo Lee¹

¹National University of Singapore, Singapore; ²National Tsing Hua University, Taiwan.

A unique process, which utilizes a membrane based vertically grown carbon nanotubes (CNTs) as nanofilters for integration with polymer based microneedle, is presented here. The CNT nanofilters are mounted at the bottom of microneedles and sharp tips are assembled on top of microneedles. Pressure and electric field are allowed to be given for drug molecules to pass through the CNT nanofilters. Drugs of different molecular weight and physical dimension could pass through the CNT nanofilter by different conditions. A new method, double drawing lithography, is developed to assemble and strengthen the sharp tips on top of microneedles. Results show that the microneedles can penetrate into skin and drugs could be delivered through CNT nanofilters into skin.

ID: 643

PO-02: 43

Attachment design of an automatic thrombus monitoring system using multiple optical emitters and detectors for an extracorporeal pulsatile artificial heart

Shinichi Tsujimura and Yoshiyuki Sankai

University of Tsukuba, Japan.

Since patients with extracorporeal pulsatile artificial hearts are always exposed to thromboembolic risk, medical staff is forced to regularly conduct visual observation of adherent thrombi inside the artificial heart over the long term. In order to reduce the burden on medical staff and accomplish objective and continuous thrombus monitoring, the purpose of this study was to propose an automatic thrombus monitoring system using multiple optical emitters and detectors for an extracorporeal pulsatile artificial heart, and design its attachment for accurate measurement. The proposed system monitors thrombi by distinguishing a difference in the light absorption and scattering characteristics between the thrombus and the whole blood, on the external surface of the artificial heart without blood contact. To accurately monitor adherent thrombi inside the artificial heart over a wide area, the system needs to firmly attach multiple optical emitters and detectors to the surface of the artificial heart. An attachment including an inner cover and an outer cover was designed. The inner cover where multiple optical emitters and detectors can be arrayed was designed based on the

external shape data of an extracorporeal pulsatile artificial heart which were obtained by using a 3D scanner. The outer cover was designed to attach the inner cover to the external surface of the artificial heart. The outer cover connects to the inner cover via spring mechanism, firmly attaching the inner cover to that of the artificial heart by the spring force when the outer cover is closed. The result of an installation test using the prototype attachment showed that the measurement error due to the installation was less than 2% and has little influence on the thrombus monitoring. We conclude that the attachment has the capability to firmly fix the measurement points for accurate monitoring.

ID: 652

PO-02: 44

Genipin cross-linked polyelectrolyte multilayer films for controllable endothelialization of cardiovascular devices

Aldona Ilona Mzyk¹, Justyna Gostek², Jacek Polit³, Roman Major¹, Piotr Wilczek⁴ and Boguslaw Major¹

¹Institute of Metallurgy and Materials Science, Polish Academy of Sciences, 25 Reymonta Street, 30-059 Krakow, Poland; ²The Henryk Niewodniczanski Institute of Nuclear Physics, Polish Academy of Sciences, 152 Radzikowskiego Street, 31-342 Krakow, Poland; ³University of Rzeszow, Department of Microelectronics and Nanotechnology, 16a Reytana Street, 35-959 Rzeszow, Poland; ⁴Foundation for Cardiac Surgery Development, 345a Wolnosci Street, 41-800 Zabrze, Poland.

The integration of biomedical implants in human organism is dependent on the chemical composition and topography of the surface as well as the mechanical properties of an applied materials. While in the past most of the clinically used materials were developed only based on their acceptance by the body, today beneficial interactions of implants with cells and proteins gather more and more importance. Current development in cardiovascular devices is related to the biocompatibility improvement through manufacturing surfaces mimicking extracellular matrix components. This dynamic microenvironment facilitates covering an internal surface of implant by cell monolayer which mask the material from an inflammatory response and reduce risk of thrombosis. The aim of this study was to improve properties of blood contacting material such as polyurethane, by the "layer by layer" polyelectrolyte multilayer film formation on its surface in order to control implant endothelialisation. However, application of polyelectrolyte coatings as biomaterials for cell attachment has been limited due to their gel like characteristics. Herein, we attempt to improve the cellular adhesion properties of films through chemical cross-linking with a genipin. Hyaluronan (HA), poly-L-lysine (PLL) and alginate (ALG) were used to assemble

[PLL-HA]_n and [PLL-ALG]_n films in two different thickness variants, 12 and 24 bi-layers respectively. The effects of genipin cross-linking on the internal composition, surface topography, nano-hardness of multilayers and as a consequence on cellular processes were investigated. Fourier Transform Infrared Spectroscopy (FTIR) measurements shown a slight changes in the internal structure of multilayers cross-linked with various genipin concentration. Atomic force microscopy (AFM) confirmed that cross-linking affected each of the films topography and stiffness differently. Cellular adhesion, proliferation and functionality studies using endothelial cells, carried out on both films demonstrated differences. The [PLL-ALG]_n film was shown to better improve endothelialization, especially for high bi-layer numbers and using higher concentrations of the cross-linker.

ID: 724

PO-02: 45

Radiofrequency Instrument for office hysteroscopy

Jan Grepl and Marek Penhaker

VSB-TU Ostrava, Czech Republic.

The work includes the design and implementation of radio-frequency tools for outpatient hysteroscopy. The research and cooperation with leading professional medical workplace designed a unique system of size 6 Fr. The requirement for a system for the safe bipolar hysteroscopy was respected for the purpose of elimination of soft tissue injury of the uterus. Subsequently BYR implemented and tested a prototype instrument made of ABS plastic resistant to 120°C, supplemented by an innovative mechanical system opening. Mechanical tests confirmed the assumption grip and distribution of neoplasms in size 0–10 mm with operating power of 1–3.8N. Radiofrequency excitation were successfully improved with a commercial RF generator RITA 1500x generator operating at 460kHz and 100V. The principle of this newly designed tool is registered with the national, patent Czech Republic.

ID: 736

PO-02: 46

Evaluation of chitosan thermosensitive hydrogel as a sustained insulin delivery system

Farzaneh Ghasemi Tahrir, Fariba Ganji and Alireza Mani

Tarbiat Modares University, Iran.

Recently, great attention has been paid to in situ gel forming chitosan/ β -glycerol-phosphate (chitosan/ β -Gp) solution due to its good biodegradability, biocompatibility and thermosensitivity. This in situ gel

forming system is injectable fluid that can be introduced into the body in a minimally invasive manner prior to solidifying within the desired tissue. This hydrogel could be used as a good candidate for achieving a prolonged drug delivery system for insulin, considering its high molecular weight. Insulin and β -Gp in different concentration were loaded in chitosan/ β -Gp solutions and in vitro drug release was studied. Results indicated that the release of insulin from chitosan/ β -Gp gel decreased by increasing in β -Gp salt and initial insulin concentration. The best formulation was chosen for in vivo experiment to control the plasma glucose of diabetic mice models after subcutaneous injection. Our obtained results showed that insulin loaded chitosan/ β -Gp hydrogels could control the blood glucose level for 5 days.

ID: 741

PO-02: 47

Preliminary study for developed foot plantar surface temperature monitoring system by reducing pressure effect

Ho Suk Ryou¹, Soo Young Sim¹, Han Byul Kim¹, Jung Min Han¹ and Kwang Suk Park²

¹Interdisciplinary Program of Bioengineering, Seoul National University, Republic of Korea; ²Department of Biomedical Engineering, Seoul National University College of Medicine, Republic of Korea.

The diabetic foot is one of the major complications in diabetic patients. Many studies revealed that monitoring temperature differences of the corresponding points on the foot plantar surface is important to prevent the foot ulceration. However, even though there are many wearable devices developed for monitoring plantar surface temperature, no studies have investigated how the person's pressure can effect on the temperature sensors while monitoring the plantar temperature when the people stand on the insole. This pressure effect can change the monitoring result which will produce the wrong diagnosis. In this study, we propose two methods; each is corresponding to estimate the standing habit of the person, and to correct the monitoring result which is affected by the pressure. Although it cannot correct the error in certain situation and it is limited to steady state, these two methods were able to correct the error caused by the pressure on the sensor.

ID: 747

PO-02: 48

High-resolution auditory brainstem response system

Arlyana Ramli, Rumaisa Abu Hasan, N. Izayu A. Rahman, Sh-Hussain Salleh and Arief R. Harris

Universiti Teknologi Malaysia, Malaysia.

Auditory Brainstem Response (ABR) can be described as the early part of auditory Evoked Potential (EP). EP is electrical response of the brain recorded from scalp obtained from acoustical stimuli. ABR signal often difficult to capture since it is small relative to the ambient noise. Electrodes placed on the scalp not only pick up ABR potential, but any physiological potential from multiple sources such as Electrooculogram (EOG), Electrocardiogram (ECG) and Electromyogram (EMG). The noise can be reduced by implementing high-resolution analogue to digital converter (ADC) into signal acquisition circuit. A high resolution ABR measurement circuit has been developed and evaluated with ABR signals. The signal acquisition circuit consists of ADS1299 as integrated amplifier and also as ADC and AT91SAM3X8E in Arduino Due as microcontroller. The microcontroller is programmed to control the serial peripheral interface (SPI) connections and send the signal to computer through USB connection. The signal is displayed, processed and saved in MATLAB environment. With the used of high-resolution ADC it gives advantage to higher signal to noise ratio of the prototype. Furthermore, the system has low input-referred noise which means it possesses only small deviation from ideal ADC. The system is able to show the ABR signals with low number of trials which is less than 300. Thus, the prototype has high potential for further development to become a reliable device.

ID: 754

PO-02: 49

A reliable handwash detector for automated hand hygiene documentation and reminder system in hospitals

S. Mohamed Rabeek¹, Andrew Norman², Minkyu Je¹, M. Kumarasamy Raja¹, Ruey Feng Peh² and Michael K. Dempsey³

¹Institute of Microelectronics, A-STAR, Singapore; ²A* MedTech Initiative Office, A-STAR, Singapore; ³MGH & the Center for Integration of Medicine and Innovative Technology (CIMIT), Boston MA, USA.

This paper presents a design of a reliable hand wash detector for the automated hand hygiene documentation and reminder system (AHHDRS). AHHDRS helps to reduce number of healthcare associated infections mainly caused by lack of hand hygiene among health care providers. This is a social problem and costs about \$35.7– \$45 billion annually

in direct medical costs to the U.S hospitals and a lot more worldwide.

AHHDRS works by creating ultrasonic hotspots with unique Identifier which gets tagged into the clinicians badge ultrasonically for a predefined movement between Wash zone/Bed zone hot spots for hand hygiene compliance. Accumulated hand hygiene compliance data pulled out by the Wireless Reader in 915MHz RF link and pushed to the AHHDRS server through Wi-Fi link.

Proposed hand wash detector can complement or replace the existing vibration based wash sensor in the AHHDRS. Existing hand wash sensor is based on vibrations and leads to lot of false positives for the hand hygiene compliance. The three pronged detection system proposed in the hand wash sensor enables the reliable detection of hand wash and hence the hand hygiene compliance. It identifies hand wash by the clinicians in hospitals based on 1) Measuring pressure applied to the wash dispenser's plunger by a pressure sensor 2) Measuring Infrared emitted by the presence of human hand in the vicinity of the wash dispenser by a Passive Infrared sensor 3) Detecting alcohol residue in the user's hand after the hand wash. Combination of the three parameters enables the wash sensor to reliably identify the hand wash event and hence the hand hygiene compliance.

ID: 758

PO-02: 50

The effect of microwave treatment on the drug release property of gelatin microspheres

Kuofeng Chou, Li Wen Wang, Pei Yong Chen, Wei Lin Xiao, Han Sheng Chiu, Jia Hui Lin, Wan Yu Huang and Ting Kai Chen

Yuanpei University, Taiwan.

This study was to investigate the effect of microwave treatment on the swelling ratio of the gelatin, the diameter and drug release behavior of gelatin microspheres. The results can be applied to the drug delivery system, wound dressings and so on. In the experiment gelatin was mixed with D.I. water with the ratio of 3:10. The UV treatment active functional groups of gelatin, so that secondary interactions between the molecular chains form. Gelatin was exposed on 2.5GHz microwave with radiation dose of 0~5150J. In the study, the temperature of mixture was used to control the diameter of gelatin microspheres. The temperature is controlled at the range of 40°C~70°C. The diameter distribute at the range of 0.05mm~0.6mm. The diameter of microsphere increases with the increasing of temperature, and the distribution is dispersed. The effect of microwave on the swelling ratio and degradation rate of gelatin were investigated. Microwave treatment for short term would raise the swelling ratio to 25%. However,

the swelling ratio and degradation rate would become low as the time of microwave treatment was over a critical value.

ID: 762

PO-02: 51

Measurement device for the repetitive saliva swallowing test using multiple magnetic sensor

Shin Kudo¹, Masatake Akutagawa², Takahiro Emoto², Yohsuke Kinouchi², Yoshinori Tegawa³, Seiko Hongama³ and Shinsuke Konaka²

¹Graduate School of Advanced Technology and Sciences, The University of Tokushima, Japan; ²Institute of Technology and Science, The University of Tokushima, Japan; ³Institute of Health Biosciences, University of Tokushima, Japan.

In the area of rehabilitation and treatment at home, there is a growing interest in dysphagia. Video Fluorography and Video Endoscopy are widely used as a definitive diagnosis of dysphagia. However these methods are invasive and have a risk of exposure. Therefore, a noninvasive screening test is necessary. Conventionally a physician has conducted the Repetitive Saliva Swallowing Test (RSST) by palpation. The disadvantage of this method is that only a skilled physician can operate this system. In addition, evaluation criteria are differ from time to time.

Purpose of this study is to automate the RSST, and to establish an evaluation method with standard evaluation criteria. In this study, three-dimensional magnetic sensors is used to measure deglutition. It reflects terrestrial magnetic field in correspondence to the body movement. There are two magnetic sensors used. One is a magnetic sensor that measures both body movement and swallowing, another is magnetic sensor that measures only body movement. Measurement result is obtained by subtraction of these values. The posture, measurement time and the number of swallowing are identical with the RSST. For an evaluation of the validity of the result of a measurement with the magnetic sensor, video is used to observe the movement of the laryngeal prominence and a throat microphone to record swallowing sound. When the body of the subject move during the measurement, only swallowing waveform is extracted using two magnetic sensor.

The future works is to apply this method to diagnose dysphagia patient. Swallowing waveform patterns would be analyzed to count the swallowing automatically.

ID: 765

PO-02: 52

Evaluation of optimum retention force of a cup yoke type dental magnetic attachment

Aggrey Kaliba¹, Tegawa Yoshinori², Kinouchi Yohsuke³, Konaka Shinsuke³, Akutagawa Masatake³ and Emoto Takahiro³

¹Graduate School of Advanced Technology and Science, The university of Tokushima; ²Institute of Health Biosciences, The University of Tokushima; ³Institute of Technology and Science, The University of Tokushima.

A dental magnetic attachment is a device to retain dental prostheses such as over dentures by magnetic attraction. As compared with mechanical attachments, the dental magnetic attachment has superior characteristics such as easy insertion, good esthetics and less lateral pressure to its abutment tooth. Because of these characteristics, it has come to be used widely. There are various types of dental magnetic attachments. There are two commercialized magnetic attachments; cup yoke type and sandwich type in Japan, and several types of dental magnetic attachments in other countries.

In this work, we determined the retentive characteristics of a cup yoke type closed-field dental magnetic systems. A finite element method based static magnetic simulation technique was used to assess the real actual dimensions of a commercialized cup yoke magnetic attachment. The objective was to reach optimum dimensions of a cup yoke magnetic attachment with relatively higher retention force than the current commercialized magnetic attachment. Where retention force was defined by the magnetic attraction with a gap between a magnetic assembly embedded in a denture base and a stainless steel keeper set on the abutment tooth. The effect of the space between the magnet and its keeper on the retention force was evaluated. The magnetic flux saturation created in the magnetic assembly would generate a stable attraction force between the magnetic assembly and the keeper that would stand the space created between during use. The maximum retention values of the magnetic system were tested with this simulation. Various spaces were developed between the magnetic assembly and the keeper, as the space increased between the magnetic assembly and keeper, the attraction force diminished rapidly but with an increasing retention force values.

The newly proposed optimum dimensions may provide flexible retention performance useful for more effective and extensive applications of a magnetic attachment.

ID: 800

PO-02: 53

Melamine in milk with surface enhanced Raman spectroscopy

Afaf Rozan Mohd Radzol, Khuan Yoot Lee and Wahidah Mansor

Universiti Teknologi Mara, Malaysia.

Melamine is rich in nitrogen and easily confound with natural protein present in dairy products. It is added to diluted milk to increase the protein concentration. However, interaction of melamine and cyanuric acid in our bladder triggers the formation of kidney stones, which results in acute kidney failure. The significance of this is accentuated in the case of infant formula, which is the sole source of food for infants, with several feedings a day. Raman spectroscopy is a photonic method capable of identifying unknown molecule through a biochemical fingerprint, from its scattering spectrum. It is simple, rapid, portable and pre-treatment is unnecessary. Our work here explores detection for traces of melamine in infant formula using Raman spectroscopy with gold substrate. A Raman spectra unique of melamine is first established. The characteristic peak at 676cm^{-1} signatures the Raman fingerprint for melamine. Then mixtures of milk and melamine, in liquid and powder form, are examined. The characteristic peak of melamine is found in the spectra of all the mixtures adulterated with melamine. It can be concluded that Raman spectroscopy with gold substrate is capable to detect for traces of melamine in infant formula, in different forms, to ensure a safe complementary and substitute for breast milk.

ID: 801

PO-02: 54

An injection moulded microfluidic chip for polymerase chain reaction (PCR) thermo-cycling and imaging of droplets to detect food-borne pathogens campylobacter spp

Carl Esben Poulsen¹, Dang Duong Bang², Anders Wolff¹ and Martin Dufva¹

¹DTU-Nanotech, Technical University of Denmark, Denmark;

²DTU-Food, Technical University of Denmark, Denmark;.

Summary: This paper reports a disposable injection moulded chip for storing, PCR amplification and imaging droplets to detect food-borne pathogens. The chip can easily be mass produced and is designed to enable single or multiple fluorescence signals to be detected using a standard fluorescence microscope. The combination of microscopy and a disposable chip enhances multiple detection capability and reduces the cost of conducting droplet based PCR.

Achievements: The chips droplet incubation chamber is designed to exploit the positive buoyancy of the droplets to facilitate optimal droplet packing regardless of the droplet production rate and water-to-oil flow-rate ratio. Two PDMS squeeze valves and a dedicated priming outlet were included. The height of the chamber restricts the droplets to pack into a single layer enabling fluorescence read out using fluorescence microscopy.

The chips were fabricated by injection moulding of cyclic olefin copolymer (COC)(5013TOPAS®) using an injection moulder fitted with a micro machined aluminium shim, harvesting the channel design, and a 12-Luer counter-shim. The injection moulded chip and a 150µm TOPAS sheet were bonded by ultrasonic welding using a USP4700 (Telsonic).

Droplets were generated using a Droplet Junction Chip, Part#3000301, (Dolomite). 2% Pico-Surf™1 in FC40 (Dolomite) was used as the continuous phase. The dispersed phase consisted of PCR master mixture for detection of *Campylobacter* spp. Additionally, to confirm successful droplet loading, 10µM Sulphorhodamine101 was added to the PCR mixture and EvaGreen (Biotium) was used to confirm DNA amplification. The flow rates of 2 and 18µl/min for the dispersed and continuous phase were used, respectively.

Droplets were imaged using a LaVision BioAnalyzer 4F/4S fitted with Cy3 and FITC filter cubes using exposure times of 20 and 100ms, respectively. Images were subsequently analysed using a MATLAB algorithm for size statistics. Using the two fluorophores, *Campylobacter* spp PCR amplified droplets could be discriminated from non-amplified droplets.

ID: 802

PO-02: 55

An efficient method for decellularizing liver

Ming-Xin Pan¹, Yi Gao^{1,2}, Yuan Cheng¹ and Yan Wang^{1,2}

¹Department of Hepatobiliary Surgery, Southern Medical

University Zhujiang Hospital, China; ²Institute of Regenerative Medicine, Southern Medical University Zhujiang Hospital, China.

Currently decellularized scaffold is recognized as the important biomaterials for engineering internal organs, such as liver and kidney. Aim for efficient decellularization of the original tissue, we optimized the preparation procedure for decellularized liver scaffold using gradient ionic detergents, i.e. EDTA, hypotonic alkaline solution, Triton X-100, and gradient sodium dodecyl sulfate (1%, 0.5%, and 0.1%, respectively), to continuously perfuse through the hepatic vascular system. Decellularization of the liver tissue was performed with different reagents buffer and washing protocol. Preservation of the original

extracellular matrix was observed with scanning electron microscopy. The scaffold was embedded in the dorsal muscle of rabbit and the inflammation features including the surrounding cell infiltration and changes of the scaffold architecture were detected to analyze its biocompatibility. The cell-attachment ability was detected by perfusion culture of HepG2 cells with the scaffold. Using gradient ionic detergents, the decellularization process could be completed by approximately 5 h, which was shorter than 10 hours in previous experiments ($p < 0.001$). The framework of the scaffold was kept relatively intact. There was no obvious inflammatory cellular infiltration or structural damage in the grafted tissue. The engraftment efficiency of HepG2 were $86 \pm 5\%$ ($n = 8$). The levels of albumin and urea synthesis of the cells cultured with decellularized scaffold were significantly superior to the ones in traditional two-dimensional culture. In conclusion, the present method can be used efficiently to produce decellular liver scaffold which have satisfying biocomparability for potential application both *in vivo* and *in vitro*.

ID: 806

PO-02: 56

A VB simulation model for ISFET sensitive to histamine ion

Yoot Khuan Lee, S. F. Mohammed Esa, R. Jarmin and M Yakup
Universiti Teknologi MARA, Malaysia.

Histamine is a type of toxins produced in the fish muscles tissue. Human suffers from Scombroid poisoning, or histamine fish poisoning, if histamine over the tolerant limit is ingested, which brings on allergic reaction. The consequence can be fatal if trachea is blocked owing to swelling of the esophagus. Besides high performance liquid chromatography, which requires pre-treatment, complex procedure that calls for skilled laboratory engineers as well as expensive and non-portable, there has been no other method to detect for level of histamine concentration in fish. Ion Sensitive Field Effect Transistor is a biosensor, product of CMOS technology. It is highly sensitive in ion selection, low cost, portable and low power consumption, features suitable for miniaturization. ISFET fabrication is similar to MOSFET base-structure, except that the gate of MOSFET is replaced with a reference electrode, electrolyte and insulator of ISFET. It is this subtle difference that enables ISFET to produce gate voltage output, in response to change between electrolyte and electrostatic. Being a novel technique, it is necessary to parameterize the ISFET and characterize it for measuring level of concentration of Histamine. Our work here develops simulation model for ISFET biosensor for histamine ions, subsequence of our previous work in developing the

theoretical model, using VB 6.0. The input is concentration of histamine between 0–300 ppm. The output is gate source voltage predicted at the Si_3N_4 gate of ISFET. Graphs of potential of electrolyte-insulator interface versus concentration of histamine, drain-source current versus drain-source voltage and drain-source current versus gate-source voltage are standard displays of the simulation model to identifying parameters for the ISFET model, which are then used to produce the characterization of ISFET. This allows iterative improvement to parameterization and characterization until an optimal ISFET model is obtained before fabrication, without incurring any hardware cost.

ID: 808

PO-02: 57

PC based wireless vital sign monitor using zigbee communication

Achmad Rizal, Sugondo Hadiyoso, Jondri Jondri, Adri R. Fikar and Anugrah Rahman

Telkom University.

Electrocardiogram (ECG), SpO₂ and body temperature are vital sign for human body. In some condition, these signals are monitored using vital sign monitor to determine patient's health condition. Vital sign monitor usually placed beside patient's bed and doctor need to come to monitor patient's condition.

In this research, we design low cost wireless PC based vital sign monitor. The design device consist of acquisition moduls to capture ECG signal, SpO₂ and body temperature and additional device to monitor flow rate of fluid from infussion pump. All the signal are displayed into a tiny graphic LCD while the all signal's data transmitted into PC via zigbee communication. In PC display, we show ECG and SpO₂ signal, body temperatur, heartrate and flow rate.

From device testing, the device worked well for maximum transmission distance of 50 meters. By this condition, we can monitored patient's vital sign from another room. So doctor or nurse does not need to come to patient's room to monitor patient's vital sign.

ID: 817

PO-02: 58

Engineering design and manufacturing of custom craniofacial implants

Marcela Arango Ospina^{1,3} and Carlos Julio Cortes Rodriguez^{2,3}

¹Biomedical Engineering Program, Faculty of Medicine, National University of Colombia; ²Department of Mechanical Engineering and Mechatronics, National University of Colombia; ³Biomechanics Research Group GIBM, National University of Colombia.

Custom implants for cranioplasty applications have the aim to restore the brain protection that the skull provided and improve the surface appearance after suffering a trauma or to correct a malformation.

Major drawbacks of the procedure of cranioplasty include the individualization of the geometry and mechanical properties of the implant to make it functional. The aim of our investigation was to propose an integrated methodology to biomechanical design and manufacturing of cranial implants and apply it to a case study of a craniofacial custom implant for the frontal bone made with Polymethylmethacrylate (PMMA) that meets the suitable geometry and mechanical properties for its functionality. The first process step was to obtain the medical data from the patient through computed tomography; then the images were processed to create a 3D model of the interest region by an imaging processing software InVesalius; we designed the implant using CAD software and finally we used rapid prototyping technology and CNC Machining to create the implant mold to produce the final geometry of the implant. The used methodology allowed us to obtain an implant according to the geometric and mechanical requirements. Likewise, it was observed that the final costs of developing individualized implant are competitive with surgical time savings and further there is an increased quality of the procedure.

ID: 834

PO-02: 59

The differences in osteogenesis between the GFP transfected hESCs and the normal hESCs

Lulu Li, Mingming Li, Intekhab islam, Sriram Gopu and Tong Cao
National University of Singapore, Singapore.

Because of the increasing clinical demand, research and development in bone tissue engineering has advanced a lot in the past few years. Osteogenic cultures of human embryonic stem cells (hESCs) play an important role in the research of skeletal reconstruction and therapies for bone defects. Osteogenesis is one of the key components of periodontal tissue development as well as regeneration. However, in

transplanting osteogenic lineage cells derived from hESCs in animal defects, it is difficult to identify grafted cells from the host tissue without performing biochemical assays. We transfected the green fluorescent protein (GFP) stably into both H1 and H9 hESCs lines in a non-viral approach. When the GFP hESCs was transplanted to the animal model, defect healing can be tracked through *in vivo* imaging system without euthanizing the hosts. Here we present the first part of our study, to investigate the differences in osteogenesis between the hESCs transfected by GFP and the normal hESCs. GFP hESCs and normal hESCs were cultured for 21 days in osteogenic media which is composed of DMEM high glucose, 10% FBS supplemented with Dexamethason, β -glycerol phosphate and ascorbic acid. Four groups were established for each lines (i) differentiation from EB stage GFP hESC; (ii) differentiation without EB stage GFP hESC; (iii) differentiation from EB stage hESC; (iv) differentiation without EB stage hESC. After 21 days of differentiation, the cultures were characterized for mineralization using alizarin red staining, osteolineage marker alkaline phosphates and osteocalcin expression by immunocytochemical staining. Polymerase Chain Reaction was also performed for the cells collected on Day 21 for osteogenic related genes expression.

ID: 837

PO-02: 60

In vivo automated haemodialysis catheter cleaner

Azmall Fraiszudeen and Kok Zuea Tang
National University of Singapore, Singapore.

Currently, ultrasonic Thrombolysis devices exist for breaking clots in blood vessels. However, this application has not been extended to haemodialysis catheters, which when develop blood clots, renders the entire catheter a hazard for renal failure patients. A third of Singapore's End stage Renal Disease (ESRD) patients undergo haemodialysis via catheter, with the rest using them for some period. The Haemodialysis Catheter is currently removed via a surgical procedure under local anaesthesia when congested with a blood clot. On average, renal failure patients undergo this procedure every 6 months. This has numerous medical, economic and psychological side-effects for the patient community. The use of Ultrasonic waves to emulsify clots *in vitro* and in arteries has been lauded in literature. Hence, an Ultrasonic probe to emulsify clots from the inner lumens of catheter can serve to increase lifespan of catheters when clotting occurs and reduces the trauma and economic burden patients face from surgical removal procedure. The main aim of this project is to develop an in vivo automated haemodialysis

catheter cleaner that automatically detects and removes clots on the intra luminal surfaces of the catheter via ultrasound, in an in-vivo setting. This proposed automated catheter cleaning system is hypothesized to be more effective in the removal of the clots of the catheter compared to current methods. It consists of ultrasonic probe, haemostasis adaptor and automation unit, and operates in simple stepped fashion. Proof of Concept experiments were conducted with various Frequency ultrasound and power to observe and quantify for effectiveness in blood clot emulsification, leading to the first manual version of the prototype. Current efforts are to incorporate the automation and safety elements to ensue less need for a medical expert supervision or operation. This device would impact communities scare of economic resources by lowering cost and need of specialised medical service for haemodialysis catheter maintenance.

ID: 843

PO-02: 61

Human endothelial cell morphogenesis within 3-dimensional PEGylated fibrinogen hydrogel

Rufaihah Abdul Jalil¹, Wan Xian, Esther Tan¹, Qian Hui, Kimberly Oen¹, Marian Plotkin², Thi Di Thien Do², Theodoros Kofidis^{1,3} and Dror Seliktar⁴

¹Department of Surgery, National University of Singapore, Singapore; ²NUS Nanoscience and Nanoengineering Institute, Singapore; ³National University Heart Centre, National University Health System, Singapore; ⁴Faculty of Biomedical Engineering, Technion-Israel Institute of Technology, Haifa, Israel.

The generation of functional vascular networks remains to be a crucial step in the development of clinically relevant tissue constructs. In the last decades, our understanding of the role of extracellular matrix (ECM) in vascular morphogenesis has been increased tremendously due to well-defined *in vitro* angiogenesis model using natural and in recent years synthetic ECM. However, little is known about the vascular morphogenesis by endothelial cells in biosynthetic hybrid matrix that has the ability to provide a more controllable and clinically relevant alternative for regenerative medicine.

In this study, we used a biosynthetic hydrogel with tunable stiffness consisting of a fibrinogen backbone that is covalently bound to difunctional polyethylene glycol (PEG) side chains as three-dimensional matrix for capillary-like structure formation from endothelial cells. We observed that the endothelial cell morphology was significantly influenced by the stiffness of the matrix. The softer matrices with local delivery of vascular endothelial growth factor within the matrices resulted in longer capillary length and larger tube area. The endothelial cells were capable of aligning and organizing themselves within the matrix, hence

assembling to form capillary-like structures with organized actin fibers. We found that these morphogenic events were regulated by two integrins, $\alpha_v\beta_3$ and $\alpha_5\beta_1$ since blockage of these integrins inhibited the assembly of capillary-like structures in the PEG-fibrinogen hydrogel. Collectively, our findings establish the initial design criteria that need to be considered when engineering vascularized tissue constructs using PEG-fibrinogen hydrogels.

ID: 865

PO-02: 62

A crosslinking gelatin ink for freeform fabrication of tissue engineered cell encapsulating scaffold

Animesh Agrawal¹, Scott A. Irvine¹, Bae Hoon Lee¹, Huiyee Chua¹, Kok Yao Low¹, Marcelle Machluf^{1,2} and Subbu S. Venkatraman¹

¹School of Materials Science and Engineering, Nanyang Technological University Singapore; ²Faculty for Biotechnology and Food engineering, Technion, Haifa, Israel.

Freeform fabrication and 3D printing have recently captured the public imagination for their wide potential for controlled design. They may also prove to be significant as a tool for precise patterning of biological and synthetic materials to fabricate bioengineered scaffolds, tissue constructs or organs. One proposed application is the direct production of cell bearing scaffolds to produce bioactive constructs. Here we present "bioink" that allows the deposition of cells within crosslinking protein (i.e. gelatin) matrix, that can be deposited by robotic free form fabrication into precise predetermined patterns. The bioink demonstrates suitable viscosity to avoid ink bleeding upon deposition and a cross linking time sufficient to deposited 200micron width and 6m long cell containing ink pattern. The encapsulated cells remained viable and proliferated for the entire one week period of monitoring.

ID: 877

PO-02: 63

Modelling viscoelastic properties of collagen networks under dynamic shear loading

Long Hui Wong¹, C. W. Chung², N. A. Kurniawan³, H. P. Too^{1,4}, M. Buist² and R. Rajagopalan⁵

¹Chemical and Pharmaceutical Engineering, Singapore-MIT Alliance, Singapore; ²Department of Bioengineering, National University of Singapore, Singapore; ³FOM Institute AMOLF, The Netherlands; ⁴Department of Biochemistry, National University of Singapore, Singapore; ⁵Skolkovo Institute of Science and Technology, The Russian Federation.

Collagen is a key participant in determining the mechanical integrity of human tissues, including the

heart, blood vessels, ligaments, bones and cartilage. Mechanical shearing of soft collagenous tissue is important in numerous physiological functions, such as in the myocardium and collateral ligaments. A hallmark of collagen networks is its strain-dependent viscoelasticity, which continues to be a subject of intense research. Although a large number of theoretical and numerical models have been generated to model nonlinear viscoelastic behavior of biopolymer networks, these models primarily focused on macroscopic tensile stretching of collagen and/or fibrils.

In this study, continuous shear rheometry was used to measure the rheological properties of collagen networks reconstituted in vitro as a function of the applied shear strain. To describe the rich mechanical properties of collagen in response to dynamic shear loading, we derived a minimal, compact model using the nonlinear viscoelastic solid (NVS) model with 12 different combinations of elastic and viscous elements. The developed model that fits all the experimental rheological data ($R^2 = 0.99$) was found to contain exponential, linear, and linear elements for the parallel elastic component (PEC), series elastic component (SEC) and series viscous component (SVC) respectively. The selected minimal model was able to capture the experimental stress-strain relations at different shear strain amplitude of collagen at different concentrations and in the presence of permanent cross-linkers.

Overall, this model allows simple quantification of the complex mechanical response of collagen networks and aids in effort to unravel the physicochemical origins. Proper modelling of the strain-dependent mechanical properties of the collagen networks will be beneficial in various cell studies and clinical applications of collagen.

ID: 881

PO-02: 64

An interfacial pressure and shear stress sensor for lower limb prosthetics

Liudi Jiang¹, P. Laszczak¹, D. L. Bader², D. Moser³ and S. Zahedi³

¹Faculty of Engineering and the Environment, University of Southampton, United Kingdom; ²Faculty of Health Sciences, University of Southampton, United Kingdom; ³Chas A Blatchford & Sons Ltd, Endolite Technology Centre, United Kingdom.

The majority of millions of lower limb amputees worldwide use prosthetic limbs to enable their mobility and daily activities. However, residual stumps of lower limb amputees are particularly vulnerable to soft tissue breakdown due to the prolonged mechanical loads at the stump-socket interface which are not naturally sustainable for the built-in soft tissue of the stumps. This is particularly crucial for many amputees who suffer from various co-morbidities

including diabetes, peripheral vascular disease and peripheral neuropathy each of which compromises their soft tissue status and limits their healing capacity. As a result, stump ulcers have been observed in many lower limb amputees who may reject the prostheses and even result in life-threatening deep tissue injuries. Both pressure (normal to skin) and shear (tangential to skin) stresses exist at the stump-socket interface which have been identified as key external factors affecting socket fit, patient comfort, and stump health. There are no existing sensors that can measure pressure and shear as well as being able to be routinely applied within a clinical setting.

To address this unmet need, a novel capacitive sensor has been developed. Experimental results will be presented to demonstrate the key electromechanical performance of the sensors when subjected to typical pressure and shear loads at the stump-socket interface. Real time results from initial clinical tests will also be presented which was obtained by locating the sensor within the prosthetic socket. The results demonstrate significant potential of the sensor for development of socket fit assessment instruments, which will lead to improved amputee care.

Day 3 – Friday, 6 December 2013

Session Poster Session 03 (PO-03)

Date / Time Friday, 6 December 2013 / 11:00–17:00 hrs

ID: 170

PO-03: 1

Evaluation of lower limb function of age change by using principal component estimation

Yohei Nomoto, Tetsuya Ohya, Yuya Onishi, Kei Sawai, Hironori Koyama and Masashi Kawasumi

University of Niigata Prefecture, Japan.

Falling is one of the most common and serious problems because advancing age has been associated with muscle weakness, reduced cutaneous sensation and deterioration of walking ability. We have investigated relation between the fall and lower limb function by development of evolution methods for lower limb function using principal component analysis so far. This paper focuses on change of the value of the evaluation of lower limb function, such as value of walking ability, value of muscle strength of lower limb and value of flexibility of ankle. The subjects were 16 healthy young volunteers (mean \pm S.D: 19.9 \pm 0.6 years) and 10 healthy aged volunteers (mean \pm S.D: 80.6 \pm 6.1 years) living in a special elderly nursing home. All subjects completed the informed consent procedures, and agreed to participate in this study. Measurement items related to lower limb function were selected from the items which we have ever used. Selected measurement items of function of lower are distance of extroversion of the toe, angle of flexion of the toe, maximum width of step, knee elevation, moving distance of greater trochanter, walking balance, toe-gap force and rotation range of ankle joint. The young group demonstrated the factor of 1.6 greater the assessment score of walking ability compared with the aged group. The young group demonstrated the factor of 1.4 greater the assessment score of muscle strength of lower limb compared with the aged group. The young group demonstrated the factor of 1.2 greater the assessment score of flexibility of ankle compared with the aged group. Parameters with significant differences between the elderly group and young group were selected and summarized by principal component analysis into lower ability assessment indices including walking ability and flexibility of ankle. The results suggested that it was possible to assess the lower limb function of aged and young numerically and to advise on their foot function.

ID: 173

PO-03: 2

Inconsistent outcomes of transcranial Direct Current Stimulation (tDCS) may be originated from individual anatomical differences

Chang-Hwan Im and Jung-Hoon Kim

Hanyang University, South Korea.

Transcranial direct current stimulation (tDCS) is a noninvasive neuromodulation method that transmits small DC currents through scalp electrodes to facilitate or inhibit cortical excitability of a particular area of the brain. Although recent studies have demonstrated that tDCS can effectively modulate excitability of various brain sites, the outcomes of tDCS are not consistent among subjects. So far, no studies have clearly elucidated the main cause of the individual variability. The hypothesis of our study was that the individual variability in the tDCS effect might be originated due to the anatomical differences among subjects. To verify our hypothesis, we investigated the relationship between the current density at dorsolateral prefrontal cortex (DLPFC) simulated using finite element method (FEM) and the behavioral outcomes of a verbal working memory (WM) task. A 3-back WM task experiment was conducted with twenty-five healthy subjects before and after the transcranial DC stimulation, when the cathode and anode electrodes were attached to right supraorbital area and F3 location, respectively. Our results showed that participants who showed enhanced WM task performance after tDCS had a significantly larger current density on DLPFC, suggesting that the inconsistent behavioral outcomes of tDCS might be originated in part due to the anatomical differences among subjects.

ID: 213

PO-03: 3

Direct application of mechanical stimuli to cell adhesion sites using magnetic-driven micropillar substrates

Kazuaki Nagayama, Takuya Inoue, Yasuhiro Hamada, Shukei Sugita and Takeo Matsumoto

Nagoya Institute of Technology, Japan.

Traction force generated at focal adhesions (FAs) of cells plays an essential role in regulating various cellular functions. The force can be measured by plating cells on a flexible substrate to observe local

displacement of the substrate caused by the forces (1–100 nN). Approaches employing this method include using microfabricated arrays of PDMS micropillars that bend by cellular traction forces. If you could apply forces to individual FAs independently by actively moving micropillars, it should become a powerful tool to delineate the cellular mechanotransduction mechanisms.

Here we developed magnetic micropillar array substrate made of PDMS that can be utilized for the mechanical stimulation of individual FAs of cells as well as the measurement of associated traction forces. The diameter, length, and center-to-center spacing of the micropillars were 3, 9, and 9 μm , respectively. We successfully embedded an enough amount of iron particles into the micropillars, so that the pillars could bend in response to an external magnetic field, and also successfully controlled their location on the substrate. By applying the magnetic field of 0.3 T, the pillars bent by $\sim 4 \mu\text{m}$ and external force could be transferred to actin cytoskeletons through individual FAs formed on the pillar top. With this approach, we investigated change in the traction forces of cultured aortic smooth muscle cells (SMCs) after local compressive stimuli to release cell pretension. The traction forces of SMCs looked fluctuated markedly during the local compression. The root mean square (RMS) of traction forces significantly increased during the compression, and it decreased to the baseline level after its release. These results may indicate that the fluctuation of forces may be caused by active reorganization of actin cytoskeleton and/or their dynamic interaction with myosin molecules. Our magnetic micropillar substrate would be useful in investigating the mechanotransduction mechanisms of the cells.

ID: 214

PO-03: 4

The differences of three dimensional gait mechanics of normal- and flat-arched feet in adults

Tulaya Prachgosin¹, Chong Yok Rue Desmond²,
Wipawan Leelasamran³, Pruittikorn Smithmaitrie⁴ and
Surapong Chatpun¹

¹Institute of Biomedical Engineering, Faculty of Medicine, Prince of Songkla University, Songkhla 90110 Thailand; ²Engineering Design and Innovation Centre (EDIC) and Department of Bioengineering, Faculty of Engineering, National University of Singapore 117576, Singapore; ³Department of Orthopaedic Surgery and Physical Medicine, Faculty of Medicine, Prince of Songkla University, Songkhla 90110 Thailand; ⁴Department of Mechanical Engineering, Faculty of Engineering, Prince of Songkla University, Songkhla 90110 Thailand.

Background: The malposition of the flat-arched foot during gait cycle directly increases stress injury to

arch stabilizers' structure and the malposition also transforms through ankle, knee and hip joints. The pathomechanics are not only in the kinematic aspect but also in the kinetics. In this study, we evaluated and identified the differences in the gait mechanics of foot, ankle, knee and hip joints between normal- and flat-arched feet.

Methods: We recruited 20 adult participants without neuro-musculoskeletal diseases. The participants had been identified their foot type by the modified Murley's protocol including footprint and radiography. Each gait cycle was captured by VICON system using Oxford foot and Plug-in Gait models. The foot, ankle, knee and hip joints angle, moment and ground reaction force were analyzed. The difference of the mechanics between two groups was tested with independent t-test.

Results: The average participant age was 29 ± 9 without the difference in BMI between two groups. Flat-arched group had significantly increased in ranges of motion of the foot, ankle, knee and hip joints in frontal and transverse planes. From joint moment in frontal plane, flat-arched group had a greater abduction moment at the ankle, knee and hip joints, which were 24.08 ± 10.68 , 43.83 ± 55.64 , and 93.40 ± 91.75 N.mm respectively. However, there was not significant between groups in the difference of ground reaction force along the stance.

Conclusion: The significantly greater moment of lower extremity joints in flat-arched group during walking may increase stress injury and consequently painful. These differences between normal- and flat-arched groups in this study can be used as the reference for the mechanical correction with the orthosis to reduce the moment at those joints.

Acknowledgement: The authors would like to thank Asst. Prof. Tan Ken Jin from Department of Orthopaedic Surgery, Yong Loo Lin School of Medicine, National University of Singapore for his assistance.

ID: 218

PO-03: 5

Influence of the bulging sinus size of the ePTFE valve conduit on the flow and opening area of the valve conduit

Toshinosuke Akutsu¹ and Koichi Okuyama²

¹Kanto Gakuin University, Japan; ²Graduate School of Engineering, Kanto Gakuin University, Japan.

There is no optimal substitute for right ventricular outflow tract (RVOT) reconstruction in congenital heart defects yet. Good clinical records seem to show

expanded polytetrafluoroethylene (ePTFE) valve conduits may be a good choice for treating this defect. Bulging sinus of the ePTFE valve seem to have favorable effect on hemodynamic performance, however, fluid mechanical research proving this effect has been limited. This research aims to study the effect of the bulging sinus size of the ePTFE valve on a flow phenomenon inside the conduit.

Several valve conduit models with different bulging sinus sizes were used. Considering bulging sinus size proportion similar to natural Aorta being "normal", straight model, reduced 50% model, normal model and enlarged 150% model were prepared. Effect of the bulging sinus size on a flow field inside the valve conduit was analyzed using Dynamic PIV system running at 1900 frames/s and valve opening areas were directly recorded using high speed digital camera running at 300 frames/s.

Comparison of flow field results between a straight model and normal model showed that the valve with normal model had strong vortex close to the leaflet location and resulted in wider valve opening area compared to a straight model.

Flow field of valve conduits with normal and enlarged 150% model generated strong vortex immediately behind the leaflet edge. Valve opened and closed early with normal and enlarged 150% model compared to reduced 50% model. Direct observation of the opening area of the valve showed that wider opening area was observed with normal and enlarged 150% model.

Valve with normal and enlarged 150% model shows strong vortex close to the leaflet location and resulted in wider valve opening area. Relative location of vortex seems to play important roll on valve open and close mechanism.

ID: 252

PO-03: 6

Hemodynamic analysis of intracranial aneurysms with atherosclerosis

Shin-ichiro Sugiyama¹, Kenichi Funamoto², Toshio Nakayama³, Kuniyasu Niizuma⁴ and Teiji Tominaga⁴

¹KOHNAN HOSPITAL, JAPAN; ²Institute of Fluid Science, Tohoku University, Japan; ³Graduate School of Tohoku University, Japan; ⁴Tohoku University Graduate School of Medicine, Japan.

Intracranial aneurysms can have atherosclerotic wall properties that may be important in predicting aneurysm history. This study aimed to investigate hemodynamic characteristics of atherosclerotic lesions in intracranial aneurysms. We conducted computational fluid dynamic analyses of 30 aneurysms using patient-derived geometries and inlet flow rates. Among 30 aneurysms, seven atherosclerotic lesions with remarkable yellow lipid

deposition were identified in five aneurysms. All seven atherosclerotic lesions were spatially agreed with the area exposed to stagnant blood flow. Univariate analysis revealed that male ($P = 0.031$), cigarette smoking ($P = 0.047$) and the exposure to stagnant blood flow ($P = 0.024$) are significantly related to atherosclerotic lesion formation on the aneurysmal wall. Of those variables that influenced atherogenesis, the variable male ($P = 0.0046$) and the exposure to stagnant flow ($P = 0.0037$) remained significant in the multivariate regression model. In conclusion, male sex and stagnant blood flow inside aneurysms were independent risk factors for atherosclerosis in intracranial aneurysms.

ID: 255

PO-03: 7

Cellular biomechanics assessment using a non-invasive technique

Jeremy Teo

Khalifa University, United Arab Emirates.

Association studies relating the biomechanical response of cells to cellular phenotype and behavioral dynamics, have shown good correlation between cell stiffness and human disease. Current cellular biomechanical assessment methods are unable to keep up with experimental requirements. As *in vitro* studies progressively moves away from standard two-dimensional (2D) petri dishes, towards recreation of three-dimensional (3D) biomimetic cellular microenvironment, there is a need for new assessment methods. Furthermore, new experimental demands to have high-throughput time-lapse imaging, with introduced biomechanical forces and biochemical cues into the cell microenvironment, further challenges the ability of current assessment methods to provide the necessary measurements. Here, we introduce a non-invasive method to measure cellular biomechanics in any biomimetic 2D/3D microenvironment.

ID: 267

PO-03: 8

Orientation and deformation of HAp crystals and elastic modulus of single trabecula in bovine femur

Satoshi Yamada, Sakurako Fukuda and Shigeru Tadano

Hokkaido University, Japan.

Cancellous bone has a hierarchical structure, spanning from the trabecular network, the single trabecula, to the hydroxyapatite (HAp) crystals and collagen fibrils level. The mechanical properties in the hierarchical structure may affect the elastic modulus and strength of cancellous bone; however, the

relationship has not been elucidated. Further, the differences in the mechanical properties between single trabecula and cortical bone have not been fully investigated. The aim of the study was to quantify the orientation and deformation behavior of HAp crystals and the elastic modulus of single trabeculae. In the experiments, single trabecular specimens were taken from the proximal cancellous bone of an adult bovine femur and were air-dried. The specimens were fixed to thin metal jigs, where the gauge length was set to 3 mm. To measure the elastic modulus of the specimens, the tensile tests were conducted using a small tensile testing device under microscopic observation and the deformation was measured using the gauge length. The specimens were irradiated with characteristic Mo-K α X-rays and diffracted X-rays were detected with an X-ray imaging plate to measure the c-axis orientation of HAp crystals in the specimens. Further, to measure the deformation behavior of HAp crystals, tensile tests were also conducted under X-ray irradiation and the deformation of interplanar spacing was measured. As a result, the c-axis of HAp crystals was aligned with the longitudinal direction of the trabecular specimens, even though the c-axis was aligned with the longitudinal direction of the diaphysis in the cortical bone of bovine femur. The elastic modulus and the deformation of HAp crystals in the trabecular specimens were smaller than those in the cortical bone of bovine femur.

ID: 270

PO-03: 9

Age-related residual stresses at diaphyseal surface of bovine femur measured by XRD-IP system

Mai Onuma, [Satoshi Yamada](#) and Shigeru Tadano

Hokkaido University, Japan.

The presence of residual stress in the diaphysis of quadrupedal extremities has been reported. Residual stress is defined as the stress that remains in bone tissue without any external forces. It is one of the stresses applied to bone tissue, as well as static stresses due to the body weight and dynamic stresses due to the movement. The bone residual stress can be measured from the deformation state of hydroxyapatite (HAp) crystals in bone tissue using X-ray diffraction. The authors proposed a $\sin^2\psi$ method of X-ray diffraction for detecting residual stress at the diaphyseal surface of extremities. However, the previous system required a complicated experimental set up, long irradiation time, and a limitation of sample size. Here, X-ray imaging plate (IP) can detect the two dimensional distribution of the diffracted X-rays from the HAp crystals in one irradiation. The aim of the study was to establish a simple measurement

system using an X-ray diffraction technique with IP (XRD-IP) for obtaining the residual stress at the diaphyseal surface of extremities and to apply this system to residual stress measurements of young and mature bovine femurs. In the experiments, the mid-diaphysis part of femurs taken from a less-than-1-month-old and a 23-month-old bovine were used. The diaphysis specimen was irradiated with characteristic Mo-K α X-rays, and the X-ray diffraction pattern was detected by an IP. The part of Debye ring from the (211) plane of HAp crystals was obtained in the pattern and the residual stress in the bone axis was calculated from the deformation state of the ring. The magnitude of residual stresses in the mature bone corresponded approximately to the results of the previous method. Further, it was demonstrated that the residual stresses at diaphyseal surface varied with age and location.

ID: 277

PO-03: 10

Preliminary experiment with the influence of sound distraction on a vigilance test

[Christina Lassfolk](#)¹, [Matti Linnavuo](#)¹, [Sanna Talvitie](#)², [Marja Hietanen](#)³ and [Raimo Sepponen](#)¹

¹Aalto University, Finland; ²ORTON Foundation, Finland; ³Helsinki University Central Hospital, Finland.

This paper presents a preliminary experiment with the influence of sound distraction on a vigilance test planned for rehabilitation of hemispatial neglect.

The experiment included five similar but not identical vigilance tasks that were performed on a laptop computer by 10 healthy, right-handed participants. Participants responded to the tasks by clicking the mouse. During the task performance they were wearing headphones over which four different sounds were played, whereas the fifth task acted as a control task without an audio track.

A drilling sound improved performance whereas a conversation impaired performance in the vigilance task. The preliminary data can direct the development of the vigilance task.

ID: 293

PO-03: 11

Evaluation of the in vivo impingement between components in cruciate-retaining and posterior-substituting total knee arthroplasty

Takeshi Shimoto¹, Satoru Ikebe², Hidehiko Higaki², Kazuho Nishimatsu³, Yoshitaka Shiraishi³, Hiromasa Miura³, Satoshi Hamai⁴, and Yukihide Iwamoto⁴

¹Fukuoka Institute of Technology, Japan; ²Kyushu Sangyo University, Japan; ³Ehime University, Japan; ⁴Kyushu University, Japan.

Impingement problem of femoral component and polyethylene insert after total knee arthroplasty (TKA) has been recently brought to light by contact pressure analysis using the knee joint simulator. Therefore, adequate motion analysis is important for estimating the impingement between components and improving postoperative exercise. In this respect, our fluoroscopic analysis was able to reproduce the in vivo relation of contact between a femoral component and polyethylene insert on a computer. The purpose of this paper is to analyze the impingement of TKA components during kneeling and stair claiming activities in vivo.

Twelve patients with cruciate-retaining (CR) TKA and nine patients with posterior-stabilized (PS) TKA were examined in kneeling activity. Also, twelve patients with CR TKA and ten patients with posterior-stabilized (PS) TKA were examined in stair claiming activity. All patients were able to walk without support. Continuous sagittal x-ray images of kneeling and stair climbing activities for each subject were taken by using a flat panel detector. The 3-D position and orientation of the implant components were determined using image matching technique. The 6-DOF of each component was able to be reproduced on 3-D CAD. Kinetic relation between the femoral component and polyethylene insert was calculated, and then the impingement was analyzed.

In the CR subjects, the femoral intercondylar notch was considered impinging the tibial eminence in hyperextension of stair claiming activity, but there was no such case. In the PS subjects, impingement of the femoral intercondylar notch and anterior aspect of the tibial post was observed in extension of stair claiming activity. In addition, it was observed that femoral cam impinge the posterior surface of tibial post in deep flexion of kneeling activity.

This study helps the surgeon be more aware about impingement between components under some conditions and is useful to improve the design of artificial knee joint.

ID: 295

PO-03: 12

Fractal dimension of self-assembled 50 bp poly(dA)-poly(dT) DNA on HOPG surface

Ryosuke Nii, Kentaro Doi and Satoyuki Kawano

Graduate School of Engineering Science, Osaka University, Japan.

Deoxyribonucleic acid (DNA) has attracted much attention to be utilized for technological applications of its various cellular functions and possibility to fabricate nano-scaled patterns on various substrate surfaces. Several techniques have also been applied to manipulate biomacromolecules. In our previous studies, self-assembled network patterns of poly(dA)-poly(dT) DNA on mica and highly oriented pyrolytic graphite (HOPG) surface could be fabricated and observed by atomic force microscopy (AFM), which is preprocessed by a specific solution concentration of MgCl₂. Although negatively charged DNA molecules repulsively interact with negatively polarized HOPG surfaces, we built our fabrication techniques to produce self-assembled DNA. Focusing on the associated self-assembly mechanism, we develop and perform coarse-grained molecular dynamics simulations, in which 50 base-pairs (bp) long DNA fragments are modeled considering both intra- and inter-molecular interactions between the DNA and HOPG surface in aqueous solution. Using this model, we carry out Langevin dynamics simulations. As a result, the network pattern formations, in which DNA fragments make bonds and bundle structures, are replicated. Our results also indicate that thermal fluctuations in solution work effectively to enhance the assembly process. In this study, characteristics of self-assembly of DNA are classified by the fractal dimension, which is associated with various time and spatial scales.

ID: 300

PO-03: 13

The relationship between body composition and ball speed in youth baseball pitchers

Chun Kai Chang¹, Shiang-Yun Huang¹ and Yung-Shen Tsai²

¹Department of Sports Sciences, Taipei Physical Education College, Taiwan; ²Graduate Institute of Sports Equipment Technology, Taipei Physical Education College, Taipei, Taiwan.

Introduction: Previous studies revealed that ball speed may be affected by body height and weight in youth baseball players. The relationship between body composition and ball speed has not been researched. The purpose of the study was to investigate the relationship between body composition and ball speed in youth baseball pitchers.

Methods: Twenty seven youth male pitchers (age: 11.7 ± 0.7 years, height: 154.9 ± 4.8 cm; and mass: 49.0 ± 13.5 kg) participated in this study. Body composition was measured using Dual Energy X-ray Absorptiometry. Ball speed was collected by a sports radar gun. Pearson Correlation Coefficients were used to investigate the relationships between body height, body weight, body composition and ball speed.

Results: The average ball speed of these players was 24.4 ± 2.2 m/s. Body height ($r=0.74$, $p=0.00$) and weight ($r=0.44$, $p=0.02$) were significantly correlated with ball speed. There were significant relationships between upper extremity ($r=0.44$, $p=0.01$), lower extremity ($r=0.57$, $p=0.00$), and trunk ($r=0.65$, $p=0.00$) bone density and ball speed. There were significant relationships between upper extremity ($r=0.62$, $p=0.00$), lower extremity ($r=0.65$, $p=0.00$), and trunk ($r=0.63$, $p=0.00$) lean muscle mass and ball speed. No relationships were observed between body fat and ball speed.

Conclusion: Improving bone density and lean muscle mass through training may increase ball speed in youth baseball pitchers.

ID: 309

PO-03: 14

Electrical stimulation of anterior cingulate cortex for the suppression of neuronal hyperactivity in ventral posterolateral nucleus in neuropathic pain model rats

Sang Baek Ryu¹, Jeong Woo Choi¹, Jin Hyung Kim^{2,3}, ChangKyun Im⁴, Jin Woo Chang^{2,3}, Hyung-Cheul Shin⁴ and Kyung Hwan Kim¹

¹Department of Biomedical Engineering, College of Health Science, Yonsei University, Wonju, 220-710, Korea; ²Brain Korea 21 Project for Medical Science and Brain Research Institute, Yonsei University College of Medicine, Seoul, 120-752, Korea; ³Department of Neurosurgery, Yonsei University College of Medicine, Seoul, 120-752, Korea; ⁴Department of Physiology, College of Medicine, Hallym University, Chuncheon, 200-702, Korea.

It has been recently reported that electrical stimulation to anterior cingulate cortex (ACC) is effective to relieve symptoms of neuropathic pain. To understand its mechanism, it is necessary to observe how neuronal activities in the pain-related area are affected by the stimulation. In this study, we investigated pain-related characteristics of neuronal activities in ventral posterolateral nucleus (VPL) of thalamus and analyzed how they are affected by ACC electrical stimulation.

Spared nerve injury rats were used as models of neuropathic pain. Single unit activities and local field potentials (LFPs) were recorded from the VPL. Press

stimulus was applied to the hind paw. Biphasic electrical pulse was applied to an electrode placed in the ACC (pulse amplitude: $100 \mu\text{A}$, pulse duration: $60 \mu\text{s}$, frequency: $10\text{--}130$ Hz).

In single unit activities, firing rate was increased during the press stimulation both in normal and neuropathic pain model rats. However, firing rate was increased significantly higher and lasted much longer (after-discharge) in neuropathic pain model rats. According to the press stimulus, spectral power of LFPs was increased in high gamma band ($80\text{--}150$ Hz) and decreased in low frequency band ($1\text{--}10$ Hz). Similarly to the single unit activities, changes in LFPs also were sustained longer in neuropathic pain model rats. By the electrical stimulation of the ACC, the hyperactivity in single unit activities including the after-discharge was suppressed. The duration of increased/decreased LFP spectral powers were also reduced to near-normal levels by the ACC stimulation. The ACC stimulation became effective when the stimulation frequency was higher than 50 Hz.

Our results suggest that the abnormal single unit activities and LFPs are distinctive features of neuropathic pain, and high frequency electrical stimulation of the ACC is an effective way to reduce these pain-specific features.

Acknowledgement: The Ministry of Knowledge Economy of Korea (10033812), The Ministry of Education, Science and Technology (2011-0031867)

ID: 312

PO-03: 15

Biomechanical analysis of stop-jump movement in female college and high school basketball players

Chiu-Yu Hsiang, Chia-Wei Chiu and Yung-Shen Tsai
Taipei Physical Education College, Taiwan.

Introduction: According to previous studies, college female basketball players seem to have greater risks in ACL injury rate than high school female basketball players. To examine the kinematics, kinetics and muscle activities of knee and hip joint during stop-jump movement in female college and high school basketball players. We also compared knee and hip muscle strength between these two groups.

Methods: Ten female college basketball players and seven female high school basketball players participated in this study. Vertical stop-jump movement was captured by a 3D electromagnetic motion analysis system. Myoelectrical activity of the knee musculature during stop-jump movement was recorded by a surface electromyographic system (EMG). Maximum isokinetic concentric contraction strength of the knee joint and maximum isometric

concentric contraction strength of the hip abduction and extension were measured by the Biodex isokinetic dynamometer.

Results: Knee flexion angle, knee abduction moment and hip abduction moment at initial contact in female high school basketball players were greater than those in female college basketball players. Knee flexion angle, proximal tibia anterior shear force, knee abduction moment, hip flexion angle, and hip abduction moment in female high school basketball players were significantly greater than those in female college basketball players at the time of the peak posterior ground reaction force. Maximal knee and hip abduction moment were greater in female high school players. No significant differences were observed in maximum hip and knee muscle strength and EMG activities between these two groups.

Conclusion: The knee joint stress during vertical stop jump in high school female basketball players seem to be greater than college female basketball players. Further study is needed to understand why the college female basketball players had higher ACL injury risks reported than high school female players.

ID: 319

PO-03: 16

Driving cell cycle of endothelial cells by hydrostatic pressure

Daisuke Yoshino¹, Kakeru Sato² and Takehiko Sato¹

¹Institute of Fluid Science, Tohoku University, Japan; ²Graduate School of Engineering, Tohoku University, Japan.

Hydrostatic pressure treatment has already been in widespread clinical use for promoting wound healing. Although neoangiogenesis of blood capillary may become a main factor for promoting wound healing, the effects of hydrostatic pressure on angiogenesis have still remained unclear. In this study, we focus on the cell cycle and morphology of endothelial cells after applying hydrostatic pressure, and discuss the effects of hydrostatic pressure on endothelial functions associated with angiogenesis.

Human umbilical vein endothelial cells (HUVECs, Cell Applications) were used in this study. The hydrostatic pressure chamber (HP chamber) was mounted onto 60 mm cell-cultured dish. The HP chamber was filled with the Medium 199 (Gibco), which contains 10% heat-inactivated fetal bovine serum (Gibco) and 0.1% penicillin/streptomycin (Gibco). HUVECs were exposed to ± 50 mmHg by volume compression and expansion of the media for 6, 12, and 24 hours. After pressure exposure, HUVECs were fixed with 4% paraformaldehyde, and the cell morphology was observed with the phase

contrast microscope (Carl Zeiss). The cells were harvested from the dish by using 0.05% Trypsin-EDTA (Gibco), and fixed with ice-cold 70% ethanol after three-times washing by PBS(-). Then, we adjusted the cell concentration to 500 cells/ μ l. After staining the cells with Guava Cell Cycle Regent (Millipore), we analyzed the cell cycle using Guava easyCyte™ HT flow cytometer (Millipore).

No morphological change was observed after hydrostatic pressure exposure for 6, 12, and 24 hours. We could also confirm the cell cycle, which remained at rest in consequence of contact inhibition in HUVECs, was forcibly driven by hydrostatic pressure. After pressure exposure, the rate of cells in S and G2/M phases has increased up to twice from that in the static condition. These results suggest that the expression of cell cycle-related proteins, such as cyclin D1, were encouraged by the hydrostatic pressure.

ID: 323

PO-03: 17

The ankle-subtalar joint axes using the articular surfaces of the talus

Ho-Jung Cho, In-Beom Kim, Yong-Seok Nam and Dai-Soon Kwak
The Catholic University of Korea, South Korea.

The shape of human bone has variance among the populations, and the range of motion is related with the articular shape. The talus is a bone in the tarsal bone that plays an important role in the articulation of the joints of the foot and ankle. Parr WC *et al.* (2012) introduced a new method using 3D talus models for calculating the talocrural joint (TCJ) and subtalar joint (STJ) axes. The aims of this study are the TCJ, STJ axes analysis using talus articular surfaces, and comparison with the previous study.

We used the 3D reconstruction models of Korean talus. The principle axis (PA) was calculated by STL Cad program (3-matic, Ver. 7.0, Materialise, Belgium). The TCJ axis was calculated by least square sphere fitting method. The lateral and the medial part of the superior facet of trochlea were used to make two spheres, and connected the center point of each sphere. The connected line defined as the TCJ axis. The STJ axis was calculated by the similar method. One sphere was fitted to the posterior calcaneal articular facet and the other sphere was fitted to the anterior and middle facet for calcaneus. The PA was used to reference coordination of the TCJ and the STJ axes.

The PA in the axial plane was opposite declination compared to the previous study (Parr WC *et al.*, 2012). The result of the STJ axis was 15.6° (deviation), 45.8° (inclination). We could not find any difference inclination angle between this study and the study of Parr WC *et al.* (2012) (P=0.75). However, the result of

deviation was larger than the study of Parr WC et al. (2012) ($P < 0.01$). The TCJ axis was 22.3° (deviation), 86.9° (inclination). At the STJ axis, the larger deviation angle in this study may be caused by the shape of the talus.

ID: 333

PO-03: 18

Plastic design of polyethylene inserts of knee prostheses

Kensei Tanaka, Rina Sakai and Kiyoshi Mabuchi

Kitasato University, Japan.

In a strength design, the yield stress as physical-properties strength of material must be sufficiently larger than the loading actually presumed. However, the strength of a ultra-high molecular weight polyethylene (UHMWPE) insert will be less than this criterion in major total knee prostheses. In the present study, we performed indentation tests of UHMWPE plates together with finite element (FE) analysis under conditions similar to those within a total knee prosthesis and discuss the fracture parameter.

Flat plates made of conventional or cross linked UHMWPE were molded as test pieces. The indentation test using a loading machine was performed. Flow pressure was calculated after the test as a ratio of the impressio area and the maximum load. Deformation of the plate was estimated by displacement at the edge. Additionally, the FE analysis was performed on a virtual model using the same conditions as in the experiments.

In indentation test, there was no influence of plate thickness in flow pressure. The values of the flow pressure were measured as a mean of 47.01 MPa for conventional UHMWPE, and as a mean of 58.42 MPa for cross-linked UHMWPE. The displacement of the UHMWPE plate edge was evaluated. It increased with decreasing thickness of the plate. The deformation estimated by FE analysis was similar to that of the experimental findings. Furthermore, shear strain in the UHMWPE plate of FE model increased as the thin plate, decreased as the thick plate.

The findings showed that stress value cannot use failure criterion in a plastic design. In contract, strain is possible for evaluation of a plastic design since it was shown large value in thin plate compared other thickness plate. Therefore, the failure criterion of joint prostheses must be presented by not only the stress but also the strain in a UHMWPE insert.

ID: 343

PO-03: 19

Motion analysis of patellofemoral joints before and after total knee arthroplasty

Satoru Ikebe¹, Hidehiko Higaki¹, Takeshi Shimoto², Yoshitaka Nakanishi³, Kazuho Nishimatsu⁴, Yoshitaka Shiraishi⁴, Masami Ishimaru⁴ and Hiromasa Miura⁴

¹*Kyushu Sangyo University, Japan;* ²*Fukuoka Institute of Technology, Japan;* ³*Kumamoto University, Japan;* ⁴*Ehime University, Japan.*

In the field of biomechanics in vivo, the analytic techniques of motion in the artificial knee joints using shape of each component on the X-ray images. However, the patellar components in the artificial knee joints are made with ultrahigh molecular weight polyethylene, the shape can't be obtained on X-ray images. Therefore, motion analysis of patellar components has been difficult in vivo. And so, we developed the six-degrees-of-freedom motion analysis using window analysis technique and image correlation of single plane X-ray images. Motion of patella can analyze using this technique, patellar component can be determined by positional relation between patella and patellar component. In this study, in vivo motion of patellar component analyzed in before and after total knee arthroplasty (TKA). Coordinate system of the bone set up same in before and after TKA, the differences in motion of knee joints were evaluated. The accuracy of this method is within 0.3 mm and 0.3 degrees for the artificial joints, and within 0.2 mm and 0.3 degrees for the natural joints.

We report analytic results of the patella before and after TKA in squatting activity. Subjects were two females and one male of the knee osteoarthritis. The helical axis of the patella with respect to the tibia was confirmed the phase of an irregular motion in before TKA, but was confirmed motion of the many medio-lateral direction in after TKA. The contact points between the femoral component and the patellar component was confirmed to two contact points, but was confirmed to one contact point from the only subject. In addition, the contact points was the confined area on articular surface of the patellar component. We were able to quantify the movement and functionality of the patella before and after TKA in vivo by using these techniques.

ID: 358

PO-03: 20

Influence of differentiation of HL-60 cells on their motion on a flat glass plate.

Yoshiro Sugiyama¹ and Atsushi Shirai²

¹Graduate School of Engineering, Tohoku University; ²Institute of Fluid Science, Tohoku University, Japan.

Rolling of leukocytes on vascular endothelium, which primarily occurs in postcapillary venules, is an early event among their inflammatory response followed by adhesion onto the endothelial cells and transmigration toward the sites of inflammation. The leukocyte rolling has been studied extensively with respect to selectin-ligand bonding. The authors, in contrast, have focused on physical interaction between endothelial cells and neutrophils, that is, influence of bumpy surface of the endothelial cell layer on motion of the leukocytes. In their previous study, behavior of HL-60 cells on human umbilical vein endothelial cells cultured on a flat glass plate was observed using an inclined centrifuge microscope. Here, promyelocytic leukemia HL-60 cells are induced to differentiate into neutrophil-like cells by some chemical stimuli. The authors have used undifferentiated cells to prevent unexpected activation of the cells during the observation, but behavior of undifferentiated HL-60 cells could differ from neutrophils because undifferentiated cells have few bonding molecules and they are stiffer than neutrophils. Therefore, in this study, the authors differentiated HL-60 cells into neutrophil-like cells by all-trans retinoic acid (ATRA), and compared their motion on a glass flat plate with undifferentiated cells with respect to adhesivity to the glass plate and moving velocity for the fundamental understanding of influence of the differentiation on their behavior. As the result, it was found that ratio of adherent cells was increased and stick-slip motion was observed by the differentiation. Mean velocity of moving cells decreased with the differentiation, but the decrement was much smaller than increment of the adhesion ratio. The decrease in the mean velocity was thought to be due to acceleration and deceleration of the cells during the stick-slip motion. Finally, it was suggested that the differentiation increases adhesivity of HL-60 cells but little influences velocity of moving cells.

ID: 371

PO-03: 21

A study on lower limb joint angles and muscle activities during maximal & sub-maximal pedaling by saddle heights

Jaehyuk Bae, Dongwon Kang, Jinseung Choi, Gyerae Tack, Y. H. Shin and J. H. Lee

Konkuk University, South Korea.

Cyclists can achieve an effective pedaling through the fitting to adjust various frame sizes by considering their physical characteristics. Among several fitting parameters, saddle height is a key factor for both injury prevention and optimal cycling performance. The purpose of this study was to analyze lower limb joint angles and muscle activities due to different saddle heights via well-known knee angle method during maximal & sub-maximal pedaling. Seven elite cyclists (Age : 34.3±3.5, Height : 174.2±4.6, Weight : 82.5±7.2) participated in 10 sec maximal (sprint) test and 3 min sub-maximal (90RPM) test with 3 different saddle heights which was set to the corresponding height by 25, 30, 35 angle between lower leg and extended shank at bottom dead center position. Movement of hip, knee, and ankle joint was obtained through 3D motion analysis system (Motion analysis Corps., USA), and EMG (Delsys Inc, USA) of biceps femoris (BF) and vastus lateralis (VL) were measured at the same time. Results showed that hip (knee angle: 35, 30) and knee (knee angle: 30, 25) joint angle were significantly increased during maximal test. There was not significantly decreased compared to 25 knee angle during maximal test, and that of biceps femoris at 35 knee angle was significantly decreased compared to 25 knee angle during the sub-maximal test. It is suggested that selection of saddle height for effective pedaling be considered with the cadence and the sport entries of cycling.

ID: 375

PO-03: 22

Normative walking spatio-temporal parameters of Malaysian aged 19–24 year old – initial findings utilizing wearable insole system

Yu Zheng Chong¹ and Jasmy Yunus²

¹Universiti Tunku Abdul Rahman, Malaysia; ²Faculty of Biosciences and Medical Engineering, Universiti Teknologi Malaysia, Skudai, Malaysia.

This paper described data collection of Spatio-Temporal characteristics of Malaysian Adults aged between 19–24 year old. Spatio-temporal characteristics are important in distinguishing between normal and pathological gait characteristics, such as cerebral palsy. Thirty (30) volunteers were recruited for the study, with equal participants from both genders. It is

found that data collected are comparable with published literatures. This preliminary work have shown promising outputs, and will serve as groundwork for further studies to be conducted on normative gait data catered for Malaysians, and as reference database in future.

ID: 381

PO-03: 23

A preliminary study on musculoskeletal model for cycle pedaling

Yoonho Shin, Jinseung Choi, Dongwon Kang, Jaehyuk Bae, Joohack Lee and Gyeræ Tack

Konkuk University, South Korea.

The purpose of this study was to develop a forward dynamic musculoskeletal model for cycle pedaling by comparing muscle activation patterns of the model and measured EMG data. Five elite cyclists (Age: 32±5.2years, Height: 171±3.5cm, Weight: 79.7±5.6kg) participated in pedaling experiment. 3D motion system (Motion analysis Corps., USA) and Trigno wireless EMG system (DELSYS, USA) were used to measure pedaling motion and muscle activation of lower limb. Biceps femoris (BF), vastus lateralis (VL), tibialis anterior (TA) and gastrocnemius medial (GM) were selected for EMG measurement. Musculoskeletal model for each subject by AnyBody program (version 5.3.0, Denmark) was developed. To compare muscle activation patterns between model and EMG, Pearson's correlation coefficient and Peak-Timing were selected. Results showed that there was a significant correlation in VL, BF, and GM between model and EMG ($p<.05$). Peak-timing of muscle activations showed a significant correlation in VL and TA ($p<.05$) which are mono-articular muscles while there were no significant correlation between BF and GM ($p>.05$) which are bi-articular muscles. Further inverse dynamic analysis is under progress by measuring reaction force at the pedal via our developed load-cell system for pedaling.

ID: 423

PO-03: 24

An in vitro stretch-injury model for elongation-controlled neuronal cells: effect of strains along neurite

Hiroimichi Nakadate¹, Shigeru Aomura¹ and Akira Kakuta²

¹Tokyo Metropolitan University, Japan; ²Tokyo National College of Technology, Japan.

Diffuse axonal injury (DAI), a major component of traumatic brain injury, is associated with rapid deformation of brain tissue resulting in the stretching of neural axons. Focal axonal beading, which is the

morphological hallmarks of DAI pathology, leads to the disconnection of neurons from tissues, resulting in cell death. Our goal is better understanding of neuronal tolerance and help to predicting the pathogenesis of DAI from mechanical loading to the head. In present study, we developed a stretch-injury model that subjected cultured neuronal cells in which the directions of neurite elongation were controlled with microfluidic culture technique to uniaxial stretch and examined the effect of strains along neurite on the cell damage. Neurites from PC 12 cells were extended at 0, 45 and 90 degrees to stretch direction using a fabricated poly(dimethylsiloxane) (PDMS) piece having microgrooves in combination with PDMS substrate. Following stretch with a strain of 0.22 and a strain rate of 27 s⁻¹, the morphology of same neurites were observed at 5 min–24 h. As a result, the beading along neurites oriented at 0 degree increased immediately following stretch and the increase was sustained until 24 h, although the beading along neurites oriented at 45 and 90 degrees transiently increased within 1 h following stretch. Many rupture of neurites was observed more in neurites oriented at 0 and 90 degrees than in neurites oriented at 45 degrees, however, the retraction and disappearance of neurites did not differ in any orientation conditions. These results suggest that the difference in strain along neurite induces different types and degrees of neurite damage and not strain of cell-cultured substrate but strain loaded to neurite is important to evaluation of neuronal injury.

ID: 431

PO-03: 25

Effect of shear stress on migration of hepatic stellate cells

Tateki Sumii¹, Ryosuke Fujita², Kazuhiro Nakashima¹ and Susumu Kudo¹

¹Kyushu university, Japan; ²Shibaura Institute of Technology, Japan.

Hepatic stellate cells (HSCs), which are located in the liver, synthesize materials inducing liver cirrhosis. HSCs produce extracellular matrix, and this matrix induce liver cirrhosis. Hence past studies said that migration of HSCs to inflamed areas developed progression of liver cirrhosis. We thought that there is relationship between migration of HSCs and shear stress, because HSCs surround blood vessel and HSCs are subjected to blood shear stress leaking from the vessel wall. However no study has been reporting about the relationship. In this study, we investigated HSCs migratory response to shear stress.

HSCs were grown to confluency, and a part of HSCs was desquamated by micropipettes. The wound of HSCs-layer was vertical to shear stress. We

use a parallel plate flow chamber as a device generating shear stress. After nine hours, we quantified HSCs-migration.

In downstream, where cells migrated to the opposite direction of flow, HSCs-migration of each shear stress increased in the following order: 2 Pa < 0.6 Pa < Static culture. On the other hands, in upper stream, where cells migrated to the same direction as flow, migration of each condition increased in the following order: 0.6 Pa < Static culture < 2 Pa.

From these results, we discuss that the direction of shear stress influences distances of HSCs-migration.

ID: 448

PO-03: 26

The coverage characteristic of tibial component for unicompartmental knee arthroplasty by finite element study

Tsung-Wei Chang, Cheng-Kuang Lu and Jiann-Jong Liao

United Orthopedic Corporation, Taiwan.

The treatment of unicompartmental knee arthritis with unicompartmental knee arthroplasty (UKA) has renewed popularity in recent years. Good coverage of tibial component and proximal resected tibial surface can be expected to improve the strength of component fixation and thus avoid component subsidence, especially for the situation that body weight mainly transfers through the cortex of the medial tibial plateau. Most of previous studies reported the effect of malalignment in UKA, but few study focused on the coverage and morphology between implant and resected surface. The purpose of this study was to investigate the force distribution over the medial tibial plateau in using this different prosthesis by FEM. A three-dimensional tibia finite element model was constructed based on computed tomography (CT) scan data of a composite tibia. Image processing software was used to extract the geometry of the cortex and cancellous outline for the construction of an intact tibia model. A compressive load of 2000 N was shared by the medial (75%) and lateral (25%) tibial condyles, simulating a one-legged weight-bearing stance. The load was applied along the long axis of the tibia and perpendicular to the distal axis of the model. The distal end of the tibia was rigidly fixed. The material properties of the composite tibia, cement, and components were assigned according to the manufacturer specifications and previous studies. Comparing the peak von Mises stress on the resected surface and cancellous bone stress around the pegs are the design of complex contour, Zimmer, could provide better stress after perfect fit design.

ID: 451

PO-03: 27

Medical equipment management support system developed from open source software

Shotaro Watanabe¹, Noritaka Mamorita², Masataka Kitama¹, Hisae Shimizu¹, Masaji Yamashita¹, Kazuyuki Kimura¹, Junji Arisawa¹, Hiroaki Arisawa³ and Taketoshi Saka³

¹Graduate School of Hokkaido Institute of Technology, Japan;

²Hokkaido Institute of Technology, Japan; ³Saka Urology Hospital, Medical Corporation Hokujuinkai, Japan.

Medical equipment is essential to modern medical practice. To ensure the safety of medical equipment, in-house clinical engineering departments (CEDs) should introduce a medical equipment management system. However, the introduction of commercial systems is difficult and dependent on the medical institution's economic status. Under such circumstances, we propose that each CED should develop its own equipment management system. However, because many institutions believe that the development of such a system is a low priority, they may not want to actively allocate time and personnel for it. In addition, because institutions cannot publish the source code, particularly when in use by other institutions, these source codes may not be readily customized to suit a specific institution.

To overcome these limitations, we developed the Open-MEMs (medical equipment management software) using open source software. Open-MEMs is a package software configured from PostgreSQL of the database server managing the equipment information and from Tomcat of the web server providing web application. Installing Open-MEMs on a PC creates a client-server system for equipment management. To test the system, we performed an introduction, customization, and operation of Open-MEMs in the CED of the 70-bed Saka Urology Hospital. The server and client use Let's note (Panasonic, Inc., Japan) and Nexus 7 (Samsung, Inc., Korea), respectively.

Because the Open-MEMs introduction includes only the hardware cost, the cost of introduction was reduced compared with other commercial systems. Regarding the operation at this point of time, the equipment information of 24 types of 227 units was centralized. We could reference the equipment information and maintenance records of operating and dialysis rooms of each department though the in-house LAN. Because the Open-MEMs source code is publishable, the system could be customized to suit each institute. In this way, Open-MEMs will promote the introduction of medical equipment management systems.

ID: 455

PO-03: 28

Morphological analysis of mouse pulmonary acini extracted from synchrotron micro-CT images with a multiscale-based segmentation algorithm

Luosha Xiao¹, Toshihiro Sera², Kenichiro Koshiyama¹ and Shigeo Wada¹

¹Department of Mechanical Science and Bioengineering, Graduate School of Engineering Science, Osaka University, Japan; ²The Center for Advanced Medical Engineering and Informatics, Osaka University, Japan.

A semi-automatic segmentation method for extracting the complete structure of pulmonary acinus from synchrotron micro-CT images was developed on the basis of the multiscale and hierarchical nature of lung structures. To verify the potential of the method for the statistical analysis of acinar morphology, we here measured and analyzed the morphological characteristics of acinus by applying the semi-automatic segmentation algorithm and specialized measurement methods of acinus to the micro-CT images of mouse lungs. The number of acinar samples for volume and surface analysis was thirty and for generation analysis was three. The number of voxels of per acinus sample was counted and the triangular patches of the internal surface were created for the analysis of acinar volume and surface. For the analysis of pathway, we applied a skeletonization algorithm to the samples. The average volume and surface area of acinus were $0.125 \pm 0.09 \text{ mm}^3$ and $10.09 \pm 6.70 \text{ mm}^3$, respectively. The peak of acinar volume distribution was 0.1 mm^3 . For a cluster of acini belonging to the same terminal bronchiole, the maximum volume of acinus occurs at the end of terminal bronchiole. The pathway lengths increase with the generation of airways. Overall morphological characteristics of acinus reasonably agree well with the histology-based estimates of previous researches.

ID: 458

PO-03: 29

Three-dimensional observation of microscopic structure of the aortas reveals their heterogeneous deformation

Shinataro Iijima¹, Sakiko Nakamura², Hideo Yokota², Kazuaki Nagayama¹ and Takeo Matsumoto¹

¹Nagoya Institute of Technology, Japan; ²Institute of Physical and Chemical Research, Japan.

Elastic laminas (ELs) in unloaded elastic arteries are corrugated, while they are almost straight in the physiological state. We noticed that the waviness of the EL is spatially heterogeneous. Such heterogeneity may indicate that the intramural stress distribution in the in vivo state is non-uniform. To reveal the cause of the heterogeneity, we observed three-dimensional

(3D) microscopic structure of rabbit thoracic aortas with a 3D Internal Structure Microscope (3D-ISM), which is a device that obtains images of serial sections by slicing a frozen sample block at $2 \mu\text{m}$ -interval. ELs were visualized by their autofluorescence excited at 488 nm and measured at 500–550 nm. The images of serial sections obtained by the 3D-ISM were reconstructed to a 3D image by a software V-Cat. We found that the corrugation of the EL was continuous in the axial direction spanning more than $300 \mu\text{m}$. When viewed its 3D shape from intraluminal side, the corrugation looks like ridges, and they were wavy in the axial direction. The waviness of the ridge, length along the curvature divided by its straight length, was 1.20 ± 0.08 (mean \pm SD, $n=7$), and was similar to the axial stretch ratio of the thoracic aortas, 1.2–1.3. This may indicate that the bending of the ridges is an artifact caused by the axial shortening of the artery. We are observing the morphology of the ELs in stretched and pressurized states. There was a patchy distribution of the ridge areas and flat areas with a representative dimension of $300 \mu\text{m}$, indicating that local shrinkage of the artery wall from the physiological to unloaded state is heterogeneous. Such heterogeneity might be caused by local heterogeneous alignment of smooth muscle cells. We are now planning to observe smooth muscle orientation to reveal their effects on the non-uniform waviness of the ELs.

ID: 461

PO-03: 30

The subliminal vibration stimulus makes the improvement of the standing balance

Masaki Yoshida and Yuuya Kawashima

Osaka Electro-Communication University, Japan.

The fall accident of the elderly person gives serious results. One of the fall prevention methods is the improvement of the standing balance ability. We have already reported that the standing balance ability is improved by the subliminal vibration stimulus to planta pedis. The stimulus to planta pedis has the problems including the possibility of the damage of the stimulator. The aim of this study is to evaluate the influence of the subliminal vibration stimulus to the bone prominence of lower leg to the standing balance ability. The stimulus points are head of fibula, lateral malleolus, malleolus medialis, tuberosity of navicular bone and 5th metatarsal bone tuberosity. The experiments are conducted under six kinds of conditions, that is, the stimulation at five places separately and no stimulus vibration. The experiment repeats five times for each condition. The stimulation intensity is 90% of the intensity to feel vibration. Therefore, a subject does not feel the vibration even if a vibration

stimulus is applied during the measurement. The subjects are five healthy males. A subject stands on one leg with closed eyes. We measured the center-of-foot-pressure (CFP) sway for 10 seconds. The standing balance was evaluated by the locus area and length of CFP sway. The stimulus to malleolus medialis or tuberosity of navicular bone or 5th metatarsal bone tuberosity significantly improved standing position balance. It became clear that the stimulation to the ankle could improve standing posture balance.

ID: 474

PO-03: 31

Relationship between angle of attack and trunk accelerations during human walking

Kei Tsunoda and Naomichi Ogihara

Keio University, Japan.

Theoretical studies on the principle mechanics of human locomotion using a spring-loaded inverted pendulum model has suggested that an appropriate control of the angle of attack (leg orientation at touchdown) is important for generation of stable locomotion utilizing self-stabilization. However, how changes in the angle of attack actually affect stability of human walking still remains unclear. In the present study, we therefore experimentally investigated the relationship between the angle of attack and the trunk accelerations during human walking. Adult male participants were asked to walk on a treadmill at 4 km/h (1.1 m/s) at a self-selected frequency, and walking kinematics was measured using an eight-camera motion capture system. The angle of attack, defined as the angle of the axis connecting center of body mass (COM) and heel marker with respect to the horizontal line, was calculated for each gait cycle. The location of COM was estimated based on the measured joint positions and published mass and COM fractions for each segment. The trunk accelerations were also recorded simultaneously with a tri-axial accelerometer attached to sternum. In order to examine the effects of the angle of attack on the trunk accelerations, we also asked the participants to walk on the treadmill while adjusting their step frequency to the beat of a metronome. As the speed of the treadmill remains constant, the change in stride frequency creates variability in stride length, and hence the angle of attack during walking. Our results demonstrated that the fluctuations of the trunk acceleration were relatively small when the variability of the angle of attack is small. Proper adjustment of the angle of attack seems important for reducing the risk of falling in actual human walking.

ID: 477

PO-03: 32

Finite element analysis of the mechanical interactions between the human foot and the ground

Tomoya Nakamura¹, Naomichi Ogihara¹, Takeo Nagura², Toshiyasu Nakamura² and Masahiro Jinzaki²

¹Department of Mechanical Engineering, Keio University, Yokohama, Japan; ²School of Medicine, Keio University, Tokyo, Japan.

Human walking is a mechanical phenomenon to move the center of body mass forward by appropriately generating the ground reaction forces onto the foot. It is therefore anticipated that mechanical characteristics of the human foot embedded in its anatomical design may greatly contribute to realize appropriate mechanical interactions between the body and the ground to facilitate generation of robust bipedal walking. In the present study, we developed a three-dimensional, anatomically detailed finite element model of the human foot in order to investigate how the anatomical design affect the way the human foot mechanically interacts with the ground. Each bone and the whole foot surfaces were extracted from computer tomography images of a human foot. The volume enclosed by each surface was meshed with tetrahedral elements. The bones were represented as a linear elastic material, and the encapsulated soft tissue was defined as a hyperelastic Ogden material. Ligaments and plantar fascia were represented by tension-only spring elements. The foot-ground contact was modeled using rigid contact surfaces. In the present study, the mechanical interactions of the foot and the ground during balanced standing were simulated by applying compressive force on the tibia and Achilles tendon force generated due to muscle contraction. Calculated plantar pressure distribution was similar to an experimentally measured pressure distribution. Using the foot model, we assessed how arthrodesis of the subtalar joint affects the mechanical interaction of the human foot with the ground. Our results demonstrated that the calcaneus was more inverted with respect to the talus and the medial longitudinal arch was more flattened because of presence of the subtalar joint. The present simulation framework can be used to clarify morpho-functional relationships between the human foot architecture and human bipedal walking.

ID: 479

PO-03: 33

A novel evaluation methodology of materials for medical devices based on molecular dynamics simulation

Miyuki Uematsu¹, Yuji Haishima¹, Ryusuke Nakaoka¹, Shingo Niimi¹, Katsunori Segawa² and Tatsuya Nakano²

¹Division of Medical Devices, National Institute of Health Sciences, Japan; ²Division of Medicinal Safety Science, National Institute of Health Sciences, Japan.

As known by recent works, many biocompatible materials contain intermediate waters. It could lead drastic cutbacks of the risk assessment process in biomaterial development by estimating the existence of intermediate waters in them utilizing a computer simulation. In this presentation, we will show results of the behavior analysis of water at biointerface of biomaterials and the validation of analyzed intermediate water by nuclear magnetic resonance spectroscopy (NMR).

Poly (2-methoxyethyl acrylate) (PMEA) is selected as the first sample of our examination since it has been reports to show good blood compatibility and contain intermediate water, which is observed by in-situ attenuated total reflection infrared spectroscopy, differential scanning calorimetry. Materials Studio (Accelrys, Inc.) was used for the simulation as follows. Firstly, adsorption energies of water were compared between oxygen atoms of three-pattern functional groups: methoxy oxygen, ester-linked carbonyl oxygen, and ester-linked oxygen. Secondly, water was placed under saturated conditions for PMEA. Finally, molecular dynamics simulation was performed for its model to calculate radial distribution function and diffusion coefficient of water in the stabilized situation. And it was attempted to capture the location of intermediate water by NMR as well.

In the simulation, some water molecules were tended to exist around the methoxy oxygens, and its adsorption energy was the most stabled among three cases. It was indicated that water behavior changes depending on the distance from the oxygens of its material, and intermediate water was situated at the 8-9 angstrom from methoxy oxygen in PMEA. By NMR measurement, water was observed around the methoxy oxygens, expected to be intermediate water.

It is concluded that intermediate water at the biointerface can be estimated by the simulation. In the future, it would be expected to reduce time for development of a new biomaterial and its practical use for medical devices.

ID: 485

PO-03: 34

Particle swarm-based vertebrae spine modelling for steering vibration impact analysis

Siti Fauziah Toha

International Islamic University Malaysia, Malaysia.

Vibrations due to steering motions always gave direct vertical impact towards human vertebrae spine. A lot of studies are carried by various researchers in this field, evaluating the injury risks to vertebrae when it exposed to vertical vibration. One of the major risks associated is low back pain which accounts to major economic loss in terms of direct and indirect costs. Therefore, an accurate vertebrae modelling is of prime important for vibration suppression analysis. The white-box model of the vertebrae is obtained using Rayleigh beam element, which account for bending and rotary inertia. Followed by the muscle strength and the inter-vertebrae fluid are represented by a spring damper system. The objective of this paper is to apply a grey-box modelling approach to model the dynamic behaviour of human vertebrae. The conjecture is that the white-box model will retain what is known about the physical behaviour of the vertebrae using mathematical modelling. The black-box modelling using particle swarm optimisation (PSO) will then use the input and output information from the white-box model to obtain an accurate transfer function parameters. In order to increase robustness to the model, effects of phenomena that are not modelled in the white-box model such as vehicle speed variation is included. The grey-box model is therefore yield an accurate model of the human vertebrae which is suitable for further investigation using active vibration suppression control. Correlation tests are carried out to determine the effectiveness of the modelling technique. It is evidence that the model complies with all the five correlation tests, indicating that the model behaviour is unbiased.

ID: 487

PO-03: 35

Towards tracking breast tumours using biomechanical models

Prasad Babarenda Gamage Thiranjai¹, Angela Lee², Duane Malcolm¹, Christopher Patrick Bradley¹, Poul Michael Fønss Nielsen³ and Peter Nash Martyn³

¹Auckland Bioengineering Institute, The University of Auckland; ²Biomedical Engineering, Division of Imaging Sciences, King's College London, UK; ³Auckland Bioengineering Institute, Department of Engineering Science, The University of Auckland.

Breast cancer is the most common cancer in women worldwide, and each year 400,000 women die from

the disease. A combination of x-ray mammography, ultrasound (US) and MR imaging is used for diagnosis, however, co-locating regions of interest between these images remains a challenge due to large deformations and different loading conditions imposed during imaging (up to 75% breast compression with mammography, surface indentation with a US probe while supine and gravity induced stretching of tissue while prone during MRI). When a tumor is detected, its location needs to be determined during radiation treatment or for its surgical removal which is also a challenge as these procedures are usually performed in a different position than during diagnostic imaging. Patient-specific biomechanical models of the breast can potentially be used to address these challenges by simulating tissue deformation during imaging to aid tumour co-location, while providing the ability to predict tumour location during treatment. Due to large deformation occurring during breast repositioning, the success of these simulations is critically dependent on the application of suitable boundary constraints to the models. Existing FE models only consider either a sliding or fixed constraints between the ribcage and pectoral muscle. This study investigates whether inclusion of a sliding interface between the pectoral muscle and the breast tissue in the retromammary space can further improve the models ability to track tumours. This is of importance as studies have shown that a large proportion of tumours are located near this interface. The hypothesis was tested by simulating prone to supine repositioning of the breast with models being created from prone MR images which are subsequently warped to supine using the resulting deformation field. These model predicted supine MR images are then registered to actual supine MR images using 3D image cross-correlation, allowing the improvement to be quantified.

ID: 495

PO-03: 36

The constraint effect on the ultracongruent polyethylene insert by FEM

Tsung-Wei Chang¹, Cheng-Kuang Lu² and Jiann-Jong Liao³

¹United orthopedic corporation, Taiwan; ²United orthopedic corporation, Taiwan; ³United orthopedic corporation, Taiwan.

The treatment of pain and disability of knee with PCL sacrifice designs of total knee arthroplasty has popularity in recent years. The insert could address the more specific needs of the young and active patients suffering of severe knee osteoarthritis. The insert is an ultracongruent polyethylene (UP) design, cruciate-sacrifice total knee arthroplasty with a fixed bearing, was designed and expected to significantly highly conforming anterior buildup to increase surface area

contact with the femoral component throughout full ROM. The purpose of this study was to investigate and compared the effect of constraint of this new inset with the tradition widespread TKA by FEM. The three-dimensional dynamic FE model utilized in this study consisted of a distal femoral component and tibial baseplate with UP insert and CR insert. Tibio-femoral contact was defined in the model and non-linear elastic-plastic material properties were used to the polyethylene model. A compressive load of 710 N was applied along the long axis of the femoral component and through the lowest point of the condyle. Three different forces, AP load, ML load and IE torque, were applied on tibial baseplate on three different models, respectively. The results of UP insert showed that the AP and ML displacement were nearly 50% and 43% of the results of CR insert, respectively. The UP insert design allows about 6° rotation freedom of the femur on the tibial component which was smaller than CR insert. The current study confirms that UP insert has more constraint and eliminate box cut with the PCL substituting design may be attributed to the benefits of mechanical substitution of the function of the PCL. The result from this investigation support the use of an ultracongruent insert as a viable alternative in primary and revision TKA surgery.

ID: 503

PO-03: 37

Evolutionary low frequency steering vibration control towards human spine

Siti Fauziah Toha

International Islamic University Malaysia, Malaysia.

This paper demonstrated a simulation study of an active vibration control using particle-swarm optimisation based proportional, integral and derivative (PSO-PID) control scheme to suppress steering vibration towards human vertebrae impact. The vertebrae dynamic model is identified based on grey-box modelling technique. This technique combines physical behaviour information of the spine via mathematical model and robust black-box model of the spine with added vehicle speed variation. The performance of PID-PSO control scheme is validated and compared with the conventional PID control scheme. PSO falls under the umbrella of evolutionary algorithms which is used to optimise and tune the PID controller parameters (K_p , K_i and K_d) based on a predefined performance index. The main objective is to minimise the mean square error (MSE) of the vibration signal. The optimum PSO-PID parameters are then used to suppress vibration induced by steering vehicles to the spine. This study showed that PSO-PID is better tuned than the conventional tuning method in terms of transient response.

ID: 513

PO-03: 38

Evaluation of blood velocity waveform features in common carotid artery for healthy subjects and cardiovascular patients

Muhamad Saleh¹, Azran Azhim¹, Zulaika Hamdon¹, Pouya Bagherpour¹, Yohsuke Kinouchi² and Fatimah Ibrahim³

¹Universiti Teknologi Malaysia, Kuala Lumpur, Malaysia;
²University of Tokushima, Japan; ³Universiti Malaya, Kuala Lumpur, Malaysia.

Blood flow velocity (BFV) provides the crucial hemodynamics data to diagnose, predict and manage cardiovascular disease including hypertension. The aim of the present study is to investigate the usefulness of envelope waveforms of BFV and its indices in the common carotid artery (CCA) by comparing it between two groups; cardiovascular patient and healthy normal subject. Data are selected to statistically analyze from normal subject (n=202, age range: 20-69) and cardiovascular patient (n=41, mean age: 68.95±10.99). A t-test is used to determine age effect on the normal subject. Multivariate analysis is used to determine the correlation of multiple BFV indices with age. In the healthy subjects, there are negative correlation of resistive index (RI) and vascular elasticity index (VEI), whereas positive correlation of velocity reflection index (VRI) with age (p<0.001). For further analysis, fifty-two healthy subjects were selected from healthy group (age mean: 57.12±4.50) as control after matching their age with cardiovascular patient group. After testing the normality of data, a Student's t-test is used to determine BFV waveform and its indices in the two groups. In the study, we found that there are significant difference of BFV and indices in cardiovascular patients and normal subjects after controlling the age and gender. In conclusion, the potential of BFV and its indices is confirmed to be used as a reference data for health-care application and clinical implications.

ID: 541

PO-03: 39

Foot loading in diabetic patients with the fifth toe deformity

Jiabing Ma and Yaodong Gu

Ningbo University, China.

The purpose of this study was to quantitatively assess plantar pressure associations with toe deformed diabetic patients. Six neuropathic diabetic subjects with the fifth toe deformity, and six age and gender matched neuropathic diabetic controls without deformity, were examined. Dynamic barefoot plantar pressures were measured with pressure platform. Peak pressure and pressure-time integral for

each of 7 foot regions were calculated. Peak pressure was significantly higher in the patients with toe deformity at heel, hallux, and other toes regions, when compared with controls. Diabetic subject with toe deformity could cause plantar contact area, pressure and gravity center variety. It shall attach importance to toe deformity situation, because it highly associated with ulcer risk especially in hallux region.

ID: 547

PO-03: 40

Stress analysis of femoral abduction osteotomy for osteoarthritis of the hip

Masaki Nakao, Rina Sakai and Kiyoshi Mabuchi

Kitasato, Japan.

Introduction: It was generally accepted that mechanical stress must be the important factor that influences the osteoarthritis. Some kinds of osteotomy, which can improve the stress distribution, are used for the surgical treatments [1]. In this study, it was shown that the stress distribution measured on model bone or analyzed by the finite element method was improved by the combined effects of Chiari pelvic osteotomy and abduction osteotomy of a femur.

Materials and method: Model bone was made by sodium chloride. That shape was followed three dimensional CT image of the hip before and after osteotomy performed for the treatment of osteoarthritis. Six model bones were formed preoperative shape and the other six were formed postoperative shape. The model bone was loaded 500N in a loading apparatus. The contact stress between the acetabulum and the femoral head was detected by a tactile sensor. Surface configuration of the model bone was digitized from the CT image by an image processing software. Tetrahedral elements, which number was about 40000 are generated. Analysis hardware was a workstation. The solver was nonlinear dynamic finite element analysis system .

On the preoperative models, the maximum stress was measured 18.0±1.9 MPa. On the postoperative models, the maximum stress was measured 6.0±3.0 MPa. The maximum stress of preoperative models were significantly higher than of postoperative models.

Discussion: In the present study, it was shown by mechanical tests on model bone together with the finite element analysis that the maximum stress was significantly lowered by the combined treatment of Chiari pelvic osteotomy with abduction osteotomy of a femur. This osteotomy must be useful because of

the dispersing effect of the high stress on the deformed hip.

ID: 560

PO-03: 41

The kinematic characteristic study on pupils walk with Heelys

Qiner Qiu, X. F. Feng and Y. D. Gu

Ningbo University, China.

Objective: The purpose of this study was to compare the gait between primary school students walking with sneakers and Heelys. Kinematic indexes were gathered when pupils wore sneakers, closed-wheel Heelys (CWH) and open-wheel Heelys (OWH).

Methods: A high-speed camera was used in this experiment to shoot the children's gait at sideline when they were walking in the three kinds of condition. Step length, stride frequency, walking velocity and landing angle were chosen as indexes in normal walking to analysis.

Conclusions: Statistics showed that wearing sneakers had the longest step length while the shortest with OWH. Stride frequency, walking velocity, landing angle presented a decreasing trend after wore sneakers, CWH and OWH. Significant different ($P < 0.01$) was all found in step length, stride frequency, walking velocity and landing angle.

ID: 564

PO-03: 42

Evaluation of range of motion of a novel artificial hip joint

Shan Wei^{1,2}, Yanping Lin¹, Dongmei Wang¹, Yuanchao Li¹, Hai Zhou¹ and Chengtao Wang¹

¹School of Mechanical Engineering, Shanghai Jiao Tong University, China; ²School of Mechanical and Automotive Engineering, Anhui Polytechnic University, China.

In Total Hip Arthroplasty, the existing ceramic-on-ceramic hip joint could not match with a large range of motion of Asian populations in the daily activities, such as sitting cross-legged, squatting and kneeling, which frequently induces dislocation of the artificial hip joint. This research proposed a novel artificial hip joint in which the ceramic acetabular liner was discretely designed. The new type of ceramic-on-ceramic hip joint included one porous metal acetabular backing, several cylindrical ceramic components, one Ti alloy bracket with several discretely distributed holes, and ceramic femoral head. This novel design changed the existing monolithic acetabular liner with the wall thickness of 8–10mm to the

several discrete cylindrical ceramic components with that of 2.5mm. Several discrete ceramic components were embedded in the bracket. Range of motion of the prosthesis was simulated using self-developed software (CMVH-HiDi) and was compared with that of the existing hip joint with femoral head diameter from 28mm to 32mm. The simulated data indicated that this novel hip joint prosthesis effectively reduced wall thickness of the existing acetabular liner, while the diameter of the existing artificial femoral head can be increased to 45mm, the size of nature femoral head for Asian populations. Compared with that of the clinically widespread hip joint, flexion/extension of this novel hip joint prosthesis distinguishingly increased, while abduction/adduction and external rotation/internal rotation had no significant change with the same head/neck ratio. The results demonstrated that this design met the requirement of the large range of motion for the Asian populations in the daily lives.

ID: 587

PO-03: 43

An investigation of gastrointestinal and cardiac sodium channelopathy

Yong Cheng Poh^{1,2} and Martin Buist^{1,2}

¹National University of Singapore; ²NUS Graduate School for Integrative Sciences and Engineering.

Motility cell-types found in the gastrointestinal tract and in the heart share the same SCN5A encoded sodium channels. Studies have demonstrated that SCN5A channels serve electrophysiological functions in these systems and affect their motility. A novel G298S mutation of the SCN5A channel was found in a patient with irritable bowel syndrome. A study investigated the G298S SCN5A channels in HEK expression systems, which revealed functional consequences of the mutation on channel behaviour. However, the effects of G298S mutation in native gastrointestinal and cardiac cells are still unknown.

To understand this, the G298S mutation was investigated computationally. Computer models describing the wild-type and G298S SCN5A channels were developed and validated based on HEK experimental data. Additionally, common SCN5A isoforms arising from polymorphism and alternative splicing were also described in these models. The SCN5A models were integrated into biophysical motility cellular models of the gastrointestinal and cardiac systems, and subjected to various simulation protocols to examine the functional consequences of the mutation and the isoforms, if any. Key characteristics of cellular behaviour that may indicate mutation impact include amplitude, frequency, resting potentials, and upstroke rate of the electrical waves.

Preliminary results showed that the G298S mutation was able to reduce sodium current density in the gastrointestinal cells, and therefore agreeing with experimental observations. The mutation in the most common SCN5A isoform caused hyperpolarization of the gastrointestinal smooth muscle cell membrane potential, while no observable change was noted in the gastrointestinal pacemaker cells. In the cardiac system, the mutation appeared to delay repolarization and reduce peak potentials in ventricular cells. Future work is required to extend the findings here, to determine concretely the consequences of the G298S mutation, and how isoforms due to alternative splicing and polymorphism modulate channel and cellular behaviour.

ID: 592

PO-03: 44

Bitter taste mediated calcium signaling in enteroendocrine cells

Zhinuo Wang¹, Edward Walker², [Vinod Suresh](#)¹ and John Ingram²

¹The University of Auckland, New Zealand; ²Plant & Food Research Ltd, New Zealand.

The T2R family of bitter taste receptors is expressed in enteroendocrine cells of the gastrointestinal tract where they modulate gastric emptying and satiety. This functionality is mediated by calcium signalling leading to the secretion of hormones involved in nutrient sensing, satiety and the control of gastrointestinal motility. In this work we present a mathematical model of calcium signalling in the HuTu 80 model of enteroendocrine cells. The model is based upon a previous description of calcium dynamics initiated by G-protein coupled receptors. It incorporates the kinetics of ligand binding; G-protein activation, inactivation and recycling; inositol triphosphate (IP3) production and degradation; calcium release from the endoplasmic reticulum and describes intracellular calcium dynamics upon exposure to bitter ligands. Model parameters were determined by fitting predictions to fluorescent measurements of intracellular calcium concentrations in HuTu 80 cells in response to chlorhexidine stimulation. Experimentally measured calcium dynamics exhibited a slow rise time and sustained response. The rise time and steady state response were dose dependent. The model was able to reproduce these features when ligand-receptor affinity and the activation/inactivation rates of the G-protein were low.

ID: 608

PO-03: 45

An efficient partial shape matching algorithm for 3D teeth recognition

[Zhiyuan Zhang](#), Xin Zhong, Sim Heng Ong and Kelvin Weng Chiong Foong

National University of Singapore, Singapore.

As a new biometric strategy, tooth recognition has drawn much attention in recent years. However, most existing work focus mainly on 2D dental radiographs which are less informative and vulnerable to noise and pose variance. Although there are already several attempts on 3D tooth recognition, the results are still inaccurate and performance is inefficient. Moreover, existing methods cannot recognize precisely when the post-mortem data contains incomplete teeth. In this work, we propose an efficient and accurate partial shape matching algorithm to recognize 3D teeth for human identification. Given the ante-mortem and post-mortem teeth models which were taken from patients using a laser scanner, we first extract a series of stable and consistent feature points on the surface of 3D teeth models using a sparse feature selection method based on the saliency map. For each feature point we then establish descriptor based on Improved Spin Images (ISI), which is able to accurately describe the local region around the feature points. Due to the small number of feature points, their correspondences can be efficiently found via the ISI descriptors. Finally, the similarity of the teeth of two input samples (ante-mortem and post-mortem data) can be determined by the sum of the distances between the corresponding ISI descriptors of the feature points. We also conduct experiments to show that the proposed method can achieve state-of-art performance for both complete and incomplete post-mortem teeth data.

ID: 635

PO-03: 46

Effect of exercise intervention and foot load changes on foot arch evaluation using foot pressure distribution data

[Kazuuya Imaizumi](#), Yumi Iwakami and Kazuhiko Yamashita

Tokyo Healthcare University, Japan.

The foot arch serves important functions in regard to shock absorption and the action of walking. Simple and quantitative classification of foot arch types such as flat foot and high arch would be helpful in health support for the elderly. The present authors have developed a classification system for foot arch type showing high reliability using foot pressure distribution data. However, effect of exercise intervention and foot load changes on foot arch evaluation using foot pressure distribution data remain unclear. The

aim of this study was to investigate the effect of exercise intervention and foot load changes on foot arch evaluation using foot pressure distribution data.

We conducted 2 field tests involving elderly individuals. 1) To investigate the effect of intervention in the elderly, foot pressure distribution data were measured before and after 12 week exercise intervention. We analyzed data from 14 elderly female individuals who had attended both the first and last sessions. 2) To investigate the load deformation characteristics of the foot arch by foot pressure distribution, foot pressure distribution data from 44 elderly were obtained by field test with elderly subjects standing on 1 leg and 2 legs.

Our results demonstrated that exercise intervention including foot care can improve foot arch function, and that these changes can be evaluated by foot pressure distribution data. From evaluation of tests involving bilateral and unilateral stance, it was suggested that that foot pressure distribution data can reflect load deformation characteristics and thus be used for evaluation. The subjects of this study were healthy and elderly, and more than half had a foot arch problem such as flat foot or high arch. Therefore, an evaluation system for foot type is considered very important in health support for the elderly.

ID: 645

PO-03: 47

A method maybe simulate eye-movements of eye disease

He Huang and Ji Wei

Jiangxi Science & Technology Normal University, China.

Eye-movements research is an interested subject for many areas researchers such as medical, physiology or robot vision. In previous studies about mathematical analysis and modeling of eye movements, the normal eye-movements were always mentioned, such as saccade, smooth pursuit, optokinetic reflex and vestibulo-ocular reflex (VOR). This paper describes a simple mathematical VOR model which is composed of components corresponding with the eye-movement nucleus and neural pathway. The model is used for understanding an physiology experimental of VOR in control technology. By comparing the result of the simulation and the physiology experiment, we think it is possible that calculate the trajectory of eye-movement in real-time, even pathologies associated oculomotor nerve. Also, it is an indirect proof of the validity of the eye-movements mathematics model.

ID: 647

PO-03: 48

Stress distribution in various fixation configurations of bilateral sagittal split osteotomy

Li-Ren Chang^{1,2}, Lain-Chyr Hwang¹, Ming-Hong Kao¹, Chih-Yu Chen² and Ting-Sheng Lin¹

¹*I-Shou University, Taiwan;* ²*E-Da Hospital, Kaohsiung, Taiwan.*

Bilateral sagittal split osteotomy (BSSO) is a common orthognathic surgery for the correction of dentofacial deformities. Many researches showed that the fixation type remained determinative for the prognosis of BSSO. The objective of this study was to investigate the stress distributions in three fixation configurations (straight miniplate, short miniplate and lag screws) of BSSO by finite element analysis. The mandible solid model was reconstructed from serial computer tomographic images and various fixation systems were assembled according to clinical suggestions. The geometry of the miniplate was referred to commercialized product (COMPACT 2.0 MF Internal Fixation System, Synthes). After the mesh models were generated, the occlusal muscle forces were applied, including masseter, temporalis and pterygoid. All modes were fixed in mandible condyle region. The von Mises stress distributions were observed to evaluate the stability of the three fixation configurations. The results showed that the greatest bone stress adjacent to the fixation screws was found in straight miniplate fixation than the other two fixations. The stress value exceeded the tensile strength of the cortical bone which might lead to screw loosening. Although the bicortical lag screw fixation revealed the best stability among these models, there are still some complications in clinical application. Short plate fixation showed similar stability with straight miniplate and might decrease the risk in surgery.

ID: 648

PO-03: 49

3D Numerical study of red blood cell doublet aggregation behaviour in shear flows

Swe Soe Ye, Meongkeun Ju and Sangho Kim

National University of Singapore, Singapore.

In this study, we investigated the dynamics of a red blood cell (RBC) doublet under shear flow. Previous studies have established that most aggregates in blood flow consist of RBC doublet-pairs and thus the aggregation interaction in a doublet has significant contribution to the overall hemodynamics of blood in microcirculatory flows. Subsequently, it has been found from our previous two-dimensional study that the RBC aggregation tendency can be significantly affected by the cell's deformability which can vary

significantly within a cell population. Due to the limited deformation and interaction freedoms represented on a two-dimensional model, the quantitative aspect of the doublet study was extended to the present three-dimensional model where a more realistic model of the doublet dynamic was constructed. To address the three-dimensional deformation behaviour of the RBC under fluidic and cell-cell interaction, the RBC membrane was discretized by a set of spring and nodes in our spring mesh membrane model where the constitutive shear, bending and area incompressibility behaviour of the physiological RBC membrane was employed to obtain the internal stresses in the RBC membrane in response to its deformation. The interaction between the pairing RBCs was simulated with our depletion theory based aggregation model using the Morse type potential function. In the final component of the computational model, the fluid-structure interaction between RBC and suspending fluid was achieved by coupling the lattice Boltzmann fluid solver with the spring mesh membrane model through the immersed boundary method. In order to capture the doublet aggregation-dissociation phenomena, we conducted the simple shear simulation in the physiologically observed range of aggregate dissociation behaviour (50 s^{-1} to 100 s^{-1}). Consequently, the three-dimensional model simulation study results confirm our major finding from the two-dimensional model study, predicting favourable RBC dissociation with an increased heterogeneity in the RBC-pair deformability.

ID: 649

PO-03: 50

The prediction of walking activity in differential sport surfaces by 3D inertial measure units

Yi-cheng Chen, Bo-Ying Chen and Chuang-Bin Tu

Graduate Institute of Sports Equipment Technology,
Taipei Physical Education College, Taiwan.

The main purpose of this project is used 2 sets 3D inertial measure units to predict the walking physical activity in different sports surfaces. Methods: Twelve healthy young adults, with 2 sets 3D-of-freedom inertial measure units on knee and ankle, were randomly walking on four different sport surfaces which were synthetic rubber, artificial grass, sand and wooden surfaces that were testing the force reductions by Berlin Artificial Athlete (EN14808). Time domain and power spectral density of ankle and knee accelerations were analyzed. Univariate ANOVA was used to test for differences among the participants in all four sport surfaces for same walking speed by SPSS v12. Results: The force reductions of different surfaces were sand (83.38%) > wooden floor (51.01%) > artificial grass (42.14%) > synthetic rubber (38.05%). The

effects of walking speed on different surfaces were non-significantly. The acceleration ratios and power spectral density of ankle-knee were non-significantly. Finally, in the path analysis, we found the model of ratio (x) of time domain and power spectral density (y) of ankle and knee accelerations is $y = -9.1962x^3 + 43.906x^2 - 67.512x + 35.019$, $R^2 = 1$. Next step, we want to prove the reliability of the walking model.

Acknowledgement: The authors would like to acknowledge Taiwan National Science Council (NSC100-2410-H-154-004) to provide the funding.

ID: 653

PO-03: 51

Effects of swing and ball velocities by different aluminum softball bats

Hong-Sheng Tsai and Yi-cheng Chen

Graduate Institute of Sports Equipment Technology, Taipei
Physical Education College, Taiwan.

Aluminum bat is characterized by lighter materials, more elastic benefit more the players swing speed and batting. But, what's difference after different alloy compositions aluminum bat hitting? This study investigated the effects of swing and ball velocities using softball bat made with differential aluminum materials.

Methods: The 20 male and right hit baseball players. Aluminum alloys components using different numbers 7250, 7150, 6061 for five balls hitting each test. The home plate sets a high-speed photography by CASIO ZR-200, and shooting frequency was 480 Hz. The image analyses were using 2D motion software Silicon Coach V.7. Totally, every three best bats for any testing will analyze the velocity of before and after bat swing hitting, the velocity of hit ball, and the reduction values of bat swing. The statistics using SPSS 18 version, measured one-way ANOVA and LSD post-hoc comparison when results have significantly different, significance value $\alpha = .05$.

Results: Each aluminum bat of the velocity of bat swing before hitting is not significant, and the velocity of bat swing after hitting is not significant. Then the velocity of ball hitting is significant ($p = .010$), it's ball velocity (BV) were $BV_{6061} > BV_{7150} > BV_{7250}$. Before and after batting the bat swing velocity reduction values (BSVR) is reached significant ($p = .043$), respectively $BSVR_{6061} > BSVR_{7150} > BSVR_{7250}$. The velocity of ball hitting and the bat swing velocity reduction values are positively correlated. The higher BSVR, the faster hit ball.

Conclusion: The velocity of ball and the bat swing velocity reduction values were positively correlated

results similar with the previous studies, In addition, batting the difference between static and dynamic sphere caused the bat swing velocity reduction values of this study showed slightly lower of the phenomenon.

Acknowledgements: The authors would like to acknowledge Taiwan National Science Council (NSC100-2622-H-154-001-CC3) to provide the funding.

ID: 655

PO-03: 52

Accurate measurement of the kinematics of the knee during cycling exercise using a 3D fluoroscopy method

Shih-Wun Hong¹, Tung-Wu Lu^{1,2}, Cheng-Chung Lin¹, Jia-Da Li¹, Yu-Huan Wu¹, Yen-Hung Liu^{1,3}, Mei-Ying Kuo⁴ and Horng-Chaung Hsu⁵

¹Institute of Biomedical Engineering, National Taiwan University, Taiwan; ²Department of Orthopaedic Surgery, School of Medicine, National Taiwan University, Taiwan; ³Department of Physical Therapy, Tzu Hui Institute of Technology, Taiwan; ⁴School of Physical Therapy, China Medical University, Taiwan; ⁵Department of Orthopaedics, China Medical University Hospital, Taichung, Taiwan.

Introduction: Cycling exercises have been used in the rehabilitation of the lower extremities especially in patients with cruciate ligament injuries or reconstruction. Knowledge of the kinematics of the knee under different pedaling patterns may help develop injury-specific cycling exercises to reduce the risk of overuse injuries and to improve the recovery rate. Therefore, the current study aimed to measure the 3D skeletal kinematics of the knee during cycling using a 3D fluoroscopy method under different pedaling patterns.

Methods: Eleven healthy young adults wearing 14 markers on the right lower limb performed cycling exercises on an ergometer with the feet placed on the pedals at neutral position, 10 degrees of inversion, and 10 degrees of internal rotation while the skeletal motions of the knee were imaged by a fluoroscopy system (ALLURA XPER FD, Philips). The knees of the subjects were also CT scanned and used to construct CT-based bone models, which were then registered to the fluoroscopy images using a fluoroscopy-to-CT registration method, giving the rotations, translations and articular contact kinematics of the knee. A one-way analysis of variance was used to analyze the effects of pedaling patterns on each of the variables ($\alpha=.05$).

Results and Discussion: Accurate 3D skeletal kinematics of the knee during cycling was measured for first time in the literature. Significantly increased

knee flexion was found in cycling exercises with the foot internal rotated. Significantly decreased contact areas of the knee in both medial and lateral compartments were found in the conditions of inverted or internal rotated foot placement. Decreased contact areas associated with inadequate foot placement may lead to abnormal pressure distributions in the articular surfaces during cycling, which may be a risk factor of failure of the knee articular cartilage.

ID: 659

PO-03: 53

Effect of extracellular matrix proteins on fluid shear stress-mediated stem cell differentiation

Surabhi Sonam and Chwee Teck Lim

Mechanobiology Institute, National University of Singapore, Singapore.

Previous studies show that stem cells growing on individual extracellular matrix proteins (ECM) proteins follow different lineages. Different integrin molecules attach to different ECM proteins and in turn activate differentiation pathways. However, under the effects of mechanical loading, differentiation patterns followed by cells seeded on different ECM proteins has not been well understood. Here, human Mesenchymal Stem Cells (hMSCs) were subjected to fluid shear stress (FSS) while growing on different ECM proteins: collagen, fibronectin and laminin. Cells seeded on collagen or fibronectin coated channels showed increased cell contractility with time. However, no change in contractility was observed in those seeded on laminin. Presence of osteogenic marker, osteopontin, showed that the cells followed osteogenic lineage on collagen and fibronectin but not on laminin. The cells also spread more on collagen and fibronectin than that on laminin. This change in spreading area of the cells can modulate the contractility and cytoskeletal arrangement of the cell on different ECM proteins which may lead the cells towards different lineages. To better understand the phenomenon, cells will be grown on ECM patterns of different sizes to control the spreading area of the cells while being exposed to FSS. Also, cells will be subjected to FSS while growing on decellularised matrices obtained from rat bone tissue and fat tissue, which have different ECM compositions. This would allow the cells to grow on tissues with different stiffness allowing different spreading areas to the cells. This study focuses on elucidating the role of ECM proteins in shear stress-mediated stem cell differentiation.

ID: 662

PO-03: 54

Computational analysis of PEEK biomaterials in a novel orthopedic plate construct.

Jason Michael Sanderson, Nobuki Murayama and Yoshitaka Nakanishi

Kumamoto University, Japan.

The present study utilizes FEM analyses to compare an original long bone plate design containing polyetheretherketone (PEEK) biomaterials with standard titanium alloy plates to determine if a PEEK fracture plate can help reduce stress shielding frequently caused by standard plates. Fracture plates were designed and analyzed in Autodesk Inventor 2013®. Original plate design consists of carbon reinforced PEEK with non-connected, cylindrical, titanium reinforcements spanning the length and width of the plate. Standard plates were equivalent in dimension to PEEK plates but were made of only titanium alloy. Locking screws with threads along the shaft were also created in Inventor 2013®. An anatomically correct human tibia model from the VAHKUM database was used to create two bone fragments, proximal and distal, with an osteotomy at the center of the tibia shaft simulating a simple fracture. The construct was loaded in an anatomical manner with separate, unequal loads on the medial and lateral condyles, and fixed distally at the talocrural joint. Screw-plate contact conditions were defined as bonded to simulate locking screws, and screw-bone contacts were separation-no sliding to simulate the ability of the screw to pull away from but not slide along the bone-screw interface. Two different screw configurations, an all Ti-alloy screw set and a Ti-alloy with PEEK end-screw set, were analyzed with both plate types. The reinforced PEEK plate consisted of approximately 3.59 million nodes and 2.32 million elements, and the standard plate contained approximate 2.72 million nodes with 1.77 million elements. Results of the FEM analysis showed that the PEEK implants were successful in reducing stress shielding when compared to standard Ti-alloy plates.

ID: 664

PO-03: 55

Finite element analysis of mechanics about different fixations for greater tuberosity fractures of the humerus

Liu Hsin-Yi

National Cheng Kung University, Taiwan.

Suture anchors and screws are commonly used for fixation of humeral greater tuberosity (GT) fractures in either arthroscopic or open surgeries, and current biomechanical studies and clinical case reports

showed a comparable outcome by using suture anchor and screw fixation, but none of these studies have dealt with the stress concentration at the site of repair. The aim of this study was to investigate the biomechanical interactions of three different fixation constructs, using suture anchors or screws, for the management of greater tuberosity fractures.

Based on our previous biomechanical study and surgical guidance of greater tuberosity fracture reconstruction, three-dimensional finite element models consisted of proximal humerus, GT fragment, and different kinds of fixation techniques. Screw fixation, Suture bridge, Double-row and Single-row fixation were included in this comparison and the bone mineral density was considered.

The findings using FEA provide quantitative evidence to identify that the suture anchor fixations shows a better result than screw fixation in low mineral density. In addition, three techniques of suture anchor fixation showed comparable displacement in the same supraspinatus tendon loading: The displacement of GT fragment by using Single-row fixation is bigger than Double-row and Suture-bridge.

ID: 665

PO-03: 56

Mechanical and FEM analysis of the rectangle double lag-screw system

Yasuaki Matsumoto¹, Hiroshi Mizuta¹, Murayama Nobuki¹, Hildehiko Higaki² and Yoshitaka Nakanishi¹

¹*Kumamoto University, Japan;* ²*KYUSHU SANGYO University, Japan.*

Recently, the incidence of proximal femoral fracture in aging patients has been increasing. Femoral nails used for treatment are made mainly of titanium alloys. However, the elastic modulus of titanium alloy is very high when compared with that of bone. This cause healing inhibition due to stress-shielding, and fracture at the distal end of the stem. These complications concern many health care professionals. Moreover, discussion of the inhibition of femoral head rotation by the lag-screw has not been adequate. Redesign of the femoral nail is suggested to resolve these problems. The development of most orthopedic implants makes great use of mechanical testing and FEM analysis however each analysis method has its own advantages and disadvantages. In mechanical testing, real world results can be easily acquired but it is difficult to evaluate the conditions within the model. Additionally, in FEM analysis, physical models do not need to be created but results can change even when something as simple as boundary conditions are chosen incorrectly. By using a 3D-scanner, it is now easy to compare displacements of physical

models with CAD models. In this study, we performed mechanical testing and FEM analysis on a proposed a new femoral nail. The new femoral nail was found to reduce interfragmentary motion as well as femoral head cut-out when compared to the traditional nail. Displacement was large in mechanical testing and results of FEM analysis became similar to mechanical testing results when some boundary conditions were changed.

ID: 671

PO-03: 57

Biomechanical changes of the lower limb joints secondary to hallux valgus during gait

Kao-Shang Shih^{1,2}, Hui-Lien Chien³, Chu-Fen Chang^{3,4} and Tung-Wu Lu^{3,5}

¹Department of Orthopedic Surgery, Shin Kong Wu Ho-Su Memorial Hospital, Taipei, Taiwan; ²School of Medicine, Fu-Jen Catholic University, New Taipei City, Taiwan; ³Institute of Biomedical Engineering, National Taiwan University, Taipei, Taiwan; ⁴Department of Physical Therapy, Tzu-Chi University, Hua-Lien, Taiwan; ⁵Department of Orthopaedic Surgery, School of Medicine, National Taiwan University, Taipei, Taiwan.

Introduction: Hallux valgus (HV) is one of the most common foot pathologies in modern society, causing pain and altered kinematics not only in the foot but also at the other joints of the lower limb. For example, the presence of HV increases disability levels in women with knee osteoarthritis (OA) and has been connected to the development of knee OA. This study aimed to investigate the kinematic and kinetic changes of the lower limb joints in patients with bilateral HV during level walking.

Methods: Eleven patients with bilateral HV and 11 healthy controls walked while the kinematic and kinetic data were measured with a motion analysis system (Vicon, Oxford Metrics, U.K.) and two force plates (AMTI, U.S.A.). The joint angles and moments at toe-off and contralateral heel strike, contralateral toe-off were obtained and the distance between the center of pressure (COP) and center of the first metatarsophalangeal joint (MPJ) was calculated when the COP passed the line joining the 1st and 2nd MPJ. All the calculated variables were analyzed using independent t-test with a significance level of 0.05.

Results and Discussion: Patients with HV were found to shift their COP laterally away from the 1st MPJ, which helped unload the joint during late stance. Lateral shift of the COP in these patients appeared to be related to the reduced toe-out angles of the foot as a result of increased internal rotation of the hip. However, this strategy increased the abductor moments at the knee, an index closely correlated

with the medial load at the knee and a predictor of the onset and progression of medial OA. Early treatment of HV may be helpful not only to reduce the foot pain and deformity but also to prevent the potentially harmful loading at the knee, especially those with medial knee OA.

ID: 686

PO-03: 58

Comparison of anticipated and unanticipated vertical stop jump between college and high school female basketball players

Chia Lo Ho¹, Chia-Wei Chiu² and Yung-Shen Tsai³

¹Department and Graduate Institute of Physical Education and Health, Taipei Physical Education College, Taiwan; ²Department of Sports Sciences, Taipei Physical Education College, Taiwan; ³Graduate Institute of Sports Equipment Technology, Taipei Physical Education College, Taiwan.

Background: Previous data revealed that college female basketball players seem to have higher ACL injury rate compared to their high school counterparts. It is not clear whether there are differences in their movements that may result in this problem.

Aim: The purpose of this study was to investigate the differences in anticipated and unanticipated vertical stop-jump between college and high school female basketball players.

Methods: 17 female basketball players (10 college and 7 high school level) participated in this study. Each player performed 5 anticipated (AN) and 5 unanticipated (UN) vertical stop jumps in a random sequence. Lower extremity movements were captured by a 3D electromagnetic motion analysis system synchronized with a force plate. Kinematics data of knee and hip joint were analyzed at 3 time points [initial contact (IC), maximal knee joint angle (MKA), and peak posterior ground reaction force (PPGRF)]. Two-way ANOVA with mixed design was used for all data analysis.

Results: At IC, both groups had less hip flexion angle under UN condition compared to AN condition. In college level, hip abduction angle at IC was greater under UN condition.

At MKA, high school players had less knee abduction angle under UN condition compared to AN condition. Both groups had greater hip abduction angle under UN condition at MKA.

At PPGRF, both groups had less knee flexion angleless knee abduction angle and less hip flexion angle.

Conclusion: Differences in vertical stop jump movement were observed between anticipated and unanticipated conditions, but not between college and high school levels of the female players.

ID: 687

PO-03: 59

Comparison of three force-position hybrid control methods of a robot-based system for biomechanical testing of the knee joint

Chih-Chung Hu^{1,3}, Tung-Wu Lu^{1,2}, Hong-Jung Hsieh⁴, Mei-Ying Kuo⁵ and Chien-Chung Kuo⁶

¹Institute of Biomedical Engineering, National Taiwan University, Taiwan; ²Department of Orthopedic Surgery, School of Medicine, National Taiwan University, Taiwan; ³Department of Mechanical Engineering, Ming Chi University of Technology, Taipei, Taiwan; ⁴Department of Mechanical and Automation Engineering, Kao Yuan University, Kaohsiung, Taiwan; ⁵School of Physical Therapy, China Medical University, Taiwan; ⁶Department of Orthopaedics, China Medical University Hospital, Taipei, Taiwan.

Introduction: Robot-based joint testing systems have been used in the study of joint biomechanics over the last decades. These systems often perform laxity tests under a force-position hybrid control method, measuring the stiffness of one degree-of-freedom (DOF) of the joint while keeping the other DOF's free to move and of loads. However, no study has evaluated quantitatively the performance of this method and other alternatives. The current study aimed to bridge the gap.

Methods: A robot-based joint testing system (RJTS) was developed for the biomechanical testing of human joints using a commercial 6-DOF robot with a 6-DOF load-cell attached at the effector. The force-position hybrid control method and two alternative methods, namely force-position alternate control, and force-position hybrid control with force-moment control, were implemented on the RJTS and their performance was compared quantitatively on a human knee cadaver in terms of the stability, precision and the time required for an antero-posterior laxity test under a maximum force of 100N.

Results and Discussion: For a complete cycle of the antero-posterior laxity test, the time required for the force-position hybrid control method was significantly less than those of the other methods, but it had the worst precision. The proximo-distal force component did not appear smoothly controlled, showing several peaks throughout the cycle. For the other DOF's that should be kept free to move and of loads, the force-position hybrid control method also had the largest non-zero force-moment deviations among the

three methods, suggesting that it was the least stable method. From the results it appeared that the force-position hybrid control with force-moment control was the best in stability and precision although requiring a bit longer than the force-position hybrid control method. It is suggested that the force-position hybrid control with force-moment control be used in future biomechanical testing studies on human joints.

ID: 693

PO-03: 60

A constitutive model for the rheological behavior of sheep rumen digesta

Helen Liley¹, German Molano², Yacine Hemar¹, David Pacheco² and Vinod Suresh¹

¹The University of Auckland, New Zealand; ²AgResearch Limited, New Zealand.

In this work we used rheometer measurements to determine a non-Newtonian model describing the small strain rheology of rumen digesta. Rumen digesta were collected from three sheep fed ryegrass and subjected to small amplitude oscillatory shear testing on a rheometer using a parallel plate geometry at a constant strain rate of 1% and a frequency range from 0.01 Hz to 100 Hz. The digesta were found to exhibit shear thinning behavior that was well described by a power law model with a flow behavior index of approximately 0.05. The storage modulus and loss modulus were frequency dependent and exhibited a crossover in the frequency range 40–60 Hz. The Cox-Merz relationship was satisfied over a limited frequency range from 0.01 Hz to 0.1 Hz. Inter-animal and intra-animal variation in the measured quantities was found to be on the order of 20%.

ID: 720

PO-03: 61

Biomechanical properties and constitutive modeling of human ventricular myocardium

Gerhard Sommer¹, Michaela Schwarz², Andreas Schrieffl¹, Heimo Wolinski³, Sepp Kohlwein³, Christian Viertler⁴, Peter Regitnig⁴ and Gerhard Holzapfel¹

¹Institute of Biomechanics, Graz University of Technology, Austria; ²Division of Surgical Research, Department of Surgery, Medical University of Graz, Austria; ³Institute of Molecular Biosciences, University of Graz, Austria; ⁴Institute of Pathology, Medical University of Graz, Austria.

In the multidisciplinary field of heart research it is of utmost importance, for the description of phenomena such as mechano-electric feedback or heart wall thickening, to accurately identify the biomechanical properties of the myocardium. Hence, mechanical

characterization of the passive human myocardium will lead to a better understanding of the mechanical deformation of the heart during the cardiac cycle, and in particular, how diseased/ischemic regions can impair pumping ability.

Therefore, this study aims at determining biaxial tensile and triaxial shear properties of the passive human myocardium. Moreover, a combination of optical clearing and multi-photon microscopy was utilized to explore the 3D microstructure of the tissue. This novel combination of biaxial and shear testing, together with the investigation of the myocardial microstructure, yielded new innovative and essential information of the material properties to fulfill the short term goals of constructing realistic myocardial models. The used newly-developed structurally-based constitutive model showed the ability to give a good representation of both the biaxial tensile and the triaxial shear responses.

The material data from this study is intended to be used in numerical (Finite Element) simulations for better understanding of fundamental underlying ventricular mechanics, a step needed for the improvement of medical treatment of heart diseases.

ID: 760

PO-03: 62

Nanoscale architecture of cadherin-mediated cell-cell junction

Cristina Bertocchi¹, Talgat Sailov¹ and Pakorn Kanchanawong^{1,2}

¹MBI National University of Singapore; ²Department of Bioengineering National University of Singapore.

Cadherins are transmembrane glycoproteins that organize with other proteins into junction complexes which mediate Ca²⁺-dependent adherence between adjacent cells, and thus are of fundamental importance in the maintenance of tissue architecture. Perturbation in the expression or function of this complex results in loss of intercellular adhesion, with possible cell transformation and tumour progression. Recently, much progress has been made in understanding the interaction between the different components of this protein complex and how this cell-cell adhesion complex is deregulated in cancer cells. However, despite the central importance of such supramolecular complexes, their molecular organization remains unknown. Deciphering the molecular-scale organization of cadherin adhesion complexes requires determination of 3D distribution of specific proteins with accuracy matching their nanometer-length scale. In a recent study involving the iPALM system with photoactivatable fluorescent proteins, a spatial resolution of at least 15–20 nm in all 3-dimensions has been achieved to study the protein complex mediating cell-matrix adhesion.

Using the same imaging tools, we are investigating the nanoscale organization of key proteins within the cadherin-mediated adhesion complexes. To obtain super resolution of the adherence complex, we are creating a library of cell-cell junction proteins expression vectors fused with photoactivatable fluorescent proteins (such as EosFP). Furthermore, high spatial resolution requires optimal optical properties of the imaging sample, thus we are optimizing a planar system with cadherin-coated substrate for iPALM imaging. This will enable us to determine spatial organization of proteins within the complex and, importantly, how they interface with the cortical actin cytoskeleton. Here we show our full experimental strategy and some preliminary results.

ID: 770

PO-03: 63

Optimal sampling of stem cells from human exfoliated deciduous teeth: opening up resources

Kristal YQ Lau¹, Yew Choy Chew², Eng Lai Tan³, Annie Tay⁴ and Suan Phaik Khoo⁵

¹University of Queensland, Australia; ²Monash University, Malaysia; ³School of Pharmacy, International Medical University; ⁴Gleneagles Intan Hospital, Kuala Lumpur, Malaysia; ⁵School of Dentistry, International Medical University.

Introduction: A population of mesenchymal stem cells (MSC) obtained from exfoliated deciduous teeth (SHED) has been of interest in recent years. The clinico-histological relationship between the exfoliated teeth and their stem cell characteristics is an important factor in achieving optimal sampling for stem cell cultivation.

Aim: To determine the clinical and histological relationship between the MSC isolated from SHED and to identify optimal sampling factors.

Methods: A total of 56 exfoliated deciduous teeth were obtained together with their clinical features. MSC suspensions were isolated from dental pulp tissue by mechanical and enzymatic disaggregation, and subsequently expanded in tissue culture dishes. Viable cell lines were grouped as anterior teeth (n=6) and posterior teeth (n=5), and female (n=6) and male (n=4). MSCs were detected using STRO-1 antibody. T-test was used to calculate and compare the mean percentage of STRO-1+ cells between groups. The pattern of STRO-1+ expression from passage P3 to P10 was identified using Pearson Correlation. Propidium Iodide was used to analyse the cell cycle of STRO-1+ cells.

Results: The percentage of STRO-1+ cells obtained from females was lower (60.47%) than that obtained

from males (72.72%). Dental pulp of anterior teeth yielded a lower proportion of STRO-1+ cells (66.20%) compared to those from the posterior teeth (71.18%). These differences however, were not statistically significant. Most STRO-1+ cells (59.40%) were in the proliferative phase and two cell lines showed high STRO-1+ expression (> 90%) as far as P10.

Conclusion: Dental pulp tissue of exfoliated deciduous teeth can produce viable and proliferative MSCs regardless of donor's gender and the dental site they were obtained from. High STRO-1+ expression across the passage of cell lines showed that the isolated MSCs can self-renew. The resource pool for quality MSCs can be opened up for future use in clinical therapy.

ID: 777

PO-03: 64

Review on simulation and evaluation of intravascular prosthetic device using finite element method and computational fluid dynamics and application to simulate aneurysm formation

Vaibhavi A. Sonetha and Jayesh R. Bellare

Indian Institute of Technology (Mumbai), India.

This paper is a review of applications of finite element method (FEM) and computational fluid dynamics (CFD) to evaluate design and performance of intravascular prosthetic devices used clinically today. This study is focused on devices such as stents, flow diverters and heart valves. A stent is a device with mesh which is placed in stenosed blood vessels to overcome flow constriction. Vascular injury and restenosis are two major drawbacks with stenting treatment. Flow diverter is a mesh structure similar to a stent which is passed across the aneurysm neck to divert blood flow from the aneurysm, allowing it to occlude over time. This technique has proven successful in many challenging aneurysm cases, post treatment hemorrhage is a serious problem reported. Mechanical heart valve is placed into the heart to replace malfunction valve. Structural failure of these valves has been reported in many patients. Numerical simulation of such devices can provide important insights about their failure. Finite element method and computational fluid dynamics are the most popular simulation techniques used for this purpose. Many researchers have studied such simulations on these prosthetic devices. It includes modeling of stent to study its mechanical behavior, modeling of deployment and expansion of flow diverter, simulation of heart valve closure etc. Studies on biological condition simulation such as blood flow simulation in human aorta, multidimensional modeling of carotid artery blood flow etc. are also discussed

in brief. Similar simulations needs to be conducted on occlusion devices used for Ventricular Septal Defect, Patent Ductus Arteriosus, Atrial Septal Defect, Patent Foramen Ovale etc. to evaluate their performance and reduce their failure in future. We apply this for the first time to show ballooning of an aneurysm.

ID: 778

PO-03: 65

Detect negative event for depression tendency from web blogs

Chia-Ming Tung and Wen-Hsiang Lu

National Cheng Kung University, Taiwan.

Many negative events happened in short period of time would trigger depressive disorder. We categorized these negative events into four groups, which are Family, Study, Jobs, and Affection. In this paper, we try to identify negative event in the web blog posts through proposed Enhanced Event Extraction method that includes Enhanced Lexicon Feature, POS pattern, and event-emotion pair. Term frequency and length had been used to calculate importance score for a long negative term in Enhanced Lexicon Feature. In POS pattern, we combined multiple POS term as negative event pattern, such VC+Nh, VC+Na, P+VC. We also consider about the distance between event terms and emotion terms. If emotion terms could be labeled in a post, we could use distance relationship to find event around emotion term. Experimental results show that the accuracy rate of Enhanced Event Extraction method is 54.9%.

ID: 782

PO-03: 66

Investigation of mechanical load on proximal left anterior descending of coronary artery

Tadashi Yamamoto^{1,2}, Kiyotaka Iwasaki¹, Jun Arai¹, Katsumi Ohori² and Mitsuo Umezu¹

¹Waseda university, TWIns, Japan; ²Hokkaido Cardiovascular Hospital.

It is clinically recognized that percutaneous coronary intervention (PCI) treatment for proximal left anterior descending (LAD) artery disease is resulting in less satisfactory in comparison with other lesions. However, the reason has not yet clarified. The purpose of this study is to investigate the mechanical loading conditions in proximal LAD artery. This study hypothesized that the coronary artery is pre-stretched in the heart. In order to investigate the pre-stretched value, porcine heart was obtained from a local slaughterhouse. Two points were marked at coronary artery and its distance was measured.

Two-dimensional distances (L1) between the dots marked on vessel centerline were measured with digital microscope. The coronary artery was separated from the heart, the distance between the points was measured again (L2). Pre-stretched ratio was calculated as $(L1-L2) / L2 \times 100\%$. 101 consecutive patients of coronary CT were taken in Hokkaido Cardiovascular Hospital from September 2012 in order to investigate dynamic loads acting on coronary artery. The distance of proximal LAD artery was measured in diastolic phase (Ld) and systolic phase (Ls) from a stretch view taken from CT. Shortening ratio was defined as $(Ld-Ls) / Ld \times 100\%$. The twist angle was defined as a sum of the following two angles and measured in end-systolic and end-diastolic phase. One is the angle between the line connecting the centers of LAD and LCX, and the perpendicular line toward abdominal to dorsal. The other is the angle between the line connecting the centers of LAD and the first septal branch, and the perpendicular line. Twisting ratio was calculated as $\theta/Ld \times 100\%$. Results showed that the pre-stretched ratio was calculated to be $7.6 \pm 2.9\%$ (mean \pm SD) in porcine LAD artery. The length of proximal LAD artery of human coronary artery was $26.6 \pm 9.3\text{mm}$ (mean \pm SD). Shortening ratio was calculated to be $6.1 \pm 6.2\%$ (mean \pm SD). And the mean twisting ratio was calculated to be $0.6^\circ/\text{mm}$. This study revealed the pre-stretched value of proximal LAD artery due to restrain from the myocardium. Moreover shortening and twisting motions in proximal LAD artery were quantified.

accuracy of the system using cognitive actions is slightly above 80 percent. This technology is very useful for the disabled and elderly people as well as for those who work in dangerous environments.

ID: 831

PO-03: 67

Analysis of brain activity while performing cognitive actions to control a car

Humaira Nisar¹, Aamir Saeed Malik², Q. W. Yeoh¹,
H. C. Balasubramaniam¹ and W. T. Wei¹

¹Universiti Tunku Abdul Rahman, Department of Electronic Engineering, Kampar, Malaysia; ²Universiti Teknologi PETRONAS Neuro-Signal Processing Group, Tronoh, Malaysia.

In this paper we will present a real time brain computer interface system that operates a LEGO Mindstorms NXT car using the EEG signals produced by the electrical activity of brain. The brain signals are acquired using an EEG device and are translated into signals that can be understood by the NXT car. The NXT car moves according to the instructions provided. The experimental prototype uses an Emotiv EPOC headset that acquires data from 14 sensors to fully control the movement of a NXT Car. We have used the Cognitive states (intent of physical actions) and Expressive states (facial expressions) to control the NXT car. The system achieves more than 90 percent accuracy by using facial expressions however the

Author Index

A

Abdullah, Haslaile 178
Abe, Tadashi 179
Abelha, António 95
Abo, Masayoshi 66
Achenbach, Stephan 48
Adachi, Taiji 70, 137
Adam, Clayton J. 23
Adnan, Khadijah 190
Agrawal, Abhishek 47
Agrawal, Animesh 202
Agudelo, Carlos 25
Agulto, Verdad Canila 190
Ahmad, Azlina 8
Ahmed, Abdella 168
Aiso, Sadakazu 159
Akutagawa, Masatake 198
Akutsu, Toshinosuke 136, 205
Alexander, Cameron 93
Alm, Martin 36
Aloni, Yoav 23
Alvarado, Diego A. Garzon 98
Amin, Hafeez Ullah 177
Amis, Andrew 68
An, Ning 61
Anderson, D. G. 132
Andersson-Svahn, Helene 123
Ando, Joji 122
Andresen, Thomas Lars 126
Anene-Nzelu, Chukwuemeka George 124
Ang, Hengpei 190
Ang, Su-Shin 135
Ang, Suan Ping 76
Anitha, D. 83
Ankam, Soneela 70
Anon, Ester 86
Aoki, Takuya 179
Aomura, Shigeru 213
Arahira, Takaaki 193, 194
Arai, Jun 229
Araki, Jun 60
Araki, Tsutomu 91
Arianto, Eko 176
Arieshanti, Isye 34
Arisawa, Hiroaki 214
Arisawa, Junji 214
Armah, Nii Armah 10
Asada, H. Harry 139
Askin, Geoff N. 23
Asvestas, Pantelis 162
Atrisandi, Amirinnisa Dyah 176
Auephanwiriyakul, Sansanee 143

Augustynek, Martin 40, 175, 189
Aylott, Jonathan W. 93
Ayukawa, Yasunori 194
Azhim, Azran 131, 145, 219

B

BS, Syam 193
Babušiak, Branko 175
Bacabac, Romel G 180, 190
Bader, D. L. 203
Badir, Sabrina 73
Badri, Cholid 40
Badrudin, Nasreen 177
Bae, J. H. 158, 163, 212, 213
Baena, Ferdinando Rodriguez y 68, 129
Bagherpour, Pouya 131, 219
Baimpas, Nikolaos 106
Balasubramanium, H. C. 230
Bang, Dang Duong 199
Banks, H. Thomas 94
Barbastathis, George 91
Barraza, Luis Carlos Hernandez 54, 146
Bashir, Rashid 59
Baumgärtner, Moritz 62
Beard, Daniel A. 74, 75
Behnia, Masud 11
Behnia, Mehrdad 11
Bellare, Jayesh R. 229
Bendali, Amel 13
Bentley, Liz 54
Berardinis, Elio de 34
Berdichevski, Sasha 50
Berg, Albert van den 58
Bergonzo, Philippe 12, 13
Bertocchi, Cristina 228
Beyer, Sebastian 22
Bezerianos, Anastasios 130
Bhakoo, Kishore 20
Bhudia, Sunil K. 119
Billones, John Philip Taroma 190
Birch, Malcolm J. 94
Birgersson, K. E. 144
Biswas, Arijit 78
Biswas, Kabir H 121
Blanik, Nikolai 105
Blazek, Vladimir 105
Blume, Holger 118
Blyakhman, Felix A. 64, 76
Bodem, Fritz 99, 100
Boer, Hans L. de 58
Boey, Freddy Yin Chiang 34, 119, 133

Bohn, Stefan 14
Bojan, Vinothkumar 170
Boland, Michael R. 97
Bongrais, Alexandre 12
Bourhis, Eric Le 106
Boyde, Alan 54
Bradley, Christopher Patrick 217
Brendle, Christian 141
Brewin, Mark P. 94
Brodland, G. Wayne 86
Bronshstein, Tomer 119, 133
Brown, Steve DM 54
Brugués, Agustí 86
Bryjova, Iveta 40
Brückner, Hans-Peter 118
Buenaobra, Bernardino Jerez 180
Buenzli, Pascal Renato 184
Buering, Michael 119
Bugenhagen, Scott M 75
Buist, M. 17, 30, 31, 202, 220
Bull, Anthony M. J. 68
Bull, Joseph Lee 120
Buranachai, Chittanon 62
Burdett, Alison 135
Bustamante, Florencio Salonoy 190
Böhm, Anna 119

C

Cai, Youzhi 8
Canali, Chiara 12, 146
Cao, Tong 3, 201
Carlo, Dino Di 28
Carminati, Marco 126
Cash, Sydney 118
Caviglia, Claudia 126
Cernohorsky, Jindrich 40
Cerny, Martin 40
Chai, Woon Huei 127
Chaichanyut, Montree 171, 172
Chaisiri, Oraphan 36
Chan, Alice H. D. 47
Chan, Barbara 101
Chan, Casey 186
Chan, Chee leong 83
Chan, Jerry 186
Chan, Lesley Y. T. 70
Chan, Wai Yee 21
Chang, Chu-Fen 226
Chang, Chun Kai 208
Chang, Herng-Hua 165, 167
Chang, Hojong 155, 156
Chang, Jin Woo 209
Chang, Kung-Chin 181

- Chang, Li-Ren 222
 Chang, Tsung-Wei 214, 218
 Chankong, Thanatip 143
 Chanunpanich, N. 36
 Chao, Ling-Hsiang 116
 Chatpun, Surapong 183, 205
 Chaw, Su Yin 34
 Chee, Johnny 150, 174
 Chemla, Yann 123
 Chen, Bichao 118
 Chen, Bo-Ying 223
 Chen, Chia-Hung 43, 49, 125, 126, 192
 Chen, Chien-Fu 13, 192
 Chen, Chih-Yu 222
 Chen, Chun-Pei 37
 Chen, Clifford 171
 Chen, Fang 61
 Chen, Guan-Hua 13
 Chen, Hao 25
 Chen, Huan-Yuan 186
 Chen, Jialin 22, 56
 Chen, Jun-You 13
 Chen, Lan 160
 Chen, Longkun 8
 Chen, Nanguang 91
 Chen, Pei Yong 197
 Chen, Peter 139, 140
 Chen, Shen-Han 114
 Chen, Ting Kai 197
 Chen, Wei-Ling 10
 Chen, Xian 80, 109
 Chen, Xiao 4, 9, 21, 35
 Chen, Xiao Dong 43
 Chen, Xiaojun 15
 Chen, Yi-cheng 223
 Chen, Yin-Lin 18
 Chen, Yu 111
 Chen, Yu-Sheng 167
 Chen, Zhongwen 121
 Cheng, Chao-Min 192
 Cheng, H. 132
 Cheng, Leo K. 30, 31, 69, 81
 Cheng, Nicholas 30
 Cheng, Yi Zhuang 61, 89
 Cheng, Yuan 120, 199
 Cheong, Fook Chiong 131
 Cheung, Carol Y. 6
 Cheung, Herman S. 7
 Chew, Yew Choy 228
 Chia, Dawn 78
 Chia, Su Shin 144
 Chiang, Chen Hsien 10
 Chiang, Yu Ju 159
 Chien, Hui-Lien 226
 Chikai, Manabu 27
 Chin, Guo Feng 93
 Chin, Khai Sing 104
 Chiu, Chia-Wei 209, 226
 Chiu, Han Sheng 197
 Cho, Ho-Jung 210
 Choi, Charles T. M. 47, 169
 Choi, Heejin 90
 Choi, Jaebong 163
 Choi, Jeong Woo 209
 Choi, Jinseung 158, 163, 212, 213
 Chong, Chuh Khiun 10, 40, 59, 138
 Chong, Desmond Y. R. 23
 Chong, Yu Zheng 24, 212
 Chongthammakun, Sukumal 139
 Chooi, Weng-Tink 177
 Chotikasemsri, Pongsathorn 113, 188
 Chou, Kuofeng 197
 Chua, Alvin 86
 Chua, Ernest 84
 Chua, Huiyee 202
 Chua, Karen S. G. 150
 Chua, Kok Poo 182
 Chua, Soo Yeng Benjamin 39
 Chuag, Shao-Hsuan 13
 Chuang, Chih Yuan 160, 161
 Chui, Chee Kong 77, 84
 Chung, C. W. 30, 104, 202
 Chung, Chunhui 52
 Chung, Minhwan 29
 Cifrek, Mario 170, 175
 Cihak, Josef 189
 Cisonni, Julien 37
 Civera, Pierluigi 26
 Cohen, J. 132
 Colombelli, Julien 86
 Conte, Vito 86
 Cornish, Jillian 96
 Corrias, Alberto 30, 31
 Costa, Marcello 16
 Cottance, Myline 13
 Cox, Roger D. 54
 Cvetkovic, Dean 178
 Czaplik, Michael 105
 Černý, Martin 175
- D**
- D., Peng 81
 Dafni, Hagit 50
 Damianou, Christakis 140
 Dang, Tram T. 132
 Das, Raj 96
 Dauwels, Justin 47, 118
 Davidson, Lance A. 86
 Davis, Graham R. 54
 Dempsey, Michael K. 197
 Deng, Ning 188
 Desmond, Chong Yok Rue 205
 Dew, Lindsey 59
 Dey, Richeek 184
 Dimitrakopoulos, Georgios 130
 Dimitrakopoulou, Konstantina 130
 Ding, Ming 151
 Dinning, Philip 16
 Do, Thi Di Thien 202
 Doi, Kentaro 32, 148, 208
 Dokmeci, Mehmet R. 34
 Doloff, J. C. 132
 Domenico, Gurzi 99
 Dorn, Sabrina 18
 Doxzen, Kevin 87
 Du, Peng 30, 31
 Duan, Bin 84
 Duan, Yubo 91
 Dufva, Martin 12, 36, 146, 199
 Durairajah, Vickneswari 15, 83
- E**
- Ebeling, Peter R. 53
 Eckhardt, Holger 99, 100
 Eguchi, Akemi 92
 Eguchi, Toru 166
 Elad, David 71
 Elgendi, Mohamed 47
 Emnèus, Jenny 12, 36, 126, 146
 Emoto, Takahiro 198
 Enezei, Hamid 8
 Enmi, Jun-ichiro 92
 Er, Kenneth Zi Jian 174
 Esa, S. F. Mohammed 200
 Esapa, Chris T. 54
 Eskofier, Bjoern M. 18, 48, 100
- F**
- Fang, Qing 183
 Fang, Weileun 195
 Fard, Mohammad 27
 Favian, Ng Chuan Fang 180
 Feng, Lin 103
 Feng, Naizhang 155
 Feng, X. F. 220
 Feng, Zhonggang 136
 Fernandez, Justin 96
 Ferrari, Giorgio 126
 Ferrua, Maria J. 17
 Fikar, Adri R. 200
 Filipovich, Mikhail A. 64
 Fong, Eileen 86
 Fong, Yong Sheng 188
 Foo, Jong Yong Abdiel 182
 Foong, Kelvin Weng Chiong 221
 Foong, Ruyi 151
 Fowlkes, J. Brian 120
 Fraiszudeen, Azmall 124, 201
 Franke, Stefan 14
 Fu, Afu 63, 125

- Fu, Jianping 28
Fuad, Norfaiza 156
Fuadah, Yunendah Nur 177
Fujinaka, Toshiyuki 81
Fujisaki, Kazuhiro 143
Fujisato, Thosia 58
Fujita, Ryosuke 213
Fukasaku, Kazuaki 108
Fukuda, Keisuke 134
Fukuda, Nobuko 46
Fukuda, Sakurako 206
Fukushima, Shuichiro 91
Funamoto, Kenichi 110, 116, 136,
142, 206
Funamoto, Kiyoe 142
Furukawa, Katsuko 145
Furuya, Kishio 85
Fürjes, Péter 26
- G**
- Gála, Michal 175
Gabsteiger, Florian 48
Gac, Séverine Le 58, 72
Gaharwar, Akhilesh 34
Ganji, Fariba 196
Gao, Jerry 31
Gao, Xinting 6
Gao, Yang 66
Gao, Yangyu 188
Gao, Yi 120, 199
Gao, Yueming 170, 175
Geraldino, Paul John Legaspi 190
Ghasemi, Mohammad Ali 187
Girard, Michael J. A. 104
Girdhar, Kiran 123
Gobee, Suresh 15, 83
Goda, Keisuke 42
Goh, Honzhen 176
Goh, James C. H. 71, 144, 145
Goh, Kay Sin 151
Gokana, Victoria 19
Golan, Lior 90
Gong, Hai-Qing 135
Gong, Xiaobo 138
Goonewardene, Mithran S. 37
Gopalai, Alpha Agape 83
Gopu, Sriram 201
Gostek, Justyna 195
Goswami, Dharitri 130
Gotoh, Shinji 173
Gouwanda, Darwin 83
Govindasamy, Gopu 113
Gradl, Stefan 48
Greenwald, Stephen E. 94
Grepl, Jan 112, 196
Gretzinger, Sarah 65
Grey, Andrew 96
Greybe, Desney 97
Groves, Jay T. 121
Gruebele, Martin 123
Gu, Shen 21
Gu, Y. D. 220
Gu, Yaodong 219
Gu, Yuan Tong 121, 70
Gu, Z. 132
Guan, Guofeng 29
Gupta, Himadri S. 54
- H**
- Hadiyoso, Sugondo 200
Haishima, Yuji 217
Hamada, Yasuhiro 204
Hamai, Satoshi 208
Hamdon, Zulaika 131, 219
Hamed, Mahyar 20
Hamidullah, Muhammad 111
Hamilton, Kirk Lee 76
Hamsan, Muthayya 180
Hamzaid, Nur Azah 84, 151
Han, Jongyoon 26, 29, 125, 160
Han, Jung Min 177, 196
Han, Kyungsup 183
Han, Yu Long 64
Hanagata, Nobutaka 58
Hannongbua, Supot 108
Hanpanich, B. S. 36
Haque, Muhammad Zeeshan Ul 81
Harada-Shiba, Mariko 51
Hari, Eswaran 74
Harinarayanan, Harini 63
Hariyani, Yuli Sun 177
Harris, Arief R. 20, 197
Hasan, MD Anwarul 34
Hasan, Rumaisa Abu 197
Hasegawa, Takuya 96
Hashem, Mohamed 111, 38, 117, 123,
136
Hayami, Takashi 185
Hayase, Toshiyuki 110, 116, 136,
142
Hayashi, Yoshifumi 55
Hebenstreit, Felix 99
Heiskanen, Arto 12, 126
Heizmann, Stefanie 62
Hemar, Yacine 227
Hemmingsen, Mette 36, 146
Hemza, Jan 184
Hennig, Friedrich 98
Hieda, Ichiro 32
Hietanen, Marja 207
Higa, Masaru 66
Higaki, Hidehiko 67, 208, 211, 255
Hikichi, Yuuki 67
Himeno, Masako 108
Himeno, Ryutaro 108
Hiraguchi, Shin 55
Hiramatsu, Yuma 158
Hirano, Yoshiaki 92, 106
Hirata, Hiroaki 87
Hirata, Masayuki 81
Hirokawa, Noriyasu 185
Hisada, Toshiaki 109
Hisari, Ayako 167
Ho, Chia Lo 226
Ho, Chia-Che 6
Ho, Dean 79
Ho, Roger 171
Hoffman, Robert M. 7, 79
Hollister-Lock, J. 132
Holzapfel, Gerhard 227
Holzapfel, Gerhard A. 16
Homma, D. 117
Homma, Dai 38
Hong, Shih-Wun 224
Hong, Tsui Ying Rachel 39
Hong, Yan 32
Hongama, Seiko 198
Hoo, Calvin C. M. 150
Horiuchi, Manabu 150
Hosoda, Koh 159
Hou, Xiyuan 147
How, Hong Siang 49
Hsiang, Chiu-Yu 209
Hsiao, Hao-Ming 37, 116
Hsieh, Hong-Jung 227
Hsieh, Ming-Fa 181, 185
Hsieh, Tsung-Hao 117
Hsieh, Wei-Chen 186
Hsin-Yi, Liu 225
Hsing, I-Ming 11
Hsu, Chin Ying Stephen 92
Hsu, Horng-Chaung 224
Hsu, M. N. 144
Hu, Changchang 56
Hu, Chih-Chung 227
Hu, Chih-Fan 195
Hu, Jiajie 35
Hu, Jie 112
Hu, Shuhua 94
Huang, Bo-Cheng 169
Huang, He 222
Huang, Huaxiong 138
Huang, Jui-Wen 186
Huang, Li 7
Huang, Ming Tsan Kao and Sen H.
161
Huang, Sen H. 160
Huang, Shang-Yi 47
Huang, Sheng Cheng 159
Huang, Shiang-Yun 208
Huang, Sihua 186

- Huang, Sunan 128
Huang, Wan Yu 197
Huang, Yu-Shin 18
Huang, Zhiwei 92
Hubbuck, Juergen 65
Hui, James H. P. 71
Hui, Qian 202
Hunter, Peter John 74, 76, 108
Huo, Yunlong 114
Hurkat, Pooja 51
Husar, Peter 38, 84
Hwang, Lain-Chyr 222
Hwang, Seonhong 23
Hyodo, Hiroshi 105
- I**
- Ibitoye, Morufu Olusola 84, 151
Ibrahim, Fatimah 131, 219
Ichinose, Izumi 60
Ii, Satoshi 81, 191
Iida, Hidehiro 92
Iijima, Shinataro 215
Iitsuka, Shinjiro 179
Ikebe, Satoru 208, 211
Ikeda, Jun 54
Im, Chang-Hwan 204
Im, ChangKyun 209
Imai, Yohsuke 17
Imaizumi, Kazuya 221
Imanishi, Nobuaki 159
Inaba, Kazuo 72
Inagaki, Katsunoki 54
Ingram, John 221
Inou, Norio 54, 167
Inoue, Takuya 204
Inoue, Yasuhiro 137
Inui, Yuma 167
Irvine, Scott A. 202
Isa, R. Mohd 156
Ishihara, Kazuhiko 25
Ishii, Daisuke 46
Ishikawa, Atsuo 157
Ishikawa, Takuji 17
Ishikawa, Takumi 33
Ishimaru, Masami 211
Islam, Intekhab 201
Islam, Syed M. S. 37
Ismail, Hanafi 21
Ito, Kohta 159
Ito, Masaaki 105
Ito, Taiki 67
Ito, Takuya 38, 111, 123, 136, 142
Itoh, Ayane 161
Itoi, Eiji 97
Iván, Kristóf 26
Iwabuchi, Yuki 55
Iwahashi, Masakuni 181
- Iwakami, Yumi 221
Iwamoto, Yukihide 67, 208
Iwasaki, Kiyotaka 229
Izatt, Maree T. 23
- J**
- Jabaseelan, Davidson 115
Jacobs, Marc D. 81
Jahidin, A. H. 156
Jain, Sanjay K. 51
Jalil, Rufaihah Abdul 132, 133, 202
Jalil, Rufaihah B. A. 34
Jarmin, R. 200
Javadzadegan, Ashkan 11
Javiel, Ng Jun Wen 180
Jayasuriya, Praveen Nisal 172
Je, Minkyu 197
Jeevan, Ranjitha Rebecca 115
Jeon, Noo Li 29
Ji, Junfeng 8, 56
Jia, Lianxi 183
Jiang, Liudi 203
Jiang, Yangzi 8
Jiang, Yu 78
Jing, Jin 118
Jing, Tengyang 125
Jinzaki, Masahiro 159, 216
Jinzhong, Song 32
Jon, Kian 84
Jondri, Jondri 200
Joon, Kim Kwang 83
Jose, Rinse 115
Joseph, Fredrick Johnson 113
Joseph, George 115
Joseph, Santhosh 115
Josyula, Poornima 39
Joucla, Sebastien 13
Ju, Meongkeun 222
Jung, Chang Jin 6
- K**
- Kabinejadian, Foad 112
Kabla, Alexandre J. 87
Kadowaki, Ren 54
Kafi, Md Abdul 59, 145
Kah, James C. Y. 66, 89
Kajiwara, Itsuro 78, 143
Kakinoki, Sachiro 58, 106, 107
Kakunai, Satoshi 66
Kakuta, Akira 213
Kaliba, Aggrey 198
Kam, Boon Horng 171
Kamikura, Hiroto 168
Kamiya, Kurodo 111, 123
Kamm, Roger 139, 186
Kan, Chung-Dann 10
Kanatharana, Proespichaya 62
- Kanchanawong, Pakorn 176, 228
Kaneeda, Toshiaki 166
Kaneko, Kazuhiro 105
Kang, Dongwon 158, 163, 212, 213
Kang, Joeng-Hung 51
Kang, Then Tze 110, 180
Kannan, Srinivasan 47
Kannan, Thirumulu Ponnuraj 21
Kano, Toru 77
Kanou, Saki 179
Kao, Ming Tsan 160
Kao, Ming-Hong 222
Karanasiou, Irene 162
Karunaratne, Angelo 54, 68
Karunaratne, Pasan Manura 172
Karunaratne, Rajith Delanka 172
Karunasekera, Hasith Ruchiran 172
Kasai, Rie 168
Kasper, F. Kurtis 3
Kato, Kazuo 157
Kawai, Tomoji 32
Kawamura, Yukio 92
Kawanaka, Hiroharu 78
Kawano, Satoyuki 32, 148, 208
Kawasaki, Hitoshi 168
Kawashima, Yuuya 215
Kawasumi, Masashi 162, 164, 204
Kee, Jack Sheng 183
Keenan, Bethany E. 23
Keeratihattayakorn, Saran 53
Kenz, Zack R. 94
Kenz, Zackary R. 94
Khademhosseini, Ali 34, 102
Khamis, Mohd 8
Khatib, Oussama 14
Khoo, Bee Luan 29
Khoo, Suan Phaik 228
Kiatpathomchai, Wansika 189
Kidoaki, Satoru 45
Kikuchi, Yohei 168
Kim, Han Byul 177, 196
Kim, In-Beom 210
Kim, Jaeuk U. 6
Kim, Ji Tae 82
Kim, Jin Hyung 209
Kim, Jung-Hoon 204
Kim, Keun Ho 6
Kim, Kyung Hwan 209
Kim, Min-Cheol 139
Kim, Sangho 222
Kim, Seunghyeon 23
Kim, Sudong 29
Kim, Sungjae 96
Kim, Sungmin 96
Kim, Youngho 23
Kimura, Hitoshi 54, 167
Kimura, Kazuyuki 214

- Kimura, Yoshihiro 185
 Kimura, Yoshitaka 142
 Kindi, Hamood Al 34
 King, Andrew J. C. 37
 Kinouchi, Yohsuke 131, 198, 219
 Kiran, Raphael 13
 Kishimoto, Hidehiro 105
 Kitagawa, Naoki 164
 Kitahara, Shigemi 55
 Kitama, Masataka 214
 Kitano, Tomoya 27
 Klimenko, Stanislav 147
 Klinkovský, Tomáš 173
 Klucken, Jochen 18
 Knoebel, Christian 140
 Kobayashi, Ikuma 17
 Kobayashi, Katsuyuki 54
 Kobayashi, Naofumi 179
 Kobayashi, Naoki 92
 Kobayashi, Shunichi 45
 Kobravi, Hamidreza 127,176
 Kofidis, Theodoros 34, 132, 133, 137, 202
 Kohlwein, Sepp 227
 Konaka, Shinsuke 198
 Konishi, Tadashi 92
 Korff, Alexander 141
 Korsunsky, Alexander M. 106
 Koseki, Michihiko 77, 96
 Koshiyama, Kenichiro 215
 Koyama, Hironori 162, 204
 Koyano, Kiyoshi 194
 Kraus, J. 175
 Kretschmer, Jörn 20, 163
 Kripfgans, Oliver D. 120
 Krishnan, R. Gokula 146
 Krithika, L. S. 63
 Krois, Igor 170, 175
 Kruse, Carola 94
 Krzok, Waldemar 171
 Krüger-Ziolek, Sabine 62
 Kuan, Yee Han 81
 Kubíček, Jan 66, 142
 Kubicek, J 112
 Kubo, Mizuho 91
 Kubo, Toshiro 55
 Kudo, Shin 198
 Kudo, Susumu 213
 Kugler, Patrick 48
 Kumagai, Hiroo 111
 Kumar, Arun 103
 Kumar, Parmod 47
 Kumar, Sathiesh 113
 Kumarsing, Ramruttun Amit 171
 Kume, Miyoko 170
 Kume, Shinnosuke 159
 Kung, Terrence 57
 Kuno, Hiroaki 127, 128
 Kuo, Chien-Chung 227
 Kuo, Mei-Ying 69, 173, 174, 224, 227
 Kurahashi, Muneshige 179
 Kuriyagawa, Motohiro 169
 Kurniawan, N. A. 202
 Kuroda, Junko 81
 Kuroiwa, Minoru 157, 166
 Kurokawa, Naoya 127, 128
 Kurumaddali, Bharath 193
 Kurzynski, Marek 164
 Kusuhara, Toshimasa 182
 Kuwata, Takeshi 33
 Kwak, Dai-Soon 210
 Kwon, Ji Yean 96
 Kyoso, Masaki 169
- L**
- Labrom, Robert D. 23
 Ladoux, Benoit 86, 87
 Laechele, Tobias 140
 Lahiri, Amitabha 78
 Lai, Mei-Chun 185
 Laki, András J. 26
 Landini, Gabriel 106
 Langer, R. 132
 Laqua, Daniel 38, 84
 Lassfolk, Christina 207
 Laszczak, P. 203
 Latief, Fourier D. E. 176
 Lau, Kristal YQ 228
 Lee, Angela 217
 Lee, Bae Hoon 202
 Lee, Chengkuo 195
 Lee, Chin-Hui 155
 Lee, Eng Hin 4
 Lee, Foong Poh 188
 Lee, Hae Ung 124
 Lee, Heow Pueh 49, 50, 56, 78, 82
 Lee, Hong Ji 155
 Lee, Hyunjae 29
 Lee, J. H. 212
 Lee, Jeong Su 155
 Lee, Joohack 158,163, 213
 Lee, Khuan Y. 46,199
 Lee, Poh Foong 93
 Lee, Seng Teik 86
 Lee, Shu Jin 49, 50, 56, 82,78
 Lee, Song Jae 155, 156
 Lee, Soo Chin 29
 Lee, Taeyong 39, 149
 Lee, Tin lap 21
 Lee, Won Kyu 155
 Lee, Yi-Hsuan 47, 169
 Lee, Yoot Khuan 200
 Leedumrongwatthanakun, Saroch 62
 Leelasamran, Wipawan 205
 Leibinger, Alexander 129
 Leo, H. L. 39, 81, 112, 124,144
 Leong, Manchun 87
 Leong, Peng 80
 Leonhardt, Steffen 105, 119, 141
 Lertprasert, Polsart 171, 172
 Leutheuser, Heike 18, 48
 Ley, Sebastian 38
 Li, Bing Nan 61, 89
 Li, Chao 183
 Li, Cheng 76
 Li, Chunyang 33, 157, 165
 Li, David S. 120
 Li, Dian-Ru 37
 Li, Hongyang 188
 Li, Jia-Da 173, 174, 224
 Li, Jiamao 103
 Li, Lulu 201
 Li, Mingming 201
 Li, Shenlong 188
 Li, Tao 121
 Li, Xiuxiang 175
 Li, Yibin 188
 Li, Yuanhao 220
 Li, Zhangyong 33, 157, 165
 Li, Zheng 160
 Liang, Sheng-Fu 18, 117, 135
 Liau, Jiann-Jong 214, 218
 Liley, Helen 227
 Lim, Alvin S. T. 29
 Lim, Aymeric 78
 Lim, Choon Kiat 57
 Lim, Chwee Teck 29, 87, 125, 131, 192, 224
 Lim, Fang Ming 151
 Lim, Karen 174
 Lim, Pang Hung 150
 Lim, Siak Piang 56, 82
 Lim, Wan-Teck 29
 Lim, Wei Sheong 150
 Lim, William 104
 Lim, Yong Gyu 155
 Lin, Cheng-Chung 69, 173, 174, 224
 Lin, Jia Hui 197
 Lin, Jinzhao 33
 Lin, Kang Ping 41,159
 Lin, Keng Hung 159
 Lin, Ting-Sheng 222
 Lin, Wen Chen 159
 Lin, Yanping 15, 220
 Lin, Yen-Ju 186
 Lin, Yi-Hsun 6
 Lin, Yu-Huan 116
 Lin, Yu-Ju 165
 Lindner, Dirk 14
 Linnavuo, Matti 207
 Liong, Yushan Kyrin Jo 78

- Liow, Tsung-Yang 183
Lissorgues, Gaëlle 12,13, 19
Liu, Fu-Tong 186
Liu, Hao 45
Liu, Huanhuan 9
Liu, Jaron Zhongliang 176
Liu, Jiang 6
Liu, Jie 33, 157, 165
Liu, Jimin 76
Liu, Shengrong 33
Liu, Xiaofeng 125
Liu, Xinyue 138
Liu, Xuening 160
Liu, Yen-Hung 224
Liu, Yisi 127
Liu, Yun Yueh 159
Liu, Yunqiao 138
Liu, Zeyu 22
Lo, Guoqiang 183
Lochmann, Matthias 48, 98, 99, 100
Loh, Wee Chuan Melvin 39
Low, Jin-Huat 146
Low, Kok Yao 202
Lu, Cheng-Kuang 214, 218
Lu, Hsuan-Lun 69
Lu, Ping 9
Lu, Tian Jian 64, 112
Lu, Tung-Wu 69, 173, 174, 224, 226, 227
Lu, Wen-Hsiang 229
Lucey, Anthony D. 37
Luo, Kathy Qian 63, 65, 125
Luo, Rong-Cong 49
Luo, Xianshu 183
Lv, Wei Fu 89
- M**
- Ma, Jiabing 219
Ma, M. 132
Mabuchi, Kiyoshi 67, 211, 219
MacNeil, Sheila 59
Machado, José 95
Machluf, Marcelle 34, 119, 133, 202
Madheswaran, Karthick 113
Maeda, Shumpei 164
Magatani, Kazushige 157, 158, 166, 179
Magnusson, Johannes Pall 93
Mahara, Atsushi 25, 92
Mahdi, Adam 75
Mahmood, Faisal 47
Mahmood, Zuliani 21
Majid, Norazman Abd. 20
Major, Boguslaw 195
Major, Roman 195
Mak, PengUn 175
Mak, PunUn 170
Malcolm, Duane 217
Malik, Aamir 109
Malik, Aamir Saeed 177, 230
Mamorita, Noritaka 214
Mani, Alireza 196
Mansor, Wahidah 46, 199
Marimuthu, Ganesan 193
Martelli, Saulo 53
Martinez, Eliana C. 22
Martinsen, Ørjan Grøttem 12
Martyr, Peter Nash 217
Marwan, M. E. 156
Masatake, Akutagawa 198
Masoudi, Mitra 127
Masouros, Spyros D. 68
Matsopoulos, George 162
Matsubara, Hisashi 78
Matsui, Shunsuke 123
Matsui, Takemi 173
Matsumoto, Takeo 9, 122, 204, 215
Matsumoto, Takuya 110
Matsumoto, Yasuaki 225
Matsuo, Satoshi 136
Matsuura, Hiroshi 166
Maturros, Thitima 189
Maurer, Manfred 73
Mazza, Edoardo 73
Meesane, Jirut 183
Mehta, Dwij 94
Mehta, Jodhbir S. 7, 102, 190
Meixensberger, Jürgen 14
Mengko, Tati L. R. 176
Meyer, Ganit 23
Mihara, Genki 51
Mikos, Antonios G. 3
Minami, Kazuyuki 194
Minamikawa-Tachino, Reiko 161
Minh, Hoang Tran 49
Misgeld, Berno 141
Misran, Misni 93
Mithraratne, Kumar 97, 147, 173
Mitragotri, Samir 79
Miura, Hidekazu 26, 38, 111, 123, 136
Miura, Hiromasa 67, 208, 211
Miura, Jiro 91
Miyagawa, Taimei 17
Miyake, Hitoshi 27
Miyamoto, Yuichi 185
Miyata, Shogo 187, 188
Mizoguchi, Hiroshi 25, 33, 104, 105, 151
Mizote, Muneaki 170
Mizuta, Hiroshi 67, 225
Moe, Aung Aung Kywe 70
Moeller, Knut 140
Mohan, Dhanya Menoth 47
Mohan, Dhruv 184
Mohan, N. Madhu 63
Mohanty, Soumyaranjan 36, 146
Mok, Qinglin 151
Molano, German 227
Monkhouse, Catriona 23
Moradihaghighat, Reyhane 187
Morimoto, Koji 185
Morimoto, Yuji 145
Morisaki, Aya 181
Morishita, Yuji 166
Moser, D. 203
Muñoz, José J. 86
Muhammad, Haseena Bashir 12, 146
Muir, Hidekazu 117
Mukhopadhyay, Jayanta 130
Murayama, Nobuki 225
Murayama, Takeshi 166
Mylonas, Nicos 140
Mythili, A 62
Mzyk, Aldona Ilona 195
Möller, Knut 15, 20, 62, 163
- N**
- NII, Ryosuke 208
Naayutaya, Surasak Sungkatat 113
Naganuma, Yoji 162
Nagaoka, Takashi 179
Nagayama, Katsuya 161
Nagayama, Kazuaki 9, 122, 204, 215
Nagel, Sarah 65
Nagura, Ken 70
Nagura, Takeo 159, 216
Nagy, Gábor Zs. 26
Nakadate, Hiromichi 213
Nakagoshi, Takuya 107
Nakajima, Atsushi 55
Nakajima, Tomoki 134
Nakajima, Yasuhiro 167
Nakamura, Gen 78, 143
Nakamura, Sakiko 215
Nakamura, Takao 182
Nakamura, Tomoya 216
Nakamura, Toshiyasu 159, 216
Nakamura, Kazuhiro 134
Nakanishi, Yoshitaka 67, 211, 225
Nakano, Tatsuya 217
Nakao, Masaki 219
Nakaoka, Ryusuke 217
Nakaoki, Takahiko 51
Nakashima, Kazuhiro 213
Nakashima, Yuta 67, 194
Nakayama, Hiroyuku 181
Nakayama, Toshio 116, 206
Nam, Ki-Chang 32
Nam, Yong-Seok 210
Nambu, Masayuki 150

- Nanayakkara, Nuwan Dayananda 172
Nanud, May Noren Dugang 190
Narayanan, N. K. 19
Narioka, Kenichi 159
Narumi, Akira 92
Naruse, Kouji 67
Natarajan, A. V. 194
Natarajan, Kannathal 174
Nathan, Saminathan S. 144
Nauman, Javid 75
Nawattanapaiboon, Kawin 189
Neeman, Michal 50
Neo, Edwin Boon-Wee 146
Neo, Puay Yong 145
Neumuth, Thomas 14
Ng, Ee Xien 23, 126
Ng, Sum Huan 124
Ngan, Weida 63
Nguyen, Evelyne 119, 133
Nguyen, Ngoc Anh Huyen 78
Nguyen, Trung Dung 70
Nguyen, Vinh-Tan 81
Niamsiri, Nuttawee 139
Nickerson, David Phillip 76
Nielsen, Poul Michael Fønss 217
Niesche, Annegret 141
Niimi, Shingo 217
Niizuma, Kuniyasu 206
Nikkhah, Mehdi 34
Ninagawa, Takako 92
Nisar, Humaira 230
Nishi, Naoki 67
Nishikawa, Kantaro 91
Nishikiori, Daisuke 185
Nishimatsu, Kazuho 208, 211
Nishitani, Kazutoshi 55
Nithya, Venkateswaran 132
Nkahara, Yukiko 181
Nobuki, Murayama 225
Noda, Shigeo 108
Nomoto, Yohei 162, 164, 204
Noor, Alias Mohd 20
Norman, Andrew 197
Nozaki, Kazunori 149, 191
- O**
- Obara, Akira 25, 104
Obika, Satoshi 51
Oelmeier, Stefan 65
Oen, Kimberly 202
Ogasawara, Masamine 166
Ogihara, Naomichi 159, 164, 216
Ogoshi, Tomoki 61
Ogura, Kiyoshi 161
Ohashi, Toshiro 123
Ohgi, Junji 80, 109
Ohi, Toshifumi 187
Ohnaka, Koichi 168
Ohuri, Katsumi 229
Ohshiro, Takahito 32
Ohta, Makoto 147
Ohtake, Masashi 147
Ohya, Tetsuya 162, 164, 204
Ohya, Yuichi 107
Ohzono, Takuya 46
Oka, Hiroyuki 80
Okada, Yoshifumi 55
Okayasu, Hiroki 166
Okuda, Satoru 137
Okuda, Yuya 188
Okuyama, Fumio 78
Okuyama, Koichi 205
Oldfield, Matthew 129
Oloyede, Adekunle 70, 121
Olufsen, Mette 75
Omari, Taher 16
Omata, Seiji 134
Omholt, Stig W. 75
Ong, Fook Rhu 150
Ong, Hian Tat 174
Ong, Sim Heng 77, 118, 221
Ong, Wai Sing 150
Ong, Weifen 171
Onishi, Yuya 162, 164, 204
Onodera, Takayuki 151
Onuma, Mai 207
Orii, Naotoshi 169
Osana, Taisuke 54
Osman, Noor Azuan Abu 107
Osochan, Tanakorn 139
Ospina, Marcela Arango 201
Otani, Tomohiro 81
Ouyang, Hongwei 4, 8, 106, 9, 21, 22, 35, 56
Ozawa, Kei 147
O'Grady, Greg 30, 69
- P**
- Pacheco, David 227
Palit, Arnab 119
Pan, Houwen Matthew 52
Pan, Ming-Xin 120, 199
Pang, Yu 33
Pant, Aakanksha 195
Park, Kwang Suk 155, 177, 196
Park, Mi Kyoung 183
Park, Sang Hyun 155
Park, Sungsu 42
Parvaneh, Tavakkoli 127
Pastorin, Giorgia 195
Paul, Arghya 34
Pearcy, Mark J. 23
Peh, Gary S. L. 190
Peh, Kah Yim 124
Peh, Priscilla 186
Peh, Ruey Feng 197
Peh, Yu Ming 63
Peng, Weng Kung 26, 160
Penhaker, Marek 40, 49, 66, 112, 173, 175, 189, 196
Penzel, T 178
Pereira, Carina Barbosa 105
Peter, L 112
Pettersen, Klas H. 75
Pettet, Graeme 23
Phee, Louis 140
Phua, Chee Teck 19
Picaud, Serge 13
Pingguan-Murphy, Belinda 107
Piro, Oreste 72
Pivonka, Peter 53
Piyush, Ranjan 178
Plotkin, Marian 132, 133, 202
Pogfai, Tawee 189
Poh, Chueh Loo 7, 141
Poh, Yong Cheng 220
Polit, Jacek 195
Portela, Filipe 95
Poulsen, Carl Esben 199
Prachgosin, Tulaya 205
Pramanik, Sumit 107
Pratondo, Agus 77
Prokop, J 112
Pun, Siohang 170, 175
Purwananto, Yudhi 34
- Q**
- Qader, Sarah Talib Abdul 21
Qian, Haisheng 90
Qian, Weixin 148
Qidwai, Uvais 109
Qin, Jing 61
Qiu, Anqi 169
Qiu, Qiner 220
- R**
- Rabeek, S. Mohamed 197
Radermacher, Klaus 141
Radzol, Afaf Rozan Mohd 199
Raghunath, Michael 22, 186
Rahman, Anugrah 200
Rahman, Ismail Ab 21
Rahman, N. Izayu A. 197
Rahman, Roselinda 8
Raja, M. Kumarasamy 197
Raja, Rangaswamy 194
Rajagopalan, R. 202
Rajaguru, Harikumar 170
Rajan, Johanna 115
Ramachandran, Gokula Krishnan 95

- Ramakrishnan, S. 142, 178
Ramanathan, R. K. 115
Ramanujam, Vaibavi S. 34,133
Ramdhani, Saumi Zikriani 176
Ramgopal, Yamini 57
Ramji, Ramesh 125, 192
Ramli, Arlyana 197
Ravichandran, Subbaraman 110, 180
Razak, Noor Hayati Abdul 8
Razali, Nur Ain Iftitah Mohamad 107
Reeth, Eric Van 7
Regitnig, Peter 227
Rehman, Shakil 91
Rein, Benjamin 141
Reis, Pedro 48
Reis, Pedro Miguel Ramos 99
Ren, Hongliang 55, 160
Ren, Xiafei 71
Riau, Andri K. 190
Riedlinger, Axel 20, 163
Rizal, Achmad 177, 200
Roberts, Clive J. 93
Rodriguez, Carlos Julio Cortes 201
Romer, Lewis H. 57
Rostami, Mostafa 187
Rousseau, Lionel 12, 13
Rua, Fernando 95
Ruelan, Mary Ann Agosto 190
Rujirojindakul, Pairaya 183
Rungrotmongkol, Thanyada 108
Ryou, Ho Suk 177, 196
Ryou, Hong Sun 82
Ryu, Jeseong 23
Ryu, Sang Baek 209
- S**
- S, Mayur Venkatesh 193
Sabri, Nurul Syazwani Ahmad 145
Safronov, Alexander P. 64
Saiki, Yoshikatsu 136
Sailov, Talgat 228
Saito, Isturo 26
Saka, Taketoshi 214
Sakai, Manabu 123
Sakai, Rina 67, 211, 219
Sakai, Yusuke 58
Sakanishi, Sanga 136
Sakata, Konomi 167
Sakuma, Ichiro 44
Saleh, Muhamad 131, 219
Salleh, Sh-Hussain 197
Salleh, Sheikh Hussain Shaikh 20
Samitsu, Sadaki 60
Sampietro, Marco 126
Sanderson, Jason Michael 225
Sandholzer, Michael A. 106
Sangi, Mehrdad 85
Sankai, Yoshiyuki 195
Sano, Hirotaka 97
Sano, Kyosuke 27, 38, 111, 123, 136
Santanirund, Pitak 189
Santos, Manuel Filipe 95
Santoya, Amos Monterroyo 190
Saputra, Gabriel Pramudita 191
Sarig, Hadar 34, 119
Sarig, Udi 34, 119, 133
Sasaki, Katsuhiko 193
Sathar, Shameer 30, 69
Sato, Kakeru 210
Sato, Takehiko 134, 210
Sawae, Yoshinori 134
Sawai, Kei 204
Scheper, Thomas 119
Schiek, Michael 131
Schmid-Schönbein, Geert W. 44
Scholl, Andrea 141
Schriefl, Andreas 227
Schuldhaus, Dominik 18, 48, 100
Schwarz, Michaela 227
Schönfeld, Uwe 171
Scorsone, Emmanuel 12, 13
Seah, Xin-Yi 190
See, Hian Hian 140
Segawa, Katsunori 217
Sekine, Masaki 167
Seliktar, Dror 34, 35, 50, 132, 133, 202
Selvam, Suvita 115
Senadeera, Wijitha 121
Sepponen, Raimo 207
Sera, Toshihiro 215
Shakir, Mohamed 109
Shalini, M. 63
Sham, Adeline 22
Shamsuddin, Rani 8
Shanshan, Lin 180
Sharan, Lalith Nag 184
Shaw, Fu-Zen 18, 135
Shaw, Simon 94
Shen, Guofang 15
Shen, Jiayi 133
Shen, Shu-Wei 192
Shen, Yi 155
Shen, Youqing 60
Shen, Zhiyuan 155
Shi, Pujiang 71, 145
Shiau, Chung-Wai 186
Shibano, Katsuhiko 81
Shibue, Tadashi 185
Shiga, Takuya 38, 111, 123
Shih, Kao-Shang 226
Shih, Po-Chung 159
Shih, Ya Ting 159
Shiina, Takayuki 104
Shimatani, Yuichi 169
Shimazu, Kenryo 67
Shimizu, Hisae 214
Shimoto, Takeshi 208, 211
Shin, Hyung-Cheul 209
Shin, Y. H. 158,212
Shin, Yoonho 163, 213
Shina, Takayuki 25
Shinsuke, Konaka 198
Shirai, Atsushi 212
Shirai, Kiyoko 182
Shiraishi, Yasuyuki 26, 27, 38, 111, 117, 123, 136
Shiraishi, Yoshitaka 208, 211
Shirlynn, Ng Wan Ern 180
Shklyar, Tatyana F. 64
Shoeibi, Ali 176
Shukla, Rohit 47
Shum-Tim, Dominique 34
SiewLokToh 42
Silva, Álvaro 95
Silveira, Miguel Hernandez 135
Sim, Soo Young 155, 177, 196
Singh, Mutum 8
Singh, R. Paul 17
Singh, Sanjleena 70
Siniakowicz, K. 132
Skolimowski, Maciej 146
Slosberg, J. E. 132
Smitha, C. K. 19
Smithmairie, Pruittikorn 205
So, Peter T. C. 90
Soga, Kohei 105
Sokabe, Masahiro 85
Sokolov, Sergey Yu. 64, 76
Sommer, Gerhard 227
Son, Jongsang 23
Sonam, Surabhi 224
Sone, Shusaku 136
Sonetha, Vaibhavi A. 229
Song, Junfeng 183
Soo, Ross A. 29
Sourina, Olga 127, 147
Spindeldreier, Christian 118
Sreenivasan, Dharshini 96
Sridhar, Adithya 58
Srihirin, Toemsak 139, 189, 191
Srinivasan, S. 62
Srivastava, Ruchir 6
Strouthidis, Nicholas 104
Suga, Mikio 143
Suganthi, S. S. 142
Sugawara, Michihito 55
Sugita, Shukei 204
Sugiura, Seiryō 109
Sugiura, Takuma 55
Sugiyama, Shin-ichiro 116, 206

- Sugiyama, Yoshiro 212
Sui, Tan 106
Sujatha, C. M. 62
Sumii, Tateki 213
Sun, Guanghao 173
Sun, Ming-Jian 117
Sun, Ying 118
Sundaram, Kiruthigha Shanmuga 115
Sung, Kun Hyuk 82
Sung-Kil, Lim 83
Suresh, Rohit 193
Suresh, Vinod 221, 227
Suresh, Vyshak 193
Surjawidjaja, Michael 54
Susanti, Dewi 66
Sutapun, Boonsong 189
Suzuki, Daichi 116
Suzuki, Hayato 78, 143
Suzuki, Kazunori 157
Suzuki, Kosuke 46
Swaminathan, Sirisha 63
Syaifudin, Achmad 193
- T**
- Tabata, Yasuhiko 57
Tack, Gyerae 158,163, 212, 213
Tadano, Shigeru 53, 78, 143, 148, 206, 207
Taeyong, Lee 83
Tagawa, Yoshihiko 127, 128
Tahrir, Farzaneh Ghasemi 196
Taib, M. N. 156
Taira, Yasunori 38, 111, 123, 136
Takada, Hiroya 85
Takahashi, Junko 33
Takahiro, Emoto 198
Takamura, Kenji 55
Takasaki, Kensuke 106
Takase, Haruhiko 78
Takeda, Ryo 68, 193
Takeda, Sunao 168, 179
Takemura, Hiroshi 33, 104, 105, 151
Takemura, Taro 58
Takeshige, Fumio 91
Takezawa, Shingo 181
Takkemura, Hiroshi 25
Tallner, Alexander 18
Talvitie, Sanna 207
Tamaddon, Houman 11
Tamamoto, Mitsuhiro 166
Tan, Beng Hao 151
Tan, Cher Heng 7
Tan, Daniel Shao-Weng 29
Tan, Eng Lai 228
Tan, Esther 202
Tan, G. T. 144
Tan, Long Bin 56, 82
Tan, Mingzhen 169
Tan, Pamela H. S. 144
Tan, Ru San 114
Tan, Xin Ji Alan 182
Tan, Zeqi 55
Tanaka, A. 27
Tanaka, Kensei 211
Tanaka, Masao 96
Tang, K. M. 132
Tang, Kok Zuea 201
Tang, Pek Yee 93
Tania, M. 144
Taniguchi, Masateru 32
Tanino, Hiromasa 66
Tao, Jiadong 56
Tavakkoli, Parvaneh 176
Tawara, Daisuke 70
Tay, Annie 228
Tegawa, Yoshinori 198
Teh, Thomas Kok Hiong 71
Teo, Benjamin Kim Kiat 57
Teo, Jeremy 206
Teo, Soo Kng 141
Teoh, Boon Yew 188
Teoh, Jee Chin 39, 149
Terrill, Nick 54
Thai, A. V. 132
Thakker, Rajesh V. 54
Thakor, Nitish 88, 124, 128
Thakur, Goutam 184
Tham, Ivan W. K. 7
Tham, Jasmine P. L. 114
Thang, Vu D. 34
Thanikachalam, Mohan 115
Thavarungkul, Panote 62
Theera-Umpon, Nipon 143
Thibbotuwawa, Noyel Deegayu 121
Thiranjia, Prasad Babarenda Gamage 217
Thompson, Benjamin 85
Thomsen, Peter 36
Ting, Gigi A. Y. C. 119
Tipmanee, Varomyalin 108
Tjin, Monica Suryana 86
Tobe, Yasutaka 55
Todo, Mitsugu 59, 145, 193, 194
Todoh, Masahiro 148
Toh, Siew Lok 42, 71,144, 145
Toh, Soon Leng 151
Toh, Yi Chin 124
Toha, Siti Fauziah 217, 218
Tominaga, Teiji 116, 206
Tomita, Sunao 78
Tong, Tong 8
Too, H. P. 202
Torigoe, Hidetaka 51
Townsend, David W. 88
Toyama, Yusuke 87
Trau, Dieter 22,52
Treat, Xavier 86
Trew, Mark L. 30, 69
Tsai, Cheng Nan 160, 161
Tsai, Hong-Sheng 223
Tsai, Tsung-Ting 192
Tsai, Yung-Shen 208, 209, 226
Tse, Kwong Ming 56, 82
Tsuboko, Yusuke 111, 117, 123, 136
Tsuji, Chizuko 179
Tsuji, Tetsuya 70
Tsuji, Shinichi 195
Tsunoda, Kei 216
Tsuruoka, Shinji 78
Tsutsui, Makusu 32
Tu, Chuang-Bin 223
Tu, Xiaoguang 183
Tuantranont, Adisorn 189
Tung, Chia-Ming 229
Tungjtkusolmun, Supan 171, 172
Tungtrakunwanit, Boonsin 113
Turley, Glen A. 119
Turuwhenua, Jason 85
Tusboko, Yusuke 38
- U**
- Uchida, Kentaro 67
Uddin, M. S. 24, 181
Uematsu, Miyuki 217
Ueno, Masaru 168
Ugsornrat, Kessararat 189
Uhlig, Axel 119
Ukiki, Mitsuhiro 122
Umezumi, Mitsuo 55, 136, 229
Undheim, Marit 68
Uno, Yohei 9
Urano, Tetsuya 179
Ushida, Takashi 145
- V**
- Vaghefi, Ehsan 85
Vai, MangI 170, 175
Vaibavi, Srirangam Ramanujam 132
Vajdíková, Ivana 175
Valencia, Santiago Rendon 98
Vasic, Željka Lučev 170, 175
Vedula, Sriram Krishna 87
Velayo, Clarissa 142
Veldhuis, Jim H. 86
Velusamy, Yugan 15
Vengadesan, S. 39
Venkateswaran, Nithya 133
Venkatraman, Subbu 34,119, 133, 202
Ventouras, Errikos 162
Ventra, Massimiliano Di 32

- Viertler, Christian 227
 Visage, Catherine Le 102
 Viswanatha, N. 115
 Viturawong, Yuvaret 139
 Vo, Nguyen 160
 Vrahatis, Aristidis 130
 Vyas, Ruchi 31
- W**
- Waasen, Stefan van 131
 Wada, Shigeo 81, 149, 191, 215
 Wahab, Ahmad Khairi Abdul 84, 151
 Walker, Edward 221
 Wan, Min 114
 Wang, Chengtao 15, 220
 Wang, Chun 37
 Wang, De Yun 49, 50
 Wang, Dongmei 220
 Wang, Hao 195
 Wang, Jaw-Lin 52
 Wang, Jing 132, 133
 Wang, Li Wen 197
 Wang, Lin 112
 Wang, ShuQi 112
 Wang, Shyh-Hau 6
 Wang, Xudong 15
 Wang, Yan 120, 199
 Wang, Yilin 176
 Wang, Yu-Lin 18, 135
 Wang, Zhinuo 221
 Wang, Zi 92
 Wangkam, Thidararat 191
 Warkiani, Majid Ebrahimi 29, 125, 135
 Watanabe, Masayuki 105
 Watanabe, Shotaro 214
 Watson, Maureen 96
 Wei, Ji 222
 Wei, Shan 220
 Wei, W. T. 230
 Weibull, Emilie 123
 Weir, G. C. 132
 Wellings, Richard 119
 Welsch, Goetz 98
 Wen, Long-Ping 88
 Wen, Yuting 61
 White, Alexander Thomas 138
 Whiteman, John R. 94
 Wicaksono, Nugroho Budi 176
 Wikantyasning, Erindyah Retno 93
 Wiklendt, Lukasz 16
 Wilczek, Piotr 195
 Williams, Mark A. 119
 Wojcik, Magdalena 36
 Wolczowski, A. 164
 Wolff, Anders 12, 36, 146, 199
 Wolinski, Heimo 227
- Wong, Christopher 109
 Wong, Chui Ching 131
 Wong, Damon 6
 Wong, Hee Kit 5
 Wong, Ken 47
 Wong, Long Hui 202
 Wong, Mark E. 3
 Wong, Paul 23
 Wong, Sum Thai 57
 Wong, Tien Y. 6
 Wongsakulyanon, Apirom 189
 Wu, Ed X. 5
 Wu, Li-Wei 116
 Wu, Pei-Shan 181
 Wu, Tim 147, 173
 Wu, Yu-Huan 173, 174, 224
- X**
- Xia, L. 144
 Xian, Wan 202
 Xiang, Zhuolin 195
 Xiao, Luosha 215
 Xiao, Wei Lin 197
 Xinming, Yu 32
 Xu, Feng 64, 112
 Xue, Zhengjun 17
- Y**
- Yagami, Hisanori 78
 Yagi, Takanobu 55
 Yahiro, Yuki 122
 Yakup, M 200
 Yam, Gary 7
 Yamada, Akahiro 117
 Yamada, Akihiro 38, 111, 123, 136
 Yamada, Naoki 194
 Yamada, Satoshi 148, 206, 207
 Yamagami, Y. 66
 Yamagishi, Masaaki 38, 136
 Yamaguchi, Daiki 158
 Yamaguchi, Takami 17
 Yamaguchi, Tomohiko 46
 Yamakoshi, Takeshi 25
 Yamamoto, Akihide 92
 Yamamoto, Kimiko 122
 Yamamoto, Naosuke 127, 128
 Yamamoto, Nobuyuki 97
 Yamamoto, Tadashi 229
 Yamamoto, Toshiyasu 127, 128
 Yamamoto, Yoshitake 182
 Yamanaka, Ryota 168
 Yamanashi, Momoko 55
 Yamaoka, Tetsuji 25, 51, 58, 92, 106, 107
 Yamashita, Kazuhiko 221
 Yamashita, Masaji 214
 Yamauchi, Kentaro 193
- Yamazaki, Sho 122
 Yambe, Tomoyuki 26, 27, 38, 111, 117, 123, 136
 Yameen, Haneen Simaan 50
 Yang, Bing-Shiang 52
 Yang, Daiwen 140
 Yang, Hsiao-Nan 116
 Yang, In Hong 124
 Yang, Kai 132
 Yang, Yin 194
 Yang, Yuxin 141
 Yanjun, Li 32
 Yao, Wang 119
 Yao, Xiao Bo 89
 Yao, Yu 131
 Yap, Chong Hao 57
 Yap, Jinq Shya 114
 Yap, Yoon Sim 29
 Yasukawa, Satoshi 157
 Ye, Swe Soe 222
 Yeh, Chun-Ting 37
 Yeh, Jui-Ming 181, 185
 Yeh, Ming-Long 10
 Yelin, Dvir 90
 Yen, Yu-Chun 13
 Yeo, Eugenia 66
 Yeoh, Jing Wui 31
 Yeoh, Q. W. 230
 Yeow, Chen-Hua 54, 95, 146
 Yeow, Siang Lin 39
 Yew, Elijah Y. S. 90
 Yiallouras, Christos 140
 Yim, Evelyn 70, 103, 57
 Yin, Fengshou 6
 Yin, Ming-Ting 116
 Yin, Zi 4, 35
 Yohsuke, Kinouchi 198
 Yokota, Hideo 215
 Yoon, Hee Nam 155
 Yoon, Yong-Jin 183
 Yos, Phanny 59, 145
 Yoshida, Hirotaka 55
 Yoshida, Masaki 167, 215
 Yoshida, Shunsuke 168
 Yoshikawa, Kogo 143
 Yoshinaga, Tsukasa 149
 Yoshino, Daisuke 134, 210
 Yoshinori, Tegawa 198
 Yoshizawa, M 27
 Yu, Boon Tat 150
 Yu, Chao 140
 Yu, Cheng-Han 121
 Yu, Ching Liang 159
 Yu, Hanry 124, 144
 Yu, Haoyong 76, 128, 151, 160
 Yu, Jing 15
 Yu, Mingbin 183

Yu, Ting 65
Yu, Wei Shin 150
Yunus, Jasmy 24, 212
Yusuke, Nakamuta 59
Yvert, Blaise 13

Z

Zabidi, Azlee 46
Zahedi, S. 203
Zaidel-Bar, Ronen 121
Zakhirehdari, Negar 127, 176
Zako, Tamotsu 105
Zeng, Kaiyang 121

Zhang, Can 9
Zhang, Guangzhi 109
Zhang, Huijuan 183
Zhang, Jun-Mei 114
Zhang, Lifang 157, 165
Zhang, Shufang 8
Zhang, Wei 22, 56
Zhang, Xiaolin 103
Zhang, Yang 188
Zhang, Yong 89
Zhang, Yuelin 148
Zhang, Zhi 120
Zhang, Zhiyuan 221

Zhao, Zhanqi 62
Zheng, Wei 92
Zheng, Yong-Ping 41
Zhi, Xu 32
Zhong, Liang 114
Zhong, Xin 221
Zhou, Hai 220
Zhou, Shengfeng 140
Zhou, Yi Ming 160
Zhu, Jian Hua 49,50
Zhu, Shouan 9
Zhu, Ting 9, 22, 35
Zifreund, Timo 140

ICBME 2013 : Programme-At-A-Glance

Time	Venue/Description					
09:00	Plenary Lecture 6 @ Auditorium Advancing Multi-modality Clinical Imaging: A Challenge for the Engineer and Physicist by David W Townsend, A*STAR-NUS Clinical Imaging Research Centre, Singapore					
09:45	Plenary Lecture 7 @ Auditorium Brain Machine Interface Technology: from Neurons to Prostheses by Nitish Thakor, SiNAPSE, Singapore					
10:30	Tea Break					
11:00	Auditorium	SR 1&2	SR 3&4	SR 5&6	SR 7&8	SR 12
	SYM-10: Nanoparticles for Bioimaging and Targeted Therapy	A7: Optical Imaging	B7: Diagnostics and Therapeutics	C7: Computational Mechanics	BES-SEC Design Awards 2013	SYM-11: Biomedical Engineering in Sport Science
12:30	Lunch					
13:30	Auditorium	SR 1&2	SR 3&4	SR 5&6	SR 7&8	SR 12
	SYM-12: Emerging Developments for Regenerative and Therapeutic Medicine	A8: Medical Imaging	B8: Biological Materials	C8: Computational Mechanics	D4: Biomedical Devices	D3: Biomedical Devices Diagnostic Device
15:00	Tea Break					
15:30	Auditorium	SR 1&2	SR 3&4	SR 5&6	SR 7&8	SR 12
	C9: Cardiovascular Mechanics	A9: Biosignal Processing	B9: Biological Materials Diagnostics and Therapeutic	C10: Mechanobiology	D5: Lab-on-Chip Micro/Nanofluidics	E3: Rehabilitation Neurotechnology
17:00						
18:30	Conference Banquet <i>*This is a ticketed event that requires prior ticket purchase*</i>					
End of Day 3						

Friday, 06 December 2013

Poster Session 3

Time	Venue/Description				
9:00	SR 1&2	SR 3&4	SR 5&6	SR 7&8	SR 12
	A10: Biosignal Processing	B10: Regenerative Medicine Tissue Engineering	D6: Biomedical Devices	C11: Cell Mechanics	E4: Bio- and Medical Robotics
10:30	Tea Break				
11:00	SR 1&2	SR 3&4	SR 5&6	SR 7&8	SR 12
	A11: Medical Imaging	B11: Tissue Engineering	C13: Biomimetics Musculoskeletal Mechanics	C12: Molecular Biomechanics Tissue Mechanics	E5: Rehabilitation
12:30	Closing & Awards Presentation				
End of Conference					

Saturday, 07 December 2013

www.icbme.org

Copyright © 2013 Biomedical Engineering Society (Singapore). All rights reserved.
Design, Typeset & Printed by **Research Publishing Services** | Email: enquiries@rpsonline.com.sg

